

SYNTHETIC AND MECHANISTIC INVESTIGATIONS OF RUTHENIUM
ALKYLIDENE-CATALYZED ALKENE-SILANE CROSS-COUPPLING REACTIONS

by

APPARAO BOKKA

Presented to the Faculty of the Graduate School of
The University of Texas at Arlington in Partial Fulfillment
of the Requirements
for the Degree of

DOCTOR OF PHILOSOPHY

THE UNIVERSITY OF TEXAS AT ARLINGTON

December 2017

Copyright © by Apparao Bokka 2017

All Rights Reserved



Acknowledgements

I would like to convey my sincere thanks and gratitude to my research supervisor, Professor Junha Jeon, for his guidance and support over the past 5 years in achieving my dream. He warmly welcomed me to his research group even though I was away from college for a quite a long time after my M. S Degree. I still remember the way he taught me the basics during my initial period in his lab. I learned many reactions and purification techniques and improved my spectroscopic knowledge under his guidance. I am really grateful for his support during my struggle in the program. I am very much inspired with his planning and execution (research and writing). I am very fortunate to have him as my mentor. I pay my sincere thanks to my committee members, Professors Carl J. Lovely, Subhrangsu S. Mandal and Alejandro Bugarin, for their continuous feedback and suggestions on my research progress. I would like to thank Drs. Lovely, Bugarin, and Foss for allowing me to borrow some chemicals from their labs which avoided delay in my research. I am very thankful to my chemistry teachers Eswararaju sir and Varaprasad sir who created interested in chemistry from my college days. I would like to say special thanks to our post-doctoral fellow Dr. Yuanda Hua (2012-2016) whose knowledge and commitment is top-notch. I appreciate his helping nature and willingness to teach new graduate students. I would like to extend my gratitude to my fellow graduate students, Parham, Udaya, Thiru and Hiep. I would like to thank our undergrads Rush and Adams for their contributions in hydrosilylation project.

I am thankful to Jill, Debbie, Jim, Jason, Beth, and Natalie for their support at various levels in my program at UTA. My sincere thanks to Drs. Brian Edwards, Roy Mc Dougald, and Chuck Savage for their trainings and help in various instruments. My heartfelt thanks to my friends Sarma, Ramya, Atchut, Surya, Ranjeeta, Prudhvi, Santosh, Swathi, Radha, Saru, and Anush. I am grateful to my parents, grandparents, and sisters for their unconditional love and affection. I

would like to thank my wife who adopted my dream and compromised in many things for my ambition. I can never forget her support to fulfil my dream. Finally, I would like to thank my in-laws and my sister from UTA Udaya who always there to understand and support my ideas.

November 20, 2017

Abstract

SYNTHETIC AND MECHANISTIC INVESTIGATIONS OF RUTHENIUM ALKYLIDENE-CATALYZED ALKENE-SILANE CROSS-COUPPLING REACTIONS

Apparao Bokka, Ph.D.

The University of Texas at Arlington, 2017

Supervising Professor: Junha Jeon

Grubbs-type ruthenium alkylidene-catalyzed intramolecular alkene hydrosilylation and intermolecular dehydrogenative silylation and hydrosilylation of vinylarenes have been achieved with high regio- and stereoselectivity. Mechanistic details to support the initial activation of ruthenium complex have been revealed.

Chapter 1 describes the uses of organosilanes in various fields. Development of transition metal-catalyzed hydrosilylations, alkene/alkyne metathesis activities of Grubbs-type ruthenium alkylidenes and non-metathetical activities including hydrosilylation of alkynes are discussed. The development of intramolecular hydrosilylation of alkenylsilyl ethers through reaction discovery and optimization is discussed. The strategy developed has been tested successfully on a variety of substrates with varying steric and electronic properties. A plausible mechanism is proposed for the activation of the ruthenium complex by direct σ -bond metathesis between Si-H and Ru-Cl. Specifically a mechanistic pathway for intramolecular alkene hydrosilylation

catalyzed by ruthenium alkylidene complexes was proposed based on experimental observations from the optimization studies, isotope labelling studies, the investigation of base and halide effects.

In Chapter 2, the synthesis and uses of vinyl and alkyl silanes and existing methods to synthesize vinylsilanes have been discussed. The discovery and development of dehydrogenative silylation and hydrosilylation of vinylarenes using Grubbs-type ruthenium alkylidene complexes are presented. Reaction optimization to selectively achieve the formation of vinyl and alkyl silanes by varying the L and X-type ligands has been demonstrated. Evaluation of sacrificial hydrogen acceptors (SHA) and the investigation on substrate scope for the dehydrogenative and hydrosilylation were explored. This chapter also rationalizes possible mechanistic pathways for dehydrogenative and hydrosilylation catalyzed by ruthenium alkylidene complexes varying L and X-type ligands. Mechanistic studies on isotope labelling experiments and ligand effect revealing the rate-determining step for both the transformations are discussed.

Table of Contents

Acknowledgements.....	iii
Abstract.....	v
List of illustrations.....	xi
List of Tables	xiv
1. Chapter 1 Introduction	1
1.1 Importance of Organosilanes	2
1.2 Alkene Hydrosilylation and Early Developments	2
1.3 Introduction to Metathesis and Non-metathetical Applications of Grubbs Ru Alkylidenes	4
1.4 Alkyne Hydrosilylation Catalyzed by Ruthenium Alkylidene Complexes	6
1.5 Alkene Hydrosilylation by Ruthenium Alkylidene Complexes and Challenges.....	9
1.6 Applications of Alkene Hydrosilylation	9
1.7 Reaction Optimization for Alkene Hydrosilylation by Ruthenium Alkylidene Complexes	
1.7.1 Synthesis of Alkenols and Alkenylsilyl Ethers	10
1.7.2 Evaluation of Grubbs Ruthenium Alkylidene Complexes for Intramolecular Alkene Hydrosilylation	12
1.7.3 Evaluation of Solvents for Intramolecular Alkene Hydrosilylation.....	14
1.7.4 Optimization of Catalyst Loading for Intramolecular Alkene Hydrosilylation	15
1.7.5 Effect of Silyl Substituent on Intramolecular Alkene Hydrosilylation	16
1.8 Substrate Scope for Intramolecular Alkene Hydrosilylation	17
1.9 Mechanistic Consideration of Hydrosilylation Using Transition Metal Catalysis.....	20
1.10 Cox's Possible Mechanism of Ruthenium Alkylidene Catalyzed Alkyne Hydrosilylation.....	21

1.11	Cosy's Possible Mechanism of Ruthenium Alkylidene Catalyzed Alkyne Hydrosilylation	22
1.12	Formation of Chlorosilane and Vinylsilane	23
1.13	Activation of Grubbs-type Ruthenium Catalysts by Silanes.....	24
1.14	Experimental Support for the Activation of Grubb's-type Ruthenium Catalysts by Silanes	26
1.14.1	Stoichiometric Reaction of Alkenylsilyl ethers: Formation of Chlorosilane	26
1.14.2	Stoichiometric Reaction of Deuteriosilane: Formation of Ruthenium Silane Complex	27
1.14.3	Detection of Ruthenium Silane Complex by ¹ H NMR spectroscopy with Ru-4 and Ru-2	28
1.15	Effect of Halides on Catalytic Activity of Ruthenium Catalysts	31
1.16	Deuterium Labeling and Crossover Studies	32
1.17	Effect of Proton Scavenger on Ruthenium Alkylidene Catalyzed Intramolecular Alkene Hydrosilylation	33
1.18	Possible Mechanism for Ruthenium Alkylidene Catalyzed Intramolecular Alkene Hydrosilylation	34
1.19	Summary of Chapter 1	36
2.	Chapter 2 Introduction	38
2.1	Uses and Applications of Vinylsilane and Alkylsilanes	38
2.2	Introduction to Dehydrogenative Silylation of Alkenes.....	39
2.3	Transition Metal Catalyzed Dehydrogenative Silylation of Alkenes.....	40
2.4	Ruthenium Alkylidene Catalyzed Dehydrogenative Silylation and Hydrosilylation	42

2.5	Optimization for Ruthenium Alkylidene Catalyzed Dehydrogenative Silylation of Alkenes.....	43
2.5.1	Evaluation of Ruthenium Alkylidene Complexes for Dehydrogenative Silylation of Alkenes.....	43
2.5.2	Evaluation of Silanes for Dehydrogenative Silylation of Alkenes.....	44
2.5.3	Effect of Solvents on Dehydrogenative Silylation of Alkenes.....	46
2.5.4	Optimization Temperature and Concentration for Dehydrogenative Silylation of Alkenes.....	48
2.5.5	Evaluation of Sacrificial Hydrogen Acceptor (SHA) for Dehydrogenative Silylation of Alkenes.....	48
2.6	Substrate Scope for Ruthenium Alkylidene Catalyzed Dehydrogenative Silylation of Alkenes.....	49
2.7	Gram Scale Synthesis of Vinylsilane.....	52
2.8	Optimization of Ruthenium Alkylidene Catalyzed Alkene Hydrosilylation.....	52
2.9	Substrate Scope for Ruthenium Alkylidene Catalyzed Hydrosilylation of Alkenes.....	53
2.10	Kinetic Isotopic Experiments.....	55
2.10.1	Isotope Labeling of Silane.....	55
2.10.2	Isotope Labeling of Alkene.....	56
2.11	Effect of Halides on Catalytic Activity of Ruthenium Catalysts (Ru-1).....	57
2.12	Possible Mechanism for Dehydrogenative Silylation of Alkenes.....	58
2.13	Possible Mechanism for Hydrosilylation of Alkenes.....	60
2.14	Effect of Proton Scavenger on Dehydrogenative and Hydrosilylation of Alkenes.....	61
2.15	Summary of Chapter 2.....	63

Appendix A List of Abbreviations.....	64
Appendix B General Experimental Procedure.....	67
Appendix C Spectral Data of Compounds.....	87
References.....	273
Biographical Information.....	284

List of Illustrations

Figure 1.1	Alkene Hydrosilylation	2
Figure 1.2	Free Radical Initiated Alkene Hydrosilylation	3
Figure 1.3	Platinum Catalyzed Alkene Hydrosilylation	3
Figure 1.4	Price Chart of Precious Metals from 2012 to 2017	4
Figure 1.5	Types of Metathesis	5
Figure 1.6	Cox's Alkyne Hydrosilylation Catalyzed by Ruthenium Alkylidenes	6
Figure 1.7	Cossy's Alkyne Hydrosilylation Catalyzed by Ruthenium Alkylidenes	7
Figure 1.8	Lee's Alkyne Hydrosilylation Catalyzed by Ruthenium Alkylidenes	8
Figure 1.9	Proposed Intramolecular Alkene Hydrosilylation Over Alkene Metathesis	8
Figure 1.10	Grubb's -Type Ruthenium Complexes	9
Figure 1.11	Synthesis of Alkenols	11
Figure 1.12	Synthesis of Alkenylsilyl Ethers	11
Figure 1.13	Chalk-Harrod Mechanisms Involving Hydrometallation and Silylmetallation	20
Figure 1.14	Cox's Possible Mechanism of Alkyne Hydrosilylation by Ruthenium Alkylidene	22
Figure 1.15	Cossy's Speculative Mechanism of Alkene Hydrosilylation by Ruthenium Alkylidenes	23
Figure 1.16	Formation of Vinylsilane and Chorosilane Observed Alkene Hydrosilylation	24
Figure 1.17	Formation of Vinylsilane and Chorosilane During Alkene Hydrosilylation	24
Figure 1.18	Addition of a Ru-Alkylidene Bond Across a Si-H Bond/HCl Elimination	25
Figure 1.19	σ -Bond Metathesis Pathway	26
Figure 1.20	Stoichiometric Reaction Alkenylsilyl Ether with Ru-2	27
Figure 1.21	Stoichiometric Reaction Deuteriosilyl Ether with Ru-2	27

Figure 1.22	Reaction Monitoring of the Stoichiometric Reaction of Silyl Ether 1-16 with Ru-4	29
Figure 1.23	Reaction Monitoring of the Stoichiometric Reaction of Silyl Ether 1-16 with Ru-2	30
Figure 1.24	Intramolecular Deuterium-Labeling Studies.....	33
Figure 1.25	Cross-Over Studies	33
Figure 1.26	Effect of Proton Scavenger on Alkene Hydrosilylation.....	33
Figure 1.27	Plausible Mechanism of Alkene Hydrosilylation Catalyzed by Ruthenium Alkylidene Complex	35
Figure 2.1	Applications of Vinyl Silanes as Synthetic Intermediates	39
Figure 2.2	Hydrosilylation of Alkynes to Produce Vinyl Silanes	40
Figure 2.3	Transition Metal Catalyzed Dehydrogenative Silylation of Alkenes	41
Figure 2.4	Hartwig's Iridium Catalyzed Dehydrogenative Silylation of Alkenes	41
Figure 2.5	Watson's Palladium Catalyzed Dehydrogenative Silylation of Alkenes	41
Figure 2.6	Chirik's Cobalt Catalyzed Dehydrogenative Silylation of Alkenes	42
Figure 2.7	Gram Scale Reaction of Ruthenium Alkylidene (Ru-1) Catalyzed Dehydrogenative Silylation of Vinylarenes	52
Figure 2.8	Isotope Labeling of Alkene–Rapid Isomerization of Alkene	55
Figure 2.9	Preliminary Mechanistic Studies- Isotope Labeling of Silane.....	56
Figure 2.10	Preliminary Mechanistic Studies- Isotope Labeling of Alkene	56
Figure 2.11	Effect of X-Type Halide Ligands.....	58
Figure 2.12	Proposed Mechanism of Dehydrogenative Silylation of Vinylarenes Catalyzed by Ru-1	59

Figure 2.13 Proposed Mechanism of Hydrosilylation of Vinylarenes Catalyzed by Ru-7	60
Figure 2.14 Effect of A Proton Scavenger on Dehydrogenative Alkene-Silane Coupling	62
Figure 2.15 Effect of A Proton Scavenger on Hydrogenative Alkene-Silane Coupling	62

List of Tables

Table 1.1	Alkenylsilyl Ethers for Alkene Hydrosilylation	12
Table 1.2	Evaluation of Grubb's-Type Ruthenium Catalysts for Intramolecular Alkene Hydrosilylation	14
Table 1.3	Evaluation of Solvents for Intramolecular Alkene Hydrosilylation	15
Table 1.4	Evaluation of Catalyst Loading for Intramolecular Alkene Hydrosilylation	16
Table 1.5	Silyl Substituent Effect Grubbs-Type Ruthenium Catalysts for Intramolecular Alkene Hydrosilylation	17
Table 1.6	Substrate Scope of Grubbs-Type Ruthenium Catalyzed Intramolecular Alkene Hydrosilylation	19
Table 1.7	Catalytic Activities Varying Halides on Ru-2-X Catalysts	32
Table 2.1	Evaluation of Grubbs-Type Ruthenium Catalysts for Dehydrogenative Silylation and Hydrosilylation of Vinylarenes	44
Table 2.2	Evaluation of Silanes for Dehydrogenative Silylation	45
Table 2.3	Evaluation of Solvents for Dehydrogenative Silylation	47
Table 2.4	Evaluation of Sacrificial Hydrogen Acceptors for Dehydrogenative Silylation	49
Table 2.5	Substrate Scope of Ruthenium Alkylidene (Ru-1) Catalyzed Dehydrogenative Silylation of Vinylarenes	51
Table 2.6	Evaluation of Solvents for Dehydrogenative Silylation	53
Table 2.7	Substrate Scope of Ruthenium Alkylidene (Ru-7) Catalyzed Hydrosilylation of Vinylarenes	54

Note

Portions of this thesis have been taken, with permission, from the following publications:

Mechanistic Insights into Grubbs-Type Ruthenium-Complex-Catalyzed Intramolecular Alkene Hydrosilylation: Direct σ -Bond Metathesis in the Initial Stage of Hydrosilylation. **Bokka, A.**; Yuanda, H.; Berlin, S. A.; Jeon, J. *ACS Catal.* **2015**, *5*, 3189–3195.

Regio- and Stereoselective Dehydrogenative Silylation and Hydrosilylation of Terminal Alkenes Catalyzed by Ruthenium Alkylidenes. **Bokka, A.**; Jeon, J. *Org. Lett.* **2016**, *18*, 5324-5327

Additional work performed while pursuing my Ph.D. that does not appear in this thesis has been published in:

Lewis Base Activation of Silyl Acetals: Iridium –Catalyzed Reductive Horner-Wadsworth-Emmons Olefination. Dakarapu, U. S.; **Bokka, A.**; Asgari, P.; Trog, G., Hua, Y.; Nguyen, H. H.; Rahman, N.; Jeon, J. *Org. Lett.* **2015**, *17*, 5792-5795.

Enhanced heat capacity via PAO-superstructure. Pournorouz, Z.; Pinto, A.; **Bokka, A.**; Jeon, J.; Shin, D. *Nanoscale Research Letters*, **2017**, 12:29.

Hydrogen Atom Transfer from Hydrosilanes by Lewis Base Catalysis. Asgari, P.; Hua, Y.; **Bokka, A.**; Thiamsiri, C.; Prasitwatcharakorn, W.; Kaderath, A.; Leem, G.; Sardar, S.; Pierce, B. S.; Nam, K.; Gao, J.; Junha Jeon, J.* (**submitted**)

Chapter 1

Mechanistic Insights into Grubbs-Type Ruthenium-Complex-Catalyzed Intramolecular Alkene

Hydrosilylation: Direct σ -Bond Metathesis in the Initial Stage of Hydrosilylation.

Apparao Bokka, Yuanda Hua, Adam S. Berlin, and Junha Jeon*

This work has been published in *ACS Catal.* 2015, 5, 3189-3195^a

^a Used with the permission of the publisher, 2015

1. Introduction

1.1 Importance of Organosilanes

Organosilanes are important building blocks and extensively used for C–C and C–O bond formation. These silanes are widely employed in organic synthesis (e.g., silicon-based blocking agents,^{1,2} reducing agents,³ cross-coupling reactions⁴⁻⁶ and silicon-based anion relay chemistry⁷), medicinal applications,^{8,9} and materials science (e.g., coating materials, silicon polymers,^{10,11} silicone-based surfactants, fluids, molding products, release coatings, and pressure sensitive adhesive^{12,13}). In addition, organosilanes, which are relatively inexpensive and a wide range of silyl precursors are commercially available, are essential synthetic moieties because they can serve as latent functional groups by Lewis base activation, and organosilanes by-products are relatively non-toxic.¹⁴⁻¹⁷

1.2 Alkene hydrosilylation and early developments

Hydrosilylation of alkenes, alkynes, and carbonyls has been utilized for syntheses of diverse organosilanes.¹⁷ Hydrosilylation is defined as the addition of silicon-hydrogen (Si–H) bonds across an unsaturated moiety (alkenes, alkynes, carbonyls, and imines) and results in a new silicon-carbon (Si–C) or silicon heteroatom (Si–O/N) bond. Specifically, alkene hydrosilylation (Figure 1.1) is an important tool to synthesize alkyl silanes,¹⁷ which can be used as silicon-containing synthetic intermediates, functionalized materials,^{10,17-19} and pharmaceutically useful molecules.²⁰⁻²²

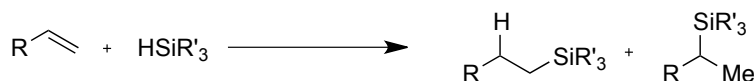


Figure 1.1 Alkene hydrosilylation.

Hydrosilylation of alkenes initiated by free-radicals²³ (Figure 1.2) has been known for almost 70 years, in a subsequent year (1957) transition metal-catalyzed alkene hydrosilylation involving platinum complexes¹⁷ (Speier's H_2PtCl_6 ²⁴⁻²⁶ Figure 1.3 and Karstedt's Pt(0) vinylsiloxane^{27,28}) revolutionized synthesis of organosilanes. In spite of its usefulness, Pt-catalyzed hydrosilylation is generally associated with inconvenience such as oligomerization, polymerization, hydrogenation, redistribution, dehydrogenation and dehydrogenative silylation.^{17,29}

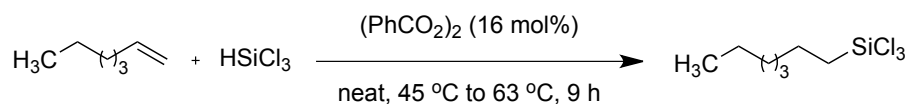


Figure 1.2 Free radical-initiated alkene hydrosilylation.

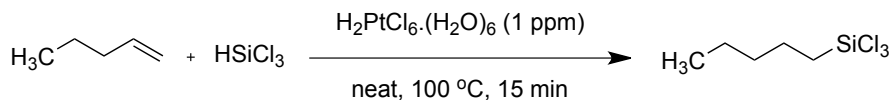


Figure 1.3 Platinum-catalyzed alkene hydrosilylation.

Apart from advances made with Pt catalysts,^{1d} various transition metals (Pd, Ir, Rh, Ru, and Ni) have been employed for the hydrosilylation of alkenes including asymmetric hydrosilylations. The choice of catalyst determines the mechanism of catalysis.¹⁷ Particularly, relative abundances and the low cost of the ruthenium made it attractive and useful for such transformation (Figure 1.4).

Platinum, Palladium, Rhodium, Iridium, Ruthenium
 Monthly Average prices between 23 Sep 2012 and 23 Sep 2017
 JM Base Price \$/Oz
 Platinum average: \$1,218.89, Palladium average: \$726.99, Rhodium average: \$985.42, Iridium average: \$689.30, Ruthenium average: \$60.10

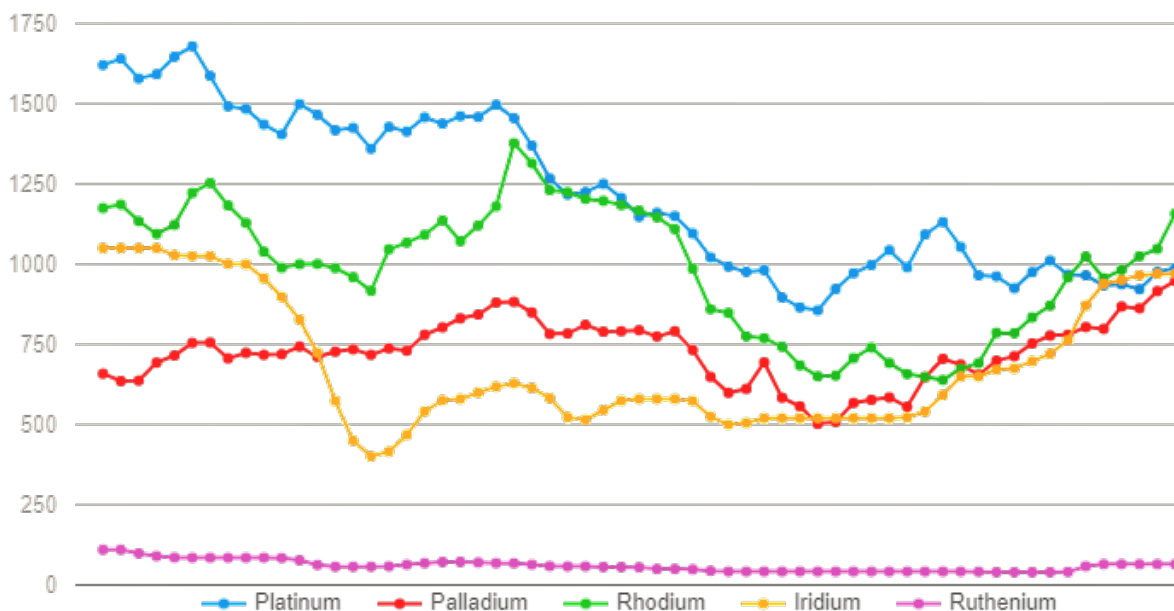


Figure 1.4 Price chart of precious metals from 2012 to 2017.

<http://www.platinum.matthey.com/prices/price-charts> (accessed in September 23, 2017)

1.3 Introduction to metathesis and non-metathetical applications of Grubbs Ru-alkylidenes

Ruthenium carbene complexes (Figure 1.5) are versatile catalysts for olefin metathesis,³⁰⁻³² metal-catalyzed redistribution of carbon-carbon double bonds (Figure 1.6). Because of their exceptional functional group tolerance, ease of operation, and insensitivity toward oxygen and water, these catalysts have revolutionized olefin synthesis through more efficient and perhaps greener methods.^{31,33,34} During the past decade researchers have begun to explore non-metathetical uses of the ruthenium alkylidene complexes as well.^{35,36} Toward this end, these catalysts have been employed to achieve various reactions such as Karasch addition,³² oxidation processes,³⁷ alkyne hydrosilylations,³⁸ alkene hydrogenation,^{39,40} cyclopropanation,^{41,42} C–H

activation,³⁶ and cycloaddition reactions.^{43,44} Surprisingly, Grubbs-type ruthenium complex-catalyzed olefin hydrosilylation to provide alkyl silanes was unknown.

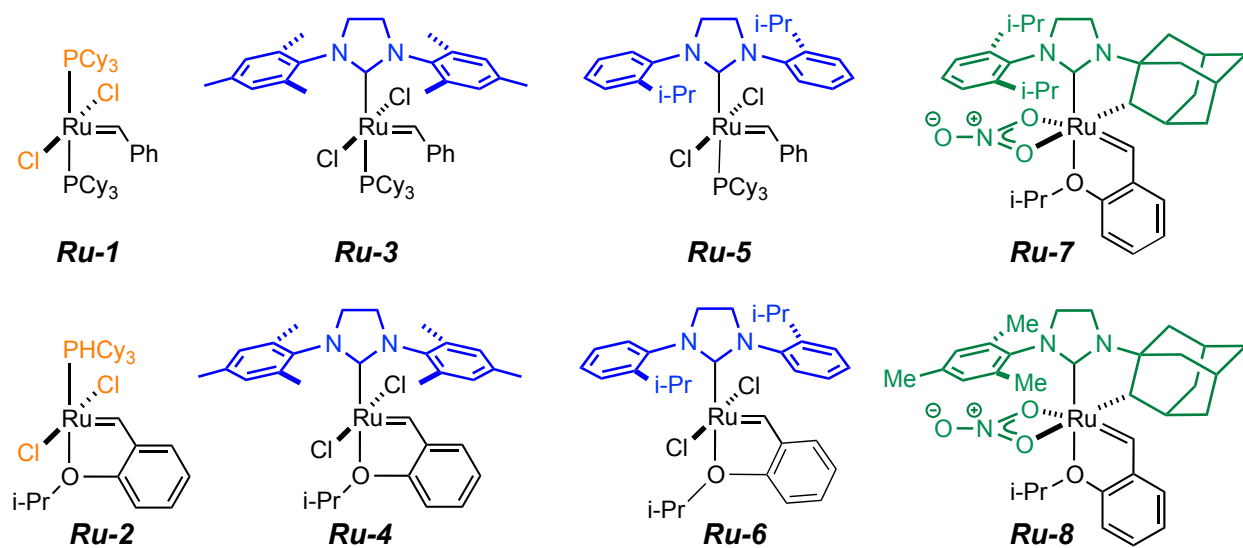


Figure 1.5 Grubbs-type ruthenium complexes

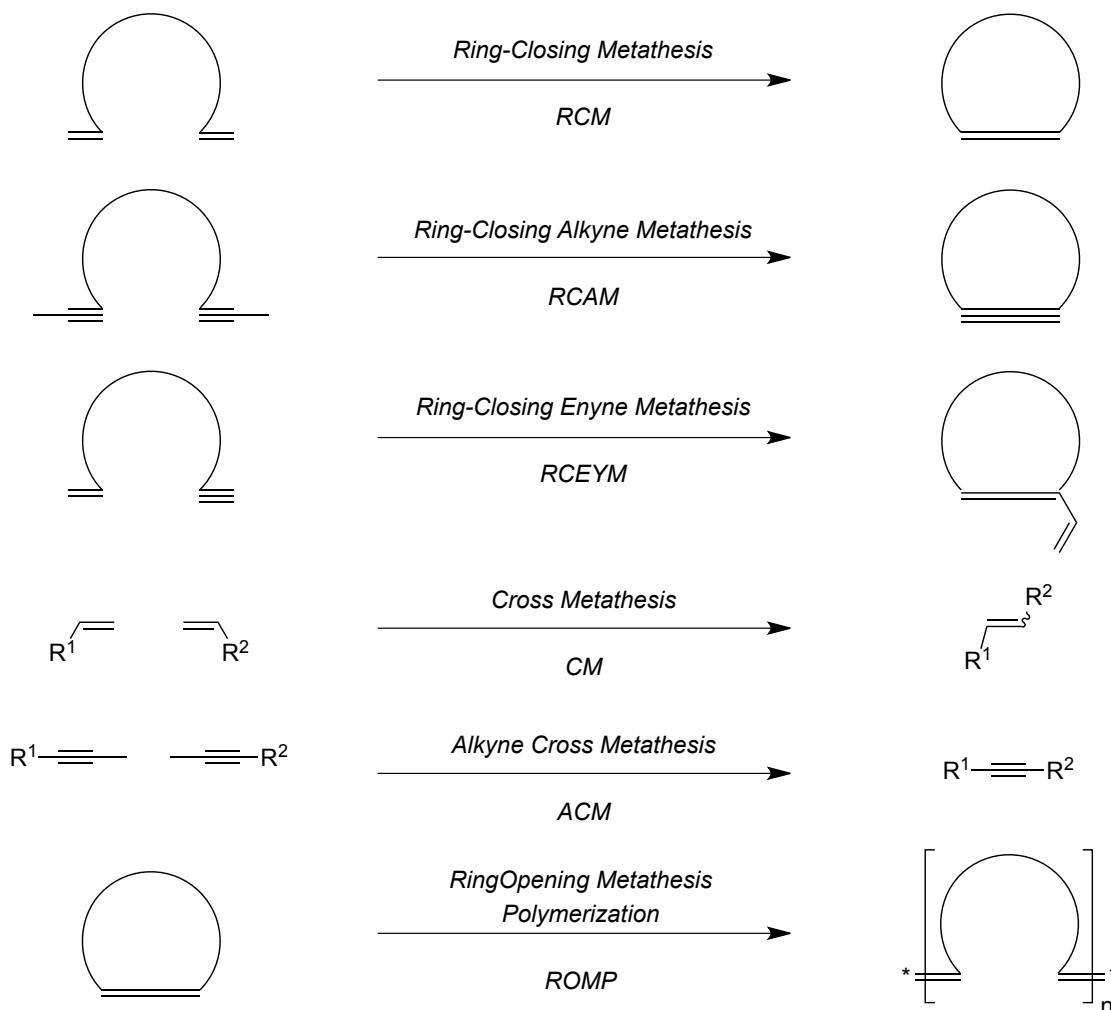


Figure 1.6 Types of metathesis

1.4 Alkyne hydrosilylation catalyzed by ruthenium alkylidene complexes

The Cox,⁴⁵ Lee,⁴⁶ and Cossy⁴⁷ laboratories demonstrated intermolecular alkyne hydrosilylation using Grubbs-type ruthenium alkylidene complexes.³²⁻³⁴ The regio- and stereochemical outcome of these processes depends on several factors including the choice of catalyst (the metal and ligands), the substituents on both reaction partners, and to a lesser extent, on other reaction parameters (e.g., reaction temperature, solvent and catalyst loading). Cox⁴⁵ reported that the choice of silane⁴⁷ governs the regioselectivity (Figure 1.7). In contrast, Cossy⁴⁷

attributed the prominent α -selectivity to stereo-electronic factors when the reaction was carried out under kinetic conditions and steric factors are responsible for the β -silyl products (Figure 1.7). Lee⁴⁶ described the formation α -silyl isomer due to the directing effect of the hydroxyl group of alkynyl alcohols (Figure 1.8).

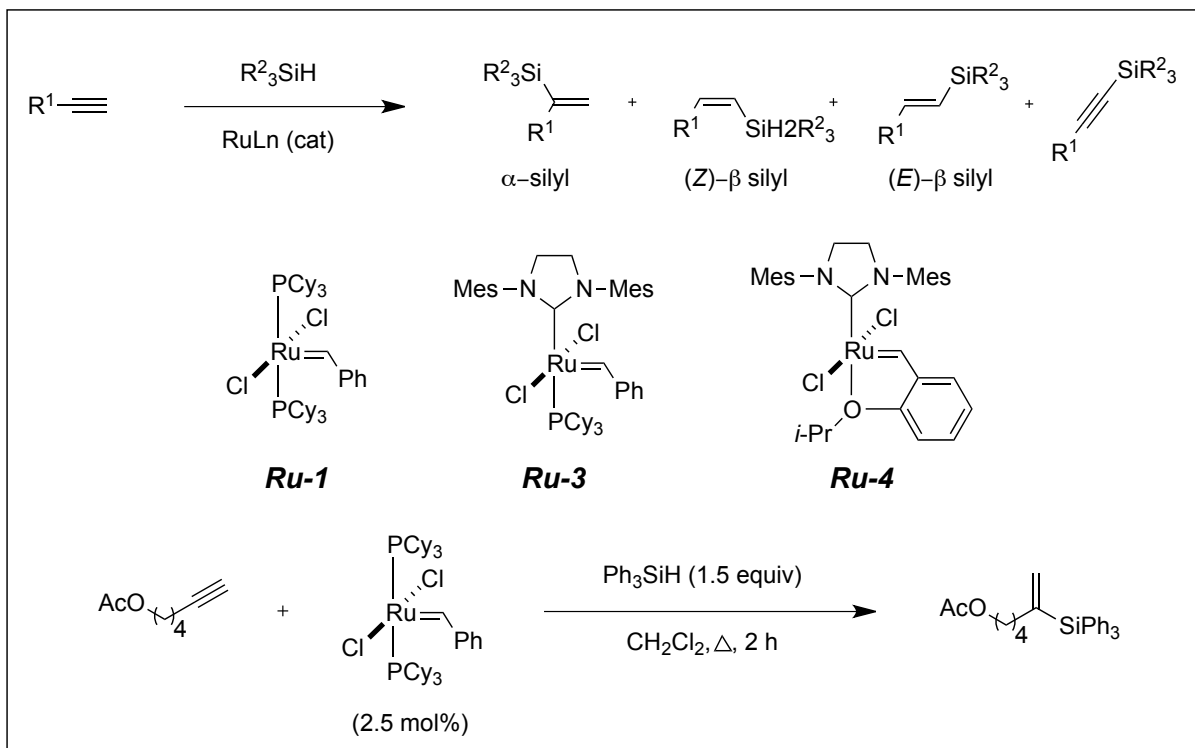


Figure 1.7 Cox's alkyne hydrosilylation catalyzed by ruthenium alkylidenes.

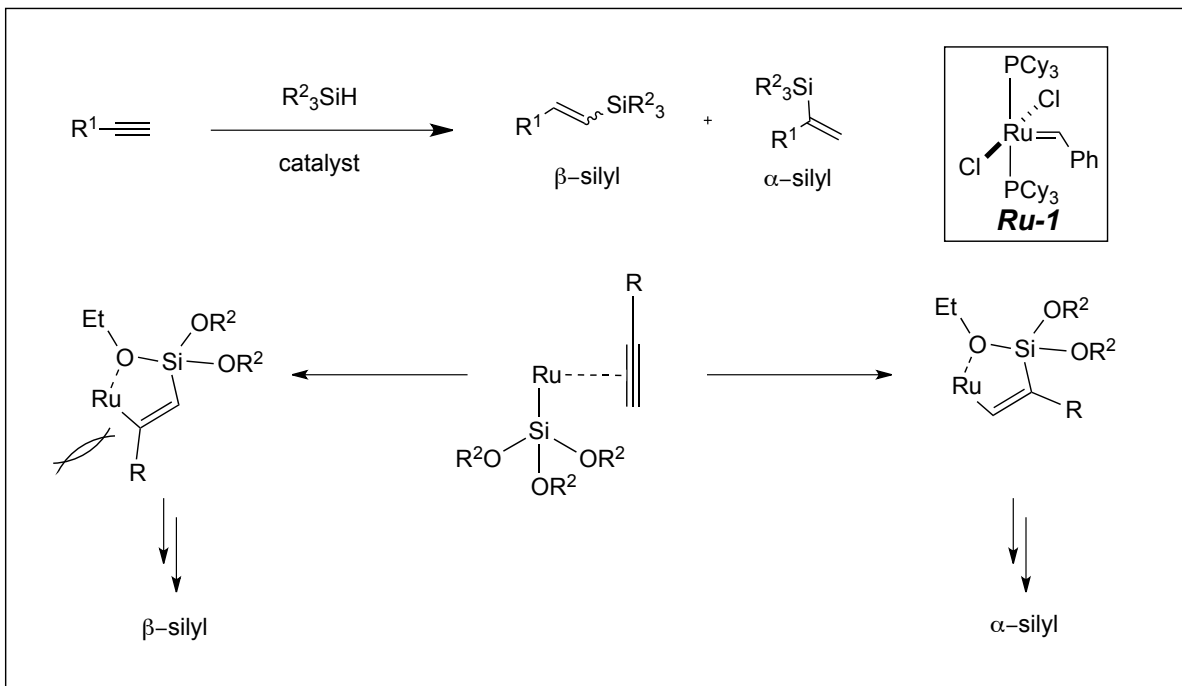


Figure 1.8 Cossy's alkyne hydrosilylation catalyzed by ruthenium alkylidenes

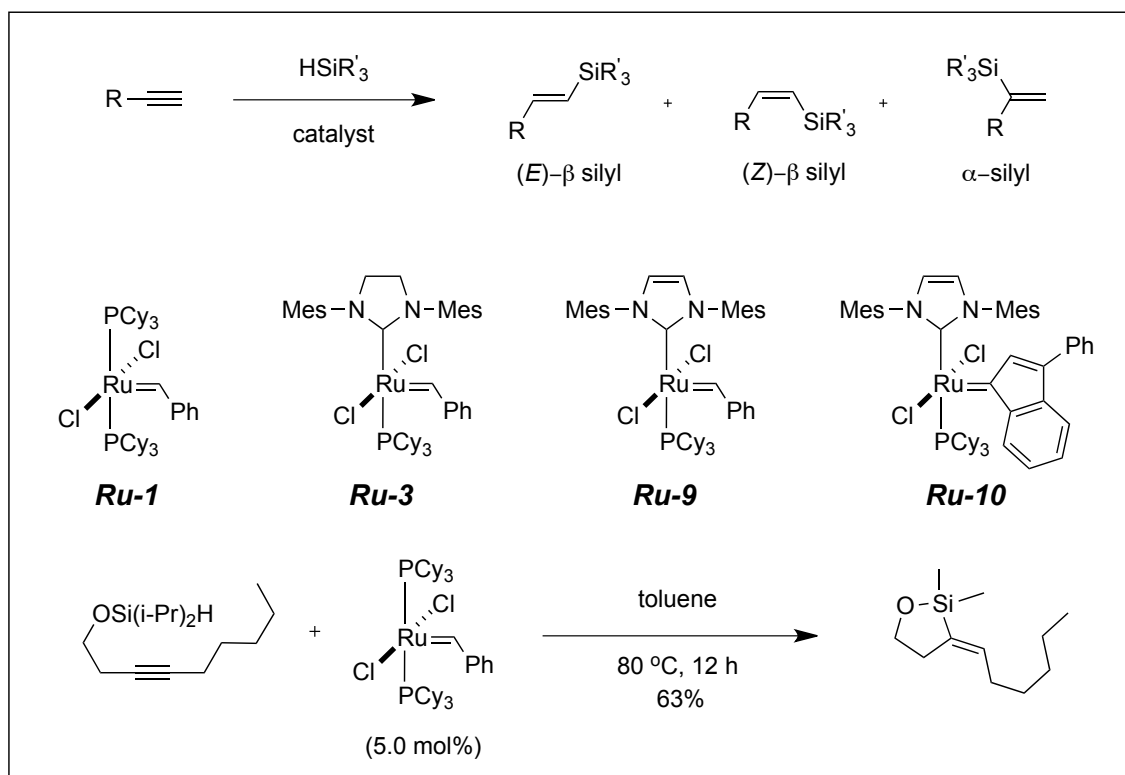


Figure 1.9 Lee's alkyne hydrosilylation catalyzed by ruthenium alkylidenes

1.5 Challenges of alkene hydrosilylation by ruthenium alkylidene complexes

Ruthenium alkylidene-catalyzed alkyne hydrosilylation was well-explored. However, inter- and intramolecular alkene hydrosilylation to provide alkyl silanes is unknown as mentioned in section 1.3. The difficulty of such processes is associated with i) diminished reactivity of alkenes compared to alkynes upon the treatment of ruthenium catalysts,^{48,49} and ii) more importantly, the competitive cross metathesis^{33,34,53} of an alkenyl silane substrate via *alkene activation over silicon-hydride*^{48,50-52} activation to afford homodimers, rather than furnishing regio- and stereoisomeric oxasilacycles (Figure 1.10). In addition, the origin of the reactivity and selectivity of the processes is unclear in which no mechanistic studies including isotope-labeling experiments, reaction kinetics, and spectroscopic observations have been reported thus far, and the regio- and diastereoselectivity remain uncertain.

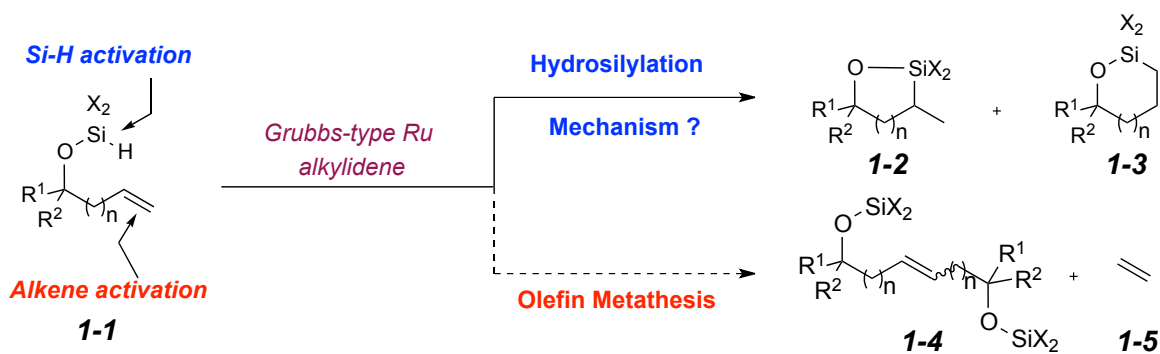


Figure 1.10 Proposed intramolecular alkene hydrosilylation over alkene metathesis

1.6 Applications of alkene hydrosilylation

Nonetheless, the outcome of these processes has merit for possessing a silicon functionality, which allows further elaboration via Hiyama-Denmark cross-coupling^{4,5,54} or Fleming-Tamao oxidation.⁵⁵ In particular, intramolecular hydrosilylation of alkenyl silyl ethers to form oxasilacycles that can be converted subsequently to 1,2-diols, 1,3-diols, and 1,4-diols⁵⁵⁻⁵⁸

after oxidative desilylation,⁵⁹ has offered an important synthetic tool in preparation of natural products and biologically relevant molecules. This research will contribute to the understanding of fundamental mechanistic aspects of non-metathetical use of the Grubbs-type ruthenium catalysts, not only hydrosilylation but other associated transformations (e.g. dehydrogenative condensation of alcohols and silanes, direct arylation, and hydrogenation) as well.

1.7 Reaction optimization for alkene hydrosilylation by ruthenium alkylidene complexes

1.7.1 Synthesis of alkenols and alkenylsilyl ethers

To test the feasibility of hydrosilylation of alkenyl silyl ethers, we designed various substrates involving allylic/homo allylic alcohol⁶⁰ and 2-allyl phenols.⁶¹ Alkenyl hydroxy/phenolic substrates were synthesized by three methods shown in Figure 1.11. These alkenyl alcohols/phenols were converted into silyl ethers by a reaction with diphenylbromosilane,⁶² which was prepared in situ from *N*-bromosuccinimide (NBS) and diphenylsilane (Figure 1.12). Some of the silyl ethers are not stable on silica gel chromatographic separation; these compounds were prepared by passing through either a pad of Celite[®] or deactivated silica gel quickly and used in the next step. A total of 16 alkenyl silyl ethers were synthesized (Table 1.1). Substrate **1-1-1** was chosen as the master substrate and used for optimization studies.

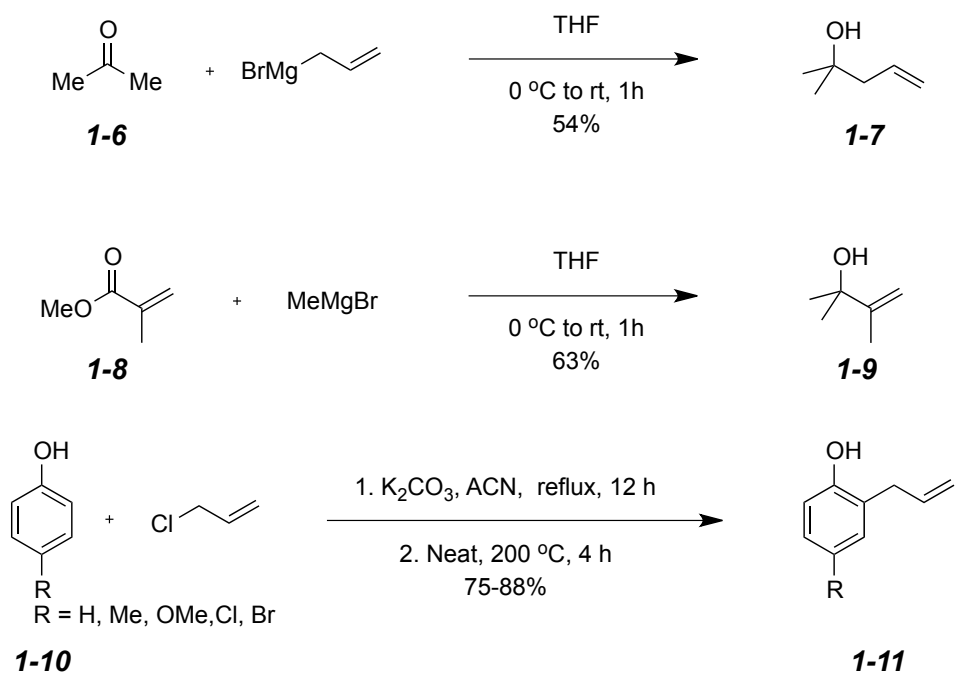


Figure 1.11 Synthesis of alkenols

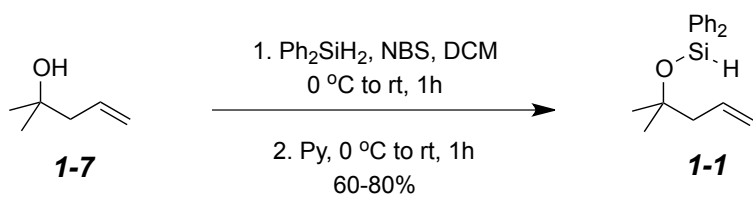


Figure 1.12 Synthesis of alkenyl silyl ethers

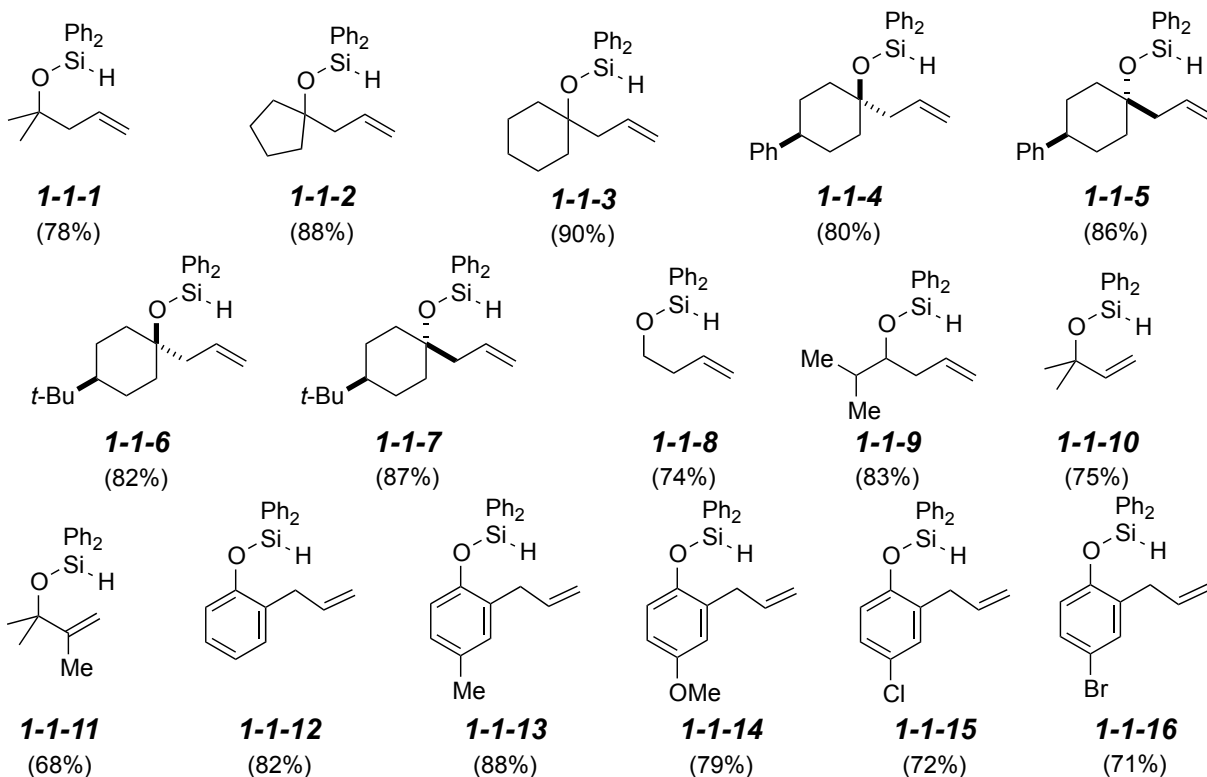


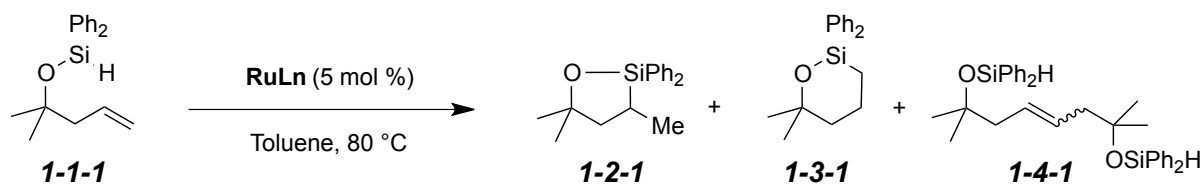
Table 1.1 Alkenylsilyl ethers for alkene hydrosilylation

1.7.2 Evaluation of Grubbs ruthenium alkylidene complexes for intramolecular alkene hydrosilylation

We started our reaction optimization studies; first, a number of ruthenium alkylidene catalysts⁶³⁻⁶⁷ were screened for this transformation. At ambient temperature, **Ru-1**⁶⁸ did not give the hydrosilylation products (i.e., **1-2-1** or **1-3-1**) and the homoallyl silyl ether **1-1-1** was recovered (Table 1.2). The desired product was first observed with **Ru-2** (first generation Hoveyda-Grubbs catalyst),⁶⁹ but even after 7 days of reaction time at room temperature the total conversion was only 20% (80% of **1-1-1** was unreacted). An improved conversion was observed by running the reaction at 80 °C (75% ¹H NMR yield with an internal standard). Seven ruthenium alkylidene catalysts (**Ru-1** to **Ru-7**) were evaluated for hydrosilylation of alkenyl silyl ethers. Among the catalysts used **Ru-2** and **Ru-3** (second generation Grubbs catalyst)⁷⁰ were

recognized as the most effective catalysts, permitting intramolecular alkene hydrosilylation of **1-1** to afford **1-2-1** (75% and 67% ¹H NMR yields with an internal standard, respectively]. To our surprise, all of the Grubbs-type ruthenium catalysts that were evaluated showed complete regioselectivity, and only regioisomer **1-2** was observed (regioisomer **1-3** was never present during the course of the reaction). When these reactions were monitored by ¹H NMR spectroscopy, no change to the resonance of a benzylidene proton on ruthenium catalyst was observed and the formation of corresponding Ru alkylidene or methyldiene intermediate was not detected in any of the reactions. Homo dimerization product (**1-4**) of alkenyl silyl ether or the styrene by-product released by the initial metathesis event were not present in the GC/MS and ¹H NMR analyses.⁷¹⁻⁷³ These results established that the regioselective synthesis of oxasilacyclopentanes **1-2** was feasible via hydrosilylative cyclization, using Grubbs-type ruthenium catalysts. Hoveyda-Grubbs second generation catalyst **Ru-4**⁷⁴ generated good yields with excellent regioselectivity, whereas Grubbs first generation catalyst **Ru-1** and other catalysts **Ru-5** and **Ru-6**^{75,76} gave poor yields including *Z*-selective catalyst **Ru-7**.⁶⁶ Together, the formation of oxasilacyclopentane **1-2-1**, as well as the absence of olefin metathesis by-product **1-4-1** confirms that the catalytic conditions performed effect the preferential Si-H bond activation over the alkene activation for metathesis.

Table 1.2 Evaluation of Grubbs-type ruthenium catalysts for intramolecular alkene hydrosilylation^a



entry	RuLn	yield (%) ^c	1-2-1:1-3-1:1-4-1 ^b
1	Ru-1	27	100:0:0
2	Ru-2	75	100:0:0
3	Ru-3	67	100:0:0
4	Ru-4	50	100:0:0
5	Ru-5	28	100:0:0
6	Ru-6	15	100:0:0
7	Ru-7	13	100:0:0

^aconditions: silane **1-1-1** (0.1 mmol), Toluene (0.01 M). ^bdetermined by GC/MS analysis.

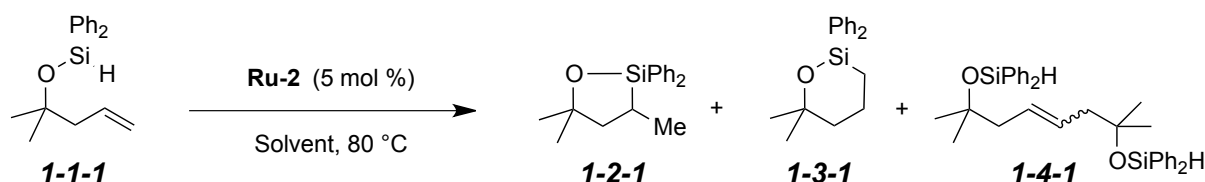
^cdetermined by ¹H NMR spectroscopy utilizing an internal standard (CH_2Br_2)

1.7.3 Evaluation of solvents for intramolecular alkene hydrosilylation

Ru-2 was identified as the best catalyst for the intramolecular alkene hydrosilylation (75% ¹H NMR yield, Table 1.2 entry 2). We wonder if there was a significant impact on yield by the choice of solvent (Table 1.3). PhMe was used as the solvent in catalyst studies, solvents routinely utilized in olefin metathesis such as; CH_2Cl_2 , PhH, PhCH_3 , and $\text{ClCH}_2\text{CH}_2\text{Cl}$ were

employed and interestingly THF (85% yield, entry 5) was superior to the rest of the solvents. Even though rest of the solvents are favorable for metathesis; not even a trace of the metathesis activity was ever detected by GC/MS.

Table 1.3 Evaluation of solvents for intramolecular alkene hydrosilylation^a



entry	Solvent	yield (%) ^c	1-2-1:1-3-1:1-4-1 ^b
1	CH ₂ Cl ₂	50	100:0:0
2	PhH	52	100:0:0
3	PhCH ₃	75	100:0:0
4	ClCH ₂ CH ₂ Cl	53	100:0:0
5	THF	85	100:0:0

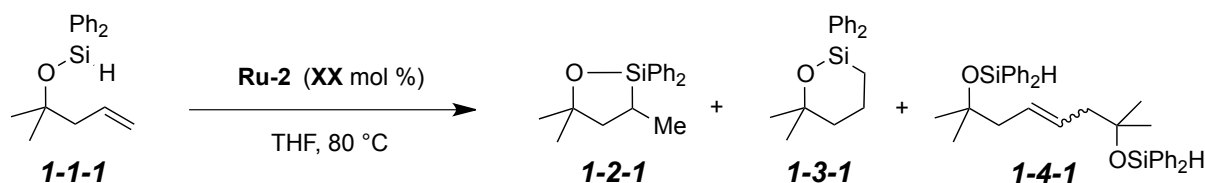
^aconditions: silane **1-1-1** (0.1 mmol), Solvent (0.2 M). ^bdetermined by GC/MS analysis.

^cdetermined by ¹H NMR spectroscopy utilizing an internal standard (CH₂Br₂).

1.7.4 Optimization of catalyst loading for intramolecular alkene hydrosilylation

Initial experiments were set up with 2 mol% of catalyst loading to give **1-2-1** (85%, ¹H NMR yield). Yield remains unchanged when the catalyst loading was lower down to 0.5 mol%. Catalyst loading of 0.1 mol% resulted in lower yield of **1-2-1** (73%, ¹H NMR yield) which was due to the left over alkenylsilylether **1-1-1**.

Table 1.4 Evaluation of catalyst loading for intramolecular alkene hydrosilylation^a



entry	Catalyst	yield (%) ^c	1-2-1:1-3-1:1-4-1 ^b
1	2 mol%	85	100:0:0
2	0.5 mol%	85	100:0:0
3	0.1 mol%	73	100:0:0

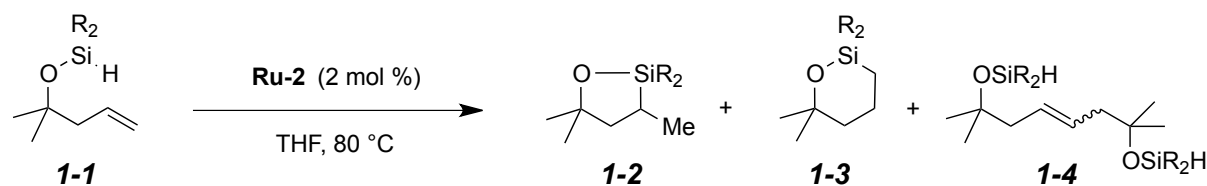
^aconditions: silane **1-1-1** (0.1 mmol), THF (0.2 M). ^bdetermined by GC/MS analysis.

^cdetermined by ¹H NMR spectroscopy utilizing an internal standard (CH₂Br₂)

1.7.5 Effect of silyl substituent on intramolecular alkene hydrosilylation

The effect of substituents on silicon was also examined. Various substitutions on a silyl moiety were studied for the intramolecular alkene hydrosilylation. Substrate possessing diphenyl substituents clearly exhibited a superior yield and conversion over those containing alkyl substituents such as dimethyl, diisopropyl and ditertiary butyl groups (Ph > Me > *i*-Pr > *t*-Bu). The later substituent had no conversion, even at elevated temperatures and extended reaction time. These experiments suggest that the silyl substituents play an important role in achieving the efficient intramolecular alkene hydrosilylation.

Table 1.5 Silyl substituent effect on Grubbs-type ruthenium catalysts for intramolecular alkene hydrosilylation^a



entry	R	yield (%) ^c	1-2-1:1-3-1:1-4-1 ^b
1	Me	63	100:0:0
2	Ph	85	100:0:0
3	<i>i</i> -Pr	20	100:0:0
4	<i>t</i> -Bu	0	NA

^aconditions: silane **1-1-1** (0.1 mmol), THF (0.2 M). ^bDetermined by GC/MS analysis.

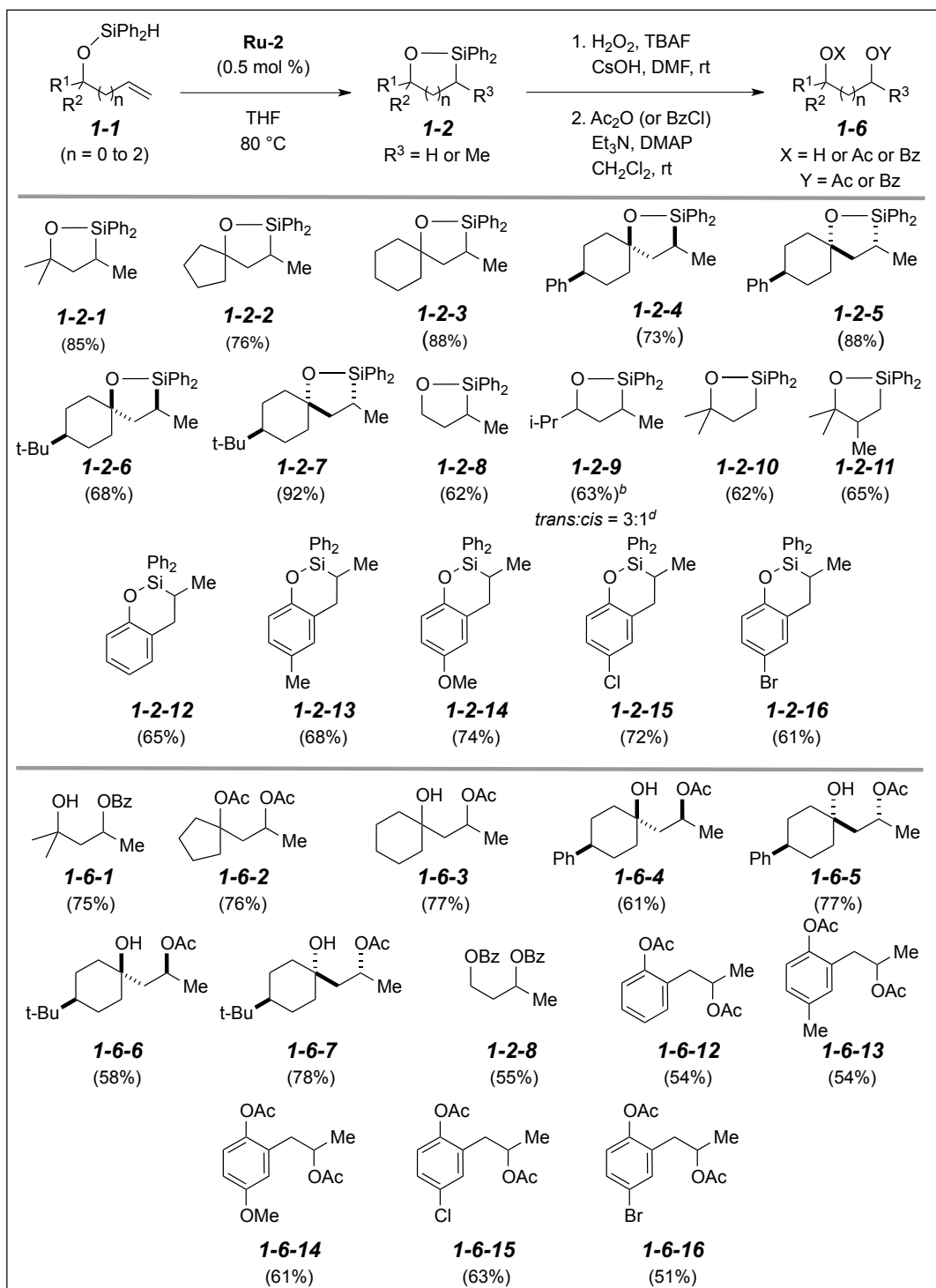
^cdetermined by ¹H NMR spectroscopy utilizing an internal standard (CH₂Br₂).

1.8 Substrate scope for intramolecular alkene hydrosilylation

With optimized reaction conditions, the homoallylic silylether **1-1-1** gave oxasilacyclopentane via a *5-exo-trig* cyclization (**1-2-1**, 85% yield), whereas allylic silylether **1-1-8** produced oxasilacyclopentane via *5-endo-trig* cyclization in 62% yield. 2-Allylphenoxy diphenylsilane **1-1-12** gave the oxasilacyclohexane **1-2-12** via a *6-exo-trig* cyclization in 65% yield. After successfully testing three substrates, we designed and synthesized a number of substrates to evaluate the regio- and stereoselectivity of Grubbs-type ruthenium alkylidene-catalyzed intramolecular alkene hydrosilylation. Substrates with 3°-alkoxy carbons exhibited excellent conversion and good yields. Cyclopentane and cyclohexane containing 3°-homoallylic

silyl ether substrates (**1-1-2** and **1-1-3**) provided hydrosilylation products **1-2-2** and **1-2-3** in very good yields (76% and 87%, respectively). Substrates **1-1-4** to **1-1-7** were designed to study the effect of stereochemistry on alkene hydrosilylation using Grubbs ruthenium alkylidenes. These substrates contain Ph or *t*-Bu groups at δ - position to the silyl ether either in either *syn* or *anti* relationship. Substrates holding *syn* relationship to each other (Ph or *t*-Bu to the silyl ether) resulted in better yields (88% for **1-2-5** and 92% for **1-2-7**), in comparison to the *trans* isomers (73% for **1-2-4** and 68% for **1-2-6**). Substrates with 1° alkoxy carbon afforded **1-2-8** in 62% yield. Substrates with 2° alkoxy carbon yielded **1-2-9** (63% yield) with a 3:1 ratio (*cis:trans*) of diastereomers. This trend supports the possible *gem*-dimethyl-like or Thorpe-Ingold effect on the cyclizations, where the slower rate in substrates holding 1° and 2° alkoxy carbon effects lower yields.⁷⁷ We also studied allylsilyl ethers, which provided **1-2-10** and **1-2-11** (62% and 65%, respectively). 2-Allylphenoxy diphenylsilanes generally afforded oxasilacyclohexanes **1-2-12** to **1-2-16** with good yields, regardless of electronic nature of substituents (Me, OMe, Cl, and Br) at *para*-position to the phenoxy group. Organosilicon heterocycles synthesized through the ruthenium alkylidene-catalyzed alkene hydrosilylation were subjected to the oxidation conditions followed by acylation or benzylation to afford diacetates, hydroxyl acetates and dibenzoates.

Table 1.6 Substrate scope of Grubbs-type ruthenium catalyzed for intramolecular alkene hydrosilylation^a



^aconditions: silane 1-1-1 (0.1 mmol), THF (0.2 M). ^bdetermined by GC/MS analysis.

^cdetermined by ^1H NMR spectroscopy utilizing an internal standard (CH_2Br_2)

1.9 General mechanistic consideration of hydrosilylation using transition metal catalysis

Hydrosilylation of alkenes catalyzed by transition metals is generally proceed by either the Chalk-Harrod mechanism⁸³ or modified Chalk-Harrod mechanism⁵²⁻⁵³ (Figure 1.13). Initial oxidative addition of hydrosilane to the metal complex provides a metal-hydrido-silyl complex B, which is coordinated with the alkene. Then complex B undergoes migratory insertion of the alkene into the M-H bond (hydrometallation) to give the complex C or D. Reductive elimination of the alkyl and silyl ligands from C or D forms the hydrosilylation product. Alternatively modified Chalk-Harrod mechanism involves an alkene insertion into the M-Si bond (silylmetallation) to form the silyl-alkyl-hydrido intermediate E or F, followed by reductive elimination to complete the hydrosilylation.

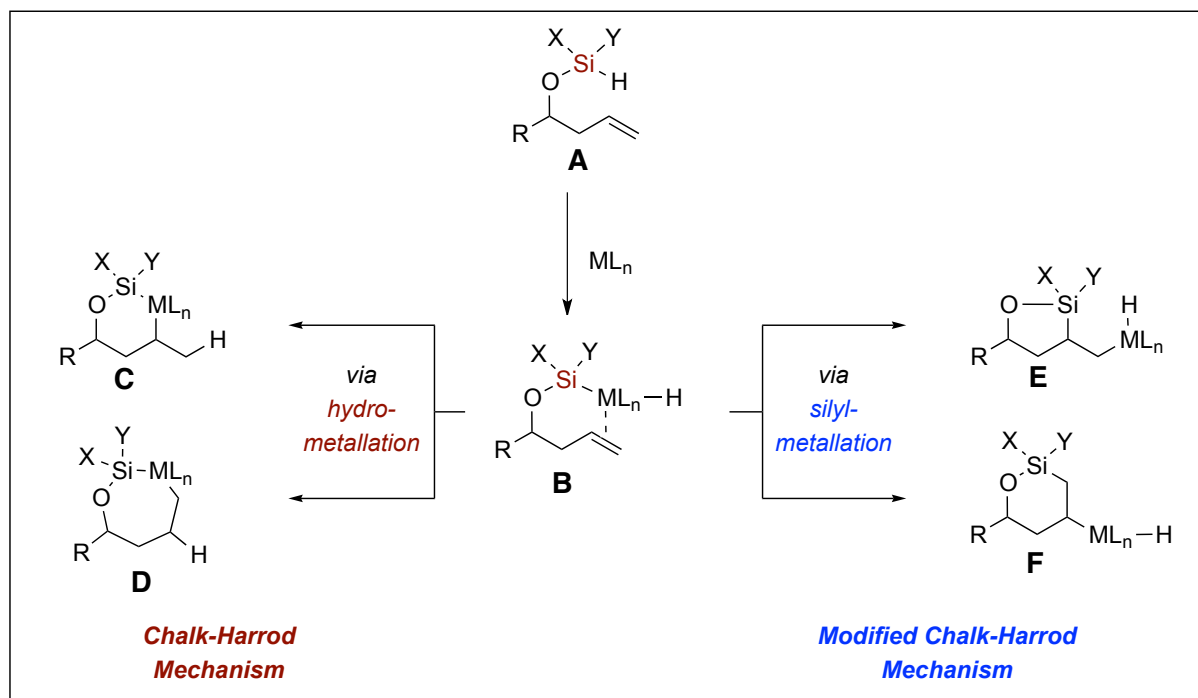


Figure 1.13 Chalk-Harrod Mechanisms involving hydrometallation and silylmetallation

1.10 Proposed mechanism of ruthenium alkylidene catalyzed alkyne hydrosilylation by Cox

Cox⁴⁵ proposed two speculative mechanisms which involves path i) activation of Ru alkylidene by hydrosilane and path ii) standard oxidative addition of silane to Ru alkylidene. Specifically, in path 1 the catalysis starts with formation of coordinatively unsaturated active ruthenium alkylidene complex **G**, generated by loss of a phosphine ligand. Ruthenium silyl intermediate **H** was formed by the reaction of the hydrosilane with the ruthenium alkylidene **G** (Chauvin-type mechanism).⁷⁸ Alkyne insertion into the Ru–Si bond proceeds in a *syn* fashion to afford a vinyl ruthenium complex **I**. Isomerization followed by β -hydride elimination would then provide the β -(*Z*)-stereoisomer vinylsilane product β -**Z** and regenerate the ruthenium alkylidene complex **G**⁷⁹ (Figure 1.14). Path ii) involves the traditional organometallic route oxidative addition, migratory insertion, and reductive elimination.⁴⁵

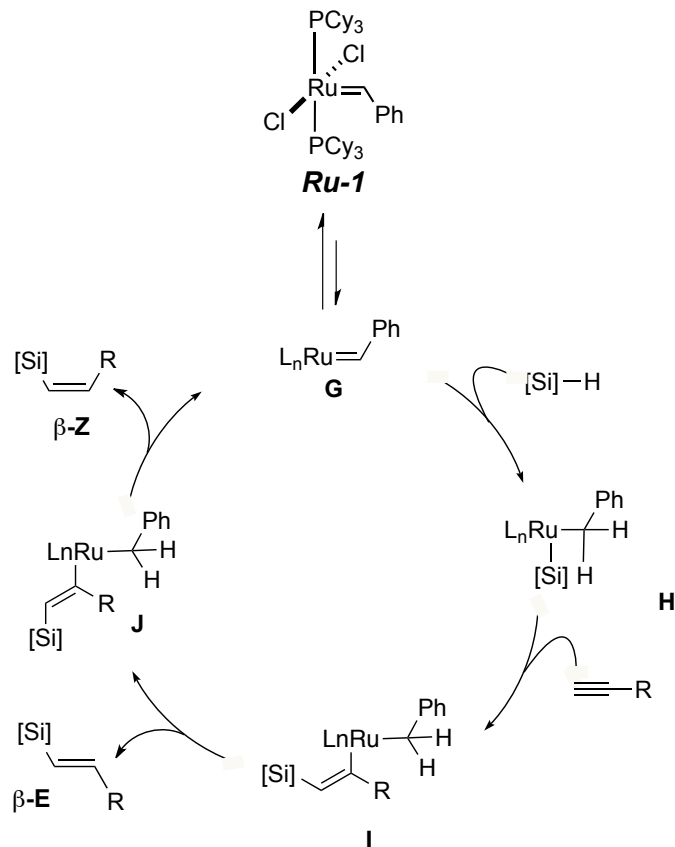


Figure 1.14 Cox's proposed mechanism of alkyne hydrosilylation by ruthenium alkylidenes

1.11 Cossy's proposed mechanism of ruthenium alkylidene-catalyzed alkyne hydrosilylation

According to Cossy,⁴⁷ the ruthenium alkylidene catalyzes the alkyne hydrosilylation through a modified Chalk-Harrod mechanism.^{48,50-52} The Ru-alkylidene pre-catalyst generates a transient 16-electron metal complex, which reacts with the alkyne and silane at the same time followed by reductive elimination of the metal to produce vinylsilanes **M** and **N** (Figure 1.15). However, neither study provided any experimental evidence, supporting any such basic processes.

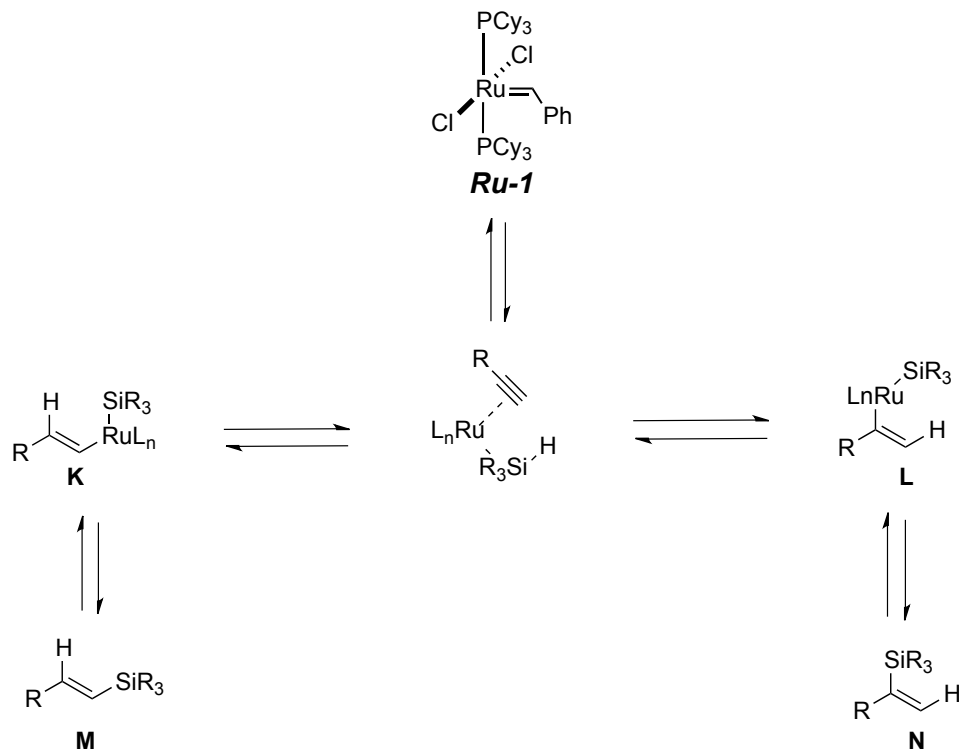


Figure 1.14 Speculative Mechanism of Alkene Hydrosilylation by Ruthenium alkylidene by Cossy

1.12 Formation of vinylsilane and chlorosilane

Experimental observations from our optimization studies addressed the initial stage of Grubbs-type ruthenium complex-catalyzed hydrosilylation within a ruthenium coordination sphere. During the reaction of silyl ether **1-1-1** with **Ru-2**, two other products were observed along with the hydrosilylation product **1-2-1**. These products were characterized by GC/MS spectrometry analysis, which were found be vinylsilane **1-12-1** (ca. 0.5%)²⁰ and chlorosilane **1-13-1** (ca. 1%)⁸⁰⁻⁸² (Figure 1.16).

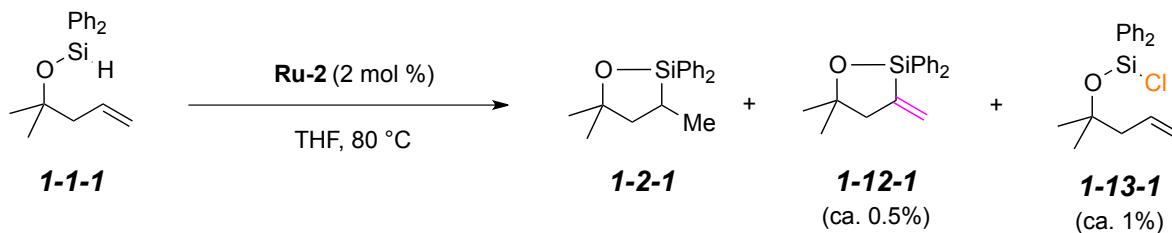


Figure 1.16 Formation of Vinylsilane and Chlorosilane Observed Alkene Hydrosilylation

Our efforts to isolate either chlorosilane or vinylsilane were not successful with the substrate **1-1-1**, but were able to isolate cyclic vinyl silane **1-12-12** (20% isolated yield) from hydrosilylation of **1-1-12** (Figure 1.17). The formation of vinylsilane **1-12-1** or **1-12-12** suggests that Grubbs-type ruthenium complex-catalyzed alkene hydrosilylation likely proceeds through a modified Chalk-Harrod mechanism (i.e., via silylruthenation)⁵¹ rather than the Chalk-Harrod (i.e., via hydorruthenation) pathway (Figure 1.10).⁸³

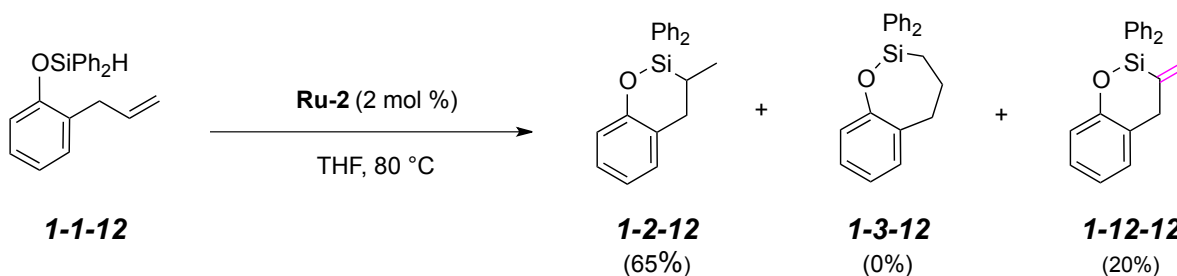


Figure 1.17 Formation of vinylsilane **1-12-12** during alkene hydrosilylation of **1-1-12**

1.13 Activation of Grubbs-type ruthenium catalysts by silanes

The formation of the chlorosilane **1-13** offers indirect information for the initial stage of the hydrosilylation. Based on these results two possible mechanisms were proposed. Departure of the PCy₃ from pre-catalyst produces the active ruthenium alkylidene complex **1-14**. **Path-A** proceeds through addition of Si-H to the π -bond of Ru-Alkylidene complex **1-14** to produce **1-14-1a**⁴⁵ followed by HCl elimination⁸⁴ to form a presumed Ru-Si complex **1-14-3**⁸⁵⁻⁸⁷ (Figure

1.18), which could be responsible for alkene hydrosilylation to provide oxasilacycle **1-2**. On the other hand, complex **1-14-1**, on reductive elimination, affords the ruthenium complex **1-14-2** and chlorosilane byproduct (e.g., **1-13**). **Path-B** Direct σ -bond metathesis between Si–H and Ru–Cl (**1-14**) via a four-centered transition state could be involved in the activation of ruthenium complex by silanes.⁸⁸⁻¹⁰⁰ Based primarily upon a bottom-face olefin coordination mechanism for olefin metathesis,⁷¹⁻⁷³ the metathesis of **1-14** and silane **1-1** may furnish either **1-14-5** via **1-14-1b** (*metal-out*: unproductive—the silicon never goes to the ruthenium metal center) or **1-14-3** via **1-14-4** (*metal-in*: productive). It could be an analogous situation where the outcome of competitive cross metathesis (CM) [i.e., productive CM: an ethylene-producing process (cf., **1-14-4** to **1-14-3**) (Figure 1.19) and unproductive CM: a degenerate metathesis (cf., **1-14-1** to **1-14-5**) is substantially dependent upon the steric hindrance of olefins, as well as the ligand set of ruthenium catalyst.¹⁰¹⁻¹⁰³

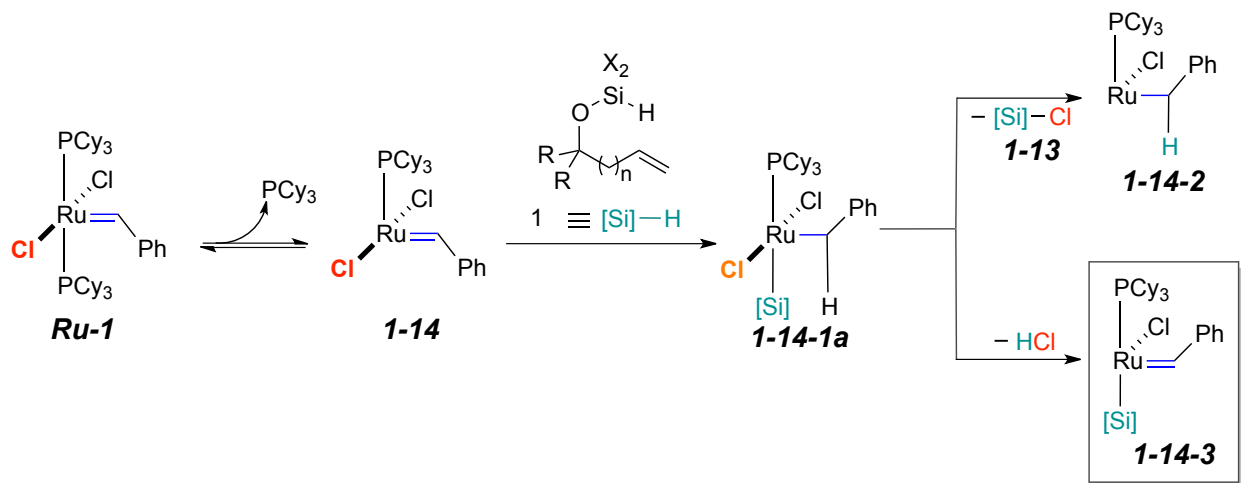


Figure 1.18 Addition of a Ru-alkylidene bond across a Si–H bond/HCl elimination

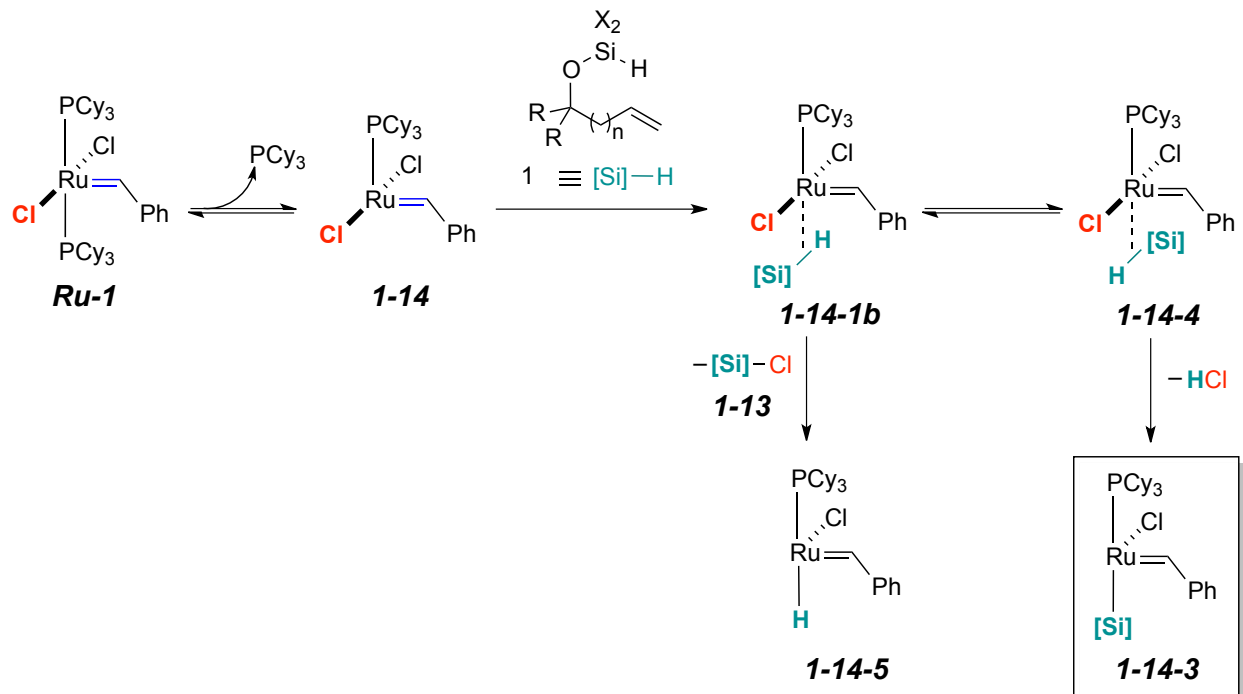


Figure 1.19 σ -Bond metathesis pathway

1.14 Experimental support for the activation of Grubbs-type ruthenium catalysts by silanes

1.14.1 Stoichiometric reaction of alkenylsilyl ethers: formation chlorosilane

To investigate these two mechanistic hypotheses for the initial stage of the catalysis, we first performed a control experiment and speculated that bulkier substituents such as a *t*-Bu group at silicon (i.e., **1-1-*t*-Bu**) could favor unproductive σ -bond metathesis to yield chlorosilyl ether **1-13-*t*-Bu** (via **1-15-1** vis-à-vis **1-15-2**). However, the formation of **1-13-*t*-Bu** via the sequential $\text{Ru}=\text{CHAr}$ addition across $\text{Si}-\text{H}$ and reductive elimination is unlikely, because an addition of di-*tert*-butylsilane **1-1-*t*-Bu** to **Ru-2** is greatly hindered—as seen in a Grubbs classification of general reactivity patterns of olefins.¹⁰⁴ When **1-1-*t*-Bu** was subjected to the reaction conditions employing 100 mol% of **Ru-2**, only **1-13-*t*-Bu** (**1-1-*t*-Bu**:**1-13-*t*-Bu**=19:81) was observed without

any notable cyclization, corroborating our mechanistic hypothesis for the σ -bond metathesis (Figure 1.20).

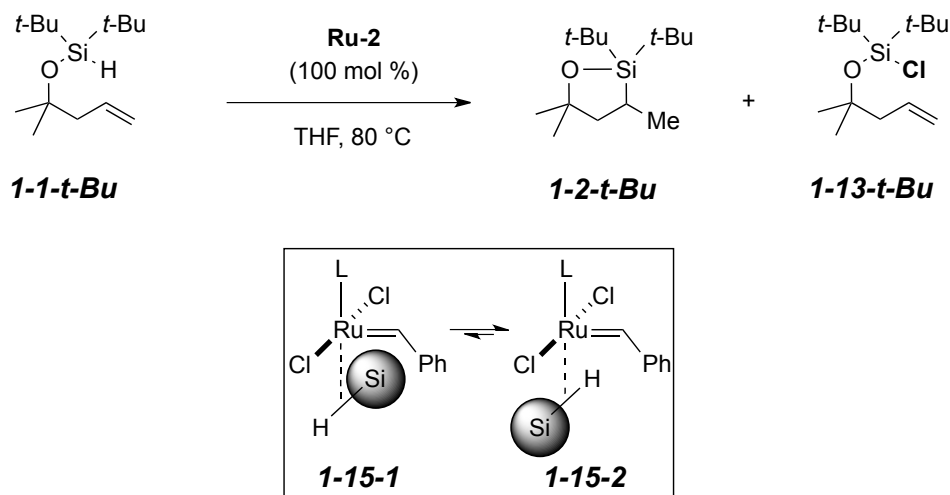


Figure 1.20 Stoichiometric Reaction Alkenylsilyl Ether (*1-1-t-Bu*) with **Ru-2**

1.14.2 Stoichiometric reaction of deuteriosilane: formation of ruthenium silane complex

In an effort to provide further support for this hypothesis, a deuterium labeling experiment was carried out using deuteriosilane **1-16-D** and **Ru-4** (Figure 1.21). The benzylidene proton within the resulting assumed ruthenium complex **1-17** remained intact; we did not detect deuterium incorporation at this position by ^2H NMR spectroscopy. This result suggests that the $\text{Ru}=\text{CHAr}$ addition across Si-H and HCl elimination cascade is unlikely.

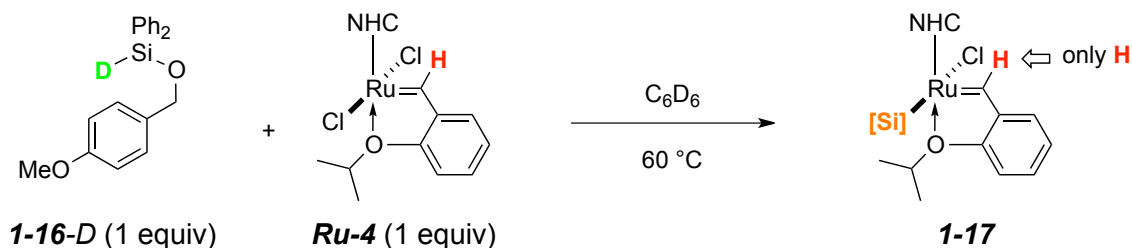


Figure 1.21 Stoichiometric reaction of deuteriosilyl ether (*1-16-D*) with **Ru-2**

1.14.3 Detection of ruthenium silane complex by ^1H NMR with Ru-4 and Ru-2

The experiment performed to directly detect ruthenium silane complex is shown in Figure 1.22. In this model, the use of an essentially equimolar ratio of **Ru-4** and silane **1-16**, which does not bear an alkene moiety, resulted in full conversion to a putative ruthenium silane complex. Over time the Si-H bond disappeared, yet benzylidene proton (H^7) and other protons within the catalyst **Ru-4** (H^7 to H^{11}) remained intact—an isopropoxy group was still anchored to the ruthenium center (H^{12} , 4.74 ppm). Interestingly, all protons in substrate **1-16-H** were shifted downfield, particularly, those at the *ortho*-position of the diphenylsilyl substituents (^1H , shifted downfield by 0.12 ppm) and the methylene protons (H^3 , shifted downfield by 0.063 ppm) within **1-16-H**. These protons were drawn closer to the ruthenium center. No additional benzylidene or alkylidene resonances were observed during this series of experiments. This experiment was also performed with **Ru-2** and silane (**1-16**) which gave the similar results as above (Figure 1.23).

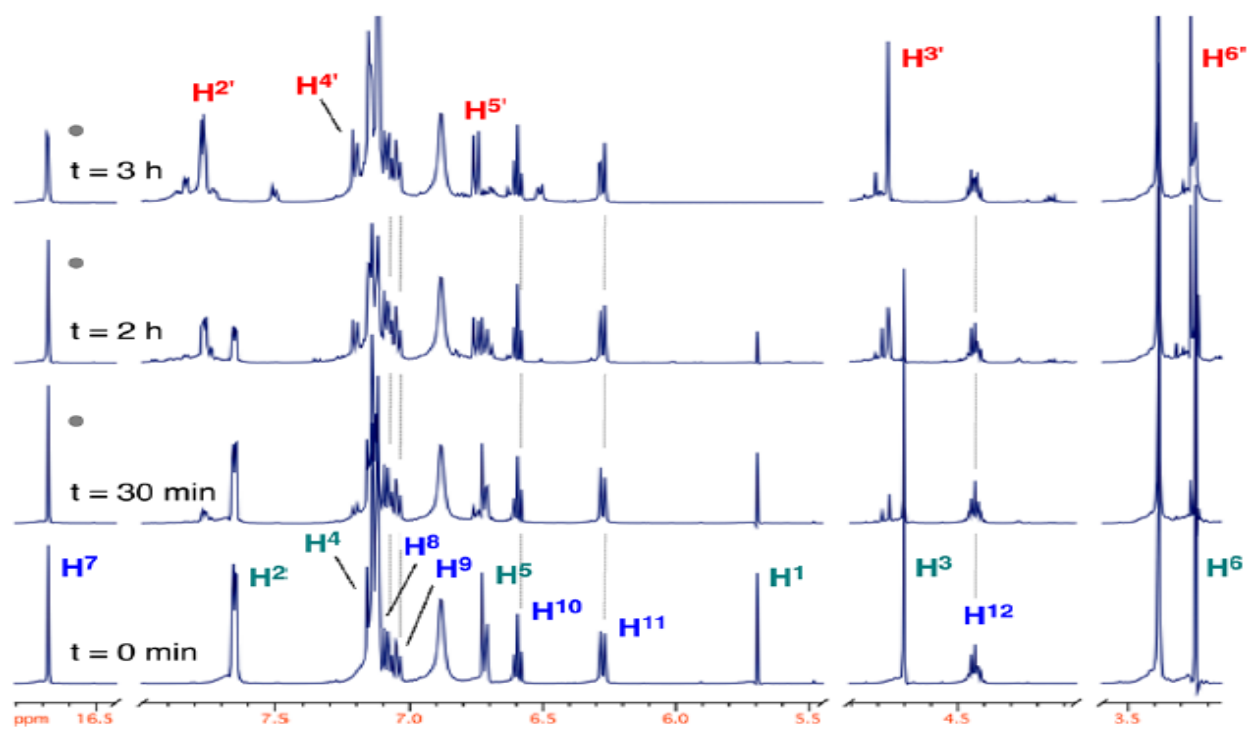
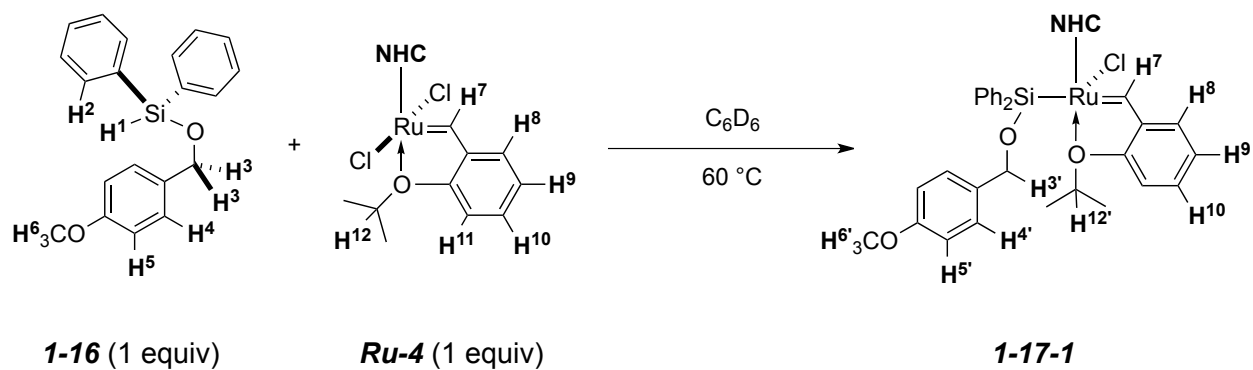


Figure 1.22 Reaction monitoring of the stoichiometric reaction of silyl ether (**1-16**) with **Ru-4**

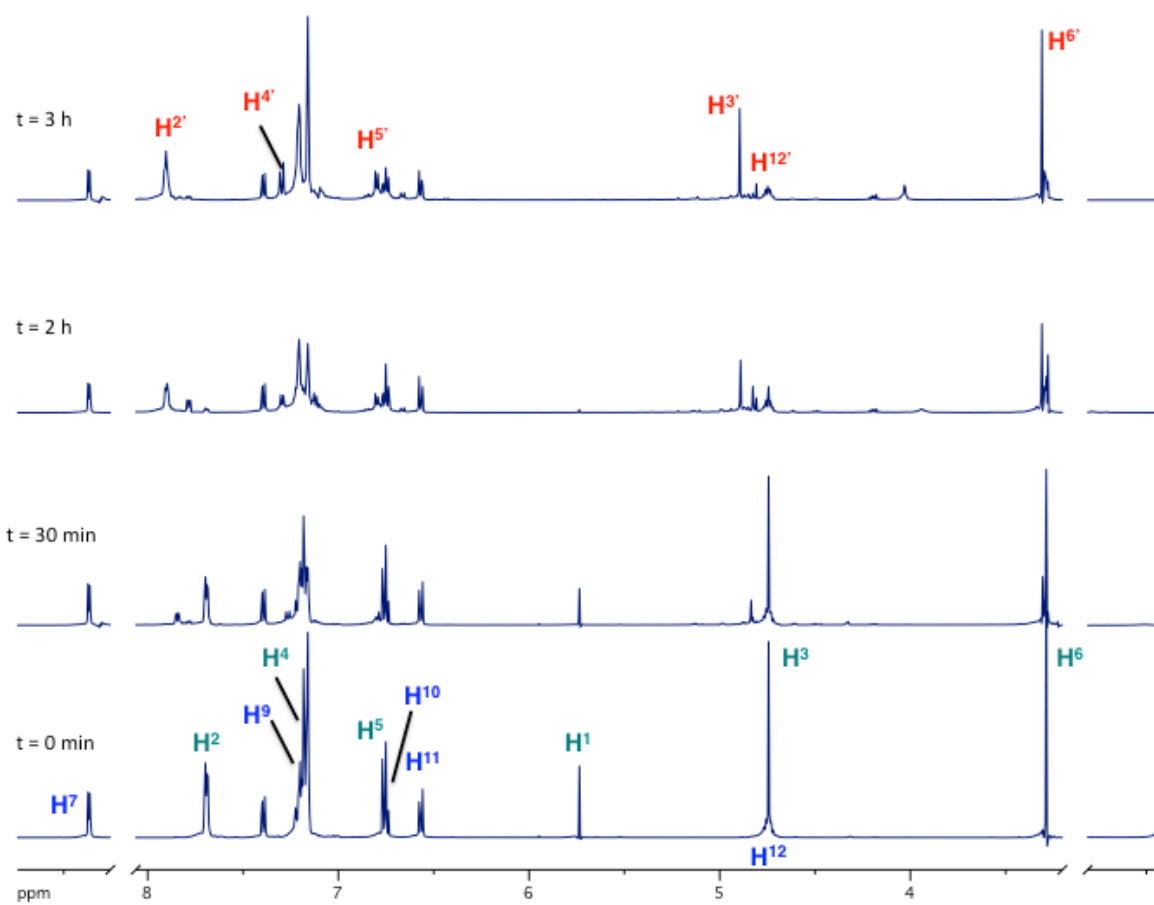
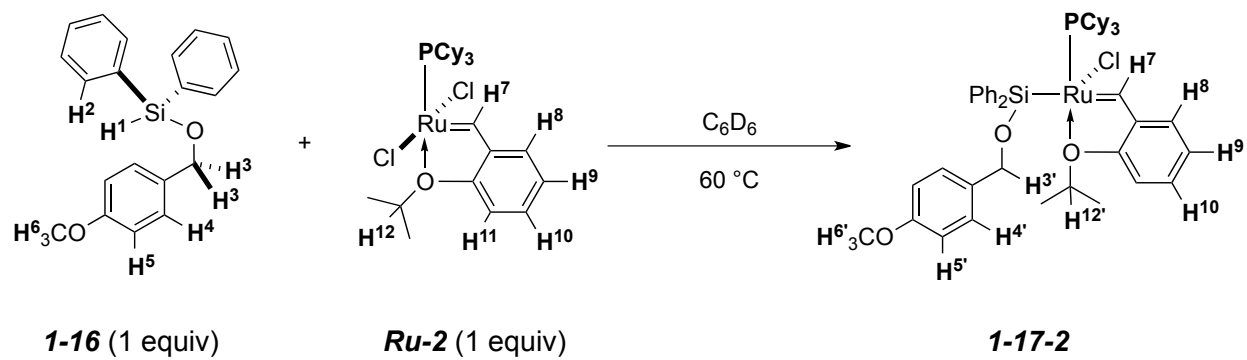
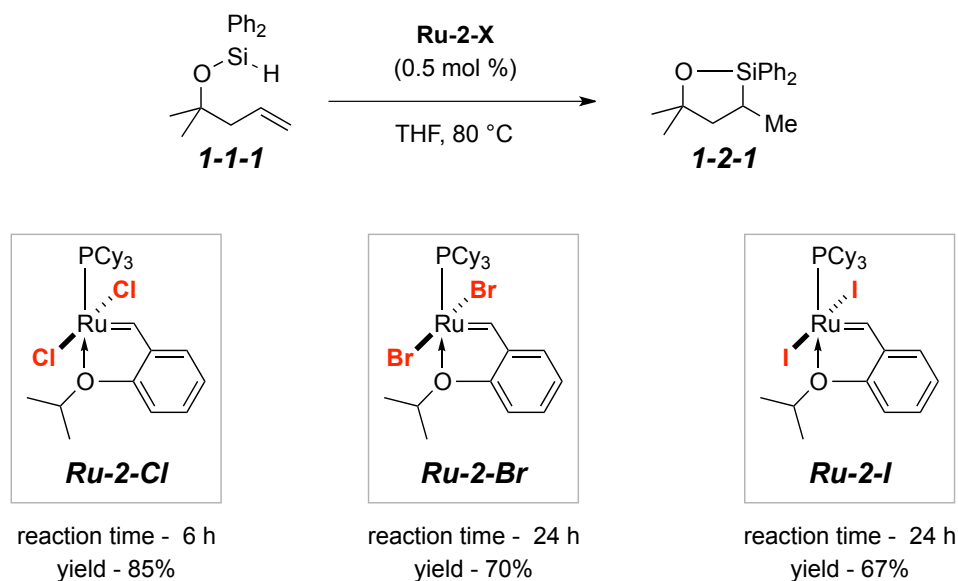


Figure 1.23 Reaction monitoring of the stoichiometric reaction of silyl ether (**1-16**) with **Ru-2**

1.15 Effect of halides on catalytic activity of ruthenium catalysts

Further insights into the reaction mechanism of the hydrosilylation were garnered by examining the impact of the halide ligands within the ruthenium catalysts (Table 1.8). The catalytic activity of the hydrosilylation was generally increased by having an electron withdrawing and smaller halide group from iodide to chloride. This trend is similar to the observed olefin metathesis reactivity of ruthenium catalyst.⁷⁵ Particularly, dichloride catalyst **Ru-2-Cl** was significantly faster than catalysts containing dibromide and diiodide (**Ru-2-Br** and **Ru-2-I**, respectively). The reasons behind the reactivity difference are unclear at this moment, but a sterically less demanding and electron withdrawing chloride ligand perhaps favors ruthenium binding to Si-H, dictating a facile σ -bond metathesis.



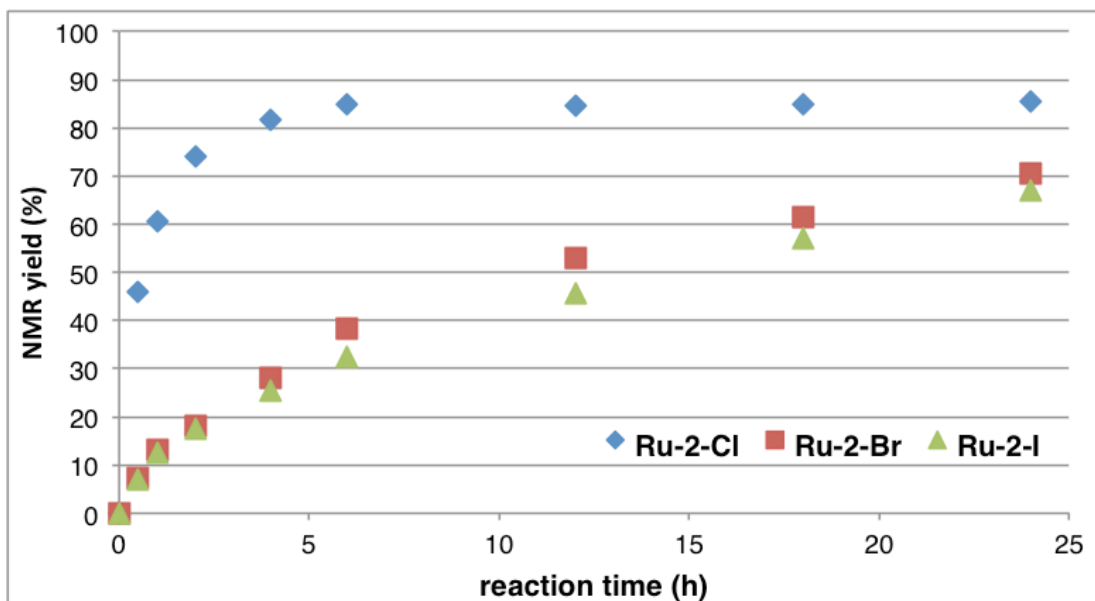


Table 1.7 Catalytic Activities Varying Halides on **Ru-2-X** Catalysts

1.16 Deuterium labeling and cross-over studies

We carried out an additional set of deuterium-labeling studies to further understand the nature of this cyclization. Under the same reaction conditions, the deuterium of **1-1-1-D** was mainly transferred to two positions of **1-1-1-D**, supporting the modified Chalk-Harrod mechanism (Figure 1.24). Furthermore, the cross-over experiment established that the proton transfer occurs intermolecularly (Figure 1.25). The hydrogen and deuterium scrambling, shown as **1-2-1H/D** and **1-2-3H/D**, reinforces our mechanistic hypothesis involving the σ -bond metathesis.

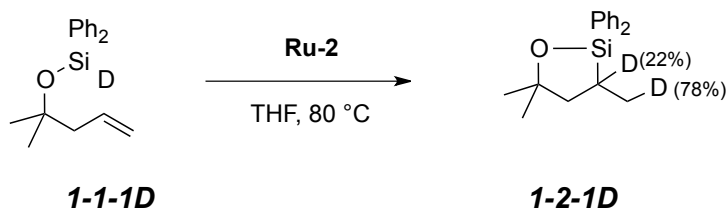


Figure 1.24 Intramolecular Deuterium-Labeling Studies

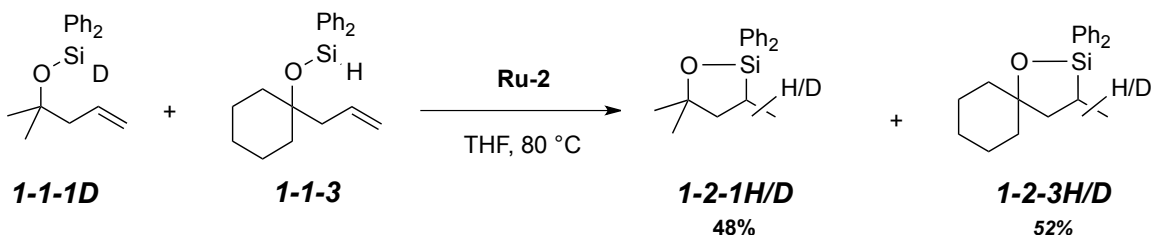


Figure 1.25 Cross-over Studies

1.17 Effect of proton scavenger on ruthenium alkylidene catalyzed intramolecular alkene hydrosilylation

Finally, we examined the reaction of **1-1-1** employing a stoichiometric amount of base [2,6-di-*tert*-butyl-4-methylpyridine (DTBMP) or NaHCO_3] (Figure 1.26). The rates of two reactions with and without base were essentially identical ($t_{1/2} = \text{ca. 40 min}$), albeit resulting in slightly diminished yields of **1-2-1**. This result indicates that the dissociated HCl did not affect the overall reaction efficiency. In addition, a potential mechanism involving heterolysis of a Si-H bond by ruthenium catalyst can be eliminated.^{84,105}

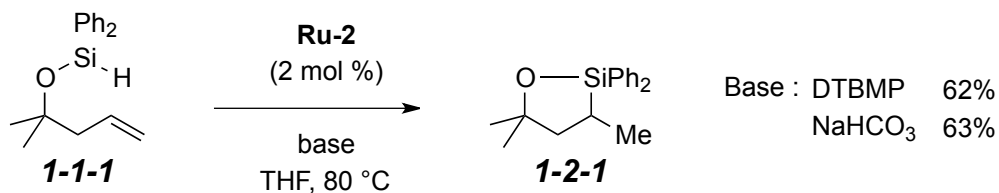
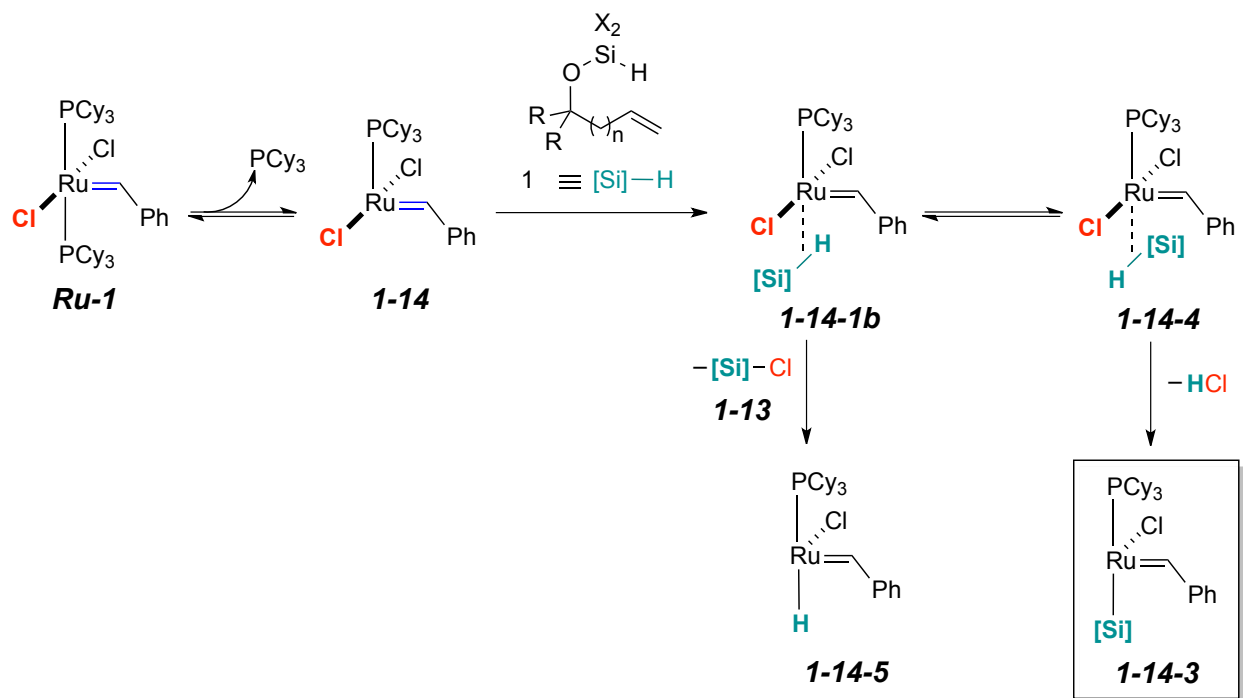


Figure 1.26 Effect of proton scavenger on alkene hydrosilylation

1.18 Possible mechanism for ruthenium alkylidene catalyzed intramolecular alkene hydrosilylation

The plausible overall mechanism, based upon our mechanistic studies and observations, is depicted in Figure 1.27. The initial productive σ -bond metathesis between ruthenium catalyst and silyl ether **1-1** affords ruthenium-silyl complex **1-14-3** (see Figure 1.19). Alkene coordination to ruthenium within **1-14-6**, followed by silylruthenation affords **1-14-7**. At this stage, either β -hydride elimination (to **1-12**) or σ -bond metathesis (to product **1-2**) via **1-14-8** takes place and regenerates **1-14-6**. Alternatively, protonation by HCl would afford **1-2** and ruthenium catalyst (RuLn).



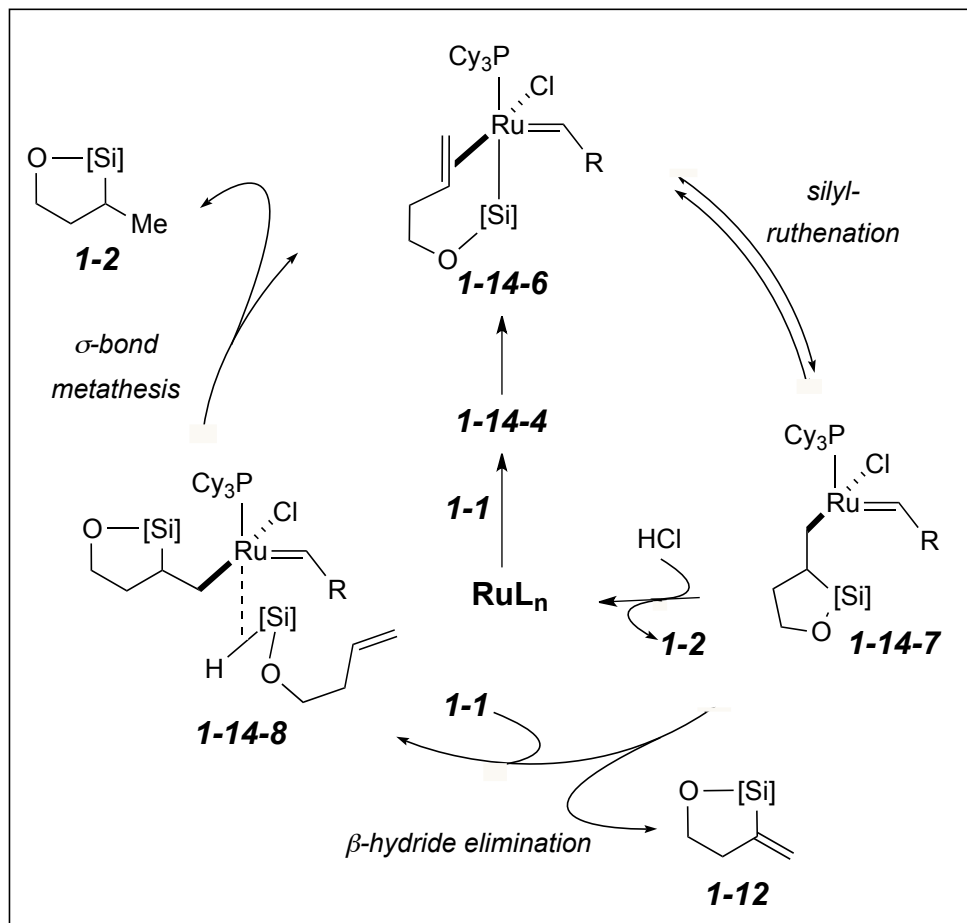


Figure 1.27 Plausible Mechanism of Alkene Hydrosilylation Catalyzed by Ruthenium Alkylidene Complex.

1.19 Summary of Chapter 1

In summary, we have developed a Grubbs-type ruthenium complex-catalyzed intramolecular alkene hydrosilylation of alkenylsilyl ethers to provide cycloalkyl silanes. Preferential silicon-hydride bond activation over alkene activation was observed, where alkene metathesis was effectively suppressed. This study expands our understanding of fundamental mechanistic aspects of non-metathetical function of Grubbs-type ruthenium catalysts for alkene hydrosilylation, with potential implications for other associated transformations such as dehydrogenative condensation of alcohols and silanes,⁴⁶ direct arylation,¹⁰⁶ and hydrogenation¹⁰⁷ Notably, the initial stage of the hydrosilylation involving the σ -bond metathesis between Si-H and Ru-Cl, is proposed. The Grubbs-type ruthenium complex-catalyzed alkene hydrosilylation follows the modified Chalk-Harrod mechanism.

Chapter 2

Regio- and Stereoselective Dehydrogenative Silylation and Hydrosilylation of Vinylarenes

Catalyzed by Ruthenium Alkylidenes.

Apparao Bokka, and Junha Jeon*

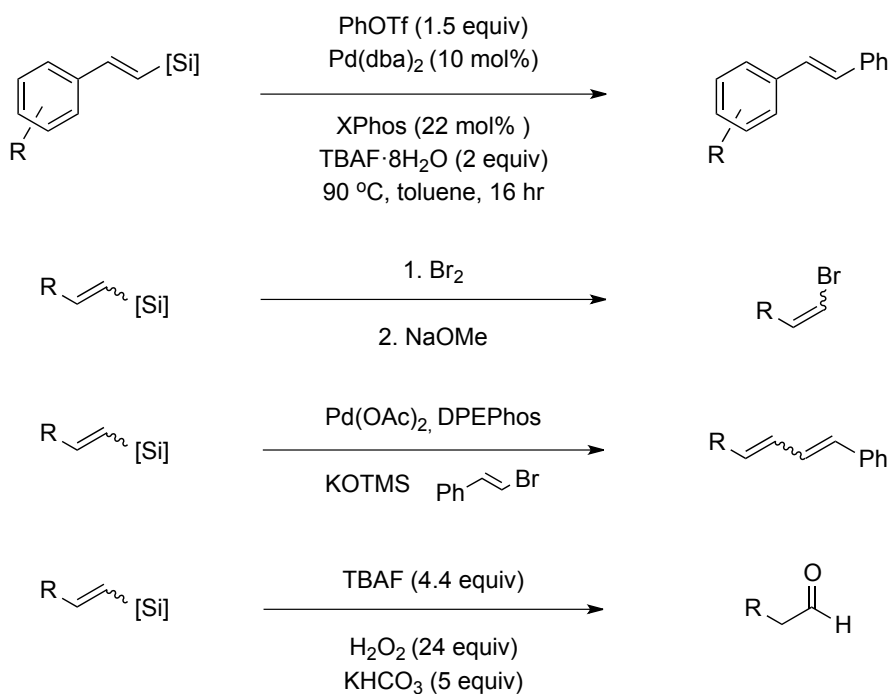
This work has been published in *Org. Lett.* **2016**, 18, 5324-5327^a

^a Used with the permission of the publisher, 2016

2. Introduction

2.1 Introduction to vinylsilanes and alkylsilanes

Vinylsilanes and alkylsilanes are important building blocks in synthesis of small molecules and polymers,^{11,16,17,108-111} based, in part, on their relatively high stability and virtually non-toxic nature.^{5,11,14,17} These organosilanes have been extensively exploited as useful synthetic intermediates whose silicon functional groups can be directly converted to many other useful moieties through further reactions. These conversion reactions include (Figure 2.1) Fleming-Tamao oxidation,^{14,109} halogenation,^{112,113} and Hiyama-Denmark cross-coupling,^{108,114} importantly, these routes allow facile access to pharmaceutical targets,^{20,21,22} and drug delivery.⁶ Unsaturated organosilanes are potent nucleophiles and highly useful intermediates in organic synthesis.^{11-14, 115-119}



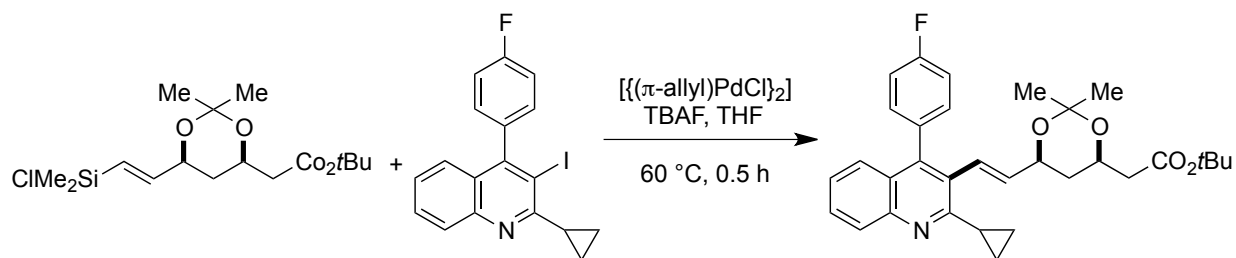


Figure 2.1 Applications of vinyl silanes as synthetic intermediates

2.2 Introduction to dehydrogenative silylation of alkenes

Vinylsilanes and alkylsilanes can be prepared primarily through organometallic addition to activated silanes (e.g., $XSiR_3$) or alkene/alkyne hydrosilylation. In addition to hydrosilylation, metal-catalyzed dehydrogenative silylation^{29,120-137} of alkenes has emerged as a powerful method to yield Si–C bonds.¹³⁶ Dehydrogenative silylation was first identified as an undesired side pathway that was competitive with metal catalyzed hydrosilylation, and catalysts that selectively furnish vinylsilanes remain rare.^{11,12,138,139} Dehydrogenative silylation of alkenes is attractive as a valuable alternative to hydrosilylation of alkynes,^{10,139,140} which has regio- and stereochemical issues.¹³⁰ Existing methods for the synthesis of vinylsilanes include the silyl-Heck reaction,^{112,141} alkyne hydrosilylation (Figure 2.2),^{45,46, 142-146} and manipulation of compounds with existing C–Si bonds;¹⁴⁷⁻¹⁵⁶ these methods have a number of drawbacks, including the commercial availability of alkynes, and limited substrate scope.^{112,84} Regio- and stereoselective dehydrogenative silylation^{7, 8, 9} to provide vinylsilanes are challenging,^{6,7} owing to either competitive hydrosilylation to afford alkylsilanes or alternative β -hydride elimination to furnish allylsilanes^{13,45-47,143, 155-163} (Figure 2.3).

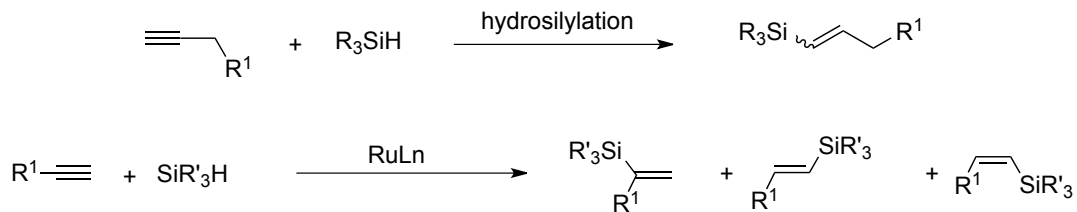


Figure 2.2 Hydrosilylation of alkynes to produce vinyl silanes

2.3 Transition metal catalyzed dehydrogenative silylation of alkenes

Based on these reports, a highly selective and more direct, alkene C–H silylation method to afford vinyl silanes thus is desired. Due to their wide accessibility, and stability, alkenes can be used as starting materials.¹⁶⁴ Iridium-catalyzed regio- and stereoselective dehydrogenative silylation of terminal alkenes was recently reported by Falck¹⁶⁵ and Hartwig (Figure 2.4)¹¹² with norbornene as a sacrificial hydrogen acceptor (SHA). These approaches were initiated by oxidative addition of Si–H bond to a metal center to afford hydridosilyl metal complexes (M = Ir). Watson demonstrated Palladium-catalyzed Silyl-Heck reaction utilizing terminal alkenes and silyl triflates (Figure 2.5).¹⁶⁴ Chirik and coworkers recently demonstrated highly selective cobalt-catalyzed dehydrogenative silylation of alkenes for preparation of allylsilanes (Figure 2.6).¹³ Activation of bis(imino)pyridine cobalt methyl complex by silane initially generates putative cobalt silyl complex and methane, rather than cobalt hydride and methylsilane. For catalytic turnover, half of the alkene served as sacrificial hydrogen acceptor to furnish simple alkanes as byproduct. Although there are a number of developments in the dehydrogenative silylation to afford vinylsilanes utilizing metal catalysts,^{29,125,127,129-131,134,136,137} such methods generally require either excess alkenes/silanes, air- and moisture sensitive catalysts, or more reactive alkylsilanes in lieu of more useful alkoxy silanes, for further manipulations.

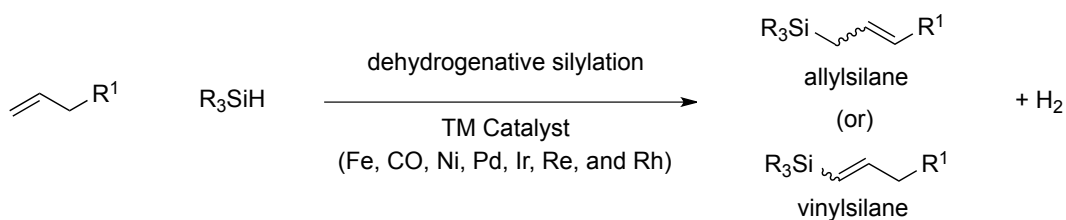


Figure 2.3 Transition metal-catalyzed dehydrogenative silylation of alkenes

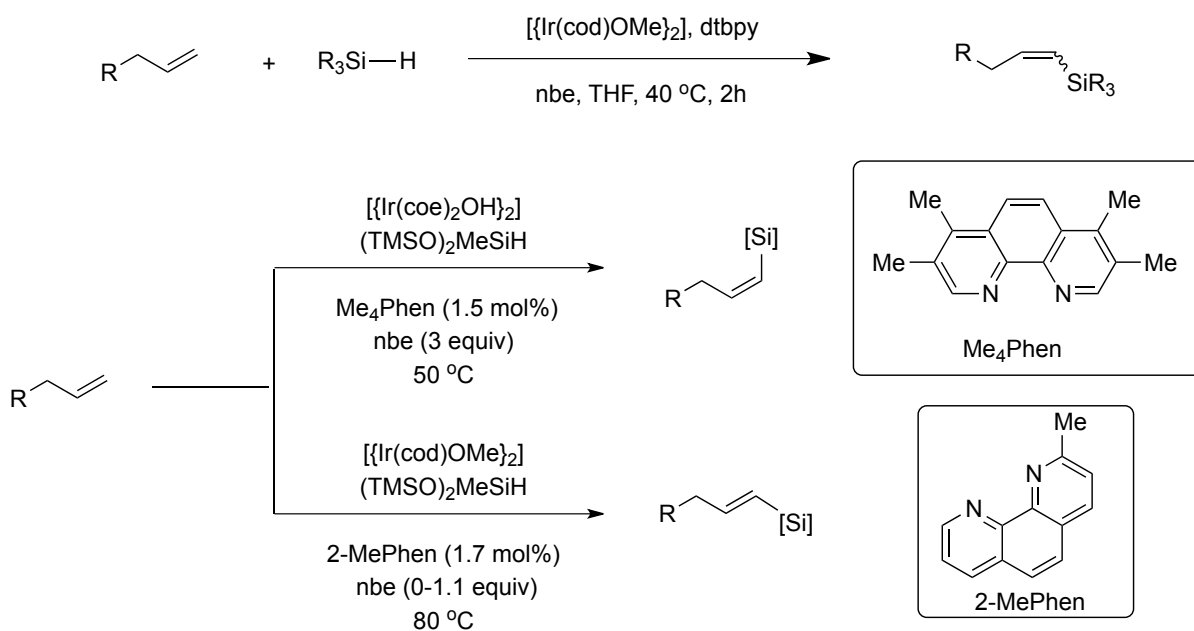


Figure 2.4 Hartwig's iridium-catalyzed dehydrogenative silylation of alkenes

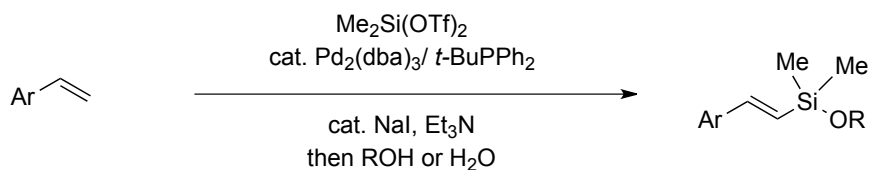


Figure 2.5 Watson's palladium catalyzed dehydrogenative silylation of alkenes

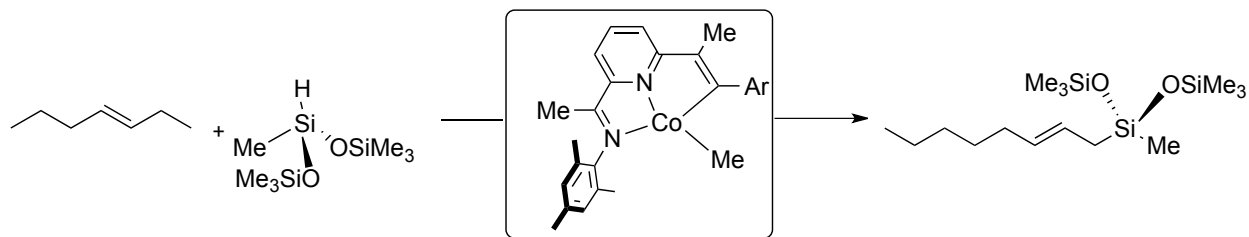


Figure 2.6 Chirik's cobalt-catalyzed dehydrogenative silylation of alkenes

2.4 Ruthenium alkylidene catalyzed dehydrogenative silylation and hydrosilylation

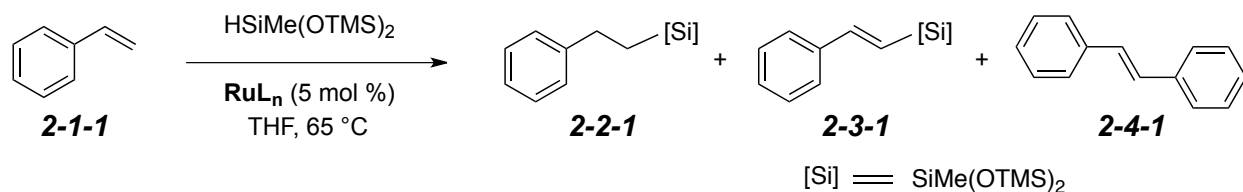
In our previous study, we demonstrated that the preferential Si–H activation over alkene activation utilizing Ru-alkylidene complexes was feasible to achieve intramolecular alkene hydrosilylation. In contrast to a generally accepted Chauvin type silylation mechanism of addition of Si–H across the π -bond of a Ru-benzylidene,^{45,47,143} a mechanism involving direct Si–H activation by Ru–Cl was proposed, based on a series of spectroscopic and isotope-labeling experiments.¹⁶⁶ However, there are no examples of this type of Si–H activation by metal alkylidenes (i.e., catalytic deprotonative silyl metalation) for dehydrogenative silylation to afford vinylsilanes (Figure 2.3).^{13,93,167,168} We focused on regio- and stereoselective dehydrogenative silylation and hydrosilylation of terminal aryl-substituted alkenes by altering the ruthenium alkylidene catalysts (L^1 and X ligand). Particularly, preparation of both alkylsilanes and vinylsilanes was achieved using a nearly equimolar ratio of alkenes and silanes.

2.5 Optimization for ruthenium alkylidene catalyzed dehydrogenative silylation of alkenes

2.5.1 Evaluation of ruthenium alkylidene complexes for dehydrogenative silylation of alkenes

We started our investigation with ruthenium alkylidene catalysts (Figure 1.10) used for our previously developed intramolecular hydrosilylation of alkenes. Styrene (**2-1-1**) was chosen as the master substrate and reactions were carried out with styrene, trisiloxane [HSiMe(OTMS)₂] and THF as the solvent at 65 °C. The results revealed three possible products alkylsilane **2-2-1**, vinylsilane **2-3-1**, and stilbene **2-4-1** from hydrosilylation, dehydrogenative silylation and olefin metathesis. The ratio of these three products is highly dependent on catalyst structure and silanes. Reaction with **Ru-1**, constituting phosphine L-type ligand and dichloride X-type ligands showed propensity towards dehydrogenative silylation (vinyl silane, Table 2.1, entry 1). The product ratio between vinylsilane and alkylsilane decreased when the **Ru-1** was replaced with **Ru-2** (Table 2.1, entry 2). Metathesis product stilbene **2-4-1** (entries 3-6) was dominant when the catalyst contains NHC/dichloride even in the presence of excess of silane. In contrast, **Ru-7** and **Ru-8**, best known for *Z*-selective olefin metathesis catalysts containing an NHC and bi-dentate nitrate ligands, as well as chelating adamantyl ligand,^{75,76} furnished alkylsilanes **2-2-1** as a major product (entries 15-16). During these reactions, 30-40% of alkene hydrogenation adduct was usually formed.

Table 2.1 Evaluation of Grubbs-type ruthenium catalysts for dehydrogenative silylation and hydrosilylation of vinylarenes.^a



entry	RuL _n	conversion (%) ^b	2-2-1:2-3-1:2-4-1 ^c
1	Ru-1	100	1:16:0
2	Ru-2	100	1:3:0
3	Ru-3	100	1:5:14
4	Ru-4	100	1:8:25
5	Ru-5	100	1:3:12
6	Ru-6	100	1:4:5
7	Ru-7	100	5:1:0
8	Ru-8	100	4:1:0

^aconditions: **2-1-1** (0.4 mmol), silane (0.44 mmol), THF (0.2 M). ^bdetermined by GC/MS analysis.

^cdetermined by GC/MS analysis and ¹H NMR spectroscopy utilizing an internal standard (CH₂Br₂)

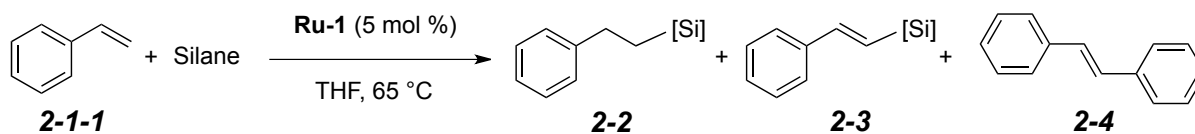
2.5.2 Evaluation of silanes for dehydrogenative silylation of alkenes

Initial catalyst screening was carried out with trisiloxane, which yielded (*E*)-vinylsilane **2-3-1** as the major product with excellent regio- and stereoselectivity (Table 2.2, entry 1).

Various silanes (mono, di, tri-hydrosilanes) were tested with **Ru-1** but the product ratio was not

improved significantly (entry 2-7). Reaction with phenyl silanes resulted in disproportionation of the silane (entries 3,5, and 6).

Table 2.2 Evaluation of silanes for dehydrogenative silylation.^a



entry	solvent	conversion (%) ^b	2-2 : 2-3 : 2-4 ^c
1	HSiMe(OSiMe ₃) ₂	100	1:16:0
2	HSi(OEt) ₃	91	1:1:0
3	HSiPh ₃	95	n.d
4	HSiEt ₃	77	1:6:0
5	H ₂ SiPh ₂	94	3:2:0
6	H ₂ SiPhMe	11	n.d
7	H ₂ Si <i>i</i> -Pr ₂	25	n.d
8	H ₂ SiEt ₂	32	n.d
9	H ₃ SiPh	60	n.d

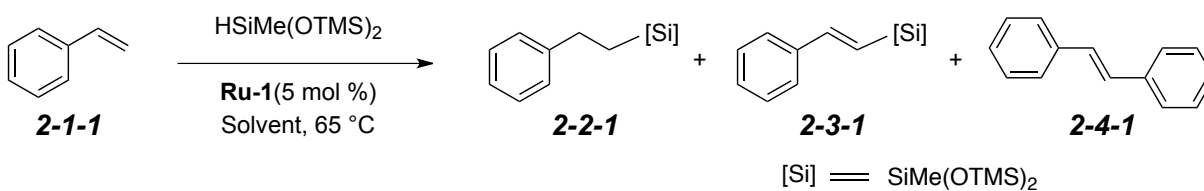
^aconditions: **2-1-1** (0.4 mmol), silane (0.44 mmol), THF (0.2 M). ^bdetermined by GC/MS analysis.

^cdetermined by GC/MS analysis and ¹H NMR spectroscopy utilizing an internal standard (CH₂Br₂)

2.5.3 Effect of solvents on dehydrogenative silylation of alkenes

With emphasis on dehydrogenative silylation, the reaction conditions were optimized, beginning with the solvent screening. As a standard condition **Ru-1** (1.0 equiv) with trisiloxane (1.1 equiv) and THF (0.1 M) resulted in excellent conversion with very good dehydrogenative silylation to the hydrosilylation (16:1) product ratio. Metathesis was never observed even the solvent was changed to DCM, toluene and benzene (solvents favorable for metathesis). When THF was replaced with other solvents the products ratio was reduced significantly (Table 2.3, entries 2-5). Pentane and hexane shown the good products ratio and surprisingly alkene hydrogenation product was greatly diminished (entries 6,7). Based on the results from THF, pentane and hexane as solvents we used the combination of THF/pentane and THF/hexane both resulted in excellent ratio with decreased hydrogenation product (entries 8, 9).

Table 2.3 Evaluation of solvents for dehydrogenative silylation.^a



entry	solvent	conversion (%) ^b	2-2-1:2-3-1:2-4-1 ^c
1	THF	100	1:16:0
2	DCM	96	2:3:0
3	Toluene	91	2:5:0
4	Benzene	95	1:3:0
5	Et ₂ O	88	1:1:0
6	Pentane	93	1:7:0
7	Hexane	94	1:8:2
8*	THF/Pentane	100	1:28:0
9*	THF/Hexane	100	1:29:0

^aconditions: **2-1-1** (0.4 mmol), silane (0.44 mmol), THF (0.2 M). ^bdetermined by GC/MS analysis.

^cdetermined by GC/MS analysis and ¹H NMR spectroscopy utilizing an internal standard (CH₂Br₂)

* solvent concentration (0.2 M)

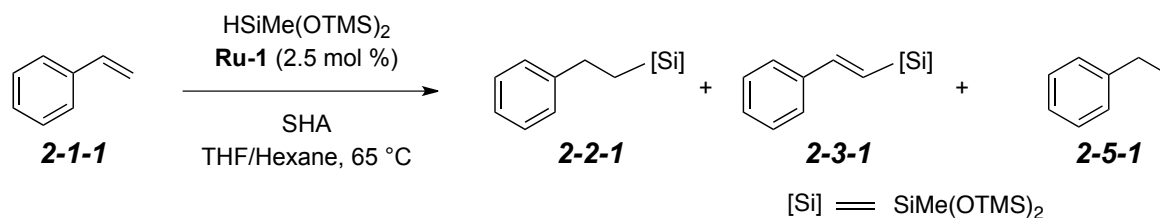
2.5.4 Optimization of temperature and concentration for dehydrogenative silylation of alkenes

These reactions were performed at different temperatures (rt, 40, 65, 85 and 100 °C), and 65 °C was suitable for this conversion. Solvent concentration of either 0.1 M or 0.2 M with catalyst loading of 5 mol% or 2 mol% resulted in good yield. Lowering down the catalyst loading to less than 1.0 mol%, was not productive with some substrates.

2.5.5 Evaluation of sacrificial hydrogen acceptor (SHA) for dehydrogenative silylation of alkenes

¹H NMR yields of the reactions were only 40-50% with these reaction conditions; hydrogenation of styrene (ethyl benzene) resulted in the formation of other major product. Earlier studies used the excess alkene which served as a sacrificial hydrogen acceptor (SHA). The external sacrificial hydrogen acceptor was employed to compensate the hydrogenation of styrene. When the well-known strained bicyclic alkenes [e.g., norbornene (nbe), norbornadiene (nbd)] were tested, we observed noticeable ring-opening metathesis polymerization (ROMP) activity of **Ru-1** in a presence of nbe or nbd. Moderately ROMP-active cycloalkenes [including cyclopentene, cyclohexene, 1,3-cyclohexadiene, cycloheptene, *cis*-cyclooctene, and *cis, cis*-1,5-cyclooctadiene (cod) **2-6**] not only afforded good yields of vinylsilane by diminishing the alkene reduction product, but also exhibited excellent selectivity of dehydrogenative silylation over hydrosilylation (Table 2.4). The trend of vinylsilane yield and the ratio of **2-2-1** and **2-3-1** was well-correlated with the ring strain of cycloalkenes, whereupon with increasing ring strain,¹⁶⁹⁻¹⁷¹ the corresponding product ratio as well as yield (**2-3-1**) proportionally increased.

Table 2.4 Evaluation of sacrificial hydrogen acceptors for dehydrogenative silylation.



entry	SHA	2-2-1:2-3-1 ^b	yield % (2-3-1:2-5-1) ^c
1	cyclopentene	1:33	65:24
2	cyclohexene	1:14	62:28
3	cycloheptene	1:28	63:25
4	cyclooctene	1:47	68:20
5	cyclooctadiene	1:50	70:9
6	norbornene	1:34	45:32
7	norbornadiene	1:26	NA

^aconditions: **2-1-1** (0.4 mmol), silane (0.44 mmol), THF (0.2 M). ^bdetermined by GC/MS analysis.

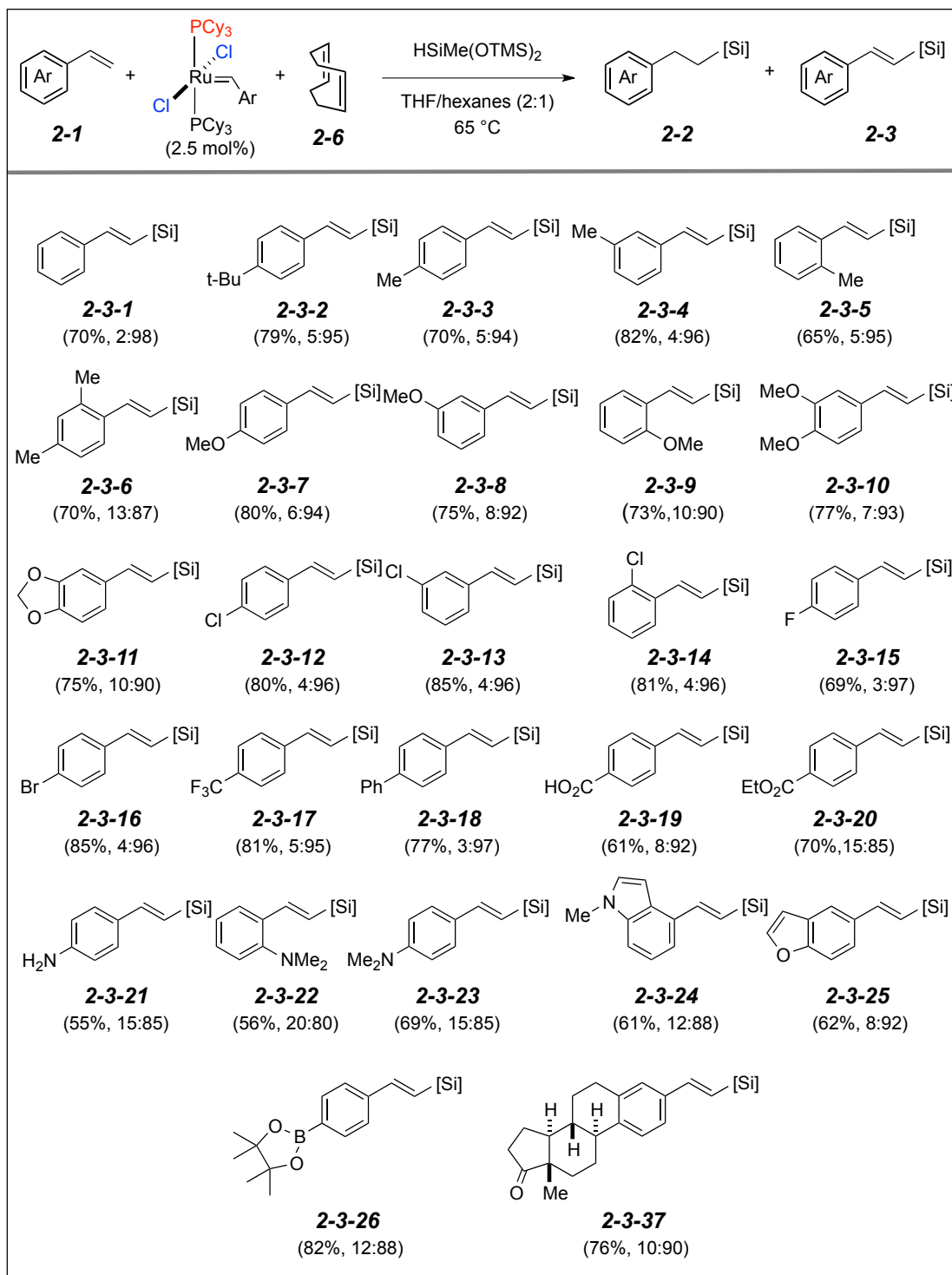
^cdetermined by GC/MS analysis and ¹H NMR spectroscopy utilizing an internal standard (CH₂Br₂)

2.6 Substrate scope for ruthenium alkylidene catalyzed dehydrogenative silylation of alkenes

With the optimized conditions, we explored the scope of Ru alkylidene-catalyzed dehydrogenative silylation of **2-1** with **Ru-1** (X = Cl and L¹ = PCy₃) to afford (*E*)-**2-3** (Table 2.6). The parent substrate styrene **2-1-1** resulted in the formation of the (*E*)-vinylsilane (**2-3-1**) in good yield and excellent stereoselectivity. Electron rich styrenes (Table 2.5, entries **2-3-2** to **2-3-**

6), styrenes with electron withdrawing substituents (entries **2-3-7** to **2-3-11**), and inductively electron withdrawing styrenes (entries **2-3-12** to **2-3-17**) produced moderate to good yields of vinylsilanes and product selectivity. Other functional groups including carboxylic acid, ester, free and protected amine, indole, benzofuran and boronate ester were well-tolerated under these conditions (entries **2-3-18** to **2-3-26**). Substrates containing amines showed little tendency towards hydrosilylation (15 to 20%) which also resulted in lower yields. The structurally complex, C3-vinyl estrone derivative yielded vinylsilane **2-3-27** in 76% yield with good product selectivity. Ru alkylidene catalytic systems unfortunately did not effect the reaction of alkyl substituted (terminal and internal) vinylarenes with an alkyl side chain.

Table 2.5 Substrate scope of ruthenium alkylidene (**Ru-1**) catalyzed dehydrogenative silylation of vinylarenes.^a



^aconditions: **2-1** (0.4 mmol), silane (0.44 mmol), THF (0.2 M) and COD (0.8 mmol). product ratio (2-2:2-3) was determined by GC/MS analysis and yields reported are isolated.

2.7 Gram scale synthesis vinylsilane

Ru alkylidene-catalyzed alkene dehydrogenative silylation strategy was successfully tested on a gram scale (Figure 2.7) on substrate **2-1-2** (7 mmol, 1.12 g) with 75% yield, good product selectivity and excellent stereoselectivity (only *E* vinyl silane).

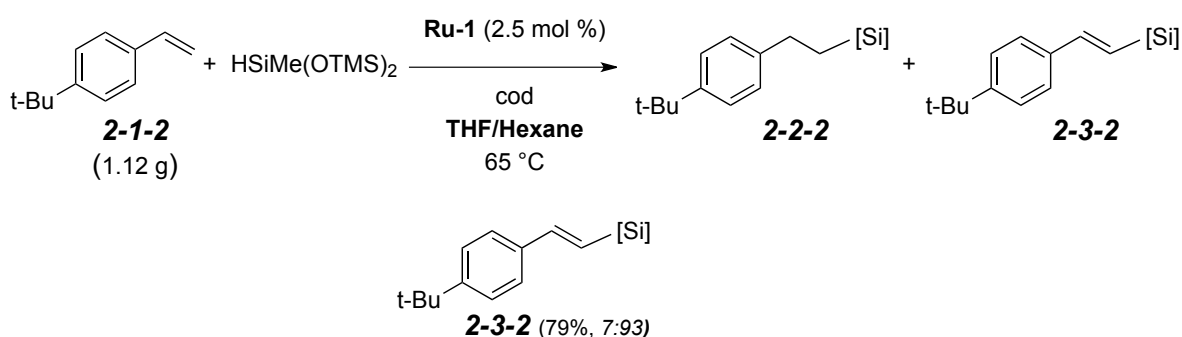
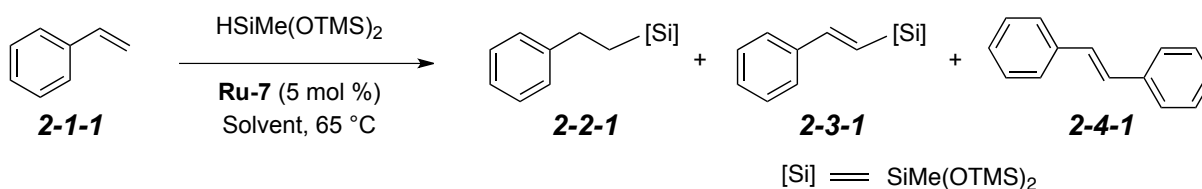


Figure 2.7 Gram scale reaction of ruthenium alkylidene (**Ru-1**)-catalyzed dehydrogenative silylation of vinylarenes.

2.8 Reaction optimization of ruthenium alkylidene-catalyzed alkene hydrosilylation

After successfully developed the dehydrogenative silylation, we turned our focus on hydrosilylation. During the catalyst screening we observed **Ru-7** ($\text{X} = \text{NO}_3$, and $\text{L}^1 = \text{NHC}$ bearing adamantyl) in the presence of silane and styrene favors the hydrosilylation to provide the alkyl silane product (Table 2.1, entries 7 and 8) over dehydrogenative silylation (**2-2-1:2-3-1**, 5:1). We started altering the conditions to achieve hydrosilylation over dehydrogenative silylation, our studies begin with temperature screening which resulted in maximum conversion at $85\text{ }^\circ\text{C}$. Then we focused our attention on solvent, like dehydrogenative silylation DCM, toluene, and hexane did not produce good product selectivity. With combinations of solvents, formation of alkylsilane is prominent, the product ratio further improved with concentrated condition [THF/Hexane 2:1, 2.0 M (Table 2.6)].

Table 2.6 Evaluation of solvents for hydrosilylation.^a



entry	solvent	conversion (%) ^b	2-2-1:2-3-1:2-4-1 ^c
1	THF	100	5:1:0
2	DCM	96	2:1:0
3	Toluene	91	1:1:0
4	Et₂O	88	2:1:0
5	Pentane	100	4:1:0
6	THF/Pentane* (2.0 M)	100	25:1:0

^aconditions: **2-1-1** (0.2 mmol), silane (0.22 mmol), THF (0.2 M). ^bdetermined by GC/MS analysis.

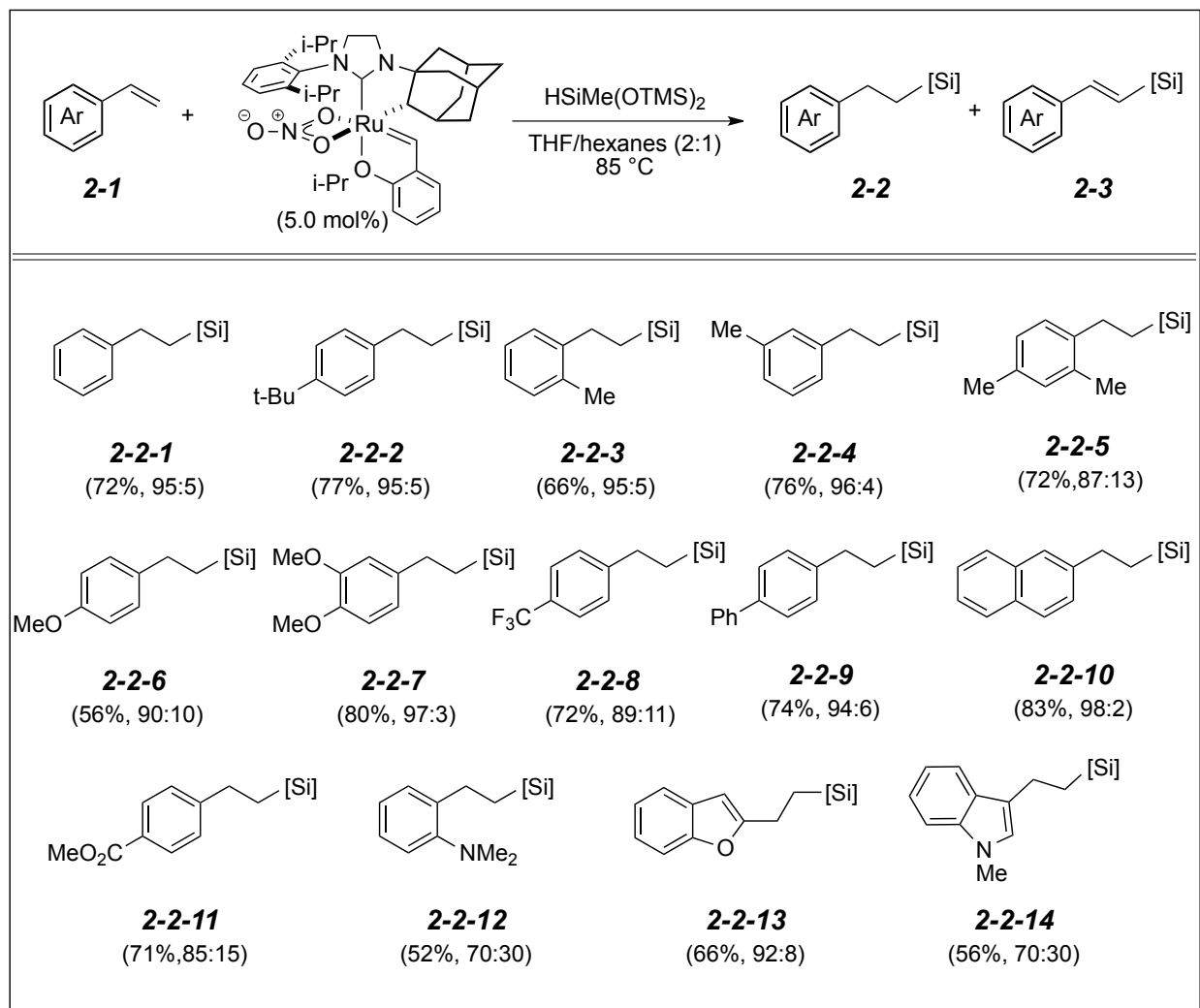
^cdetermined by GC/MS analysis and ¹H NMR spectroscopy utilizing an internal standard (CH₂Br₂)

2.9 Substrate scope for ruthenium alkylidene catalyzed hydrosilylation of alkenes

We continued to investigate the scope of Ru alkylidene-catalyzed hydrosilylation of **2-1** and HSiMe(OTMS)₂ with **Ru-7** (Table 4). When **Ru-7** (X = NO₃ and L¹ = adamantyl bearing NHC) was used, diverse mono- and disubstituted styrenes provided alkylsilanes **2-2-1** to **2-2-10** with moderate to good yields and a synthetically useful level of product selectivity of hydrosilylation over dehydrogenative silylation. Again, ester, amino, benzofuran, and indole-

containing styrenes underwent hydrosilylation to provide **2-2-11** to **2-2-14** in good yields (Table 2.7).

Table 2.7 Substrate scope of ruthenium alkylidene (**Ru-7**) catalyzed hydrosilylation of vinylarenes.^a



^aconditions: **2-1** (0.2 mmol), silane (0.25 mmol), solvent (2.0 M), reaction time 24 h.

product ratio (2-2:2-3) was determined by GC/MS analysis and yields reported are isolated.

2.10 Kinetic isotopic experiments

Kinetic isotopic experiments (KIE) were planned to illuminate some insights into the reaction mechanism of ruthenium alkylidene catalyzed dehydrogenative silylation. We assumed that when the isotope –labelled styrenes on reaction with **Ru-1** and silane will provide some valuable information regarding the stereoselectivity of the dehydrogenative silylation. Unfortunately, under the reaction conditions stereospecifically isotope-labeled alkenes (*Z*)-**2-1-1-D** or (*E*)-**2-1-1-D** were rapidly isomerized to furnish a nearly 1:1 mixture of (*Z*)-**2-1-1** and (*E*)-**2-1-1**, which hindered the studies for stereoselectivity of this process (Figure 2.8).

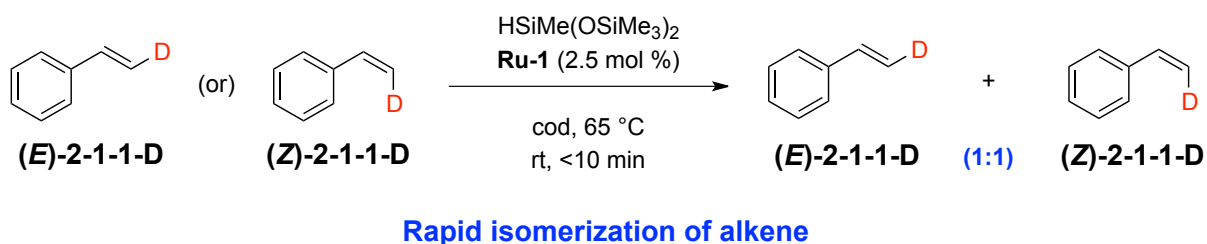


Figure 2.8 Isotope labeling of alkene–rapid isomerization of alkene

2.10.1 Isotope labeling of silane

Two independent reactions (Figure 2.9) were carried out to study the KIE of dehydrogenative silylation of vinylarenes catalyzed by ruthenium alkylidene complex. Reaction of styrene **2-1-1** and 3-deutero-1,1,1,3,5,5,5-heptamethyltrisiloxane [**DSiMe(OTMS)₂**], was monitored by ¹H NMR spectroscopy at time intervals of 6 min by taking aliquots. A parallel reaction was carried out using 1,1,1,3,5,5,5-heptamethyltrisiloxane [**HSiMe(OTMS)₂**]. Aliquots at 18 min from the independent parallel reactions were diluted with CDCl₃ at room temperature and the products were analyzed by ¹H NMR spectroscopy. The reaction with **DSiMe(OTMS)₂** produced vinyl silane in 2.7% yield, whereas **HSiMe(OTMS)₂** afforded vinyl silane in 8.7%

yield (18 min). Analysis of the products by ^1H NMR spectroscopy established KIE of 3.2 ($k_{\text{H}}/k_{\text{D}} = 3.2$, 1° KIE).

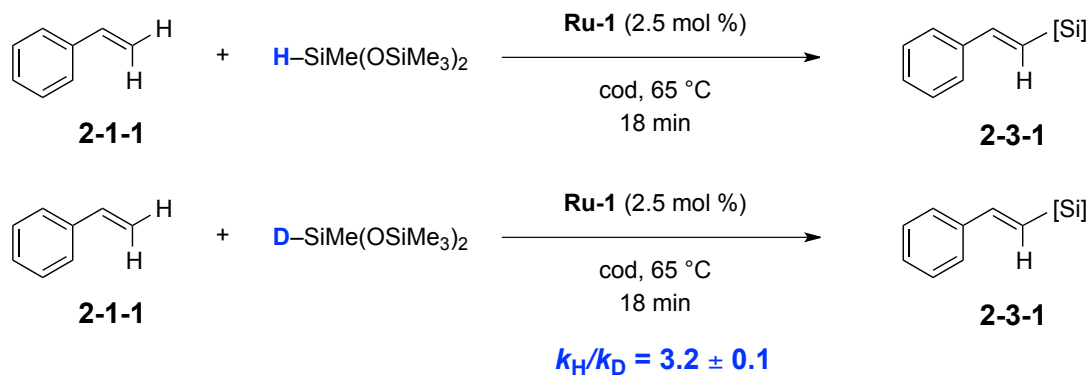


Figure 2.9 Preliminary mechanistic studies- Isotope labeling of silane

2.10.2 Isotope labeling of alkene

Reaction of styrene **2-1-1**-[2,2- H^2] and 2,2-dideuterostyrene **2-1-1**-[2,2- D_2] with silane [$\text{HSiMe}(\text{OTMS})_2$] in presence of **Ru-1** and COD (**2-6**) was monitored by ^1H NMR spectroscopy at time intervals of 5 min (Figure 2.10). The reaction furnished **2-3-1-H** in 6.2% yield and β -deutero-vinylsilane **2-3-1-D** in 4.8% yield. Analysis of the products by ^1H NMR spectroscopy established KIE of 1.3 ($k_{\text{H}}/k_{\text{D}} = 1.3$, 2° KIE) suggesting that direct C-H activation/silylation to afford vinylsilane is unlikely.

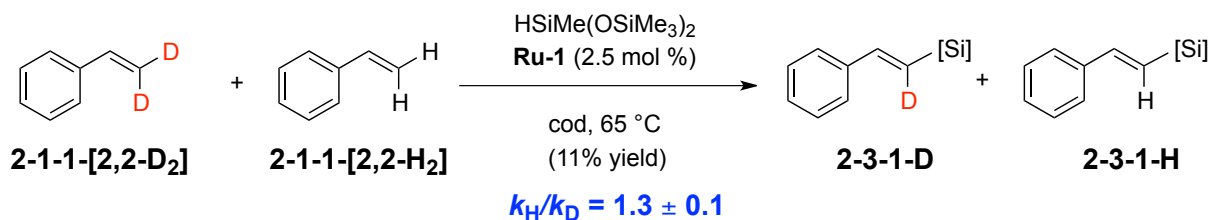


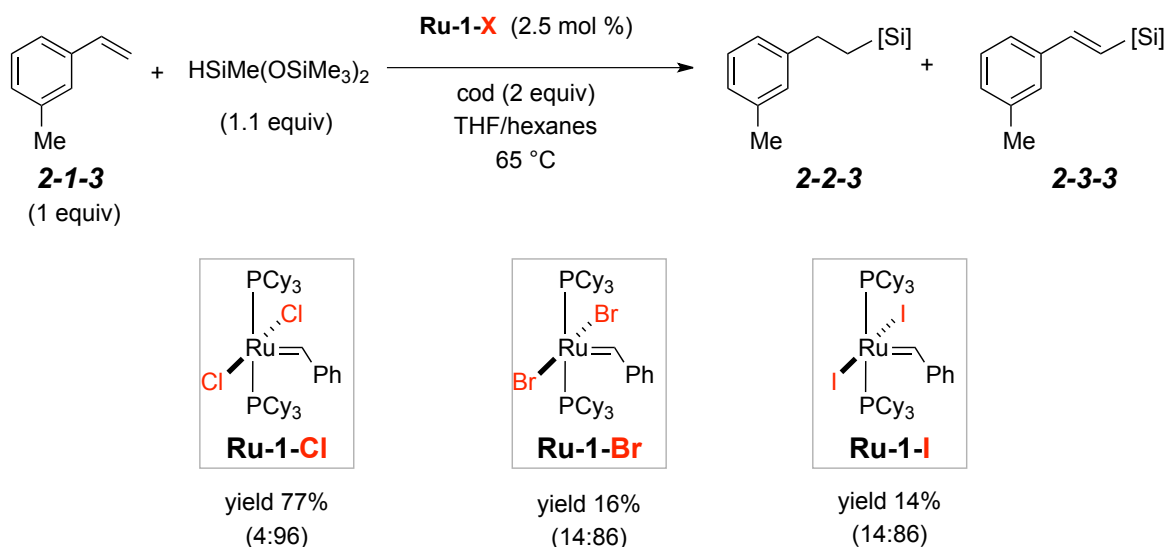
Figure 2.10 Preliminary mechanistic studies- Isotope labeling of alkene

Taken together, the observed significant KIE in the parallel isotope experiments indicates that the Si-H bond cleavage to generate the putative ruthenium silyl complex and HCl,

is the turnover-limiting step which is consistent with observation of ruthenium alkylidene (e.g. **Ru-1**) as the resting state.^{45,166}

2.11 Effect of halides on catalytic activity of ruthenium catalysts (**Ru-1**)

We further examined the influence of X-type ligands of **Ru-1** for dehydrogenative silylation. As reported in our previous work, dichloride catalyst **Ru-1-Cl** was superior to **Ru-1-Br** and **Ru-1-I**.¹⁶⁶ The propensity of product selectivity (i.e., **2-2-3** and **2-3-3**) paralleled the kinetic behavior of catalysts, whereby the reaction with **Ru-1-Cl** was considerably faster and most favorable to the formation of **2-3-3**, whereas **Ru-1-Br/Ru-1-I** produced more reduction products. This study suggests that electron-withdrawing and smaller X-type halide ligands in Ru alkylidene may facilitate rapid Si-H bond activation, as well as conformationally allow facile β -H elimination leading to **2-3-3**, relative to the analogous events with **Ru-1-Br/Ru-1-I** (Figure 2.11).^{71,75,76}



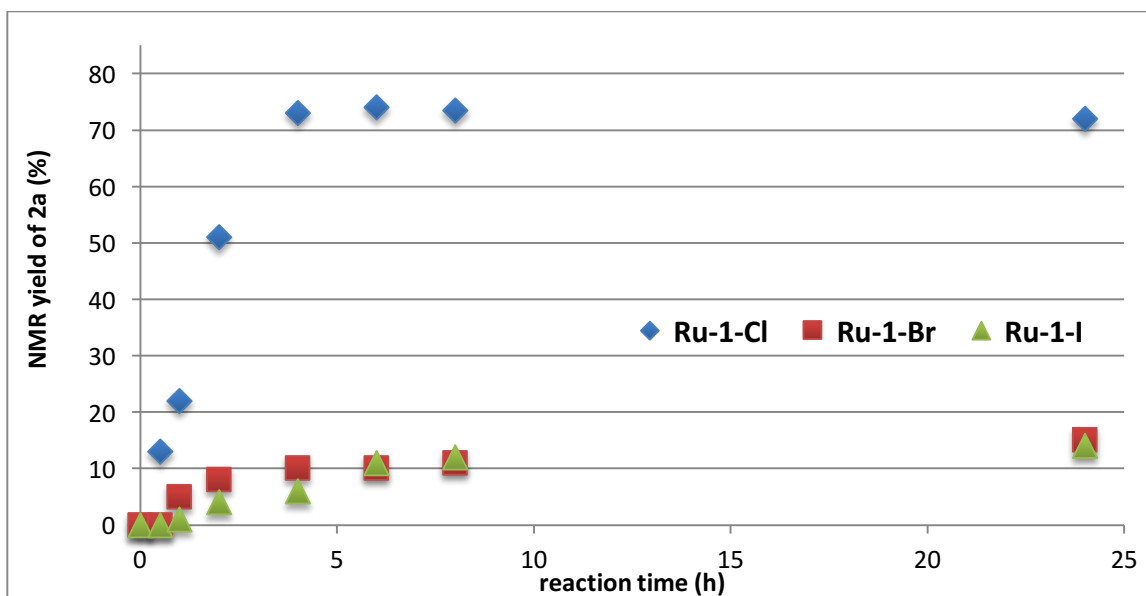


Figure 2.11 Effect of X-type Halide Ligands

2.12 Possible mechanism for dehydrogenative silylation of alkenes

The catalytic mechanisms of these processes involving catalysts such as **Ru-1** and **Ru-7** have not been yet fully elucidated. Based upon discoveries from our current studies, coupled with previous studies regarding Ru alkylidene-catalyzed intramolecular alkene hydrosilylation,¹⁶⁶ we propose mechanisms for the Ru alkylidene-catalyzed hydrosilylation and dehydrogenative silylation of alkenes (Figure 2.12). First, dehydrogenative silylation begins with the Si-H activation by the catalyst after dissociation of phosphine ligand to afford putative Ru-Si complex **2-7-3** (via **2-7-1**)¹⁷² and HCl. The resulting sub-stoichiometric amount of HCl can further react with silane to give Si-Cl and H₂. Due to this side reaction the dehydrogenative silylation requires a slight excess of silane (1.1 equiv). A similar type of a bond exchange reaction has been seen in Noyori's asymmetric hydrogenation, where early activation of H₂, by Ru(II)Cl₂, provided Ru(II)HCl and HCl.¹⁷³ Alkene coordination and olefin migratory insertion then give rise to **2-7-5** via **2-7-4**. When catalyst contains phosphine/dichloride ligands (e.g., **Ru-**

1) **2-7-6**, produced by coordination of ROMP-active cycloalkane COD (**2-6**) to ruthenium metal. This intermediate (**2-7-6**) could be responsible for the product selectivity by facilitating the C-C single bond rotation (**2-7-7**). Subsequent β -hydride elimination will produce the thermodynamic product (*E*)-vinylsilane **2-3** and Ru-H (**2-7-8**). The catalytically responsible Ru-Si (**2-7-3**) is regenerated by a sequence of olefin migratory insertion of cod into ruthenium hydride (to **2-7-9**), and reaction with silane by releasing cyclooctene (observed in ^1H NMR spectroscopy and GC-MS spectrometry).

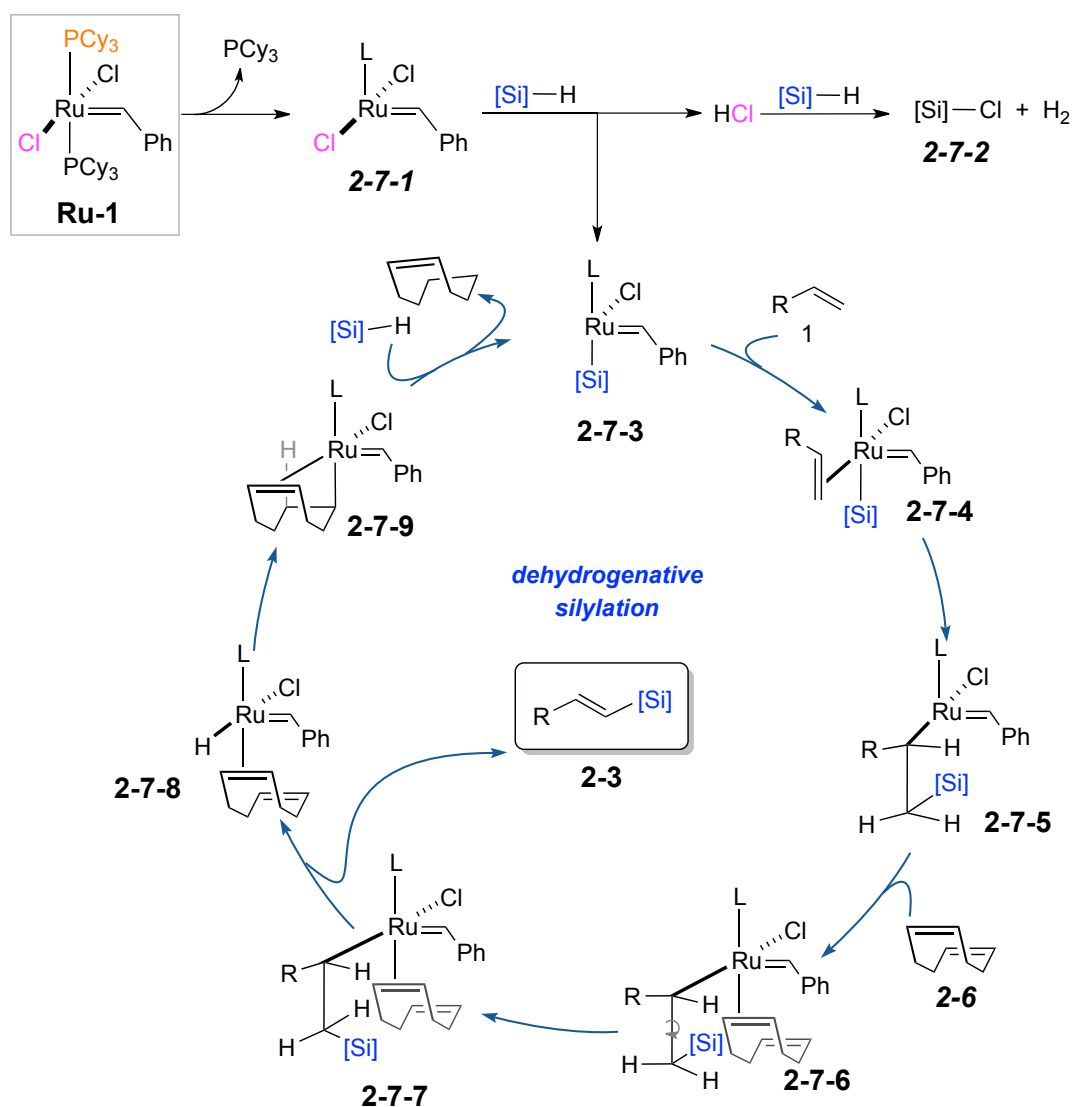


Figure 2.12 Proposed mechanism of dehydrogenative silylation of vinylarenes catalyzed by **Ru-1**

2.13 Possible mechanism for hydrosilylation of alkenes

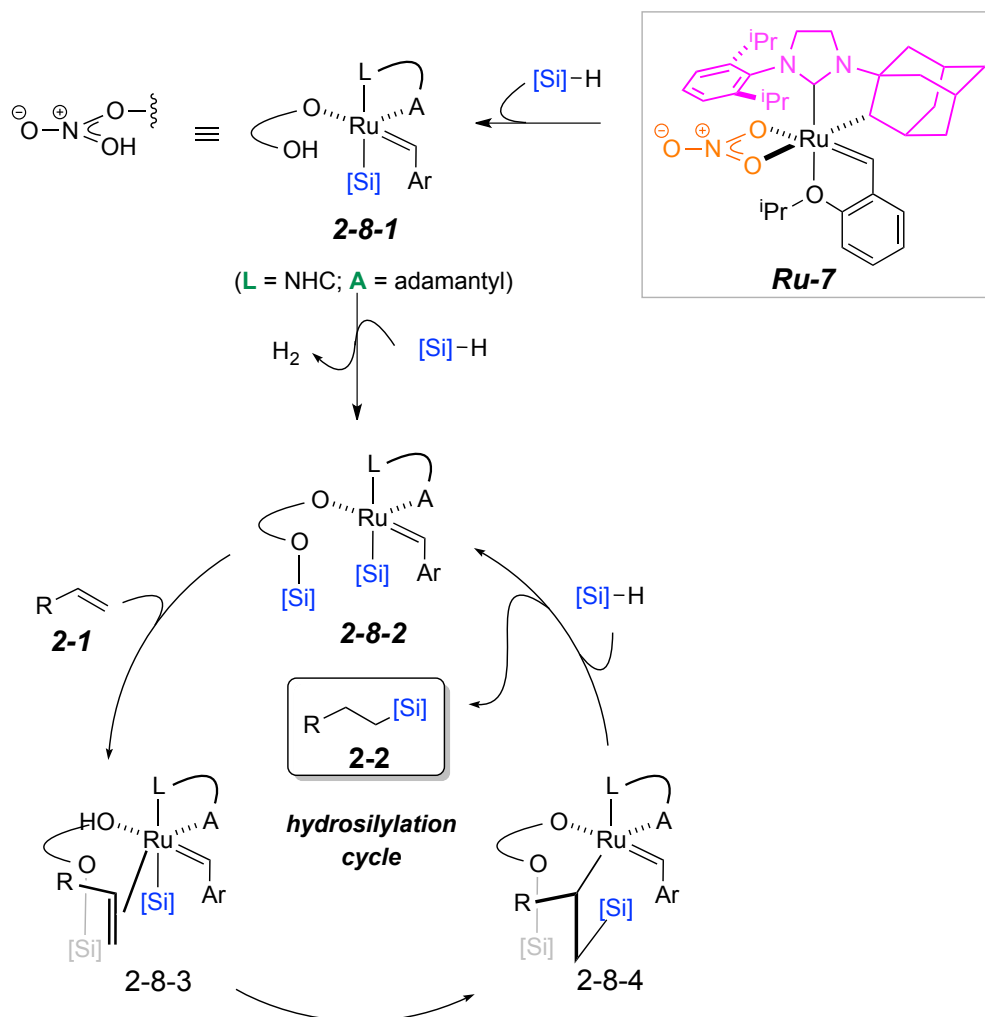


Figure 2.13 Proposed mechanism of hydrosilylation of vinylarenes catalyzed by **Ru-7**

Hydrosilylation catalyst **Ru-7**, which includes NHC, nitrate, and adamantyl ligands, activates the Si-H bond to furnish the putative Ru silyl complex **2-8-1**. The resulting mono-bound nitrate can quickly react with additional silane to afford bis-silyl Ru complex **2-8-2**. As shown in Table 2.7, the hydrosilylation necessitates use of slightly more silane (1.25 equiv, cf. 1.1 equiv for dehydrogenative silylation). Side-bound olefin in **2-8-3** then undergoes olefin migratory insertion to provide **2-8-4**. Finally, reaction of **2-8-4** with silane releases alkylsilanes

2-2 and produce the active silyl complex **2-8-2**. We observed that this hydrosilylation is nearly four-times slower compared to dehydrogenative silylation ($t_{1/2} = 30$ min for dehydrogenative silylation of **2-1-4** and $t_{1/2} = 120$ min for hydrosilylation of **2-1-4**), presumably resulting from added steric hindrance with the Ru complex. Moreover, we conjecture that bulky 2,6-diisopropyl groups in NHC ligand and other moieties in the metal-ligand sphere such as adamantyl and silylated nitrate ligands likely impede the propensity of β -hydride elimination (cf. **2-7-7** to **2-7-8** and **2-3**) by restricted conformational change for requisite *syn*-elimination within **2-7-7**. A structurally similar catalyst **Ru-8** holding the smaller mesityl group in NHC reduces product selectivity, shown in Table 2.1, entry 8.

2.14 Effect of proton scavenger on dehydrogenative and hydrosilylation of alkenes

In order to better understand potential impact of liberated HCl or the putative protonated nitrate moiety within Ru complex (e.g., **2-8-1**), we carried out the dehydrogenative silylation and hydrosilylation of **2-1-2** doped with 2,6-di-*tert*-butyl-4-methylpyridine (DTBMP) (1 equiv). In fact, the reaction rates were basically identical to those without DTBMP. These results indicate that the dissociated HCl and the protonated nitrate moiety were consumed by the rapid reactions with silane to release Si-Cl and H₂ or O₂NOSi and H₂ under the reaction conditions, thereby such strong acids did not affect the overall reaction efficiency.

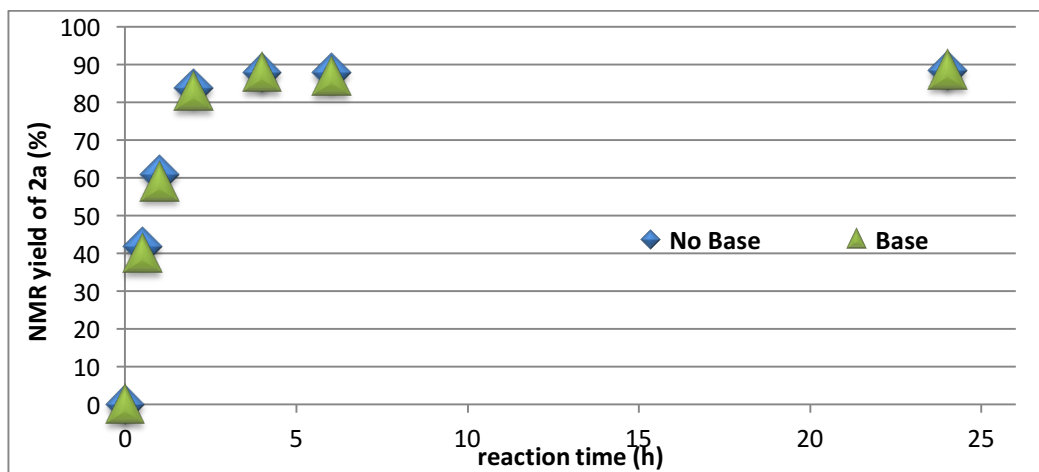
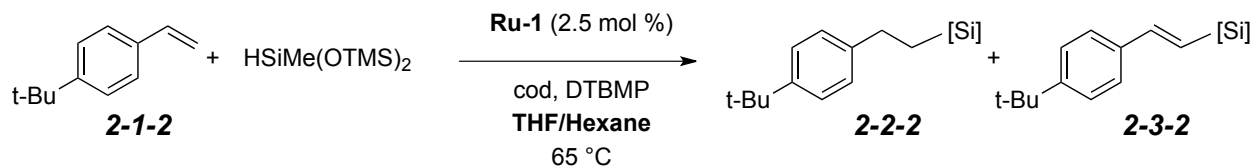


Figure 2.14 Effect of a proton scavenger on dehydrogenative alkene-silane coupling

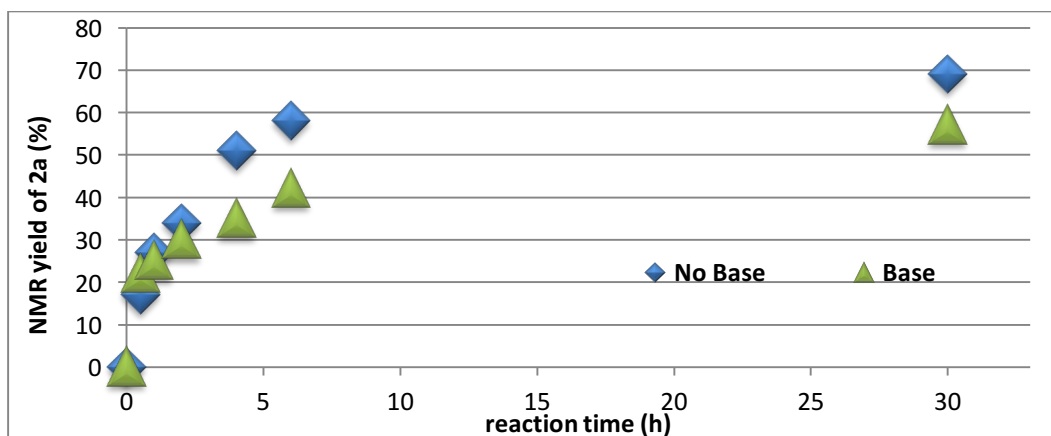
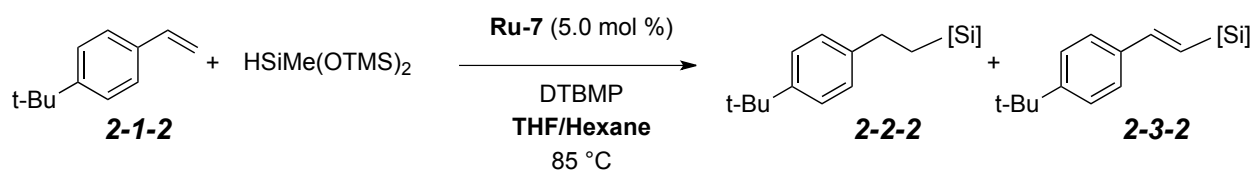


Figure 2.15 Effect of a proton scavenger on hydrogenative alkene-silane coupling

2.15 Summary of Chapter 2

In summary, we have developed selective dehydrogenative silylation and hydrosilylation of a virtually equimolar ratio of alkenes and alkoxy silanes exploiting ruthenium alkylidene catalysts to access vinylsilanes and alkylsilanes. Notably, variation of catalyst structure, specifically both L- and X-type ligands at ruthenium, greatly altered reaction pathways to dehydrogenative silylation and hydrosilylation. The readily accessible catalysts, with a newly discovered *cis,cis*-1,5-cyclooctadiene hydrogen acceptor for the dehydrogenative silylation, exhibited relatively broad functional group tolerance and high regio- and stereoselectivity. Although a variety of non-metathetical synthetic applications of Grubbs-type ruthenium alkylidenes are known, including silylation reactions, a mechanistic understanding of non-metathetical catalytic function of such catalysts is still limited. Our preliminary studies on dehydrogenative silylation exhibited that the turnover-determining step is the Si-H cleavage by Ru alkylidene. The origin of such ligand-controlled selectivity regarding dehydrogenative silylation and hydrosilylation as well as their detailed mechanism are currently under investigation.

Appendix A: List of Abbreviations

δ : chemical shift (ppm)

μL : microliter

Ac: acetate

Ad: adamantyl

Ar: aryl group or substituent, general

Bn: benzyl

Bu: butyl

*t*Bu: tert-butyl

C: Celsius

calcd: calculated

cat.: catalyst, catalytic amount

COD: 1,5-cyclooctadiene

cf: compare

Cy: cyclohexyl

DCM: dichloromethane

Eq.: equation

equiv.: equivalent

Et: ethyl

g: gram

GCMS: gas chromatography mass spectrometry

h: hours

HRMS: high resolution mass spectrometry

Hz: hertz

IR: infrared spectroscopy

J: coupling constant, NMR spectroscopy

M: metal, general

M: molar

[M⁺]: molecular ion

Me: methyl

min.: minutes

mg: milligram

MHz: megahertz

mL: milliliter

mmol: millimole

MW: molecular weight

n/a: not applicable

nfom (non-first-order multiplet)

NHC: *N*-heterocyclic carbene ligand

NMR: nuclear magnetic resonance spectroscopy

Appendix B: Experimental Procedures

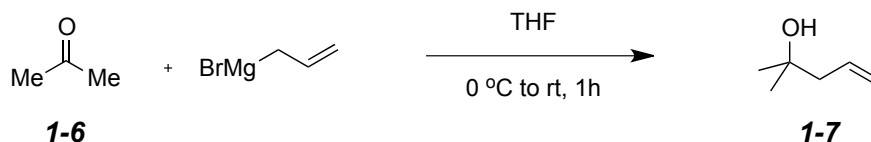
General Experimental

Reactions requiring anhydrous conditions were performed under an atmosphere of nitrogen or argon in a VAC glovebox or using standard Schlenk techniques with flame or oven dried glassware. Anhydrous tetrahydrofuran (THF) and diethyl ether (Et₂O) were distilled from sodium and benzophenone. Triethylamine and pyridine were distilled from KOH. DMF and DMSO were stored over 4Å molecular sieves. All other solvents and reagents from the commercial sources were used as received. ¹H, ²H, and ¹³C NMR spectra were recorded on JEOL Eclipse Plus 500 (500 MHz) and JEOL ECX 300 (300 MHz) spectrometers. ¹H NMR chemical shifts are referenced to chloroform (7.26 ppm), THF-*d*₈ (1.72 ppm), and benzene-*d*₆ (7.16 ppm). ²H NMR chemical shifts are referenced to chloroform (7.26 ppm) and benzene (7.16 ppm). ¹³C NMR chemical shifts are referenced to ¹³CDCl₃ (77.23 ppm). The following abbreviations are used to describe multiplets: s (singlet), d (doublet), t (triplet), q (quartet), pent (pentet), m (multiplet), nfom (non-first-order multiplet), and br (broad). The following format was used to report peaks: chemical shift in ppm [multiplicity, coupling constant(s) in Hz, integral, and assignment]. ¹H NMR assignments are indicated by structure environment, e.g., CH_aH_b. Coupling constant analysis was guided by method described elsewhere.¹⁷⁴ ¹H NMR and ¹³C NMR were processed with iNMR software program. Infrared (IR) spectra were recorded on a Bruker Alpha-P FT-IR spectrometer using neat (for liquid compound) or a thin film from a concentrated DCM solution. Absorptions are reported in cm⁻¹. Only the most intense and/or diagnostic peaks are reported. MPLC refers to medium pressure liquid chromatography (25-200 psi) using hand-packed columns of Silasorb silica gel (20-45 μm, spherical, 70 Å pore size), a Waters HPLC pump, and a Waters R401 differential refractive index detector. High-resolution mass spectra (HRMS) were recorded in electrospray ionization time-of-flight (ESI-TOF) mode

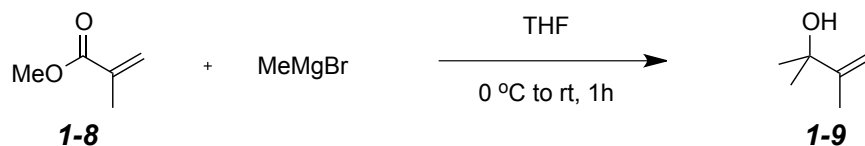
using a Shimadzu LC/MS IT-TOF. Samples were introduced as solutions in mixed solution of methanol and methylene chloride (DCM). GC/MS data were recorded on a Varian 450-GC/Varian 240-MS System. The methods used are noted parenthetically: 5025015 refers to 2 min @ 50 °C – 20 °C/min – 3 min @ 250 °C (a 50 °C initial temperature that was held for 2 minutes followed by a 20 °C/min ramp to a final temperature of 250 °C that was held for 3 minutes for a total run time of 15 minutes). 5029017 refers to: 2 min @ 50 °C – 20 °C/min – 3 min @ 290 °C. 5029019 refers to: 2 min @ 50 °C – 20 °C/min – 5 min @ 290 °C. 5032021 refers to: 2 min @ 50 °C – 20 °C/min – 5 min @ 320 °C. Analytical TLC experiments were performed on EMD Merck F254 plate, 250 µm thickness. Detection was performed by UV light or potassium phosphomolybdic acid, permanganate, *p*-anisaldehyde staining.

General Experimental Procedure: Chapter 1

General Procedure for Preparation of Alkenol by organometallic addition reactions^{175,176}:

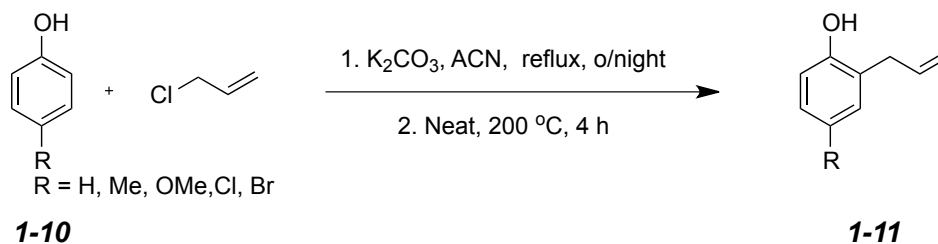


To a solution of allylmagnesium chloride in anhydrous THF (15.3 mL, 2 M, 30.6 mmol, 1.50 equiv) at 0 °C was slowly added acetone (1.50 mL, 1.18 g, 20.4 mmol, 1 equiv). After 15 min at 0 °C, the reaction mixture was stirred for 1 h at rt. The reaction mixture was then poured into a saturated aqueous NH₄Cl solution (20 mL) and extracted with diethyl ether (300 mL). The combined organic extracts were washed with a saturated aqueous NaHCO₃ solution (25 mL), dried over MgSO₄, filtered, and concentrated under reduced pressure. Distillation under reduced pressure (10–15 bar, bp 50 °C) gave the product (1.1 g, 54%) as colorless oil.



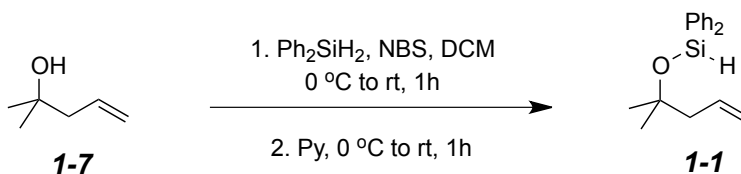
To a solution of methylmagnesiumbromide in anhydrous THF (100 mL, 0.3 M, 75 mmol, 2.50 equiv) at 0 °C was slowly added methyl methacrylate (3.0 g, 30 mmol, 1 equiv). After 15 min at 0 °C, the reaction mixture was stirred for 4 h at rt. The reaction mixture was then poured into a saturated aqueous NH₄Cl solution (20 mL) and extracted with ethyl acetate (300 mL). The combined organic extracts were washed with a saturated aqueous NaHCO₃ solution (25 mL), dried over MgSO₄, filtered, and concentrated under reduced pressure. Distillation under reduced pressure gave the product (1.9 g, 63%) as colorless oil.

General Procedure for Preparation of Alkenols by Claisen Rearrangement:



To a mixture of phenol (0.4 g, 2.3 mmol) and K_2CO_3 (0.62g, 4.6 mmol) in acetonitrile (9.2 mL, 0.25 M) was added allyl chloride (0.352 g, 4.6 mmol). The reaction mixture was heated to reflux for 6-8 h. Reaction progress was monitored by GC-MS. Upon completion of the reaction pour the reaction mixture into water and extract the product into ethyl acetate (3*30 mL). Combined organics were washed with brine solution and dried over Na_2SO_4 and evaporated to get the crude product. The crude product (>90% pure by GC-MS) from this stage is used as starting material for the next stage. The crude allyl ether was charged in a 4 mL glass vial with a screw cap u/nitrogen atmosphere. The reaction was heated to 200 °C for 4-6 h. Reaction progress was monitored by GS-MS. Crude product **1-11** was purified by column chromatography using 10% ethyl acetate in hexane as the eluent.

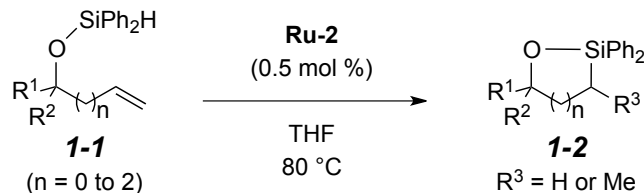
General Procedure for Preparation of Alkenylsilyl Ethers (1-1):



Diphenylsilane (2.07 mL, 11.2 mmol) was dissolved in DCM (30 mL, 0.33 M), and the reaction mixture was cooled to 0 °C with an ice bath and stirred at 0 °C for 5 min. NBS (1.95 g, 11.0 mmol) was added to the mixture in three portions (caution: exothermic), and the reaction mixture was warmed to rt and stirred for 1 h. During this process, the reaction mixture turned

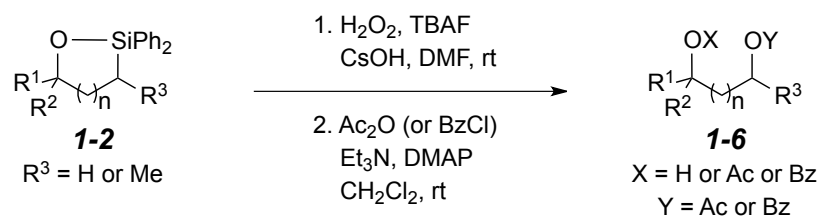
colorless from orange. The reaction mixture was again cooled to 0 °C with an ice bath, and stirred at 0 °C for 5 min. Pyridine (0.96 mL, 12.0 mmol) and alkenols (10.0 mmol, non-commercial substrates were synthesized through either vinylic or allylic organometallic addition reactions for **1a-1i**, **1j-1k** or Claisen rearrangement for **1l-1p**⁴) were added to the reaction mixture dropwise, which was warmed to rt and stirred for 1 h. The volatiles were removed *in vacuo*. Pentane was added to the resulting mixture, which was filtered through a pad of Celite[®] and concentrated *in vacuo* to afford the alkenylsilyl ethers **1**. The resulting crude material was purified by MPLC (hexanes/EtOAc = 80:1, 8 mL/min, retention time 5-10 min), unless otherwise notices – partial decomposition of some alkenylsilyl ethers was observed during the MPLC separation.

General Procedure for Ru-Catalyzed Hydrosilylation of Alkenylsilyl Ethers:



Ruthenium catalyst, **Ru-2** (0.9 mg, 0.5 mol %) was dissolved in degassed THF (1.5 mL, 0.2 M). Alkenylsilyl ether (0.3 mmol) was added to the reaction mixture, and the septum on the vial was replaced by a screw cap with a Teflon liner. The mixture was warmed to 80 °C and stirred for 8 to 18 h. Volatiles were removed *in vacuo*. Hexanes was added to the resulting mixture and stirred for 10 min, which was filtered through a pad of Celite[®] and concentrated *in vacuo*. The yield of the reaction was determined by ¹H NMR spectroscopy by an addition of CH₂Br₂ (21 μL, 0.3 mmol) as an internal standard. The resulting crude mixture was purified by MPLC, unless otherwise notices a partial decomposition of some oxasilacycles was observed during the MPLC separation.

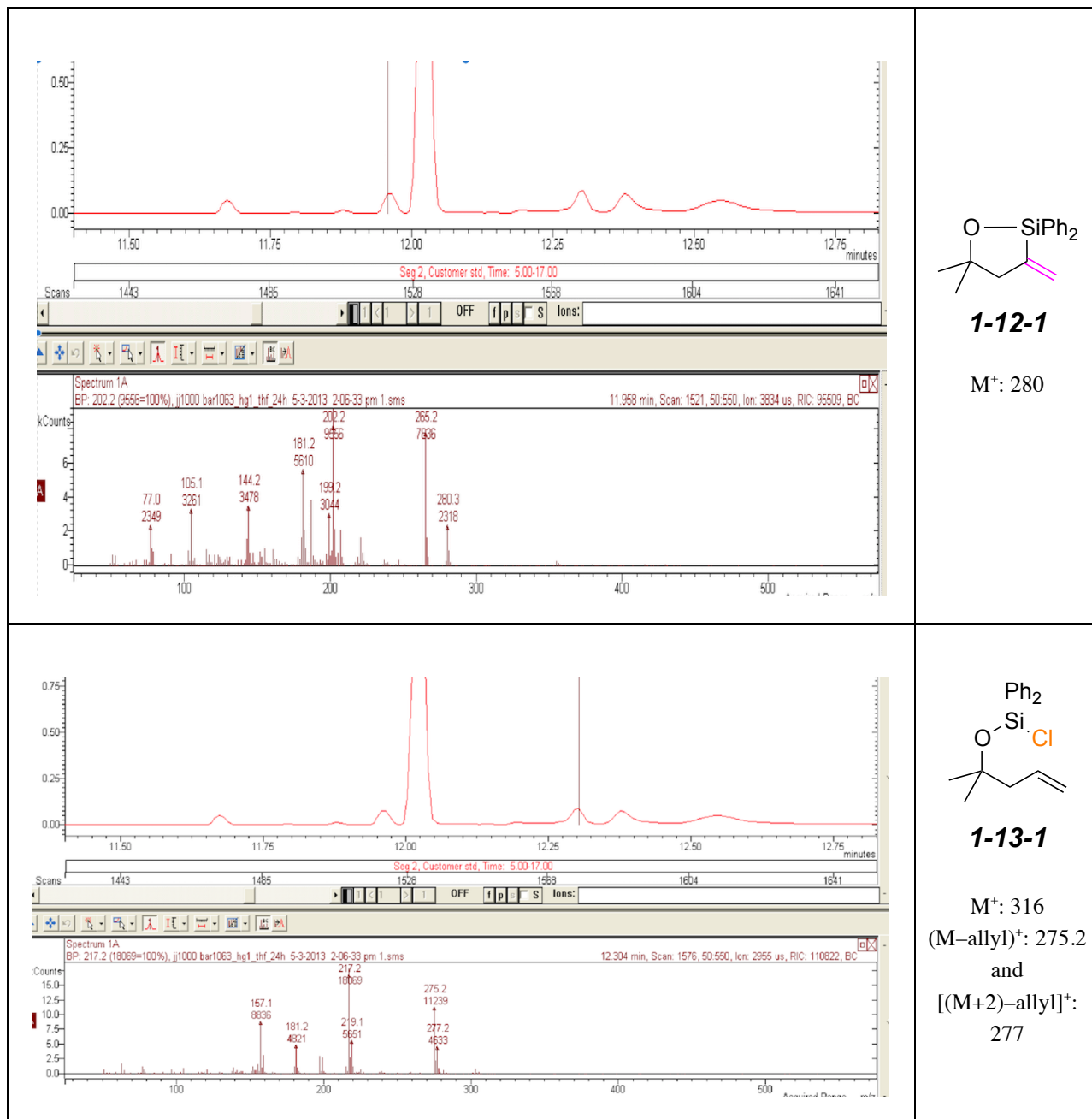
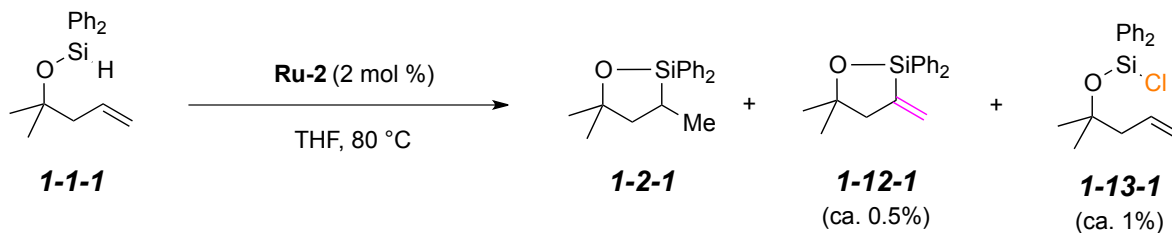
General Procedure for Oxidation and Acetylation or Benzoylation of Oxasilacycles:



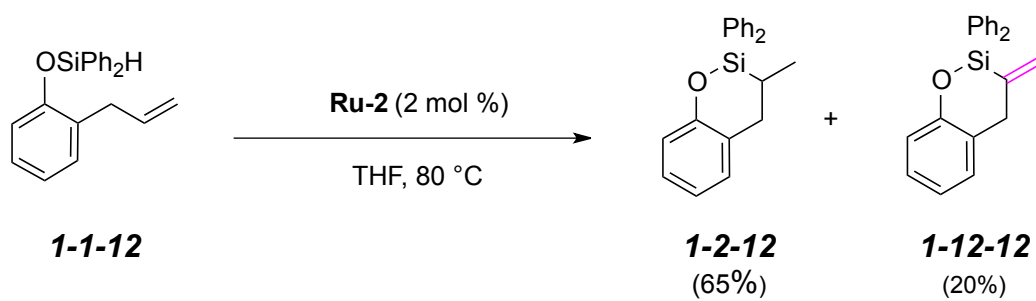
KHCO_3 (1.0 mmol), hydrogen peroxide (30% in H_2O , 3.0 mmol), and a 1:1 mixture of DMF (1.0 mL, 0.5 M) and THF (1 mL, 0.5 M) were added to a vial. Tetrabutylammonium fluoride (TBAF, 1.0 M in THF solution, 1.0 mmol) and oxasilacycles (0.20 mmol) were added to the mixture at rt, which was stirred for 2-12 h. The reaction mixture was carefully quenched with saturated aqueous sodium thiosulfate and stirred for 10 min. The mixture was extracted with EtOAc (20 mL \times 3), and the combined organic extract was washed with aqueous HCl (1.0 M, 20 mL), saturated aqueous sodium bicarbonate (20 mL), brine (20 mL), and dried over anhydrous sodium sulfate. The volatiles were removed under reduced pressure to afford the crude diol, which was directly used for a subsequent reaction without further purification.

Diol (0.2 mmol), DMAP (0.04 mmol), and Et_3N (1.2 mmol) were dissolved in DCM (0.15 M). acetic anhydride (1.2 mmol) or benzoyl chloride (1.2 mmol) was added to the reaction mixture, which was stirred for 4 to 8 hr at rt. The reaction mixture was quenched with water and extracted with EtOAc (3 \times 20 mL), and the combined organic layer was washed with brine solution, and dried over Na_2SO_4 . The volatiles were removed *in vacuo*. The resulting crude mixture was purified by MPLC (hexanes/EtOAc = 3.5:1 to 10:1, 8 mL/min).

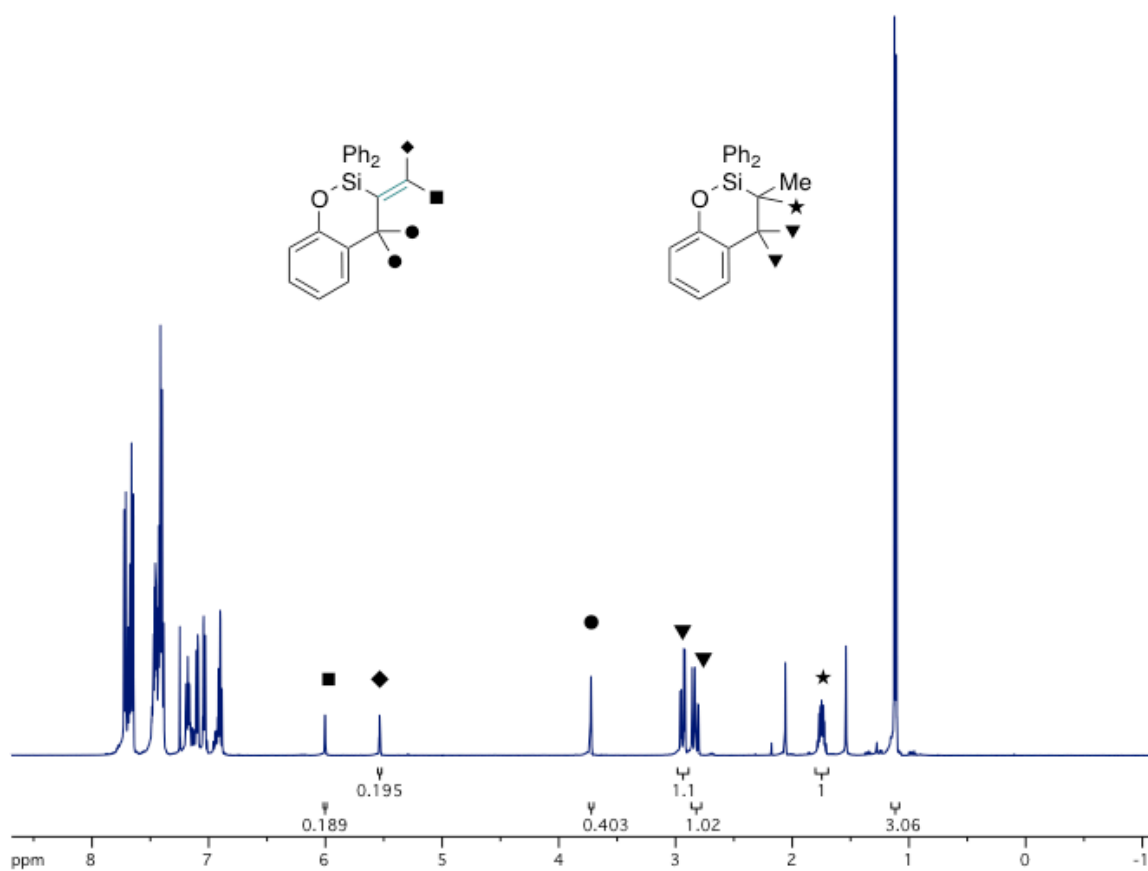
Formation of vinylsilane 1-12 and chlorosilane 1-13 from alkenylsilyl ether 1-1-1:



¹H NMR spectrum for 1-2-12 and 1-12-12:



¹H NMR (CDCl₃, 500 MHz):



GC/MS for 1-13-*t*-Bu:

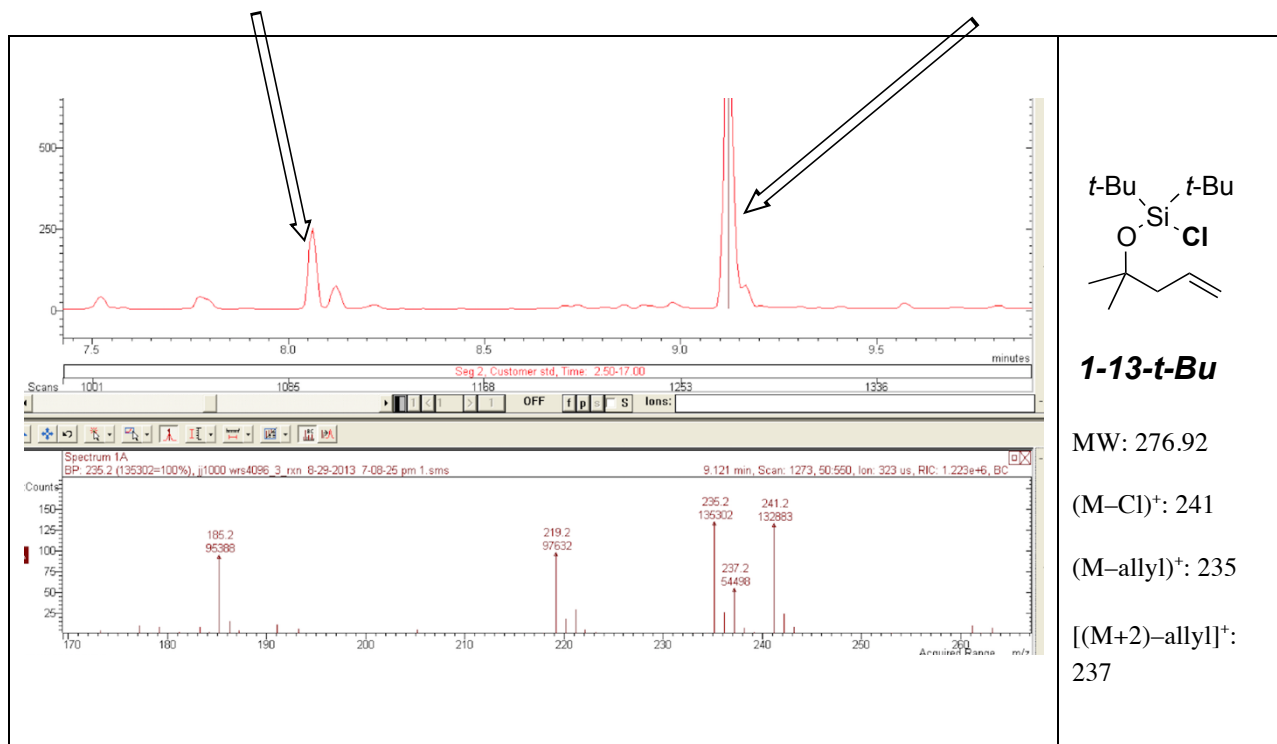
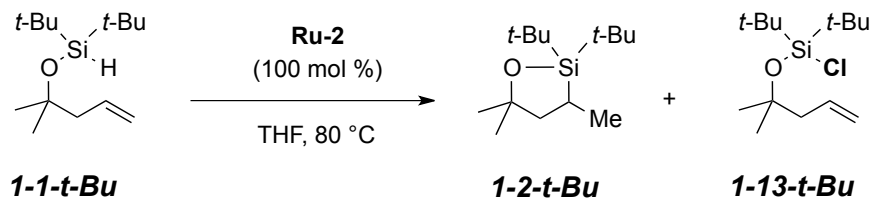
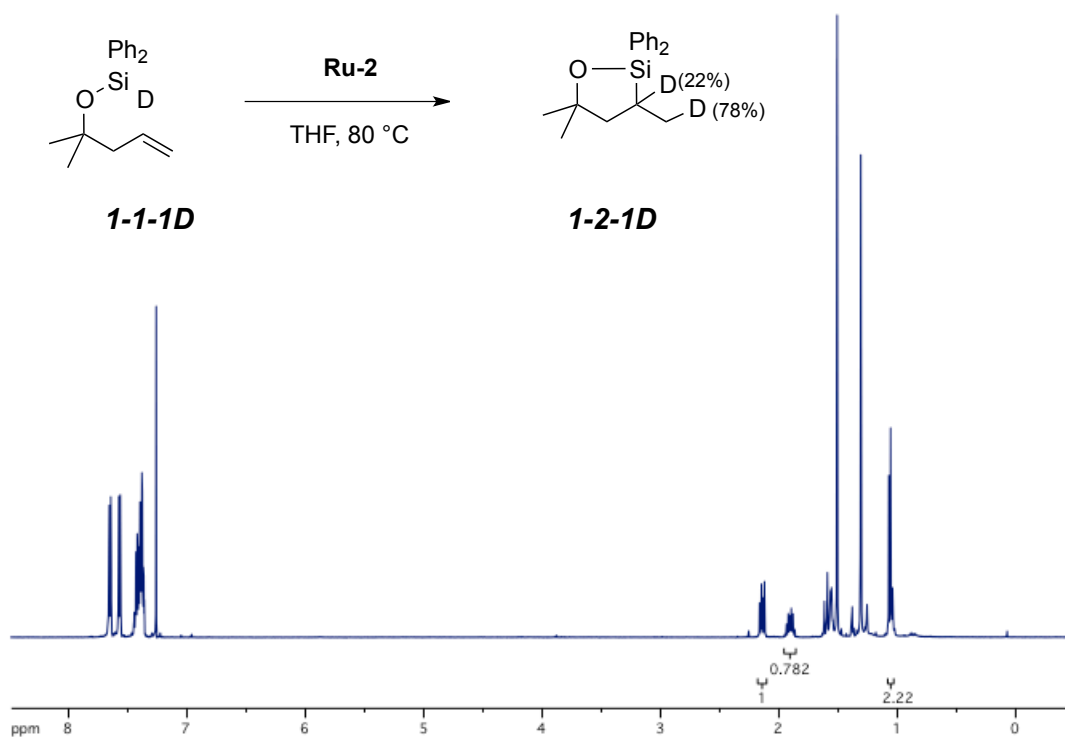


Figure 1.24: ^1H NMR Spectrum (CDCl_3 , 500 MHz):



^2H NMR Spectrum (CHCl_3 , 300 MHz):

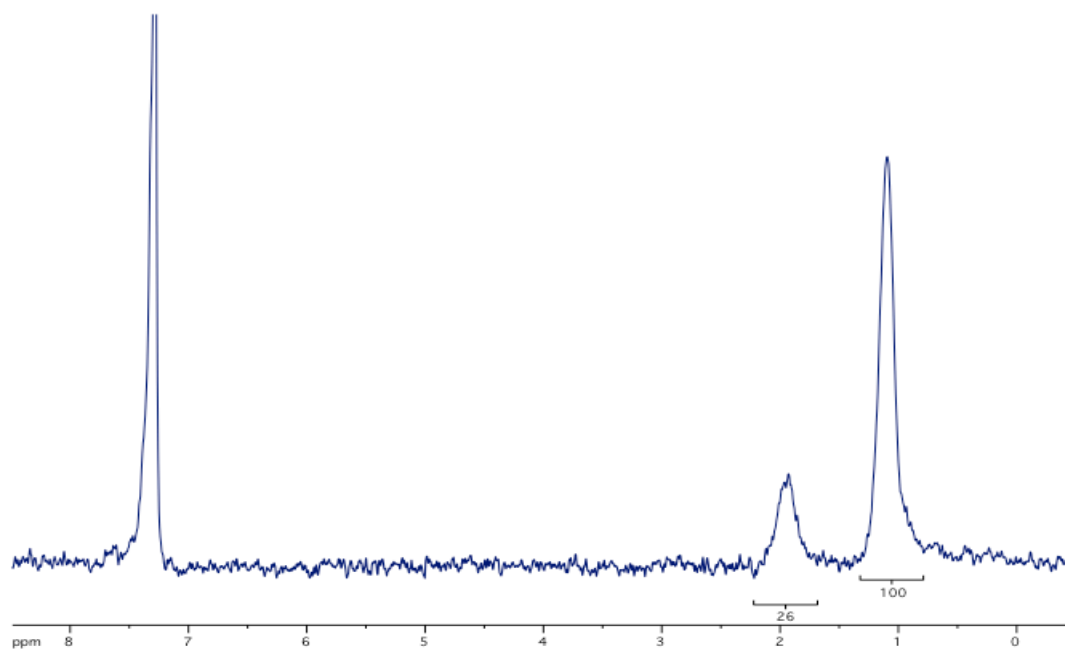
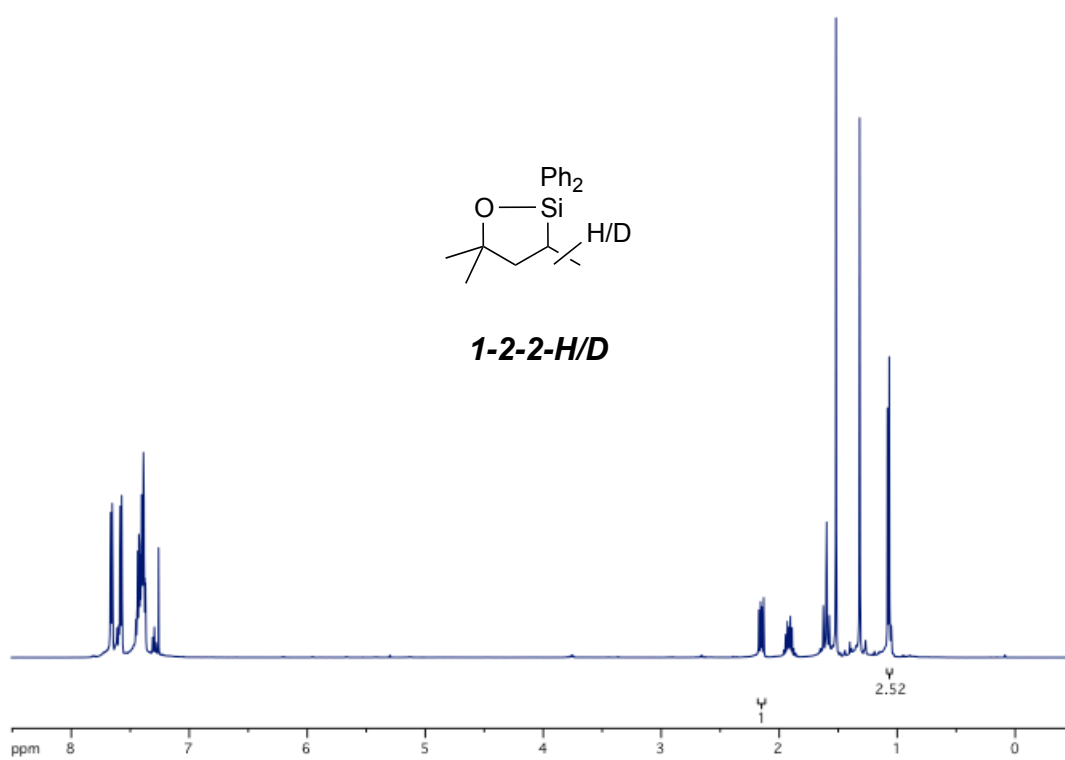
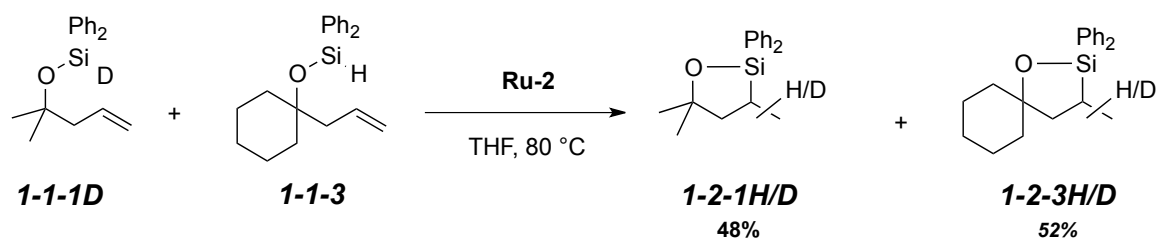
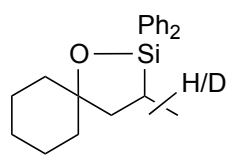
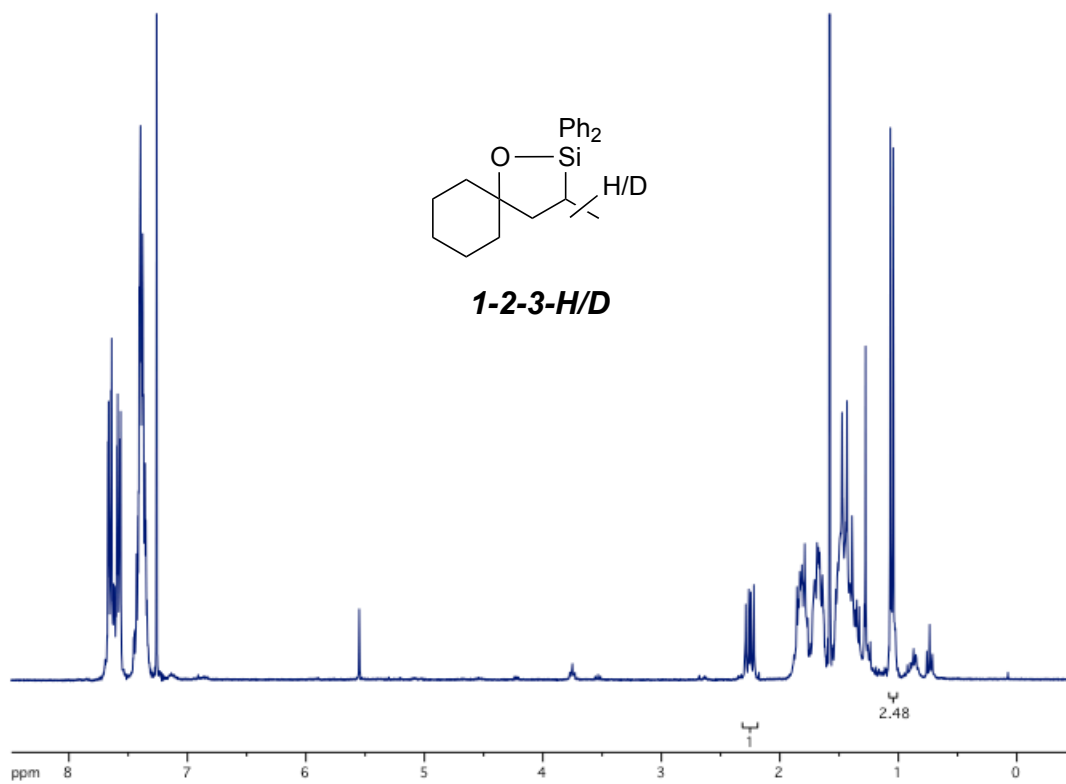


Figure 1.25: ^1H NMR (CDCl_3 , 500 MHz):

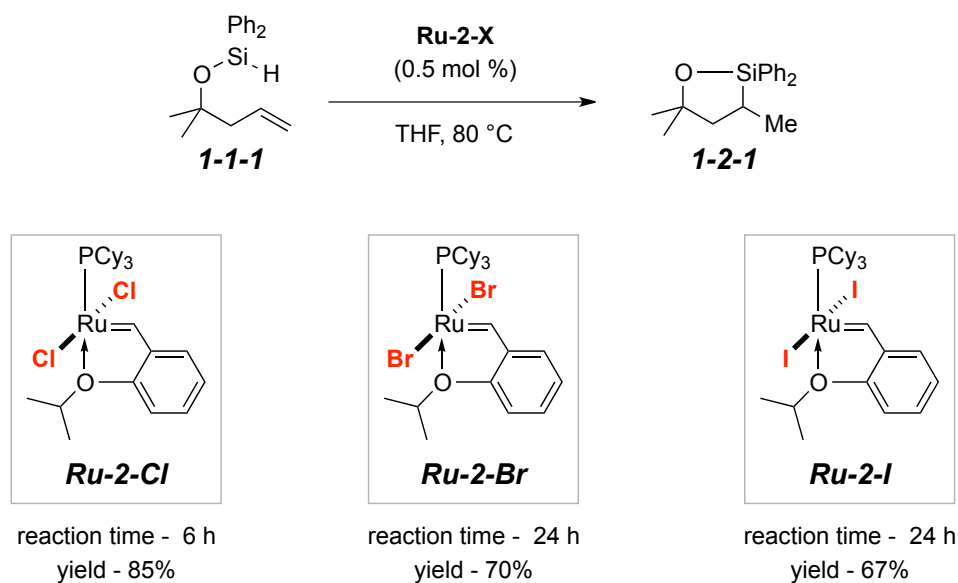




1-2-3-H/D



Catalytic activities varying halides on Ru-2



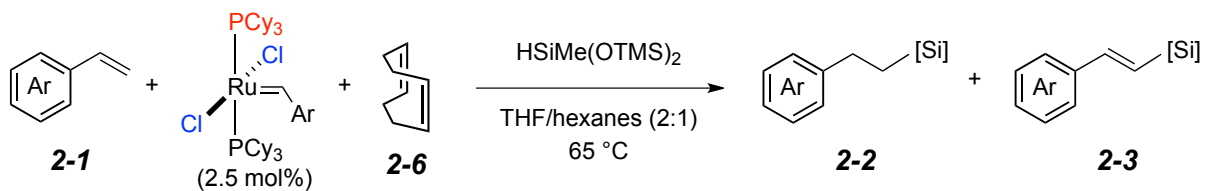
For synthesis of **Ru-2-Br** and **Ru-2-I**, see the following reference.

M. S. Sanford, J. A. Love, R. H. Grubbs, *J. Am. Chem. Soc.* **2001**, *123*, 6543-6554.

Ruthenium catalyst (0.3 mg, 0.5 mol%) was placed in an oven-dried J-Young tube and d_8 -THF (0.5 mL, 0.2 M) was added. Alkenylsilyl ether (28 mg, 0.1 mmol) and CH_2Br_2 (0.1 mmol) as an internal standard were added to the reaction mixture. The septum on the NMR tube was replaced by a TFE plug with a Viton O-ring seal. The mixture was warmed to 80 °C and the reaction progress was monitored and the yield of the reaction was determined by ^1H NMR spectroscopy.

General Experimental Procedure: Chapter 2

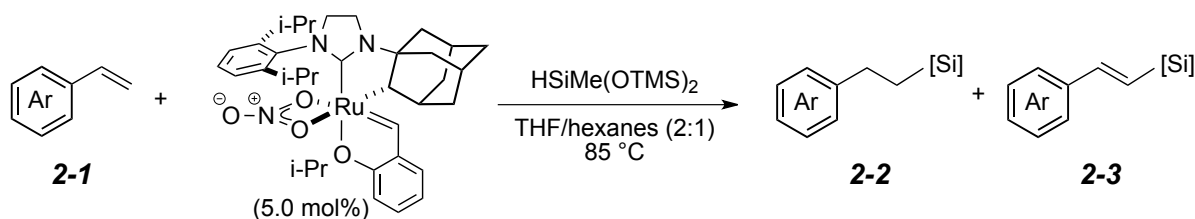
General Procedure for Ruthenium Alkylidene-Catalyzed Dehydrogenative Alkene-Silane Coupling:



Ru-1 (4.1 mg, 2.5 mol %) and degassed THF/hexanes (0.7 mL/0.35 mL, 0.2 M) were added to a flame-dried, nitrogen-purged septum-capped vial. 1,1,1,3,5,5,5-Heptamethyltrisiloxane [HSiMe(OTMS)₂], 56 μ L, 0.22 mmol], alkene **1** (0.2 mmol), and cyclooctadiene (49 μ L, 0.4 mmol) were added to the mixture. The septum on the vial was replaced by a screw cap with a Teflon liner under a N₂ atmosphere. The reaction mixture was stirred for 8-18 h at 65 °C. Volatiles were removed *in vacuo*, and hexanes was added to the resulting mixture, which was stirred for 10 min, filtered through a pad of Celite[®], and concentrated *in vacuo*. The crude product was purified by MPLC to afford vinyl silanes **2-3**.

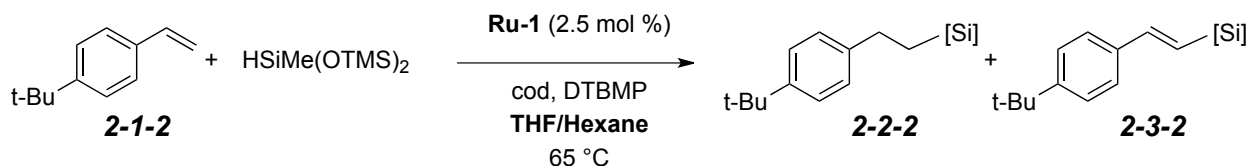
General Procedure for Ruthenium Alkylidene-Catalyzed hydrogenative Alkene-Silane

Coupling:



Ru-7 (6.8 mg, 5.0 mol %) and degassed THF/hexanes (0.13 mL/0.065 mL, 2 M) were added to a flame-dried, nitrogen-purged septum-capped vial. 1,1,1,3,5,5,5-Heptamethyltrisiloxane [HSiMe(OTMS)₂, 63 μ L, 0.25 mmol] and alkenes **1** (0.2 mmol), were added to the mixture. The septum on the vial was replaced by a screw cap with a Teflon liner under a N₂ atmosphere. The reaction mixture was stirred for 18-30 h at 85 °C. Volatiles were removed *in vacuo*, and hexanes was added to the resulting mixture, which was stirred for 10 min, filtered through a pad of Celite[®], and concentrated *in vacuo*. The crude product was purified by MPLC to afford alkyl silanes **2-2**.

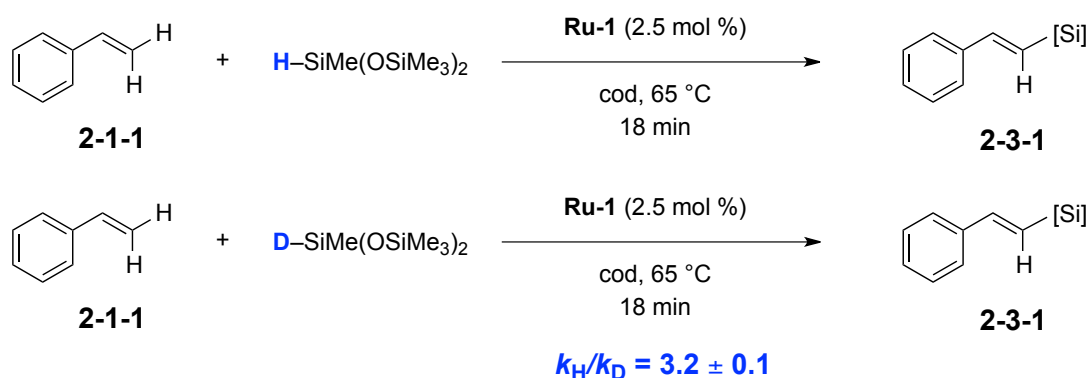
Addition of a Proton Scavenger for Dehydrogenative Silylation



Ru-1 (4.1 mg, 2.5 mol %) and degassed THF/hexanes (0.7 mL/0.35 mL, 0.2 M) were added to a flame-dried, nitrogen-purged septum-capped vial. 1,1,1,3,5,5,5-Heptamethyltrisiloxane [HSiMe(OTMS)₂, 56 μ L, 0.22 mmol], alkene **2-1** (32 mg, 0.2 mmol), cyclooctadiene (49 μ L, 0.4 mmol), and DTBMP (2,6-di-*tert*-butyl-4-methylpyridine, 41.1 mg, 0.2 mmol) were added to the mixture. The septum on the vial was replaced by a screw cap with

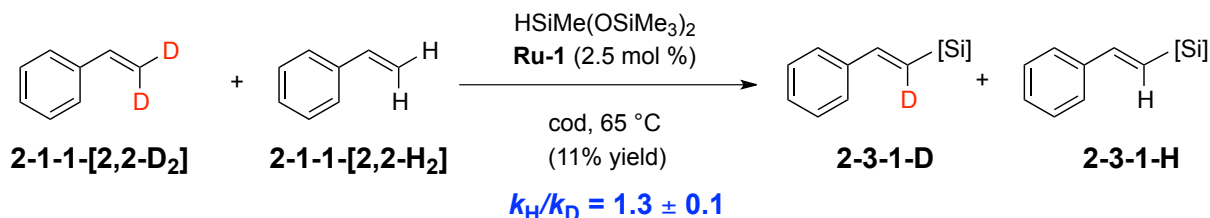
a Teflon liner under a N₂ atmosphere. The mixture was warmed to 65 °C and stirred for 24 hr. Reaction progress was monitored by ¹H NMR using EtOAc (20 μL, 0.2 mmol) as an internal standard.

Isotope Labeling of Silane-Independent Parallel Experiments:



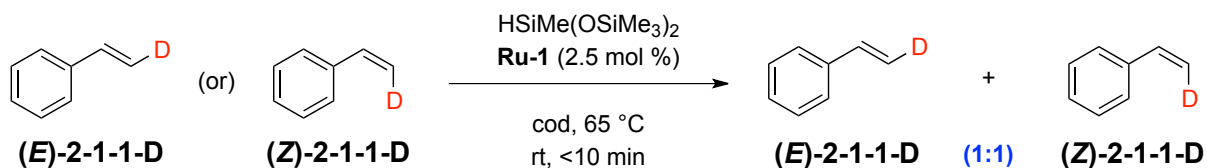
Ru-1 (4.1 mg, 2.5 mol %) and degassed THF/hexanes (0.7 mL/0.35 mL, 0.2 M) were added to a flame-dried, nitrogen-purged septum-capped vial. 3-Deutero-1,1,1,3,5,5,5-heptamethyltrisiloxane [DSiMe(OTMS)₂, 56 μL, 0.22 mmol], styrene (23 μL, 0.2 mmol), cyclooctadiene (49 μL, 0.4 mmol), and ethyl acetate (internal standard, 20 μL, 0.2 mmol) were added to the mixture. The septum on the vial was replaced by a screw cap with a teflon liner under a N₂ atmosphere. The reaction mixture was heated to 65 °C and the reaction progress was monitored by ¹H NMR spectroscopy at time intervals of 6 min by taking aliquots. A parallel reaction was carried out using 1,1,1,3,5,5,5-heptamethyltrisiloxane [HSiMe(OTMS)₂]. Aliquots at 18 min from the independent parallel reactions were diluted with CDCl₃ at room temperature and the products were analyzed by ¹H NMR spectroscopy. The reaction with DSiMe(OTMS)₂ produced vinyl silane in 2.7% yield, whereas HSiMe(OTMS)₂ afforded vinyl silane in 8.7% yield. Analysis of the products by ¹H NMR spectroscopy established KIE of 3.2 (1° KIE).

Isotope Labeling of Alkene–Competition Experiment



Ru-1 (4.1 mg, 2.5 mol %) and degassed THF/hexanes (0.7 mL/0.35 mL, 0.2 M) were added to a flame-dried, nitrogen-purged septum-capped vial. 1,1,1,3,5,5,5-Heptamethyltrisiloxane [HSiMe(OSiMe₃)₂, 50 μL, 0.2 mmol], styrene **1a**-[2,2-H₂] (23 μL, 0.2 mmol), 2,2-dideuterostyrene **1a**-[2,2-D₂] (23 μL, 0.2 mmol), cyclooctadiene (49 μL, 0.4 mmol), and ethyl acetate (internal standard, 20 μL, 0.2 mmol) were added to the mixture. The septum on the vial was replaced by a screw cap with a Teflon liner under a N₂ atmosphere. The reaction mixture was heated to 65 °C and the reaction progress were monitored by ¹H NMR spectroscopy at time intervals of 5 min by taking aliquots. An aliquot at 25 min from the competition reaction was diluted with CDCl₃ at room temperature and the products were analyzed by ¹H NMR spectroscopy. The reaction furnished **3a**-H in 6.2% yield and deuterio-vinylsilane **3a**-D in 4.8% yield. Analysis of the products by ¹H NMR spectroscopy established KIE of 1.3 (2° KIE).

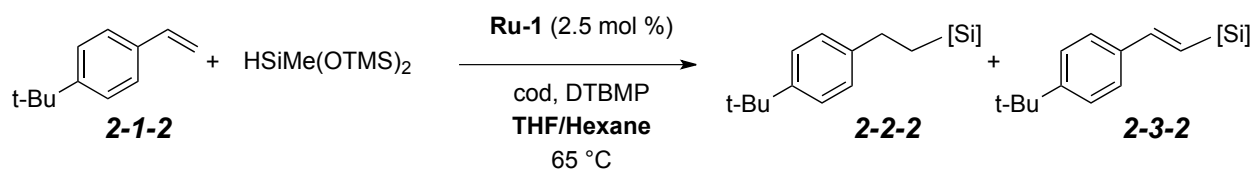
Isotope Labeling of Alkene–Rapid Isomerization of Alkene



Rapid isomerization of alkene

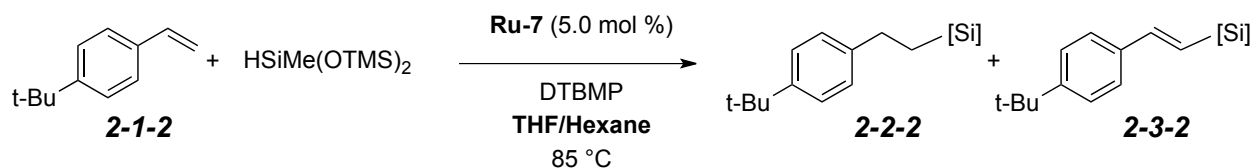
Two separate reactions were set up in the above mentioned procedure with *cis*-styrene-(β)-d (23 μL , 0.2 mmol) and *trans*-styrene-(β)-d (23 μL , 0.2 mmol). Rapid isomerization to furnish a nearly 1:1 mixture of (*Z*)-1a and (*E*)-1a were observed in both the cases, which unfortunately hindered studies for stereoselectivity of the dehydrogenative silylation.

Addition of a Proton Scavenger for Dehydrogenative Silylation



Ru-1 (4.1 mg, 2.5 mol %) and degassed THF/hexanes (0.7 mL/0.35 mL, 0.2 M) were added to a flame-dried, nitrogen-purged septum-capped vial. 1,1,1,3,5,5,5-Heptamethyltrisiloxane [HSiMe(OTMS)_2 , 56 μL , 0.22 mmol], alkene **1b** (32 mg, 0.2 mmol), cyclooctadiene (49 μL , 0.4 mmol), and DTBMP (2,6-di-*tert*-buthyl-4-methylpyridine, 41.1 mg, 0.2 mmol) were added to the mixture. The septum on the vial was replaced by a screw cap with a Teflon liner under a N_2 atmosphere. The mixture was warmed to 65 °C and stirred for 24 hr. Reaction progress was monitored by ^1H NMR using EtOAc (20 μL , 0.2 mmol) as an internal standard.

Addition of a Proton Scavenger for Hydrosilylation

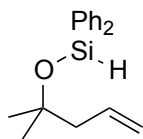


Ru-7 (6.8 mg, 5 mol %) and degassed THF/hexanes (0.13 mL/0.065 mL, 2 M) were added to a flame-dried, nitrogen-purged septum-capped vial. 1,1,1,3,5,5,5-Heptamethyltrisiloxane [HSiMe(OTMS)₂, 63 μ L, 0.25 mmol], alkene **1b** (32 mg, 0.2 mmol), and DTBMP (2,6-di-*tert*-butyl-4-methylpyridine, 41.1 mg, 0.2 mmol) were added to the mixture. The septum on the vial was replaced by a screw cap with a Teflon liner under a N₂ atmosphere. The mixture was warmed to 65 °C and stirred for 24 hr. Reaction progress was monitored by ¹H NMR using EtOAc (20 μ L, 0.2 mmol) as an internal standard.

Appendix C

Spectral data of the compounds

[(2-Methylpent-4-en-2-yl)oxy]diphenylsilane (1-1-1)



1-1-1

Physical Appearance: Colorless clear liquid.

¹H NMR (CDCl₃, 500 MHz): δ 7.62 [dd, *J* = 7.9, 1.5 Hz, 4H, Si{C₆(*H*_{ortho})₂H₃}₂], 7.43-7.35 [m, 6H, Si{C₆(*H*_{ortho})₂(*H*_{meta})₂*H*_{para}}₂], 5.91 (dddd, *J* = 17.5, 10.3, 7.2, 7.2 Hz, 1H, CH₂=CH), 5.57 (s, 1H, SiH), 5.07 (dddd, *J* = 10.3, 2.4, 1.2, 1.2 Hz, 1H, CH_{trans}H_{cis}=CH), 5.05 (dddd, *J* = 17.5, 2.4, 1.2, 1.2 Hz, 1H, CH_{trans}H_{cis}=CH), 2.34 (ddd, *J* = 7.2, 1.2, 1.2 Hz, 2H, CH₂CH=CH₂), and 1.30 [s, 6H, OC(CH₃)₂].

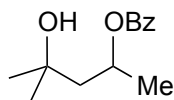
¹³C NMR (CDCl₃, 125 MHz): δ 136.2, 135.1, 134.7, 130.1, 128.1, 117.7, 75.4, 49.1, and 29.4.

GC-MS (5029017): *t*_R = 11.70 min, *m/z* 281 [(M-H)⁺, 100], 241 [(M-allyl)⁺, 15], and 205 (10).

IR (neat): 2972 (m), 2119 (m), 1428 (m), 1111 (s), 1246 (m), 816 (s), and 695 (s) cm⁻¹.

HRMS (ESI/TOF): Calcd for (C₁₈H₂₃OSi)⁺: 283.1513. Found: 383.1521.

4-Hydroxy-4-methylpentan-2-yl benzoate (1-6-1)



1-6-1

Physical Appearance: Colorless clear liquid.

Purified by MPLC (hexanes/EtOAc = 3:1, 8 mL/min).

Physical Appearance: Colorless clear liquid.

¹H NMR (CDCl₃, 500 MHz): δ 8.02 [dd, *J* = 8.3, 1.4 Hz, 2H, Ph*H*_{ortho}], 7.54 [tt, *J* = 7.4, 1.4 Hz, 1H, Ph*H*_{para}], 7.43 [ddd, *J* = 8.3, 7.4, 1.4 Hz, 2H, Ph*H*_{meta}], 5.42 [dq, *J* = 8.8, 6.2, 3.3 Hz, 1H, CH₂CH(OBz)CH₃], 2.06 [dd, *J* = 14.9, 8.8 Hz, 1H, C(OH)CH_aH_b], 1.76 [dd, *J* = 14.9, 3.3 Hz, 1H, C(OH)CH_aH_b], 1.39 [d, *J* = 6.2 Hz, 3H, CH₂CH(OBz)CH₃], and 1.27 [s, 3H, CH₃CH₃C(OH)] and 1.25 [s, 3H, CH₃CH₃C(OH)].

^{13}C NMR (CDCl_3 , 125 MHz): δ 166.3, 133.1, 130.6, 129.6, 128.5, 70.1, 69.5, 49.2, 30.0, 29.8, and 21.9.

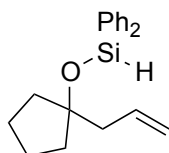
TLC: R_f = 0.40 in 3:1 hexanes: EtOAc.

GC-MS (5032021): t_R = 10.04 min, m/z 222.7 $[(\text{M}-\text{H})^+]$ and 205 $[(\text{M}-\text{OH})^+, 100]$

IR (neat): 3455 (w), 2972 (m), 1712 (s), 1273 (s), 1111 (s), and 709 (s) cm^{-1} .

HRMS (ESI/TOF): Calcd for $(\text{C}_{13}\text{H}_{19}\text{O}_3)^+$: 223.1329. Found: 223.1320

[(1-Allylcyclopentyl)oxy]diphenylsilane (1-1-2)



1-1-2

Physical Appearance: Colorless clear liquid.

^1H NMR (CDCl_3 , 500 MHz): δ 7.65 [dd, J = 7.7, 1.6 Hz, 4H, $\text{Si}\{\text{C}_6(\text{H}_{ortho})_2\text{H}_3\}_2$], 7.45-7.38 [m, 6H, $\text{Si}\{\text{C}_6(\text{H}_{ortho})_2(\text{H}_{meta})_2\text{H}_{para}\}_2$], 5.95 (dddd, J = 17.2, 10.3, 7.1, 7.1 Hz, 1H, $\text{CH}_2=\text{CH}$), 5.59 (s, 1H, SiH), 5.07 (dddd, J = 10.2, 2.2, 1.2, 1.2 Hz, 1H, $\text{CH}_{trans}\text{H}_{cis}=\text{CH}$), 5.05 (dddd, J = 17.2, 2.2, 1.2, 1.2 Hz, 1H, $\text{CH}_{trans}\text{H}_{cis}=\text{CH}$), 2.46 (ddd, J = 7.1, 1.2, 1.2 Hz, 2H, $\text{CH}_a\text{H}_b\text{CH}=\text{CH}_2$), 1.87 (ddd, J = 11.6, 2.9, 2.9 Hz, 2H, cyclopentyl H_2 and H_5), 1.75 (dddd, J = 11.6, 5.9, 5.9, 3.4, 3.4 Hz, 2H, cyclopentyl H_3 and H_4), and 1.67-1.57 (m, 4H, cyclopentyl H_2 , H_3 , H_4 , and H_5).

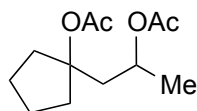
^{13}C NMR (CDCl_3 , 125 MHz): δ 136.1, 135.3, 134.7, 130.1, 128.0, 117.5, 86.6, 45.6, 39.1, and 23.7.

GC-MS (5029017): t_R = 12.744 min, m/z 307 $[(\text{M}-\text{H})^+, 100]$, 267 $[(\text{M}-\text{allyl})^+, 60]$, and 231 (100).

IR (neat): 2955 (m), 2127 (m), 1738 (w), 1428 (m), 1114 (m), 818 (s), and 695 (s) cm^{-1} .

HRMS (ESI/TOF): Calcd for $(\text{C}_{20}\text{H}_{25}\text{OSi})^+$: 309.1669. Found: 309.1676.

1-(1-Acetoxypropyl)cyclopentyl acetate (1-6-2)



1-6-2

Physical Appearance: Colorless clear liquid.

Purified by MPLC (hexanes/EtOAc = 5:1, 8 mL/min).

¹H NMR (CDCl₃, 500 MHz): δ 5.04 [dq, *J* = 8.6, 6.3, 3.6 Hz, 1H, CH₂CH(OAc)CH₃], 2.31 [dd, *J* = 15.1, 3.6 Hz, 1H, cyclopentane(OAc)CH_aH_b], 2.21 [d, *J* = 15.0, 3.4 Hz, 1H, cyclopentane(OAc)CH_aH_b], 2.01 [s, 3H, CH(O₂CCH₃)], 1.97 [s, 3H, CH(O₂CCH₃)], 1.72-1.56 (m, 8H, cyclopentyl CH₂), and 1.21 [d, *J* = 6.3 Hz, 3H, CH₂CH(OAc)CH₃].

¹³C NMR (CDCl₃, 125 MHz): δ 171.0, 170.7, 91.2, 68.5, 42.3, 38.3, 38.1, 23.9, 23.5, 22.5, 21.7, and 21.5.

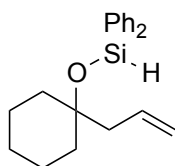
TLC: R_f = 0.5 in 5:1 hexanes: EtOAc.

GC-MS (5032021): t_R = 8.0 min, m/z 169 [(M-OAc)⁺, 40], 111(60) and 84(100).

IR (neat): 2875 (s), 1736 (s), 1370 (s), 1240 (s), 1079(s) and 1035 (s) cm⁻¹.

HRMS (ESI/TOF): Calcd for (C₁₂H₂₁O₄)⁺: 229.1434. Found: 229.1425.

[(1-Allylcyclohexyl)oxy]diphenylsilane (1-1-3)



1-1-3

Physical Appearance: Colorless clear liquid.

¹H NMR (CDCl₃, 500 MHz): δ 7.63 [dd, *J* = 7.9, 1.5 Hz, 4H, Si{C₆(H_{ortho})₂H₃}₂], 7.42-7.34 [m, 6H, Si{C₆(H_{ortho})₂(H_{meta})₂H_{para}}₂], 5.86 (dddd, *J* = 17.2, 10.2, 7.2, 7.2 Hz, 1H, CH₂=CH), 5.59 (s, 1H, SiH), 5.02 (dddd, *J* = 10.2, 2.2, 1.2, 1.2 Hz, 1H, CH_{trans}H_{cis}=CH), 4.98 (dddd, *J* = 17.2, 2.2, 1.2, 1.2 Hz, 1H, CH_{trans}H_{cis}=CH), 2.32 (ddd, *J* = 7.2, 1.2, 1.2 Hz, 2H, CH_aH_bCH=CH₂), and 1.68-1.25 (m, 10H, cyclohexyl CH₂).

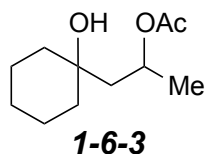
¹³C NMR (CDCl₃, 125 MHz): δ 136.4, 134.8, 134.6, 130.1, 128.0, 117.7, 76.9, 53.26 (CH₂Cl₂), 46.3, 37.6, 25.8, and 22.6.

GC-MS (5029017): t_R = 13.23 min, m/z 321 [(M-H)⁺, 100], 281 [(M-allyl)⁺, 10] and 245.

IR (neat): 2931 (m), 2119 (m), 1738 (w), 1428 (m), 814 (s), and 695 (s) cm⁻¹.

HRMS (ESI/TOF): Calcd for (C₂₁H₂₇OSi)⁺: 323.1826. Found: 323.1814.

1-(1-Hydroxycyclohexyl)propan-2-yl acetate (1-6-3)



Physical Appearance: Colorless clear liquid.

Purified by MPLC (hexanes/EtOAc = 5:1, 8 mL/min).

¹H NMR (CDCl₃, 500 MHz): 5.09 [dq, *J* = 8.6, 6.3, 3.4 Hz, 1H, CH₂CH(OAc)CH₃], 2.26 [dd, *J* = 15.3, 8.6 Hz, 1H, CH_aH_bCH(OAc)], 2.25-2.20 (m, 1H, cyclohexyl CH_aH_b), 2.17-2.12 (m, 1H, cyclohexyl CH_aH_b), 2.10 [dd, *J* = 15.3, 3.4 Hz, 1H, CH_aH_bCH(OAc)], 2.00 [s, 3H, CH(O₂CCH₃)], 1.57 [dddd, *J* = 17.0, 8.5, 4.2, 1.2, 1.2 Hz, 1H, CH_aH_b], 1.52-1.40 (m, 4H, cyclohexyl CH₂), 1.37-1.31 (m, 2H, cyclohexyl CH₂), 1.28-1.22 (m, 1H, cyclohexyl CH_aH_b), and 1.20 [d, *J* = 6.3 Hz, 3H, CH₂CH(OAc)CH₃].

¹³C NMR (CDCl₃, 125 MHz): δ 170.7, 82.8, 67.6, 42.9, 35.1, 35.0, 25.6, 22.6, 22.0, 21.9, and 21.7.

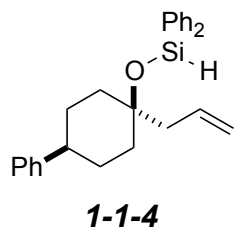
TLC: R_f = 0.5 in 5:1 hexanes: EtOAc.

GC-MS (5032021): t_r = 9.34 min, m/z 183 [(M-OAc)⁺, 70], 122 (100) and 81 (40).

IR (neat): 2926 (m), 1733 (s), 1368 (m), 1233 (s), 1015 (s), and 699 (w) cm⁻¹.

HRMS (ESI/TOF): Calcd for (C₁₃H₂₃O₄)⁺: 243.1591. Found: 343.1587.

[[1-Allyl-4-phenylcyclohexyl]oxy]diphenylsilane (1-1-4)



Physical Appearance: Colorless clear liquid.

¹H NMR (CDCl₃, 500 MHz): δ 7.70 [dd, *J* = 7.8, 1.4 Hz, 4H, Si{C₆(H_{ortho})₂H₃}₂], 7.46-7.38 [m, 6H, Si{C₆(H_{ortho})₂(H_{meta})₂H_{para}}₂], 7.25 [dd, *J* = 7.8, 7.3 Hz, 2H, Ph-H], 7.17 [dd, *J* = 7.3, 7.3 Hz, 1H, Ph-H], 7.08 [d, *J* = 7.8 Hz, 2H, Ph-H], 5.86 (dddd, *J* = 17.3, 10.2, 7.3, 7.3 Hz, 1H, CH₂=CH), 5.66 (s, 1H, SiH),

5.05 (dddd, $J = 10.2, 3.0, 1.0, 1.0$ Hz, 1H, $\text{CH}_{\text{trans}}\text{H}_{\text{cis}}=\text{CH}$), 5.01 (dddd, $J = 17.3, 3.0, 1.0, 1.0$ Hz, 1H, $\text{CH}_{\text{trans}}\text{H}_{\text{cis}}=\text{CH}$), 2.43 (dddd, $J = 11.9, 11.9, 3.3, 3.3$ Hz, 1H, PhCH), 2.39 (app d, $J = 7.3$ Hz, 2H, $\text{CH}_a\text{H}_b\text{CH}=\text{CH}_2$), 1.94-1.85 (m, 4H, Cy-H), 1.64-1.61 (m, 2H, Cy-H), and 1.55-1.48 (m, 2H, Cy-H).

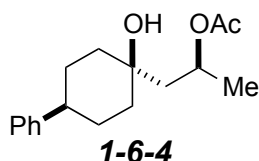
^{13}C NMR (CDCl_3 , 125 MHz): δ 147.7, 136.3, 134.8, 134.3, 130.2, 128.5, 128.1, 127.1, 126.1, 118.2, 76.0, 48.5, 44.0, 37.1, and 29.4.

GC-MS (5032021): $t_{\text{R}} = 16.91$ min, m/z 397 [(M-H) $^+$, 20], 357 [(M-allyl) $^+$, 80], 321(30), 279 (20), 199 (90) and 157 (100).

IR (neat): 2931 (w), 2128 (m), 1738 (w), 1428 (m), 1112 (m), 1054 (m), 812 (s), 730 (s) and 694 (s) cm^{-1}

HRMS (ESI/TOF): Calcd for $(\text{C}_{27}\text{H}_{31}\text{OSi})^+$: 399.2139. Found: 399.2144.

1-(1-Hydroxy-4-phenylcyclohexyl)propan-2-yl acetate (1-6-4)



Physical Appearance: Colorless clear liquid.

Purified by MPLC (hexanes/EtOAc = 3:1, 8 mL/min).

^1H NMR (CDCl_3 , 500 MHz): δ 7.29 [dd, $J = 8.0, 7.2$ Hz, 2H, Ph- H_{meta}], 7.23 [dd, $J = 8.0, 1.4$ Hz, 2H, Ph- H_{ortho}], 7.18 [dddd, $J = 7.2, 7.2, 1.4, 1.4$ Hz, 1H, Ph- H_{para}], 5.24 [dq, $J = 8.6, 6.3, 3.4$ Hz, 1H, $\text{CH}_2\text{CH}(\text{OAc})\text{CH}_3$], 2.45 (dddd, $J = 12.2, 12.2, 3.5, 3.5$ Hz, 1H, PhCH), 2.06 [s, 3H, $\text{CH}(\text{OCOCH}_3)$], 2.01 (br s, 1H, CyOH), 1.91 [dd, $J = 15.0, 8.6$ Hz, 1H, $\text{Cy}(\text{OH})\text{CH}_a\text{H}_b$], 1.90-1.68 (m, 6H, Cy-H), 1.63 [dd, $J = 15.0, 3.4$ Hz, 1H, $\text{Cy}(\text{OH})\text{CH}_a\text{H}_b$], 1.47 (dddd, $J = 13.4, 13.4, 4.0, 2.9$ Hz, 2H, $\text{H}_{2\text{ax}}$ and $\text{H}_{6\text{ax}}$), and 1.29 [d, $J = 6.3$ Hz, 3H, $\text{CH}_2\text{CH}(\text{OAc})\text{CH}_3$].

^{13}C NMR (CDCl_3 , 125 MHz): δ 171.1, 147.3, 128.5, 127.1, 126.2, 69.8, 68.4, 49.8, 44.2, 38.2, 37.5, 29.34, 29.28, 22.1, and 21.8.

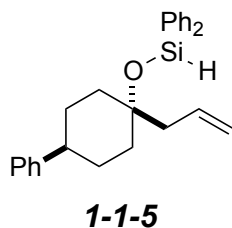
TLC: $R_f = 0.4$ in 3:1 hexanes: EtOAc.

GC-MS (5032021): $t_{\text{R}} = 12.88$ min, m/z 259 [(M-OH) $^+$, 100], 198 (10), 156 (10) and 128 (10).

IR (neat): 3481 (b), 2926 (m), 1733 (s), 1371 (m), 1244 (s), 1128 (m), 1034 (m), 757 (m), and 698(s) cm^{-1}

HRMS (ESI/TOF): Calcd for (C₁₇H₂₅O)⁺: 277.1798. Found: 277.1791.

[[1-Allyl-4-phenylcyclohexyl]oxy]diphenylsilane (1-1-5)



Physical Appearance: Colorless clear liquid.

¹H NMR (CDCl₃, 500 MHz): δ 7.66 [dd, *J* = 7.9, 1.6 Hz, 4H, Si{C₆(H_{ortho})₂H₃}₂], 7.45-7.38 [m, 6H, Si{C₆(H_{ortho})₂(H_{meta})₂H_{para}}₂], 7.30 [dd, *J* = 7.8, 7.3 Hz, 2H, Ph-*H*], 7.22-7.18 [m, 3H, Ph-*H*], 6.04 (dddd, *J* = 17.3, 10.4, 7.1, 7.1 Hz, 1H, CH₂=CH), 5.66 (s, 1H, SiH), 5.13 (dddd, *J* = 10.2, 2.4, 1.2, 1.2 Hz, 1H, CH_{trans}H_{cis}=CH), 5.11 (dddd, *J* = 17.3, 2.4, 1.2, 1.2 Hz, 1H, CH_{trans}H_{cis}=CH), 2.54 (app d, *J* = 7.1 Hz, 2H, CH_aH_bCH=CH₂), 2.51 (dddd, *J* = 12.2, 12.2, 3.3, 3.3 Hz, 1H, PhCH), 2.02 (dddd, *J* = 12.9, 3.3, 3.3, 3.3 Hz, 2H, H_{3_{eq}} and H_{5_{eq}}), 1.85-1.81 (m, 2H, H_{2_{eq}} and H_{6_{eq}}), 1.76 (ddd, *J* = 12.9, 12.9, 3.3 Hz, 2H, H_{2_{ax}} and H_{6_{ax}}), and 1.57 (dddd, *J* = 13.4, 12.2, 12.2, 3.3 Hz, 2H, H_{3_{ax}} and H_{5_{ax}}).

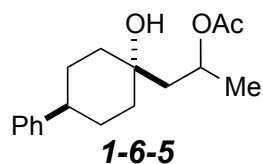
¹³C NMR (CDCl₃, 125 MHz): δ 146.6, 136.3, 134.7, 134.5, 130.1, 128.6, 128.1, 127.0, 126.3, 117.7, COSiPh₂H (overlap with CDCl₃ peaks between 77.4 to 76.9; inferred by **1e/1f/1g**), 43.4, 41.8, 38.5, and 31.3.

GC-MS (5032021): t_R = 17.97 min, m/z 397 [(M-H)⁺, 20], 357 [(M-allyl)⁺, 10], 321(30), 279 (20), 199 (90) and 157 (100).

IR (neat): 2931 (w), 2128 (m), 1738 (w), 1428 (m), 1112 (m), 1054 (m), 812 (s), 730 (s) and 694 (s) cm⁻¹.

HRMS (ESI/TOF): Calcd for (C₂₇H₃₁OSi)⁺: 399.2139. Found: 399.2144.

1-[(1-Hydroxy-4-phenylcyclohexyl)propan-2-yl] acetate (1-6-5)



Physical Appearance: Colorless clear liquid.

Purified by MPLC (hexanes/EtOAc = 3:1, 8 mL/min).

¹H NMR (CDCl₃, 500 MHz): δ 7.30 [dd, *J* = 8.0, 7.2 Hz, 2H, Ph-*H*_{meta}], 7.22 [dd, *J* = 8.0, 1.4 Hz, 2H, Ph-*H*_{ortho}], 7.20 [dddd, *J* = 7.2, 7.2, 1.4, 1.4 Hz, 1H, Ph-*H*_{para}], 5.20 [dq, *J* = 8.6, 6.3, 3.5 Hz, 1H, CH₂CH(OAc)CH₃], 2.58 [dddd, *J* = 11.6, 11.6, 3.5, 3.5 Hz, 1H, PhCH], 2.23 (br s, 1H, CyOH), 2.04 [s, 3H, CH(O₂CCH₃)], 2.03 [dd, *J* = 15.0, 8.6 Hz, 1H, CH_aH_bC(OAc)], 1.91-1.80 [m, 5H, Cy-*H* or CH_aH_bC(OAc)], 1.67-1.45 [m, 4H, CyH or CH_aH_bC(OAc)], and 1.32 [d, *J* = 6.2 Hz, 3H, CH(OAc)CH₃].

¹³C NMR (CDCl₃, 125 MHz): δ 170.9, 146.4, 128.6, 127.0, 126.4, 71.4, 68.8, 43.5, 42.7, 39.1, 38.9, 31.3, 31.2, 22.0, and 21.8.

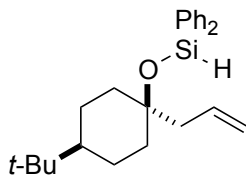
TLC: R_f = 0.3 in 3:1 hexanes: EtOAc.

GC-MS (5032021): t_R = 12.65 min, m/z 259 [(M-OH)⁺, 100], 198 (10), 156 (10) and 128 (10).

IR (neat): 3453 (b), 2930 (m), 1731 (s), 1493 (m), 1371 (s), 1242 (s), 1024 (m), 756 (m), and 698 (s) cm⁻¹.

HRMS (ESI/TOF): Calcd for (C₁₇H₂₅O)⁺: 277.1798. Found: 277.1791.

[{1-Allyl-4-(*tert*-butyl)cyclohexyl}oxy]diphenylsilane (1-1-6)



1-1-6

Physical Appearance: Colorless clear liquid.

¹H NMR (CDCl₃, 500 MHz): δ 7.63 [dd, *J* = 7.8, 1.5 Hz, 4H, Si{C₆(*H*_{ortho})₂H₃}₂], 7.42-7.34 [m, 6H, Si{C₆(*H*_{ortho})₂(*H*_{meta})₂*H*_{para}}₂], 5.79 [dddd, *J* = 17.1, 10.2, 7.1, 7.1 Hz, 1H, CH₂=CH], 5.60 (s, 1H, SiH), 4.99 [dddd, *J* = 10.2, 2.2, 1.2, 1.2 Hz, 1H, CH_{trans}H_{cis}=CH], 4.95 [dddd, *J* = 17.1, 2.2, 1.2, 1.2 Hz, 1H, CH_{trans}H_{cis}=CH], 2.32 [dddd, *J* = 15.9, 7.3, 1.2, 1.2 Hz, 1H, CH_aH_bCH=CH₂], 2.28 [dddd, *J* = 15.9, 7.3, 1.2, 1.2 Hz, 1H, CH_aH_bCH=CH₂], 1.82 [dddd, *J* = 13.8, 3.1, 3.1, 3.1 Hz, 2H, H₂_{eq} and H₆_{eq}], 1.49 (m, 2H, H₃_{eq} and H₅_{eq}), 1.42 [ddd, *J* = 13.1, 11.8, 3.3 Hz, 2H, H₂_{ax} and H₆_{ax}], 1.32 [dddd, *J* = 13.1, 11.8, 11.8, 4.3 Hz, 2H, H₃_{ax} and H₅_{ax}], 0.97 [dddd, *J* = 11.8, 11.8, 3.3, 3.3 Hz, 1H, ^tBuCH], and 0.79 [s, 9H, C(CH₃)₃].

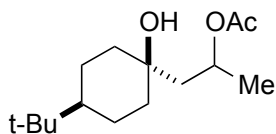
NMR (CDCl₃, 125 MHz): δ 136.4, 134.8, 134.6, 130.1, 128.0, 117.8, 76.3, 48.5, 47.8, 37.3, 32.6, 27.7, 22.5.

GC-MS (5029017): t_R = 14.8 min, m/z 377 [(M-H)⁺, 100], 337 [(M-allyl)⁺, 20] and 301 (20).

IR (neat): 2940 (s), 2119 (w), 1738 (w), 1428 (m), 1111 (m), 814 (s), and 696 (s) cm^{-1} .

HRMS (ESI/TOF): Calcd for $(\text{C}_{25}\text{H}_{35}\text{OSi})^+$: 379.2452. Found: 379.2445.

1-[4-(*tert*-Butyl)-1-hydroxycyclohexyl]propan-2-yl acetate (1-6-6)



1-6-6

Physical Appearance: Colorless clear liquid.

Purified by MPLC (hexanes/EtOAc = 3.5:1, 8 mL/min).

^1H NMR (CDCl_3 , 500 MHz): δ 5.24 [dq, $J = 8.6, 6.1, 3.3$ Hz, 1H, $\text{CH}_2\text{CH}(\text{OAc})\text{CH}_3$], 2.02 [s, 3H, $\text{CH}(\text{O}_2\text{CCH}_3)$], 1.85 (br s, 1H, CyOH), 1.82 [dd, $J = 14.9, 8.6$ Hz, 1H, Cy(OH) CH_aH_b], 1.68 (nfom, 2H, Cy-H), 1.59-1.53 (m, 2H, Cy-H), 1.55 [dd, $J = 14.9, 3.4$ Hz, 1H, Cy(OH) CH_aH_b], 1.37-1.26 (m, 4H, Cy-H), 1.24 [d, $J = 6.2$ Hz, 3H, $\text{CH}_2\text{CH}(\text{OAc})\text{CH}_3$], 0.94-0.88 (m, 1H, $^t\text{BuCH}$), and 0.84 [s, 9H, $\text{CyC}(\text{CH}_3)_3$].

^{13}C NMR (CDCl_3 , 125 MHz): δ 170.8, 69.9, 68.3, 49.6, 47.8, 38.2, 37.8, 32.5, 27.6, 22.4, 22.3, 21.9 and 21.6.

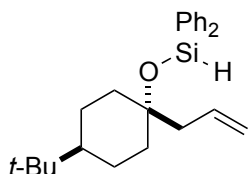
TLC: $R_f = 0.5$ in 3.5:1 hexanes: EtOAc.

GC-MS (5032021): $t_R = 10.51$ min, m/z 239 [$(\text{M}-\text{OH})^+$, 100], 180 (10), 164(5) and 138 (5).

IR (neat): 3482 (b), 2939 (s), 1735 (s), 1367 (s), 1242 (s), 1040 (m), and 950 (w) cm^{-1} .

HRMS (ESI/TOF): Calcd for $(\text{C}_{15}\text{H}_{29}\text{O}_3)^+$: 257.2111. Found: 257.2105.

[[1-Allyl-4-(*tert*-butyl)cyclohexyl]oxy]diphenylsilane (1-1-7)



1-1-7

Physical Appearance: Colorless clear liquid.

¹H NMR (CDCl₃, 500 MHz): δ 7.61 [dd, *J* = 7.8, 1.5 Hz, 4H, Si{C₆(H_{ortho})₂H₃}₂], 7.42-7.34 [m, 6H, Si{C₆(H_{ortho})₂(H_{meta})₂H_{para}}₂], 5.99 (dddd, *J* = 17.2, 10.2, 7.1, 7.1 Hz, 1H, CH₂=CH), 5.60 (s, 1H, SiH), 5.08 (dddd, *J* = 10.3, 2.4, 1.4, 1.4 Hz, 1H, CH_{trans}H_{cis}=CH), 5.05 (dddd, *J* = 17.0, 2.4, 1.4, 1.4 Hz, 1H, CH_{trans}H_{cis}=CH), 2.40 (dd, *J* = 16, 7.1 Hz, 1H, CH_aH_bCH=CH₂), 2.38 (dd, *J* = 16, 7.1 Hz, 1H, CH_aH_bCH=CH₂), 1.92 (dddd, *J* = 12.2, 3.3, 3.3, 3.3 Hz, 2H, H3_{eq} and H5_{eq}), 1.62 (m, 2H, H2_{eq} and H6_{eq}), 1.55 (ddd, *J* = 12.8, 12.8, 3.3 Hz, 2H, H2_{ax} and H6_{ax}), 1.07 (dddd, *J* = 12.8, 12.8, 12.2, 3.3 Hz, 2H, H3_{ax} and H5_{ax}), 0.98 (dddd, *J* = 12.2, 12.2, 3.3, 3.3 Hz, 1H, ^tBuCH), and 0.83 [s, 9H, C(CH₃)₃].

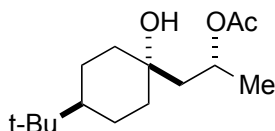
¹³C NMR (CDCl₃, 125 MHz): δ 136.5, 134.8, 134.7, 130.1, 128.0, 117.4, 77.4, 47.4, 41.5, 38.7, 32.4, 27.8 and 24.6.

GC-MS (5029017): t_R = 14.8 min, m/z 377 [(M-H)⁺, 100], 337 [(M-allyl)⁺, 20] and 301 (20).

IR (neat): 2940 (m), 2122 (m), 1738 (w), 1428 (m), 1352 (w), 1113 (s), 1058 (s), 843 (s), 731 (s) and 696 (s) cm⁻¹.

HRMS (ESI/TOF): Calcd for (C₂₅H₃₅OSi)⁺: 379.2452. Found: 379.2443.

1-[1-Hydroxy-4-(*tert*-butyl)cyclohexyl]propan-2-yl acetate (1-6-7)



1-6-7

Physical Appearance: White fluffy solid.

Purified by MPLC (hexanes/EtOAc = 3:1, 8 mL/min).

¹H NMR (CDCl₃, 500 MHz): δ 5.24 [dq, *J* = 8.6, 6.2, 3.6 Hz, 1H, CH₂CH(OAc)CH₃], 2.16 (br s, 1H, CyOH), 2.03 [s, 3H, CH(O₂CCH₃)], 1.88 [dd, *J* = 15.1, 8.6 Hz, 1H, Cy(OH)CH_aH_b], 1.79-1.65 [m, 5H, Cy-H and Cy(OH)CH_aH_b], 1.37 (dddd, *J* = 12.9, 12.9, 12.9, 3.7 Hz, 2H, H3_{ax} and H5_{ax}), 1.28 [d, *J* = 6.2 Hz, 3H, CH₂CH(OAc)CH₃], 1.15-0.94 (m, 3H, Cy-H and ^tBuCH), and 0.84 (s, 9H, CyC(CH₃)₃).

¹³C NMR (CDCl₃, 125 MHz): δ 170.7, 71.6, 68.7, 47.5, 42.1, 39.1, 39.1, 32.3, 27.7, 24.6, 24.4, 21.8 and 21.6.

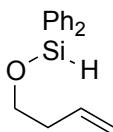
TLC: R_f = 0.3 in 3:1 hexanes: EtOAc.

GC-MS (5032021): $t_R = 10.51$ min, m/z 239 [(M-OH)⁺, 100], 180 (10), 164(5) and 138 (5)

IR (neat): 3454 (b), 2939 (s), 1735 (s), 1366 (m), 1243 (m), 1129 (m), and 950 (s) cm⁻¹.

HRMS (ESI/TOF): Calcd for (C₁₅H₂₉O₃)⁺: 257.2111. Found: 257.2119.

(But-3-en-1-yloxy)diphenylsilane (1-1-8)



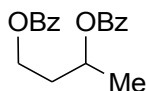
1-1-8

1h was not stable on SiO₂ column chromatography (flash or MPLC). The crude **1h** (ca. 95% ¹H NMR yield) was directly used for the hydrosilylation.

Physical Appearance: Colorless clear liquid.

GC-MS (5029017): $t_R = 10.97$ min, m/z 253 [(M-H)⁺, 100], 180 (20) and 154 (5).

Butane-1,3-diyl dibenzoate (1-2-8)



1-2-8

Physical Appearance: Colorless clear liquid.

Purified by MPLC (hexanes/EtOAc = 10:1, 8 mL/min).

¹H NMR (CDCl₃, 500 MHz): δ 8.04 [dd, $J = 8.0, 1.4$ Hz, 2H, Ph-*H*_{ortho}], 8.01 [dd, $J = 8.0, 1.4$ Hz, 2H, Ph-*H*_{ortho}], 7.54 [dddd, $J = 7.2, 7.2, 1.4, 1.4$ Hz, 1H, Ph-*H*_{para}], 7.53 [dddd, $J = 7.2, 7.2, 1.4, 1.4$ Hz, 1H, Ph-*H*_{para}], 7.41 [dddd, $J = 8.0, 7.2, 1.4, 1.4$ Hz, 2H, Ph-*H*_{meta}], 7.40 [dddd, $J = 8.0, 7.2, 1.4, 1.4$ Hz, 2H, Ph-*H*_{meta}], 5.40 [dq, $J = 8.0, 6.3, 4.6$ Hz, 1H, CH₂CH(OBz)CH₃], 4.50 [ddd, $J = 11.2, 6.1, 6.1$ Hz, 1H, (BzO)CH_aH_b], 4.43 [ddd, $J = 11.2, 7.6, 5.7$ Hz, 1H, (BzO)CH_aH_b], 2.23 [dddd, $J = 14.2, 8.0, 6.1, 5.7$ Hz, 1H, (BzO)CH₂CH_aCH_b], 2.15 [dddd, $J = 14.2, 7.6, 6.1, 4.6$ Hz, 1H, (BzO)CH₂CH_aCH_b], and 1.45 [d, $J = 6.3$ Hz, 3H, CH₂CH(OBz)CH₃],

¹³C NMR (CDCl₃, 125 MHz): δ 166.6, 166.2, 133.1, 133.0, 130.6, 130.2, 129.8, 129.7, 128.4 (2), 68.9, 61.6, 35.2 and 20.4.

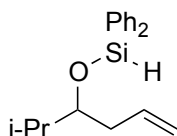
TLC: $R_f = 0.5$ in 10:1 hexanes: EtOAc.

GC-MS (5032021): $t_R = 14.14$ min, m/z 299 [(M-H)⁺, 100], 177 [(M-OBz)⁺, 100], and 105 (5).

IR (neat): 2977 (w), 1711 (s), 1450 (m), 1263 (s), 1095 (s), 1068 (s), 1025 (s), and 705 (s) cm^{-1} .

HRMS (ESI/TOF): Calcd for (C₁₈H₁₉O₄)⁺: 299.1278. Found: 299.1289.

(2-Methylhex-5-en-3-yloxy)diphenylsilane (1-1-9)



1-1-9

Physical Appearance: Colorless clear liquid.

¹H NMR (CDCl₃, 500 MHz): δ 7.67-7.65 [nfom, 4H, Si{C₆(H_{ortho})₂H₄}₂], 7.46-7.38 [m, 6H, Si{C₆H₂(H_{meta})₂H_{para}}₂], 5.81 (dddd, $J = 17.2, 10.1, 7.1, 7.1$ Hz, 1H, CH₂=CH), 5.49 (s, 1H, SiH), 5.05 (dddd, $J = 17.2, 2.2, 1.2, 1.2$ Hz, 1H, CH_{trans}H_{cis}=CH), 5.01 (dddd, $J = 10.2, 2.2, 1.2, 1.2$ Hz, 1H, CH_{trans}H_{cis}=CH), 3.67 (ddd, $J = 6.6, 5.1, 5.1$ Hz, 1H, SiOCHCH₂), 2.32 (dddd, $J = 14.2, 6.6, 6.6, 1.2, 1.2$ Hz, 1H, CH_aH_bCH=CH₂), 2.28 (dddd, $J = 14.2, 6.8, 5.1, 1.2, 1.2$ Hz, 1H, CH_aH_bCH=CH₂), 1.80 [qqd, $J = 6.8, 6.8, 5.1$ Hz, 1H, SiOCHCH(Me)₂], 0.93 (d, $J = 6.8$ Hz, 3H, CH₃), and 0.91 (d, $J = 6.8$ Hz, 3H, CH₃).

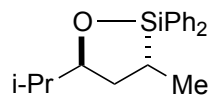
¹³C NMR (CDCl₃, 125 MHz): δ 135.7, 135.00, 134.96, 130.4, 128.1, 117.0, 79.3, 38.7, 33.0, 19.1, and 17.5.

GC-MS (5029017): $t_R = 11.727$ min, m/z 295 [(M-H)⁺, 100], and 219 (40).

IR (neat): 3069 (w), 2125 (m), 1640 (w), 1590 (w), 1467 (m), 812 (s), and 695 (s) cm^{-1} .

HRMS (ESI/TOF): Calcd for (C₁₉H₂₅OSi)⁺: 297.1669. Found: 297.1660.

Trans-5-Isopropyl-3-methyl-2,2-diphenyl-1,2-oxasilolane (trans-1-2-9)



trans 1-2-9

Physical Appearance: Colorless clear liquid.

¹H NMR (CDCl₃, 500 MHz): δ 7.66-7.61 [m, 4H, Si{C₆(H_{ortho})₂H₃}₂], 7.44-7.38 [m, 6H, Si{C₆H₂(H_{meta})₂H_{para}}₂], 3.99 (ddd, *J* = 7.9, 7.3, 5.0 Hz, 1H, SiOCH), 2.01 (ddd, *J* = 13.2, 7.9, 7.4 Hz, 1H, CH_aH_bCHMeSiPh₂), 1.78 (ddd, *J* = 13.2, 5.0, 5.0 Hz, 1H, CH_aH_bCHMeSiPh₂), 1.72 (qqd, *J* = 7.3, 6.6, 6.6 Hz, 1H, CHMe₂), 1.74 (qdd, *J* = 7.6, 7.4, 5.0 Hz, 1H, SiCHMe), 1.04 [d, *J* = 6.6 Hz, 3H, (CH₃)₂CH], and 1.01 (d, *J* = 7.6 Hz, 3H, SiCHCH₃), and 0.91 [d, *J* = 6.6 Hz, 3H, (CH₃)₂CH].

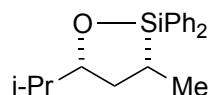
¹³C NMR (CDCl₃, 125 MHz): δ 135.7, 135.1, 134.6, 133.7, 130.14, 130.06, 128.1, 127.9, 82.9, 38.2, 34.6, 19.5, 18.7, 17.1, and 15.8.

GC-MS (5029017): t_R = 13.062 min, m/z 253 [(M-iPr)⁺, 100], 199 (45), and 175 (70).

IR (neat): 3068 (w), 2925 (m), 1453 (m), 1117 (m), 697 (s), and 499 (s) cm⁻¹.

HRMS (ESI/TOF): Calcd for (C₁₉H₂₄NaOSi)⁺: 319.1489. Found: 319.1473.

Cis-5-Isopropyl-3-methyl-2,2-diphenyl-1,2-oxasilolane (cis-1-2-9)



cis 1-2-9

Physical Appearance: Colorless clear liquid.

Purified by MPLC (hexanes/EtOAc = 10:1, 8 mL/min).

¹H NMR (CDCl₃, 500 MHz): δ 7.64 [dd, *J* = 7.8 Hz, 1.4 Hz, 2H, Si{C₆(H_{ortho})₂H₃}], δ 7.57 [dd, *J* = 7.8 Hz, 1.4 Hz, 2H, Si{C₆H₂(H_{meta})₂H_{para}}₂], 7.45-7.36 [m, 6H, Si{C₆(H_{ortho})₂H₃}₂], 3.75 (ddd, *J* = 10.8, 6.8, 3.8 Hz, 1H, SiOCH), 2.22 (ddd, *J* = 12.7, 7.3, 3.8 Hz, 1H, CH_aH_bCHMeSi), 1.85 (qqd, *J* = 6.8, 6.8, 6.8 Hz, 1H, CHMe₂), 1.72 (dq, *J* = 12.7, 7.3, 7.3 Hz, 1H, SiCHMe), 1.36 (ddd, *J* = 12.7, 12.7, 10.8 Hz, 1H, CH_aH_bCHMeSi), 1.08 (d, *J* = 7.3 Hz, 3H, SiCHCH₃), 1.07 [d, *J* = 6.8 Hz, 3H, (CH₃)₂CH], and 0.96 [d, *J* = 6.8 Hz, 3H, (CH₃)₂CH].

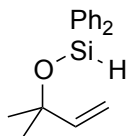
^{13}C NMR (CDCl_3 , 125 MHz): δ 135.4, 135.2, 134.8, 133.7, 130.3, 130.07, 128.1, 127.9, 83.7, 39.2, 35.1, 19.7, 19.6, 18.5, and 14.8.

GC-MS (5032021): $t_{\text{R}} = 13.270$ min, m/z 253 [$(\text{M}-i\text{Pr})^+$, 100] and 175 (90).

IR (neat): 3068 (w), 2925 (m), 1453 (m), 1117 (m), 697 (s), and 499 (s) cm^{-1} .

HRMS (ESI/TOF): Calcd for $(\text{C}_{19}\text{H}_{24}\text{NaOSi})^+$: 319.1489. Found: 319.1473.

[(2-Methylbut-3-en-2-yl)oxy]diphenylsilane (1-1-10)



1-1-10

Physical Appearance: Colorless clear liquid.

^1H NMR (CDCl_3 , 500 MHz): δ 7.62 [dd, $J = 7.8, 1.4$ Hz, 4H, $\text{Si}\{\text{C}_6(\text{H}_{ortho})_2\text{H}_3\}_2$], 7.42-7.34 [m, 6H, $\text{Si}\{\text{C}_6(\text{H}_{ortho})_2(\text{H}_{meta})_2\text{H}_{para}\}_2$], 5.97 (dd, $J = 17.2, 10.6$ Hz, 1H, $\text{CH}_2=\text{CH}$), 5.53 (s, 1H, SiH), 5.20 (dd, $J = 17.2, 1.2$ Hz, 1H, $\text{CH}_{trans}\text{H}_{cis}=\text{CH}$), 4.97 (dd, $J = 10.6, 1.2$ Hz, 1H, $\text{CH}_{trans}\text{H}_{cis}=\text{CH}$), and 1.39 [s, 6H, $\text{OC}(\text{CH}_3)_2$].

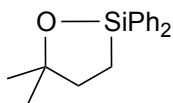
^{13}C NMR (CDCl_3 , 125 MHz): δ 145.7, 136.0, 134.8, 130.1, 128.0, 111.7, 75.4, and 29.8.

GC-MS (5029017): $t_{\text{R}} = 10.88$ min, m/z 267 [$(\text{M}-\text{H})^+$, 100], 253 [$(\text{M}-\text{CH}_3)^+$, 5] and 181 (5).

IR (neat): 2974 (w), 2123 (m), 1428 (m), 1111 (m), 1033 (s), 815 (s), 730 (s) and 696 (s) cm^{-1} .

HRMS (ESI/TOF): Calcd for $(\text{C}_{17}\text{H}_{20}\text{OSi})^+$: 269.1356. Found: 269.1356.

5,5-Dimethyl-2,2-diphenyl-1,2-oxasilolane (1-2-10)



1-2-10

Physical Appearance: Colorless clear liquid.

Purified by MPLC (hexanes/EtOAc = 40:1, 7 mL/min).

¹H NMR (CDCl₃, 500 MHz): δ 7.61 [dd, *J* = 7.9, 1.4 Hz, 4H, Si{C₆(*H*_{ortho})₂H₃}₂], 7.43-7.35 [m, 6H, Si{C₆(*H*_{ortho})₂(*H*_{meta})₂*H*_{para}}₂], 1.95 (t, *J* = 7.7 Hz, 2H, CH₂CH₂Si), 1.37 [s, 6H, OC(CH₃)₂] and 1.32 (t, *J* = 7.7 Hz, 2H, CH₂CH₂Si).

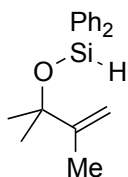
¹³C NMR (CDCl₃, 125 MHz): δ 135.6, 134.7, 130.2, 128.1, 80.9, 38.2, 30.0 and 10.1.

GC-MS (5032021): *t*_R = 11.50 min, *m/z* 267 [(M-H)⁺, 5], 253 [(M-CH₃)⁺, 100], 225 (10), 182 (100) and 152 (20).

IR (neat): 3069 (w), 2969 (m), 1738 (s), 1428 (s), 1117 (s), 819 (s), and 696 (s) cm⁻¹.

HRMS (ESI/TOF): Calcd for (C₁₇H₂₀OSi)⁺: 269.1356. Found: 269.1348.

[(2,3-Dimethylbut-3-en-2-yl)oxy]diphenylsilane (1-1-11)



1-1-11

Physical Appearance: Colorless clear liquid.

¹H NMR (CDCl₃, 500 MHz): δ 7.62 [dd, *J* = 7.8, 1.5 Hz, 4H, Si{C₆(*H*_{ortho})₂H₃}₂], 7.42-7.34 [m, 6H, Si{C₆(*H*_{ortho})₂(*H*_{meta})₂*H*_{para}}₂], 5.53 (s, 1H, SiH), 5.01 (qd, *J* = 1.5, 0.8 Hz, 1H, CH_{trans} H_{cis}=CH), 4.77 (dq, *J* = 1.5, 1.5 Hz, 1H, CH_{trans} H_{cis}=CH), and 1.80 [dd, *J* = 1.5, 0.8 Hz, 3H, C(CH₃)=CH₂], and 1.42 [s, 6H, OC(CH₃)₂].

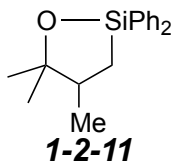
¹³C NMR (CDCl₃, 125 MHz): δ 151.1, 136.1, 134.7, 130.1, 128.0, 109.5, 77.4, 29.4 and 19.3

GC-MS (5029017): *t*_R = 11.40 min, *m/z* 281 [(M-H)⁺100], 239 (5) and 205 (70).

IR (neat): 2974 (w), 2127 (m), 1738 (w), 1428 (m), 1149 (s), 815 (s), 696 (s) and 458 (s) cm⁻¹.

HRMS (ESI/TOF): Calcd for (C₁₈H₂₃OSi)⁺: 283.1513. Found: 283.1520.

4,5-Trimethyl-2,2-diphenyl-1,2-oxasilolane (1-2-11)



Physical Appearance: Colorless clear liquid.

Purified by MPLC (hexanes/EtOAc = 40:1, 7 mL/min).

¹H NMR (CDCl₃, 500 MHz): δ 7.62 [dd, *J* = 7.9, 1.4 Hz, 2H, Si{C₆(H_{ortho})₂H₃}], 7.59 [dd, *J* = 7.9, 1.4 Hz, 2H, Si{C₆(H_{ortho})₂H₃}], 7.43-7.35 [m, 6H, Si{C₆(H_{ortho})₂(H_{meta})₂H_{para}}₂], 2.12 [dq, *J* = 12.6, 6.7, 6.4 Hz, 1H, CH₃CHCH₂Si], 2.0 (unidentifiable impurities), 1.42 [s, 3H, OC(CH₃)(CH₃)], 1.37 (dd, *J* = 14.8, 6.4 Hz, 1H, H_aH_bCSi), 1.15 [s, 3H, OC(CH₃)(CH₃)], 1.09 (dd, *J* = 14.8, 12.6 Hz, 1H, H_aH_bCSi), and 1.08 (d, *J* = 6.7 Hz, 3H, CH₃CCH₂Si).

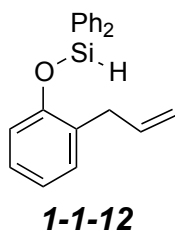
¹³C NMR (CDCl₃, 125 MHz): δ 135.6, 135.0, 134.8, 134.7, 130.2, 130.1, 130.1, 128.0, 83.0, 43.5, 29.5, 28.9, 23.8, and 19.0.

GC-MS (5032021): t_R = 11.93 min, m/z 281 [(M-H)⁺, 5], 267 [(M-CH₃)⁺, 100], 225 (5) and 152 (5).

IR (neat): 2929 (m), 1738 (w), 1428 (m), 1110 (s), 958 (s), 911 (s), 731 (s), 695 (s), 524 (s), and 472 (s) cm⁻¹.

HRMS (ESI/TOF): Calcd for (C₁₈H₂₃O₂Si)⁺: 283.1513. Found: 283.1521.

(2-Allylphenoxy)diphenylsilane (1-1-12)



Physical Appearance: Colorless clear liquid.

¹H NMR (CDCl₃, 500 MHz): δ 7.70 [d, *J* = 8.0 Hz, 4H, Si{C₆(H_{ortho})₂H₃}₂], 7.48 [app t, *J* = 7.3 Hz, 2H, SiPhH], 7.42 [app t, *J* = 7.2 Hz, 4H, SiPhH], 7.17 (dd, *J* = 7.5, 1.7 Hz, 1H, H3 or H6), 7.05 (ddd, *J* = 7.7, 7.7, 1.7 Hz, 1H, H4 or H5), 6.93 (ddd, *J* = 7.4, 7.4, 1.2 Hz, 1H, H4 or H5), 6.87 (dd, *J* = 8.0, 1.2 Hz, 1H, H3 or H6), 5.98 (dddd, *J* = 16.8, 10.7, 6.6, 6.6 Hz, 1H, CH₂=CH), 5.77 (s, 1H, SiH), 5.044 (dddd, *J* =

10.6, 1.5, 1.5 Hz, 1H, $\text{CH}_{\text{trans}}\text{H}_{\text{cis}}=\text{CH}$), 5.036 (dddd, $J = 16.8, 1.6, 1.6$ Hz, 1H, $\text{CH}_{\text{trans}}\text{H}_{\text{cis}}=\text{CH}$), and 3.45 (dt, $J = 6.6, 1.5$ Hz, 2H, $\text{ArCH}_2\text{CH}=\text{CH}_2$).

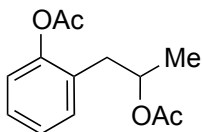
^{13}C NMR (CDCl_3 , 125 MHz): δ 153.4, 137.0, 134.9, 133.3, 130.9, 130.7, 130.4, 128.4, 127.5, 122.1, 118.2, 115.9, and 34.8.

GC-MS (5029017): $t_{\text{R}} = 13.58$ min, m/z 316 [M^+ , 100], 287 (10) and 238 (10).

IR (neat): 3069 (w), 2135 (m), 1489 (m), 1428 (m), 1245 (s), 1113 (s), 918 (s), 813 (s), 731 (s), 695 (s) and 495 (s) cm^{-1} .

HRMS (ESI/TOF): Calcd for $(\text{C}_{21}\text{H}_{21}\text{OSi})^+$: 317.1356. Found: 317.1348.

1-(2-Acetoxyphenyl)propan-2-yl acetate (**1-6-12**)



1-6-12

Physical Appearance: Colorless clear liquid.

Purified by MPLC (hexanes/EtOAc = 10:1, 8 mL/min).

^1H NMR (CDCl_3 , 500 MHz): δ 7.27-7.23 (m, 2H, Ar-H), 7.17 (ddd, $J = 7.5, 7.5, 1.0$, 1H, H4 or H5), 7.04 (dd, $J = 7.5, 1.0$ Hz, 1H, H3 or H6), 5.09 [dq, $J = 7.3, 6.3, 6.3$ Hz, 1H, $\text{CH}(\text{OAc})\text{CH}_3$], 2.92 (dd, $J = 13.6, 6.3$ Hz, 1H, ArCH_aH_b), 2.62 (dd, $J = 13.6, 7.3$ Hz, 1H, ArCH_aH_b), 2.35 [s, 3H, ArO_2CCH_3], 2.0 (s, 3H, CHO_2CCH_3), and 1.19 [d, $J = 6.3$ Hz, 3H, $\text{CH}(\text{OAc})\text{CH}_3$].

^{13}C NMR (CDCl_3 , 125 MHz): δ 170.7, 169.8, 149.5, 131.7, 129.6, 128.0, 126.2, 122.7, 70.4, 36.9, 21.5, 21.2 and 19.6.

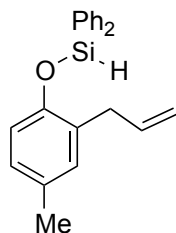
TLC: $R_f = 0.6$ in 10:1 hexanes: EtOAc.

GC-MS (5032021): $t_{\text{R}} = 9.72$ min, m/z 237 [$(\text{M}+\text{H})^+$, 100], 177 (100) and 134 (70).

IR (neat): 2982 (w), 1763 (s), 1732 (s), 1370 (m), 1241 (s), 1202 (s), 1172 (s) and 751 (s) cm^{-1} .

HRMS (ESI/TOF): Calcd for $(\text{C}_{21}\text{H}_{21}\text{O}_4)^+$: 237.1121. Found: 237.1123.

(2-Allyl-4-methylphenoxy)diphenylsilane (1-1-13)



1-1-13

Physical Appearance: Colorless clear liquid.

¹H NMR (CDCl₃, 500 MHz): δ 7.69 [app d, *J* = 6.6 Hz, 4H, Si{C₆(*H*_{ortho})₂H₃}₂], 7.47 [app t, *J* = 7.3 Hz, 2H, SiPhH], 7.41 [dddd, *J* = 7.2 Hz, 4H, SiPhH], 6.96 [d, *J* = 2.1 Hz, 1H, H3], 6.83 (dd, *J* = 8.1, 2.1 Hz, 1H, H5), 6.75 (d, *J* = 8.1 Hz, 1H, H6), 5.97 (dddd, *J* = 16.6, 10.1, 6.6, 6.6 Hz, 1H, CH₂=CH), 5.74 (s, 1H, SiH), 5.05-5.00 (m, 2H, CH_{trans}H_{cis}=CH), 3.41 (d, *J* = 6.6 Hz, 2H, ArCH₂CH=CH₂), and 2.25 [s, 3H, CH₃Ar].

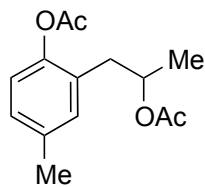
¹³C NMR (CDCl₃, 125 MHz): δ 151.1, 137.2, 134.9, 133.4, 131.3, 131.0, 130.8, 130.3, 128.3, 127.8, 118.0, 115.8, 34.8 and 20.8.

GC-MS (5032021): *t*_R = 14.03 min, *m/z* 330 [M⁺, 100], 301 (15) and 252(15).

IR (neat): 3069 (w), 2133 (m), 1498 (m), 1428 (m), 1254 (m), 1112 (s), 812 (s), 730 (s), 695 (s), and 473 cm⁻¹.

HRMS (ESI/TOF): Calcd for (C₂₂H₂₃OSi)⁺: 331.1513. Found: 331.1522.

1-(2-Acetoxy-5-methylphenyl)propan-2-yl acetate (1-6-13)



1-6-13

Physical Appearance: Colorless clear liquid..

Purified by MPLC (hexanes/EtOAc = 10:1, 8 mL/min).

¹H NMR (CDCl₃, 500 MHz): δ 7.06-7.03 [m, 2H, H3 and H5], 6.91[d, *J* = 8.0 Hz 1H, H6], 5.09 [dq, *J* =

7.5, 6.2, 6.2 Hz, 1H, $CH(OAc)CH_3$], 2.88 [dd, $J = 13.5, 6.0$ Hz, 1H, $ArCH_aH_b$], 2.57 [dd, $J = 13.5, 7.5$ Hz, 1H, $ArCH_aH_b$], 2.34 [s, 3H, $Ar(O_2CCH_3)$], 2.31 [s, 3H, $ArCH_3$], 2.0 [s, 3H, $CH(O_2CCH_3)$], and 1.18 [d, $J = 6.2$ Hz, 3H, $CH_2CH(OAc)CH_3$].

^{13}C NMR ($CDCl_3$, 125 MHz): δ 170.7, 170.0, 147.3, 135.8, 132.2, 129.2, 128.7, 122.4, 70.6, 36.9, 21.5, 21.2, 21.0, and 19.6.

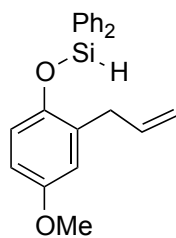
TLC: $R_f = 0.5$ in 10:1 hexanes: EtOAc.

GC-MS (5032021): $t_R = 11.19$ min, m/z 251 [(M+H) $^+$, 40], 191 [(M-OAc) $^+$, 70], and 148 (100).

IR (neat): 2936 (w), 1758 (s), 1732 (s), 1496 (m), 1369 (m), 1240 (s), 1053 (m), 806 (s), and 491 (s) cm^{-1} .

HRMS (ESI/TOF): Calcd for $(C_{14}H_{18}NaO_4)^+$: 273.1097. Found: 273.1120.

(2-Allyl-4-methoxyphenoxy)diphenylsilane (1-1-14)

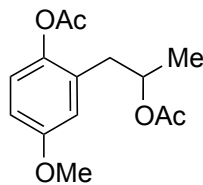


1n was not stable on SiO_2 column chromatography (flash or MPLC). The crude **1n** (ca. 95% 1H NMR yield) was directly used for the hydrosilylation.

Physical Appearance: Colorless clear liquid.

GC-MS (5029017): $t_R = 14.99$ min, m/z 346 [(M-H) $^+$, 100], 317 (10) and 269 (100).

1-(2-Acetoxy-5-methoxyphenyl)propan-2-yl acetate (1-6-14)



Physical Appearance: Pale yellow color liquid.

Purified by MPLC (hexanes/EtOAc = 10:1, 8 mL/min).

¹H NMR (CDCl₃, 500 MHz): δ 6.95 (d, *J* = 8.6 Hz 1H, H₆), 6.78 (dd, *J* = 8.6, 3.0 Hz, 1H, H₅), 6.75 [d, *J* = 3.0 Hz, 1H, H₃], 5.09 [dq, *J* = 7.3, 6.3, 6.3 Hz, 1H, CH₂CH(OAc)CH₃], 3.77 (s, 3H, H₃COAr), 2.87 [dd, *J* = 13.6, 6.3 Hz, 1H, C(OAc)CH_aH_b], 2.57 [dd, *J* = 13.6, 7.3 Hz, 1H, C(OAc)CH_aH_b], 2.33 (s, 3H, ArO₂CCH₃), 2.0 [s, 3H, CH(O₂CCH₃)], and 1.19 [d, *J* = 6.3 Hz, 3H, CH₂CH(OAc)CH₃].

¹³C NMR (CDCl₃, 125 MHz): δ 170.7, 170.2, 157.4, 143.1, 130.6, 123.3, 116.7, 112.9, 70.4, 55.7, 37.1, 21.5, 21.1 and 19.6.

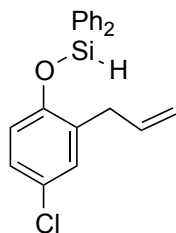
TLC: R_f = 0.5 in 10:1 hexanes: EtOAc.

GC-MS (5032021): t_R = 11.02 min, m/z 267 [(M+H)⁺, 20], 207 (40), 164 (100) and 149 (30).

IR (neat): 2937 (w), 1758 (s), 1731 (s), 1496 (m), 1369 (m), 1240 (s), 1192 (s), 1052 (m), 1032 (s), and 1011 (s) cm⁻¹.

HRMS (ESI/TOF): Calcd for (C₁₄H₁₉O₄)⁺: 251.1278. Found: 251.1260.

(2-Allyl-4-chlorophenoxy)diphenylsilane (**1-1-15**)



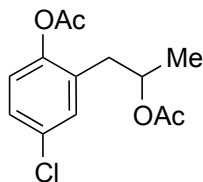
1-1-15

1o was not stable on SiO₂ column chromatography (flash or MPLC). The crude **1o** (ca. 95% ¹H NMR yield) was directly used for the hydrosilylation.

Physical Appearance: Colorless clear liquid.

GC-MS (5032021): t_R = 14.69 min, m/z 350 [M⁺, 60], 272 (50), 257 (70), 246 (60), 183 (60) and 105

1-(2-Acetoxy-5-chlorophenyl)propan-2-yl acetate (1-6-15)



1-6-15

Physical Appearance: Pale yellow color liquid.

Purified by MPLC (hexanes/EtOAc = 10:1, 8 mL/min).

¹H NMR (CDCl₃, 500 MHz): δ 7.227 [d, *J* = 2.5 Hz, 1H, H₃], 7.225 (dd, *J* = 9.2, 2.5 Hz, 1H, H₅), 7.00 [d, *J* = 9.2 Hz, 1H, H₆], 5.06 [dq, *J* = 7.0, 6.3, 6.3 Hz, 1H, CH₂CH(OAc)CH₃], 2.88 [dd, *J* = 13.6, 6.3 Hz, 1H, C(OAc)CH_aH_b], 2.59 [dd, *J* = 13.6, 7.0 Hz, 1H, C(OAc)CH_aH_b], 2.35 (s, 3H, ArO₂CCH₃), 2.00 [s, 3H, CH(O₂CCH₃)], and 1.19 [d, *J* = 6.3 Hz, 3H, CH₂CH(OAc)CH₃].

¹³C NMR (CDCl₃, 125 MHz): δ 170.7, 169.5, 148.0, 131.6, 131.5, 131.4, 128.1, 124.0, 70.0, 36.8, 21.5, 21.1, and 19.7.

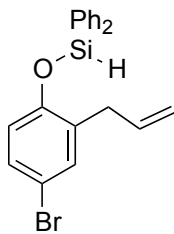
TLC: R_f = 0.5 in 10:1 hexanes: EtOAc.

GC-MS (5032021): t_R = 15.156 min, m/z 271 [(M+H)⁺, 60], 211 [(M-OAc)⁺, 60], 168 (100), 133 (20).

IR (neat): 2982 (w), 1762 (s), 1732 (s), 1482 (m), 1370 (s), 1238 (s), 1199 (s), 1165 (s), 1055 (m), 956 (m), and 825 (m) cm⁻¹.

HRMS (ESI/TOF): Calcd for (C₁₃H₁₅ClNaO₄)⁺: 293.0551. Found: 293.0570.

(2-Allyl-4-bromophenoxy)diphenylsilane (1-1-16)



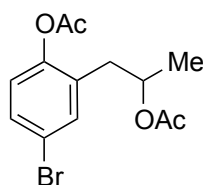
1-1-16

1p was not stable on SiO₂ column chromatography (flash or MPLC). The crude **1p** (ca. 95% ¹H NMR yield) was directly used for the hydrosilylation.

Physical Appearance: Colorless clear liquid.

GC-MS (5032021): *t_R* = 15.108 min, *m/z* 396 [(M+2)⁺, 100], 394 [M⁺, 98], 318 (40), 290 (25), 259 (30), 183 (70) and 105 (90).

1-(2-Acetoxy-5-bromophenyl)propan-2-yl acetate (1-6-16)



1-6-16

Physical Appearance: Pale yellow color liquid.

Purified by MPLC (hexanes/EtOAc = 10:1, 8 mL/min).

¹H NMR (CDCl₃, 500 MHz): δ 7.377 [d, *J* = 2.5 Hz, 1H, H₃], 7.366 (dd, *J* = 8.6, 2.4 Hz, 1H, H₅), 6.94 (d, *J* = 8.6 Hz, 1H, H₆), 5.06 [dq, *J* = 7.0, 6.3, 6.3 Hz, 1H, CH₂CH(OAc)CH₃], 2.88 [dd, *J* = 13.6, 6.3 Hz, 1H, C(OAc)CH_aH_b], 2.59 [dd, *J* = 13.6, 7.0 Hz, 1H, C(OAc)CH_aH_b], 2.35 (s, 3H, ArO₂CCH₃), 2.00 [s, 3H, CHC(O₂CCH₃)], and 1.19 [d, *J* = 6.3 Hz, 3H, CH₂CH(OAc)CH₃].

¹³C NMR (CDCl₃, 125 MHz): δ 170.6, 169.4, 148.5, 134.4, 132.0, 131.0, 124.5, 119.1, 70.1, 36.7, 21.4, 21.1, and 19.6.

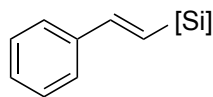
TLC: R_f = 0.4 in 10:1 hexanes: EtOAc.

GC-MS (5032021): *t_R* = 15.156 min, *m/z* 317 [{(M+2)+H}⁺, 70], 315 [(M+H)⁺, 70], 255 [(M-OAc)⁺, 50], 214/215 (100) and 133 (70)

IR (neat): 3982 (w), 1762 (s), 1734 (s), 1481 (m), 1370 (m), 1241 (s), 1201 (s), 1167 (s), 1122 (m), 1057 (m) and 1012 (m) cm⁻¹.

HRMS (ESI/TOF): Calcd for (C₁₃H₁₆BrO₄)⁺: 315.0226. Found: 315.0210.

(E)-1,1,1,3,5,5,5-Heptamethyl-3-styryltrisiloxane (2-3-1)



2-3-1

Physical Appearance: Colorless clear liquid.

Yield: 45.4 mg, 70%.

¹H NMR (CDCl₃, 500 MHz): δ 7.45 (d, *J* = 7.6 Hz, 2H, Ar-*H*), 7.34 (dd, *J* = 7.6, 7.3 Hz, 2H, Ar-*H*), 7.27 (dd, *J* = 7.3, 7.3 Hz, 1H, Ar-*H*), 6.96 (d, *J* = 19.2 Hz, 1H, ArCH=CH), 6.27 (d, *J* = 19.2 Hz, 1H, ArCH=CH), 0.19 [s, 3H, CH₃Si(OTMS)₂], and 0.13 [s, 18H, MeSi{OSi(CH₃)₃}₂].

¹³C NMR (CDCl₃, 125 MHz): δ 145.2, 138.4, 128.7, 128.5, 126.86, 126.80, 2.1, and 0.2.

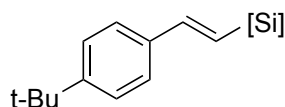
TLC: R_f = 0.6 in hexanes.

GC-MS (5029017): *t*_R = 9.26 min, *m/z* 324 [M⁺, 10], 309 [(M-CH₃)⁺, 80], 221 (100), and 73 (80).

IR (neat): 2957 (m), 1606 (w), 1574 (w), 1250 (s), 1036 (s), 990 (s), 835 (s), 751(s), and 687 (s) cm⁻¹.

HRMS (ESI/TOF): Calcd for (M+Na)⁺ (C₁₅H₂₈NaO₂Si₃)⁺: 347.1289. Found: 347.1273.

(E)-3-[4-(*tert*-Butyl)styryl]-1,1,1,3,5,5,5-heptamethyltrisiloxane (2-3-2)



2-3-2

Physical Appearance: Colorless clear liquid.

Yield: 60.1 mg, 79%; 2.00 g, 75% [7 mmol (1.12 g) scale]

¹H NMR (CDCl₃, 500 MHz): δ 7.37 (nfom, 2H, Ar-*H*), 7.36 (nfom, 2H, Ar-*H*), 6.94 (d, *J* = 19.2 Hz, 1H, ArCH=CH), 6.22 (d, *J* = 19.2 Hz, 1H, ArCH=CH), 1.32 (s, 9H, *t*-Bu), 0.17 [s, 3H, CH₃Si(OTMS)₂], and 0.13 [s, 18H, MeSi{OSi(CH₃)₃}₂].

¹³C NMR (CDCl₃, 125 MHz): δ 151.6, 145.0, 135.7, 126.5, 125.9, 125.7, 34.8, 31.5, 2.1, and 0.2.

TLC: R_f = 0.6 in hexanes.

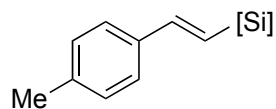
GC-MS (5029017): *t*_R = 10.98 min, *m/z* 381 [(M+H)⁺, 4], 366 [(M-CH₃)⁺, 15], 221 (100), 73 (90), and 57

(60).

IR (neat): 2957 (m), 1607 (w), 1512 (w), 1251 (s), 1037 (s), 988 (s), 836 (s), 752 (s), and 797(s) cm^{-1} .

HRMS (ESI/TOF): Calcd for $(\text{M}+\text{Na})^+$ ($\text{C}_{19}\text{H}_{36}\text{NaO}_2\text{Si}_3$) $^+$: 403.1915. Found: 403.1947.

(E)-1,1,1,3,5,5,5-Heptamethyl-3-(4-methylstyryl)trisiloxane (2-3-3)



2-3-3

Physical Appearance: Colorless clear liquid.

Yield: 47.3 mg, 70%.

^1H NMR (CDCl_3 , 500 MHz): δ 7.34 (app d, $J = 8.1$ Hz, 2H, Ar-*H*), 7.15 (app d, $J = 7.9$ Hz, 2H, Ar-*H*), 6.93 (d, $J = 19.2$ Hz, 1H, ArCH=CH), 6.20 (d, $J = 19.2$ Hz, 1H, ArCH=CH), 2.35 (s, 3H, Ar- CH_3), 0.17 [s, 3H, $\text{CH}_3\text{Si}(\text{OTMS})_2$], and 0.12 [s, 18H, $\text{MeSi}\{\text{OSi}(\text{CH}_3)_3\}_2$].

^{13}C NMR (CDCl_3 , 125 MHz): δ 145.1, 138.4, 135.7, 129.4, 126.7, 125.5, 21.5, 2.1, and 0.2.

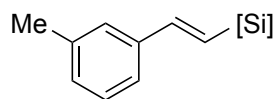
TLC: $R_f = 0.6$ in hexanes.

GC-MS (5029017): $t_R = 9.87$ min, m/z 338 [M^+ , 10], 323 [($\text{M}-\text{CH}_3$) $^+$, 80], 221 (100), 175 (40), and 73 (35).

IR (neat): 2957 (m), 1609 (w), 1510 (w), 1250 (s), 1035 (s), 988 (s), 836 (s), 783 (s), and 752(s) cm^{-1} .

HRMS (ESI/TOF): Calcd for $(\text{M}+\text{Na})^+$ ($\text{C}_{16}\text{H}_{30}\text{NaO}_2\text{Si}_3$) $^+$: 361.1446. Found: 361.1434.

(E)-1,1,1,3,5,5,5-Heptamethyl-3-(3-methylstyryl) trisiloxane (2-3-4)



2-3-4

Physical Appearance: Colorless clear liquid.

Yield: 55.5 mg, 82%.

^1H NMR (CDCl_3 , 500 MHz): δ 7.26-7.21 (m, 3H, Ar-*H*), 7.09 (d, $J = 6.9$ Hz, 1H, Ar-*H*), 6.94 (d, $J = 19.2$ Hz, 1H, ArCH=CH), 6.25 (d, $J = 19.2$ Hz, 1H, ArCH=CH), 2.36 (s, 3H, Ar- CH_3), 0.18 [s, 3H,

$\text{CH}_3\text{Si}(\text{OTMS})_2$], and 0.12 [s, 18H, $\text{MeSi}\{\text{OSi}(\text{CH}_3)_3\}_2$].

^{13}C NMR (CDCl_3 , 125 MHz): δ 145.3, 138.33, 138.29, 129.3, 128.6, 127.5, 126.6, 123.9, 21.6, 2.1, and 0.2.

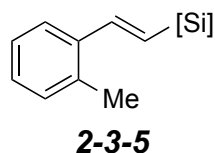
TLC: $R_f = 0.6$ in hexanes.

GC-MS (5029017): $t_R = 9.77$ min, m/z 338 [M^+ , 12], 323 [$(\text{M}-\text{CH}_3)^+$, 100], 221 (100), 175 (35), and 73 (40).

IR (neat): 2957 (m), 1609 (w), 1582 (w), 1250 (s), 1035 (s), 988 (s), 836 (s), 783 (s), and 753(s) cm^{-1} .

HRMS (ESI/TOF): Calcd for $(\text{M}+\text{Na})^+$ ($\text{C}_{16}\text{H}_{30}\text{NaO}_2\text{Si}_3$) $^+$: 361.1446. Found: 361.1464.

(E)-1,1,1,3,5,5,5-Heptamethyl-3-(2-methylstyryl)trisiloxane (2-3-5)



Physical Appearance: Colorless clear liquid.

Yield: 44 mg, 65%.

^1H NMR (CDCl_3 , 500 MHz): δ 7.54-7.50 (m, 1H, Ar-*H*), 7.20 (d, $J = 19.0$ Hz, 1H, ArCH=CH), 7.21-7.14 (m, 3H, Ar-*H*), 6.18 (d, $J = 19.0$ Hz, 1H, ArCH=CH), 2.42 (s, 3H, Ar- CH_3), 0.19 [s, 3H, $\text{CH}_3\text{Si}(\text{OTMS})_2$], and 0.14 [s, 18H, $\text{MeSi}\{\text{OSi}(\text{CH}_3)_3\}_2$].

^{13}C NMR (CDCl_3 , 125 MHz): δ 142.9, 137.7, 135.8, 130.5, 128.6, 128.2, 126.3, 125.6, 19.9, 2.1, and 0.4.

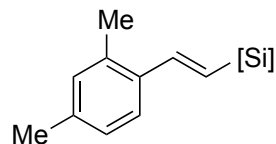
TLC: $R_f = 0.6$ in hexanes.

GC-MS (5029017): $t_R = 9.71$ min, m/z 323 [$(\text{M}-\text{CH}_3)^+$, 65], 221 (100), 175 (35) and 73 (40).

IR (neat): 2957 (m), 1609 (w), 1582 (w), 1250 (s), 1035 (s), 988 (s), 836 (s), 783 (s), and 753(s) cm^{-1} .

HRMS (ESI/TOF): Calcd for $(\text{M}+\text{Na})^+$ ($\text{C}_{16}\text{H}_{30}\text{NaO}_2\text{Si}_3$) $^+$: 361.1446. Found: 361.1420.

(E)-3-(2,4-Dimethylstyryl)-1,1,1,3,5,5,5-heptamethyltrisiloxane (2-3-6)



2-3-6

Physical Appearance: Colorless clear liquid.

Yield: 49.3 mg, 70%.

¹H NMR (CDCl₃, 500 MHz): δ 7.43 (d, *J* = 7.9 Hz, 1H, Ar-*H*), 7.21 (d, *J* = 19.1 Hz, 1H, ArCH=CH), 7.01 (d, *J* = 7.9 Hz, 1H, Ar-*H*), 6.97 (s, 1H, Ar-*H*), 6.13 (d, *J* = 19.1 Hz, 1H, ArCH=CH), 2.36 (s, 3H, ArCH₃), 2.31 (s, 3H, ArCH₃), 0.18 [s, 3H, CH₃Si(OTMS)₂], and 0.13 [s, 18H, MeSi{OSi(CH₃)₃}₂].

¹³C NMR (CDCl₃, 125 MHz): δ 142.7, 138.0, 135.7, 134.8, 131.3, 127.3, 127.1, 125.5, 21.3, 19.8, 2.1, and 0.4.

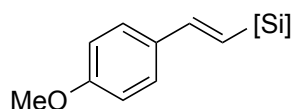
TLC: R_f = 0.7 in hexanes.

GC-MS (5029017): *t*_R = 10.27 min, *m/z* 353 [(M+H)⁺, 16], 338 [(M-CH₃)⁺, 100], 221 (100), 189 (35), and 73 (40).

IR (neat): 2957 (m), 1600 (w), 1479 (w), 1250 (s), 1035 (s), 900 (s), 835 (s), 783 (s), and 749(s) cm⁻¹.

HRMS (ESI/TOF): Calcd for (M+Na)⁺ (C₁₇H₃₂NaO₂Si₃)⁺: 375.1602. Found: 375.1660.

(*E*)-3-(4-Methoxystyryl)-1,1,1,3,5,5,5-heptamethyltrisiloxane (2-3-7)



2-3-7

Physical Appearance: Colorless clear liquid.

Yield: 56.7 mg, 80%.

¹H NMR (CDCl₃, 500 MHz): δ 7.39 (app d, *J* = 8.7 Hz, 2H, Ar-*H*), 6.90 (d, *J* = 19.2 Hz, 1H, ArCH=CH), 6.87 (app d, *J* = 8.7 Hz, 2H, Ar-*H*), 6.10 (d, *J* = 19.2 Hz, 1H, ArCH=CH), 3.82 (s, 3H, Ar-OCH₃), 0.17 [s, 3H, CH₃Si(OTMS)₂], and 0.13 [s, 18H, MeSi{OSi(CH₃)₃}₂].

¹³C NMR (CDCl₃, 125 MHz): δ 160.0, 144.6, 131.3, 128.1, 124.1, 114.1, 55.5, 2.1, and 0.3.

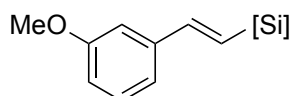
TLC: R_f = 0.3 in hexanes:EtOAc = 100:1.

GC-MS (5029017): $t_R = 10.74$ min, m/z 355 [(M+H)⁺, 80], 340 [(M-CH₃)⁺, 100], 265 (20), 221 (30), and 73 (50).

IR (neat): 2956 (m), 1606 (m), 1509 (s), 1248 (s), 1170 (m), 1032 (s), 988 (s), 835 (s), 793 (s), and 752 (s) cm⁻¹.

HRMS (ESI/TOF): Calcd for (M+Na)⁺ (C₁₆H₃₀NaO₃Si₃)⁺: 377.1395. Found: 377.1441.

(E)-3-(3-Methoxystyryl)-1,1,1,3,5,5,5-heptamethyltrisiloxane (2-3-8)



2-3-8

Physical Appearance: Colorless clear liquid.

Yield: 53 mg, 75%.

¹H NMR (CDCl₃, 500 MHz): δ 7.25 (dd, $J = 8.1, 7.7$ Hz, 1H, Ar-*H*), 7.04 (ddd, $J = 7.7, 1.3, 1.3$ Hz, 1H, Ar-*H*), 6.98 (dd, $J = 2.6, 1.3$ Hz, 1H, Ar-*H*), 6.93 (d, $J = 19.2$ Hz, 1H, ArCH=CH), 6.83 (ddd, $J = 8.1, 2.6, 1.3$ Hz, 1H, Ar-*H*), 6.25 (d, $J = 19.2$ Hz, 1H, ArCH=CH), 3.83 (s, 3H, Ar-OCH₃), 0.18 [s, 3H, CH₃Si(OTMS)₂], and 0.12 [s, 18H, MeSi{OSi(CH₃)₃}₂].

¹³C NMR (CDCl₃, 125 MHz): δ 160.0, 145.0, 139.9, 129.7, 127.2, 119.6, 114.1, 111.9, 55.5, 2.1, and 0.2.

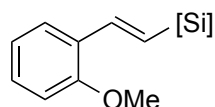
TLC: $R_f = 0.4$ in hexanes:EtOAc = 100:1.

GC-MS (5029017): $t_R = 10.55$ min, m/z 355 [(M+H)⁺, 80], 340 [(M-CH₃)⁺, 100], 265 (15), 221 (50), and 73 (60).

IR (neat): 2956 (m), 1601 (w), 1577 (w), 1251 (s), 1036 (s), 988 (s), 836 (s), 782 (s), 752 (s), and 684 (s) cm⁻¹.

HRMS (ESI/TOF): Calcd for (M+Na)⁺ (C₁₆H₃₀NaO₃Si₃)⁺: 377.1395. Found: 377.1369.

(E)-3-(2-Methoxystyryl)-1,1,1,3,5,5,5-heptamethyltrisiloxane (2-3-9)



2-3-9

Physical Appearance: Colorless clear liquid.

Yield: 51.7 mg, 73%.

¹H NMR (CDCl₃, 500 MHz): δ 7.53 (dd, *J* = 7.6, 1.6 Hz, 1H, Ar-*H*), 7.40 (d, *J* = 19.5 Hz, 1H, ArCH=CH), 7.25 (ddd, *J* = 8.3, 7.6, 1.6 Hz, 1H, Ar-*H*), 6.94 (dd, *J* = 7.6, 7.6 Hz, 1H, Ar-*H*), 6.87 (dd, *J* = 8.3, 0.7 Hz, 1H, Ar-*H*), 6.24 (d, *J* = 19.5 Hz, 1H, ArCH=CH), 3.85 (s, 3H, Ar-OCH₃), 0.19 [s, 3H, CH₃Si(OTMS)₂], and 0.14 [s, 18H, MeSi{OSi(CH₃)₃}₂].

¹³C NMR (CDCl₃, 125 MHz): δ 157.1, 139.6, 129.5, 127.5, 127.0, 126.4, 120.8, 111.2, 55.7, 2.1, and 0.3.

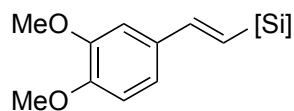
TLC: R_f = 0.3 in hexanes:EtOAc = 100:1.

GC-MS (5029017): *t_R* = 10.32 min, *m/z* 355 [(M+H)⁺, 60], 340 [(M-CH₃)⁺, 100], 265 (20), 221 (30), and 191 (60).

IR (neat): 2901 (m), 1598 (m), 1485 (m), 1243 (s), 1029 (s), 995 (s), 835 (s), 782 (s), and 747 (s) cm⁻¹.

HRMS (ESI/TOF): Calcd for (M+Na)⁺ (C₁₆H₃₀NaO₃Si₃)⁺: 377.1395. Found: 377.1423.

(*E*)-3-(3,4-Dimethoxystyryl)-1,1,1,3,5,5,5-heptamethyltrisiloxane (2-3-10)



2-3-10

Physical Appearance: White color semi solid.

Yield: 59.2 mg, 77%.

¹H NMR (CDCl₃, 500 MHz): δ 7.01 (d, *J* = 1.9 Hz, 1H, Ar-*H*), 6.98 (dd, *J* = 8.3, 1.9 Hz, 1H, Ar-*H*), 6.89 (d, *J* = 19.2 Hz, 1H, ArCH=CH), 6.83 (d, *J* = 8.3 Hz, 1H, Ar-*H*), 6.10 (d, *J* = 19.1 Hz, 1H, ArCH=CH), 3.92 (s, 3H, Ar-OCH₃), 3.89 (s, 3H, Ar-OCH₃), 0.18 [s, 3H, CH₃Si(OTMS)₂], and 0.14 [s, 18H, MeSi{OSi(CH₃)₃}₂].

¹³C NMR (CDCl₃, 125 MHz): δ 149.6, 149.2, 144.9, 131.6, 124.4, 120.3, 111.1, 108.9, 56.14, 56.03, 2.1, and 0.3.

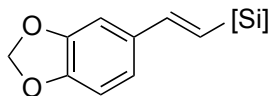
TLC: R_f = 0.5 in hexanes:EtOAc = 200:1.

GC-MS (5029017): *t_R* = 11.56 min, *m/z* 386 [(M+2H)⁺, 100], 370 [(M-CH₃)⁺, 100], 221 (25), and 73 (90).

IR (neat): 2956 (m), 1602 (w), 1579 (w), 1513 (s), 1465 (s), 1249 (s), 1163 (m), 1024 (s), 988 (s), 834 (s), 788 (s), and 751(s) cm^{-1} .

HRMS (ESI/TOF): Calcd for $(\text{M}+\text{Na})^+$ ($\text{C}_{17}\text{H}_{32}\text{NaO}_4\text{Si}_3$)⁺: 407.1501. Found: 407.1551.

(E)-3-{2-(Benzo[d][1,3]dioxol-5-yl)vinyl}-1,1,1,3,5,5,5-heptamethyltrisiloxane (2-3-11)



2-3-11

Physical Appearance: Colorless clear liquid.

Yield: 55.2 mg, 75%.

¹H NMR (CDCl_3 , 500 MHz): δ 7.00 (d, $J = 1.7$ Hz, 1H, Ar-*H*), 6.87 (ddd, $J = 7.9, 1.7, 0.4$ Hz, 1H, Ar-*H*), 6.85 (d, $J = 19.1$ Hz, 1H, ArCH=CH), 6.77 (d, $J = 7.9$ Hz, 1H, Ar-*H*), 6.05 (d, $J = 19.1$ Hz, 1H, ArCH=CH), 5.96 (s, 2H, ArOCH₂O), 0.16 [s, 3H, CH₃Si(OTMS)₂], and 0.11 [s, 18H, MeSi{OSi(CH₃)₃}₂].

¹³C NMR (CDCl_3 , 125 MHz): δ 148.3, 148.0, 144.6, 133.1, 124.6, 122.0, 108.4, 105.8, 101.3, 2.1, and 0.2.

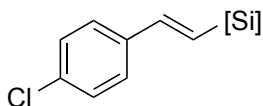
TLC: $R_f = 0.3$ in hexanes.

GC-MS (5029017): $t_R = 11.28$ min, m/z 369 [(M+H)⁺, 25], 353 [(M-CH₃)⁺, 20], 279 (25), 115 (30), and 73 (100).

IR (neat): 2957 (m), 1737 (w), 1594 (w), 1503 (m), 1489 (s), 1445 (m), 1247 (s), 1205 (w), 1034 (s), 986 (s), 836 (s), 786 (s), and 752(s) cm^{-1} .

HRMS (ESI/TOF): Calcd for $(\text{M}+\text{Na})^+$ ($\text{C}_{16}\text{H}_{28}\text{NaO}_4\text{Si}_3$)⁺: 391.1188. Found: 391.1218.

(E)-3-(4-Chlorostyryl)-1,1,1,3,5,5,5-heptamethyltrisiloxane (2-3-12)



2-3-12

Physical Appearance: Colorless clear liquid.

Yield: 57.3 mg, 80%.

¹H NMR (CDCl₃, 500 MHz): δ 7.46 (app d, *J* = 8.4 Hz, 2H, Ar-*H*), 7.30 (app d, *J* = 8.4 Hz, 2H, Ar-*H*), 6.89 (d, *J* = 19.2 Hz, 1H, ArCH=CH), 6.25 (d, *J* = 19.2 Hz, 1H, ArCH=CH), 0.18 [s, 3H, CH₃Si(OTMS)₂], and 0.13 [s, 18H, MeSi{OSi(CH₃)₃}₂].

¹³C NMR (CDCl₃, 125 MHz): δ 143.8, 137.3, 131.8, 128.3, 127.9, 122.3, 2.1, and 0.2.

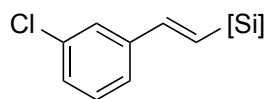
TLC: R_f = 0.7 in hexanes.

GC-MS (5029017): *t*_R = 10.17 min, *m/z* 345 [(M+2)–CH₃]⁺, 4], 343 [(M–CH₃)⁺, 2], 221 (50), and 195 (100).

IR (neat): 2957 (m), 1605 (w), 1486 (m), 1445 (m), 1250 (s), 1036 (s), 987 (s), 835 (s), 788 (s), and 752 (s) cm⁻¹.

HRMS (ESI/TOF): Calcd for (M+H)⁺ (C₁₅H₂₈ClO₂Si₃)⁺: 359.1080. Found: 359.1118.

(*E*)-3-(3-Chlorostyryl)-1,1,1,3,5,5,5-heptamethyltrisiloxane (2-3-13)



2-3-13

Physical Appearance: Colorless clear liquid.

Yield: 60.9 mg, 85%.

¹H NMR (CDCl₃, 500 MHz): δ 7.42 (dd, *J* = 1.8, 1.8 Hz, 1H, Ar-*H*), 7.30 (ddd, *J* = 7.3, 1.8, 1.8 Hz, 1H, Ar-*H*), 7.27 (dd, *J* = 7.3, 7.3 Hz, 1H, Ar-*H*), 7.24 (ddd, *J* = 7.3, 1.8, 1.8 Hz, 1H, Ar-*H*), 6.89 (d, *J* = 19.2 Hz, 1H, ArCH=CH), 6.28 (d, *J* = 19.2 Hz, 1H, ArCH=CH), 0.18 [s, 3H, CH₃Si(OTMS)₂], and 0.14 [s, 18H, MeSi{OSi(CH₃)₃}₂].

¹³C NMR (CDCl₃, 125 MHz): δ 143.6, 140.3, 134.8, 130.0, 128.8, 128.3, 126.7, 125.0, 2.1, and 0.2.

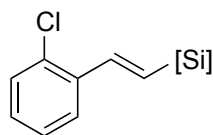
TLC: R_f = 0.7 in hexanes.

GC-MS (5029017): *t*_R = 10.26 min, *m/z* 345 [(M+2)–CH₃]⁺, 5], 343 [(M–CH₃)⁺, 10], 221 (100), 175 (15), 149 (15), and 73 (10).

IR (neat): 2957 (m), 1606 (w), 1563 (w), 1470 (w), 1250 (s), 1192 (w), 1037 (s), 987 (s), 836 (s), 813 (s), 538 (s), and 677 (s) cm⁻¹.

HRMS (ESI/TOF): Calcd for (M+H)⁺ (C₁₅H₂₈ClO₂Si₃)⁺: 359.1080. Found: 359.1124.

(E)-3-(2-Chlorostyryl)-1,1,1,3,5,5,5-heptamethyltrisiloxane (2-3-14)



2-3-14

Physical Appearance: Colorless clear liquid.

Yield: 58 mg, 81%.

¹H NMR (CDCl₃, 500 MHz): δ 7.59 (dd, *J* = 7.7, 1.8 Hz, 1H, Ar-*H*), 7.40 (d, *J* = 19.2 Hz, 1H, ArCH=CH), 7.35 (dd, *J* = 7.7, 1.5 Hz, 1H, Ar-*H*), 7.24 (dddd, *J* = 7.7, 7.7, 1.5, 0.6 Hz, 1H, Ar-*H*), 7.20 (ddd, *J* = 7.7, 7.7, 1.8 Hz, 1H, Ar-*H*), 6.27 (d, *J* = 19.2 Hz, 1H, ArCH=CH), 0.20 [s, 3H, CH₃Si(OTMS)₂], and 0.14 [s, 18H, MeSi{OSi(CH₃)₃}₂].

¹³C NMR (CDCl₃, 125 MHz): δ 140.9, 136.3, 133.6, 130.1, 129.8, 129.2, 126.92, 126.81, 2.0, and 0.2.

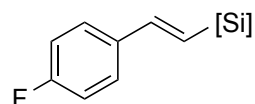
TLC: R_f = 0.7 in hexanes.

GC-MS (5029017): *t*_R = 10.12 min, *m/z* 345 [(M+2)-CH₃]⁺, 5], 343 [(M-CH₃)⁺, 10], 221 (50), 195 (100), and 143 (20).

IR (neat): 2957 (m), 1601 (w), 1466 (w), 1439 (w), 1250 (s), 1037 (s), 989 (m), 835 (s), 811 (m), 782 (s), 746 (s), and 686 (s) cm⁻¹.

HRMS (ESI/TOF): Calcd for (M+H)⁺ (C₁₅H₂₈ClO₂Si₃)⁺: 359.1080. Found: 359.1096.

(E)-3-(4-Fluorostyryl)-1,1,1,3,5,5,5-heptamethyltrisiloxane (2-3-15)



2-3-15

Physical Appearance: Colorless clear liquid.

Yield: 47.2 mg, 69%.

¹H NMR (CDCl₃, 500 MHz): δ 7.41 (nfom, 2H, Ar-*H*), 7.02 (nfom, 2H, Ar-*H*), 6.91 (d, *J* = 19.2 Hz, 1H, ArCH=CH), 6.17 (d, *J* = 19.2 Hz, 1H, ArCH=CH), 0.18 [s, 3H, CH₃Si(OTMS)₂], and 0.13 [s, 18H,

MeSi{OSi(CH₃)₃}₂].

¹³C NMR (CDCl₃, 125 MHz): δ 162.7 (d, ¹J_{F-C} = 247 Hz), 143.9, 134.6 (d, ⁴J_{F-C} = 2.5 Hz), 128.39 (d, ³J_{F-C} = 8.4 Hz), 126.6, (d, ⁵J_{F-C} = 2.2 Hz), 115.5 (d, ²J_{F-C} = 21.7 Hz), 2.1, and 0.2.

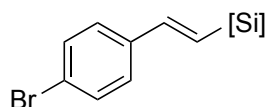
TLC: R_f = 0.6 in hexanes.

GC-MS (5029017): t_R = 9.22 min, m/z 342 [M⁺, 2], 327 [(M-CH₃)⁺, 10], 221 (100), 175 (20), 143 (15) and 91 (10).

IR (neat): 2957 (m), 1602 (m), 1507 (m), 1410 (w), 1251 (s), 1230 (m), 1036 (s), 987 (s), 836 (s), 785 (s), 752 (s) and 687 (s) cm⁻¹.

HRMS (ESI/TOF): Calcd for (M+Na)⁺ (C₁₅H₂₇FNaO₂Si₃)⁺: 365.1195. Found: 365.1201.

(E)-3-(4-Bromostyryl)-1,1,1,3,5,5,5-heptamethyltrisiloxane (2-3-16)



2-3-16

Physical Appearance: Colorless clear liquid.

Yield: 68.3 mg, 85%.

¹H NMR (CDCl₃, 500 MHz): δ 7.46 (app d, J = 8.4 Hz, 2H, Ar-H), 7.31 (app d, J = 8.4 Hz, 2H, Ar-H), 6.89 (d, J = 19.2 Hz, 1H, ArCH=CH), 6.25 (d, J = 19.2 Hz, 1H, ArCH=CH), 0.18 0.19 [s, 3H, CH₃Si(OTMS)₂], and 0.13 [s, 18H, MeSi{OSi(CH₃)₃}₂].

¹³C NMR (CDCl₃, 125 MHz): δ 143.8, 137.3, 131.8, 128.3, 127.9, 122.3, 2.1, and 0.2.

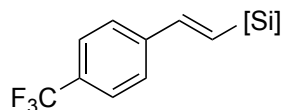
TLC: R_f = 0.8 in hexanes:EtOAc = 100:1.

GC-MS (5029017): t_R = 10.87 min, m/z 389 [(M+2)-CH₃)⁺, 15], 387 [(M-CH₃)⁺, 15], 221 (100), 143 (20), and 73 (10).

IR (neat): 2957 (m), 1605 (w), 1486 (m), 1397 (w), 1250 (s), 1037 (s), 987 (w), 835 (s), 788 (s), 752 (s) and 664 (m) cm⁻¹.

HRMS (ESI/TOF): Calcd for (M+Na)⁺ (C₁₅H₂₇BrNaO₂Si₃)⁺: 425.0394. Found: 425.0400.

(E)-1,1,1,3,5,5,5-Heptamethyl-3-[4-(trifluoromethyl)styryl]trisiloxane (2-3-17)



2-3-17

Physical Appearance: Colorless clear liquid.

Yield: 63.5 mg, 81%.

¹H NMR (CDCl₃, 500 MHz): δ 7.46 (d, *J* = 8.4 Hz, 2H, Ar-*H*), 7.31 (d, *J* = 8.4 Hz, 2H, Ar-*H*), 6.89 (d, *J* = 19.2 Hz, 1H, ArCH=CH), 6.25 (d, *J* = 19.2 Hz, 1H, ArCH=CH), 0.18 [s, 3H, CH₃Si(OTMS)₂], and 0.13 [s, 18H, MeSi{OSi(CH₃)₃}₂].

¹³C NMR (CDCl₃, 125 MHz): δ 143.5, 141.7, 130.2, 130.1 (²*J*_{F-C} = 32 Hz), 126.9, 125.7 (³*J*_{F-C} = 3.6 Hz), 124.4 (¹*J*_{F-C} = 272 Hz), 2.1, and 0.2.

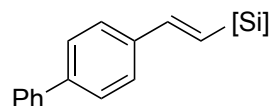
TLC: R_f = 0.8 in hexanes.

GC-MS (5029017): *t*_R = 9.10 min, *m/z* 377 [M⁺, 15], 151 (15), 128 (10), and 73 (100).

IR (neat): 2957 (m), 1613 (w), 1574 (w), 1411 (w), 1324 (s), 1252 (s), 1165 (m), 1127 (m), 1041 (s), 988 (m), 835 (s), 781 (s), 752 (s) and 623 (m) cm⁻¹.

HRMS (ESI/TOF): Calcd for (M+Na)⁺ (C₁₆H₂₇F₃NaO₂Si₃)⁺: 415.1163. Found: 415.1234.

(*E*)-3-[2-((1,1'-Biphenyl)-4-yl)vinyl]-1,1,1,3,5,5,5-heptamethyltrisiloxane (2-3-18)



2-3-18

Physical Appearance: Colorless clear liquid.

Yield: 61.6 mg, 77%.

¹H NMR (CDCl₃, 500 MHz): δ 7.63-7.60 (m, 2H, Ar-*H*), 7.59 [nfom, 2H, Ar-*H* (*styryl*)], 7.53 [nfom, 2H, Ar-*H* (*styryl*)], 7.45 (app dd, *J* = 7.9, 7.4 Hz, 2H, Ar-*H*), 7.35 (dddd, *J* = 7.9, 6.7, 1.3, 1.3 Hz, 1H, Ar-*H*), 7.01 (d, *J* = 19.2 Hz, 1H, ArCH=CH), 6.32 (d, *J* = 19.2 Hz, 1H, ArCH=CH), 0.21 0.19 [s, 3H, CH₃Si(OTMS)₂], and 0.14 [s, 18H, MeSi{OSi(CH₃)₃}₂].

¹³C NMR (CDCl₃, 125 MHz): δ 144.7, 141.2, 140.9, 137.4, 129.0, 127.58, 127.44, 127.24, 127.20, 127.0, 2.1, and 0.2.

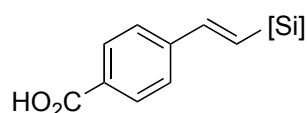
TLC: $R_f = 0.6$ in hexanes:EtOAc = 100:1.

GC-MS (5029017): $t_R = 13.12$ min, m/z 400 [M^+ , 15], 385 [$(M-CH_3)^+$, 22], 221 (30), 59 (35), and 73 (100).

IR (neat): 2957 (m), 1604 (w), 1486 (w), 1406 (w), 1250 (s), 1035 (s), 988 (m), 835 (s), 781 (s), 752 (s), 694 (m), and 593 (w) cm^{-1} .

HRMS (ESI/TOF): Calcd for $(M+Na)^+$ ($C_{21}H_{32}NaO_2Si_3$) $^+$: 423.1602. Found: 423.1608.

(E)-4-[2-(1,1,1,3,5,5,5-Heptamethyltrisiloxan-3-yl)vinyl]benzoic acid (2-3-19)



2-3-19

Physical Appearance: Yellow color semi solid.

Yield: 44.9 mg, 61%. [containing ca. 6% of hydrosilylation product (alkyl silane) and 3% of hydrogenation product (ethyl benzene)]

1H NMR ($CDCl_3$, 500 MHz): δ 8.09 (d, $J = 8.2$ Hz, 2H, Ar-*H*), 7.53 (d, $J = 8.2$ Hz, 2H, Ar-*H*), 7.00 (d, $J = 19.2$ Hz, 1H, ArCH=CH), 6.43 (d, $J = 19.2$ Hz, 1H, ArCH=CH), 0.20 [s, 3H, $CH_3Si(OTMS)_2$], and 0.12 [s, 18H, $MeSi\{OSi(CH_3)_3\}_2$].

^{13}C NMR ($CDCl_3$, 125 MHz): δ 171.8, 143.9, 143.5, 130.84, 130.77, 130.61, 126.8, 2.1, and 0.2.

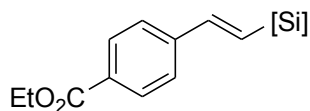
TLC: $R_f = 0.5$ in hexanes:EtOAc = 5:1.

GC-MS (5029017): $t_R = 12.96$ min, m/z 353 [$(M-CH_3)^+$, 100], 262 (25), 145 (25), and 73 (100).

IR (neat): 3200-2500 (b), 2956 (m), 1683 (s), 1604 (m), 1419 (m), 1286 (m), 1249 (s), 1031 (s), 991 (m), 836 (s), 809 (s), 786 (s), 753 (s), 630 (m), and 577 (w) cm^{-1} .

HRMS (ESI/TOF): Calcd for $(M-H^+)$: 367.1217. Found: 367.1210.

(E)-Ethyl 4-[2-(1,1,1,3,5,5,5-Heptamethyltrisiloxan-3-yl)vinyl]benzoate (2-3-20)



2-3-20

Physical Appearance: Colorless clear liquid.

Yield: 55.5 mg, 70%.

¹H NMR (CDCl₃, 500 MHz): δ 8.01 (app d, *J* = 8.4 Hz, 2H, Ar-*H*), 7.49 (app d, *J* = 8.4 Hz, 2H, Ar-*H*), 6.98 (d, *J* = 19.2 Hz, 1H, ArCH=CH), 6.39 (d, *J* = 19.2 Hz, 1H, ArCH=CH), 4.38 (q, *J* = 7.1 Hz, 2H, ArCO₂CH₂CH₃), 1.40 (t, *J* = 7.1 Hz, 3H, ArCO₂CH₂CH₃), 0.19 [s, 3H, CH₃Si(OTMS)₂], and 0.11 [s, 18H, MeSi{OSi(CH₃)₃}₂].

¹³C NMR (CDCl₃, 125 MHz): δ 166.6, 144.0, 142.5, 130.14, 130.09, 130.06, 126.6, 61.2, 14.6, 2.1, and 0.2.

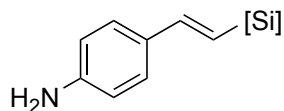
TLC: R_f = 0.3 in hexanes:EtOAc = 100:1 .

GC-MS (5029017): *t_R* = 11.91 min, m/z 397 [(M+H)⁺, 20], 272 [(M-CH₃)⁺, 25], 143 (30), 131 (100), and 73 (30).

IR (neat): 2957 (m), 1718 (s), 1606 (w), 1409 (w), 1366 (w), 1272 (s) 1250 (s), 1038 (s), 989 (m), 836 (s), 808 (s), 782 (s), 751 (s), 688 (m), and 631 (w) cm⁻¹.

HRMS (ESI/TOF): Calcd for (M+Na)⁺ (C₁₈H₃₂NaO₄Si₃)⁺: 419.1501. Found: 419.1536.

(*E*)-4-[2-(1,1,1,3,5,5,5-Heptamethyltrisiloxan-3-yl)vinyl]aniline (2-3-21)



2-3-21

Physical Appearance: Light brown color clear liquid.

Yield: 37.3 mg, 55%. [containing ca. 10% of hydrosilylation product (HS)]

¹H NMR (CDCl₃, 500 MHz): δ 7.27 (app d, *J* = 8.4 Hz, 2H, Ar-*H*), 6.86 (d, *J* = 19.2 Hz, 1H, ArCH=CH), 6.65 (app d, *J* = 8.4 Hz, 2H, Ar-*H*), 6.02 (d, *J* = 19.2 Hz, 1H, ArCH=CH), 3.72 (br s, 2H, NH₂), 0.16 [s, 3H, CH₃Si(OTMS)₂], and 0.12 [s, 18H, MeSi{OSi(CH₃)₃}₂].

¹³C NMR (CDCl₃, 125 MHz): δ 146.9, 145.1, 129.3 (DS or HS), 128.7 (DS or HS), 128.1, 122.1, 115.5 (HS), 115.1, 2.1, and 0.3.

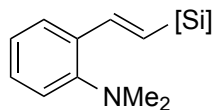
TLC: R_f = 0.6 in hexanes:EtOAc = 7:1 .

GC-MS (5029017): $t_R = 11.32$ min, m/z 340 [(M+H)⁺, 1000], 324 [(M-CH₃)⁺, 25], 176 (30), and 73 (30).

IR (neat): 3465 (w), 3386 (w), 2956 (m), 1619 (m), 1601 (m), 1513 (s), 1250 (s), 1173 (m), 1032 (s), 988 (m), 835 (s), 792 (s), 752 (s), 686 (m), and 510 (m) cm⁻¹.

HRMS (ESI/TOF): Calcd for (M+H)⁺ (C₁₅H₃₀NO₂Si₃)⁺: 340.1579. Found: 340.1640.

(E)-2-[2-(1,1,1,3,5,5,5-Heptamethyltrisiloxan-3-yl)vinyl]-N,N-dimethylaniline (2-3-22)



2-3-22

Physical Appearance: Light brown color clear liquid.

Yield: 41 mg, 56%.

¹H NMR (CDCl₃, 500 MHz): δ 7.49 (dd, $J = 7.4, 1.5$ Hz, 1H, Ar-*H*), 7.35 (d, $J = 19.4$ Hz, 1H, ArCH=CH), 7.23 (ddd, $J = 8.3, 7.4, 1.5$ Hz, 1H, Ar-*H*), 7.00 (m, 2H, Ar-*H*), 6.17 (d, $J = 19.4$ Hz, 1H, ArCH=CH), 2.73 [s, 6HArN(CH₃)₂], 0.20 [s, 3H, CH₃Si(OTMS)₂], and 0.13 [s, 18H, MeSi{OSi(CH₃)₃}₂].

¹³C NMR (CDCl₃, 125 MHz): δ 152.2, 143.4, 132.5, 128.8, 127.1, 125.8, 122.3, 118.1, 44.9, 2.1, and 0.2.

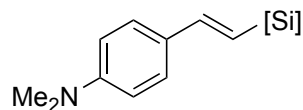
TLC: R_f = 0.3 in hexanes:EtOAc = 200:1 .

GC-MS (5029017): $t_R = 10.42$ min, m/z 368 [(M+H)⁺, 90], 252 [(M-CH₃)⁺, 30], 143 (40), 131 (100), and 73 (60).

IR (neat): 2956 (m), 1597 (m), 1484 (m), 1321 (w), 1250 (s), 1036 (s), 947 (m), 835 (s), 815 (s), 781 (s), 752 (s), 687 (m), and 559 (w) cm⁻¹.

HRMS (ESI/TOF): Calcd for (M+H)⁺ (C₁₇H₃₄NO₂Si₃)⁺: 368.1892. Found: 368.1942.

(E)-4-[2-(1,1,1,3,5,5,5-Heptamethyltrisiloxan-3-yl)vinyl]-N,N-dimethylaniline (2-3-23)



2-3-23

Physical Appearance: Red color liquid.

Yield: 50.7 mg, 69%.

¹H NMR (CDCl₃, 500 MHz): δ 7.35 (app d, *J* = 8.8 Hz, 2H, Ar-*H*), 6.89 (d, *J* = 19.2 Hz, 1H, ArCH=CH), 6.69 (app d, *J* = 8.8 Hz, 2H, Ar-*H*), 6.02 (d, *J* = 19.1 Hz, 1H, ArCH=CH), 2.98 (s, 6H, ArNMe₂), 0.17 [s, 3H, CH₃Si(OTMS)₂], and 0.13 [s, 18H, MeSi{OSi(CH₃)₃}₂].

TLC: R_f = 0.3 in hexanes:EtOAc = 200:1.

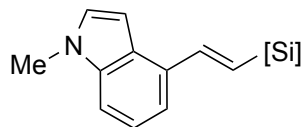
¹³C NMR (CDCl₃, 125 MHz): δ 150.8, 145.2, 127.9, 127.0, 121.2, 112.4, 40.7, 2.1, and 0.3.

GC-MS (5029017): *t*_R = 11.80min, m/z 368 [(M+H)⁺, 100], 252 [(M-CH₃)⁺, 80], 278 (10), 204 (20), 144 (25), and 73 (60).

IR (neat): 2956 (m), 1600 (m), 1519 (m), 1354 (w), 1250 (s), 1180 (m), 1036 (s), 986 (m), 869 (s), 835 (s), 812 (s), 790 (s), 751 (s), 687 (m), and 514 (w) cm⁻¹.

HRMS (ESI/TOF): Calcd for (M+H)⁺ (C₁₇H₃₄NO₂Si₃)⁺: 368.1892. Found: 368.1902.

(*E*)-4-[2-(1,1,1,3,5,5,5-Heptamethyltrisiloxan-3-yl)vinyl]-1-methyl-1*H*-indole (2-3-24)



2-3-24

Physical Appearance: Light brown color clear liquid.

Yield: 46 mg, 61%.

¹H NMR (CDCl₃, 500 MHz): δ 7.41 (d, *J* = 19.3 Hz, 1H, ArCH=CH), 7.32 (d, *J* = 7.2 Hz, 1H, Ar-*H*), 7.26 (d, *J* = 8.0 Hz, 1H, Ar-*H*), 7.23 (dd, *J* = 8.0, 7.2 Hz, 1H, Ar-*H*), 7.1 (d, *J* = 3.1 Hz, 1H, NCHCH), 6.72 (d, *J* = 3.1 Hz, 1H, NCHCH), 6.44 (d, *J* = 19.3 Hz, 1H, ArCH=CH), 3.81 (s, 3H, ArNMe), 0.23 [s, 3H, CH₃Si(OTMS)₂], and 0.15 [s, 18H, MeSi{OSi(CH₃)₃}₂].

¹³C NMR (CDCl₃, 125 MHz): δ 143.5, 137.4, 130.8, 129.3, 127.3, 127.0, 121.7, 117.1, 109.2, 99.4, 33.1, 2.1, and 0.3.

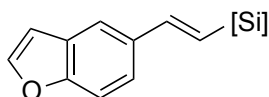
TLC: R_f = 0.3 in hexanes:EtOAc = 40:1.

GC-MS (5029017): *t*_R = 12.52 min, m/z 378 [(M+H)⁺, 80], 262 [(M-CH₃)⁺, 100], 288 (25), 221 (25), 214 (25), 198 (55), 168 (60), 154 (40), and 73 (60).

IR (neat): 2956 (m), 1594 (w), 1513 (w), 1417 (w), 1340 (w), 1288 (m), 1250 (s), 1033 (s), 988 (m), 869 (s), 835 (s), 783 (s), 740 (s), 709 (m), and 594 (m) cm⁻¹.

HRMS (ESI/TOF): Calcd for (M+H)⁺ (C₁₈H₃₂NO₂Si₃)⁺: 378.1735. Found: 378.1780.

(E)-3-[2-(Benzofuran-5-yl)vinyl]-1,1,1,3,5,5,5-heptamethyltrisiloxane (2-3-25)



2-3-25

Physical Appearance: White color clear liquid.

Yield: 45.1 mg, 62%.

¹H NMR (CDCl₃, 500 MHz): δ 7.66 (ddd, *J* = 1.7, 0.7, 0.7 Hz, 1H, Ar*H*), 7.61 (d, *J* = 2.2 Hz, 1H, OCHCH), 7.45 (ddd, *J* = 8.5, 0.7, 0.7 Hz 1H, Ar*H*), 7.45 (dd, *J* = 8.5, 1.7 Hz 1H, Ar*H*), 7.06 (app d, *J* = 19.2 Hz, 1H, ArCH=CH), 6.76 (dd, *J* = 2.2, 0.7 Hz, 1H, OCHCH), 6.24 (d, *J* = 19.2 Hz, 1H, ArCH=CH), 0.20 [s, 3H, CH₃Si(OTMS)₂], and 0.13 [s, 18H, MeSi{OSi(CH₃)₃}₂].

¹³C NMR (CDCl₃, 125 MHz): δ 155.3, 145.7, 145.4, 133.7, 127.9, 125.5, 123.3, 119.7, 111.6, 107.0, 2.2, and 0.3.

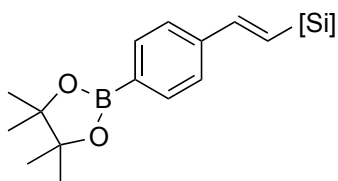
TLC: R_f = 0.4 hexanes:EtOAc = 60:1.

GC-MS (5029017): *t_R* = 11.21min, m/z 365 [(M+H)⁺, 15], 249 [(M-CH₃)⁺, 60], 221 (100), 201 (30), and 73 (15).

IR (neat): 2957 (m), 1604 (w), 1586 (w), 1465 (w) 1439 (m), 1251 (s), 1187 (m), 1030 (s), 987 (m), 836 (s), 790 (s), 752 (s), 729 (s), and 687 (m) cm⁻¹.

HRMS (ESI/TOF): Calcd for (M+Na)⁺ (C₁₇H₂₈NaO₃Si₃)⁺: 387.1238. Found: 387.1252.

(E)-1,1,1,3,5,5,5-Heptamethyl-3-[4-(4,4,5,5-tetramethyl-1,3,2-dioxaborolan-2-yl)styryl]trisiloxane (2-3-26)



2-3-26

Physical Appearance: White color semi solid.

Yield: 73.8mg, 82%.

¹H NMR (CDCl₃, 500 MHz): δ 7.78 (d, *J* = 8.0 Hz, 2H, Ar-*H*), 7.44 (d, *J* = 8.0 Hz, 2H, Ar-*H*), 6.97 (d, *J* = 19.2 Hz, 1H, ArCH=CH), 6.34 (d, *J* = 19.2 Hz, 1H, ArCH=CH), 1.35 (s, *J* = 3.2 Hz, 12H, BPin), 0.19 [s, 3H, CH₃Si(OTMS)₂], and 0.11 [s, 18H, MeSi{OSi(CH₃)₃}₂].

¹³C NMR (CDCl₃, 125 MHz): δ 145.1, 141.0, 135.2, 135.1, 128.1, 126.1, 84.0, 25.1, 2.1, and 0.2.

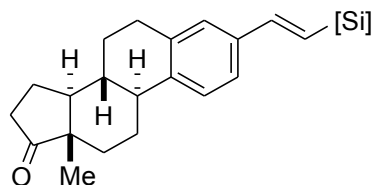
TLC: R_f = 0.3 hexanes:EtOAc = 100:1.

GC-MS (5029017): *t_R* = 10.42 min, *m/z* 452 [(M+2H)⁺, 40], 435 [(M-CH₃)⁺, 60], 351 (25), 313 (25), 221 (30), 143 (70), 83 (80), and 73 (100).

IR (neat): 2957 (m), 1606 (w), 1514 (m), 1396 (s) 1358 (m), 1252 (s), 1143 (m), 1037 (s), 993 (m), 836 (s), 796 (s), 752 (s), 669 (s), and 577 (m) cm⁻¹.

HRMS (ESI/TOF): Calcd for (M+Na)⁺ (C₂₁H₃₉BNaO₄Si₃)⁺: 473.2141. Found: 473.2107.

(8*R*,9*S*,13*S*,14*S*)-3-[(*E*)-2-(1,1,1,3,5,5,5-Heptamethyltrisiloxan-3-yl)vinyl]-13-methyl-7,8,9,11,12,13,15,16-octahydro-6*H*-cyclopenta[*a*]phenanthren-17(14*H*)-one (2-3-27)



2-2-27

Physical Appearance: White color semi solid.

Yield: 76 mg, 76%.

¹H NMR (CDCl₃, 500 MHz): δ 7.27 (d, *J* = 8.3 Hz, 1H, Ar-*H*), 7.25 (dd, *J* = 8.3, 1.2 Hz, 1H, Ar-*H*), 7.17 (d, *J* = 1.2 Hz, 1H, Ar-*H*), 6.91 (d, *J* = 19.2 Hz, 1H, ArCH=CH), 6.22 (d, *J* = 19.2 Hz, 1H, ArCH=CH), 2.94 (dd, *J* = 4.5, 4.5 Hz, 1H), 2.93-2.91 (m, 1H, alkyl-*H*), 2.51 (ddd, *J* = 19.1, 8.8, 0.7 Hz, 1H, alkyl-*H*), 2.46-2.41 (nfom, 1H, alkyl-*H*), 2.31 (ddd, *J* = 10.7, 10.7, 4.2 Hz, 1H, alkyl-*H*), 2.24 (dddd, *J* = 19.2, 9.0, 9.0 Hz, 1H, alkyl-*H*), 2.09-2.01 (m, 2H, alkyl-*H*), 1.99-1.95 (nfom, 1H, alkyl-*H*), 1.68-1.41 (m, 6H, alkyl-*H*), 1.00 [s, 3H, CH(18)₃], 0.26 [s, 3H, CH₃Si(OTMS)₂], and 0.21 [s, 18H, MeSi{OSi(CH₃)₃}₂].

¹³C NMR (CDCl₃, 125 MHz): δ 221.1, 144.9, 140.2, 136.8, 136.0, 127.5, 126.1, 125.8, 124.2, 50.7, 48.2, 44.7, 38.3, 36.1, 31.8, 29.6, 26.7, 25.9, 21.8, 14.0, 2.1, and 0.2.

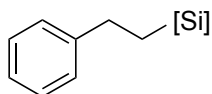
TLC: $R_f = 0.4$ in hexanes:EtOAc = 10:1.

GC-MS (5029019): $t_R = 18.9$ min, m/z 501 [(M+H)⁺, 2], 486 [(M-OH)⁺, 3], 264 (2), 151 (10) and 73 (100).

IR (neat): 2956 (m), 1738 (s), 1603 (w), 1454 (w) 1407 (w), 1250 (s), 1035 (s), 989 (m), 837 (s), 783 (s), 752 (s), 688 (s), and 579 (w) cm^{-1} .

HRMS (ESI/TOF): Calcd for (M+H)⁺ (C₂₇H₄₅O₃Si₃)⁺: 501.2671. Found: 501.2626.

1,1,1,3,5,5,5-Heptamethyl-3-phenethyltrisiloxane (2-2-1)



2-2-1

Physical Appearance: Colorless clear liquid.

Yield: 46.9 mg, 72%.

¹H NMR (CDCl₃, 500 MHz): δ 7.29 (dd, $J = 7.6, 7.4$ Hz, 2H, Ar-*H*), 7.21 (d, $J = 7.6$ Hz, 2H, Ar-*H*), 7.18 (dd, $J = 7.4, 7.4$ Hz, 1H, Ar-*H*), 2.67-2.63 (nfom, 2H, Ar-CH₂CH₂), 0.86-0.83 (nfom, 2H, Ar-CH₂CH₂), 0.12 [s, 18H, MeSi{OSi(CH₃)₃}₂], and 0.04 [s, 3H, CH₃Si(OTMS)₂].

¹³C NMR (CDCl₃, 125 MHz): δ 145.4, 128.5, 128.0, 125.7, 29.5, 19.9, 2.1, and -0.1.

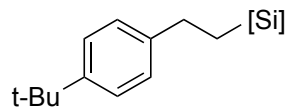
TLC: $R_f = 0.3$ in hexanes.

GC-MS (5029017): $t_R = 9.15$ min, m/z 327 [(M+H)⁺, 10], 322 [(M-CH₃)⁺, 100], 221 (100), 208 (20) and 164 (10).

IR (neat): 2957 (m), 1603 (w), 1496 (w) 1453 (w), 1251 (s), 1039 (s), 835 (s), 793 (s), 780 (s), 751 (s), 696 (s), and 572 (m) cm^{-1} .

HRMS (ESI/TOF): Calcd for (M+H)⁺ (C₁₅H₃₁O₂Si₃)⁺: 327.1626. Found: 327.1669.

3-[4-(*tert*-Butyl)phenethyl]-1,1,1,3,5,5,5-heptamethyltrisiloxane (2-2-2)



2-2-2

Physical Appearance: Colorless clear liquid.

Yield: 58.8 mg, 77%.

¹H NMR (CDCl₃, 500 MHz): δ 7.31 (d, *J* = 8.3 Hz, 2H, Ar-*H*), 7.14 (d, *J* = 8.3 Hz, 2H, Ar-*H*), 2.63-2.60 (nfom, 2H, Ar-CH₂CH₂), 1.32 (s, 9H, Ar-CMe₃), 0.85-0.82 (nfom, 2H, Ar-CH₂CH₂), 0.11 [s, 18H, MeSi{OSi(CH₃)₃}₂], and 0.03 [s, 3H, CH₃Si(OTMS)₂].

¹³C NMR (CDCl₃, 125 MHz): δ 148.5, 142.3, 127.6, 125.4, 34.5, 31.7, 28.8, 19.8, 2.1, and -0.1.

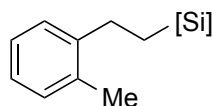
TLC: R_f = 0.6 in hexanes.

GC-MS (5029017): *t*_R = 10.89 min, *m/z* 383 [(M+H)⁺, 4], 367 [(M-CH₃)⁺, 50], 313 (15), 295 (10), and 221 (100).

IR (neat): 2957 (m), 1516 (w), 1363 (w), 1252 (s), 1041 (s), 836 (s), 796 (s), 780 (s), 753 (s), 687 (m), and 561 (m) cm⁻¹.

HRMS (ESI/TOF): Calcd for (M+H)⁺ (C₁₉H₃₉O₂Si₃)⁺: 383.2252. Found: 383.2291.

1,1,1,3,5,5,5-Heptamethyl-3-(2-methylphenethyl)trisiloxane (2-2-3)



2-2-3

Physical Appearance: Colorless clear liquid.

Yield: 44.9 mg, 66%.

¹H NMR (CDCl₃, 500 MHz): δ 7.16 (m, 2H, Ar-*H*), 7.13 (s, 1H, Ar-*H*), 7.11 (m, 1H, Ar-*H*), 2.63-2.60 (nfom, 2H, ArCH=CH), 2.31 (s, 3H, Ar-CH₃), 0.80-0.76 (nfom, 2H, ArCH=CH), 0.13 [s, 18H, MeSi{OSi(CH₃)₃}₂], and 0.07 [s, 3H, CH₃Si(OTMS)₂].

¹³C NMR (CDCl₃, 125 MHz): δ 143.5, 135.6, 130.3, 128.1, 126.2, 125.8, 26.8, 19.4, 18.5, 2.1, and -0.1.

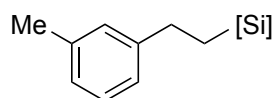
TLC: R_f = 0.6 in hexanes.

GC-MS (5029017): $t_R = 9.74$ min, m/z 341 [(M+H)⁺, 5], 325 [(M-CH₃)⁺, 100], 296 (3), 251 (5), 221 (100), 208 (20) and 179 (7).

IR (neat): 2956 (m), 1492 (w), 1457 (w), 1251 (s), 1179 (w), 1039 (s), 835 (s), 802 (s), 781 (s), 750 (s), 687 (m), and 447 (m) cm⁻¹.

HRMS (ESI/TOF): Calcd for (M+H)⁺ (C₁₆H₃₃O₂Si₃)⁺: 341.1783. Found: 341.1842.

1,1,1,3,5,5,5-Heptamethyl-3-(3-methylphenethyl)trisiloxane (2-2-4)



2-2-4

Physical Appearance: Colorless clear liquid.

Yield: 51.7 mg, 76%.

¹H NMR (CDCl₃, 500 MHz): δ 7.18 (dd, $J = 7.4, 7.4$ Hz, 1H, Ar-*H*), 7.03 (s, 1H, Ar-*H*), 7.00 (app t, $J = 8.2$ Hz, 2H, Ar-*H*), 2.63-2.60 (nfom, 2H, Ar-CH₂CH₂), 2.35 (s, 3H, Ar-CH₃), 0.85-0.82 (nfom, 2H, Ar-CH₂CH₂), 0.12 [s, 18H, MeSi{OSi(CH₃)₃}₂], and 0.04 [s, 3H, CH₃Si(OTMS)₂].

¹³C NMR (CDCl₃, 125 MHz): δ 145.4, 138.0, 128.8, 128.4, 126.4, 125.0, 29.4, 21.6, 20.0, 2.1, and -0.1.

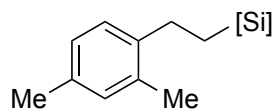
TLC: $R_f = 0.6$ in pure hexanes.

GC-MS (5029017): $t_R = 9.61$ min, m/z 341 [(M+H)⁺, 5], 325 [(M-CH₃)⁺, 100], 251 (6), 221 (100), 208 (20) and 179 (10).

IR (neat): 2957 (m), 1609 (w), 1488 (w), 1410 (w), 1251 (s), 1179 (w), 1039 (s), 835 (s), 805 (s), 780 (s), 752 (s), 689 (m), and 585 (m) cm⁻¹.

HRMS (ESI/TOF): Calcd for (M+H)⁺ (C₁₆H₃₃O₂Si₃)⁺: 341.1783. Found: 341.1837.

3-(2,4-Dimethylphenethyl)-1,1,1,3,5,5,5-heptamethyltrisiloxane (2-2-5)



2-2-5

Physical Appearance: Colorless clear liquid.

Yield: 51 mg, 72%.

¹H NMR (CDCl₃, 500 MHz): δ 7.07 (d, *J* = 8.3 Hz, 1H, Ar-*H*), 6.97 (s, 1H, Ar-*H*), 6.96 (d, *J* = 8.3 Hz, 1H, Ar-*H*), 2.60-2.57 (nfom, 2H, Ar-CH₂CH₂), 2.30 (s, 3H, Ar-CH₃), 2.28 (s, 3H, Ar-CH₃), 0.78-0.75 (nfom, 2H, Ar-CH₂CH₂), 0.13 [s, 18H, MeSi{OSi(CH₃)₃}₂], and 0.08 [s, 3H, CH₃Si(OTMS)₂].

¹³C NMR (CDCl₃, 125 MHz): δ 140.5, 135.4, 135.2, 131.1, 128.0, 126.8, 26.3, 21.1, 19.3, 18.8, 2.1, -0.2.

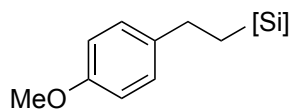
TLC: R_f = 0.7 in pure Hexanes.

GC-MS (5029017): *t_R* = 10.19 min, *m/z* 354 [M⁺, 5], 339 [(M-CH₃)⁺, 60], 265 (8), 221 (100), 208 (25) and 192 (10).

IR (neat): 2956 (m), 1503 (w), 1453 (w), 1251 (s), 1179 (w), 1039 (s), 836 (s), 798 (s), 784 (s), 751 (s), 687 (m), and 560 (m) cm⁻¹.

HRMS (ESI/TOF): Calcd for (M+Na)⁺ (C₁₇H₃₄NaO₂Si₃)⁺: 377.1759. Found: 377.1792.

3-(4-Methoxyphenethyl)-1,1,1,3,5,5,5-heptamethyltrisiloxane (2-2-6)



2-2-6

Physical Appearance: Colorless clear liquid.

Yield: 39.9 mg, 56%.

¹H NMR (CDCl₃, 500 MHz): δ 7.12 (d, *J* = 8.6 Hz, 2H, Ar-*H*), 6.83 (d, *J* = 8.6 Hz, 2H, Ar-*H*), 3.79 (s, 3H, ArOCH₃), 2.61-2.57 (nfom, 2H, Ar-CH₂CH₂), 0.82-0.79 (nfom, 2H, Ar-CH₂CH₂), 0.11 [s, 18H, MeSi{OSi(CH₃)₃}₂], and 0.03 [s, 3H, CH₃Si(OTMS)₂].

¹³C NMR (CDCl₃, 125 MHz): δ 157.7, 137.4, 128.8, 113.8, 55.4, 28.5, 20.1, 2.0, and -0.2.

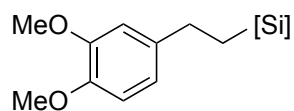
TLC: R_f = 0.4 in hexanes:EtOAc = 100:1.

GC-MS (5029017): *t_R* = 10.66 min, *m/z* 357 [(M+H)⁺, 100], and 341 [(M-CH₃)⁺, 100].

IR (neat): 2956 (m), 1612 (w), 1511 (m), 1299 (w), 1245 (s), 1174 (m), 1036 (s), 835 (s), 797 (s), 781 (s), 752 (s), 687 (m), and 516 (w) cm⁻¹.

HRMS (ESI/TOF): Calcd for (M+Na)⁺ (C₁₆H₃₂NaO₃Si₃)⁺: 379.1551. Found: 379.1622.

3-(3,4-Dimethoxyphenethyl)-1,1,1,3,5,5,5-heptamethyltrisiloxane (2-2-7)



2-2-7

Physical Appearance: Colorless clear liquid.

Yield: 61.8 mg, 80%.

¹H NMR (CDCl₃, 500 MHz): δ 6.79 (d, *J* = 8.0 Hz, 1H, Ar-*H*), 6.73 (dd, *J* = 8.0, 1.9 Hz, 1H, Ar-*H*), 6.72 (app s, 1H, Ar-*H*), 3.88 (s, 3H, ArOCH₃), 3.86 (s, 3H, ArOCH₃), 2.61-2.57 (nfom, 2H, Ar-CH₂CH₂), 0.84-0.80 (nfom, 2H, Ar-CH₂CH₂), 0.11 [s, 18H, MeSi{OSi(CH₃)₃}₂], and 0.03 [s, 3H, CH₃Si(OTMS)₂].

¹³C NMR (CDCl₃, 125 MHz): δ 149.0, 147.1, 138.1, 119.6, 111.4 (2), 56.15, 55.98, 29.0, 20.1, 2.1, and -0.1.

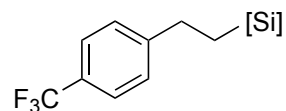
TLC: R_f = 0.7 in hexanes:EtOAc = 100:1.

GC-MS (5029017): *t_R* = 11.49 min, *m/z* 387 [(M+H)⁺, 100], 372 [(M-CH₃)⁺, 15], and 283 (15).

IR (neat): 2956 (m), 1590 (w), 1513 (s), 1464 (w), 1416 (w), 1251 (s), 1141 (m), 1030 (s), 835 (s), 795 (s), 782 (s), 752 (s), and 687 (m) cm⁻¹.

HRMS (ESI/TOF): Calcd for (M+Na)⁺ (C₁₇H₃₄NaO₄Si₃)⁺: 409.1657. Found: 409.1704.

1,1,1,3,5,5,5-Heptamethyl-3-[4-(trifluoromethyl)phenethyl]trisiloxane (2-2-8)



2-2-8

Physical Appearance: Colorless clear liquid.

Yield: 56.8 mg, 72%. [containing ca. 5% of dehydrogenative silylation (DS) product]

¹H NMR (CDCl₃, 500 MHz): δ 7.52 (d, *J* = 8.0 Hz, 2H, Ar-*H*), 7.30 (d, *J* = 8.0 Hz, 2H, Ar-*H*), 2.70-2.67 (nfom, 2H, Ar-CH₂CH₂), 0.84-0.81 (nfom, 2H, Ar-CH₂CH₂), 0.13 [s, 18H, MeSi{OSi(CH₃)₃}₂], and 0.04 [s, 3H, CH₃Si(OTMS)₂].

^{13}C NMR (CDCl_3 , 125 MHz): δ 149.5, 143.5 (DS), 128.3, 128.1 ($^2J_{\text{F-C}} = 32$ Hz), 126.9 (DS), 126.8 ($^1J_{\text{F-C}} = 271$ Hz), 125.4 ($^3J_{\text{F-C}} = 3.6$ Hz), 29.4, 19.7, 2.1, and -0.12 .

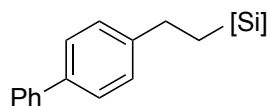
TLC: $R_f = 0.6$ in hexanes.

GC-MS (5029017): $t_R = 9.17$ min, m/z 395 [(M+H) $^+$, 2], 376 [(M-F) $^+$, 100], 221 (130), and 155 (50).

IR (neat): 2958 (m), 1618 (w), 1416 (w), 1324 (s), 1252 (s), 1163 (m), 1125 (s), 1041 (s), 836 (s), 815 (s), 797 (s), 781 (s), 752 (s), 687 (m), and 614 (w) cm^{-1} .

HRMS (ESI/TOF): Calcd for (M+Na) $^+$ ($\text{C}_{16}\text{H}_{29}\text{F}_3\text{NaO}_2\text{Si}_3$) $^+$: 417.1320. Found: 417.1280.

3-[2-((1,1'-Biphenyl)-4-yl)ethyl]-1,1,1,3,5,5,5-heptamethyltrisiloxane (2-2-9)



2-2-9

Yield: 59.5 mg, 74%.

Physical Appearance: Colorless clear liquid.

^1H NMR (CDCl_3 , 500 MHz): δ 7.60 (dd, $J = 8.3, 1.2$ Hz, 2H, Ar- H), 7.53 (d, $J = 8.2$ Hz, 2H, Ar- H), 7.44 (dd, $J = 8.3, 7.4$ Hz, 2H, Ar- H), 7.35 (ddd, $J = 7.4, 1.2, 1.2$ Hz, 1H, Ar- H), 7.29 (d, $J = 8.2$ Hz, 2H, Ar- H), 2.72-2.69 (nfom, 2H, Ar- CH_2CH_2), 0.91-0.87 (nfom, 2H, Ar- CH_2CH_2), 0.15 [s, 18H, $\text{MeSi}\{\text{OSi}(\text{CH}_3)_3\}_2$], and 0.07 [s, 3H, $\text{CH}_3\text{Si}(\text{OTMS})_2$].

^{13}C NMR (CDCl_3 , 125 MHz): δ 144.4, 141.4, 138.6, 128.8, 128.3, 127.18, 127.13, 127.05, 29.0, 19.8, 2.0, and -0.2 .

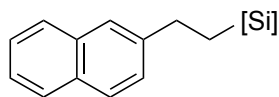
TLC: $R_f = 0.5$ in hexanes:EtOAc = 100:1.

GC-MS (5029017): $t_R = 13.11$ min, m/z 402 [M^+ , 20], 388 [(M- CH_3) $^+$, 60], and 221 (100).

IR (neat): 2956 (m), 1486 (m), 1449 (w), 1408 (w), 1251 (s), 1178 (w), 1038 (s), 1041 (s), 853 (s), 796 (s), 781 (s), 752 (s), 695 (m), 585 (m), and 501 (m) cm^{-1} .

HRMS (ESI/TOF): Calcd for (M+Na) $^+$ ($\text{C}_{21}\text{H}_{34}\text{NaO}_2\text{Si}_3$) $^+$: 425.1759. Found: 425.1803.

1,1,1,3,5,5,5-Heptamethyl-3-[2-(naphthalen-2-yl)ethyl]trisiloxane (2-2-10)



2-2-10

Physical Appearance: Colorless clear liquid.

Yield: 62.4 mg, 83%.

¹H NMR (CDCl₃, 500 MHz): δ 7.81-7.76 (m, 3H, Ar-*H*), 7.62 (s, 1H, Ar-*H*), 7.44 (ddd, *J* = 8.1, 6.8, 1.3, 1H, Ar-*H*), 7.40 (ddd, *J* = 8.1, 6.8, 1.3, 1H, Ar-*H*), 7.35 (dd, *J* = 8.4, 1.7 Hz, 1H, Ar-*H*), 2.82-2.79 (nfom, 2H, Ar-CH₂CH₂), 0.94-0.90 (nfom, 2H, Ar-CH₂CH₂), 0.13 [s, 18H, MeSi{OSi(CH₃)₃}₂], and 0.06 [s, 3H, CH₃Si(OTMS)₂].

¹³C NMR (CDCl₃, 125 MHz): δ 142.9, 133.9, 132.1, 128.0, 127.80, 127.61, 127.3, 126.0, 125.6, 125.2, 29.7, 19.9, 2.1, and 0.0.

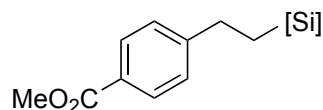
TLC: R_f = 0.7 in hexanes:EtOAc = 100:1.

GC-MS (5029017): *t_R* = 12.18 min, *m/z* 376 [M⁺, 20], 362 [(M-CH₃)⁺, 60], and 221 (100).

IR (neat): 2957 (m), 1600 (w), 1508 (w), 1251 (s), 1179 (w), 1038 (s), 835 (s), 798 (s), 781 (s), 751 (s), 687 (m), and 473 (m) cm⁻¹.

HRMS (ESI/TOF): Calcd for (M+Na)⁺ (C₁₉H₃₂NaO₂Si₃)⁺: 399.1602. Found: 399.1635.

Ethyl 4-[2-(1,1,1,3,5,5,5-Heptamethyltrisiloxan-3-yl)ethyl]benzoate (2-2-11)



2-2-11

Physical Appearance: Colorless clear liquid.

Yield: 55.5 mg, 71%.

¹H NMR (CDCl₃, 500 MHz): δ 7.95 (d, *J* = 8.3 Hz, 2H, Ar-*H*), 7.25 (d, *J* = 8.3 Hz, 2H, Ar-*H*), 4.36 (q, *J* = 7.1 Hz, 2H, ArCO₂CH₂CH₃), 2.70-2.66 (nfom, 2H, Ar-CH₂CH₂), 1.39 (t, *J* = 7.1 Hz, 3H,

ArCO₂CH₂CH₃), 0.84-0.81 (nfom, 2H, Ar-CH₂CH₂), 0.08 [s, 18H, MeSi{OSi(CH₃)₃}₂], and 0.03 [s, 3H, CH₃Si(OTMS)₂].

¹³C NMR (CDCl₃, 125 MHz): δ 167.0, 150.8, 129.9, 128.07, 128.00, 60.9, 29.6, 19.7, 14.6, 2.1, and -0.1.

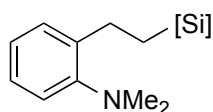
TLC: R_f = 0.3 in hexanes:EtOAc = 80:1.

GC-MS (5029017): *t_R* = 11.86 min, *m/z* 398 [M⁺, 20], 383 [(M-CH₃)⁺, 15], 353 (30), 340 (20), and 132 (100).

IR (neat): 2957 (m), 1719 (s), 1610 (w), 1414 (w), 1366 (w), 1273 (s), 1251 (s), 1178 (m), 1105 (m), 1040 (s), 835 (s), 781 (s), 752 (s), 688 (m), and 623 (w) cm⁻¹.

HRMS (ESI/TOF): Calcd for (M+Na)⁺ (C₁₈H₃₄NaO₄Si₃)⁺: 421.1657. Found: 421.1701.

2-[2-(1,1,1,3,5,5,5-Heptamethyltrisiloxan-3-yl)ethyl]-*N,N*-dimethylaniline (2-2-12)



2-2-12

Physical Appearance: Colorless clear liquid.

Yield: 38.4 mg, 52%.

¹H NMR (CDCl₃, 500 MHz): δ 7.21 (dd, *J* = 7.5, 1.6 Hz, 1H, Ar-*H*), 7.15 (ddd, *J* = 8.0, 7.3, 1.6 Hz, 1H, Ar-*H*), 7.07 (dd, *J* = 8.0, 1.6 Hz, 1H, Ar-*H*), 7.01 (ddd, *J* = 7.5, 7.3, 1.6 Hz, 1H, Ar-*H*), 2.75-2.69 (nfomm, 1H, Ar-CH₂CH₂), 2.67 (s, 6H, Ar-NMe₂), 0.87-0.81 (nfomm, 2H, Ar-CH₂CH₂), 0.11 [s, 18H, MeSi{OSi(CH₃)₃}₂], and 0.06 [s, 3H, CH₃Si(OTMS)₂].

¹³C NMR (CDCl₃, 125 MHz): δ 152.5, 140.0, 129.2, 126.3, 123.4, 119.4, 45.2, 24.0, 19.0, 2.1, and -0.1.

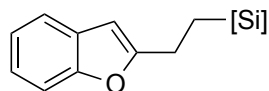
TLC: R_f = 0.3 in hexanes:EtOAc = 200:1.

GC-MS (5029017): *t_R* = 10.23 min, *m/z* 370 [(M+H)⁺, 70], 354 [(M-CH₃)⁺, 30], 221 (80), and 148 (100).

IR (neat): 2956 (m), 1597 (w), 1491 (m), 1452 (w), 1251 (s), 1039 (s), 836 (s), 800 (s), 781 (s), 751 (s), 687 (m), and 566 (w) cm⁻¹.

HRMS (ESI/TOF): Calcd for (M+H)⁺ (C₁₇H₃₆NO₂Si₃)⁺: 370.2048. Found: 370.2109.

3-[2-(Benzofuran-2-yl)ethyl]-1,1,1,3,5,5,5-heptamethyltrisiloxane (2-2-13)



2-2-13

Physical Appearance: Colorless clear liquid.

Yield: 48.3 mg, 66%.

¹H NMR (CDCl₃, 500 MHz): δ 7.49-7.46 (nfom, 1H, Ar-*H*), 7.43-7.39 (nfom, 1H, Ar-*H*), 7.20 (ddd, *J* = 7.3, 7.3, 1.9 Hz, 1H, Ar-*H*), 7.17 (ddd, *J* = 7.3, 7.3, 1.6 Hz, 1H, Ar-*H*), 6.38 (d, *J* = 0.8 Hz, 1H, Ar-*H*), 2.82-2.76 (nfom, 2H, Ar-CH₂CH₂), 0.98-0.92 (nfom, 2H, Ar-CH₂CH₂), 0.11 [s, 18H, MeSi{OSi(CH₃)₃}₂], and 0.06 [s, 3H, CH₃Si(OTMS)₂].

¹³C NMR (CDCl₃, 125 MHz): δ 161.9, 154.9, 129.3, 123.2, 122.5, 120.4, 110.9, 101.2, 22.4, 15.6, 2.1, and -0.2.

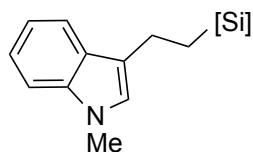
TLC: R_f = 0.8 in hexanes:EtOAc = 100:1.

GC-MS (5029017): *t_R* = 11.16 min, *m/z* 366 [M⁺, 30], 351 [(M-CH₃)⁺, 100], 278 (30), and 221 (90).

IR (neat): 2956 (m), 1600 (w), 1588 (w), 1455 (m), 1251 (s), 1183 (w), 1040 (s), 947 (w), 835 (s), 790 (s), 748 (s), 737 (s), and 687 (m) cm⁻¹.

HRMS (ESI/TOF): Calcd for (M+Na)⁺ (C₁₇H₃₀NaO₃Si₃)⁺: 389.1395. Found: 389.1445.

3-[2-(1,1,1,3,5,5,5-Heptamethyltrisiloxan-3-yl)ethyl]-1-methyl-1*H*-indole (2-2-14)



2-2-14

Physical Appearance: Colorless clear liquid.

Yield: 42.5 mg, 56%.

¹H NMR (CDCl₃, 500 MHz): δ 7.60 (d, *J* = 7.9 Hz, 1H, Ar-*H*), 7.29 (d, *J* = 8.2 Hz, 1H, Ar-*H*), 7.23 (dd, *J* = 8.2, 7.3 Hz, 1H, Ar-*H*), 7.11 (dd, *J* = 7.9, 7.3 Hz, 1H, Ar-*H*), 6.84 (s, 1H, Ar-*H*), 3.78-3.72 (s, 3H, NMe), 2.80-2.77 (m, 2H, Ar-CH₂CH₂), 0.97-0.92 (m, 2H, Ar-CH₂CH₂), 0.14 [s, 18H, MeSi{OSi(CH₃)₃}₂], and 0.07 [s, 3H, CH₃Si(OTMS)₂].

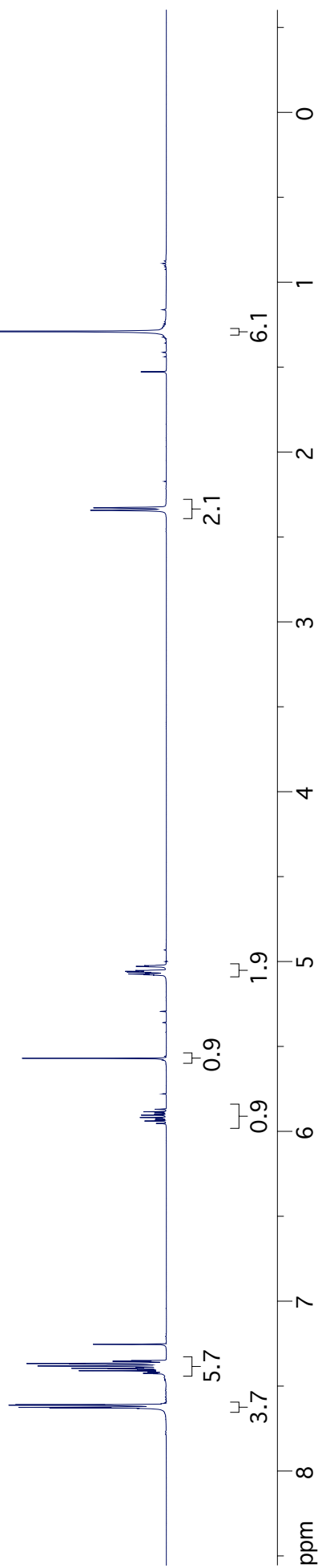
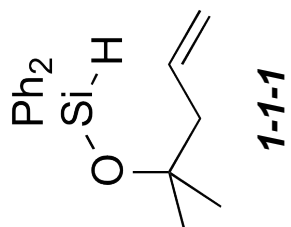
^{13}C NMR (CDCl_3 , 125 MHz): δ 137.3, 127.7, 125.5, 121.5, 119.1, 118.51, 118.33, 109.2, 32.6, 18.6, 18.4, 2.0, and -0.2 .

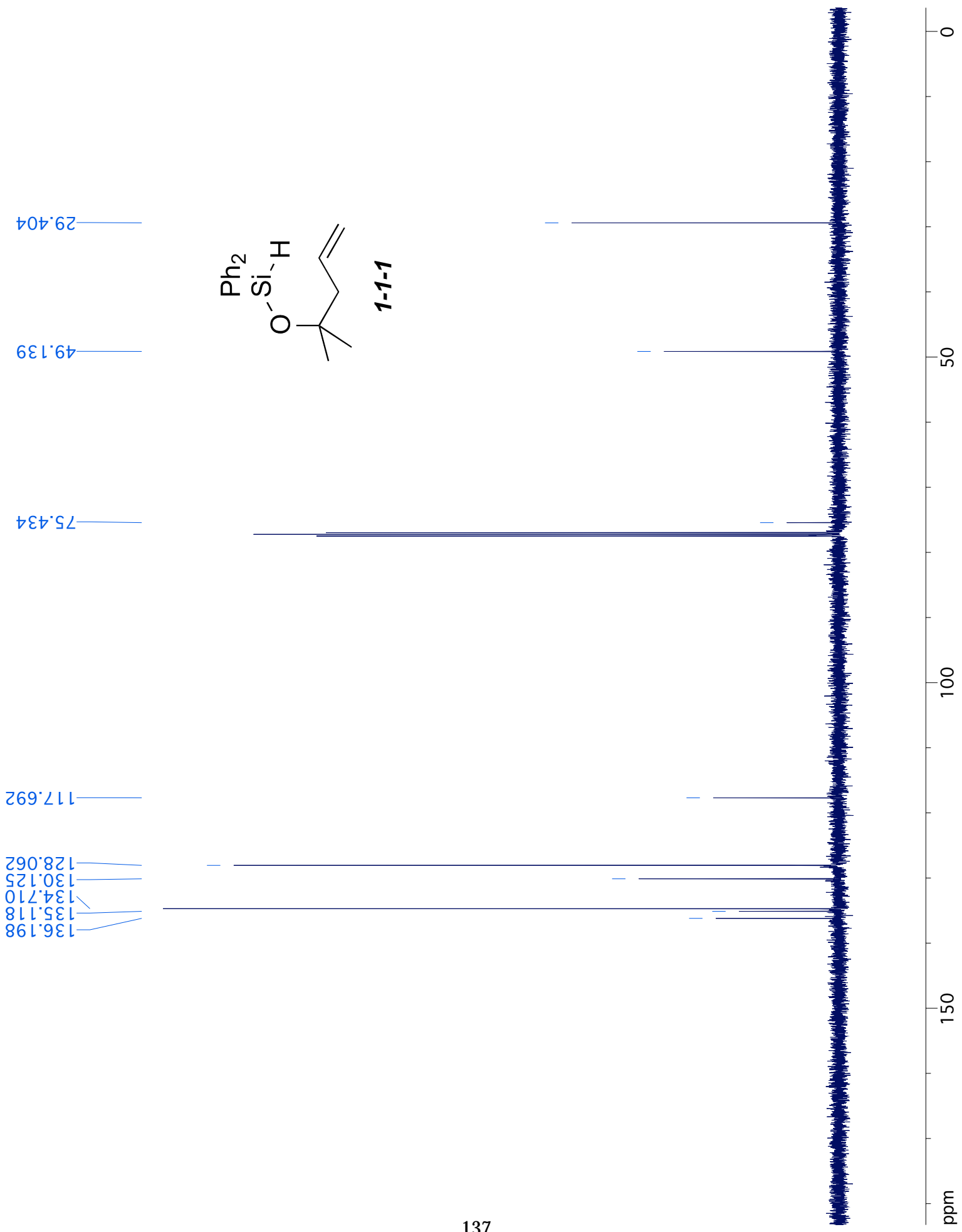
TLC: $R_f = 0.8$ in hexanes:EtOAc = 80:1.

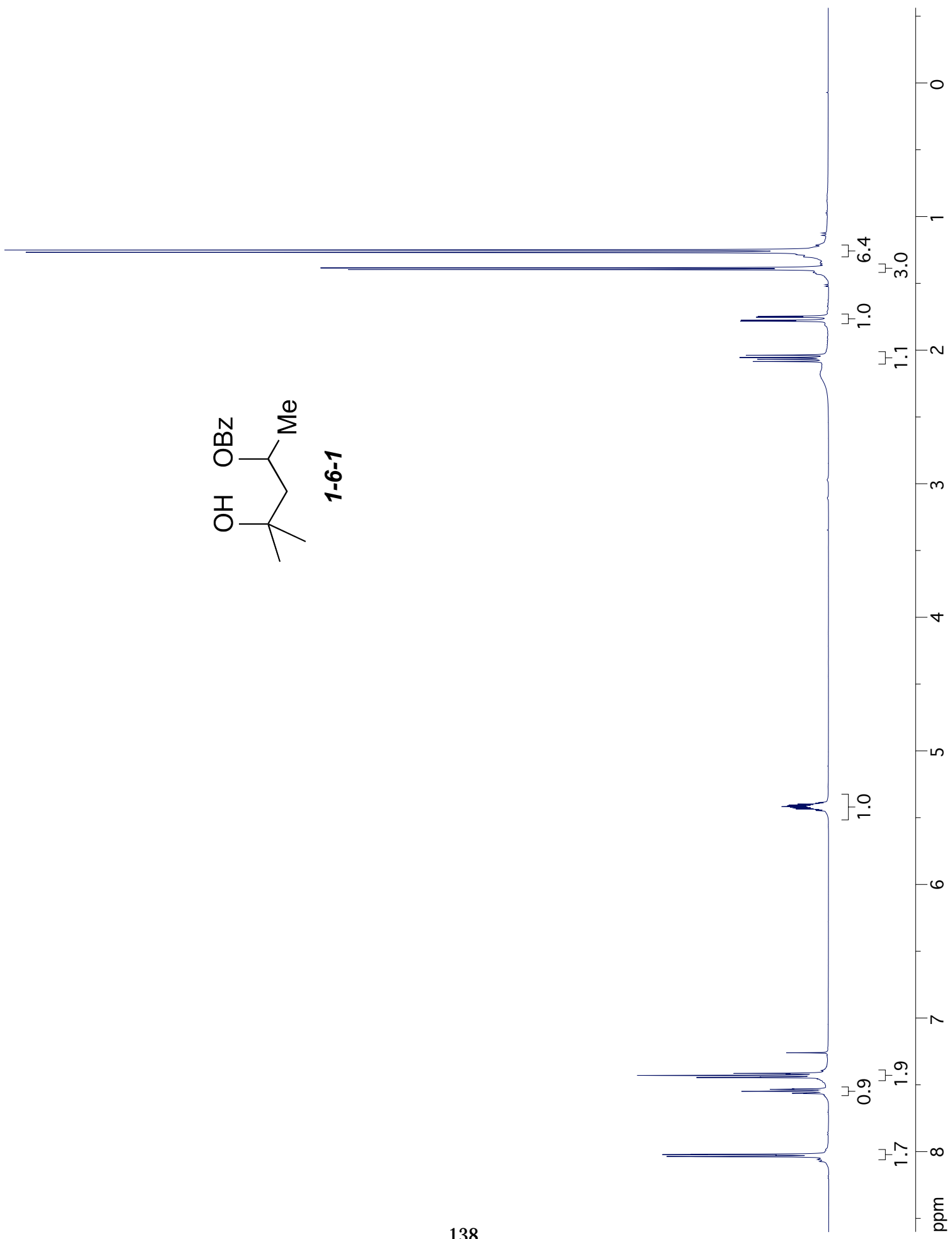
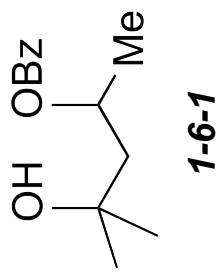
GC-MS (5029017): $t_R = 12.22$ min, m/z 379 [M^+ , 100], 366 [$(\text{M}-\text{CH}_3)^+$, 60], 337 (10), 291 (5), 280 (12), 144 (70), and 73 (5).

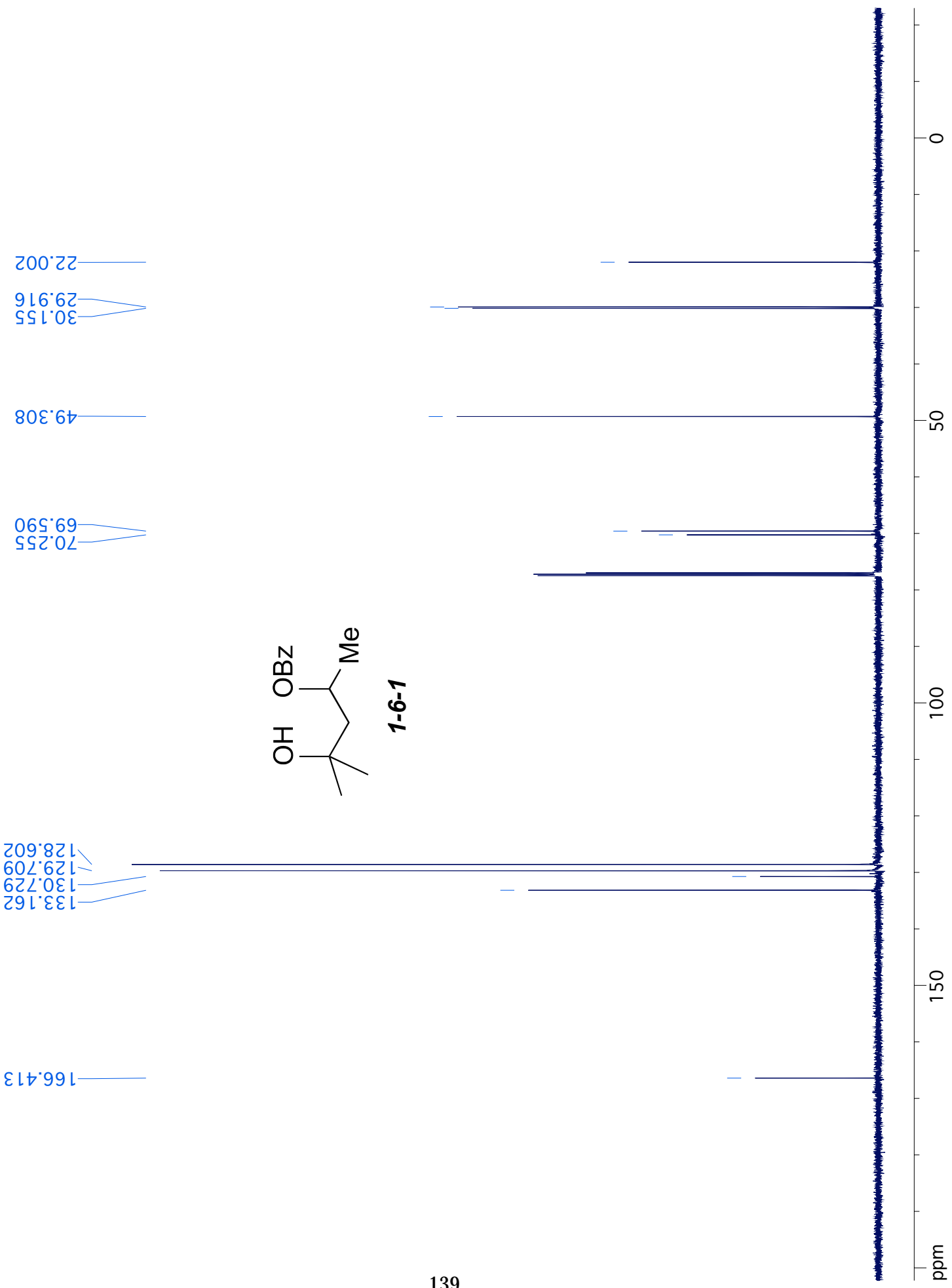
IR (neat): 2956 (m), 1615 (w), 1471 (w), 1423 (w), 1251 (s), 1037 (s), 835 (s), 785 (s), 752 (s), 733 (s), 686 (m), and 425 (w) cm^{-1} .

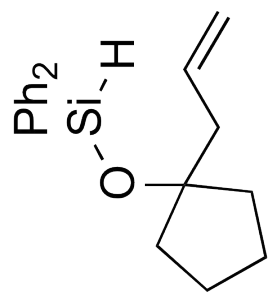
HRMS (ESI/TOF): Calcd for $(\text{M}+\text{Na})^+$ ($\text{C}_{18}\text{H}_{33}\text{NNaO}_2\text{Si}_3$) $^+$: 402.1711. Found: 402.1778



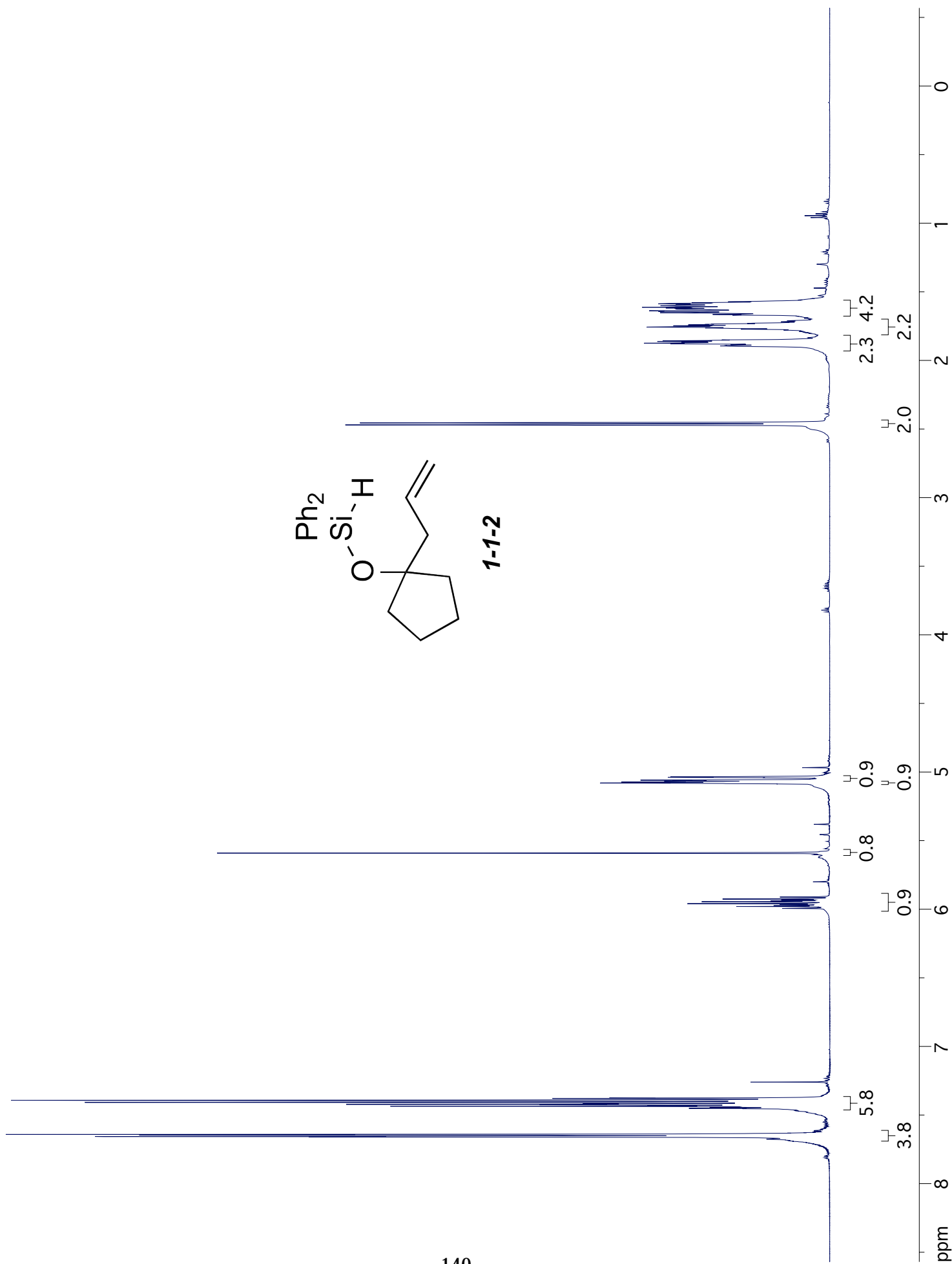


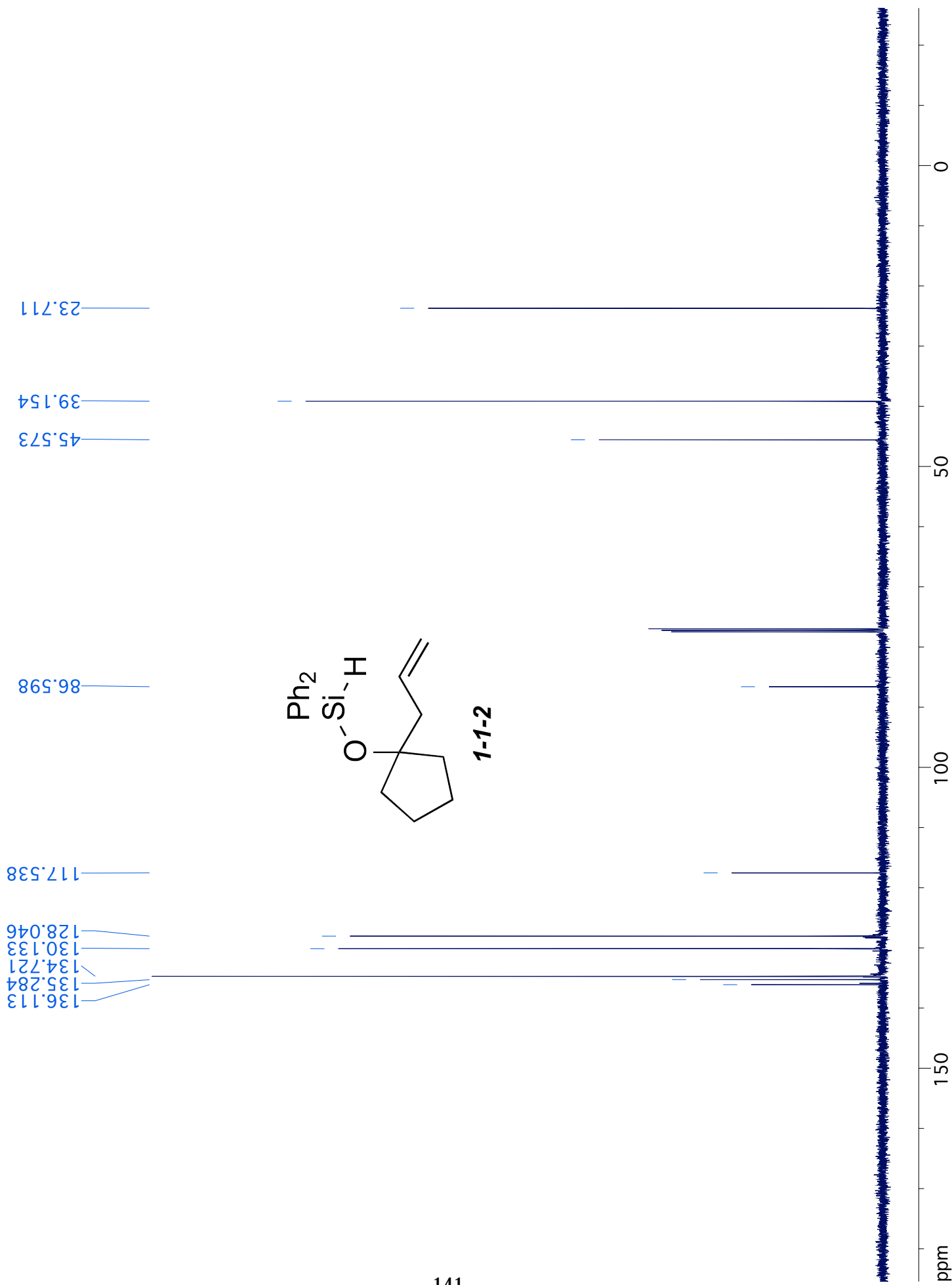


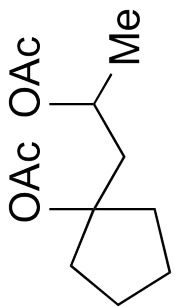




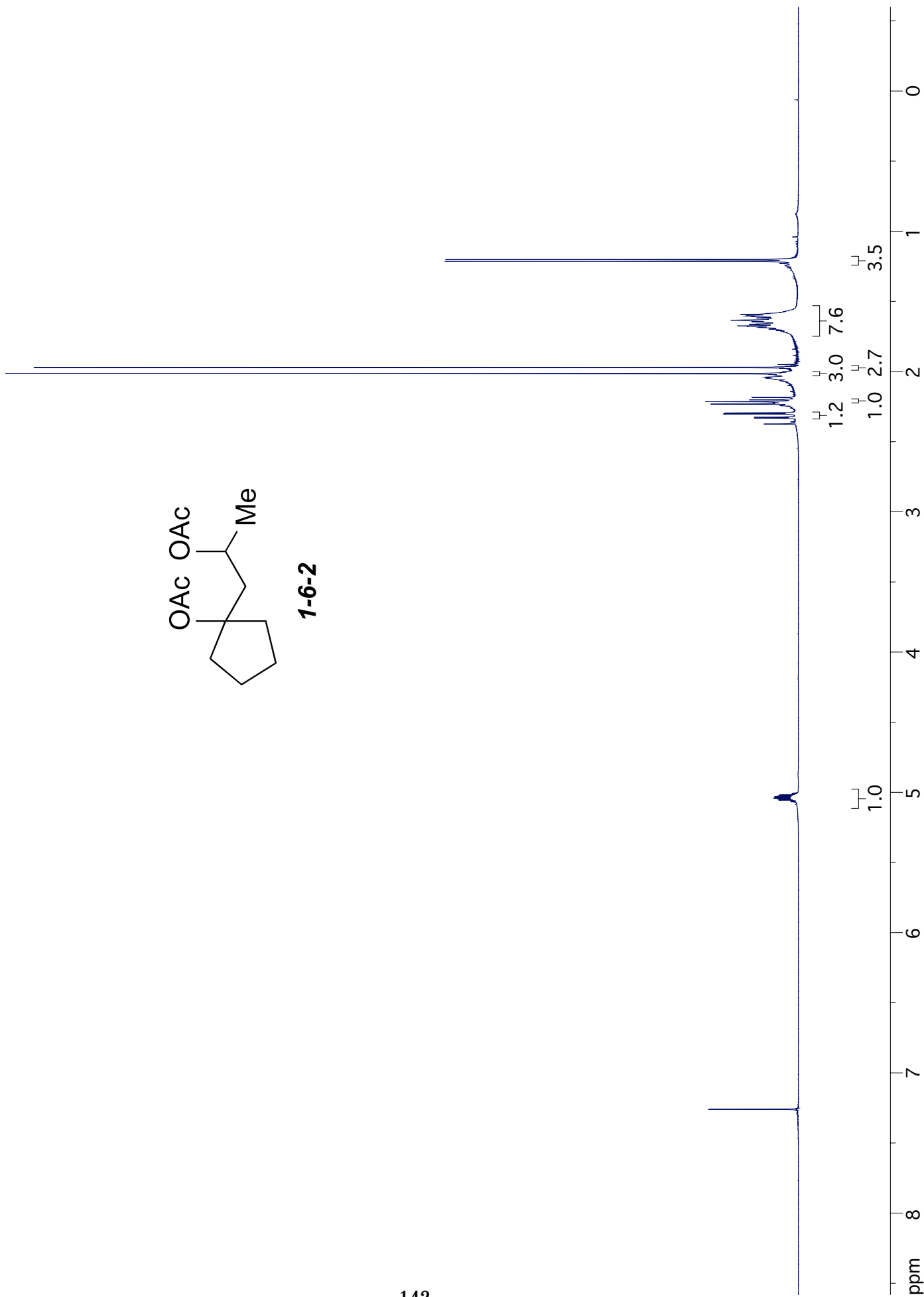
1-1-2

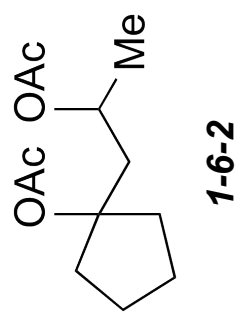
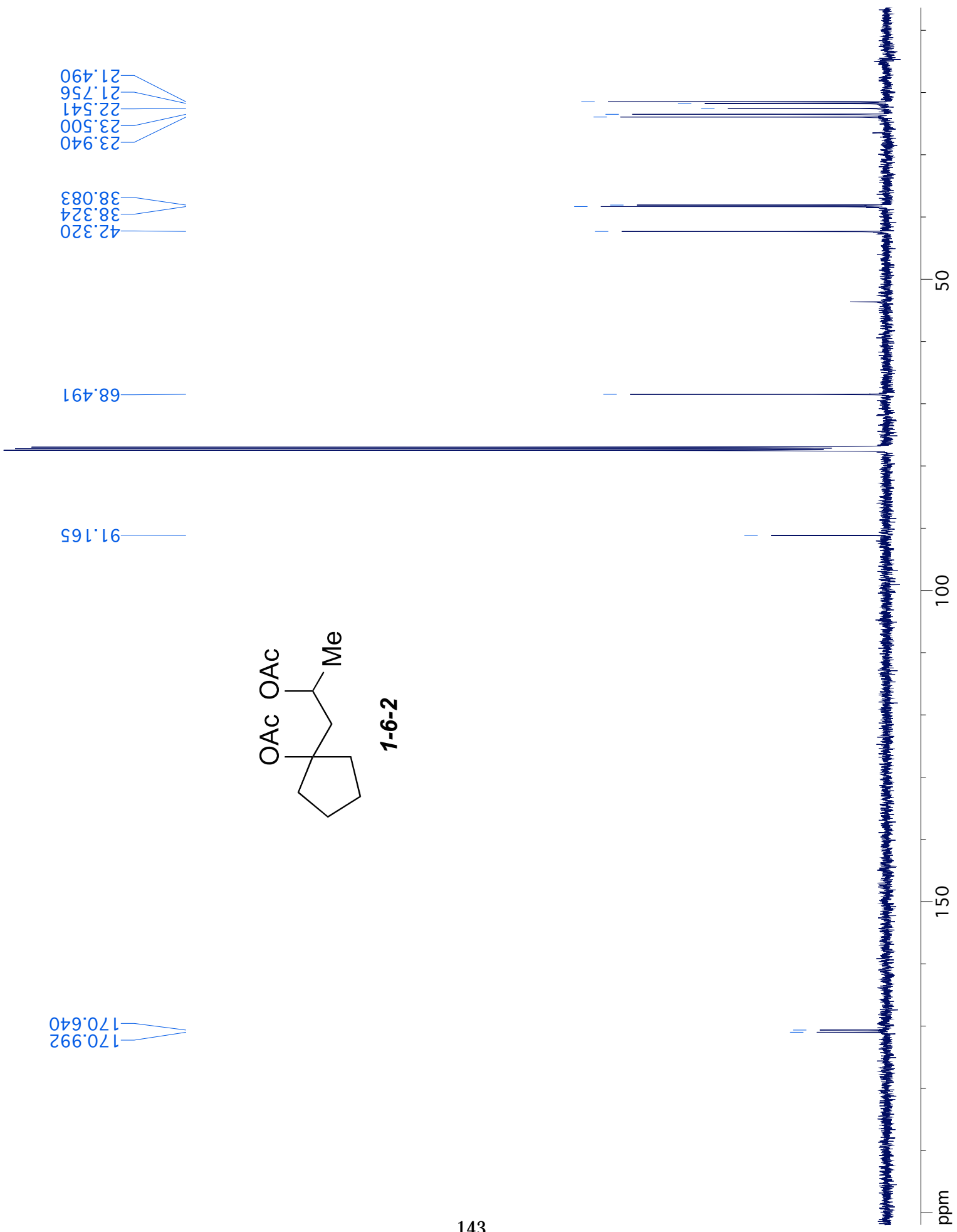


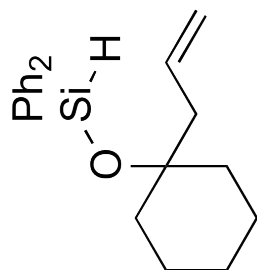




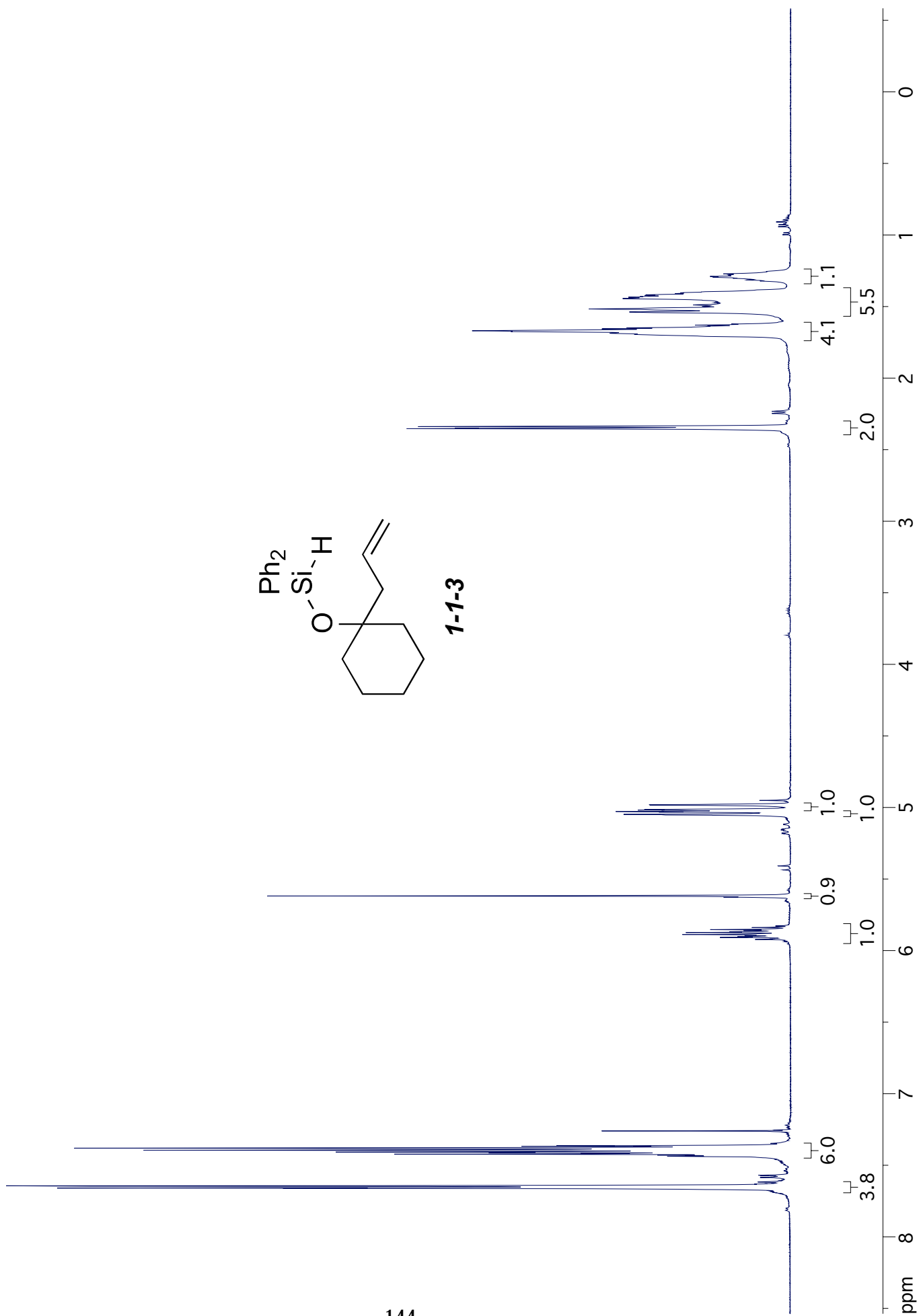
1-6-2

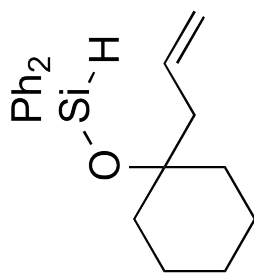






1-1-3

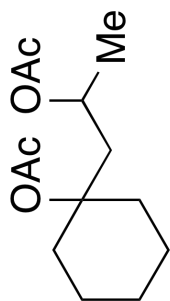




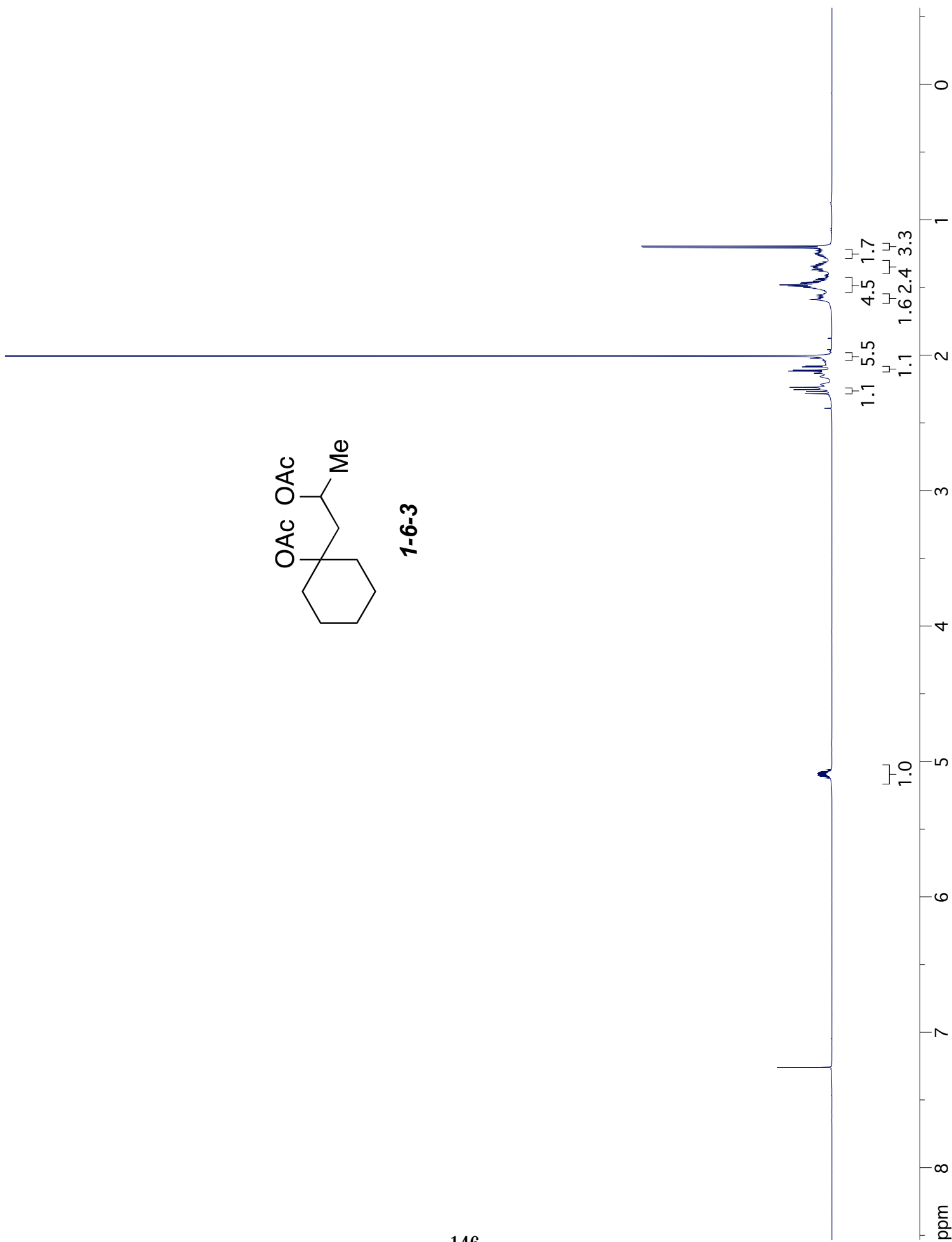
1-1-3

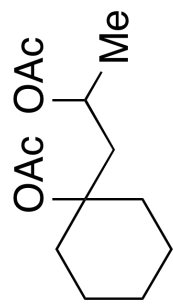
- 22.591
- 25.789
- 37.595
- 46.286
- 76.916
- 117.678
- 128.035
- 130.084
- 134.569
- 134.767
- 136.418



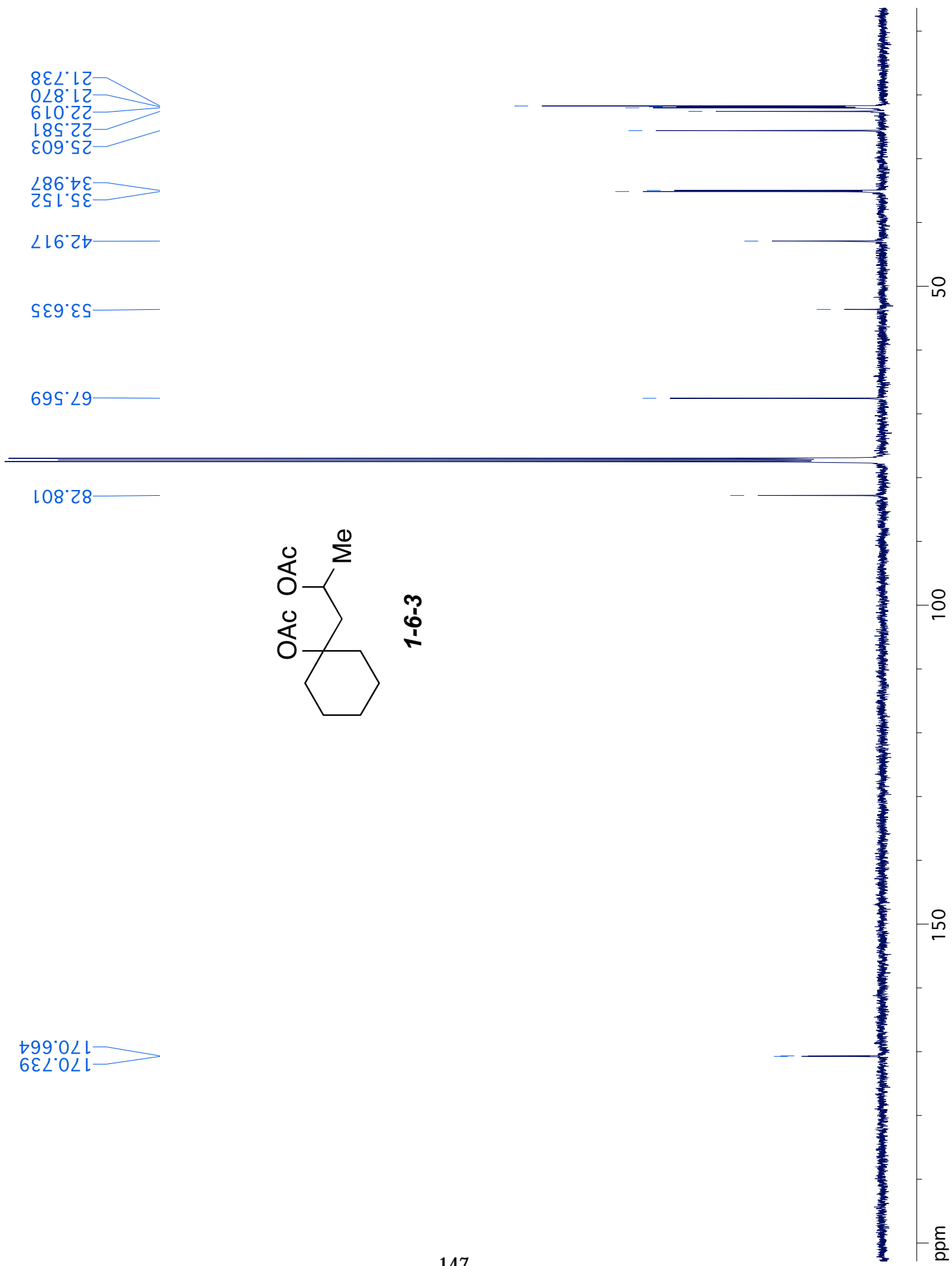


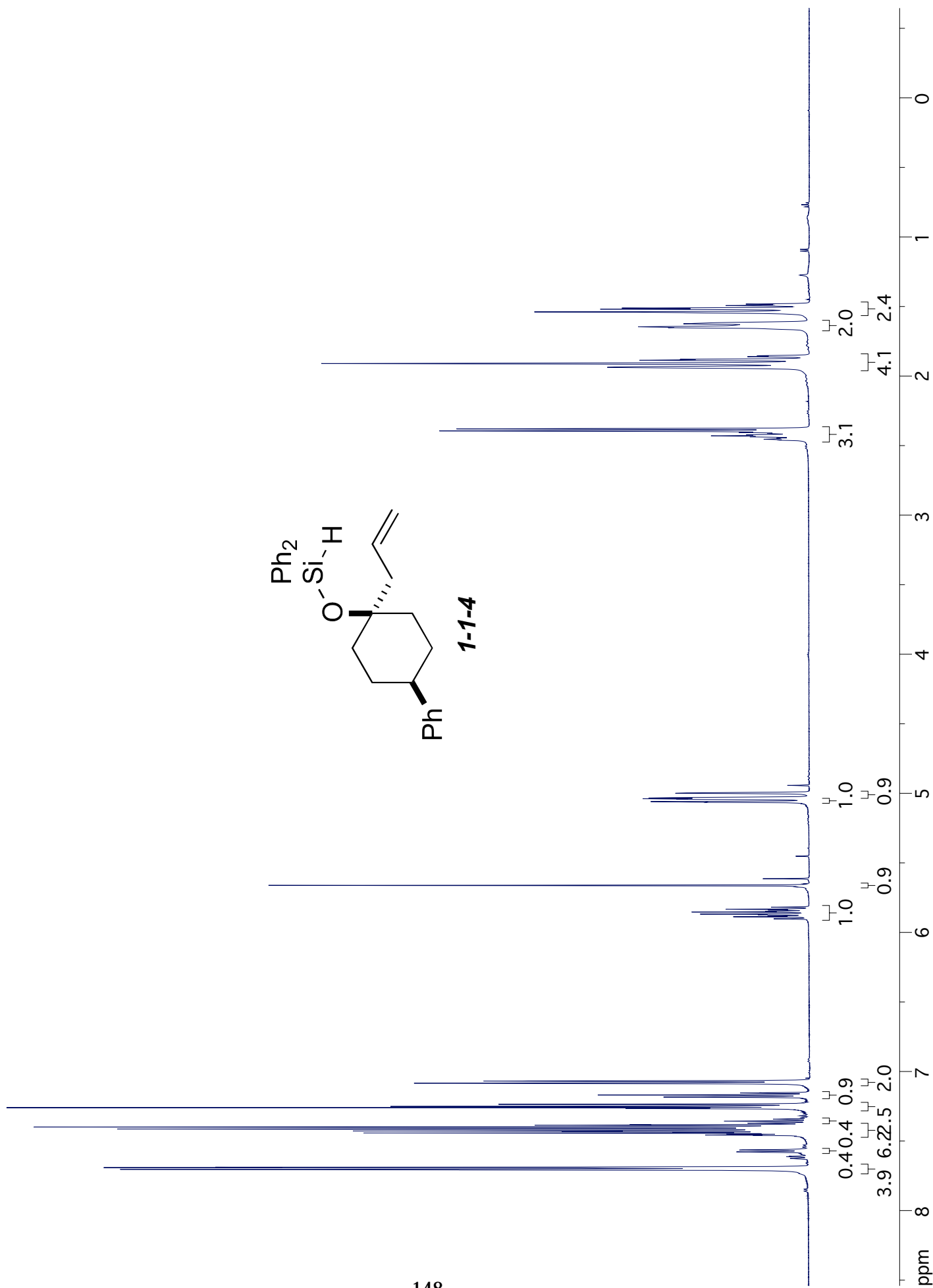
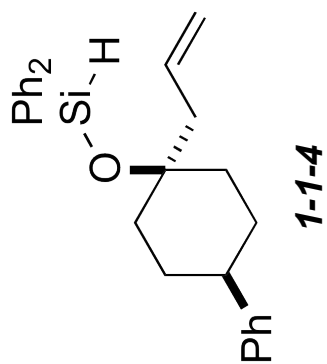
1-6-3

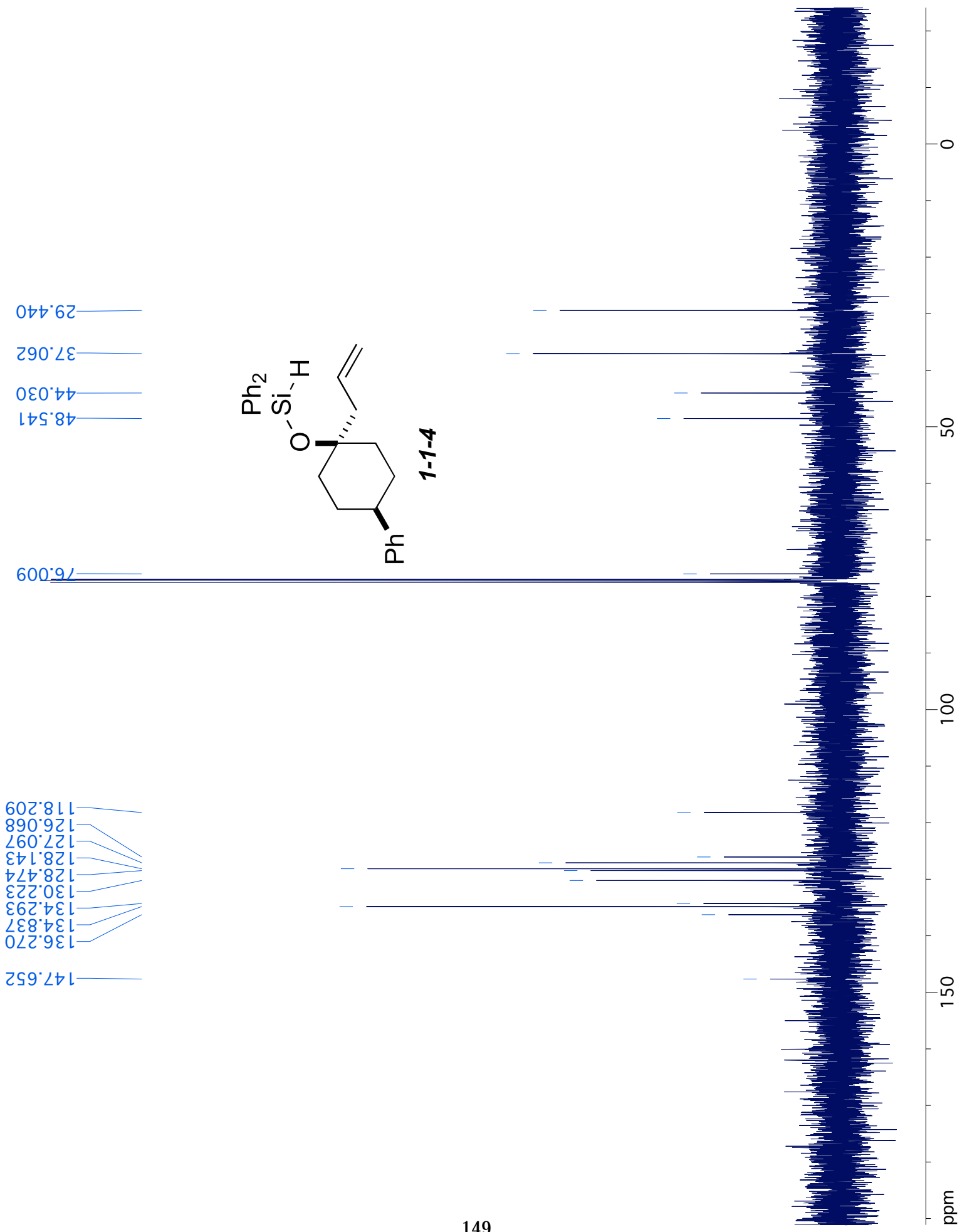


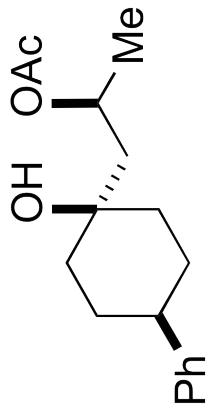


1-6-3

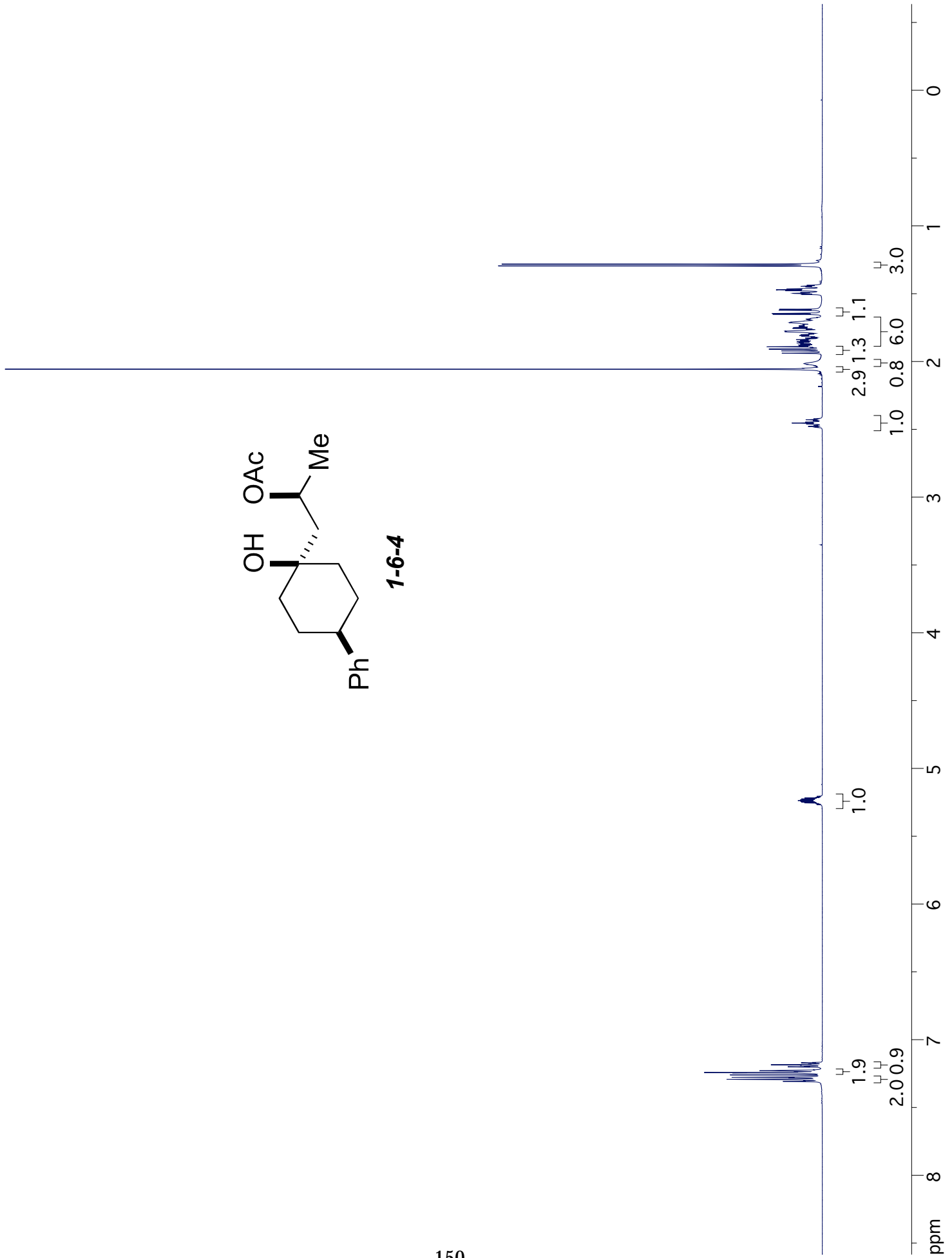




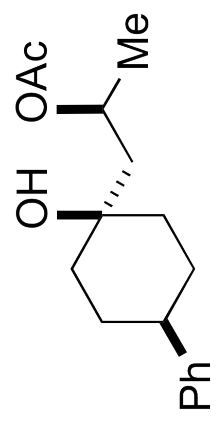




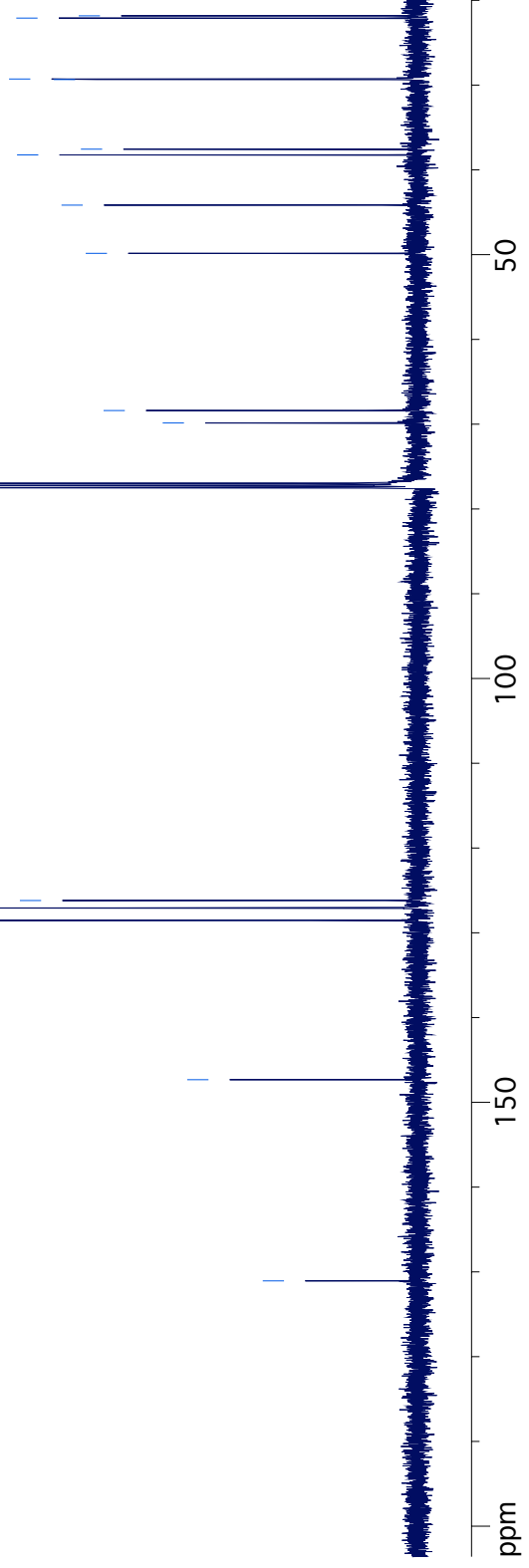
1-6-4

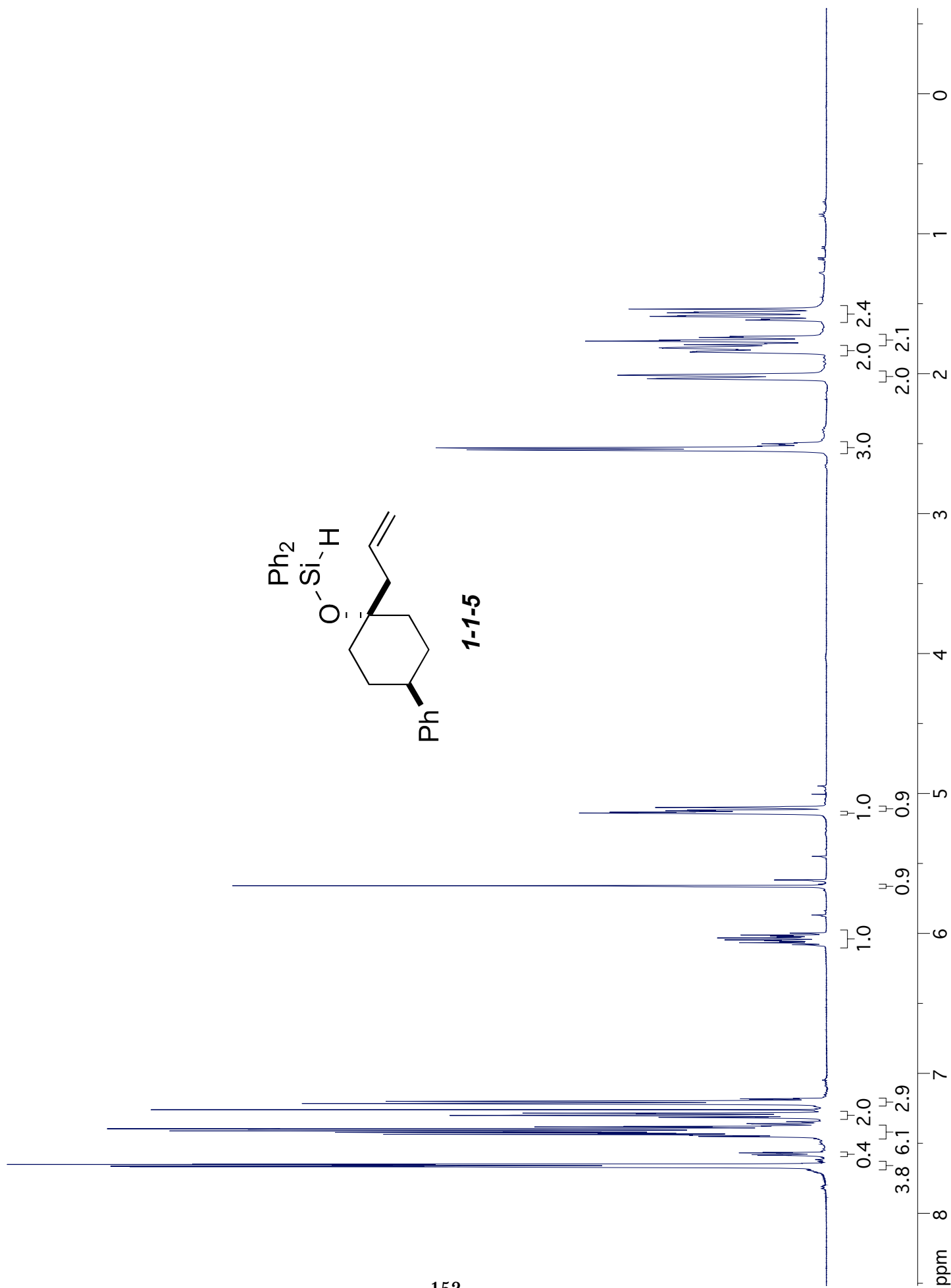
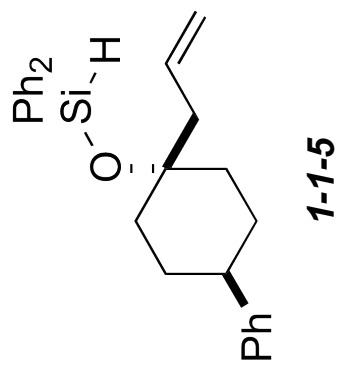


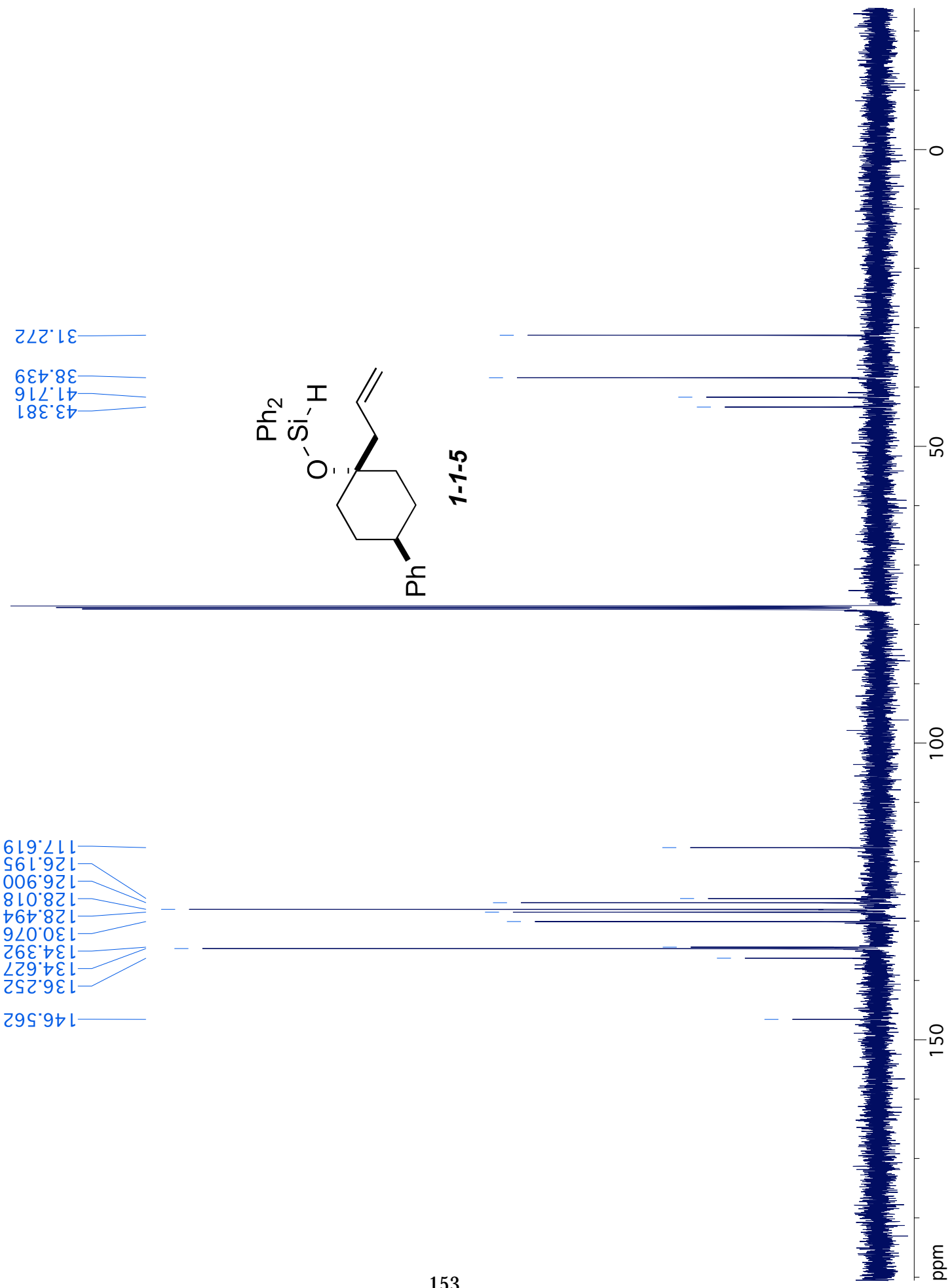
69.858
68.391
49.847
44.161
38.236
37.557
29.345
29.280
22.097
21.830

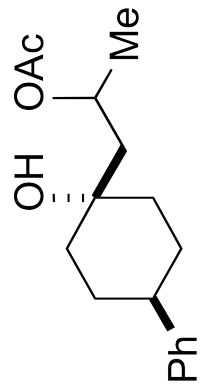


171.061
147.330
128.547
127.069
126.192

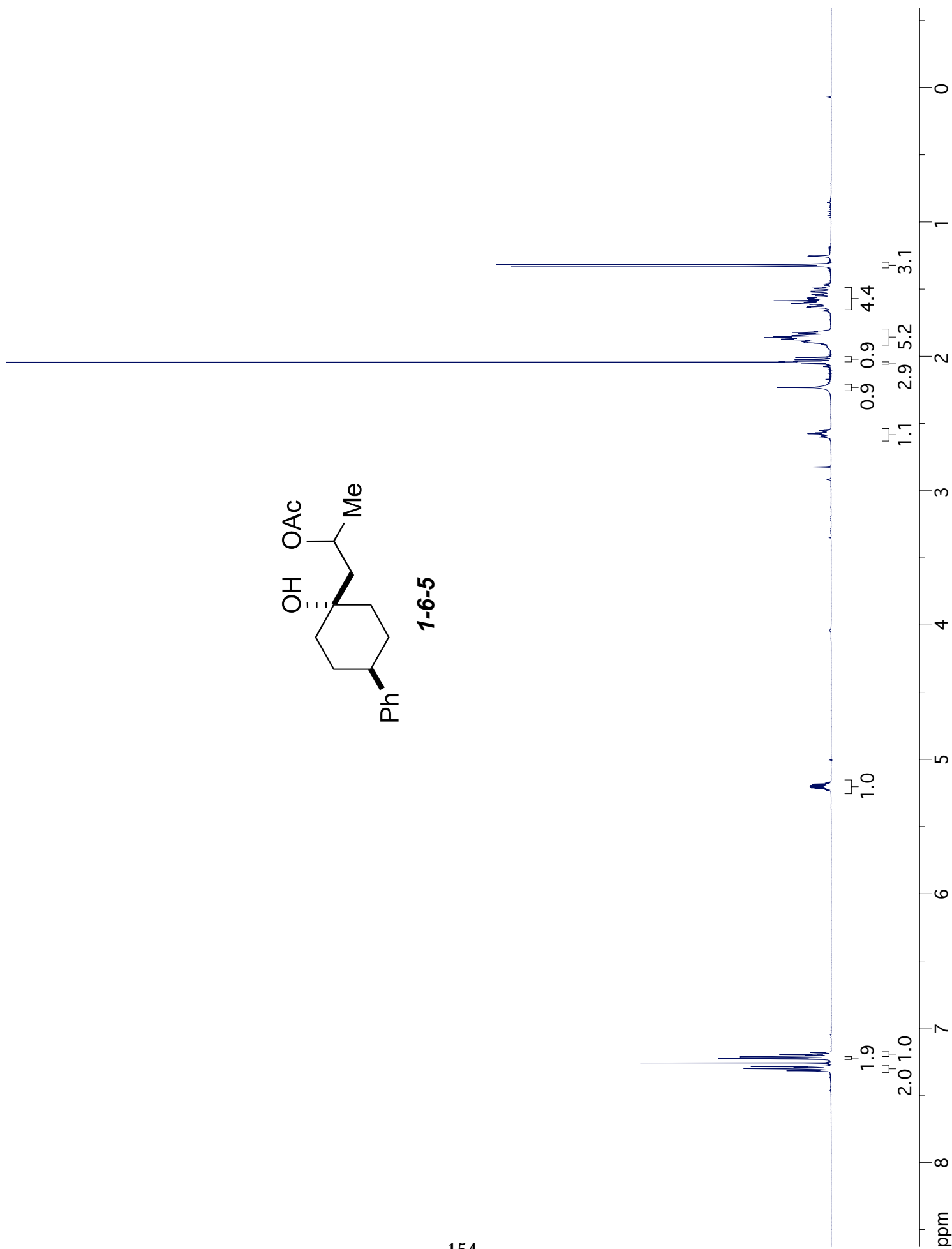


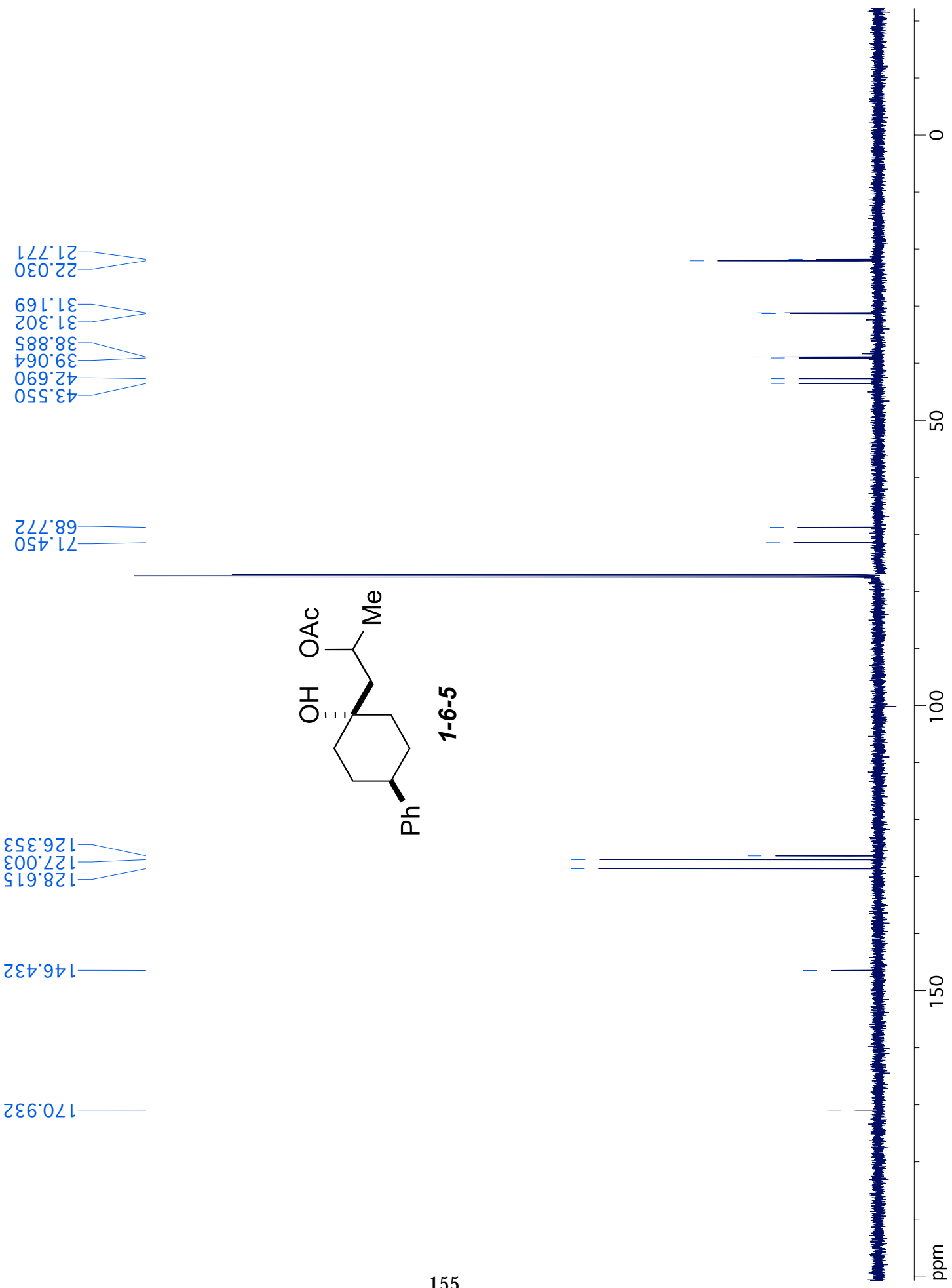


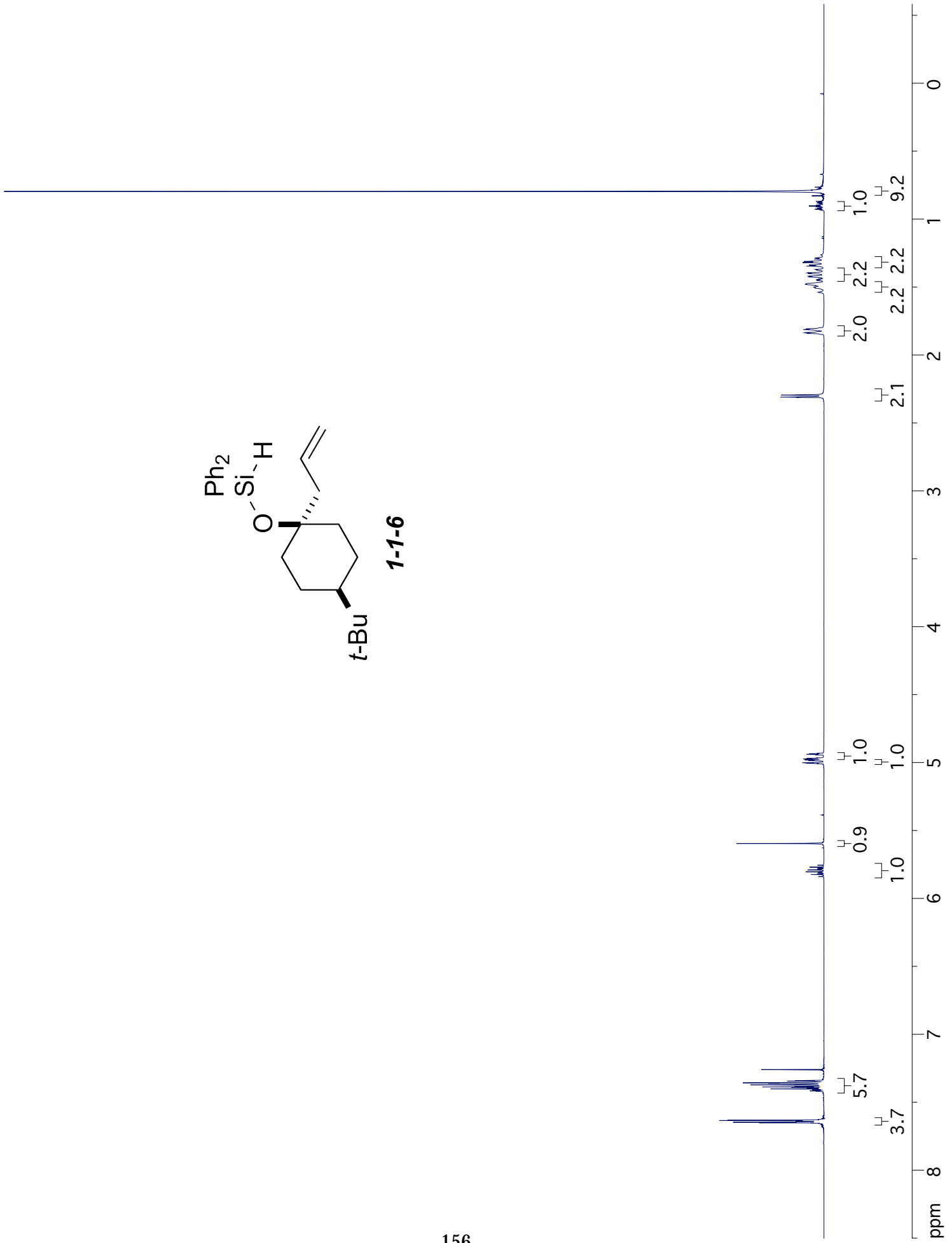
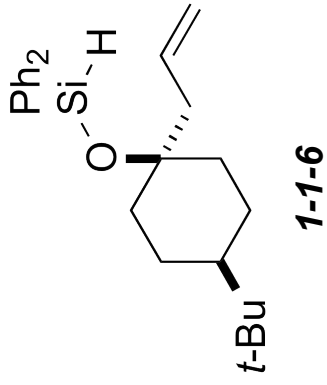




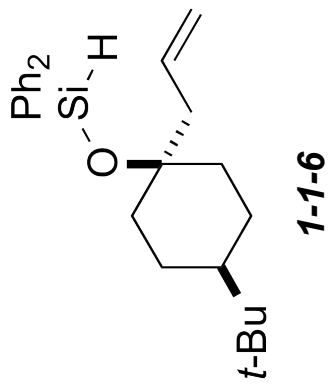
1-6-5



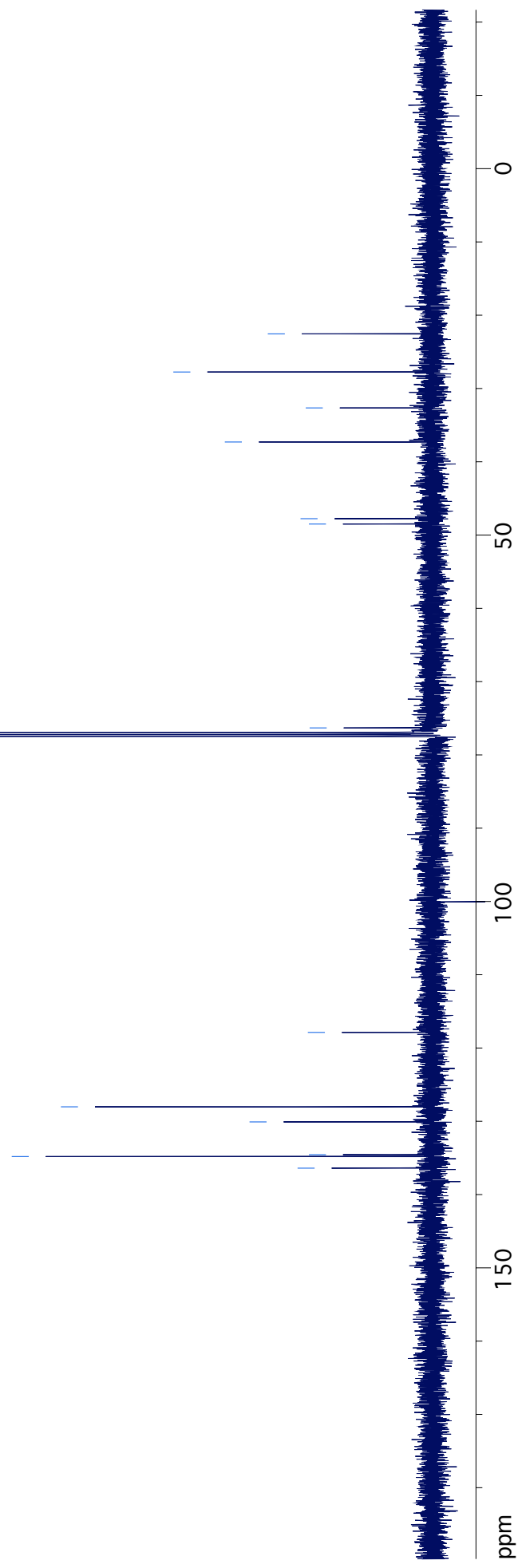


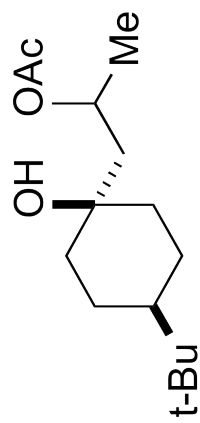


22.542
27.747
32.647
37.302
47.765
48.500
76.314

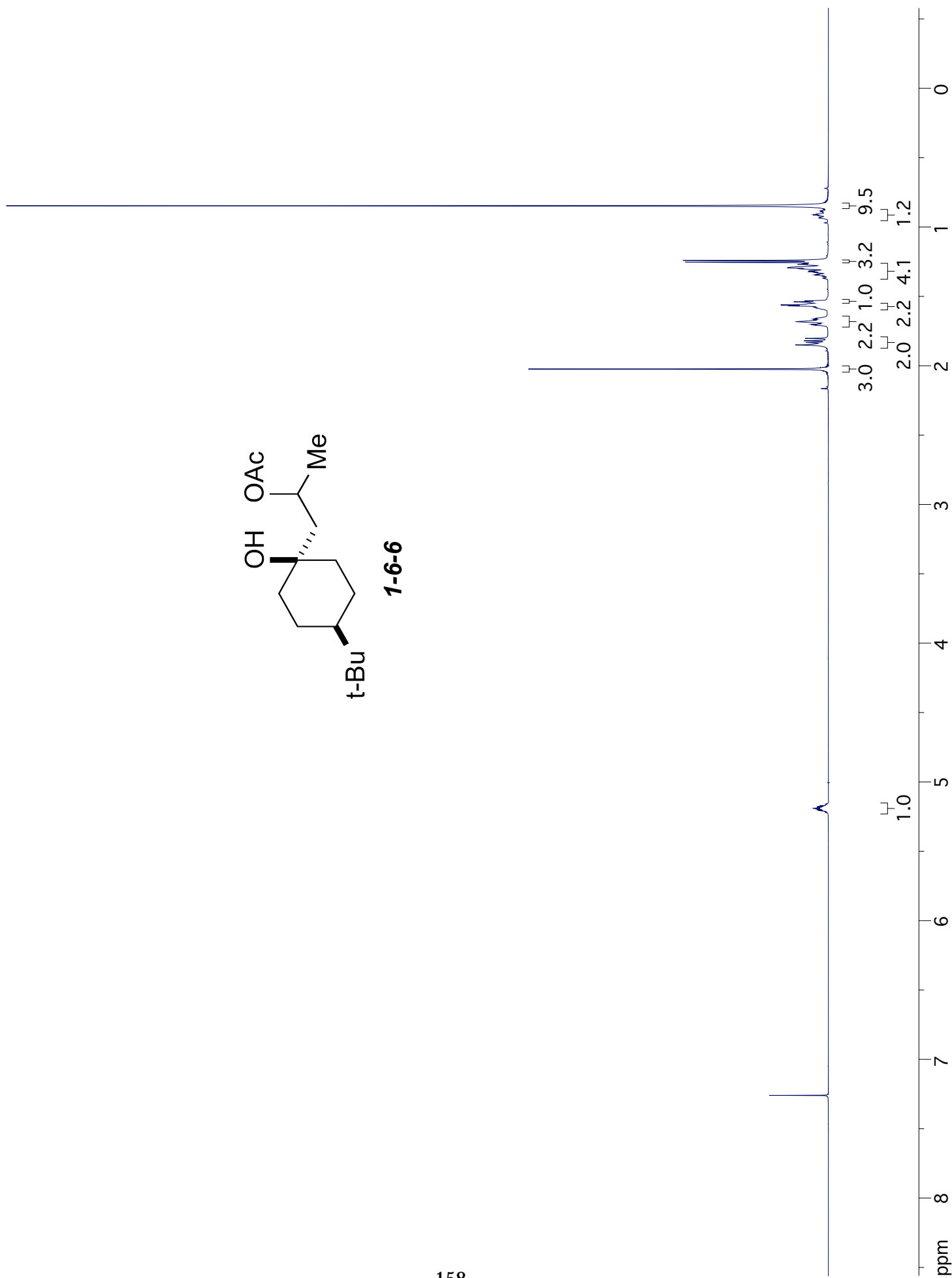


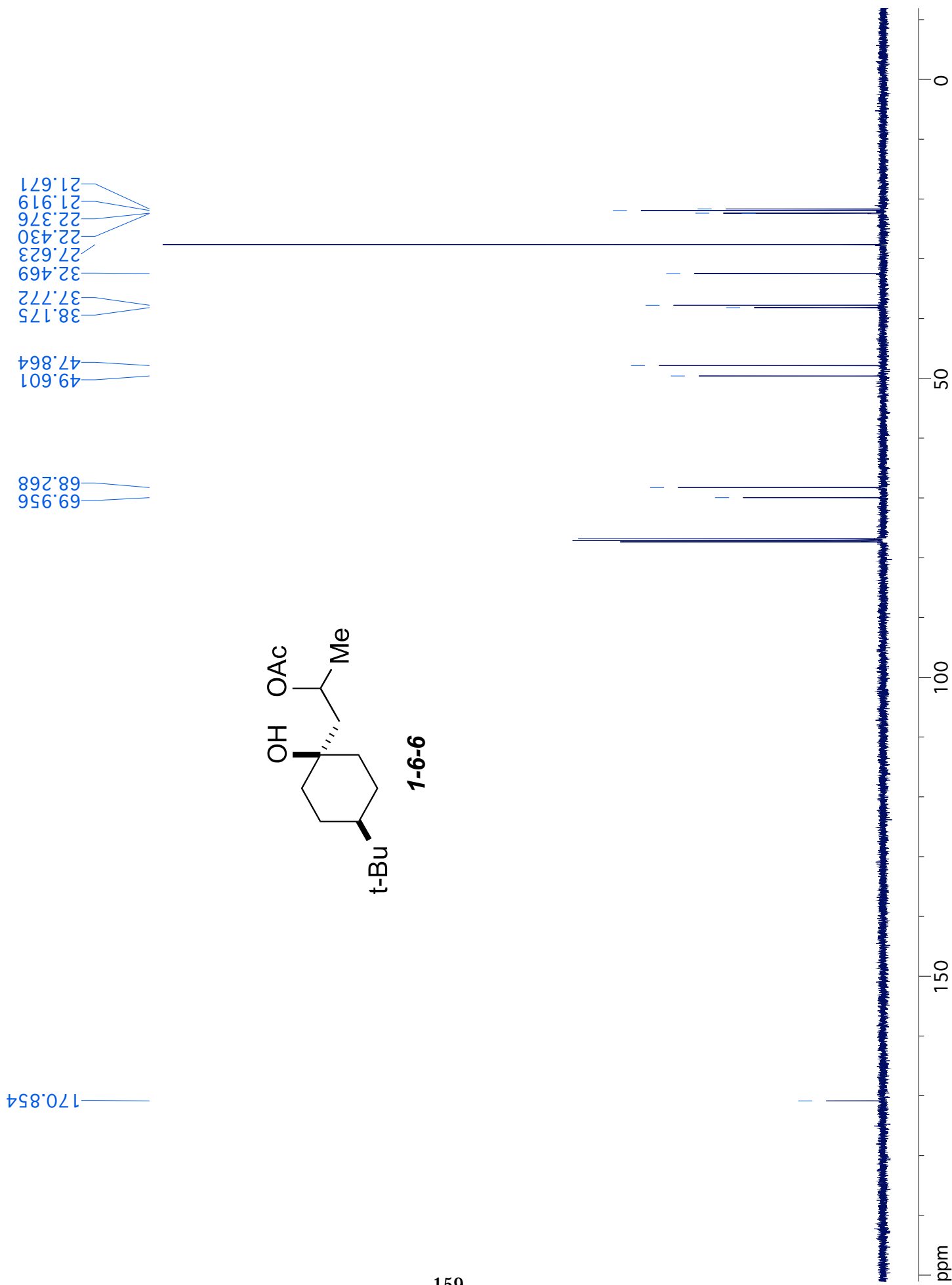
117.874
128.024
130.086
134.558
134.806
136.399

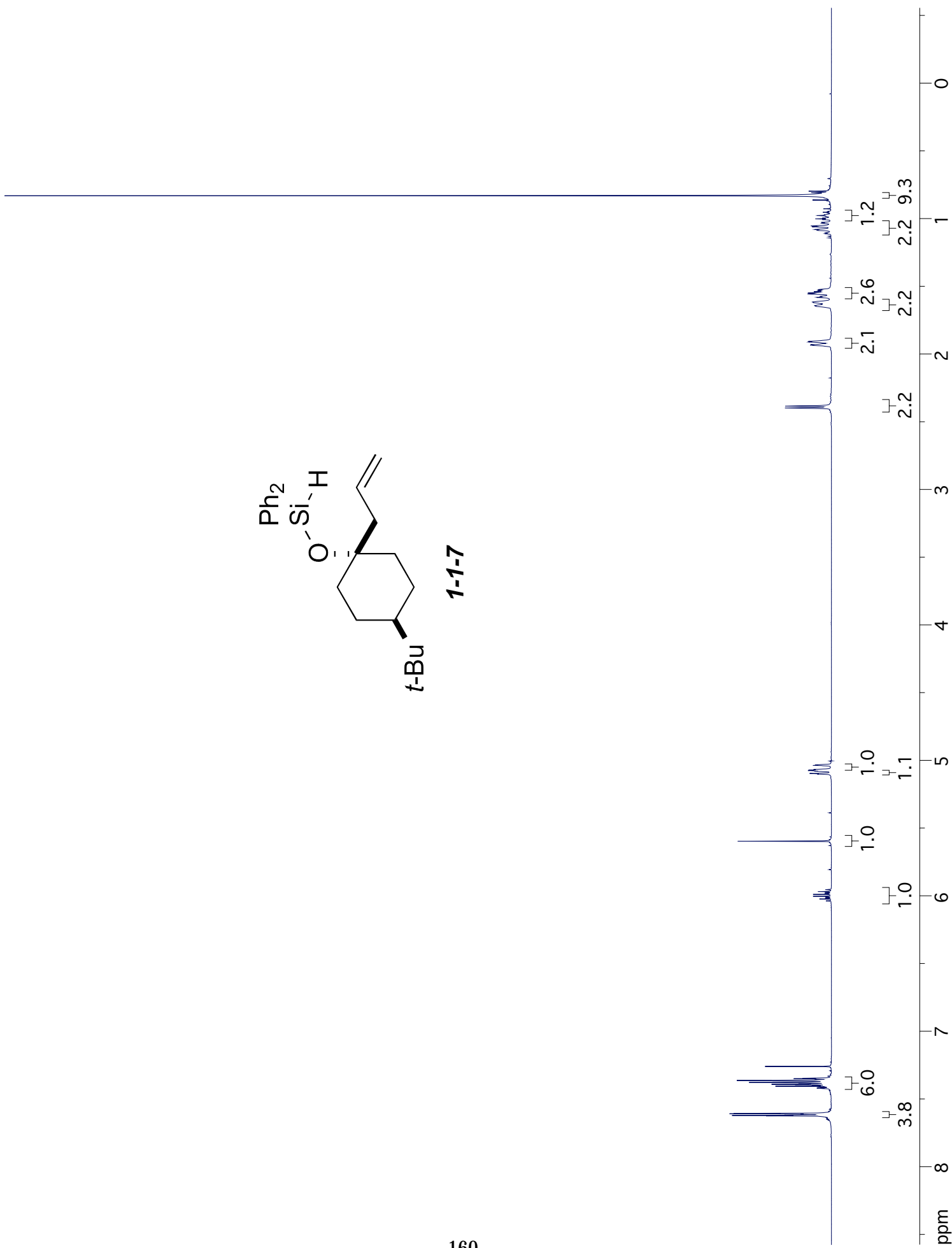
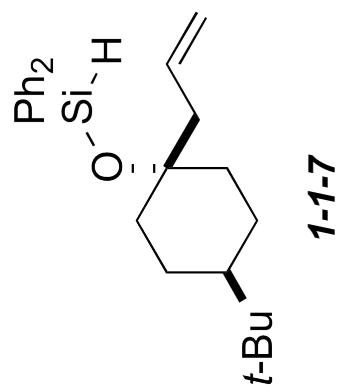


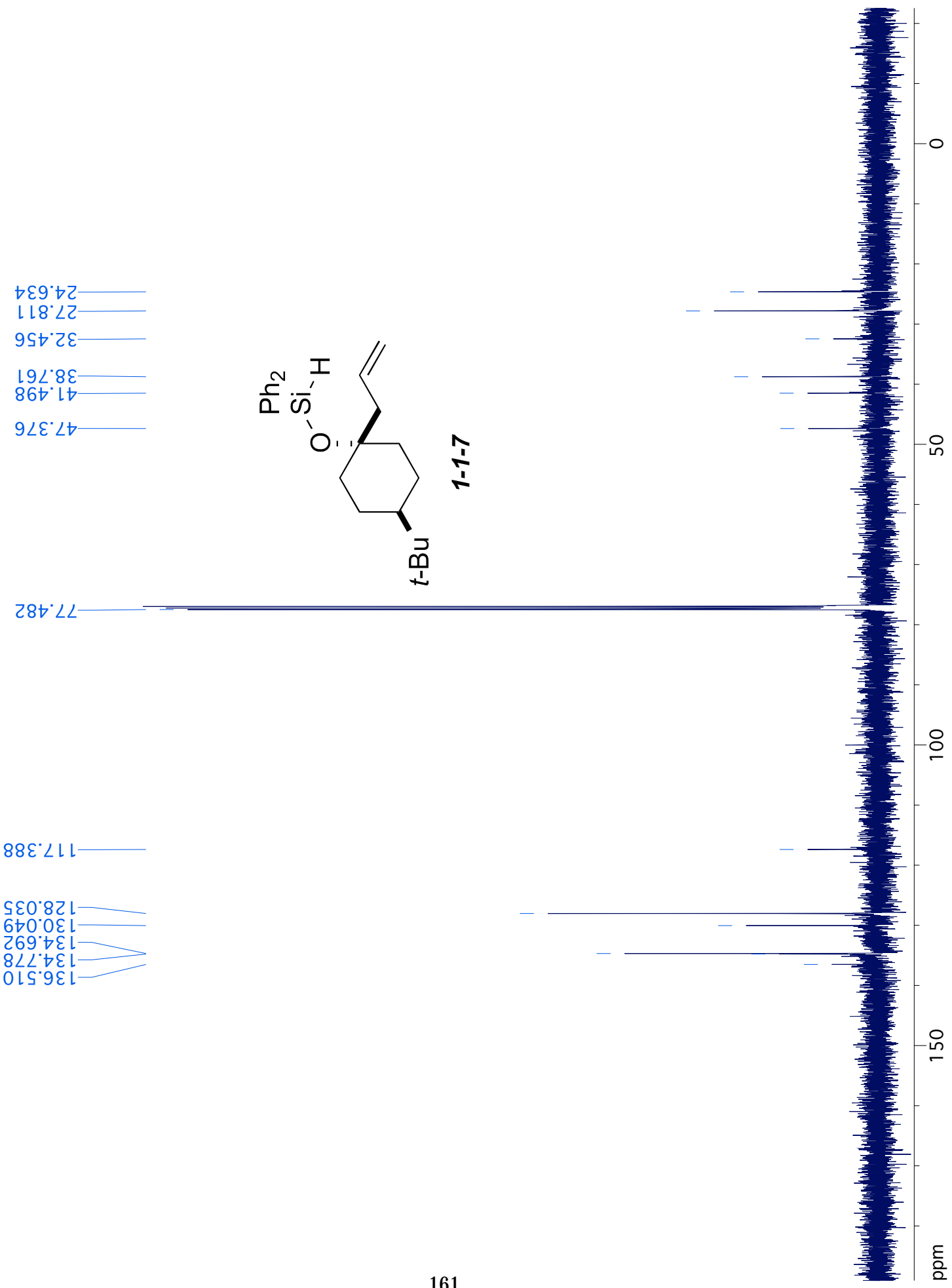


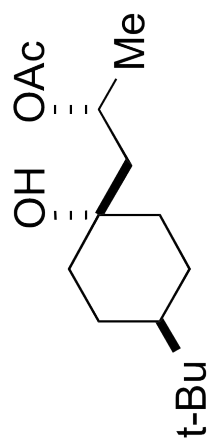
1-6-6



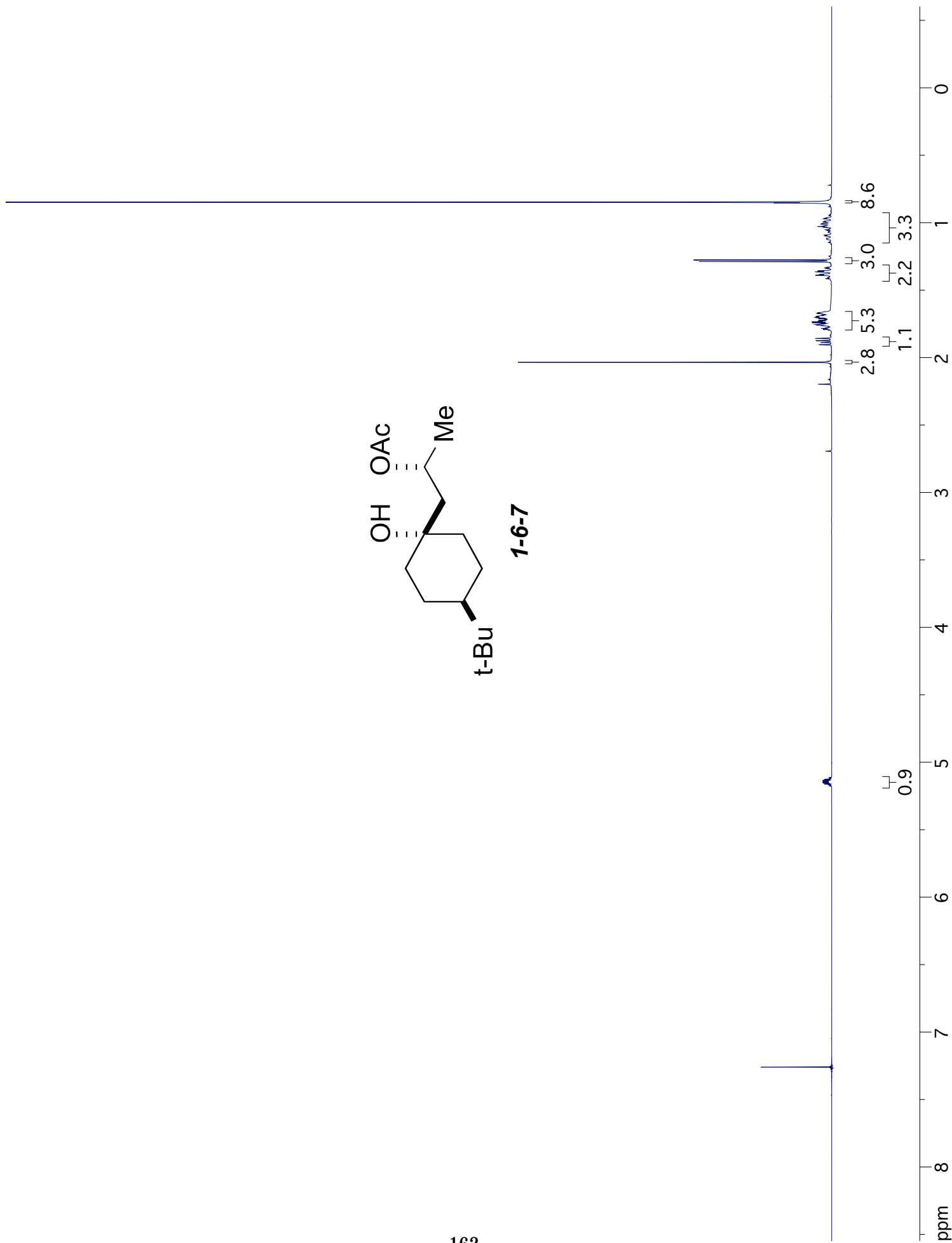


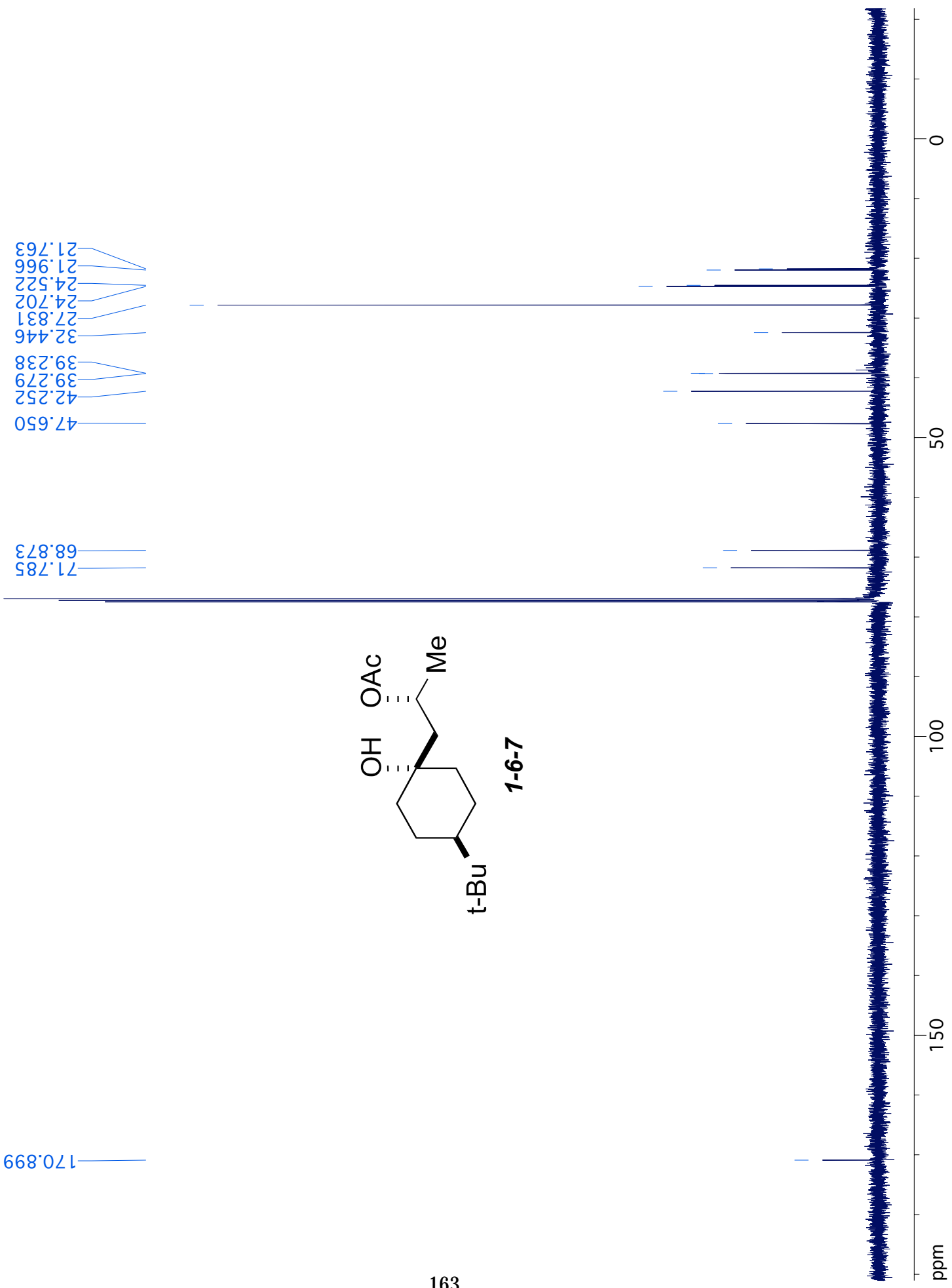


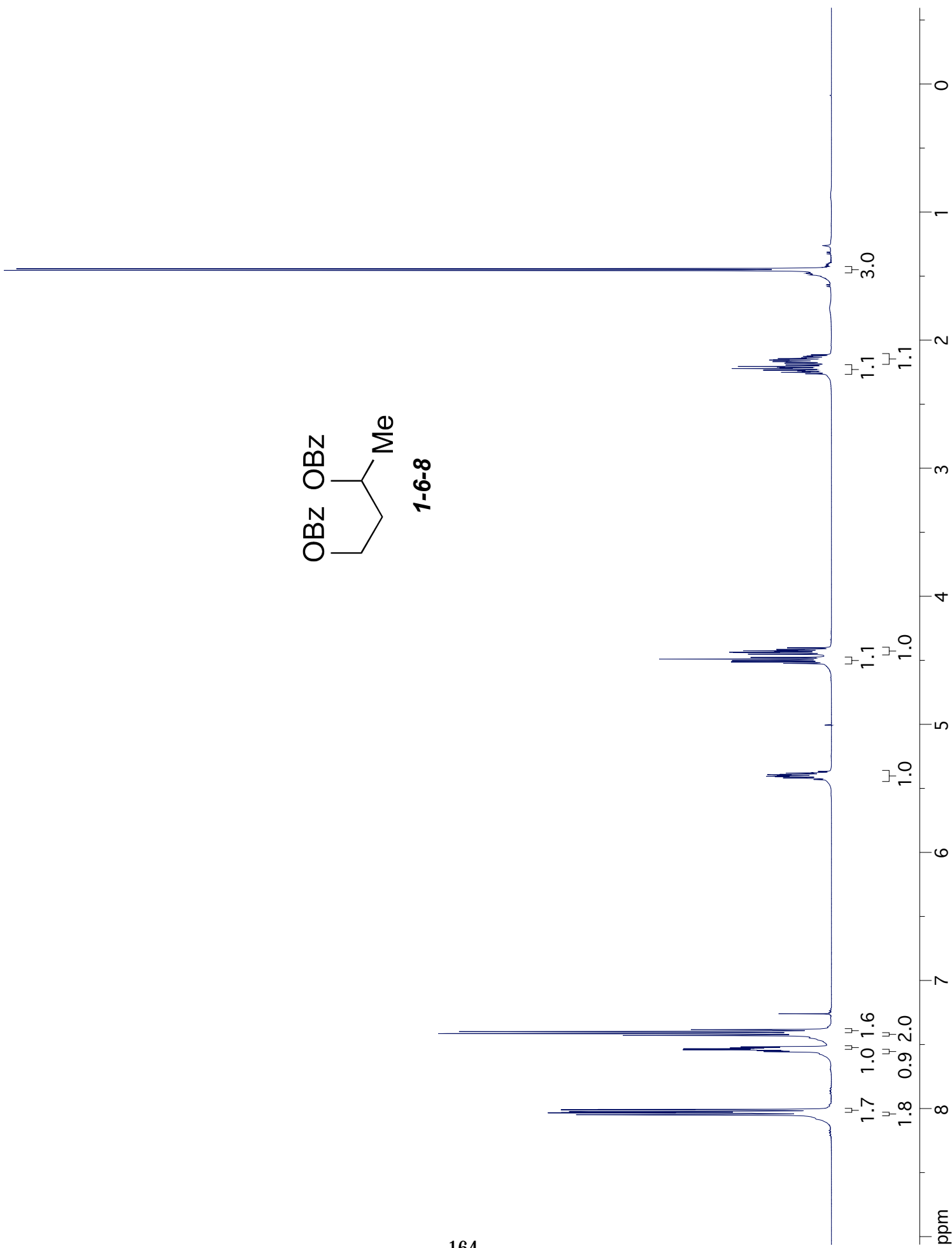
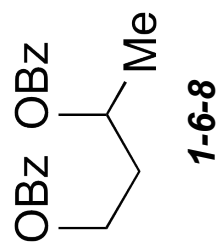


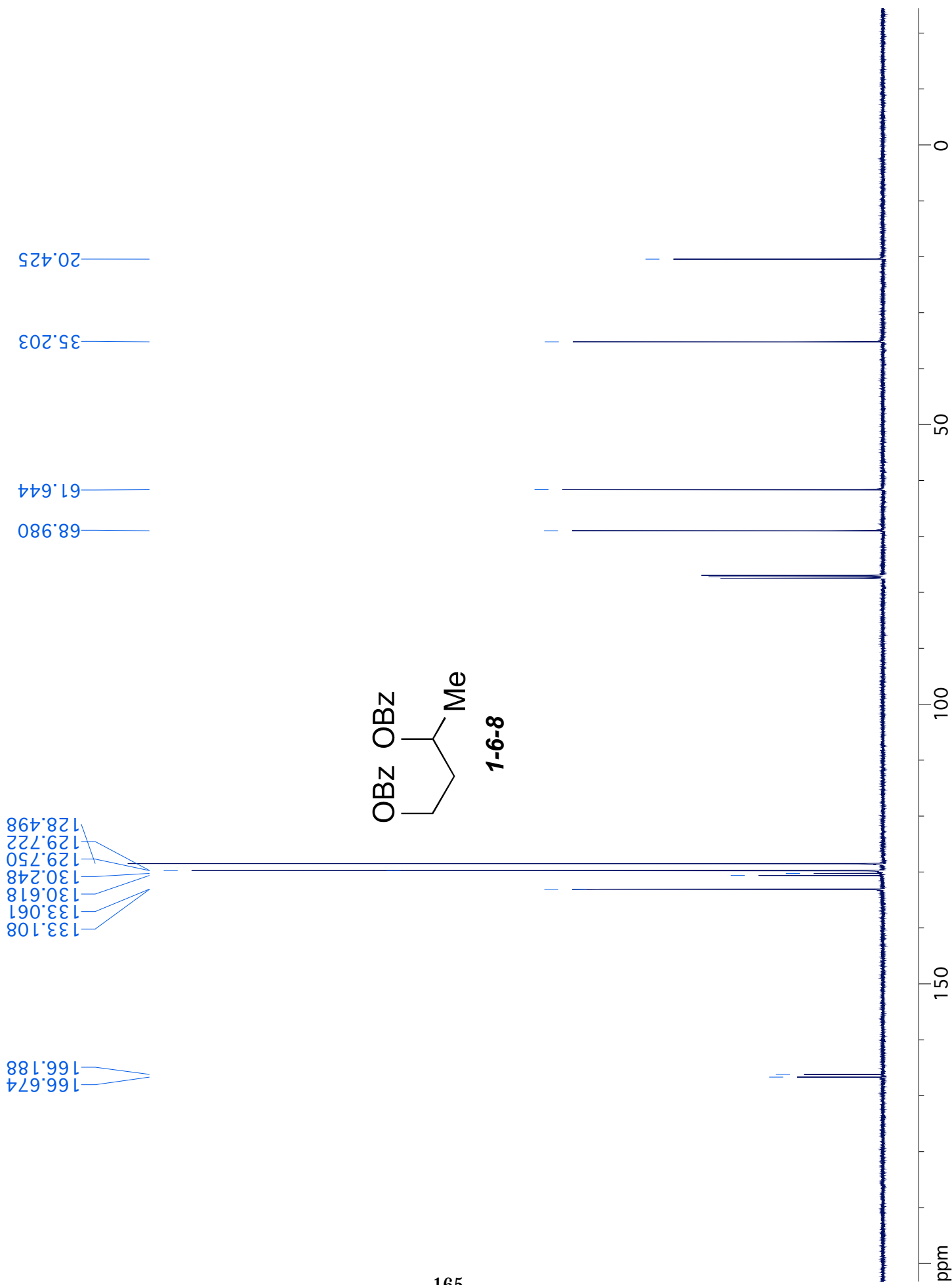


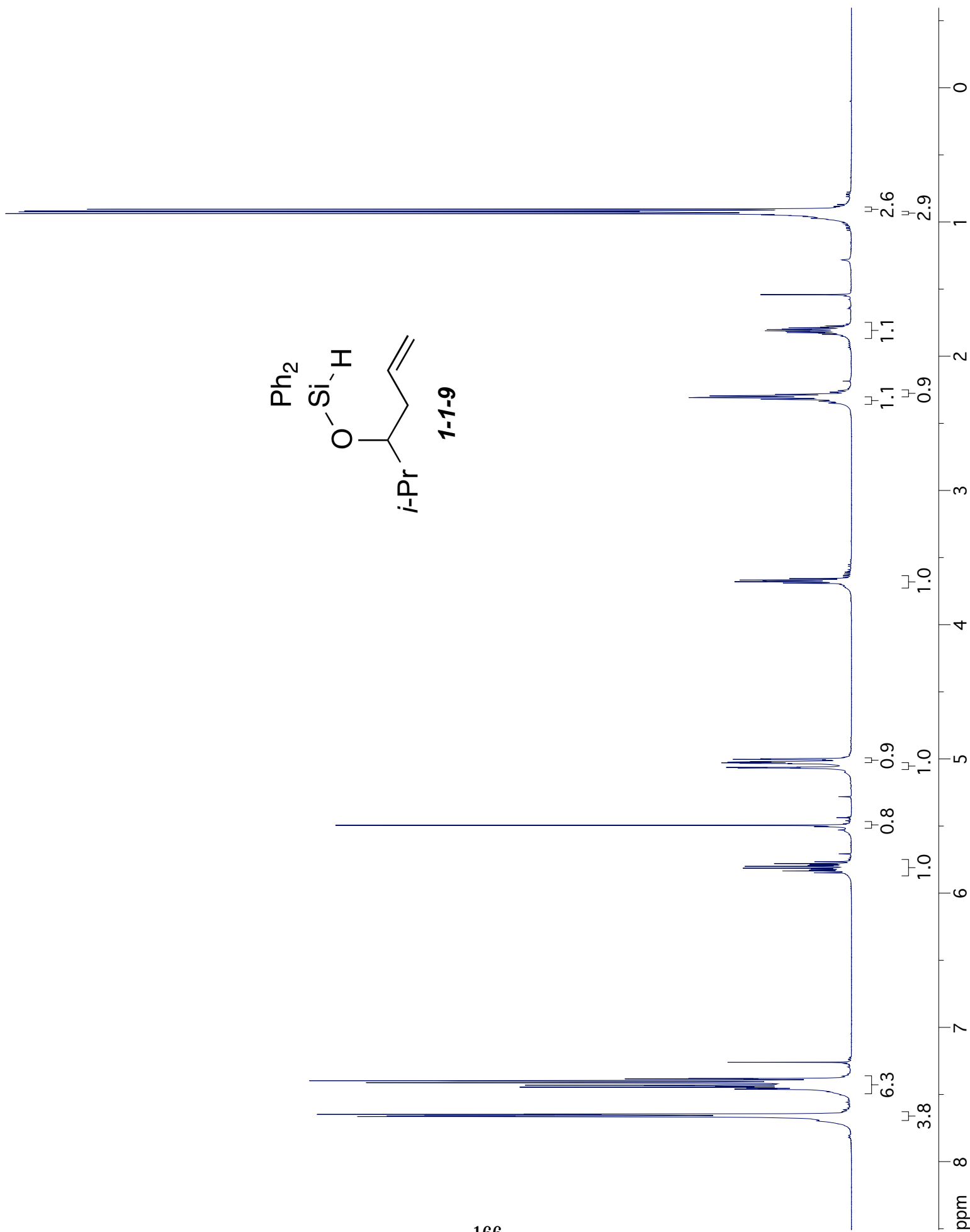
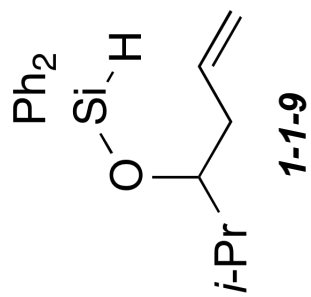
1-6-7

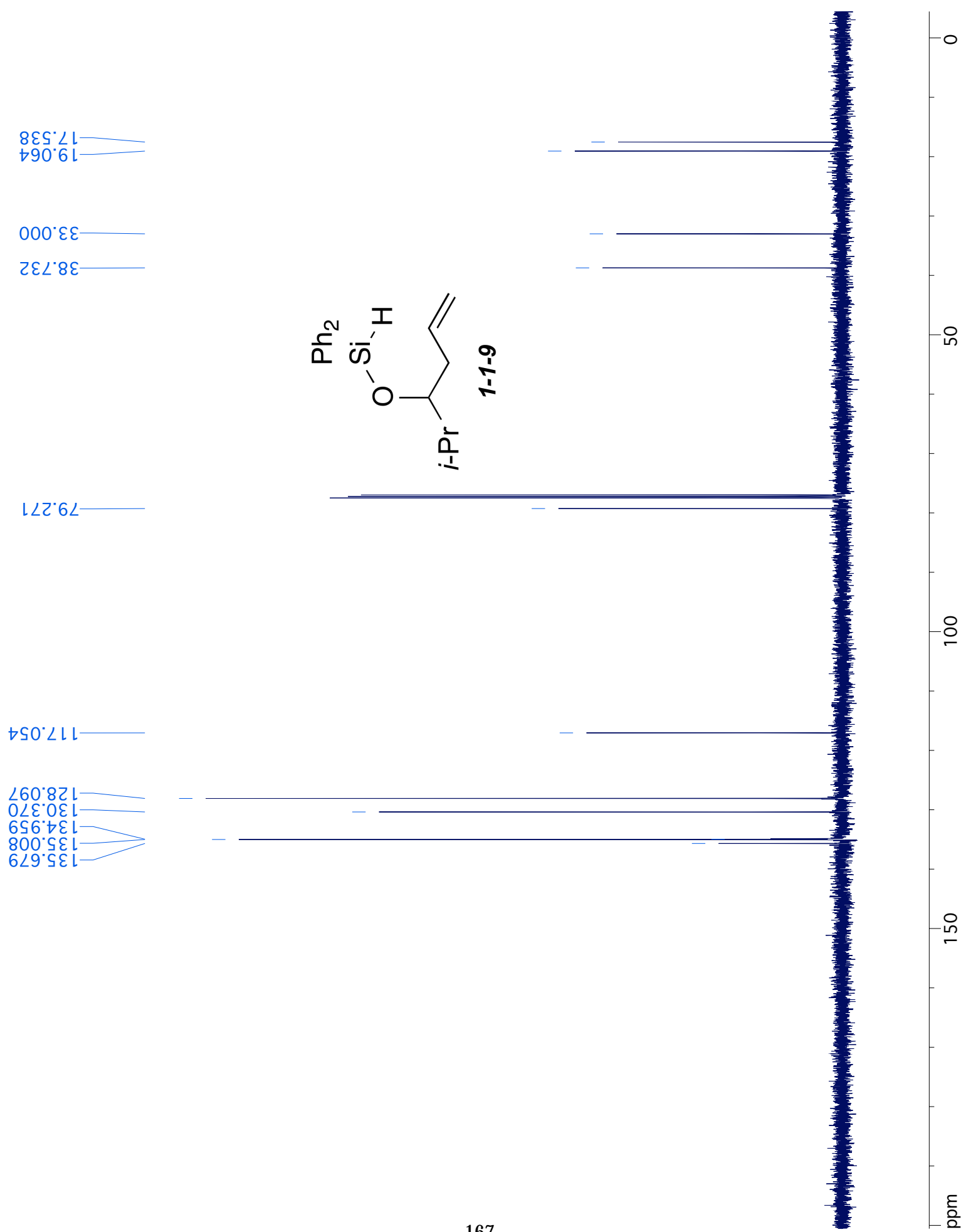


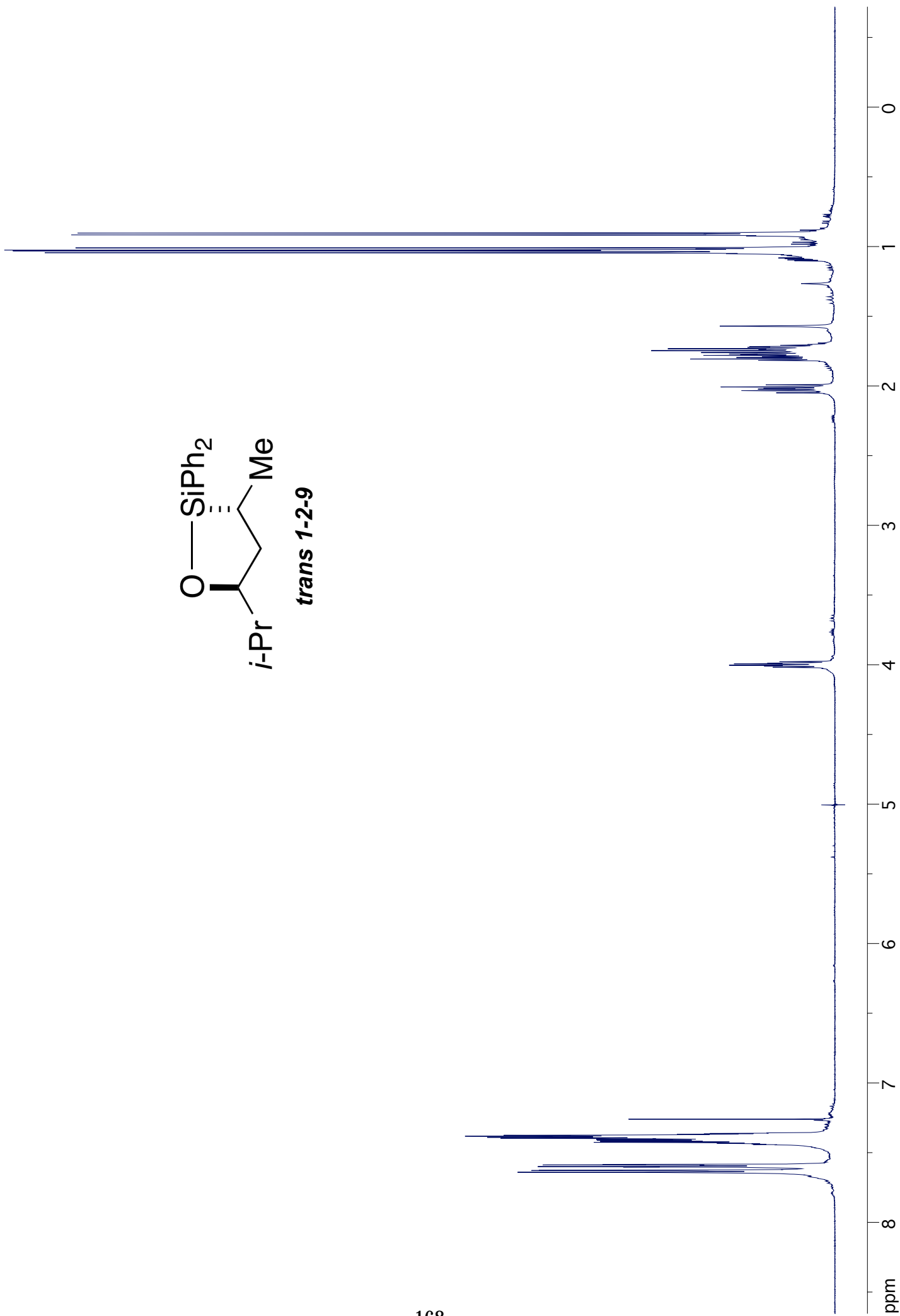
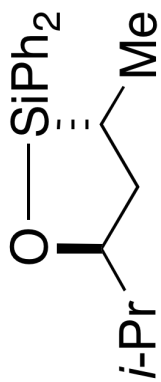


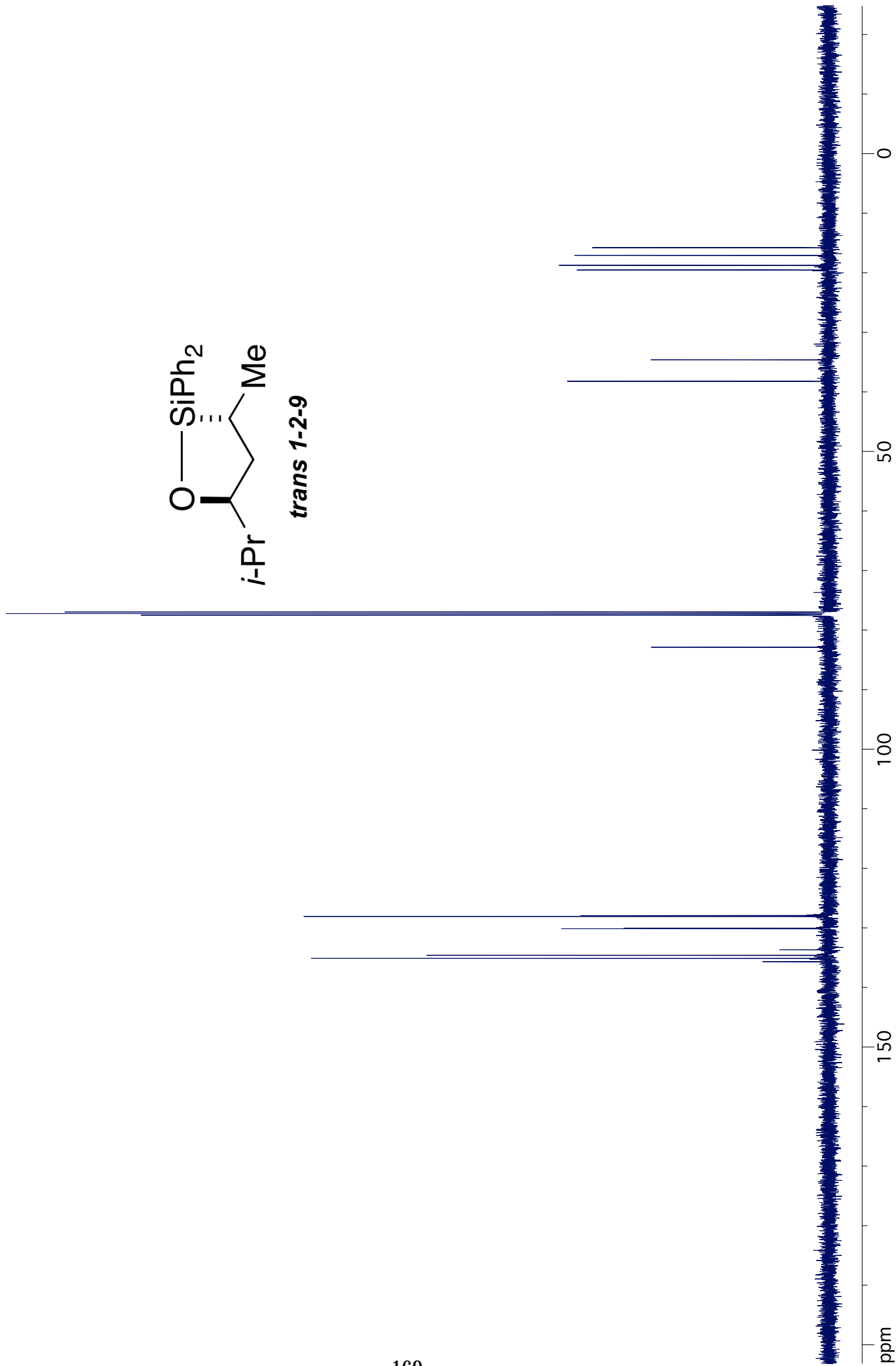
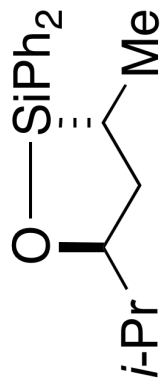


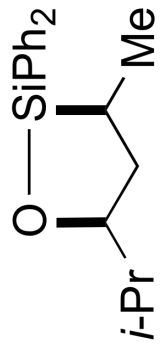




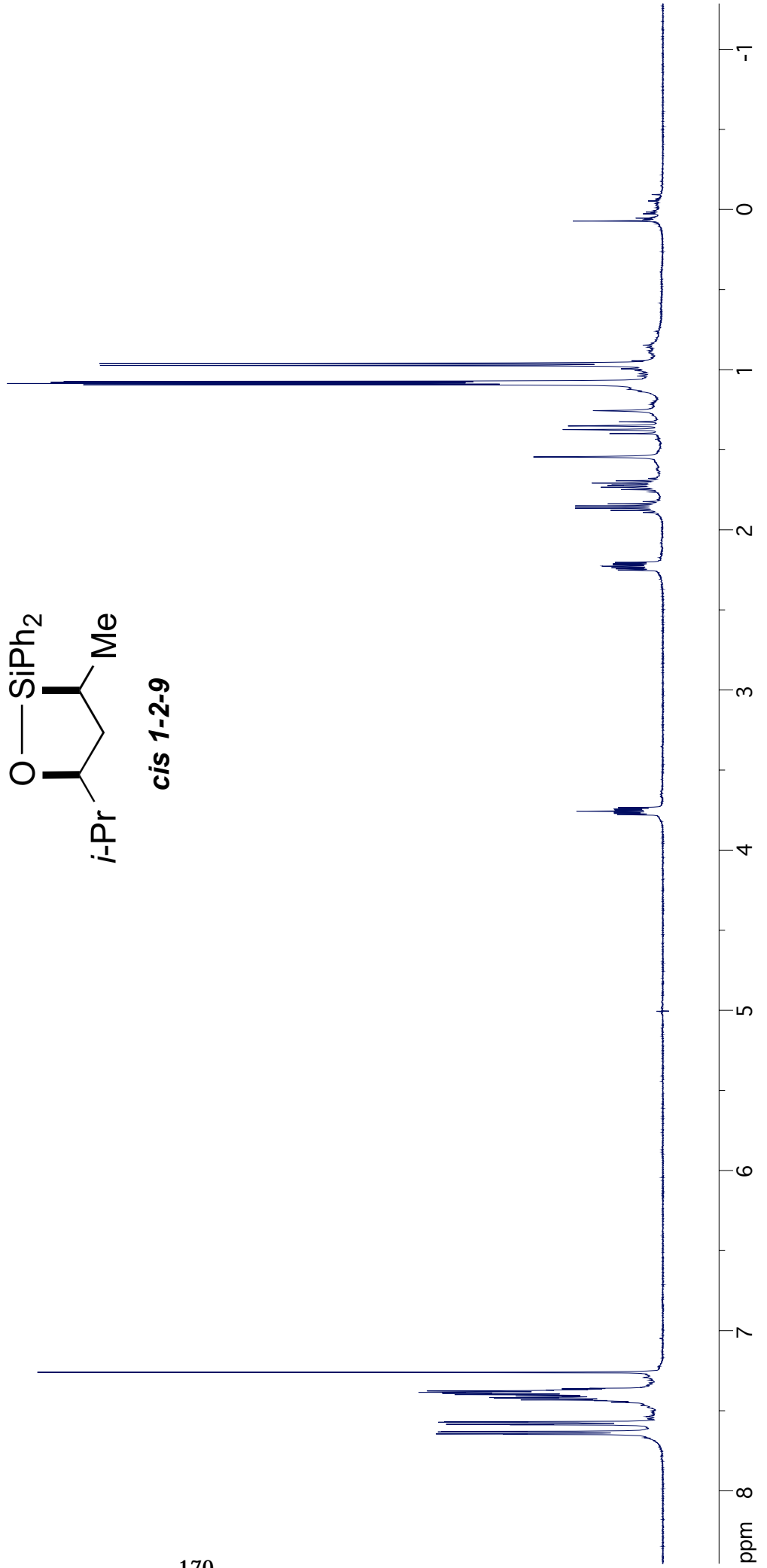


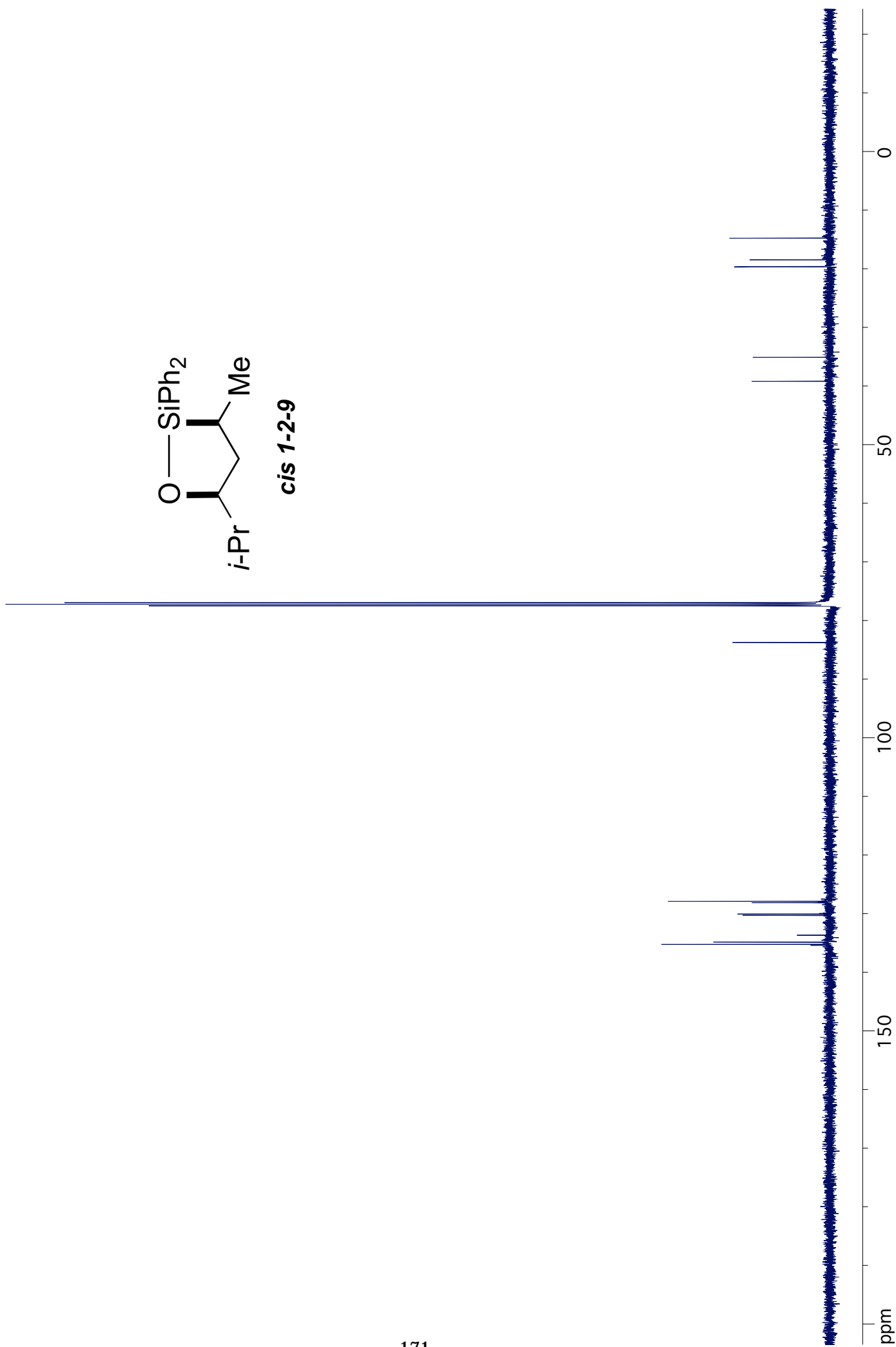
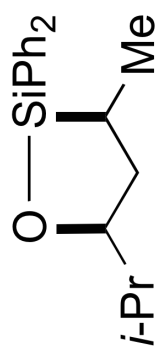


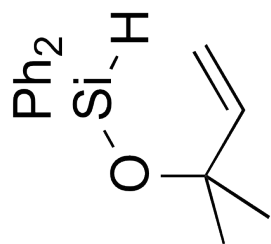




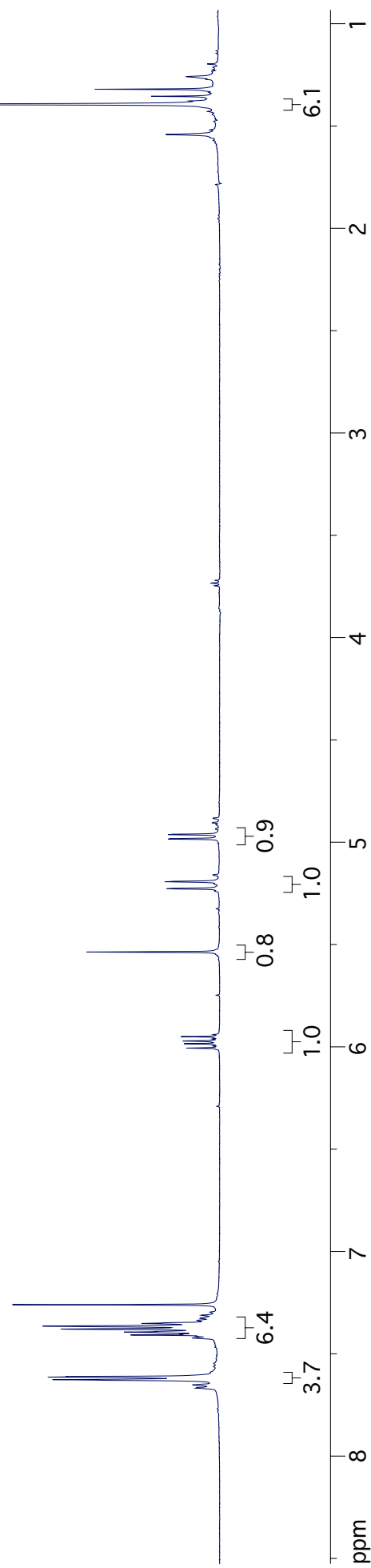
cis 1-2-9

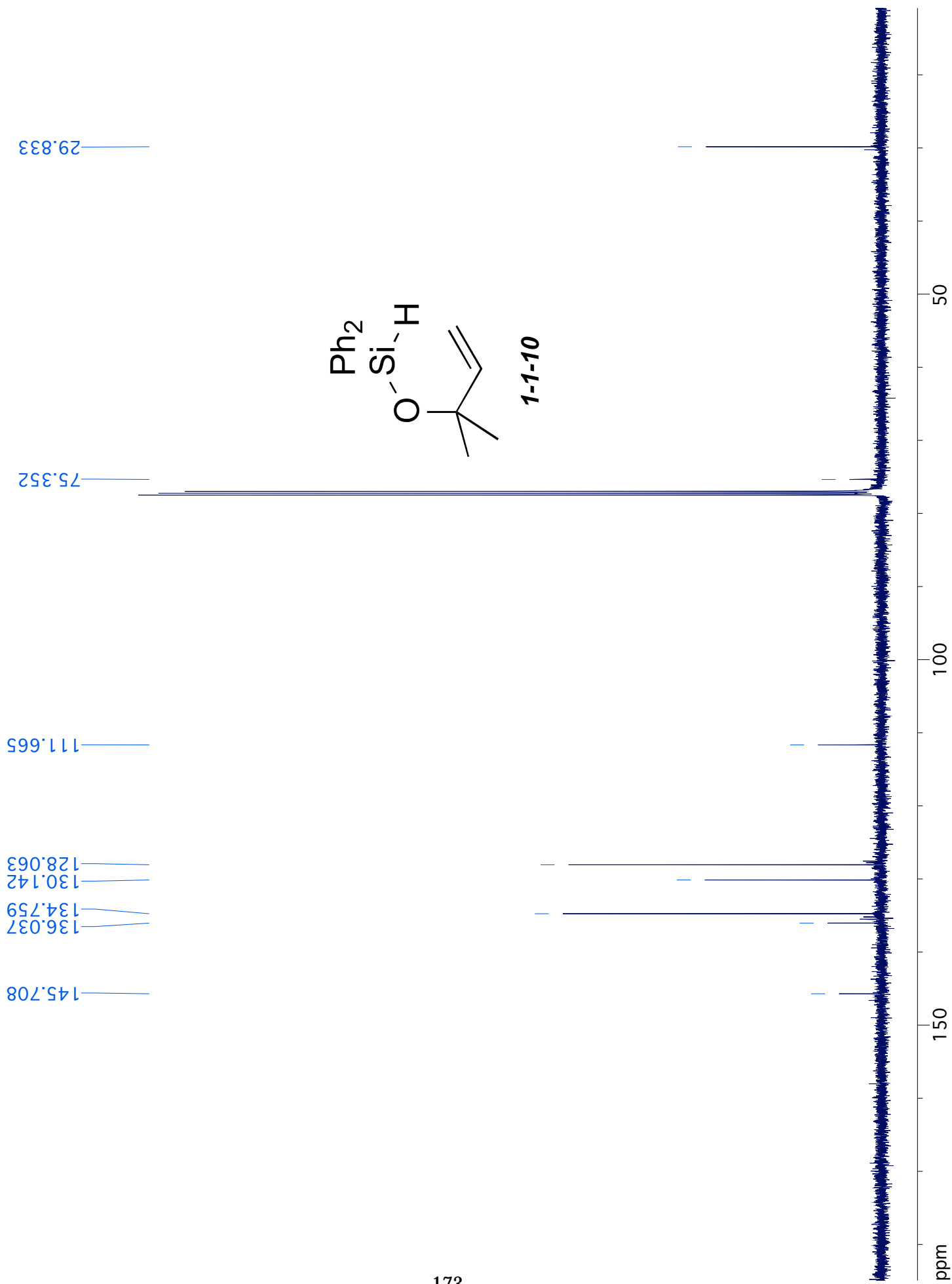


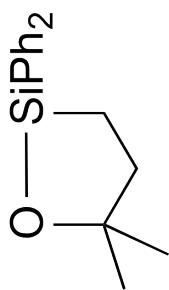




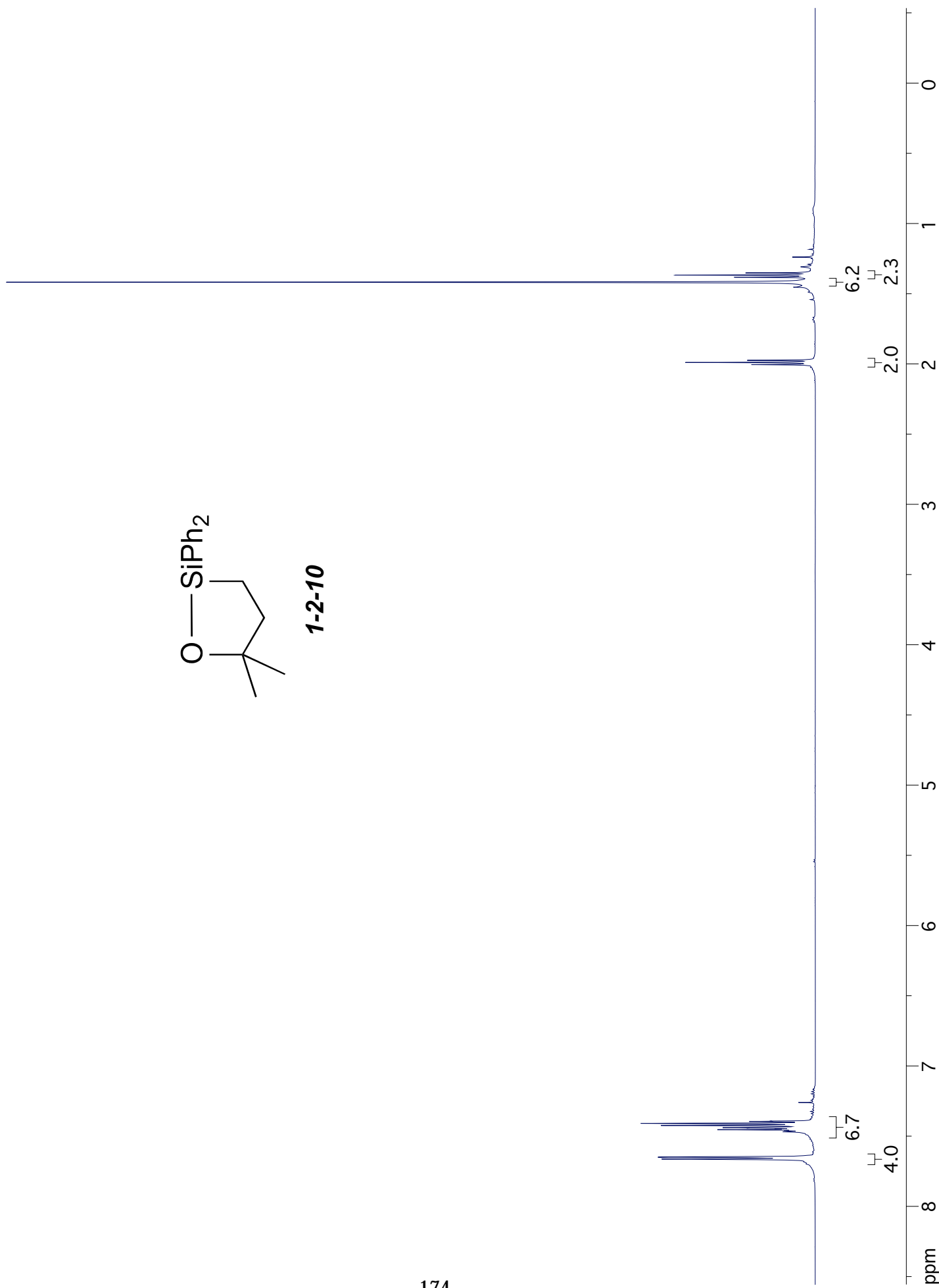
1-1-10

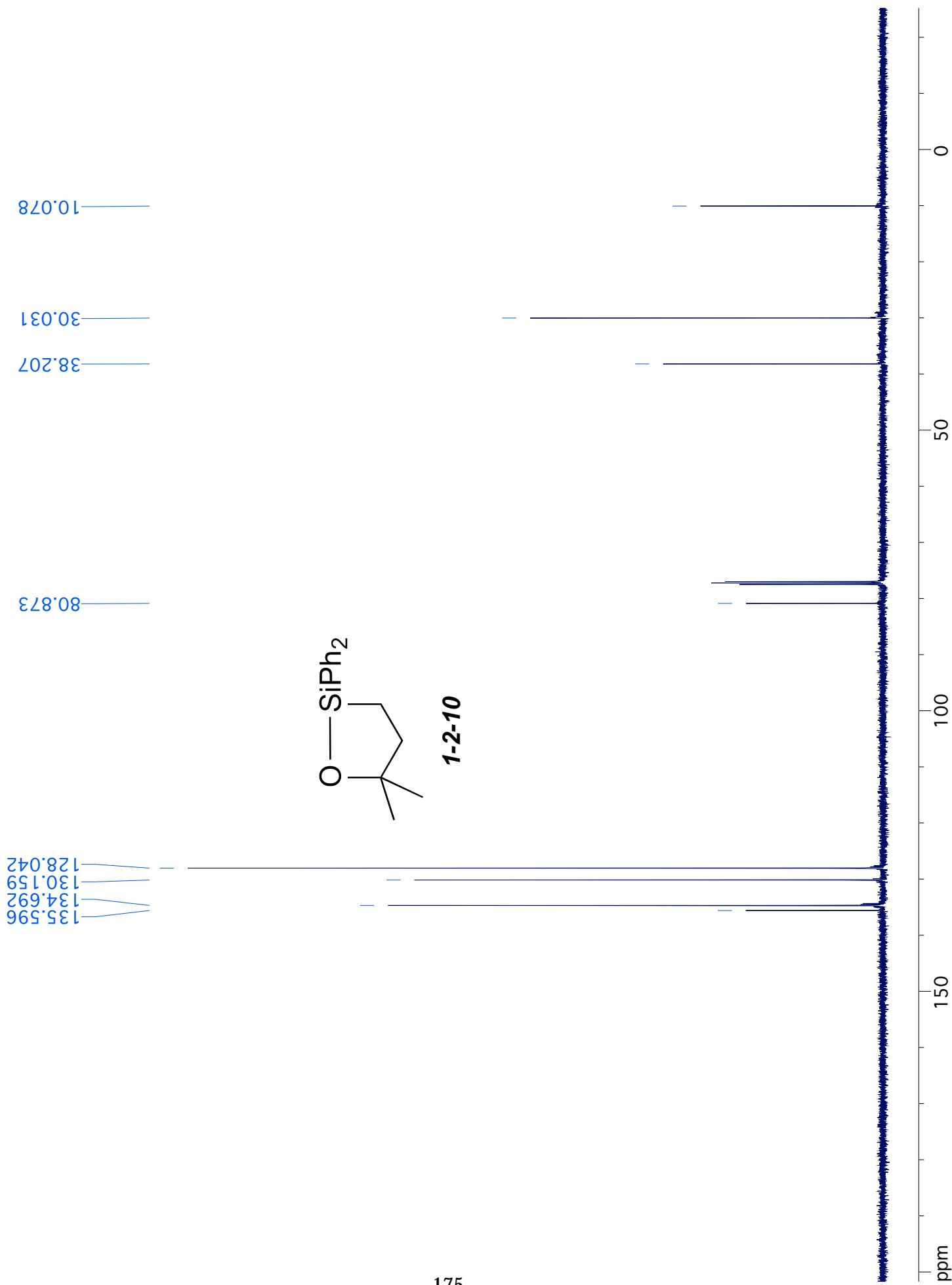


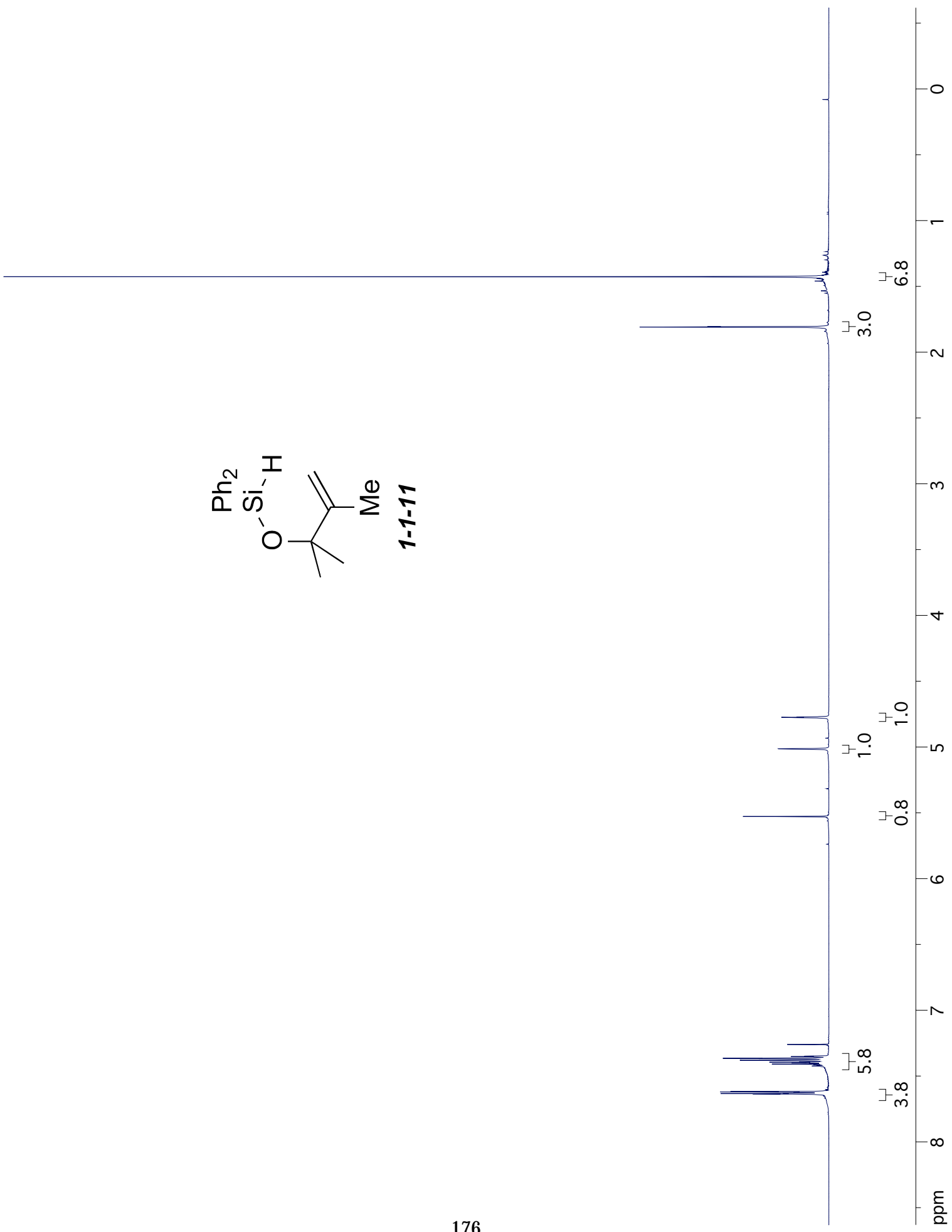
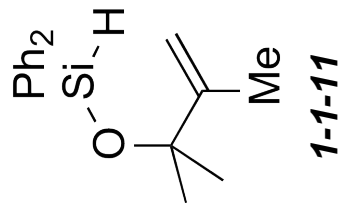


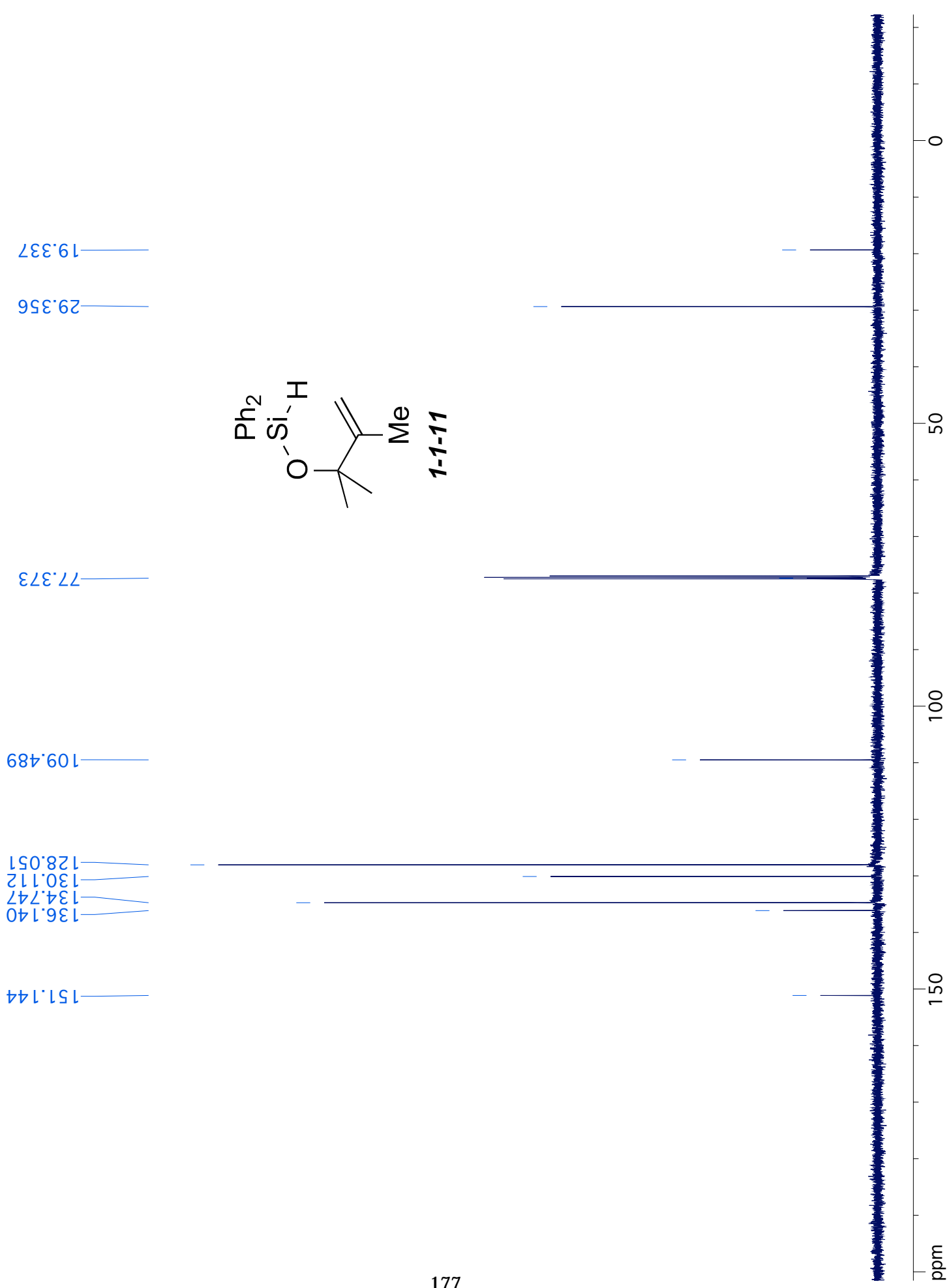
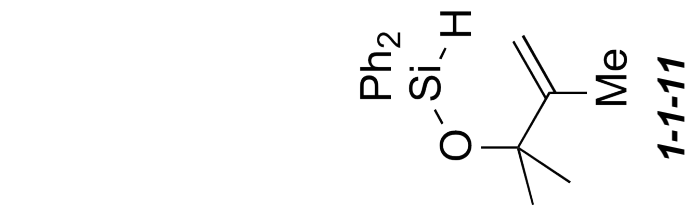


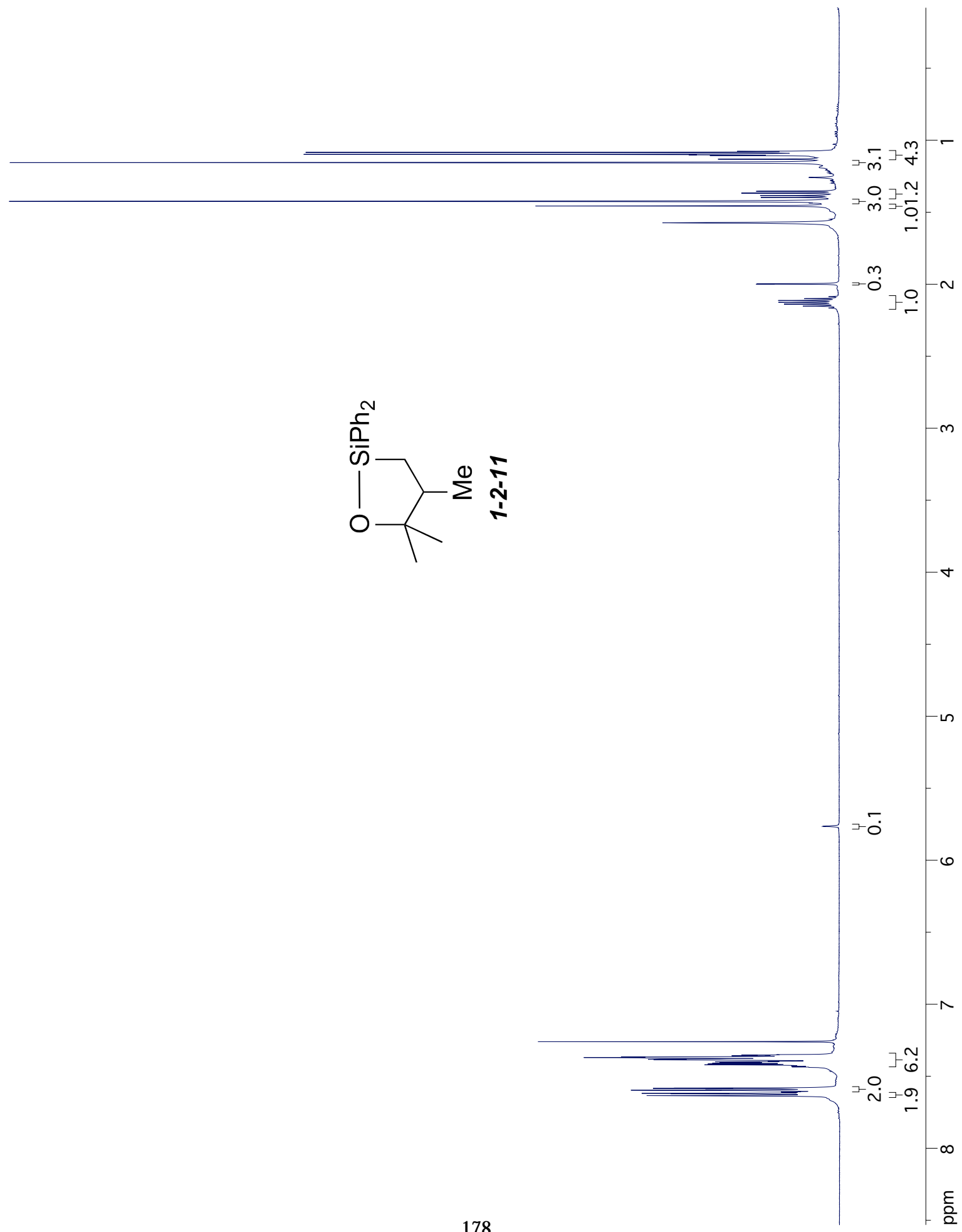
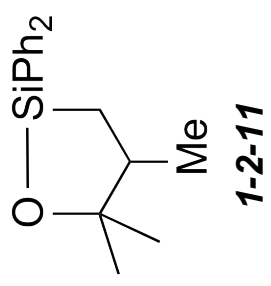
1-2-10

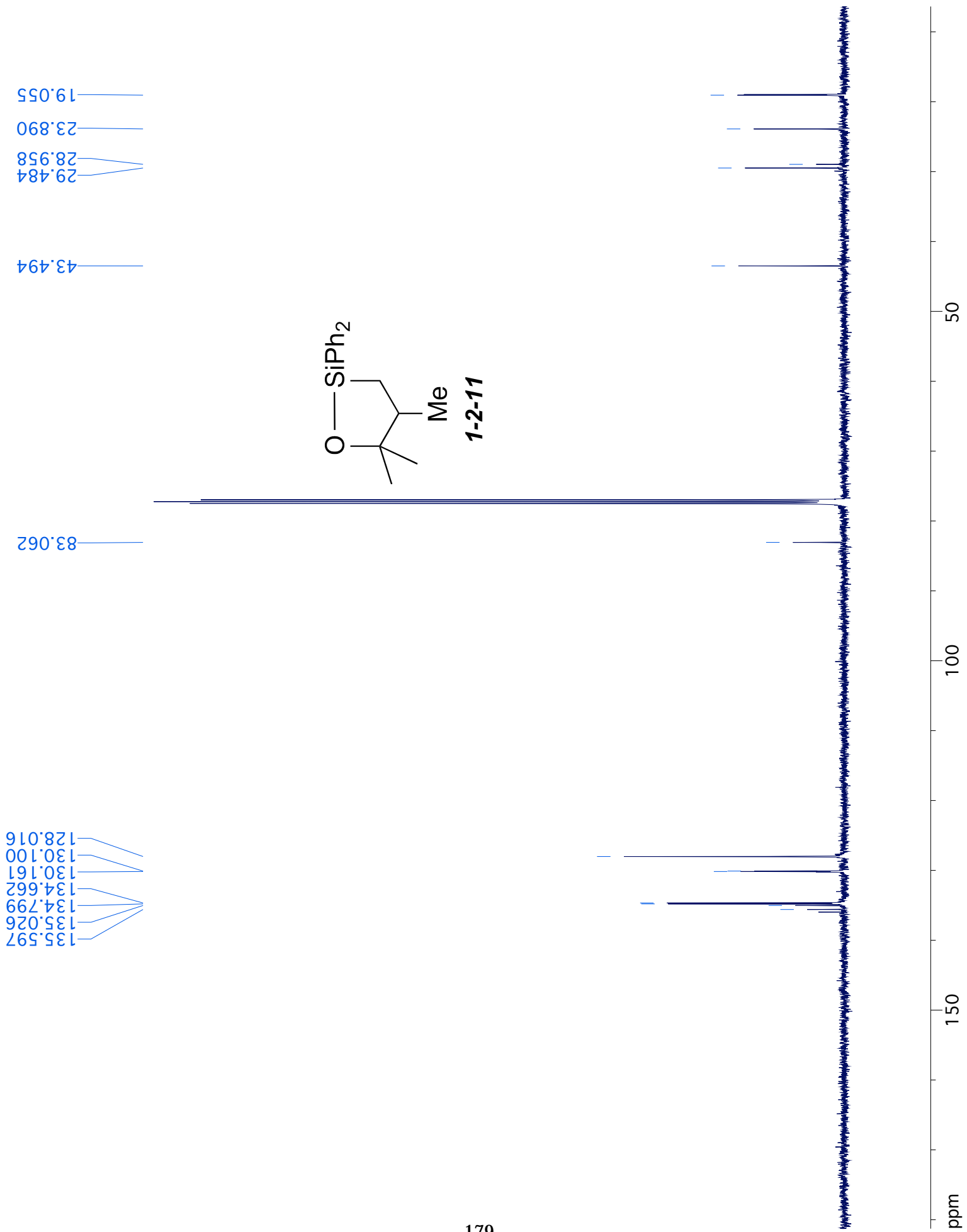


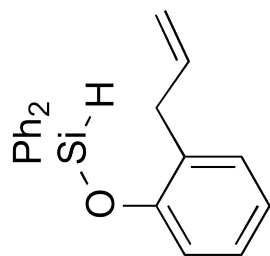




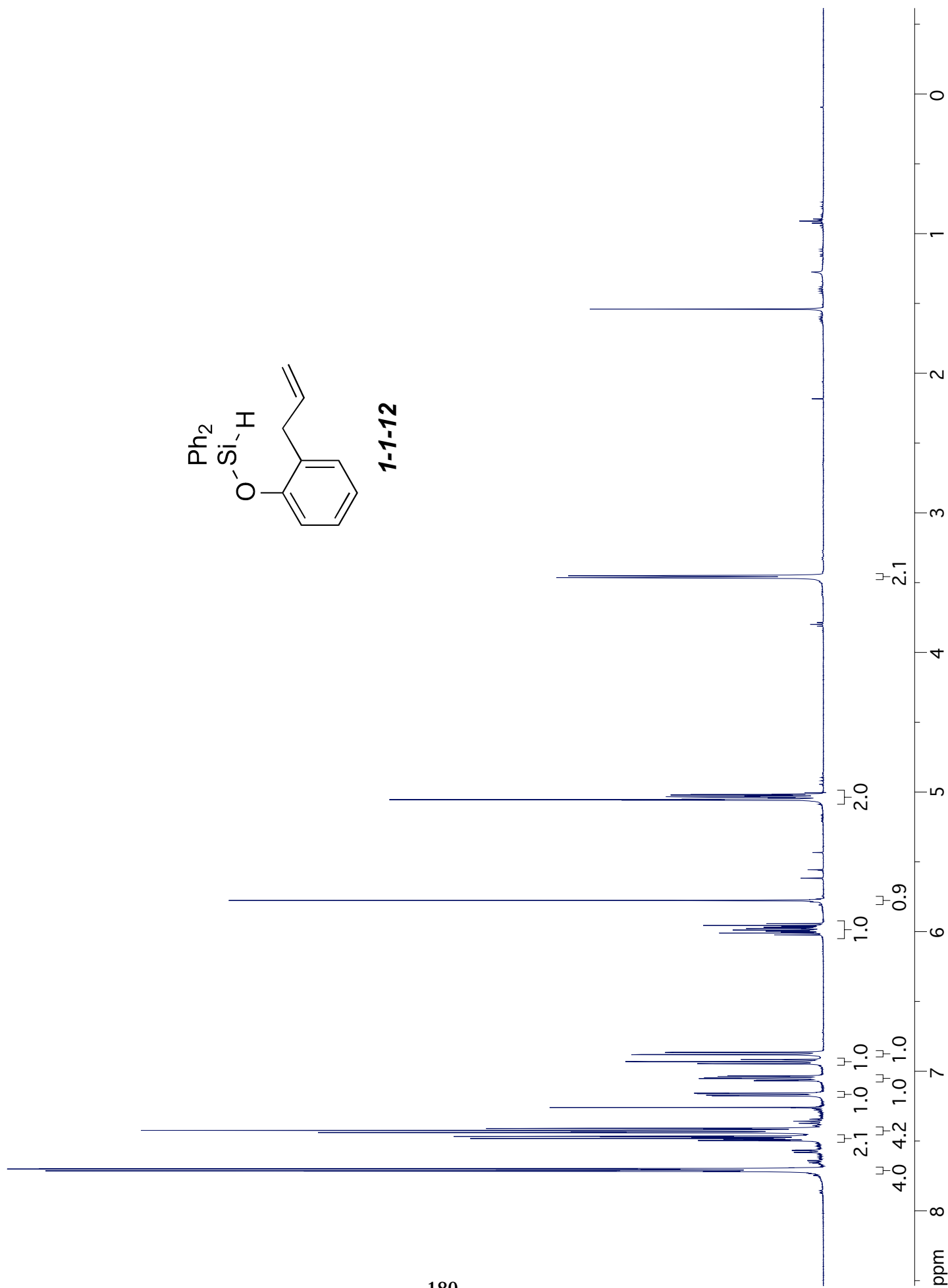


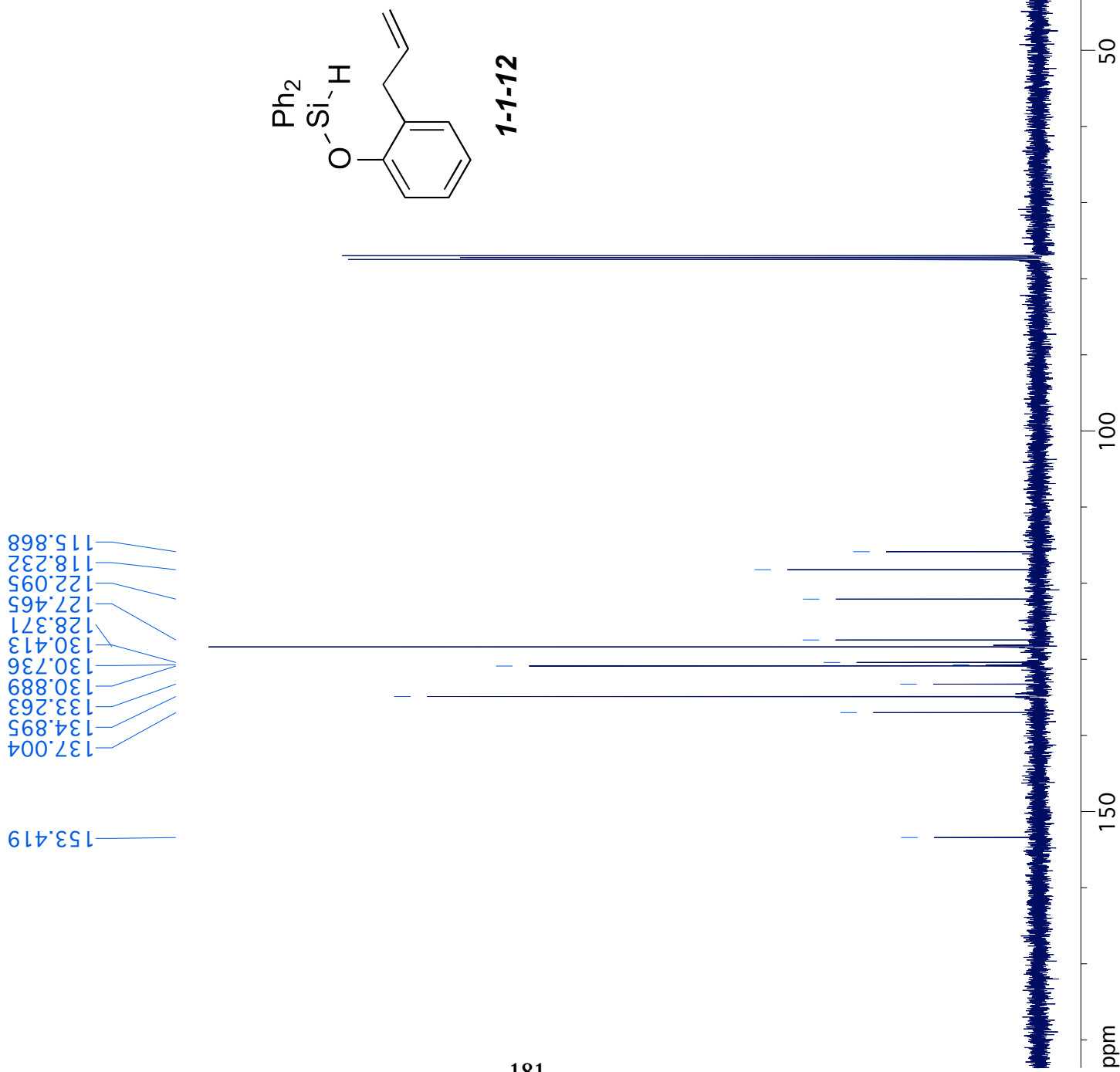


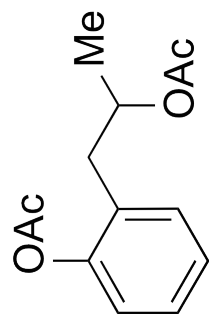




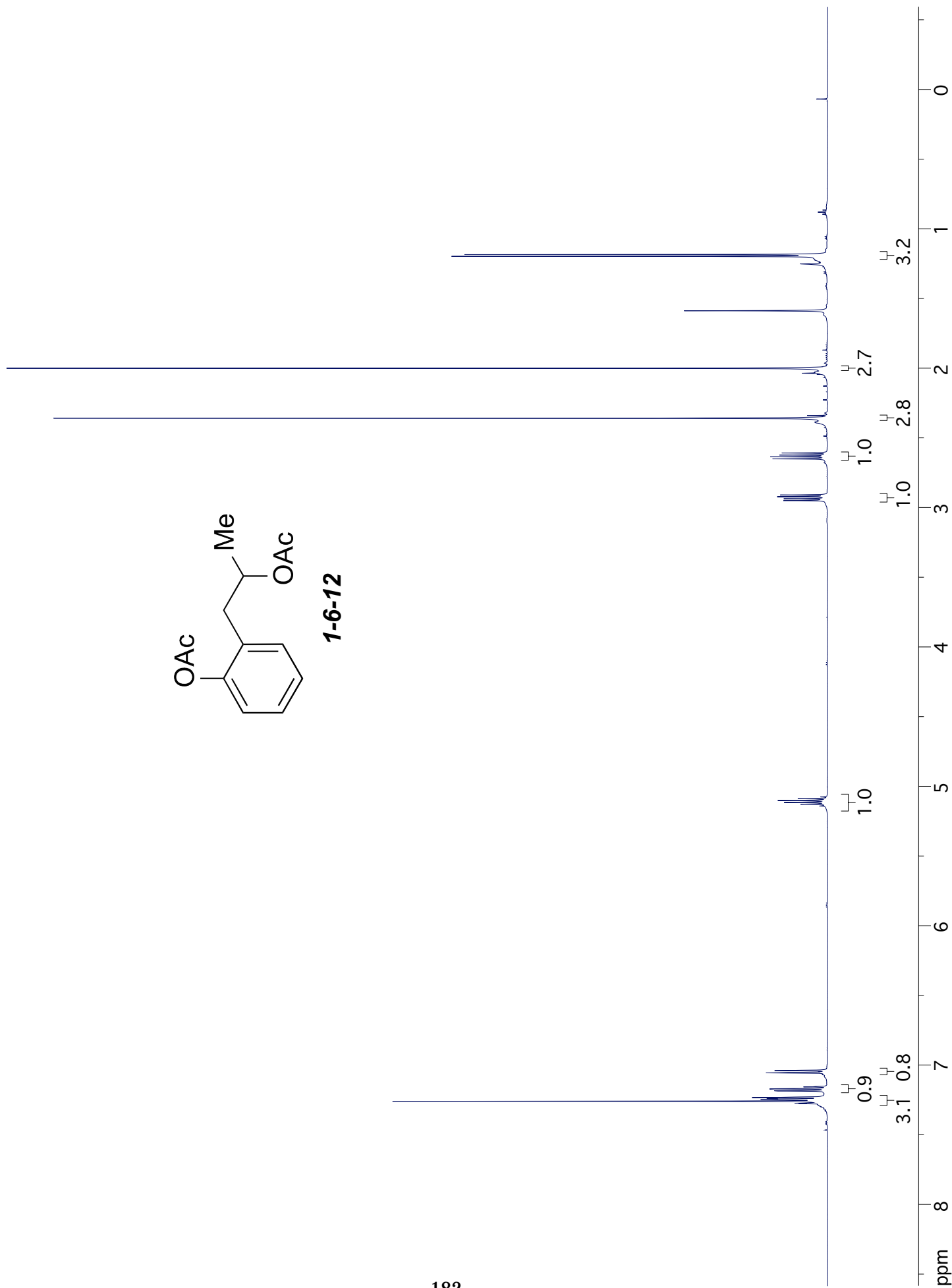
1-1-12

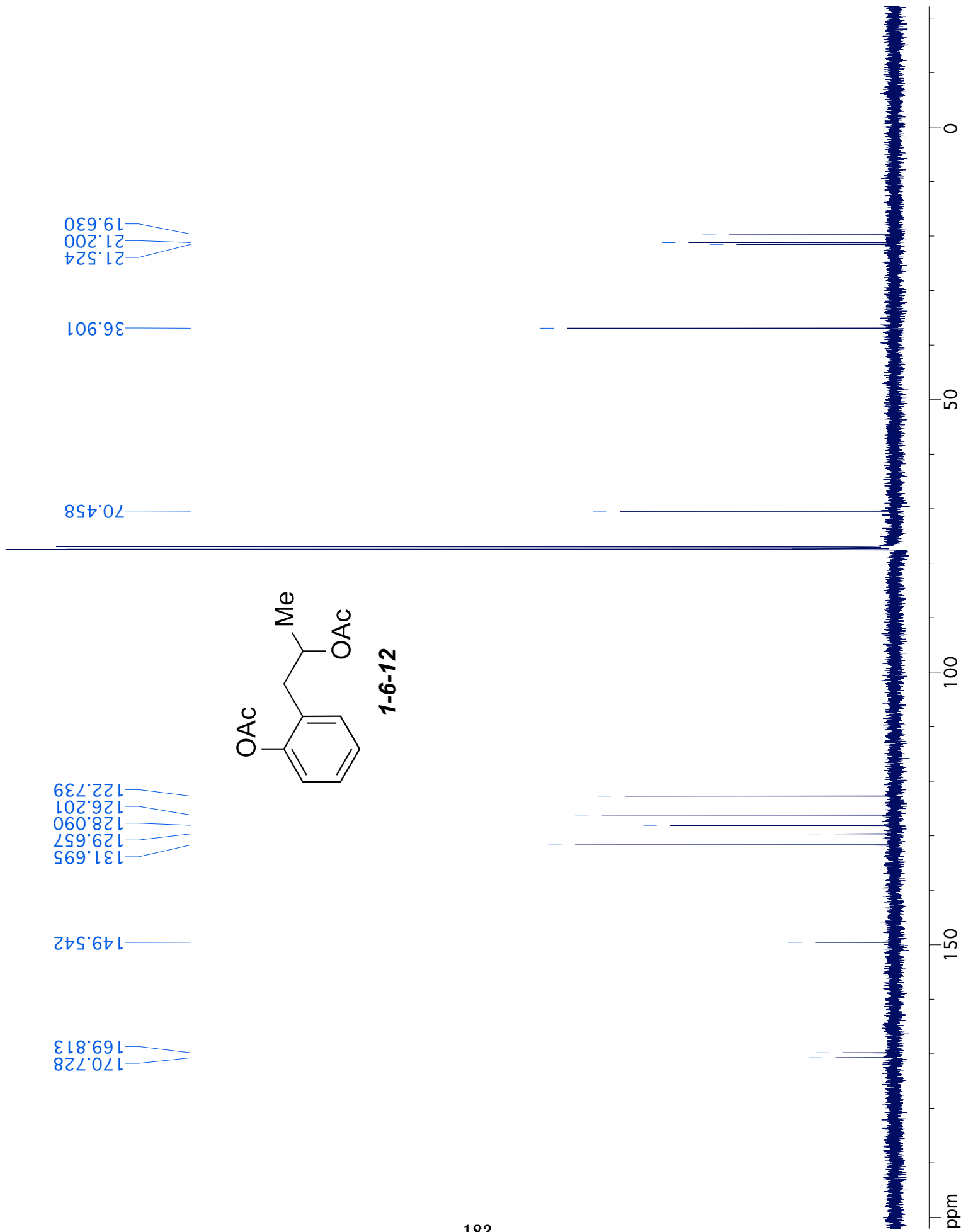


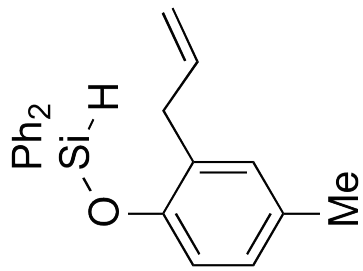




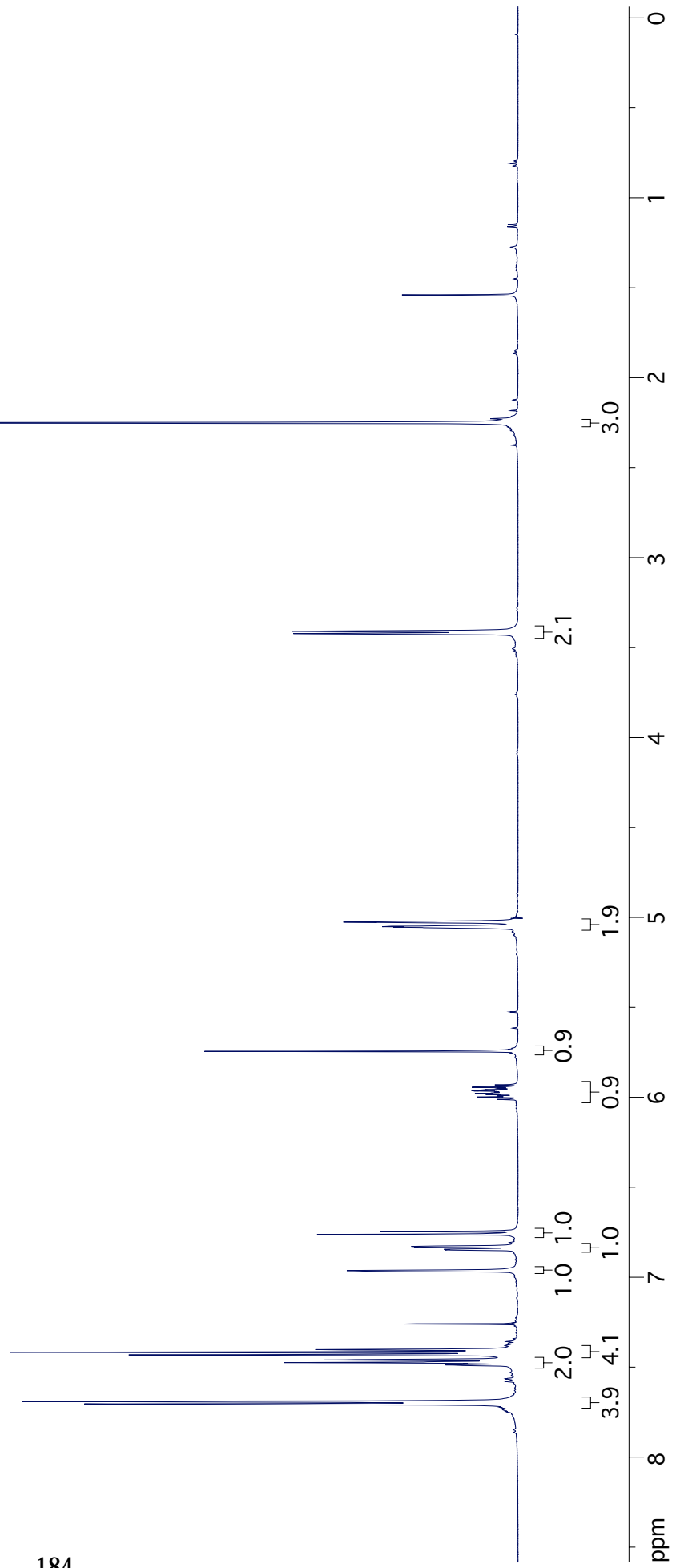
1-6-12

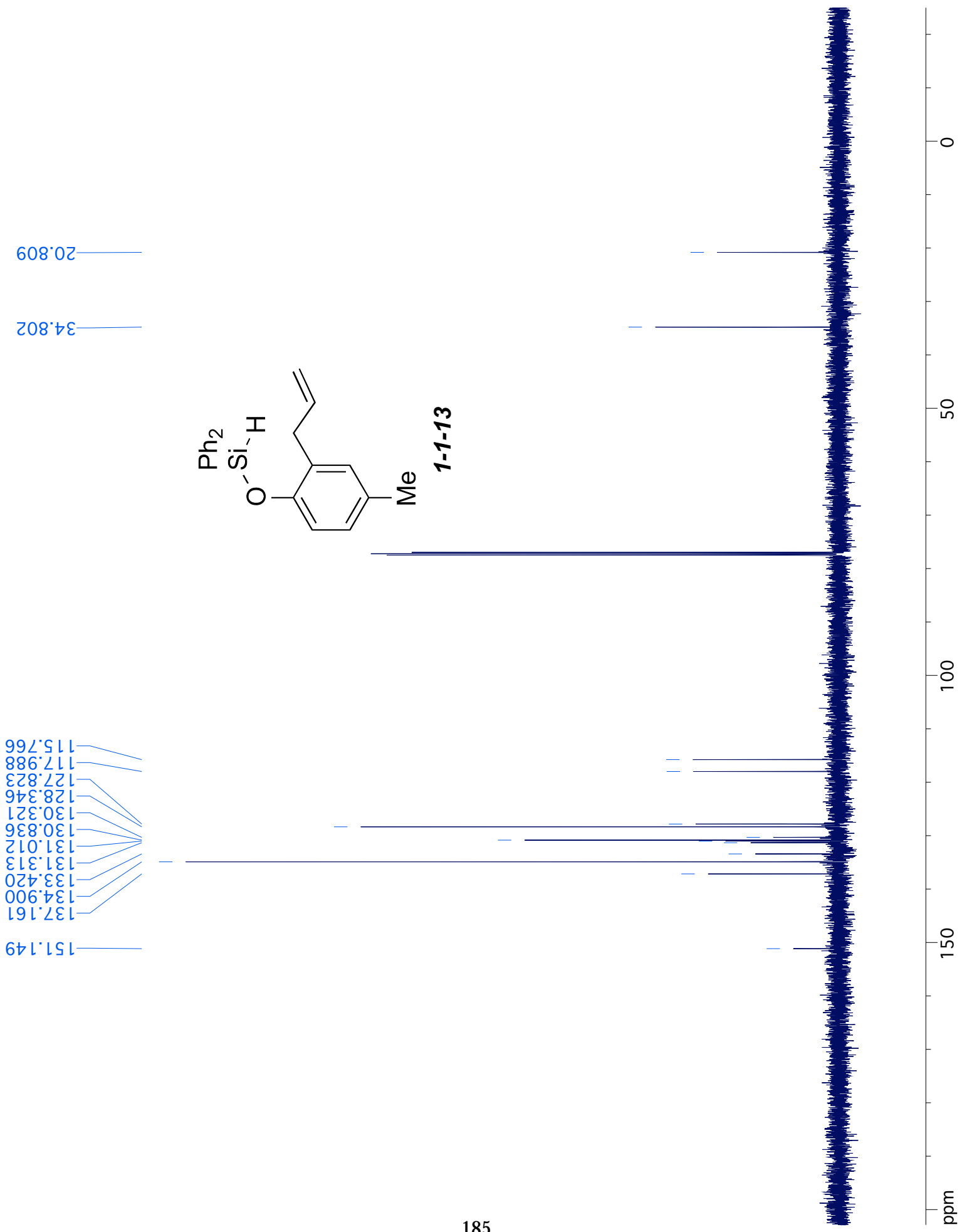


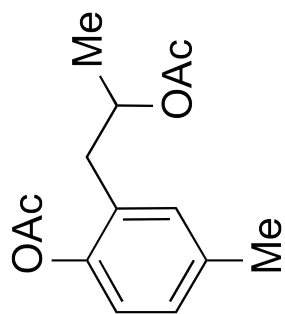




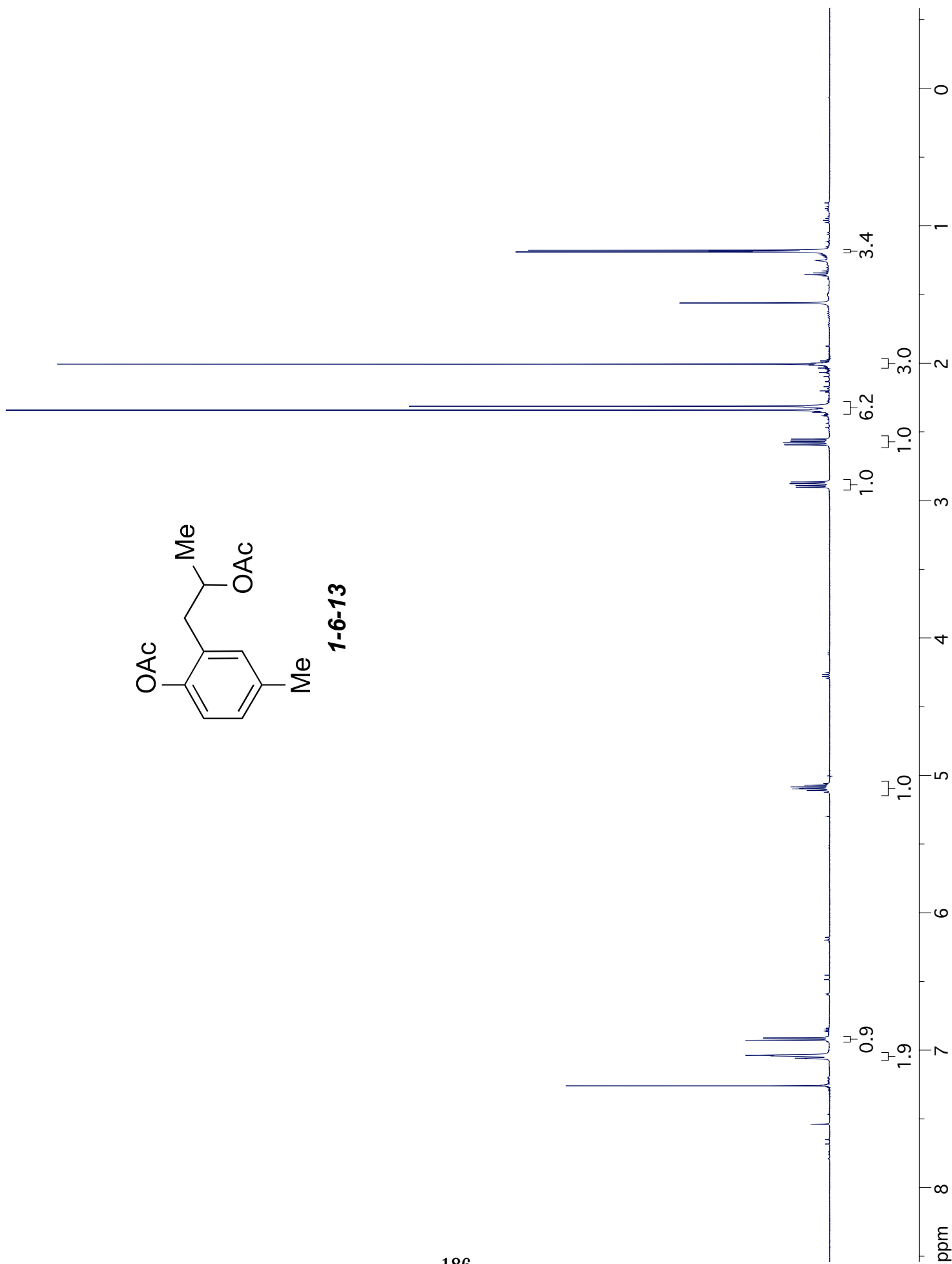
1-1-13

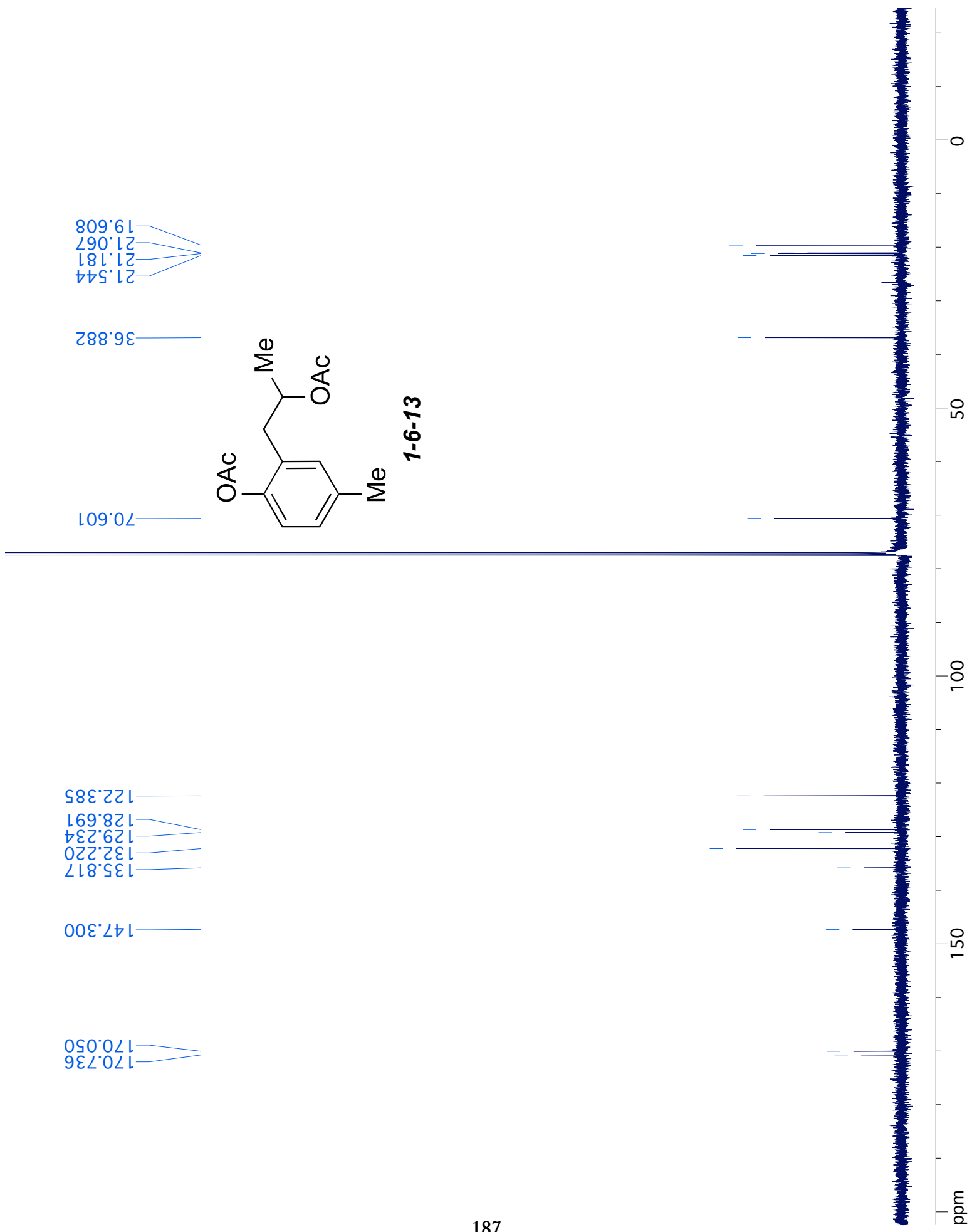


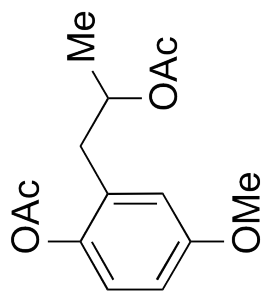




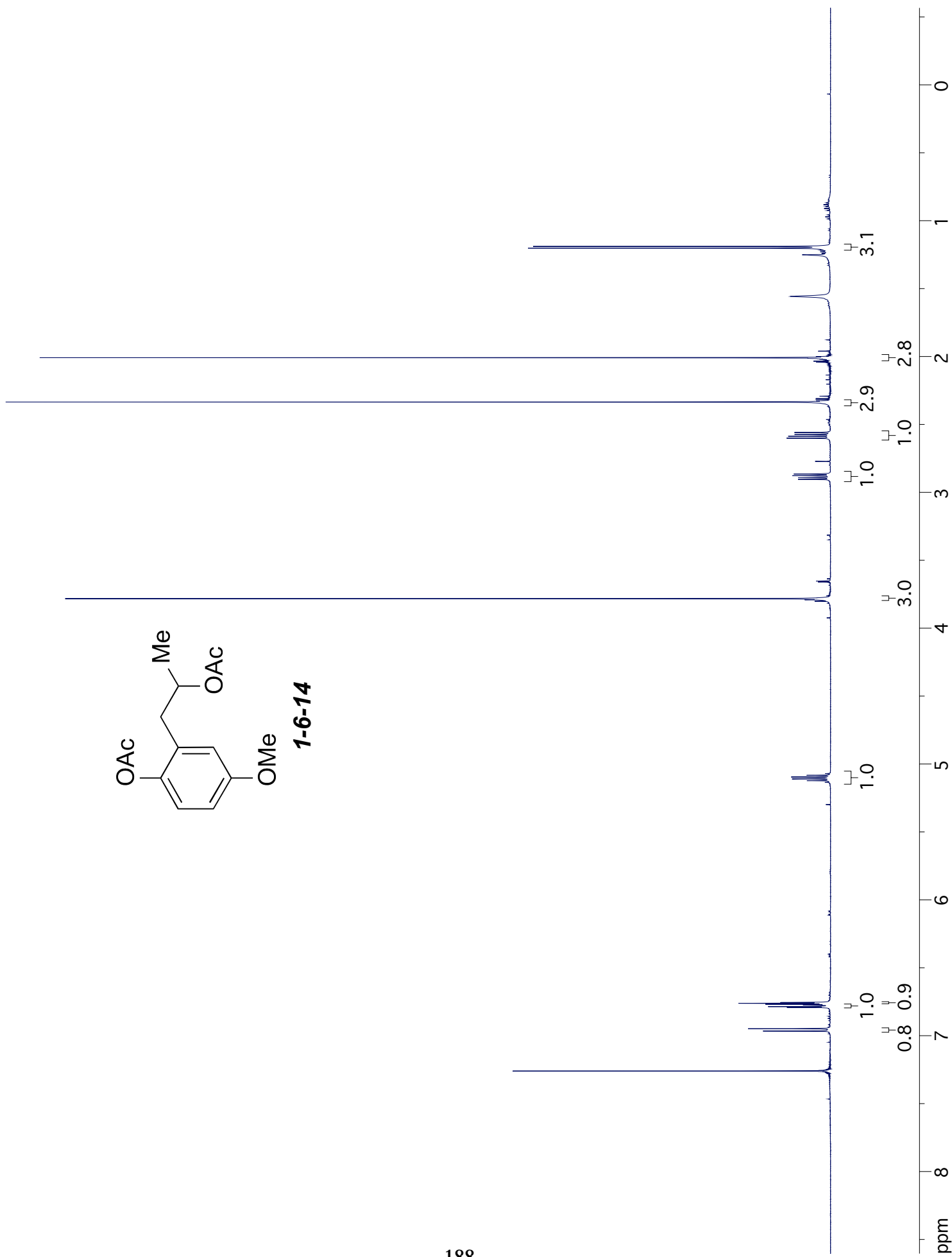
1-6-13

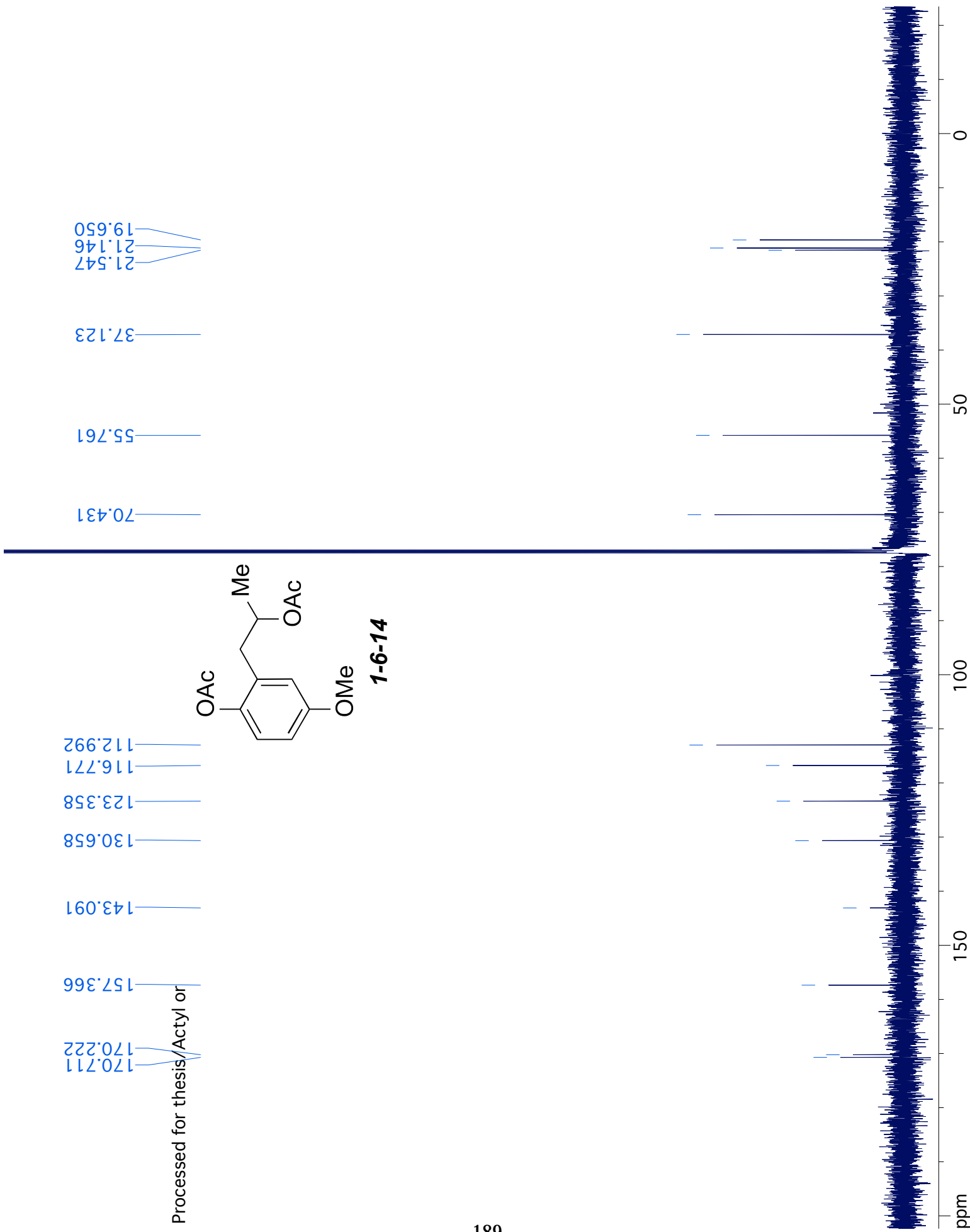


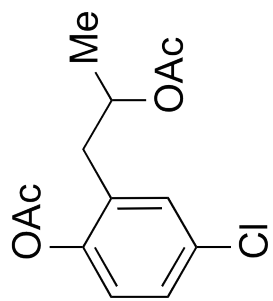




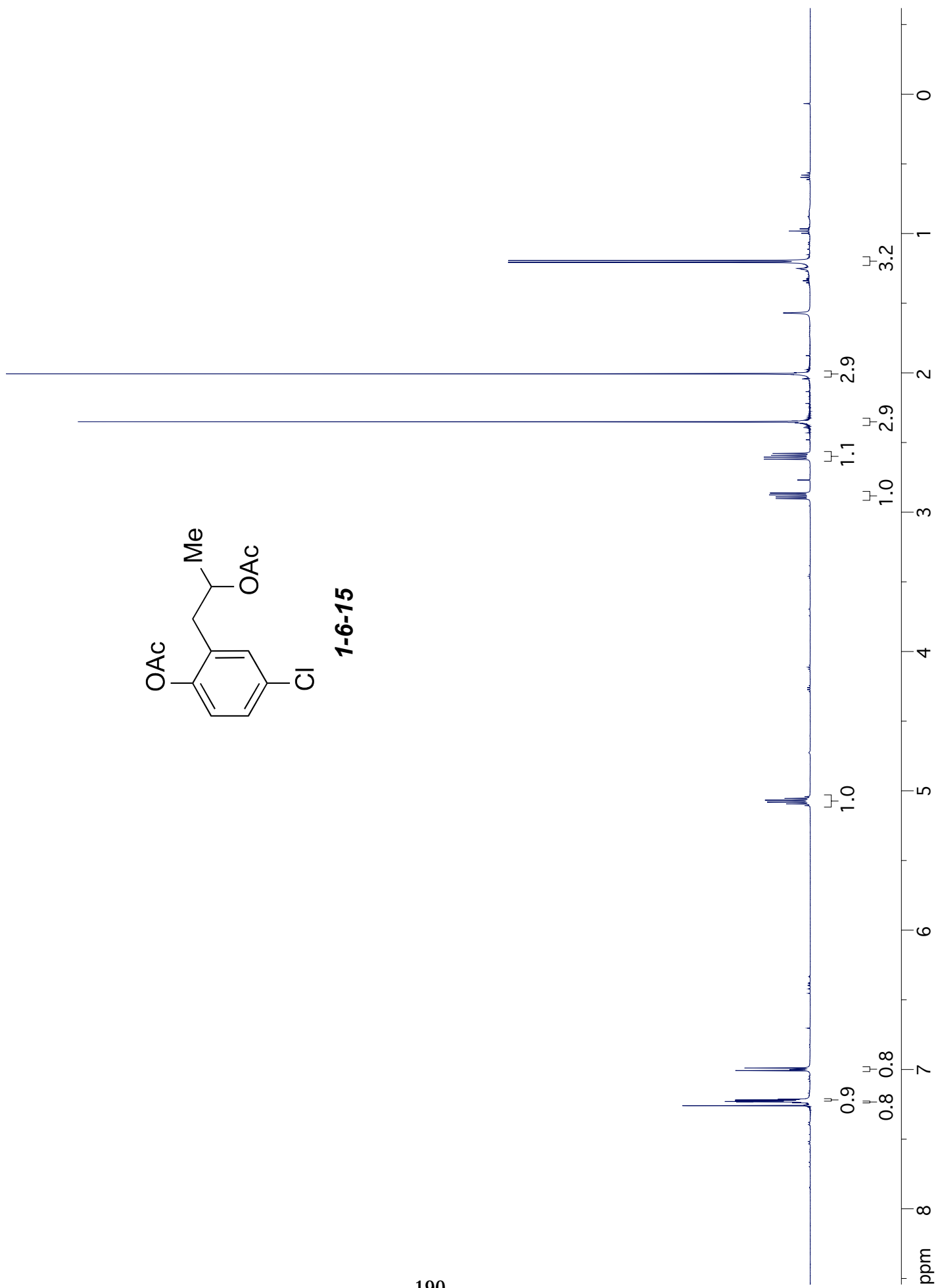
1-6-14

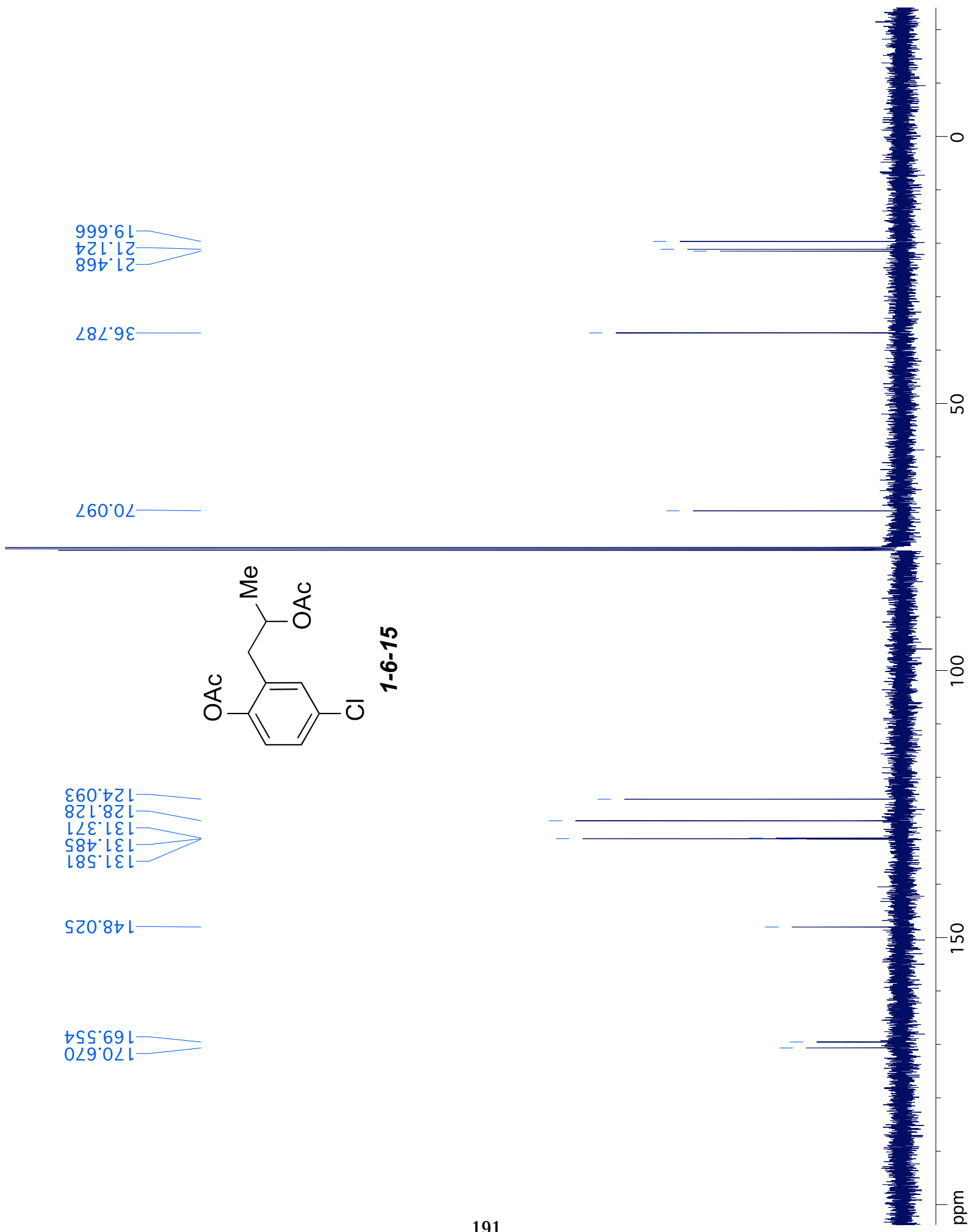


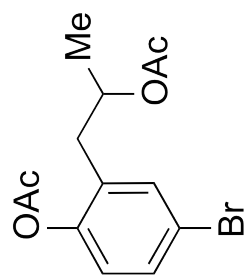




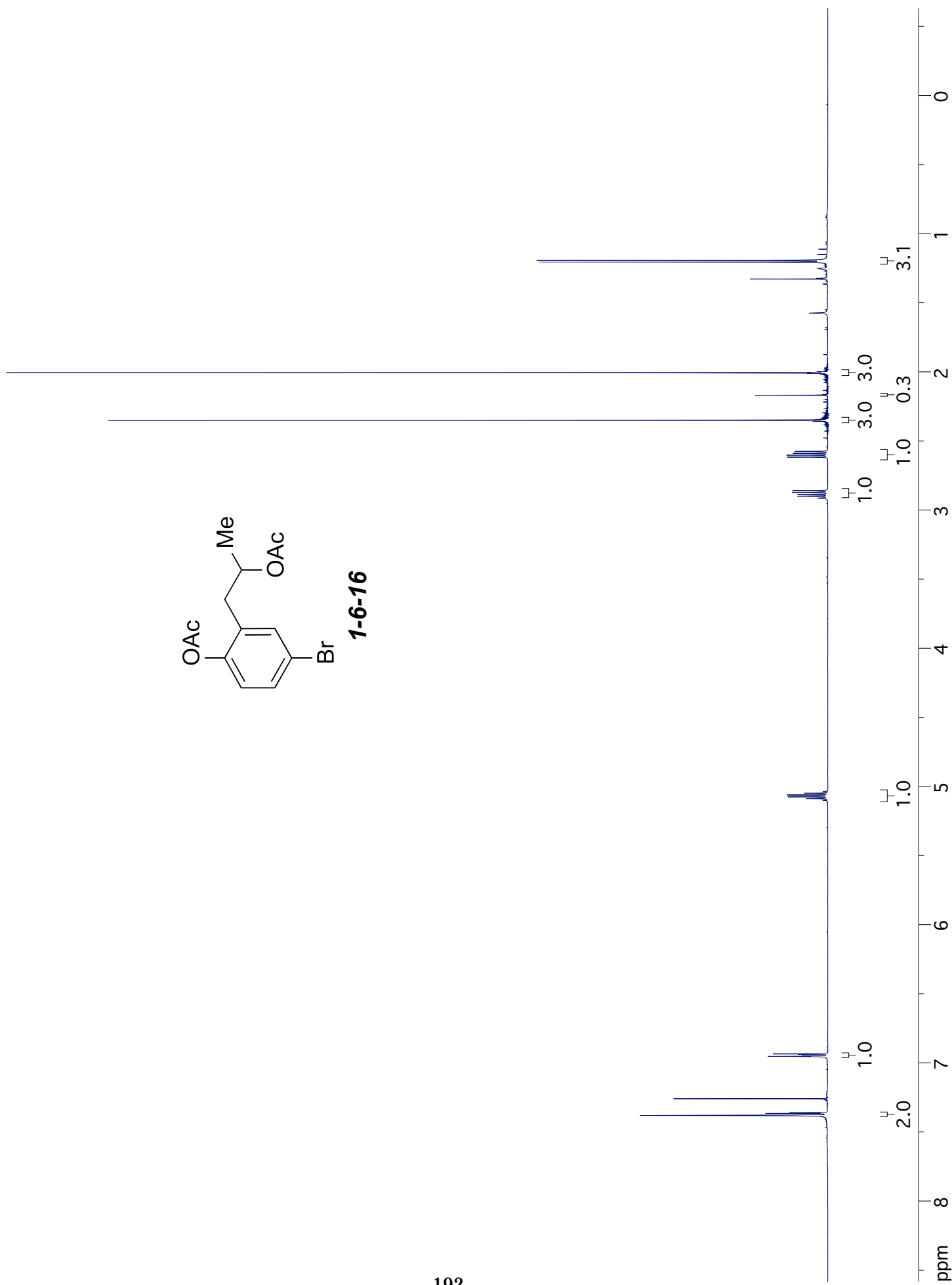
1-6-15

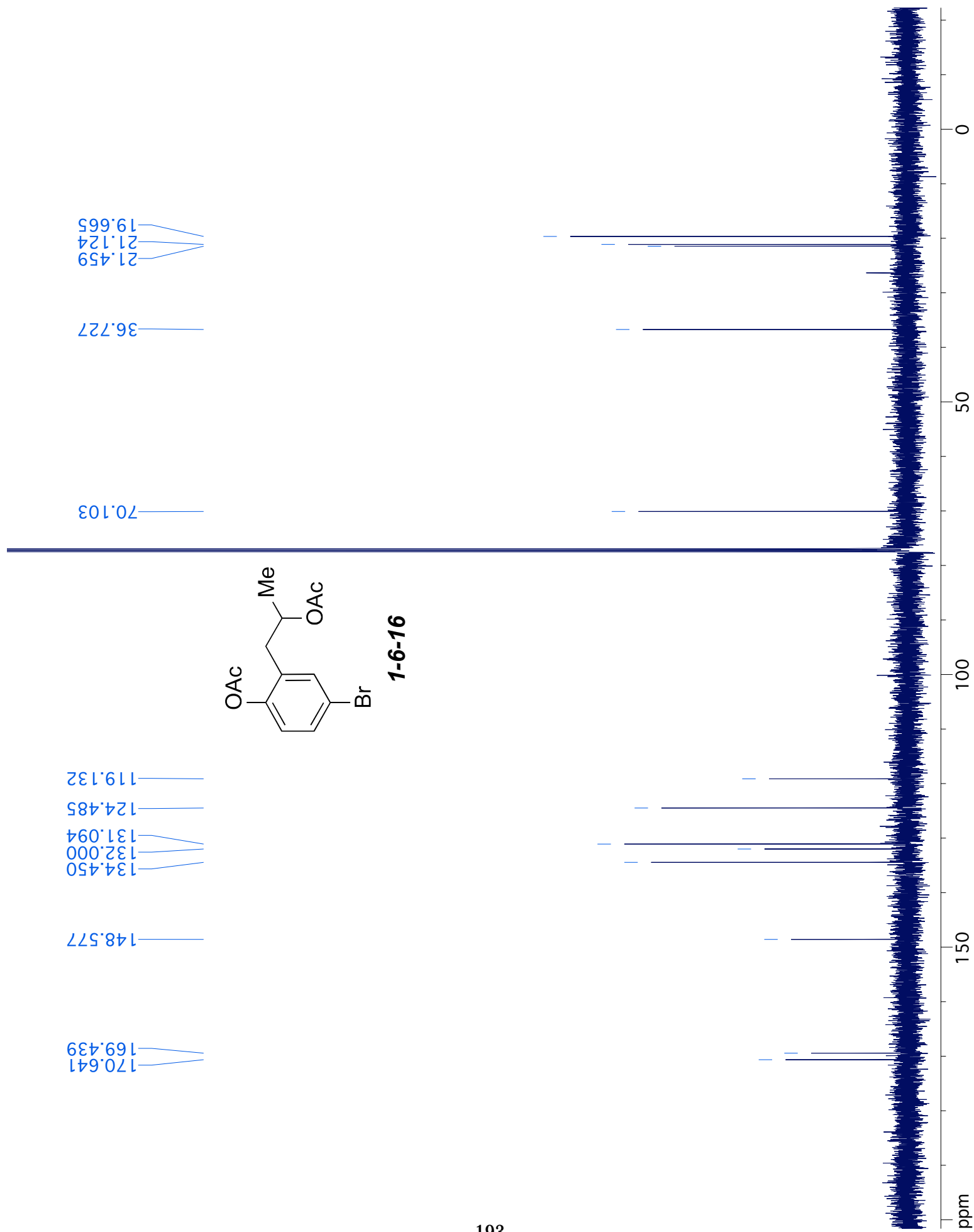


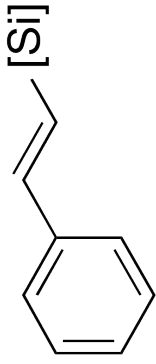




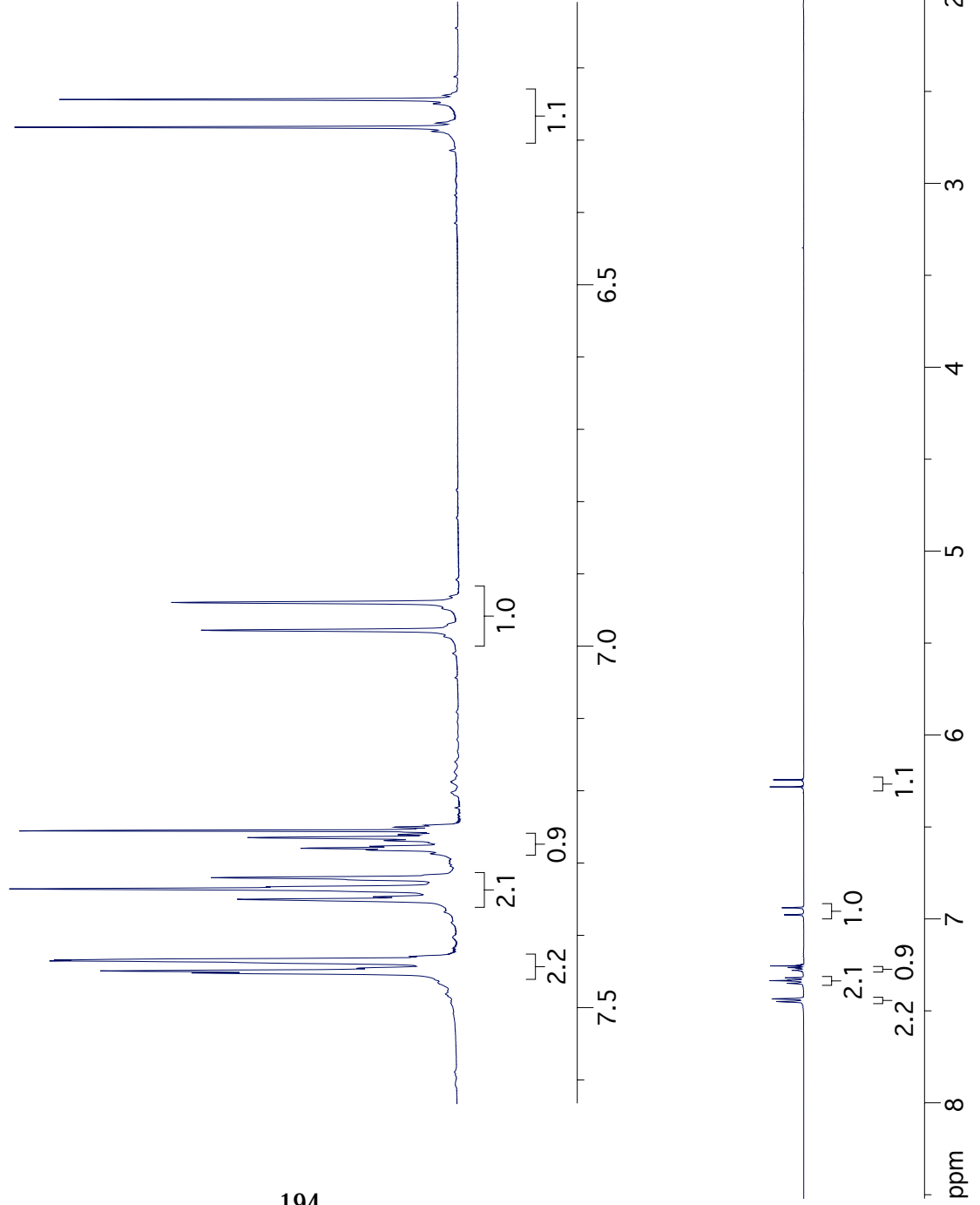
1-6-16

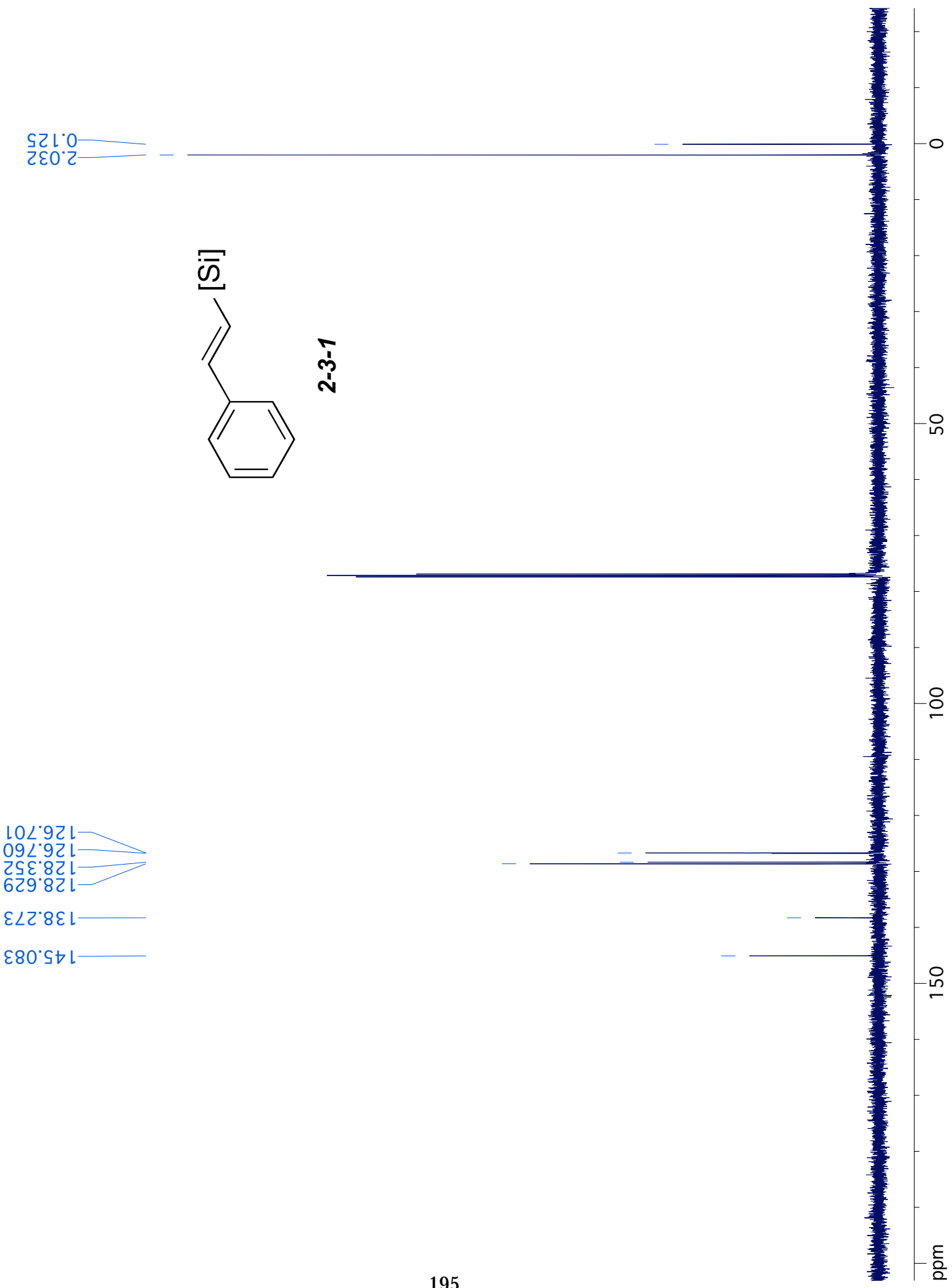


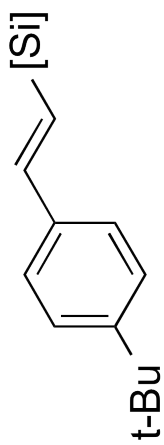




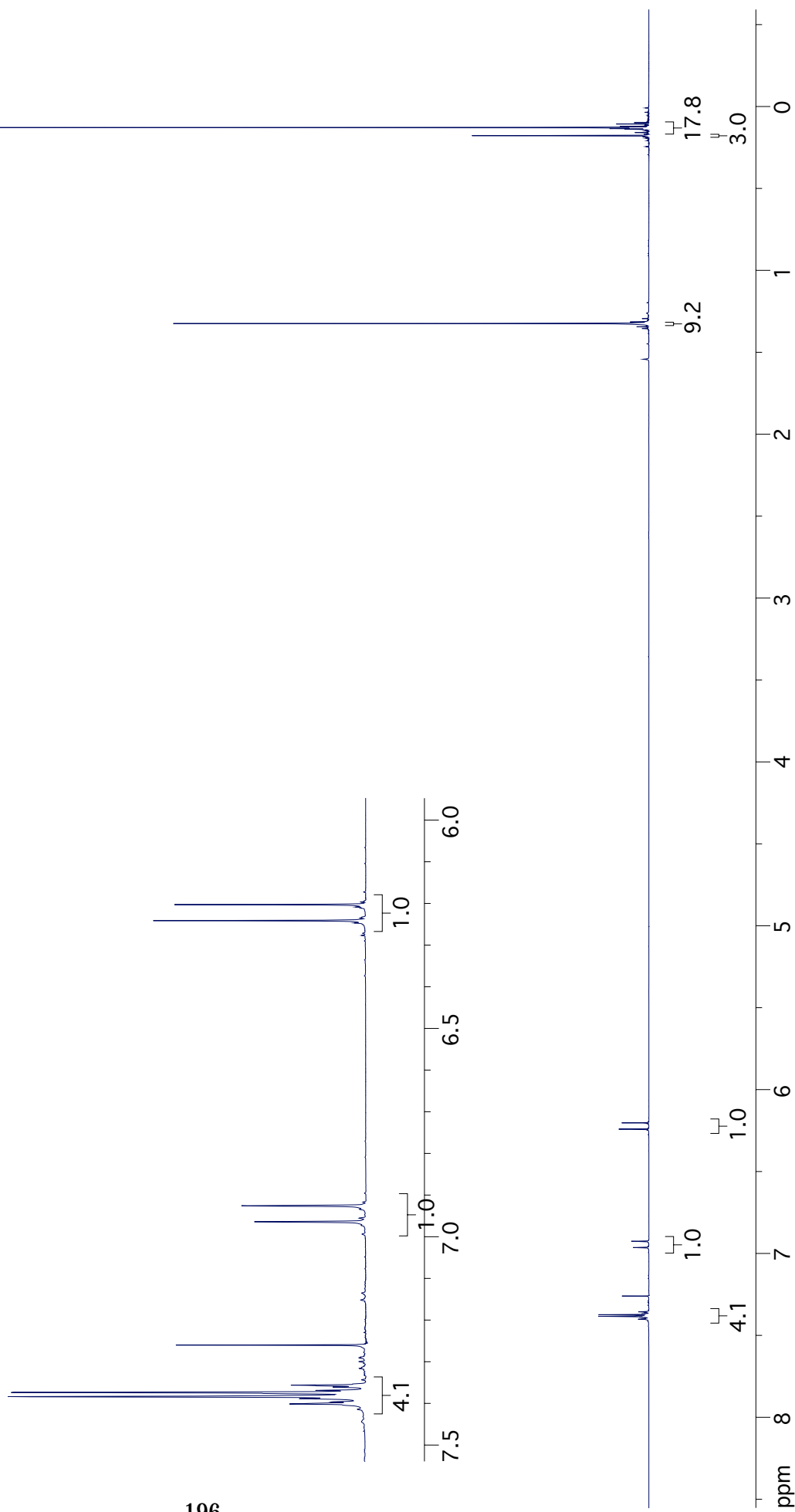
2-3-1

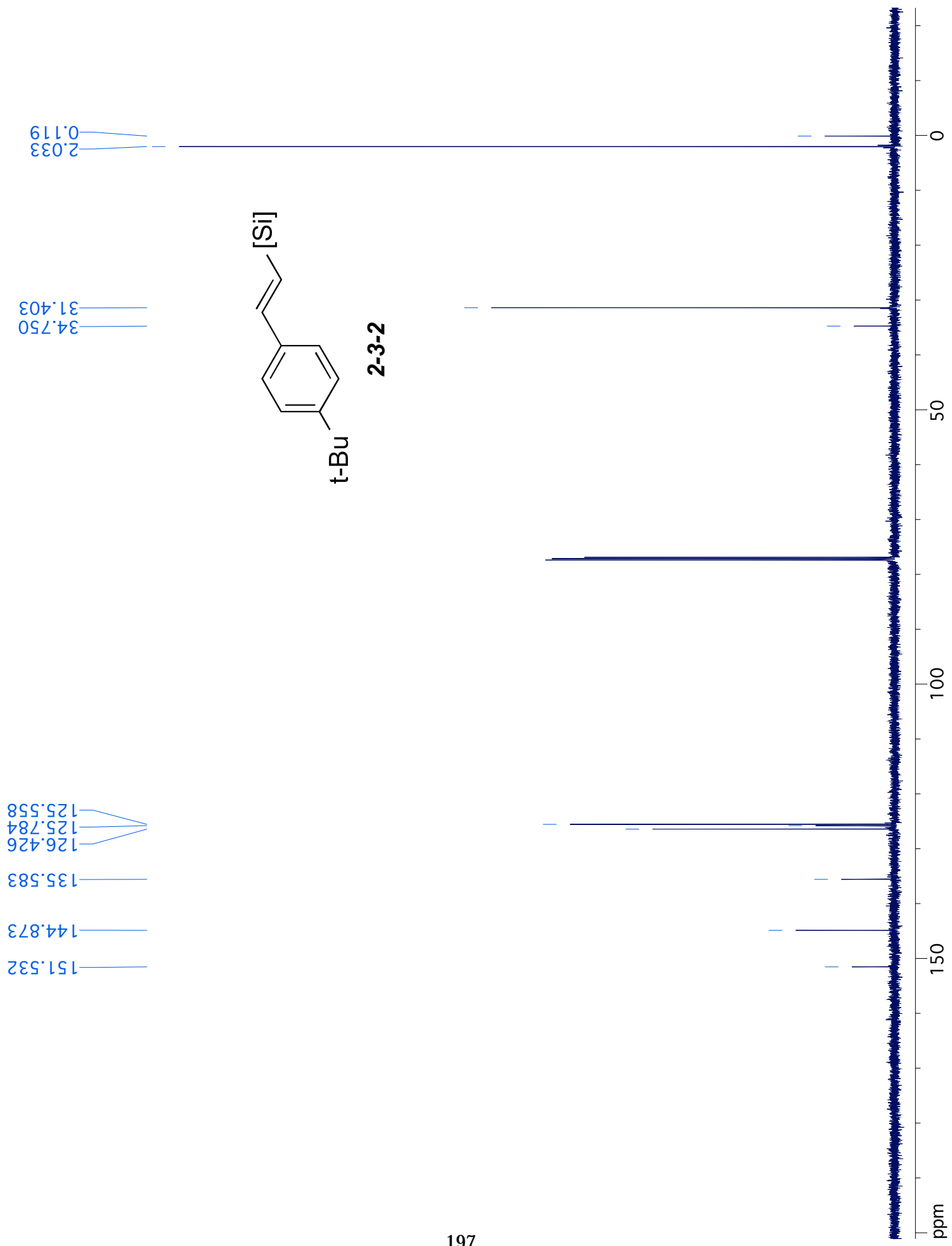


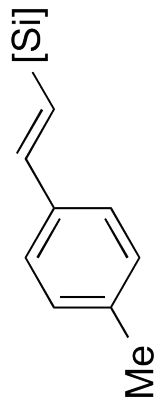




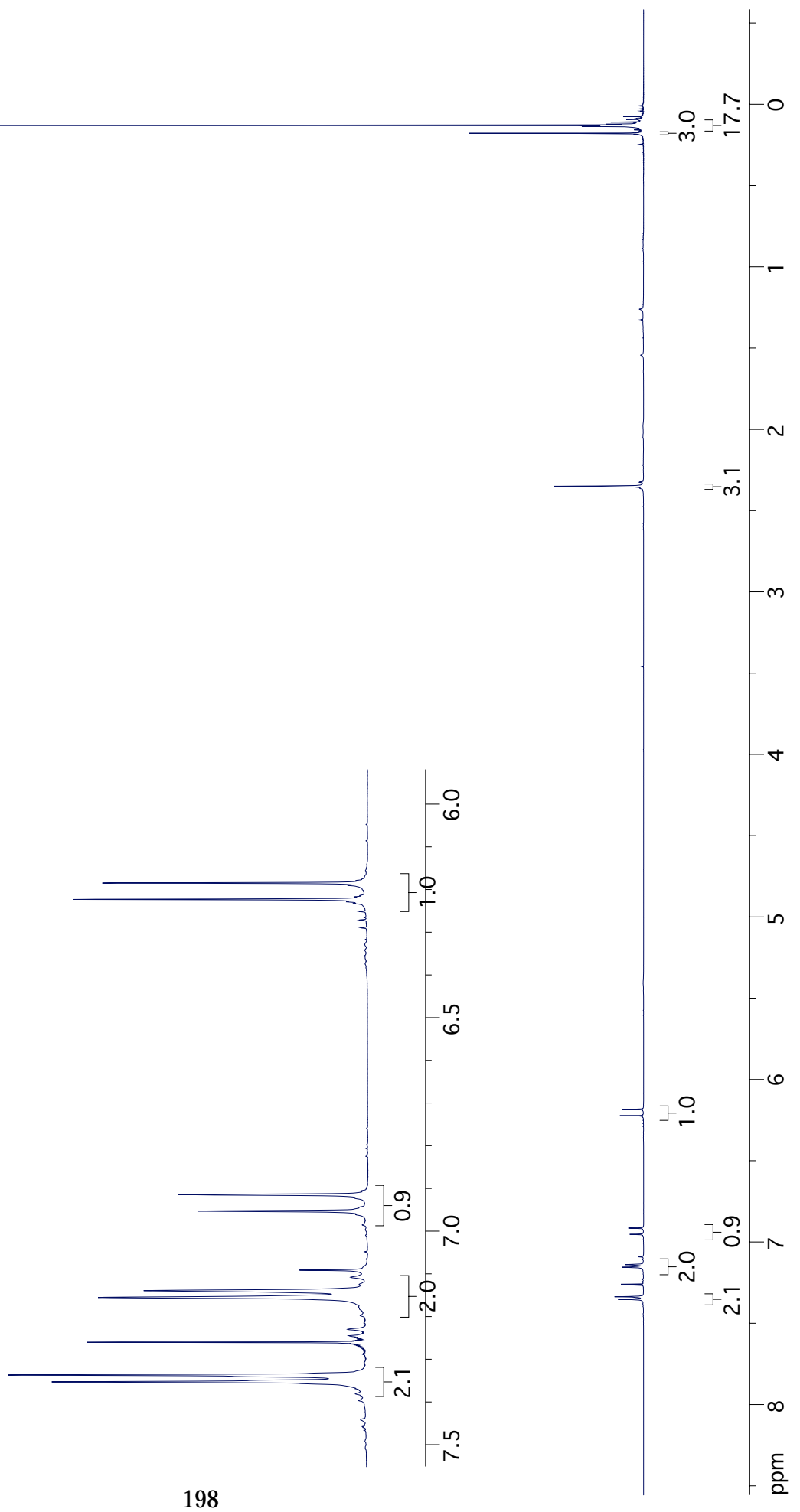
2-3-2

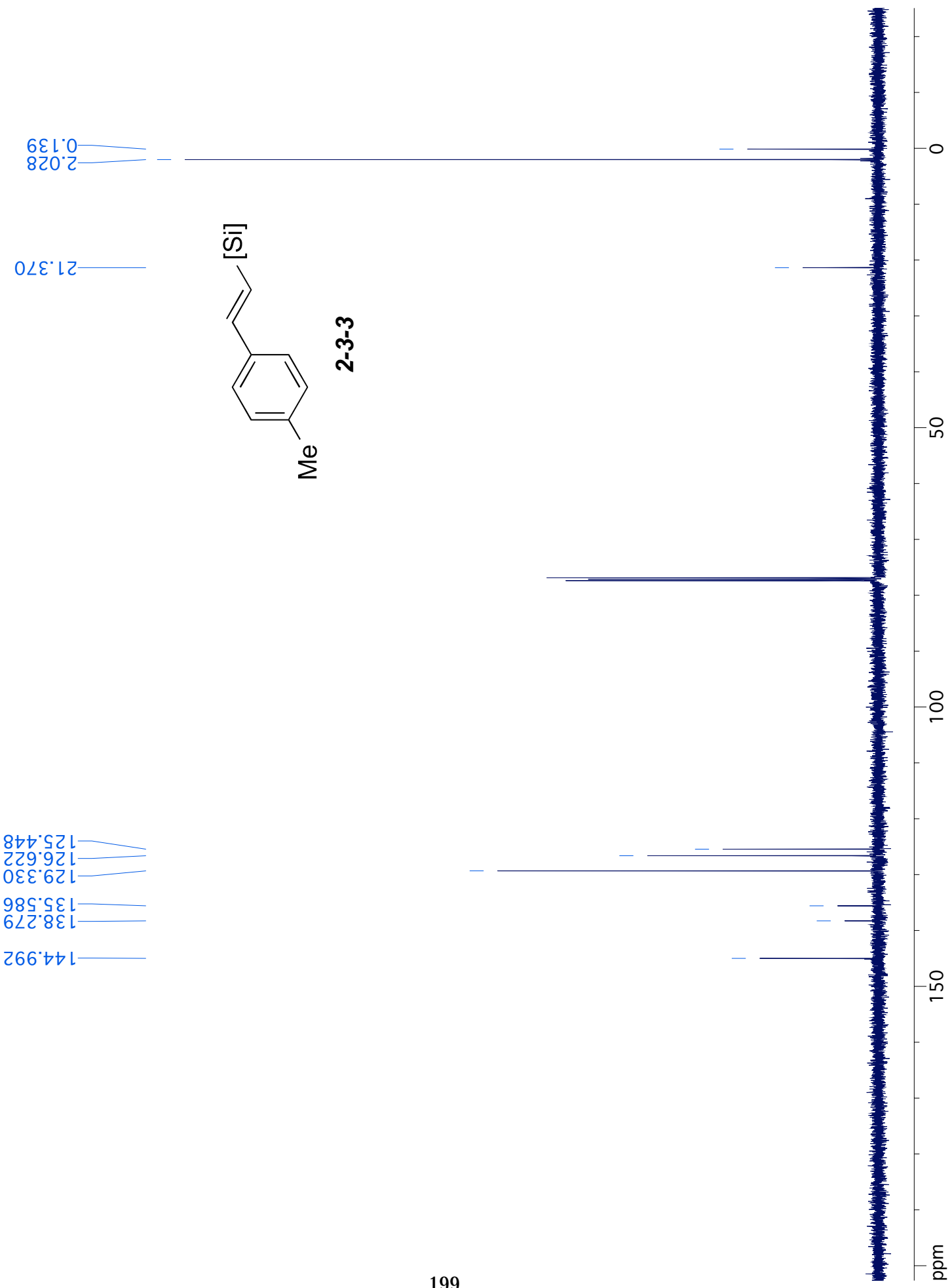


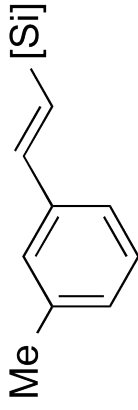




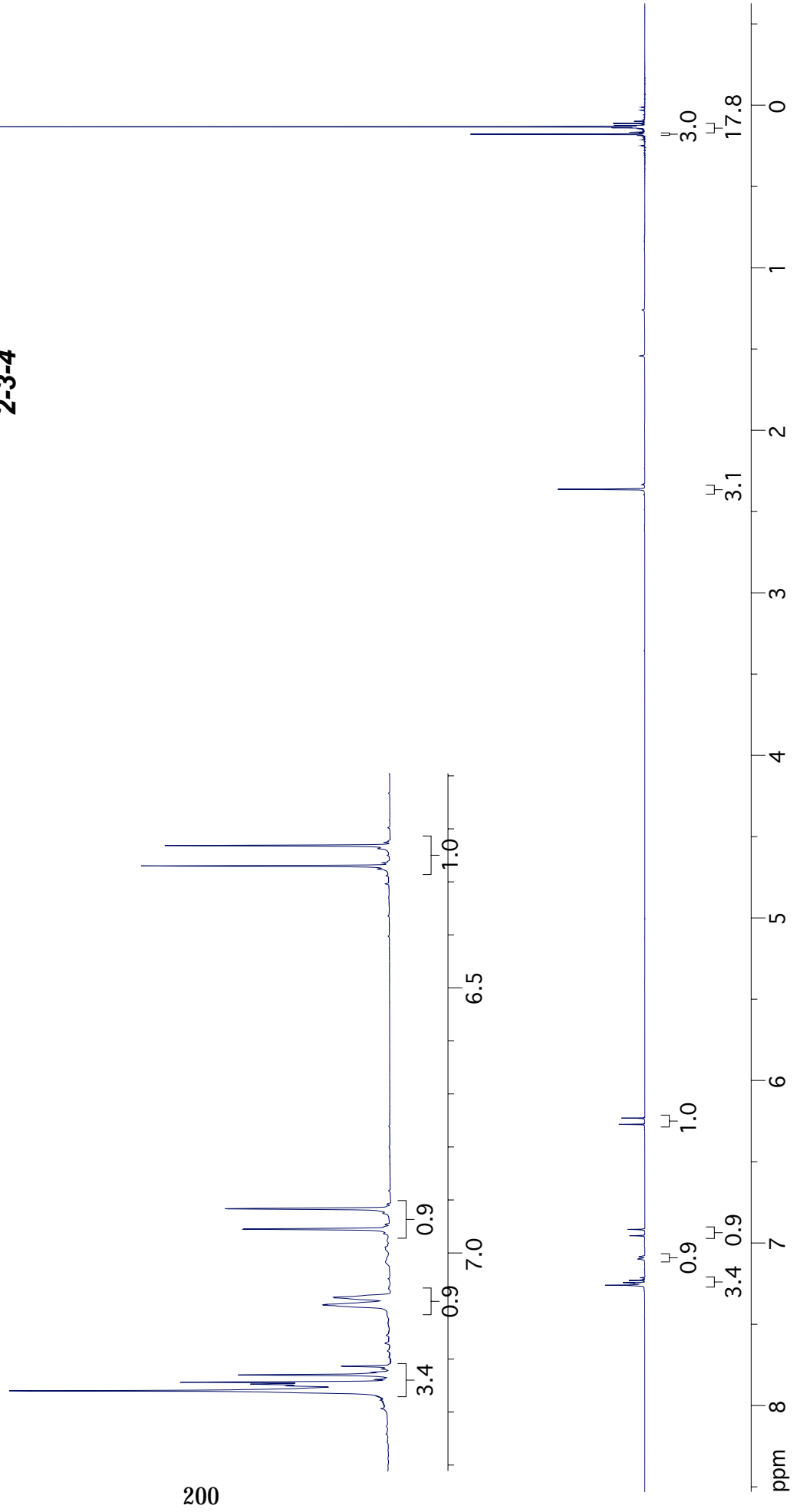
2-3-3

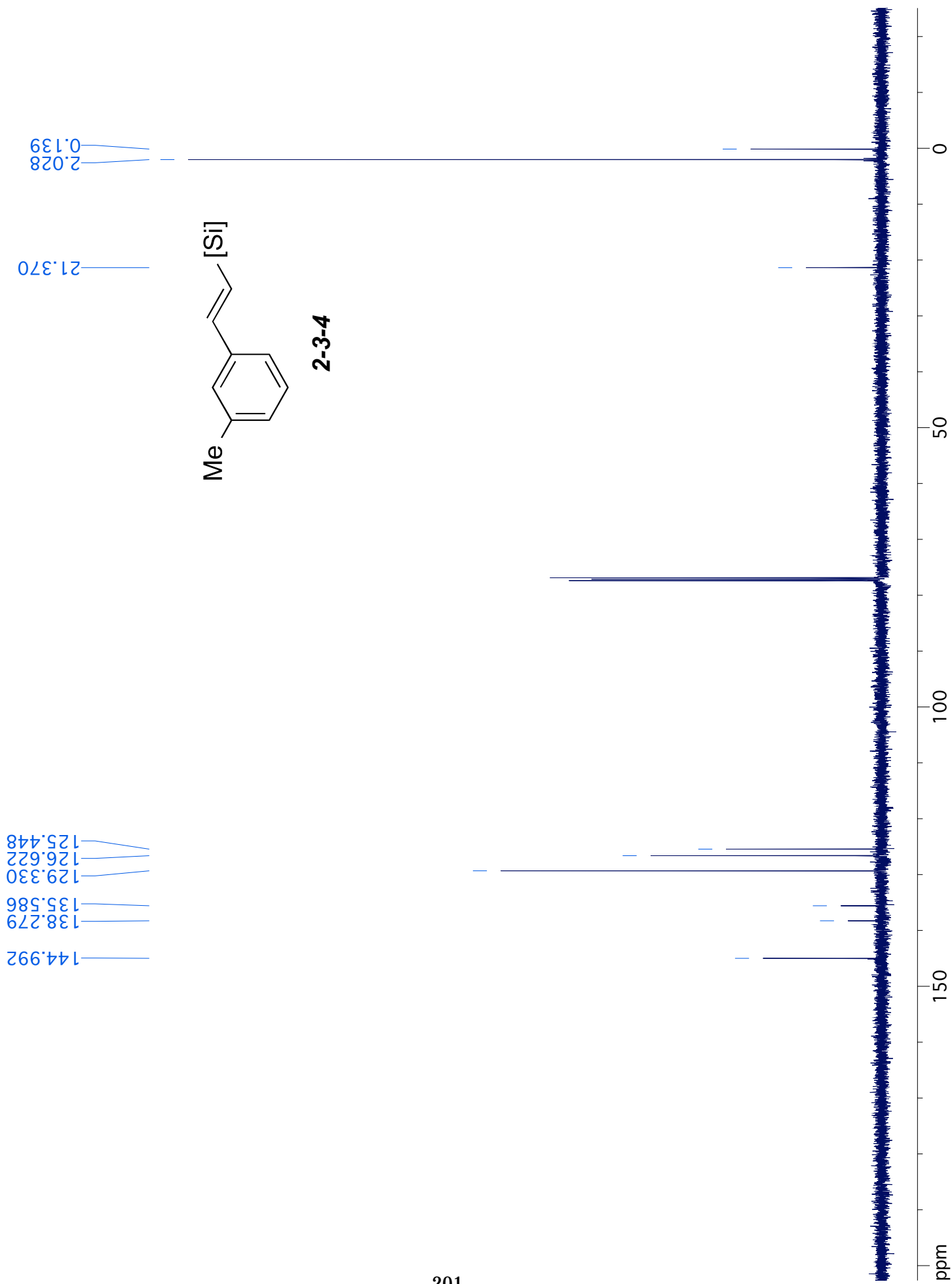


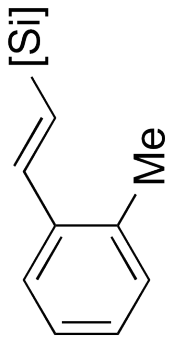




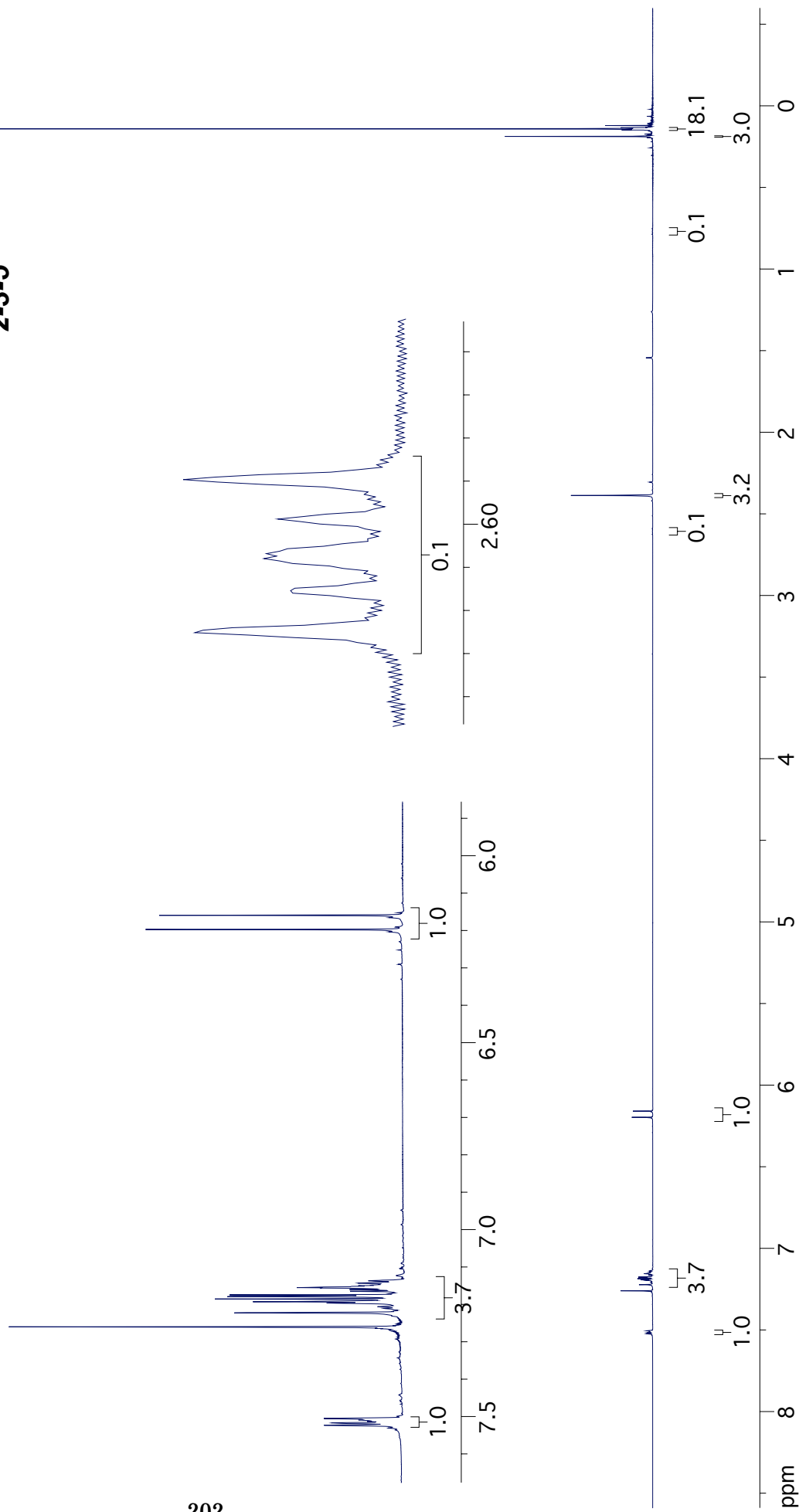
2-3-4

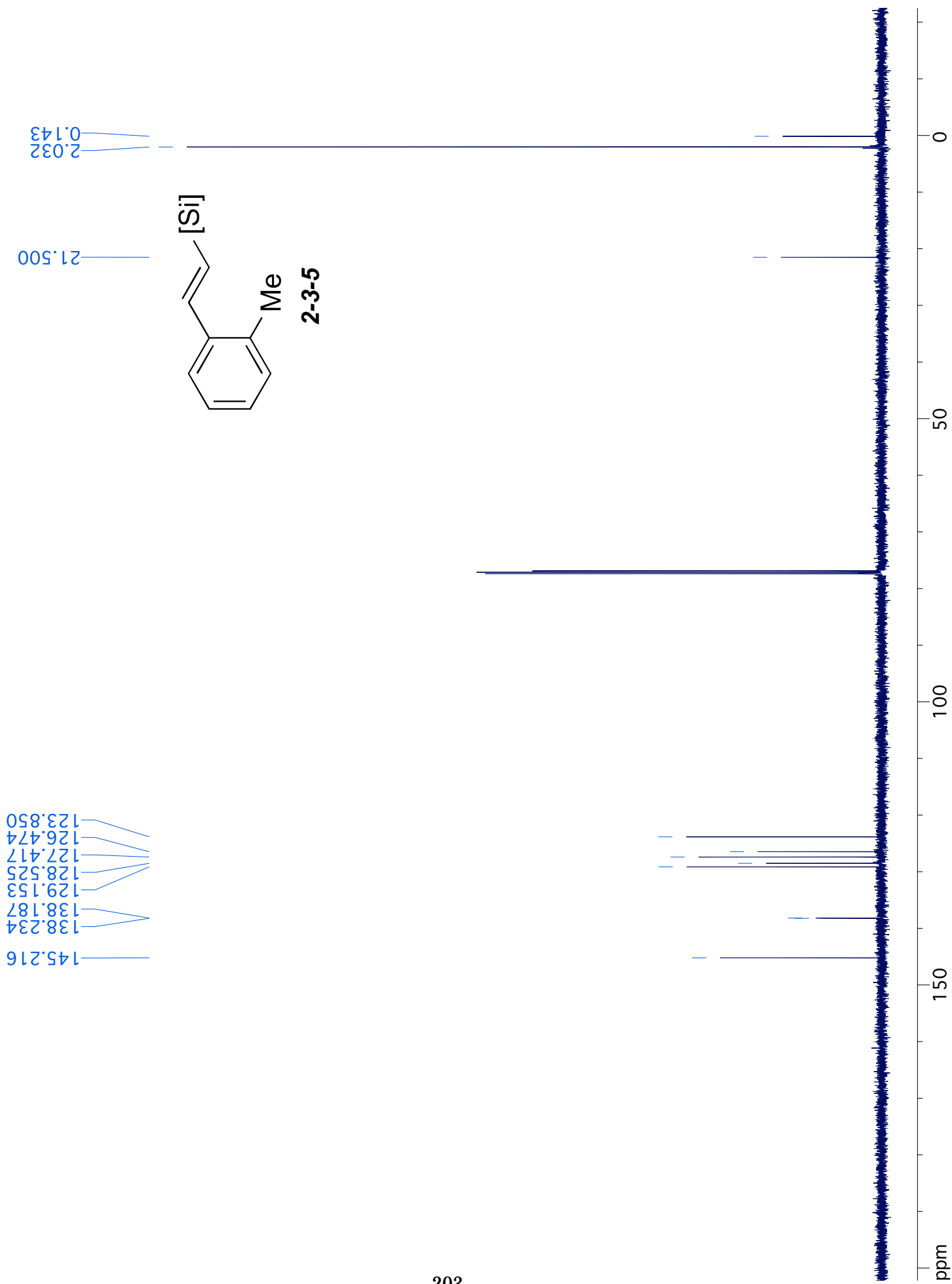


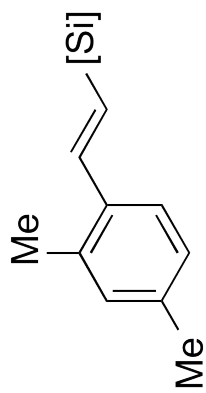




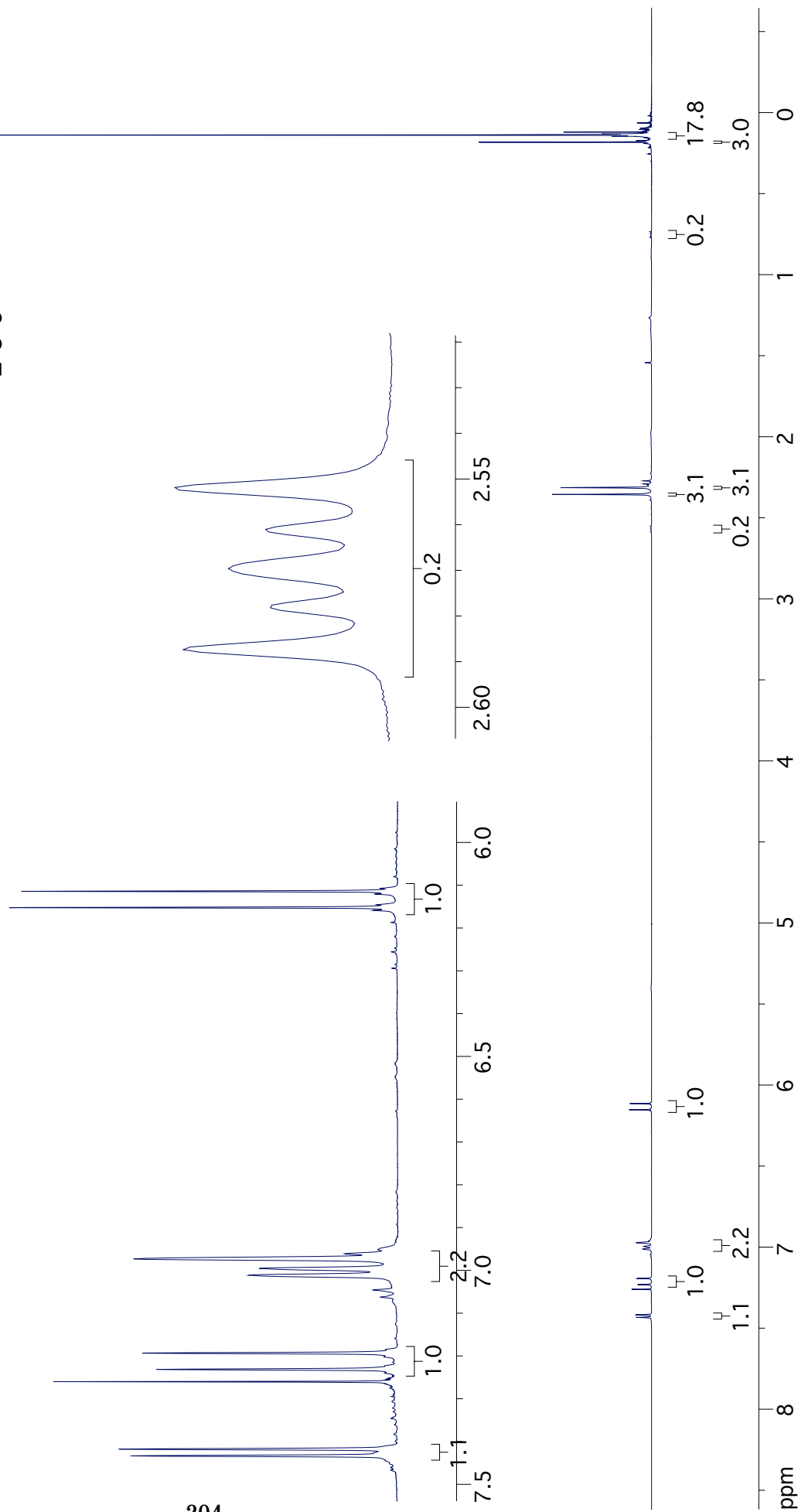
2-3-5

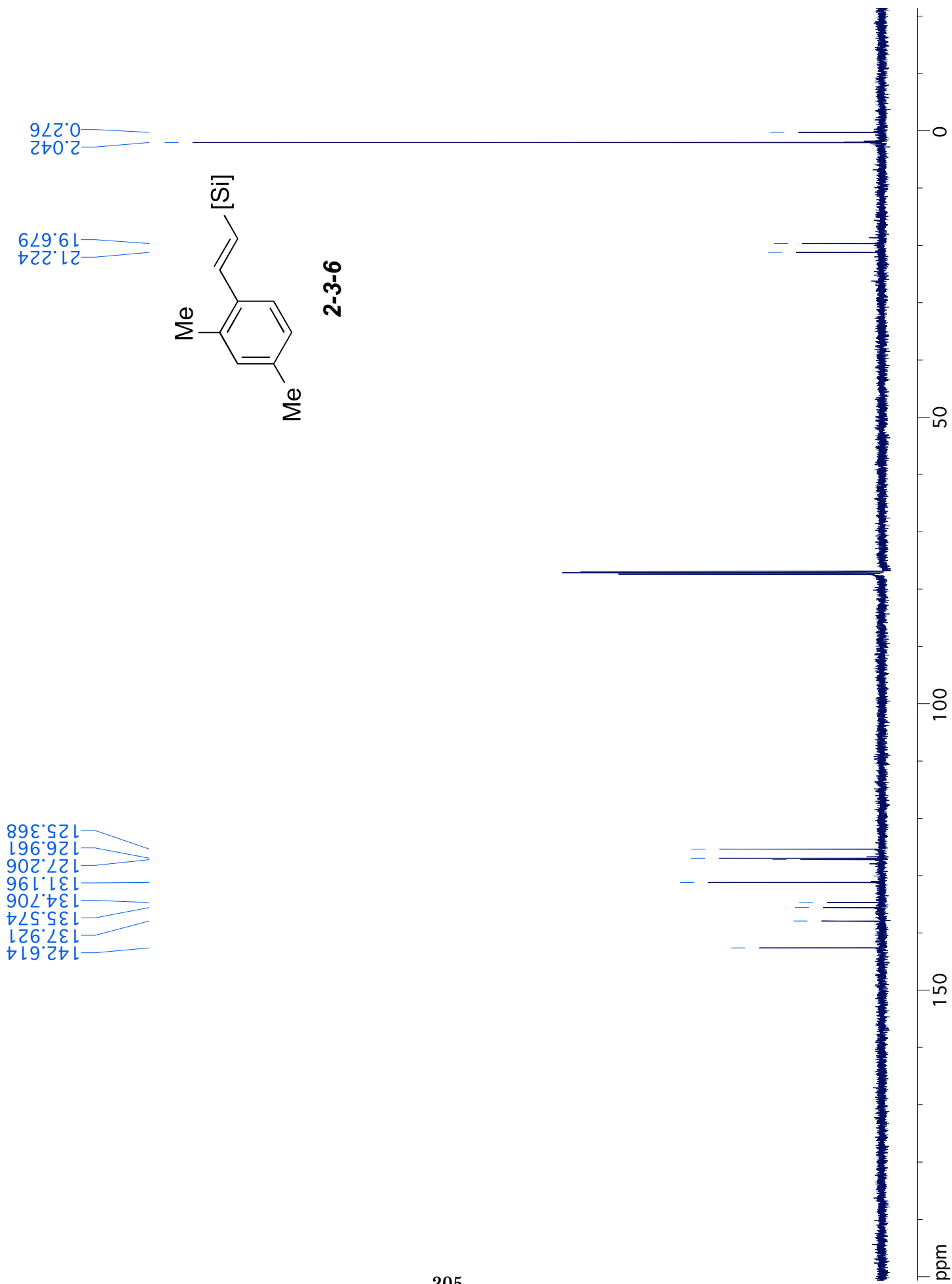


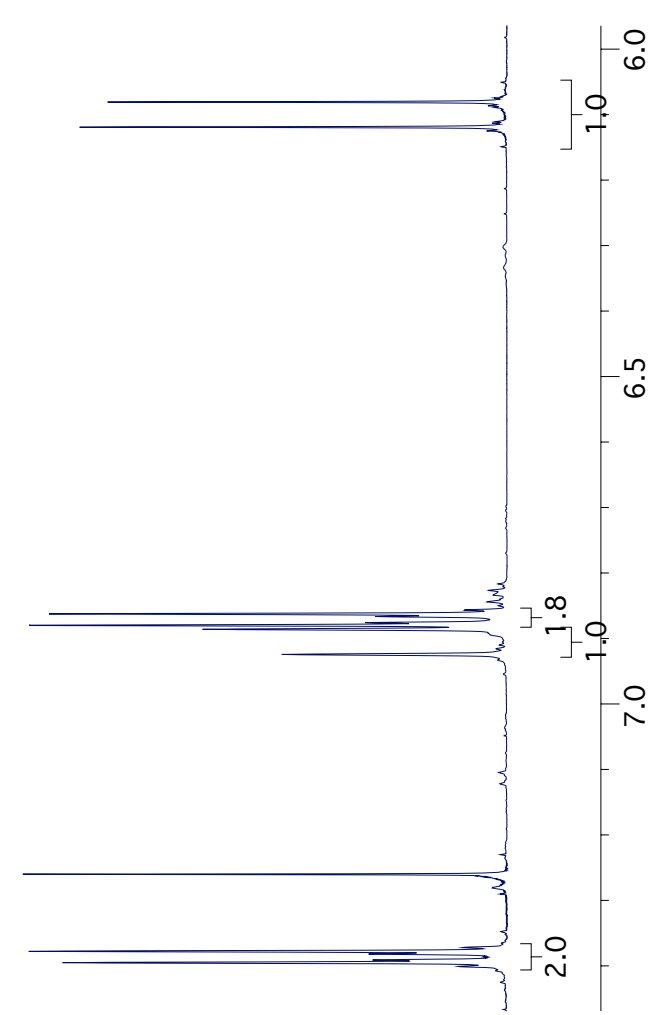
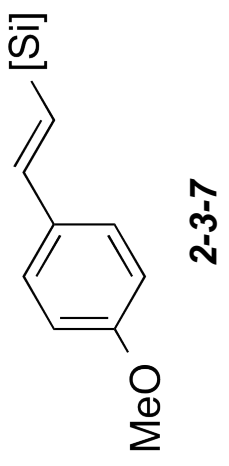




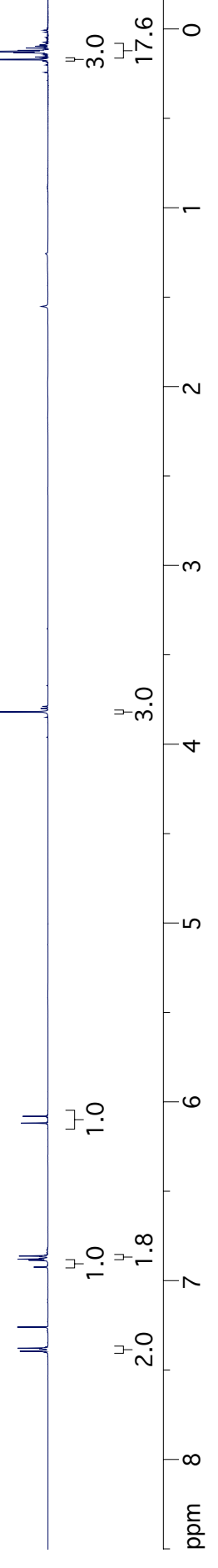
2-3-6

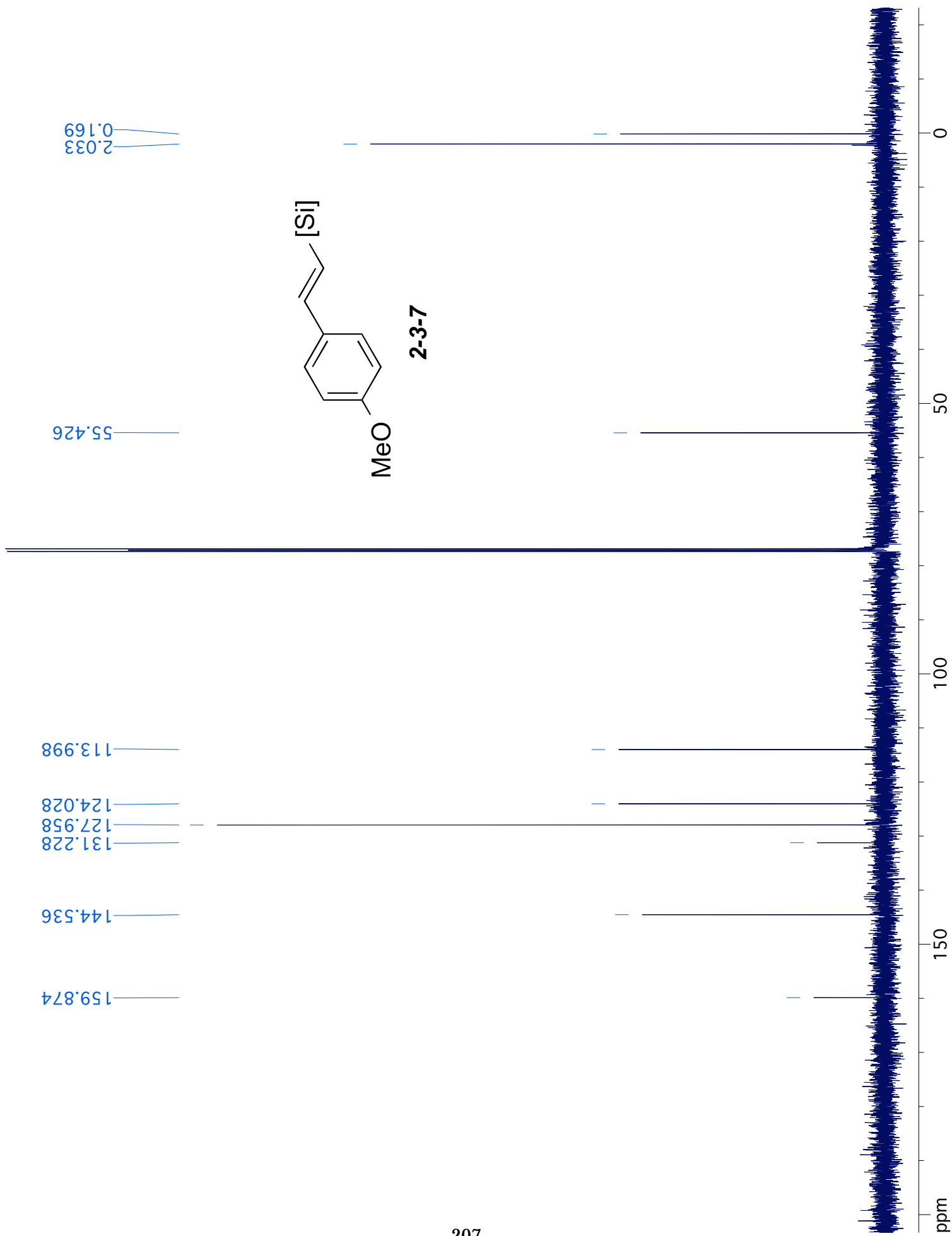


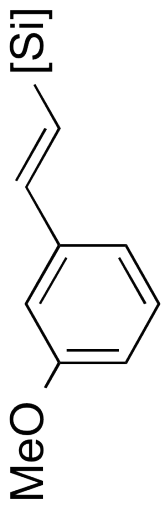




206

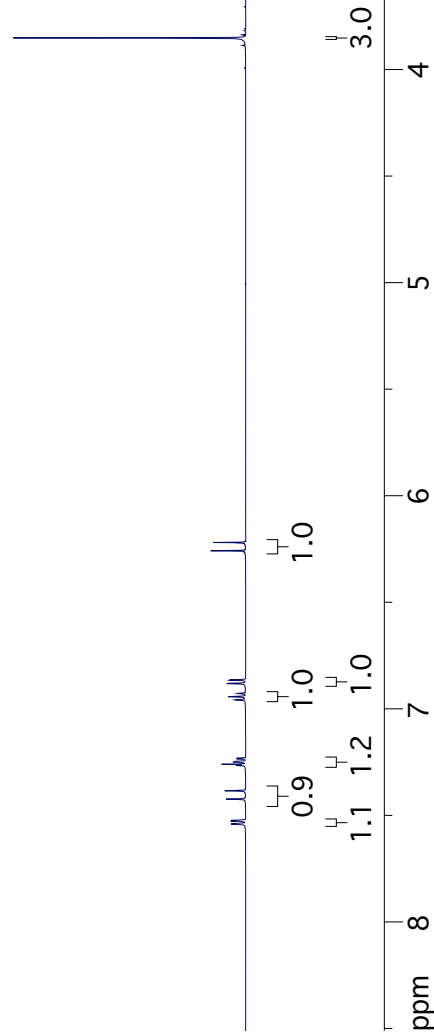
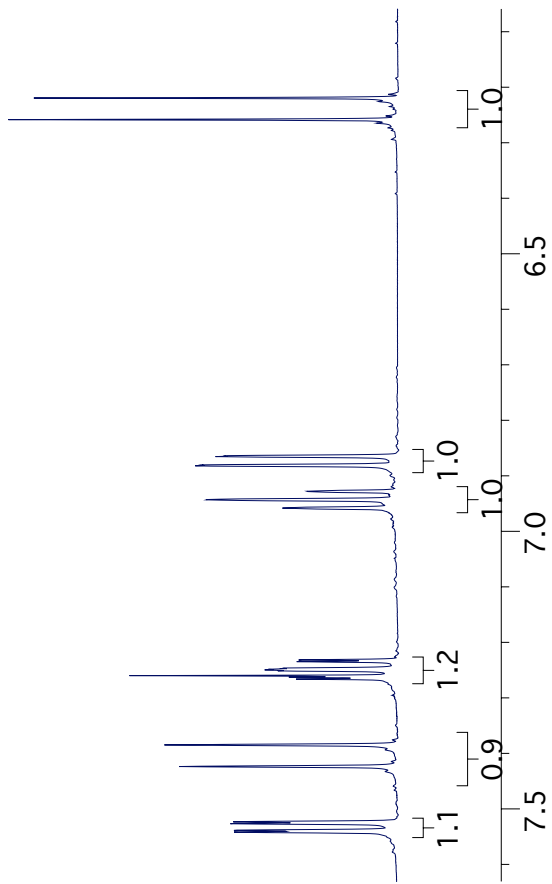


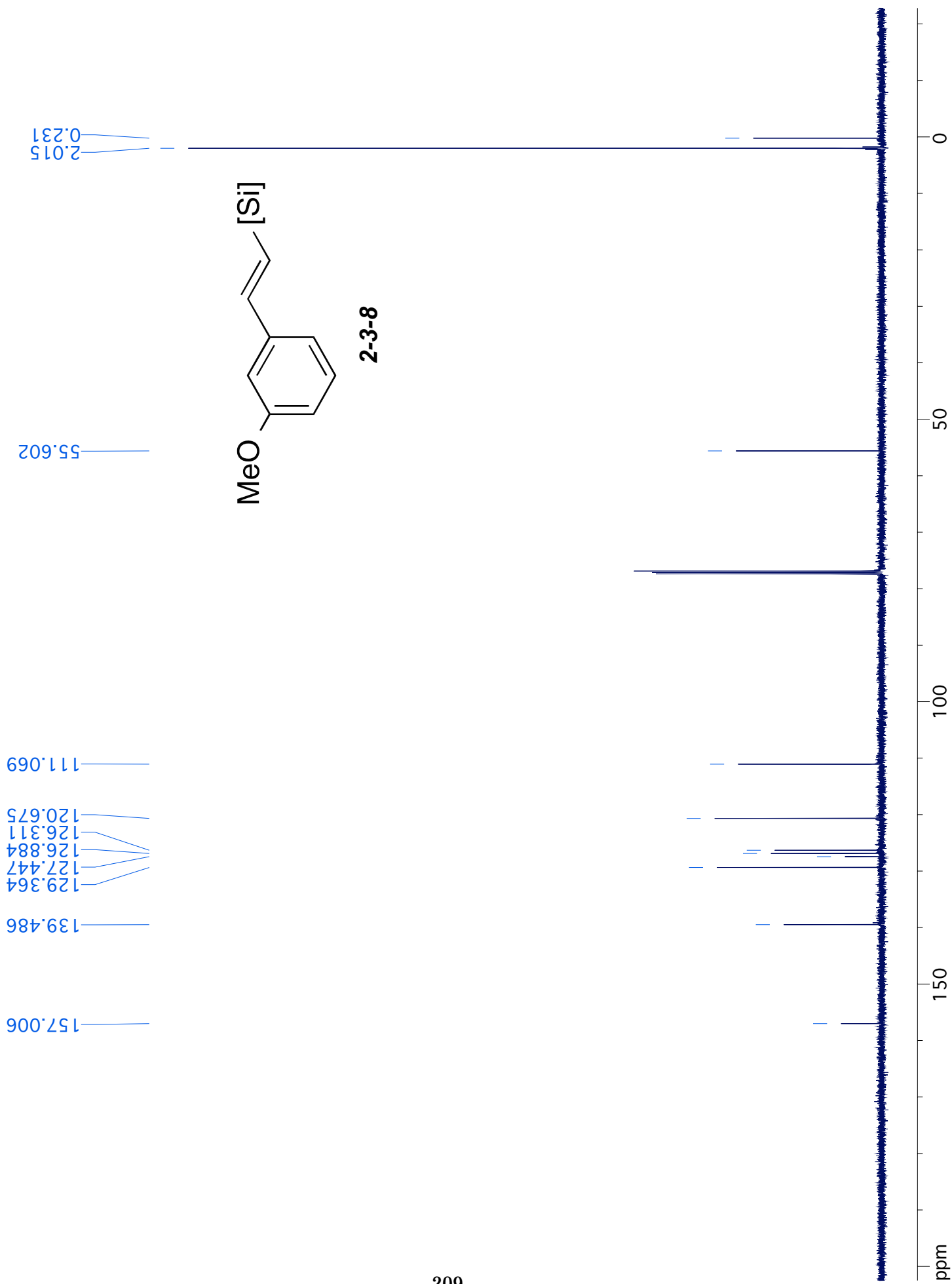


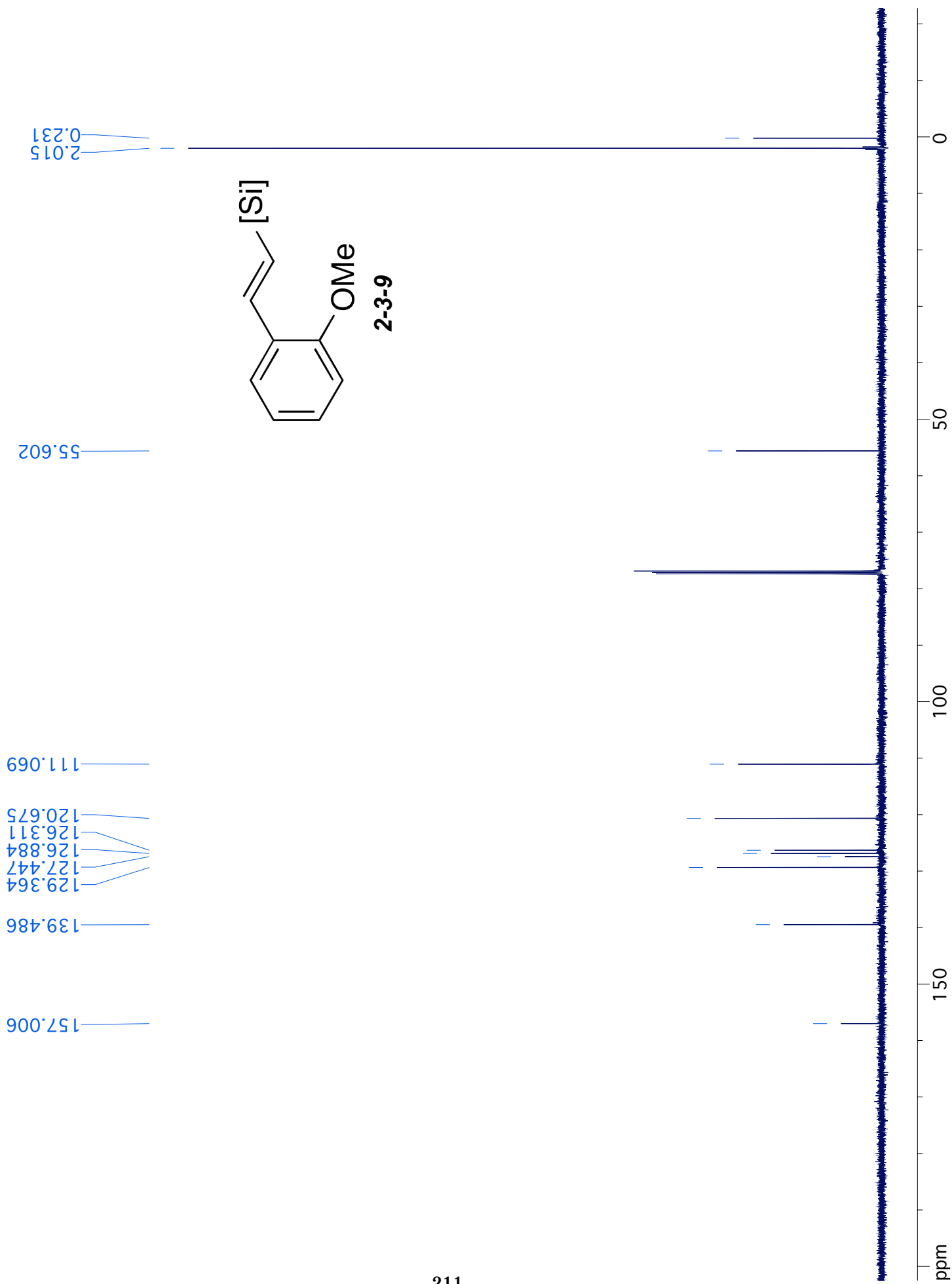


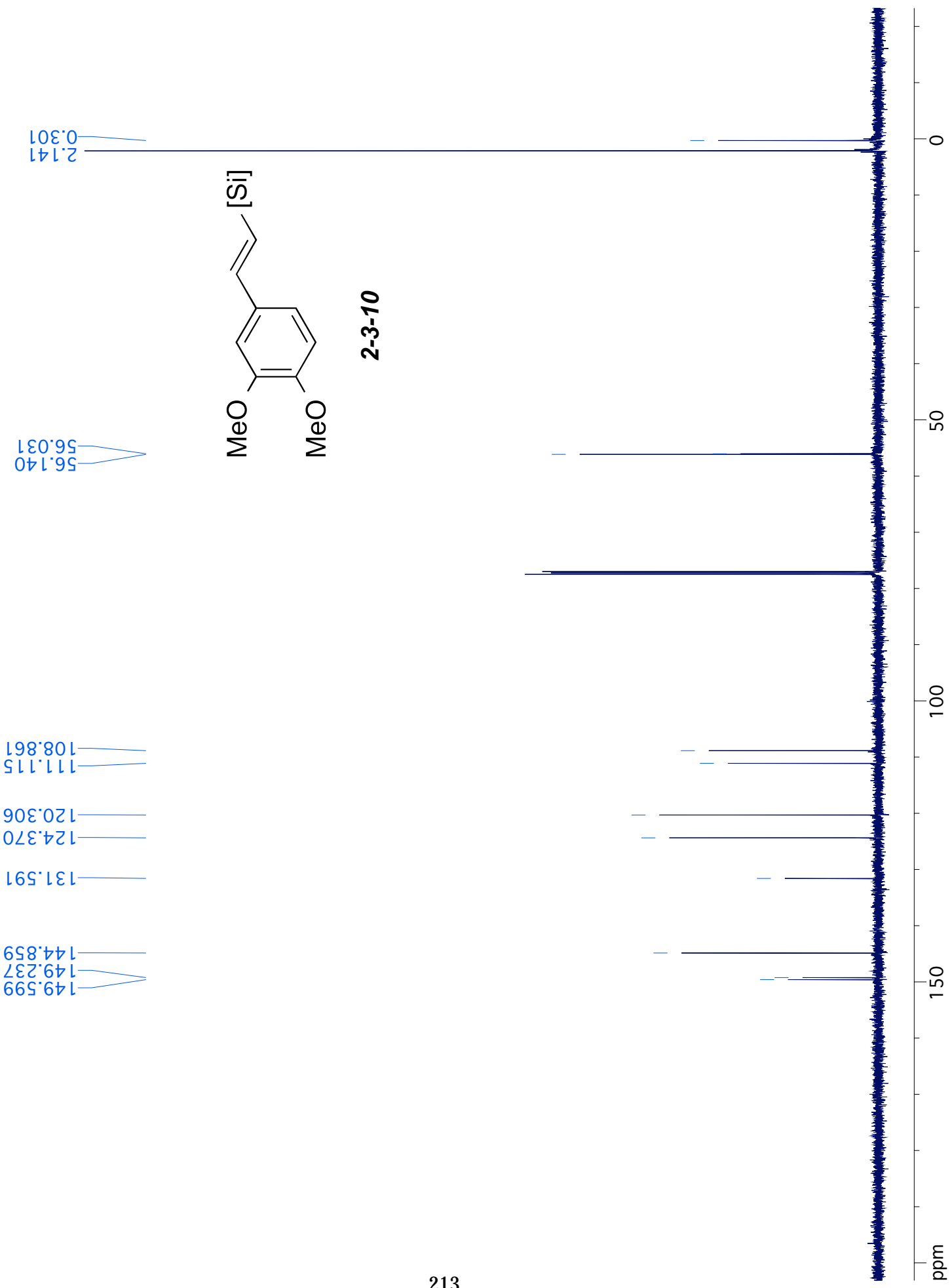
2-3-8

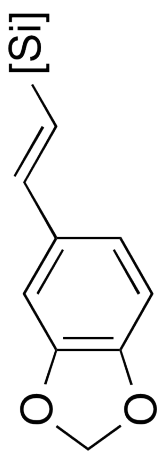
208



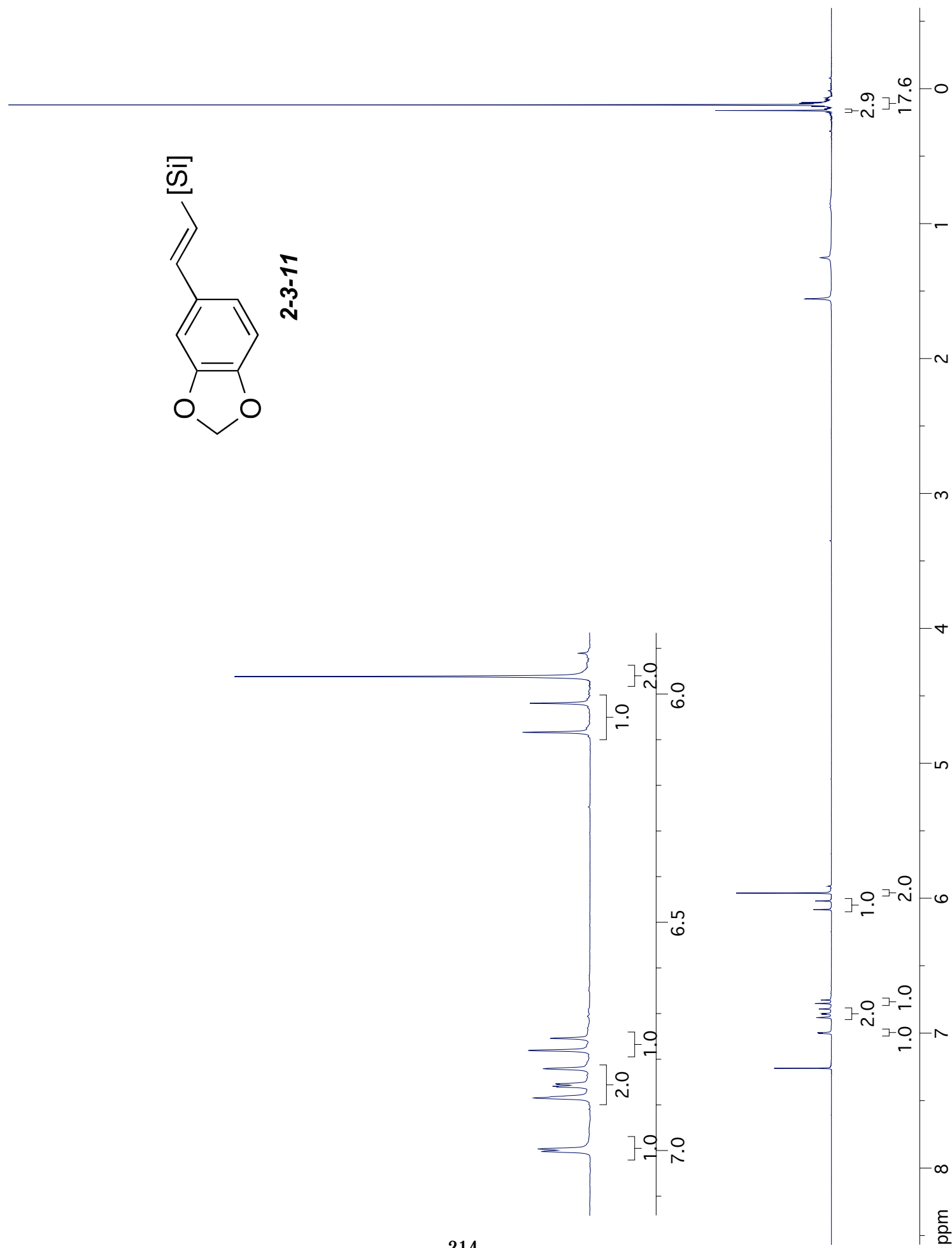


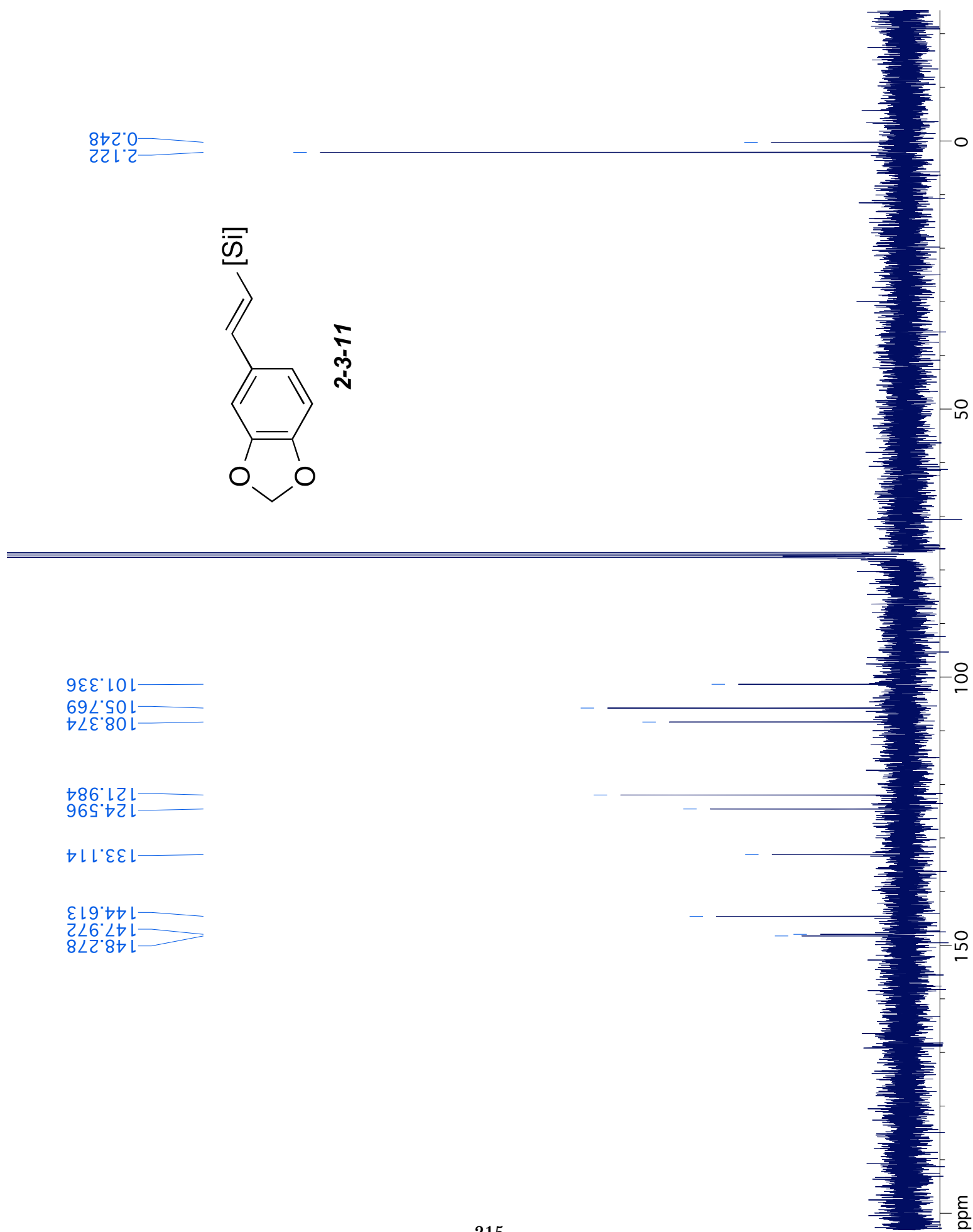


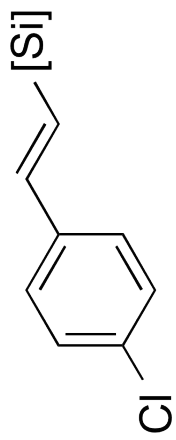




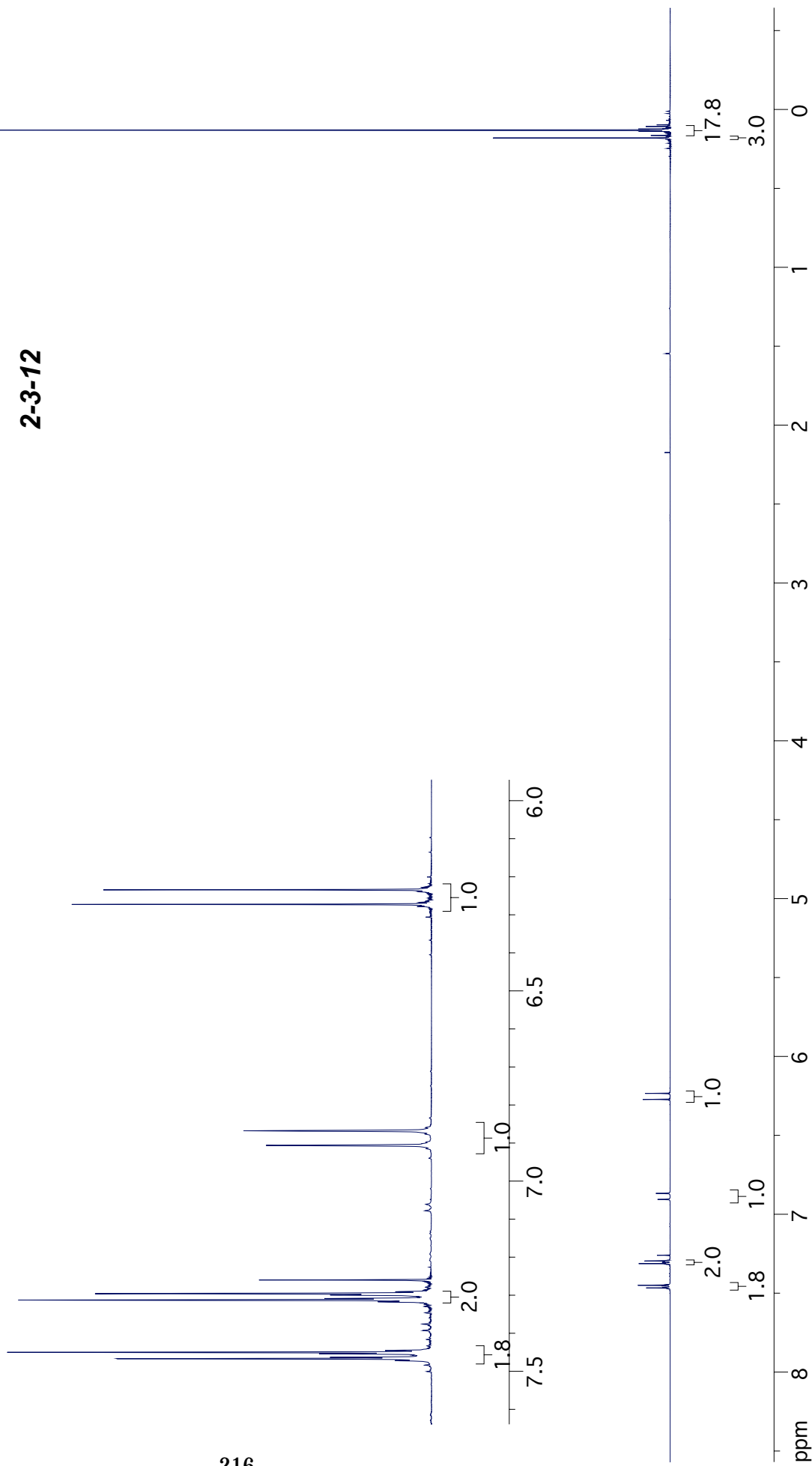
2-3-11

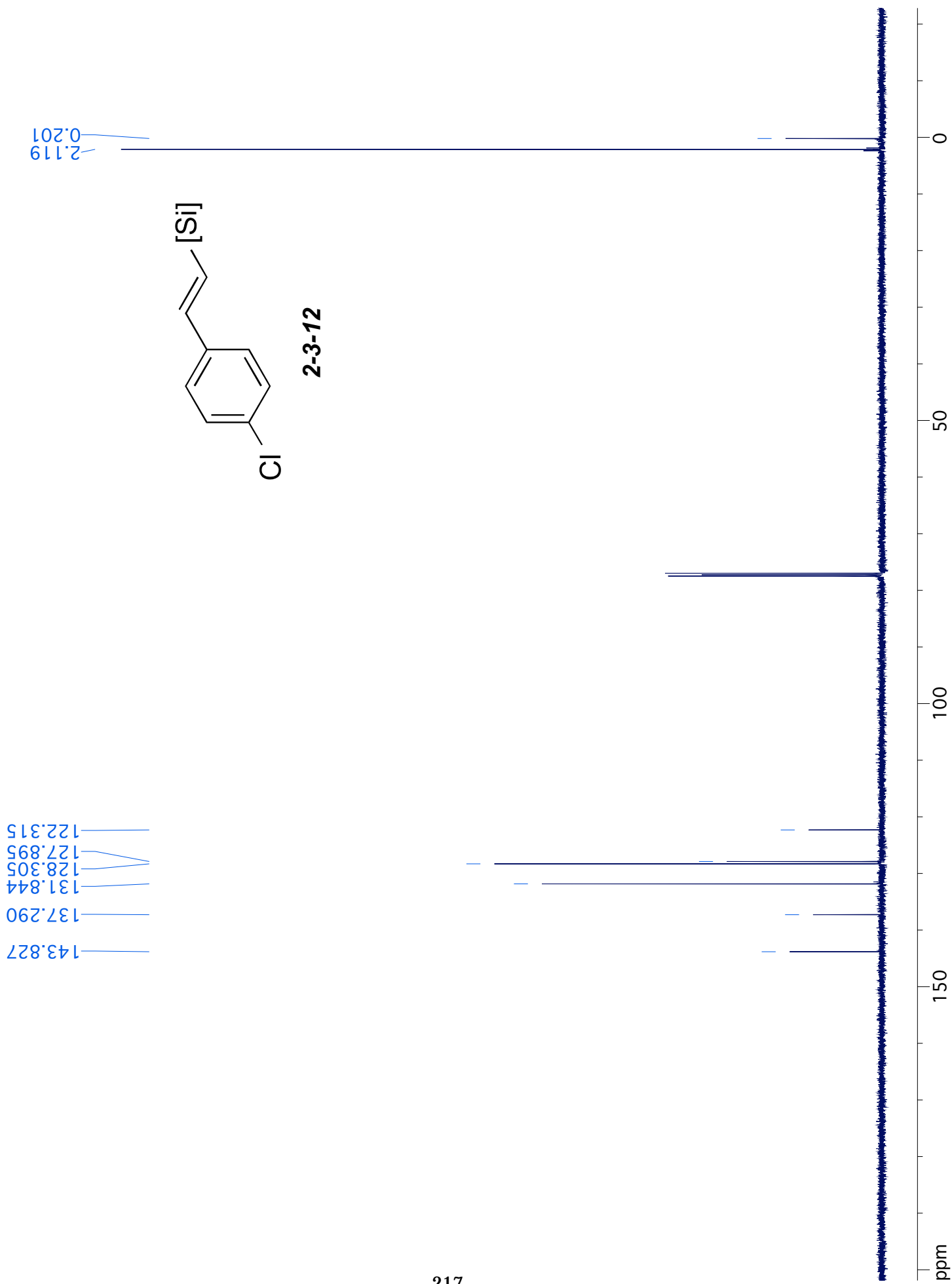


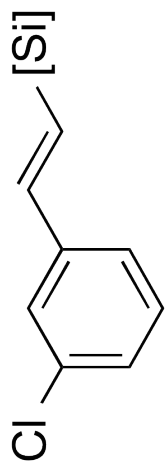




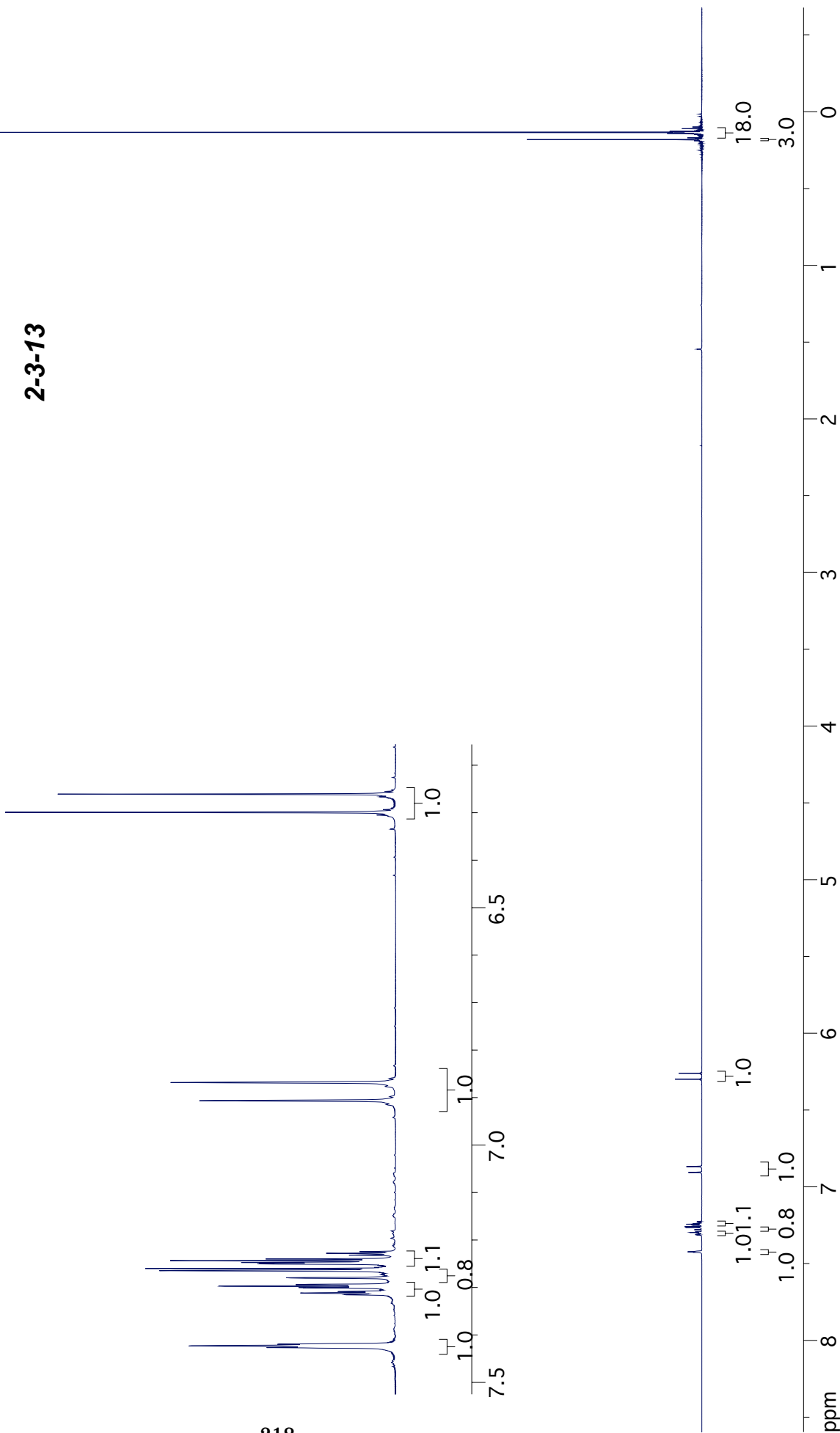
2-3-12



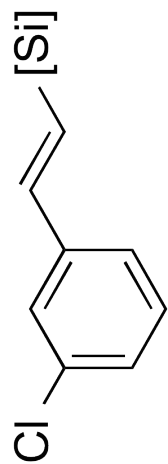




2-3-13

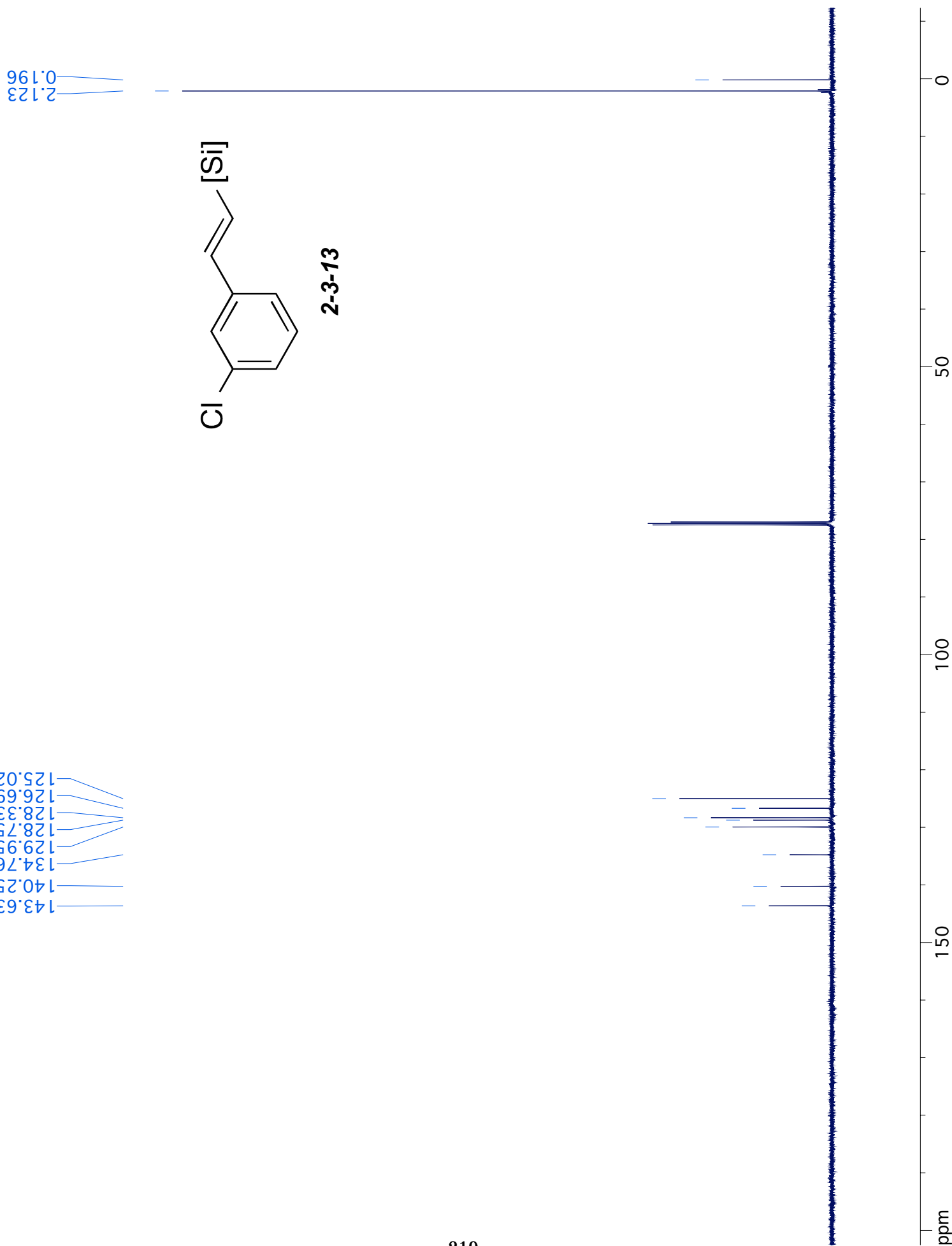


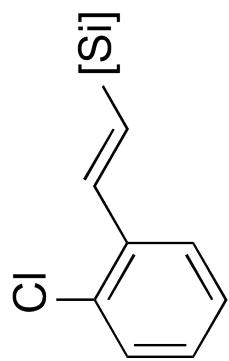
2.123
0.196



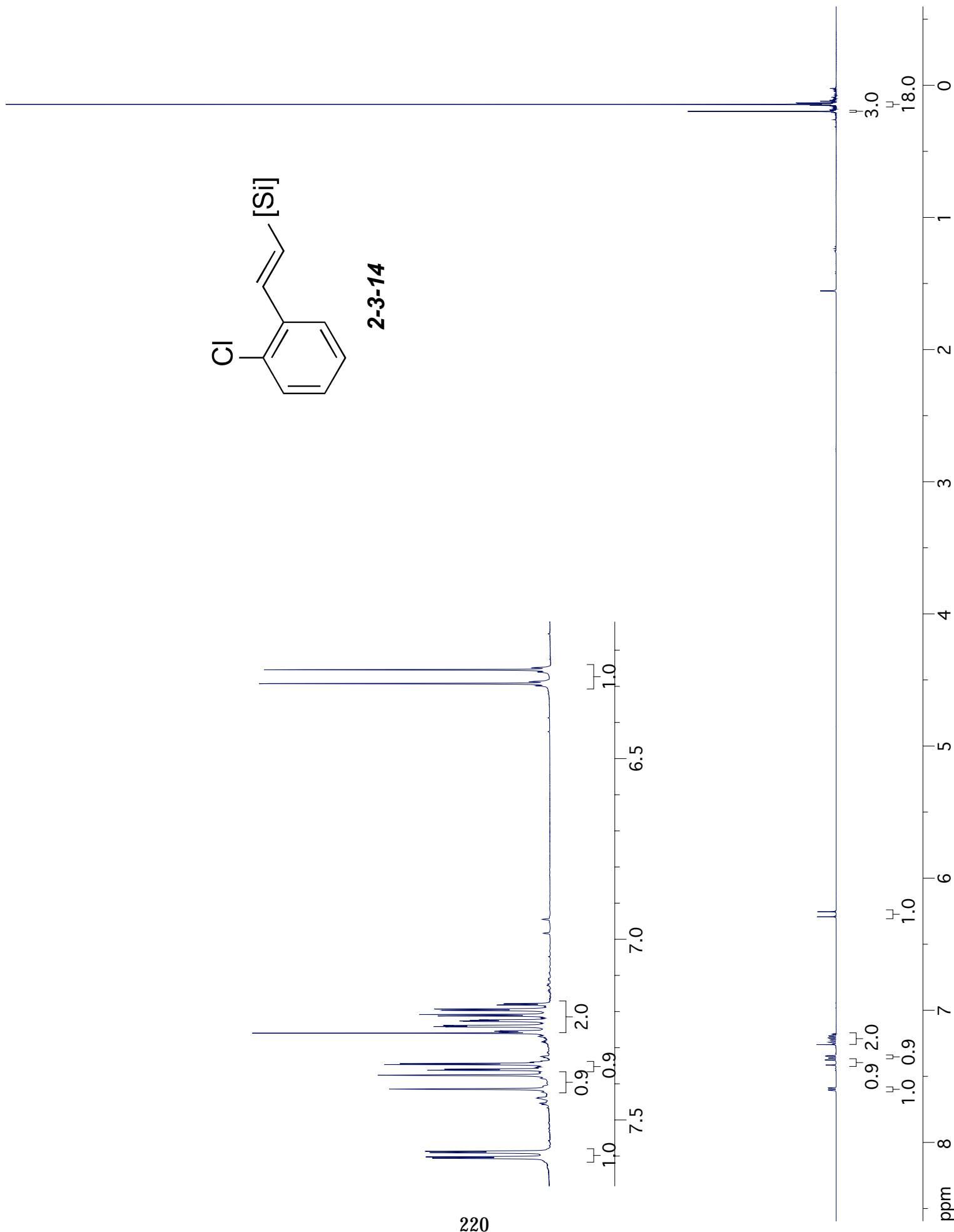
2-3-13

143.635
140.251
134.767
129.950
128.759
128.337
126.696
125.028

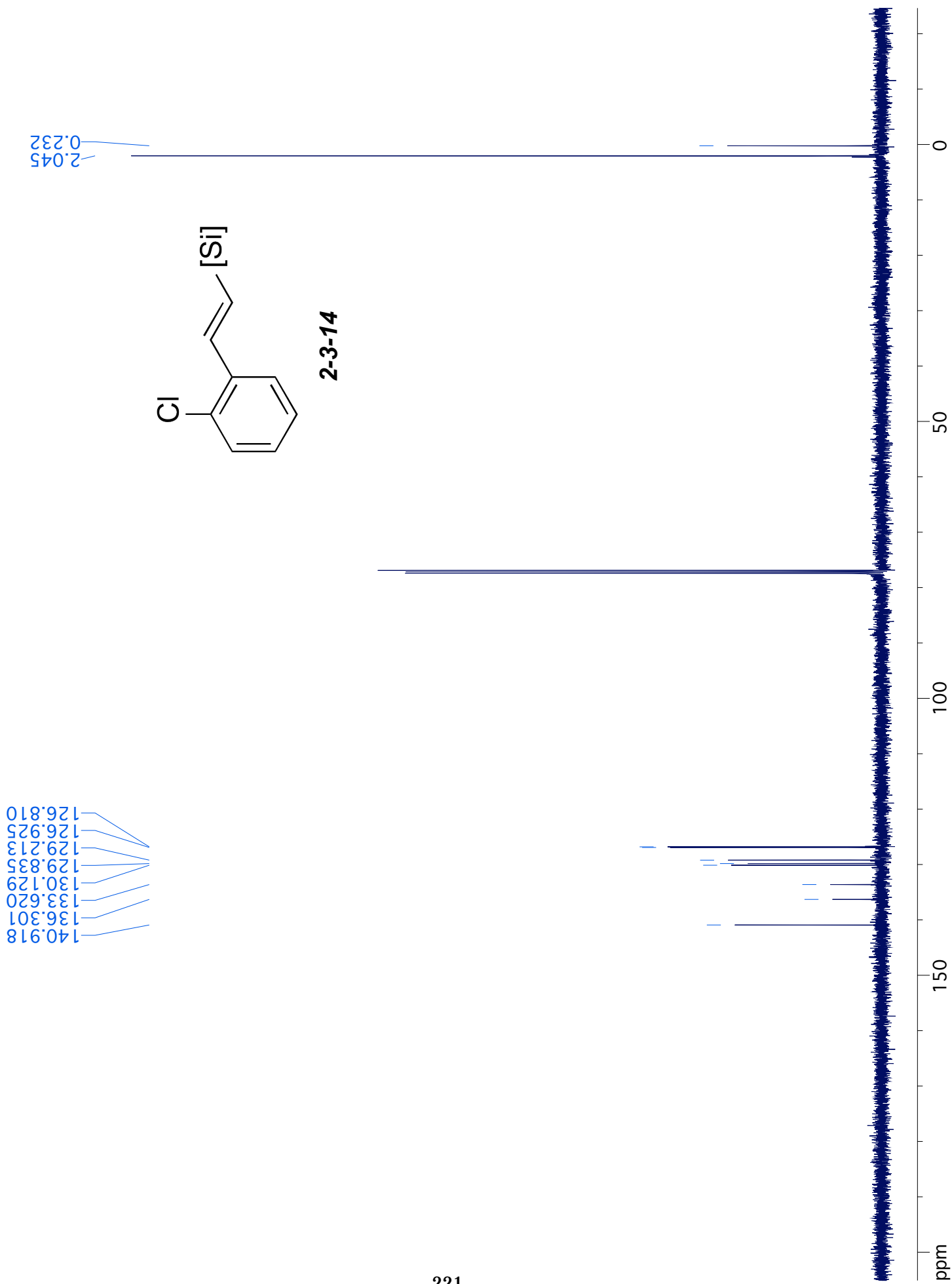


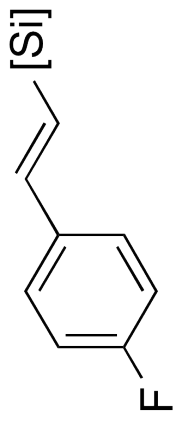


2-3-14



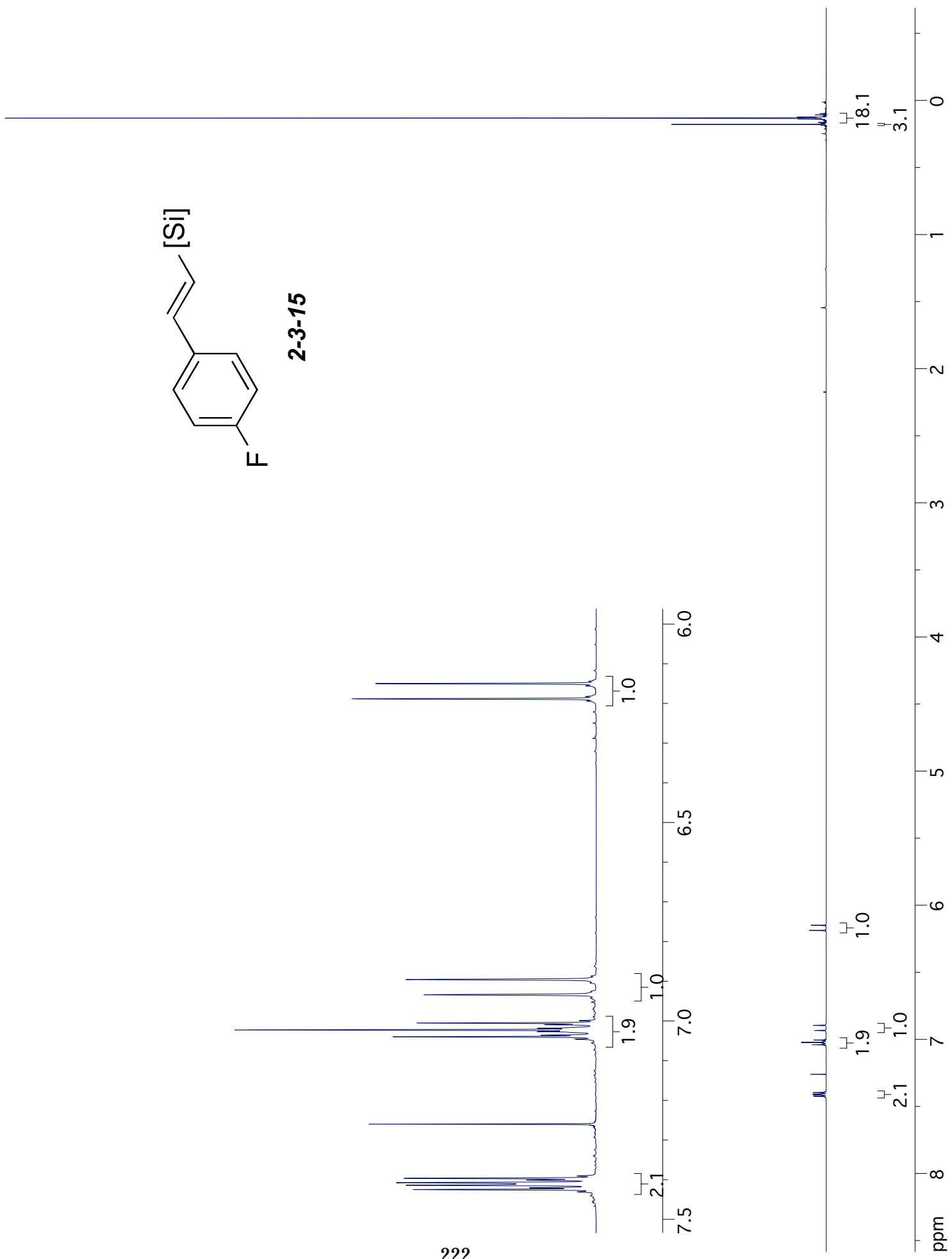
220

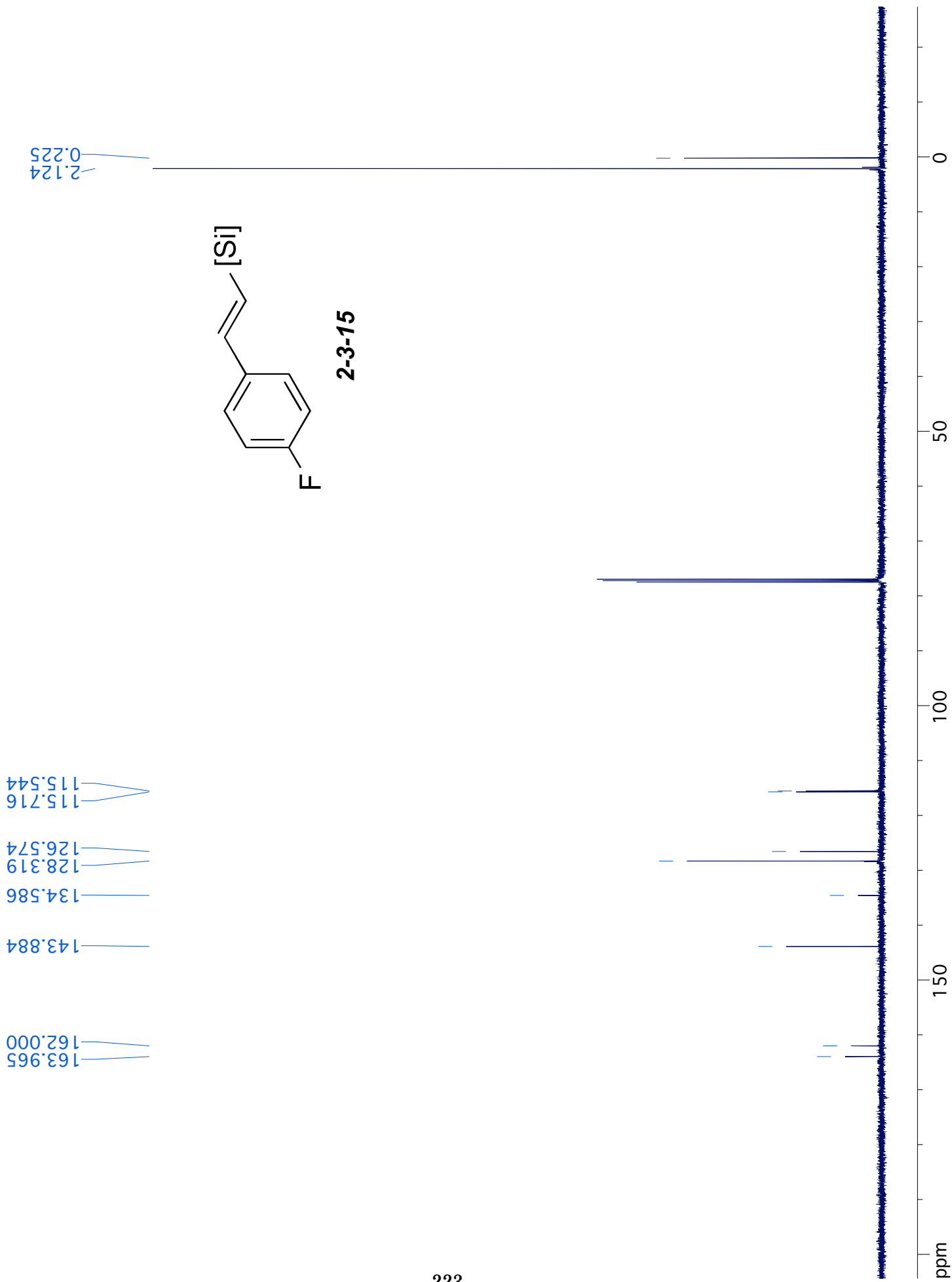


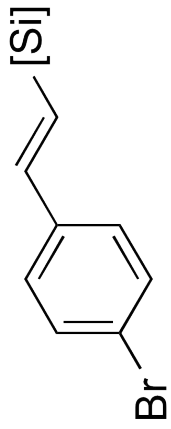


2-3-15

222

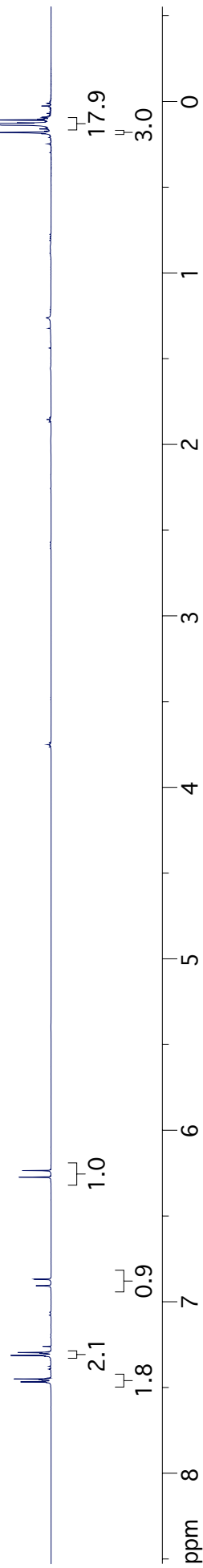
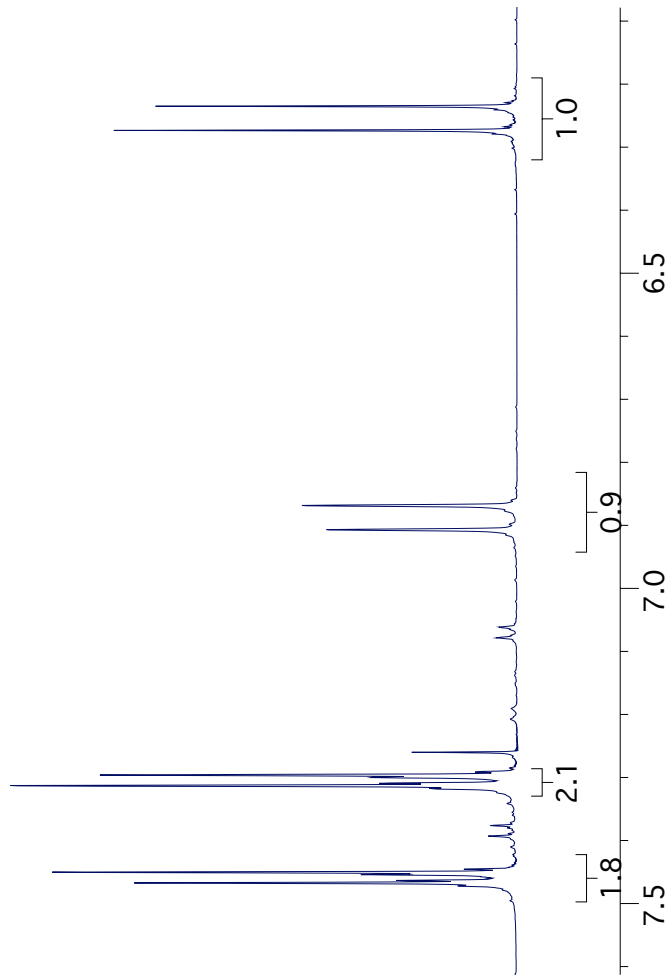


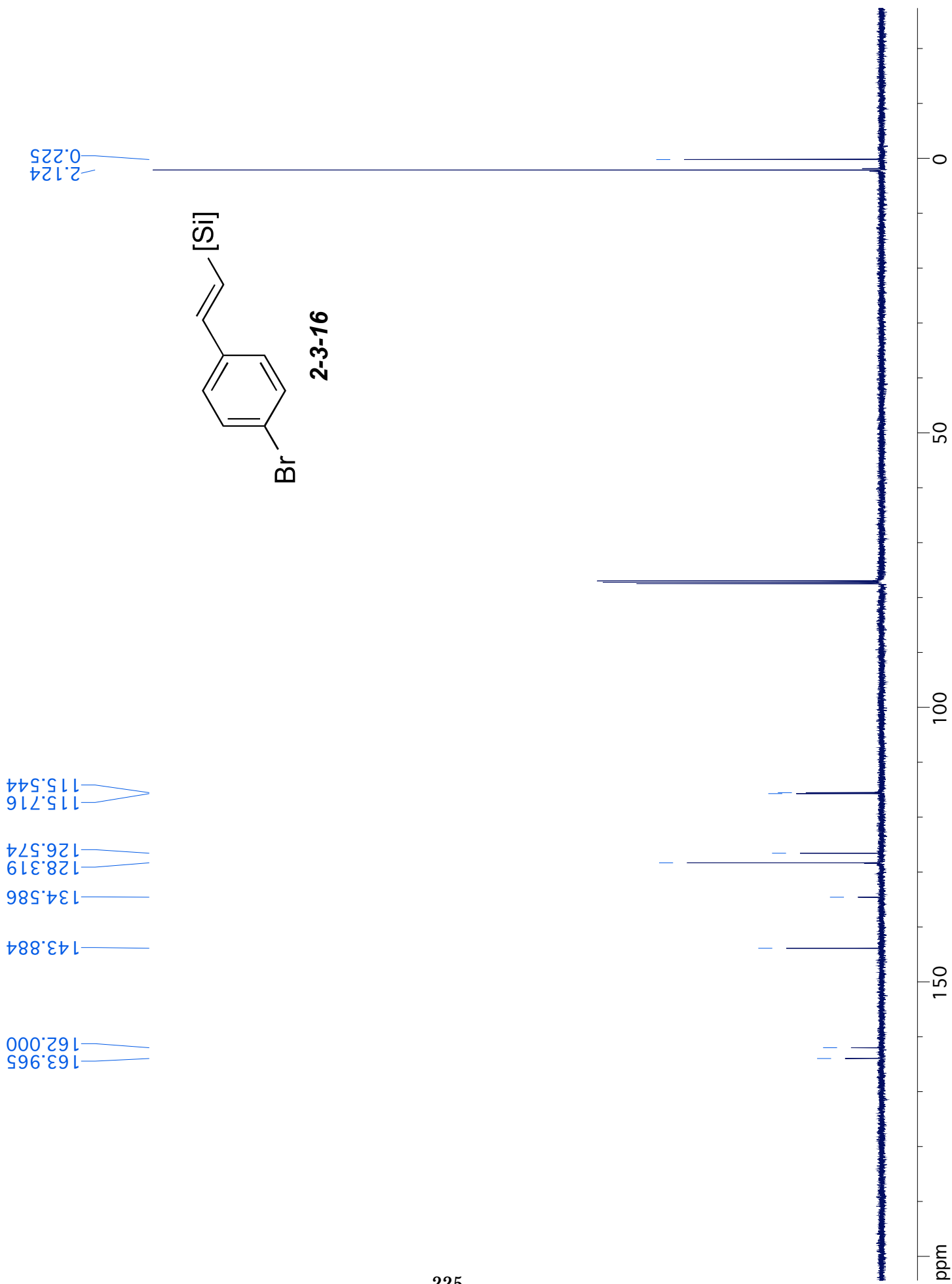


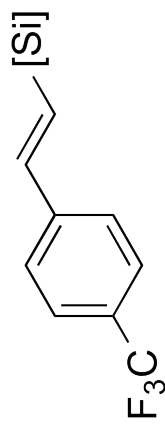


2-3-16

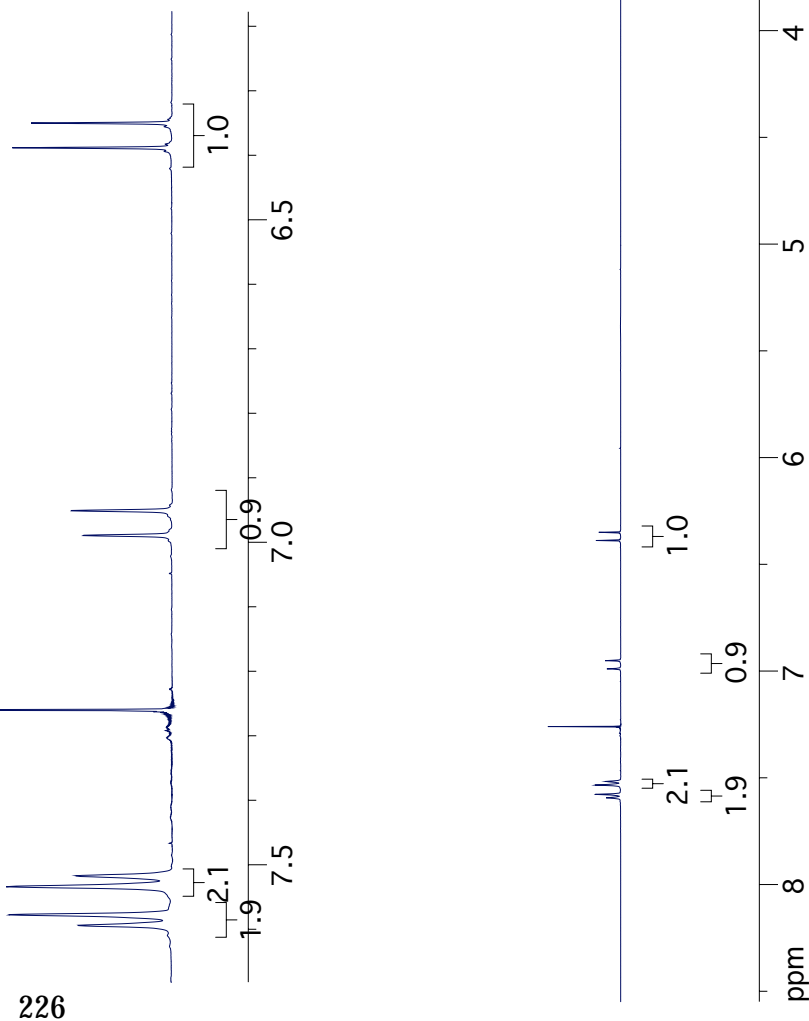
224

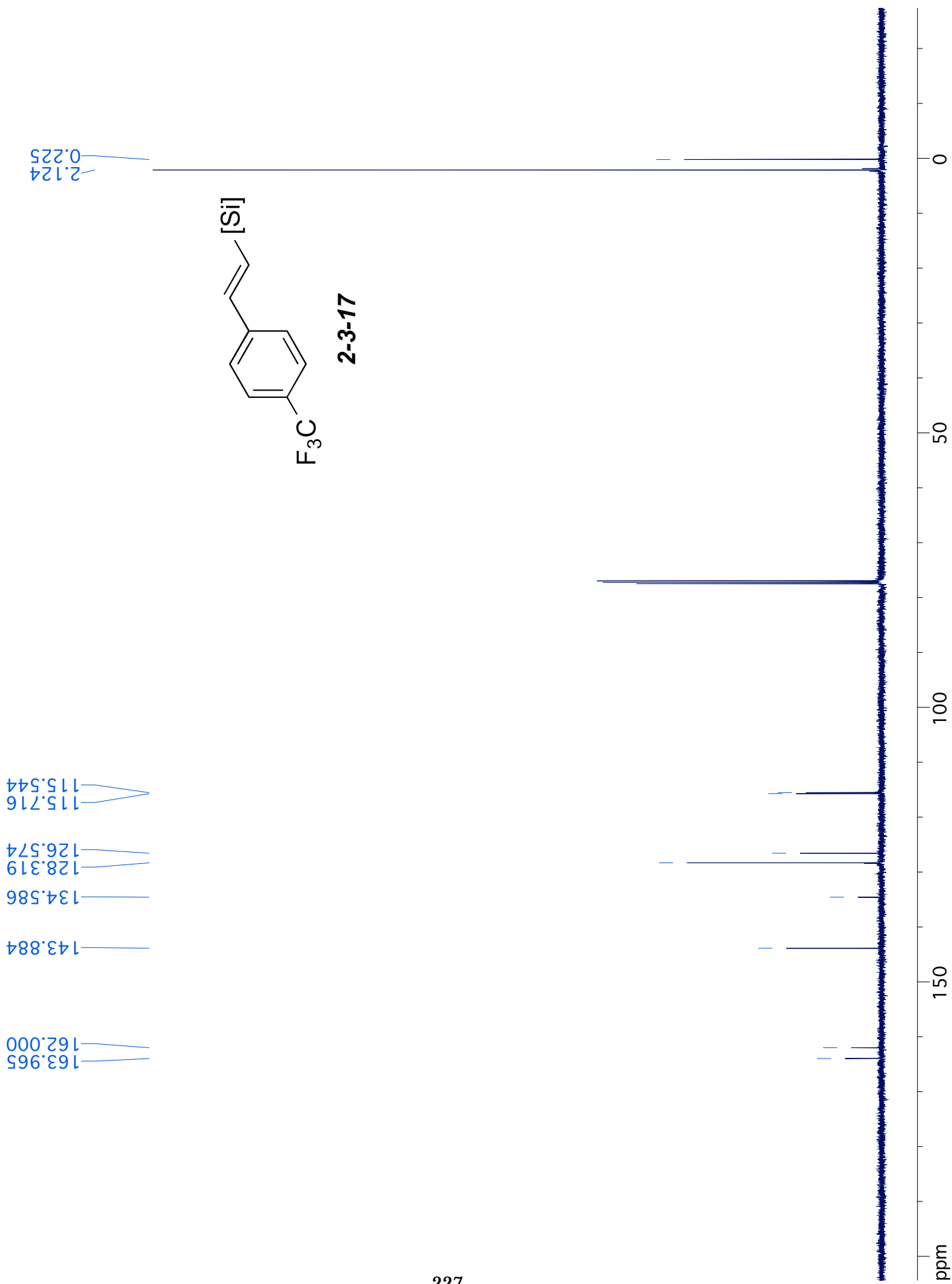


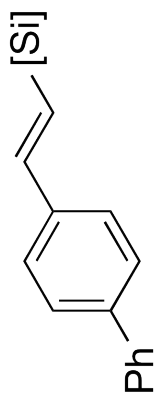




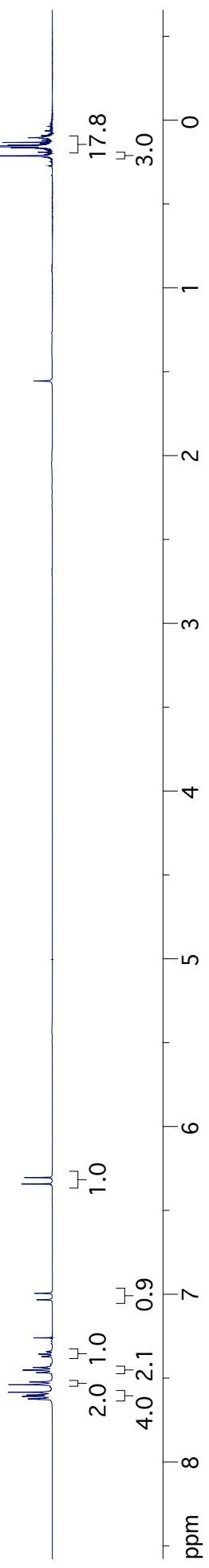
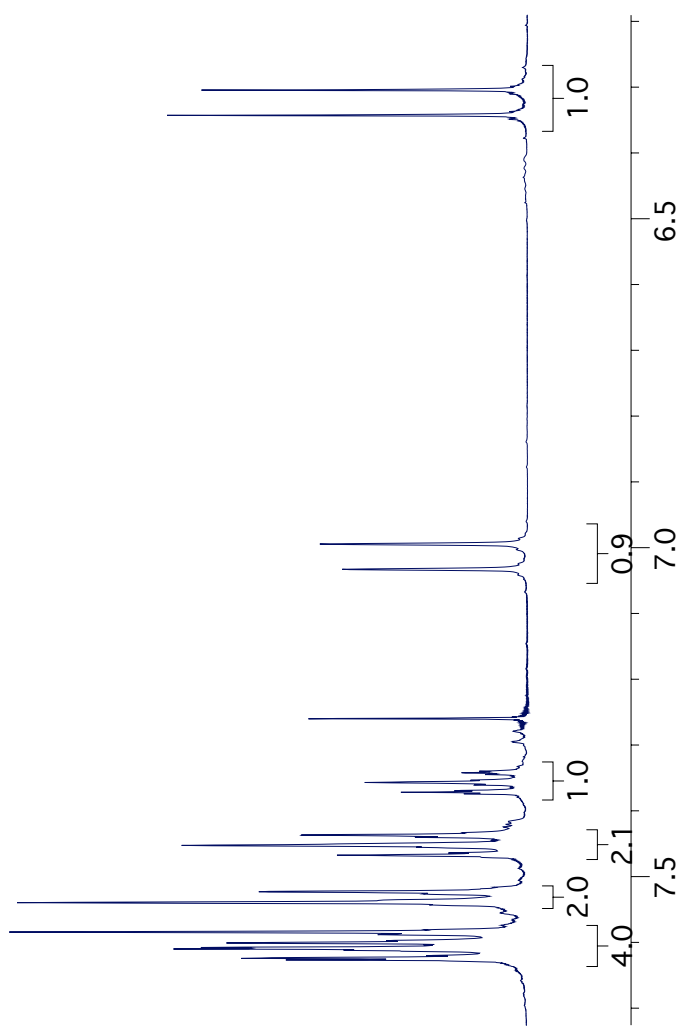
2-3-17

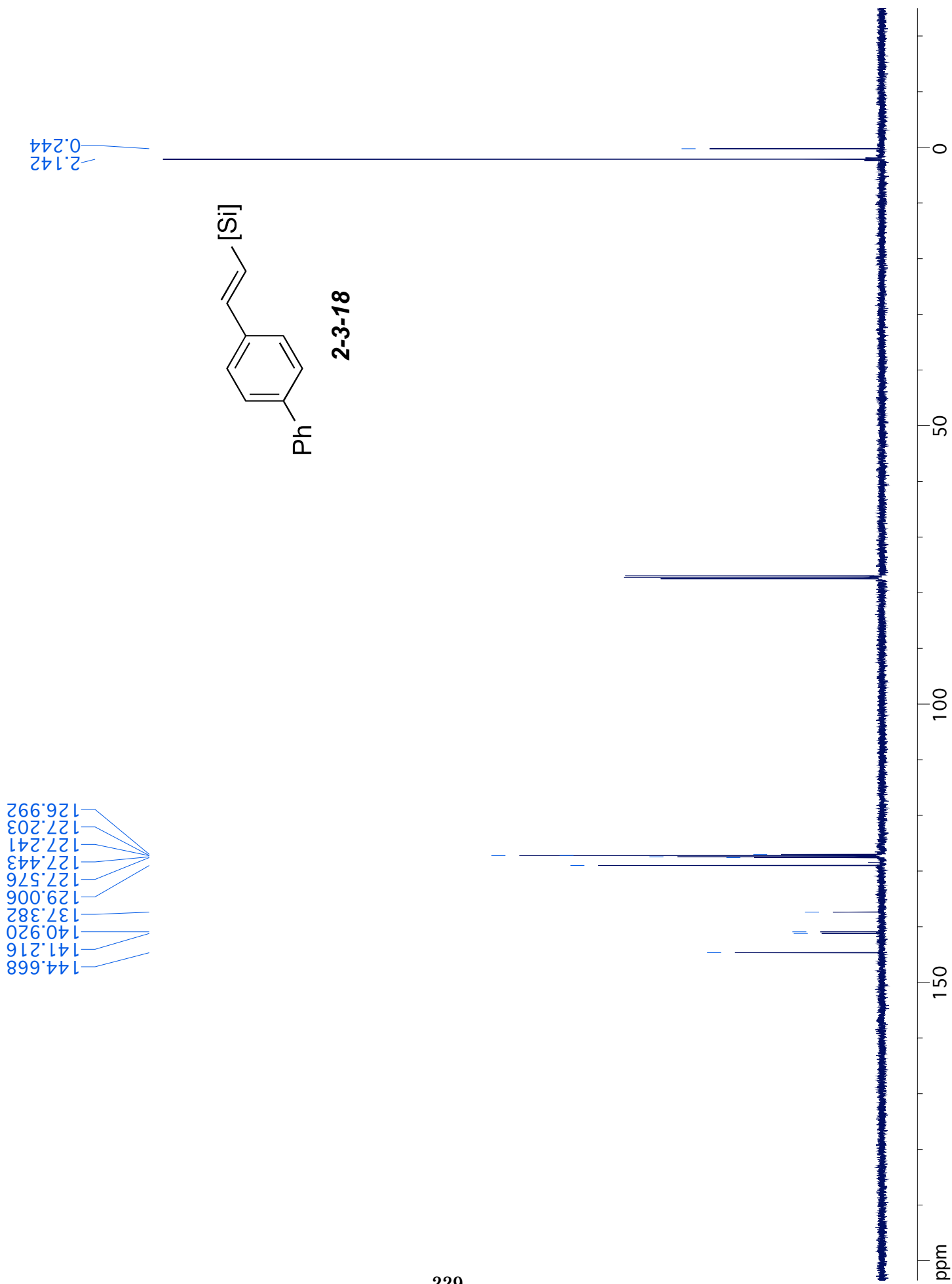


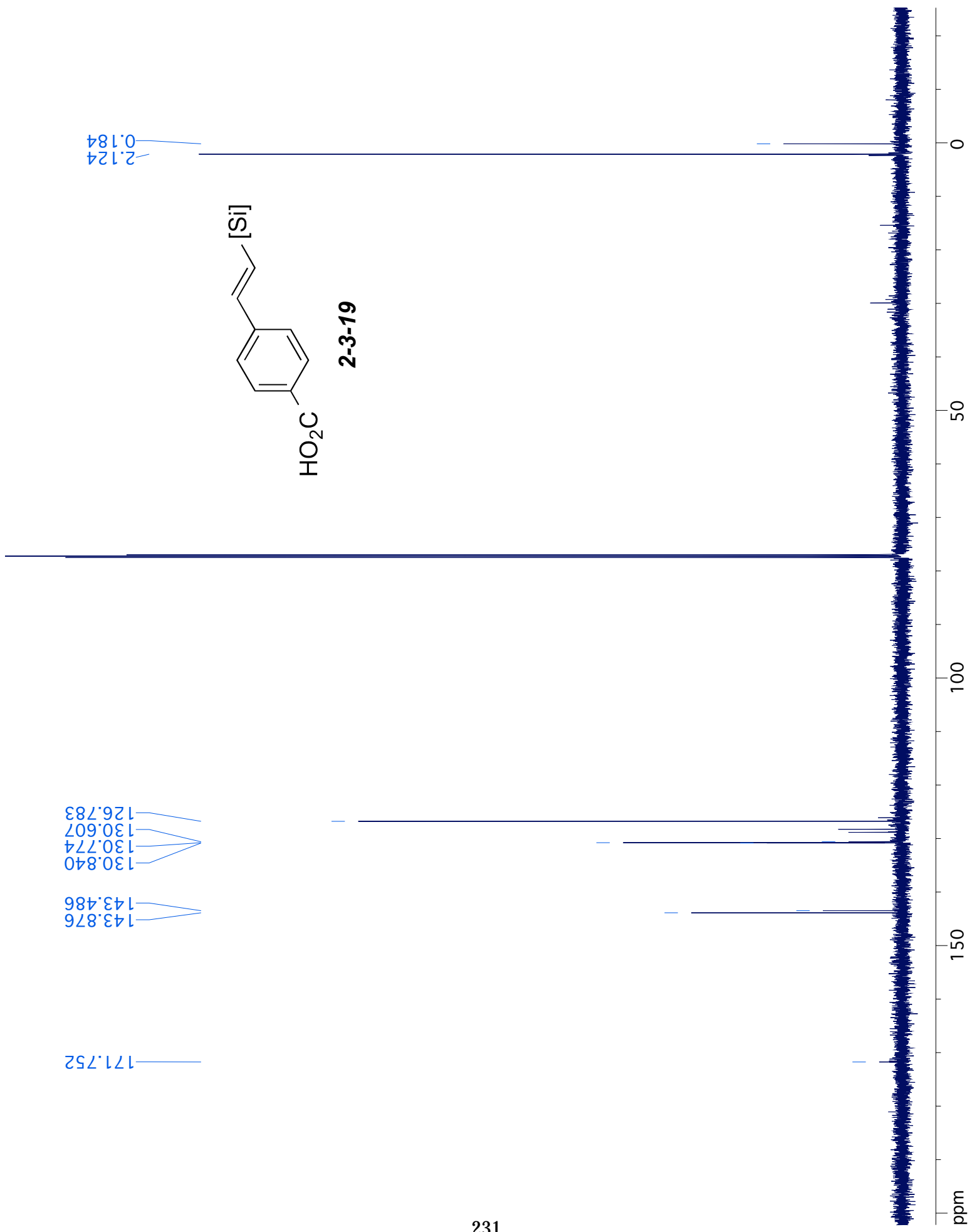


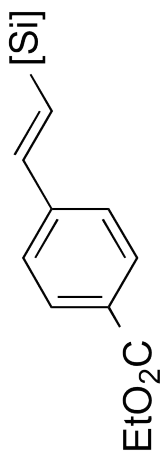


2-3-18

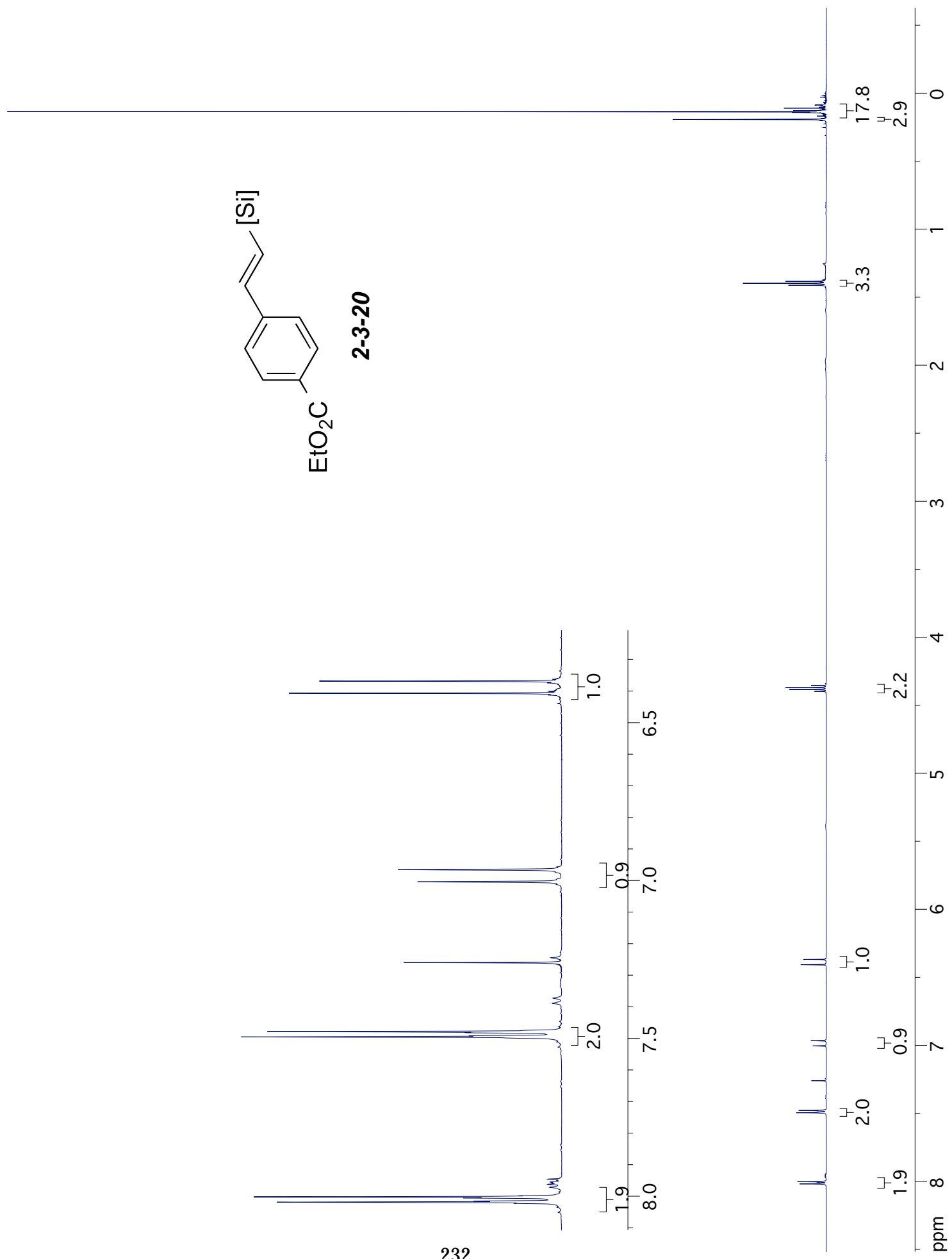


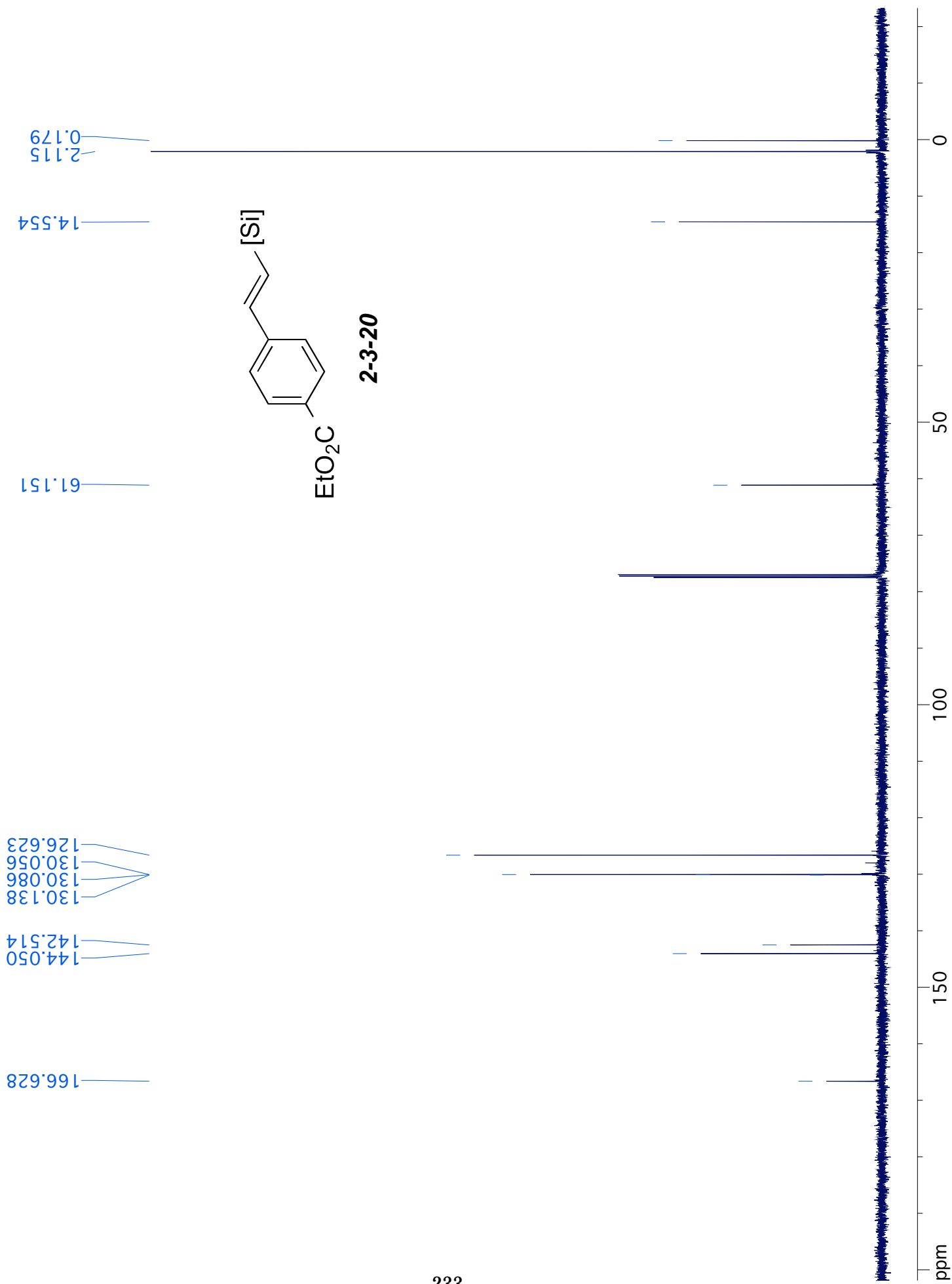


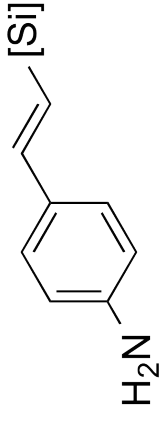




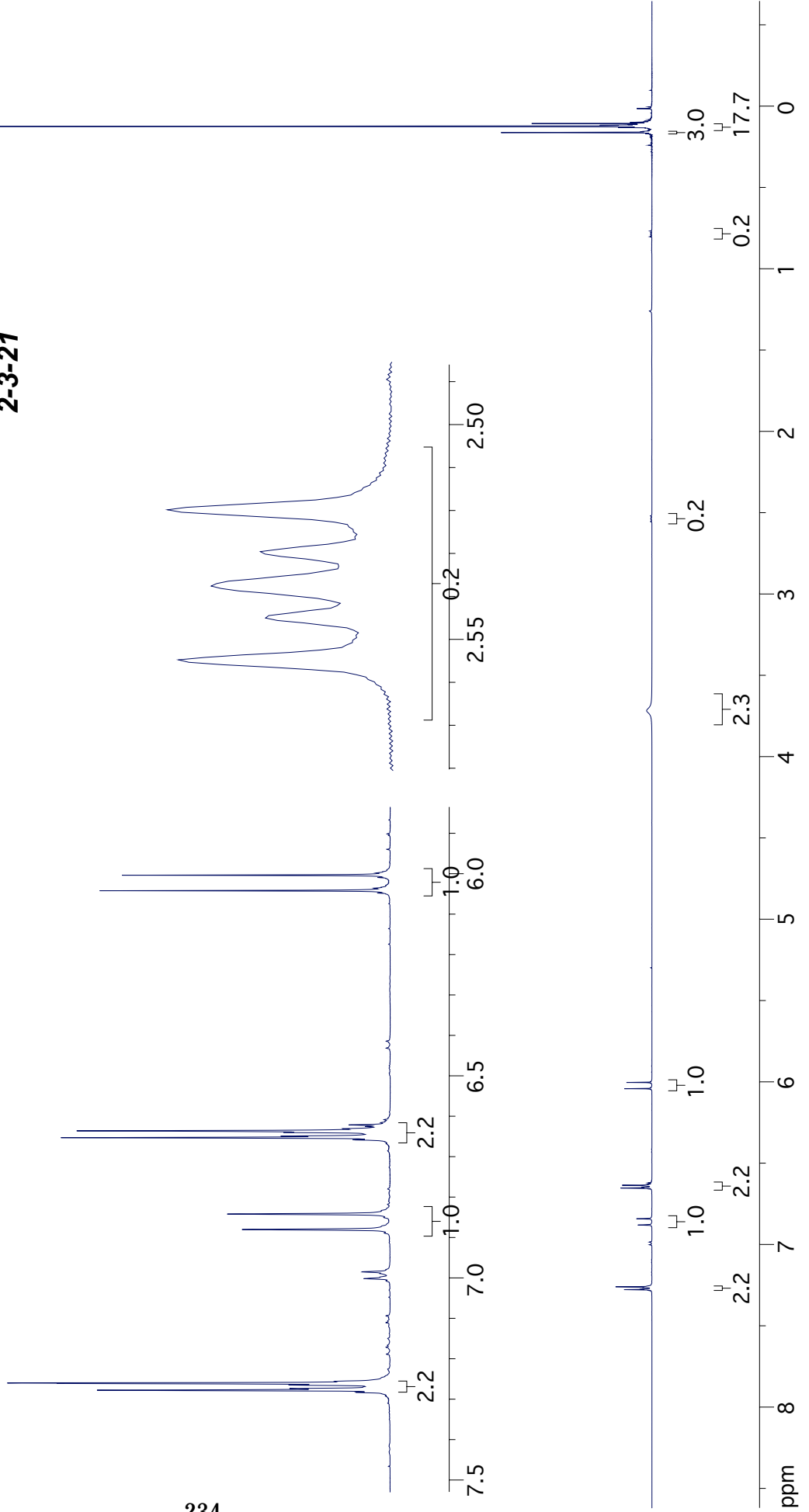
2-3-20

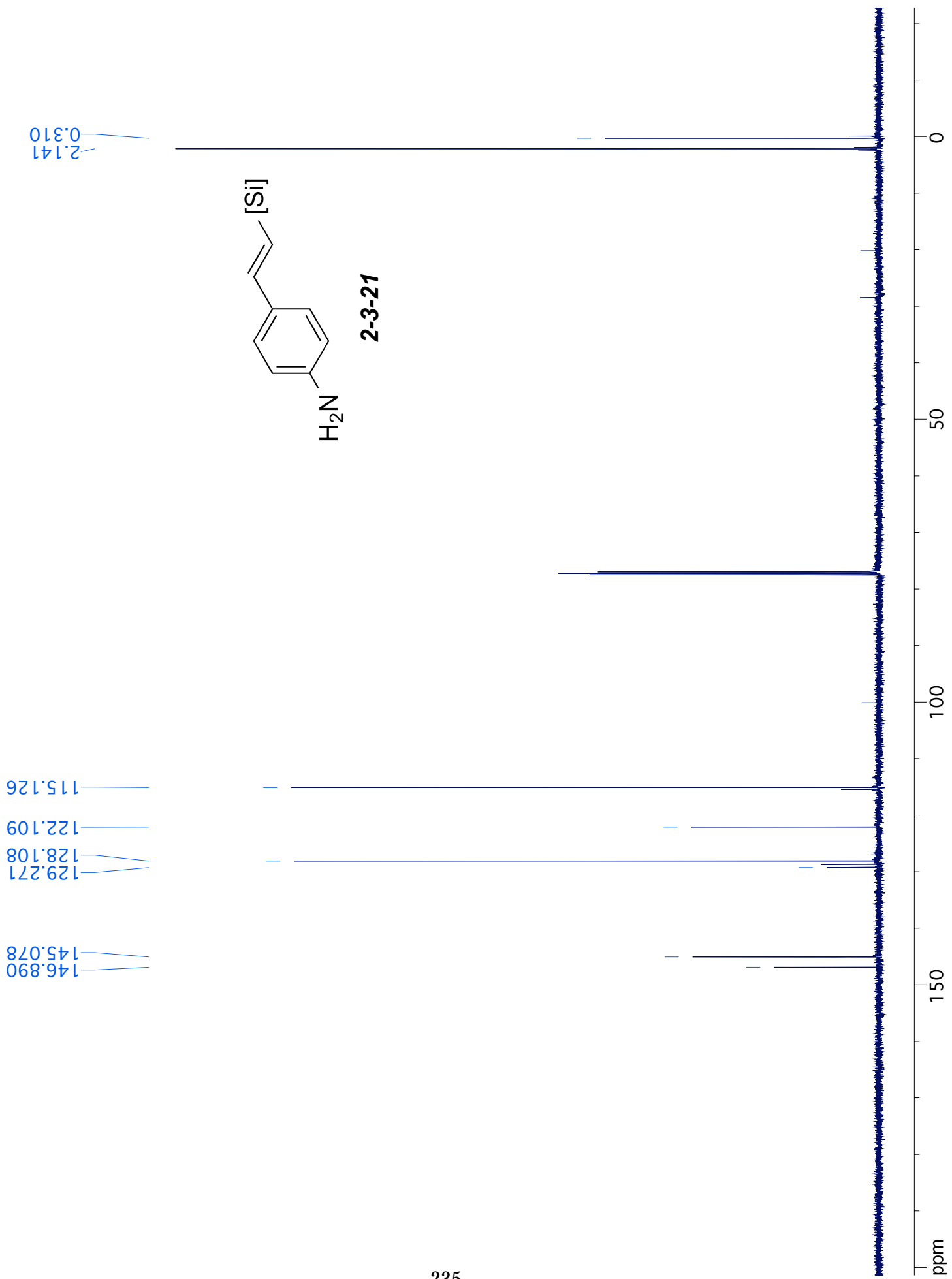


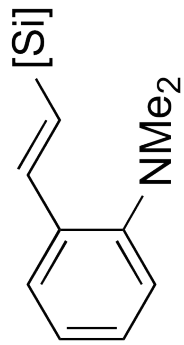




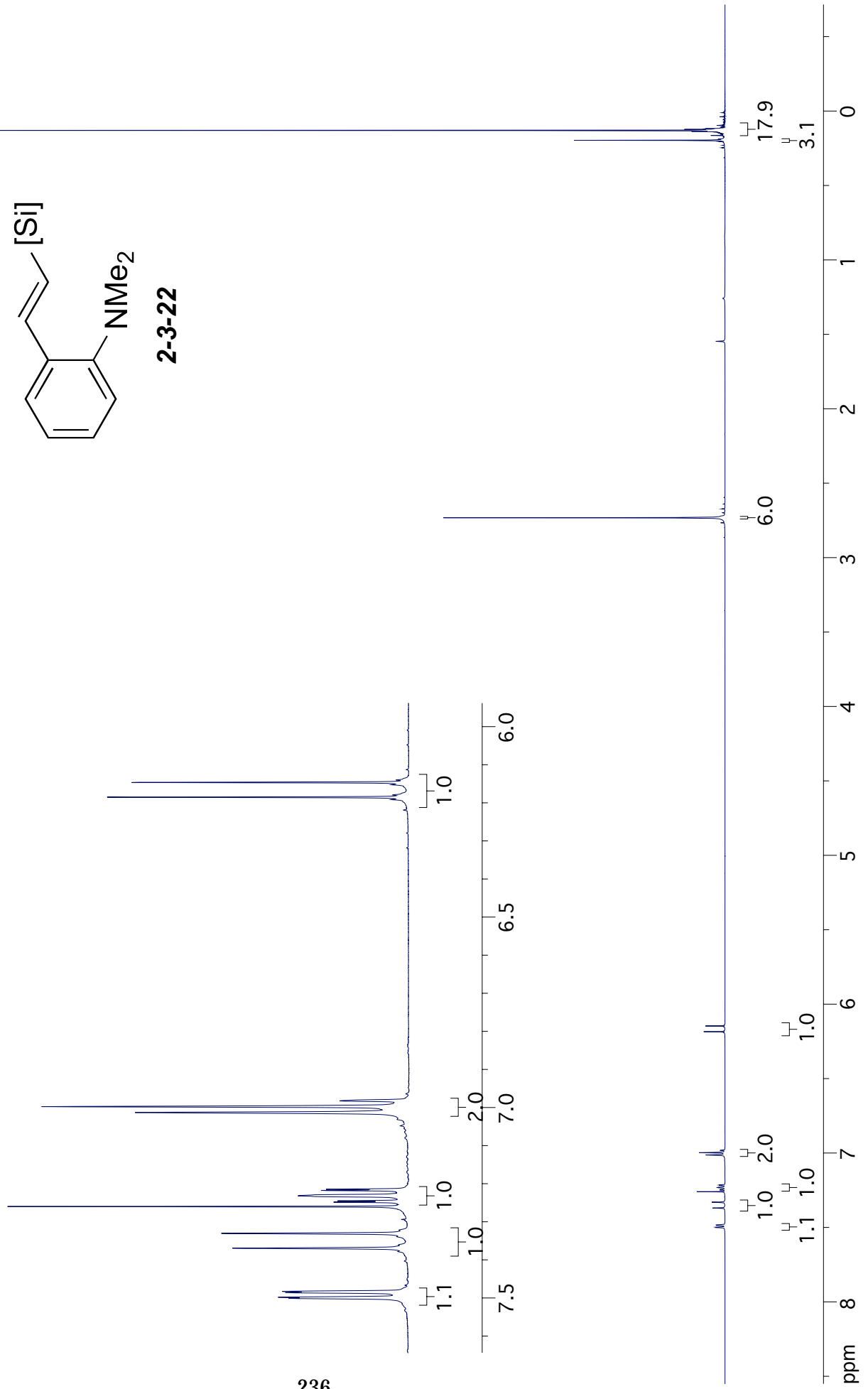
2-3-21

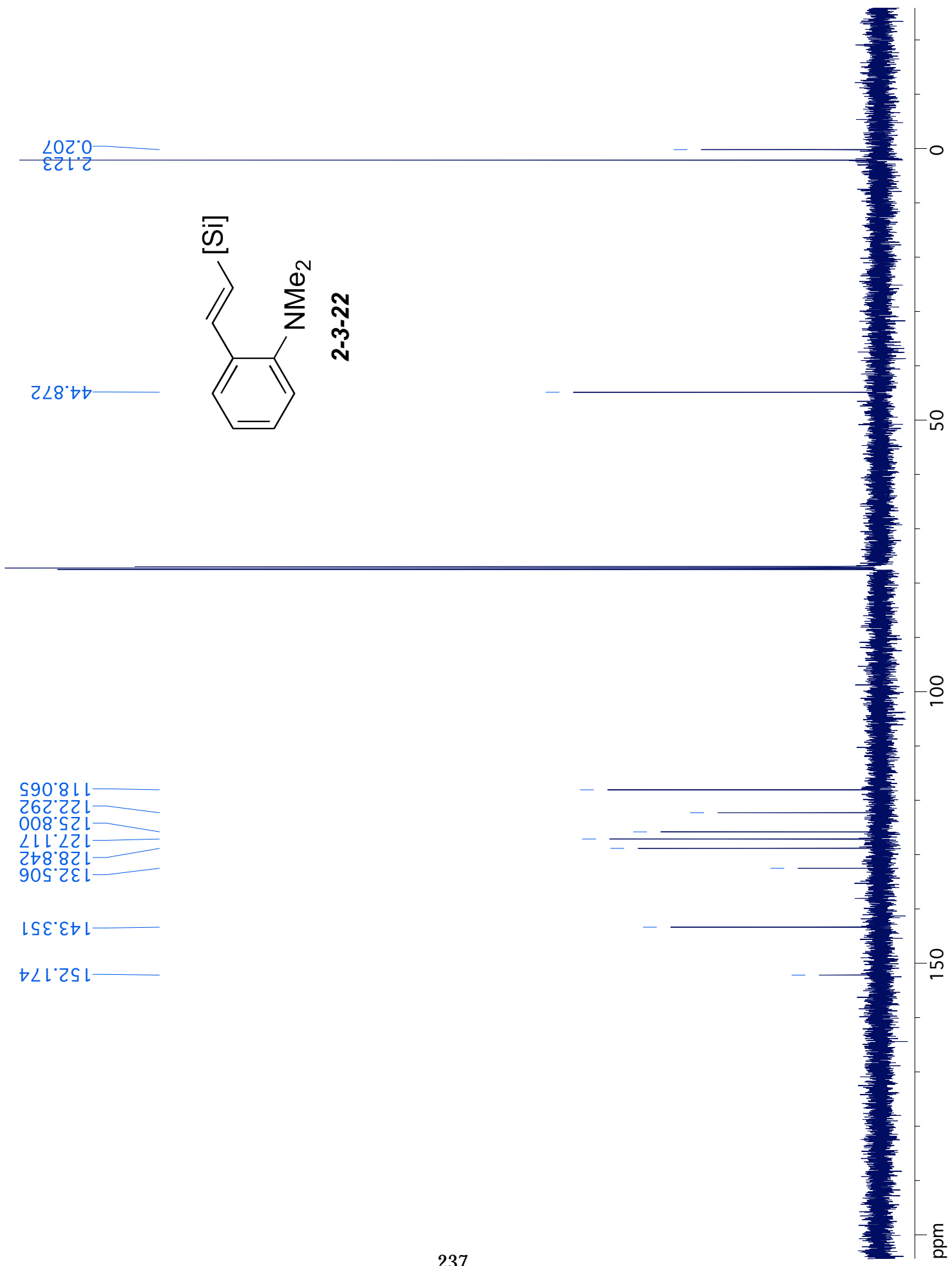


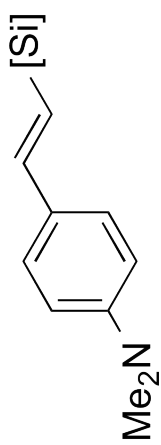




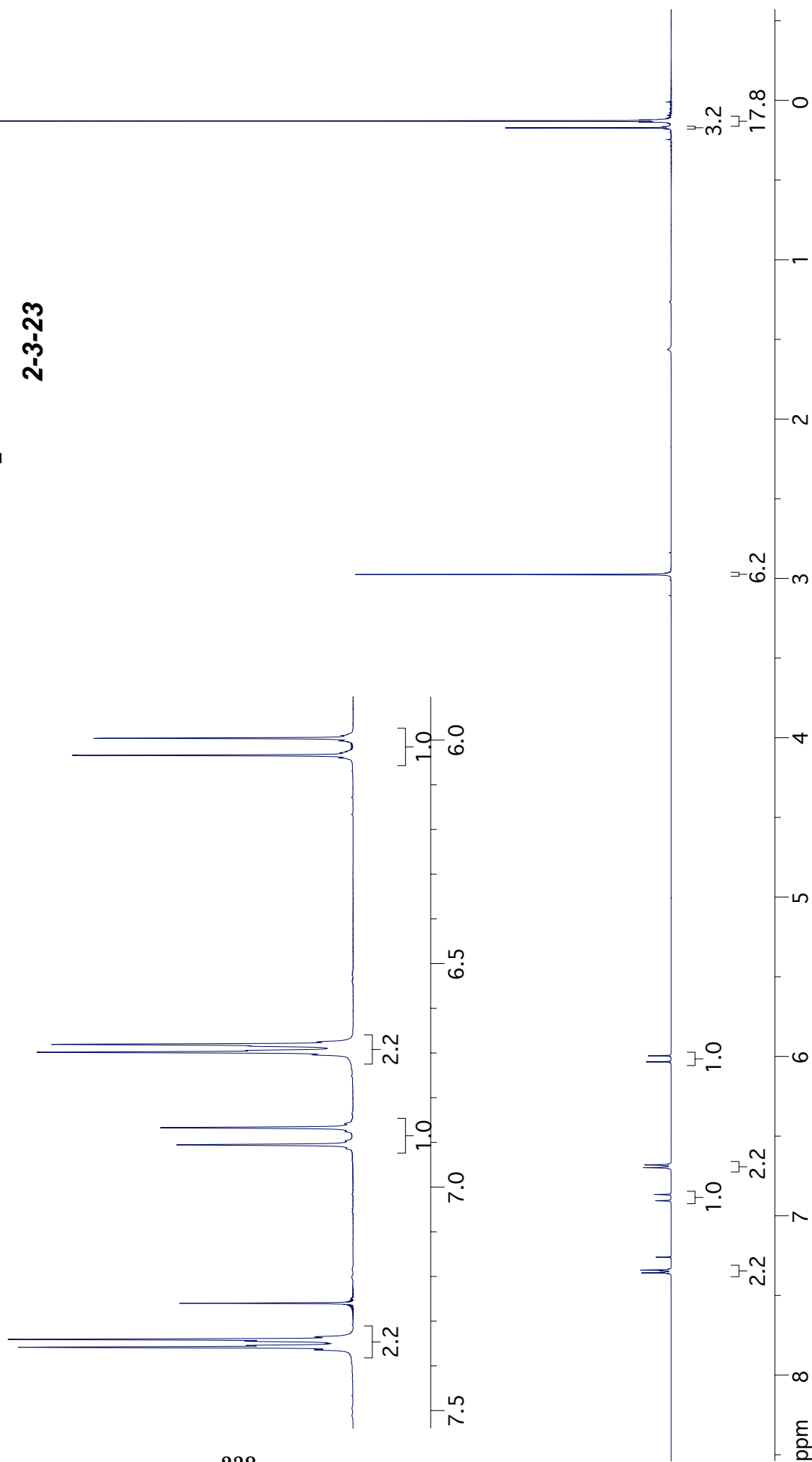
2-3-22

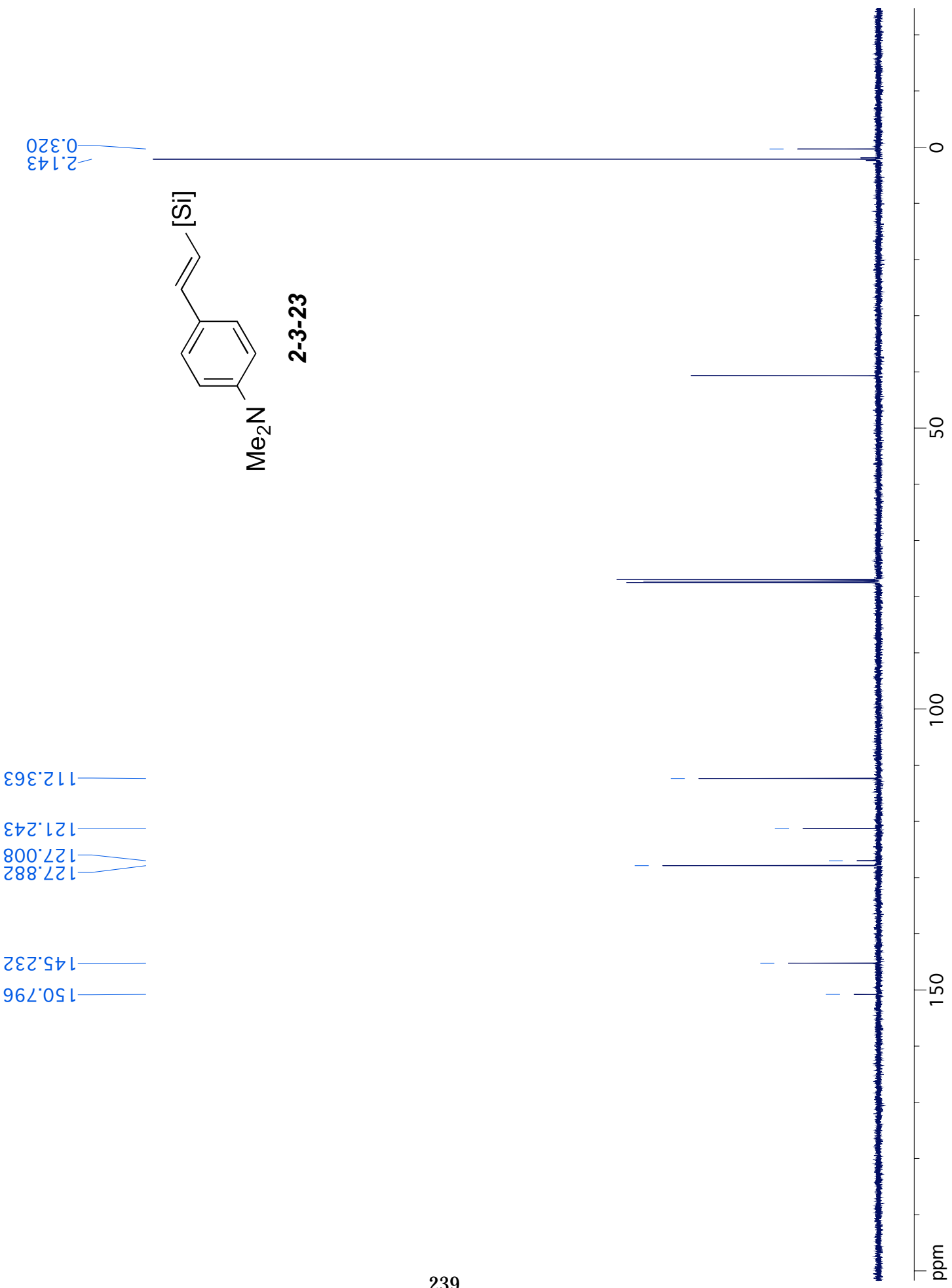


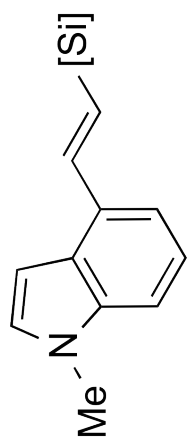




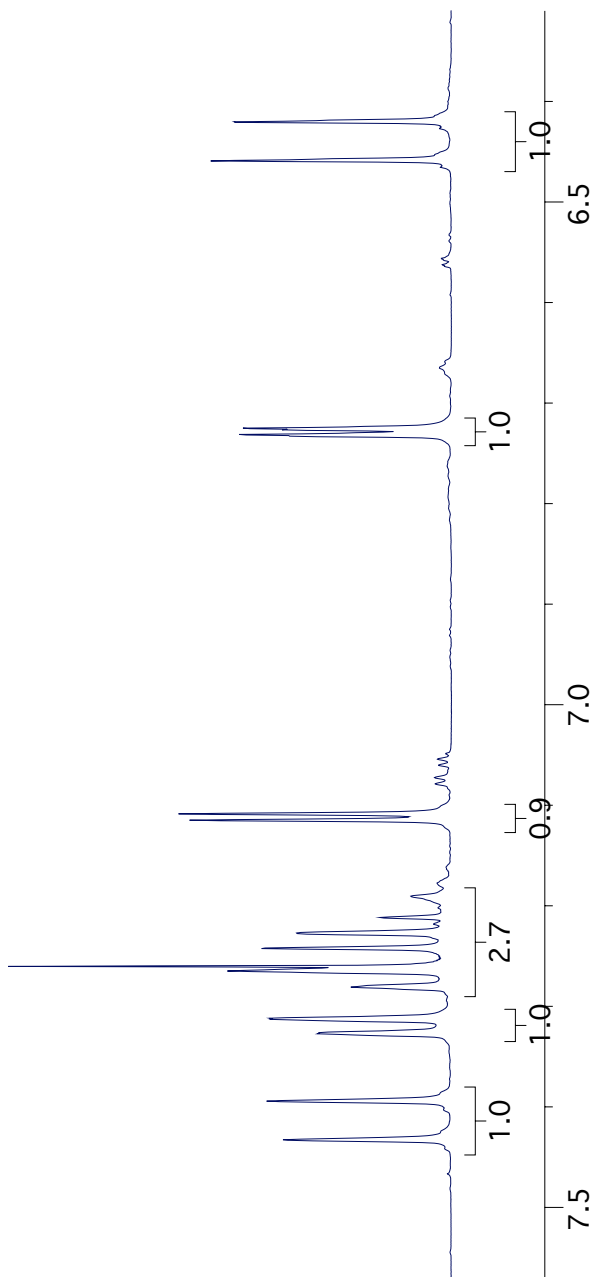
2-3-23



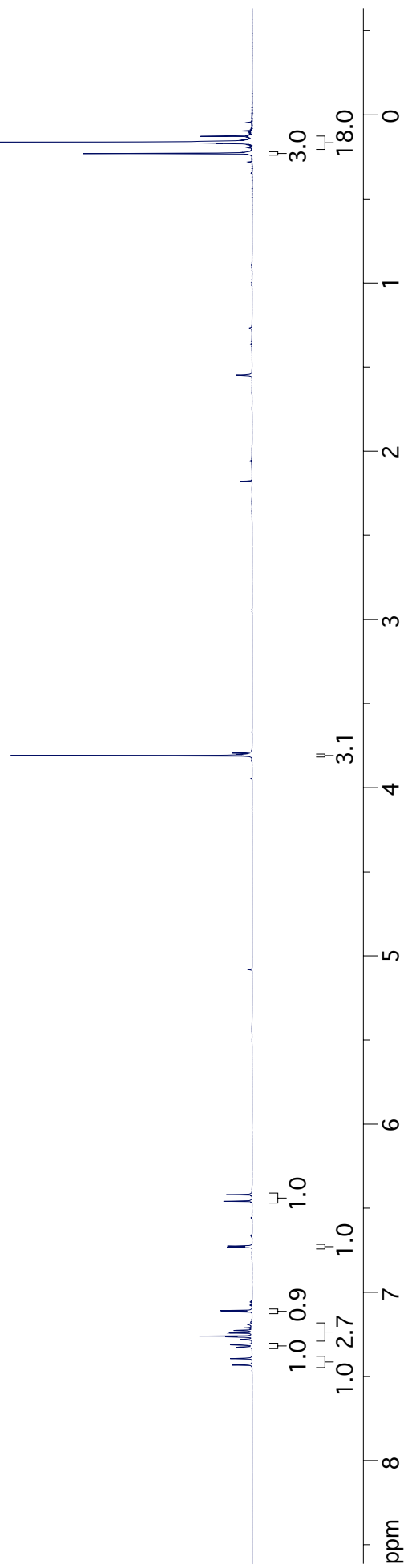


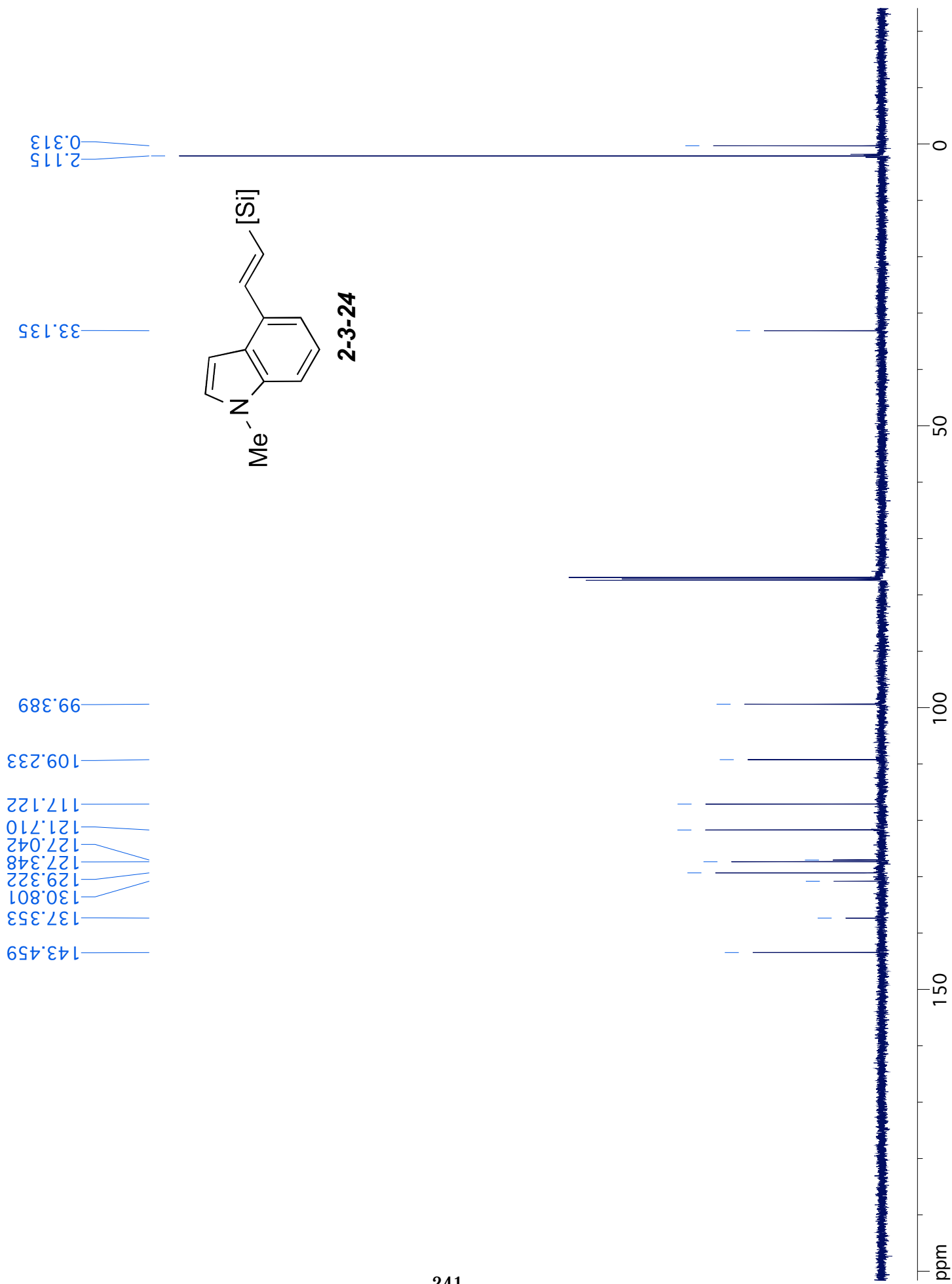


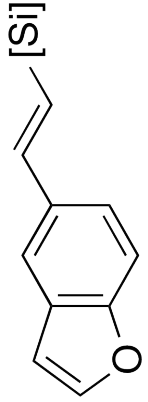
2-3-24



240

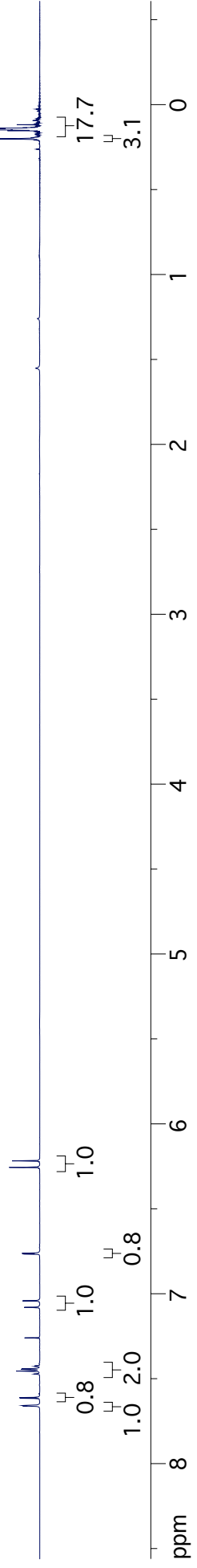
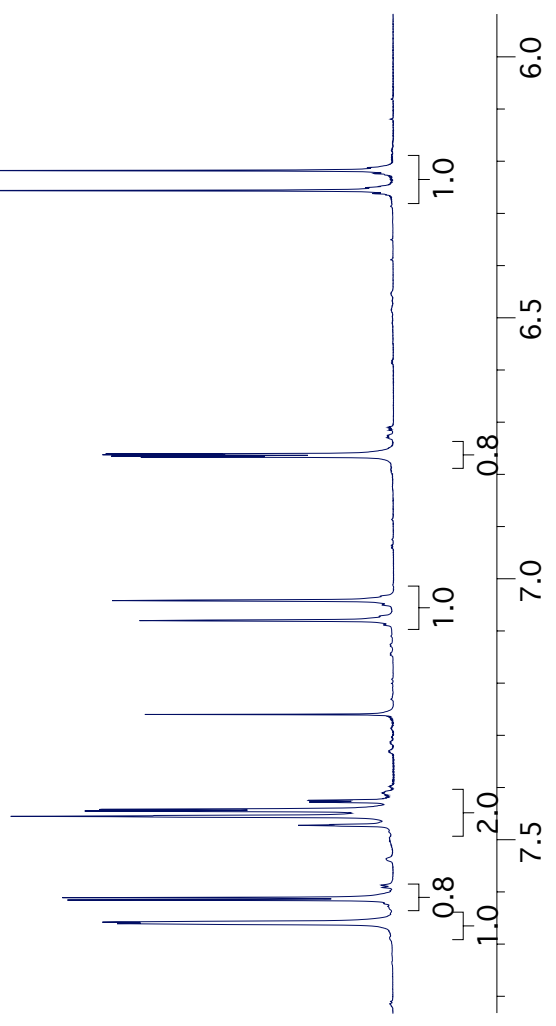


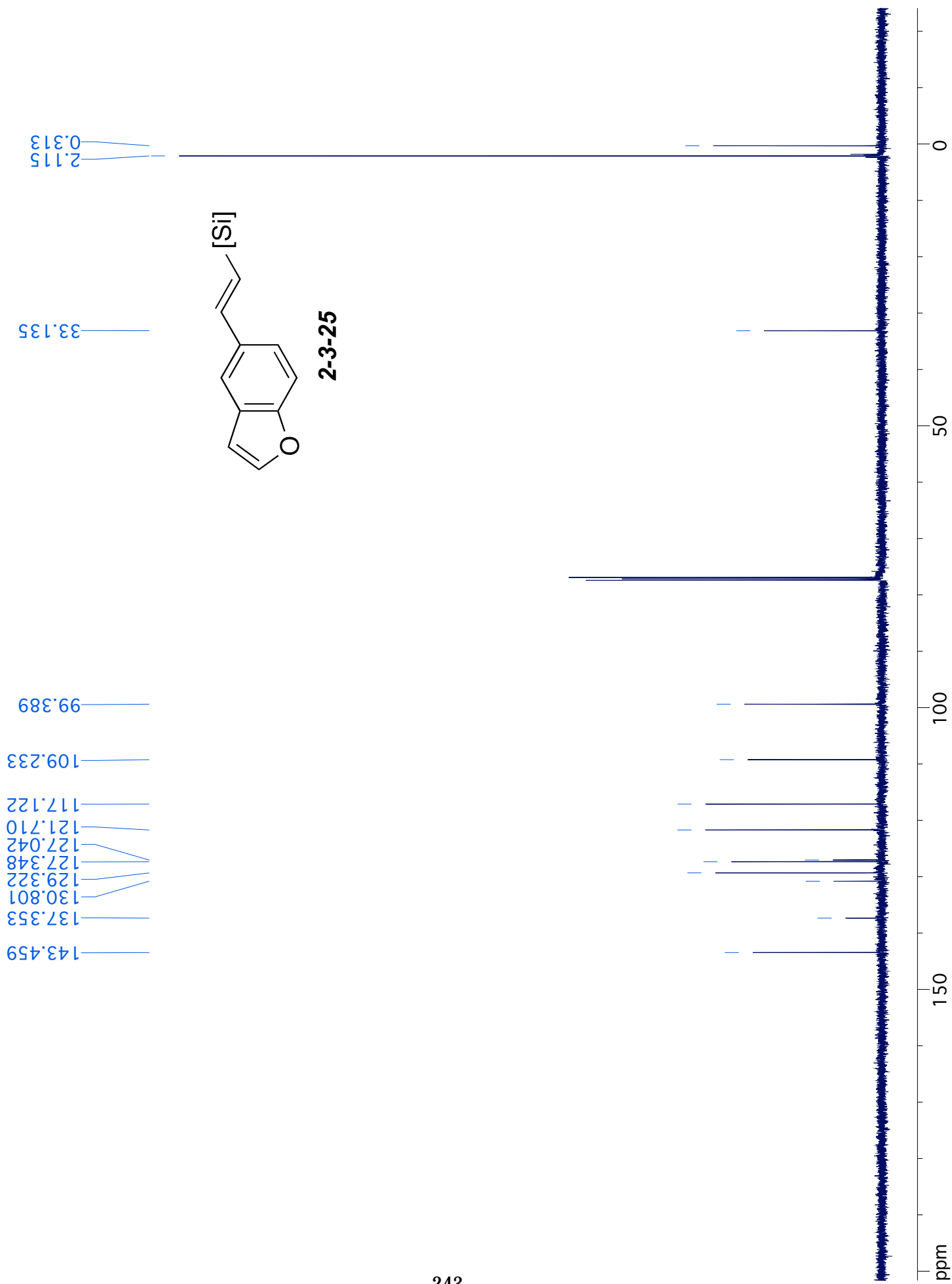


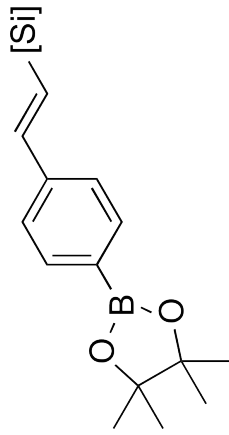


2-3-25

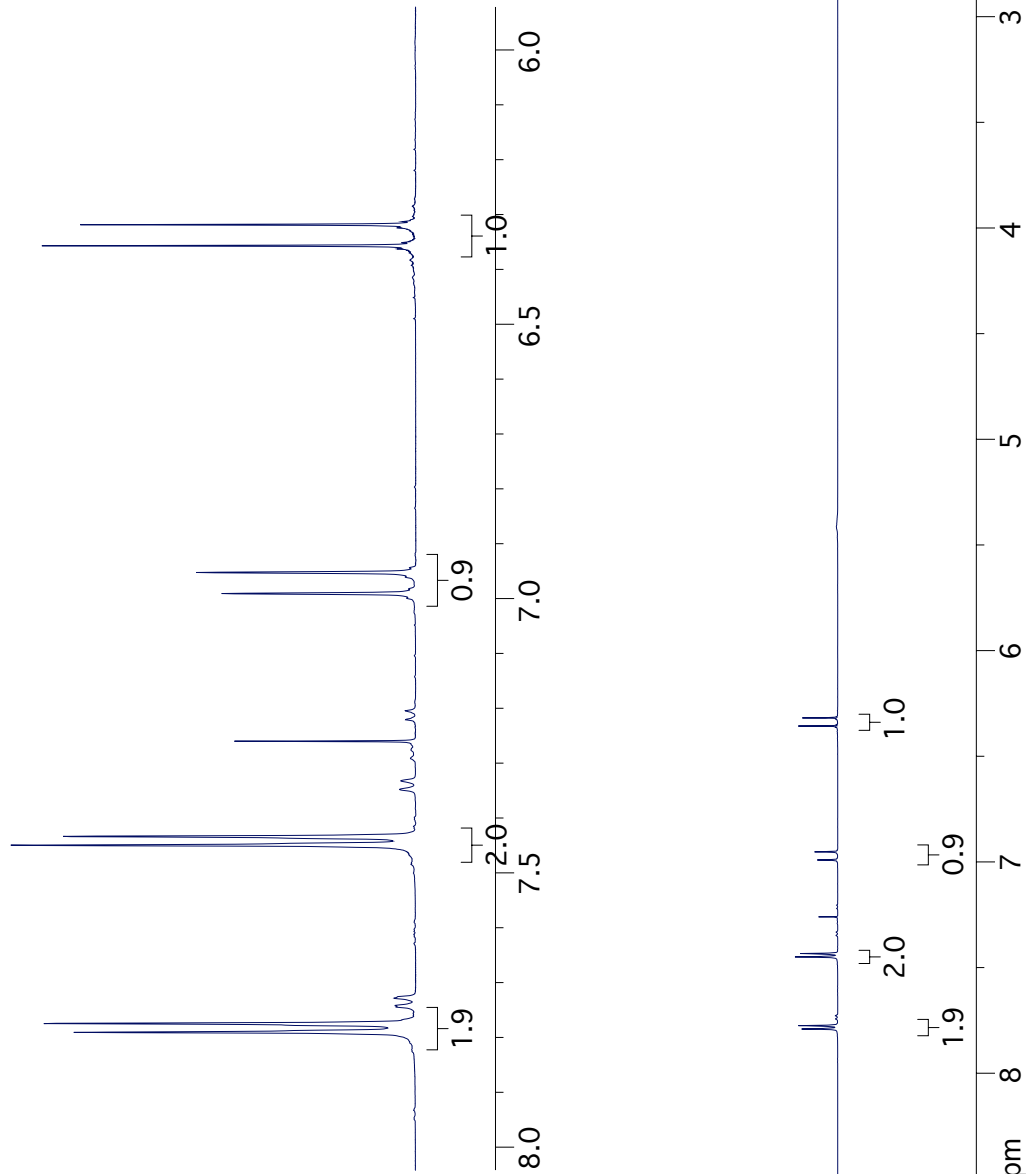
242

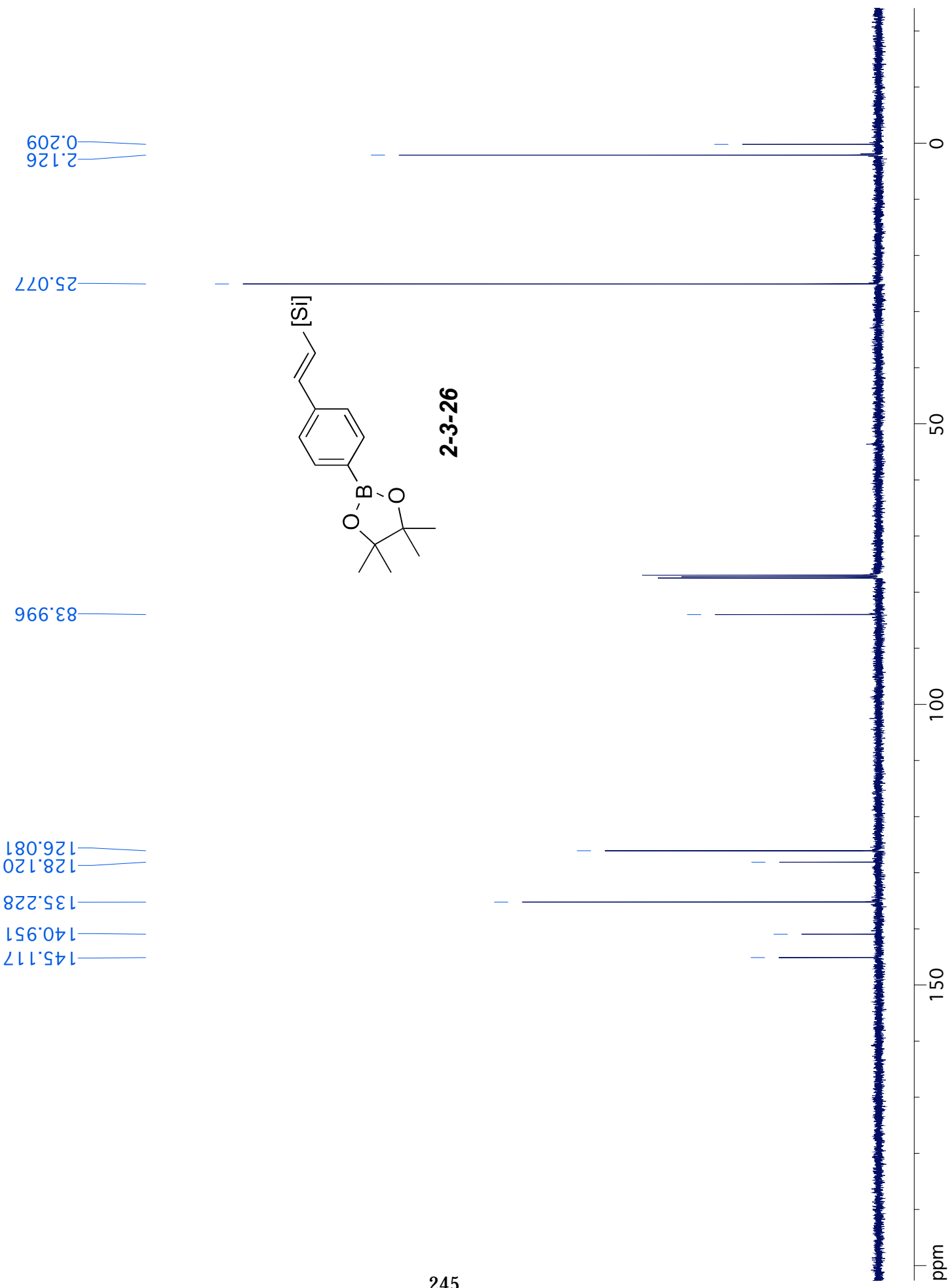


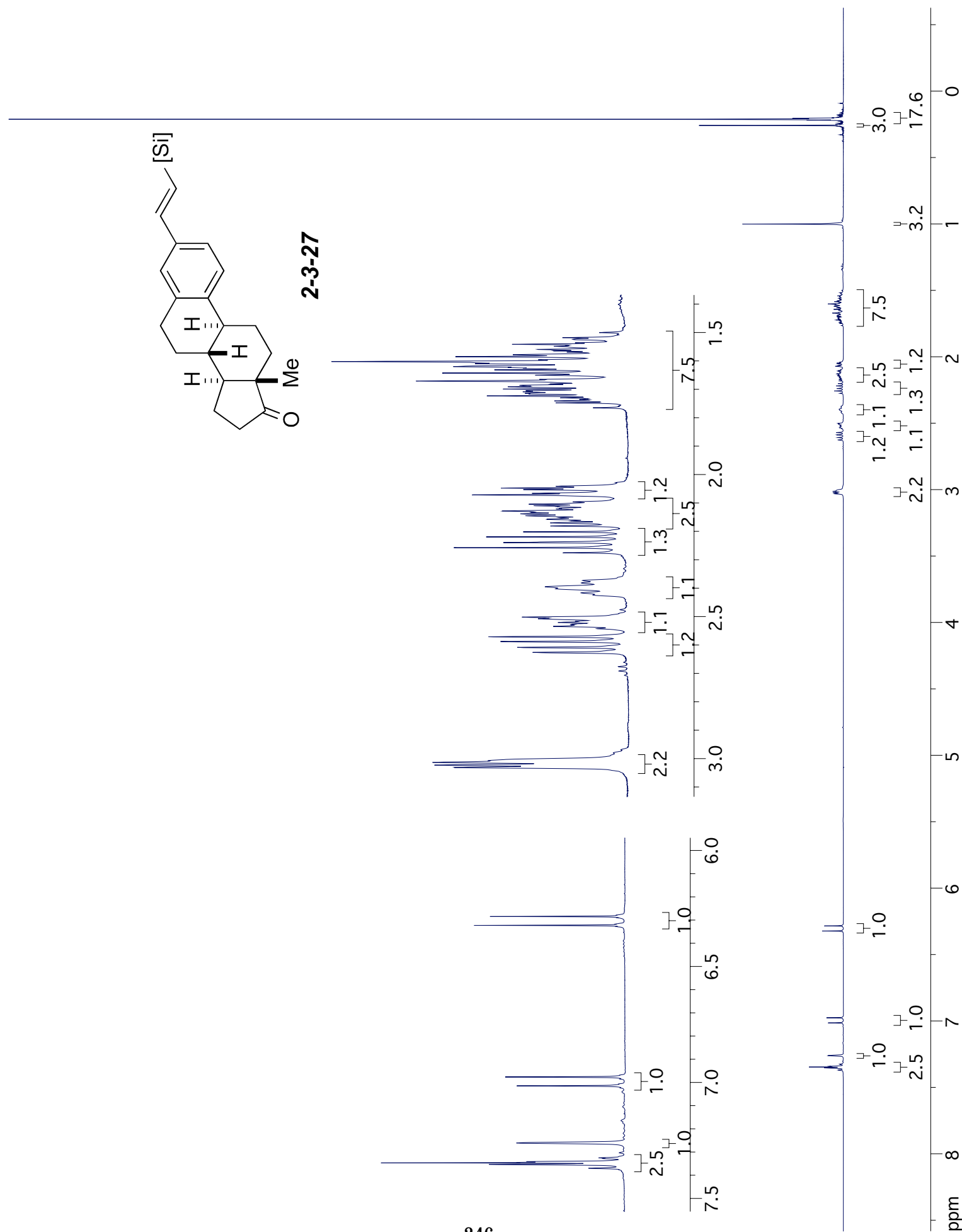
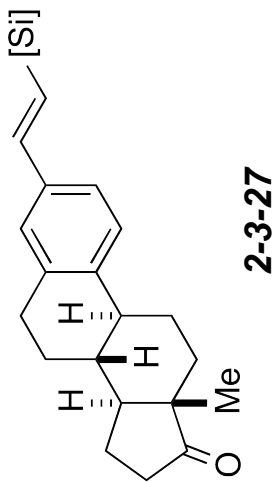


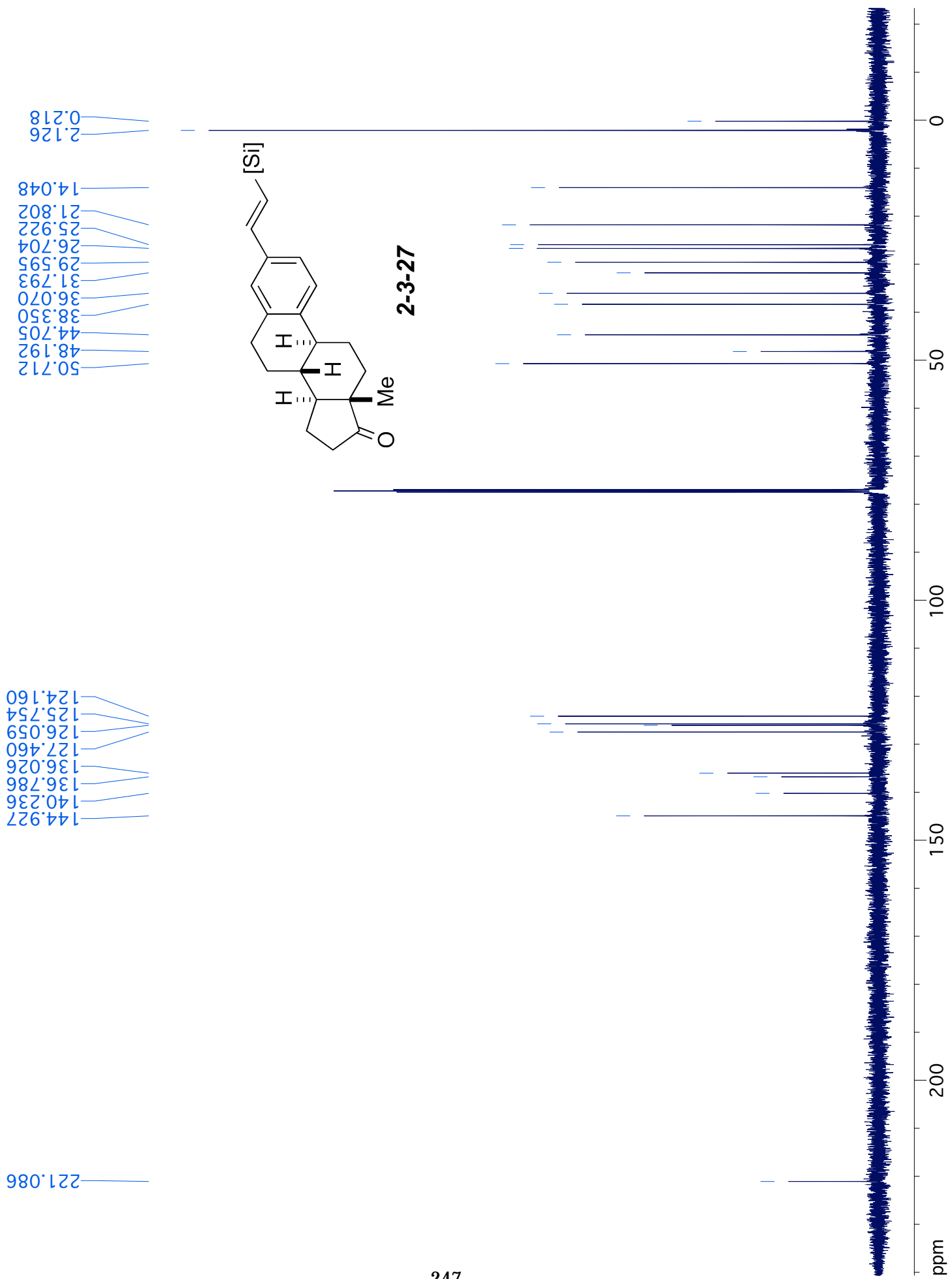


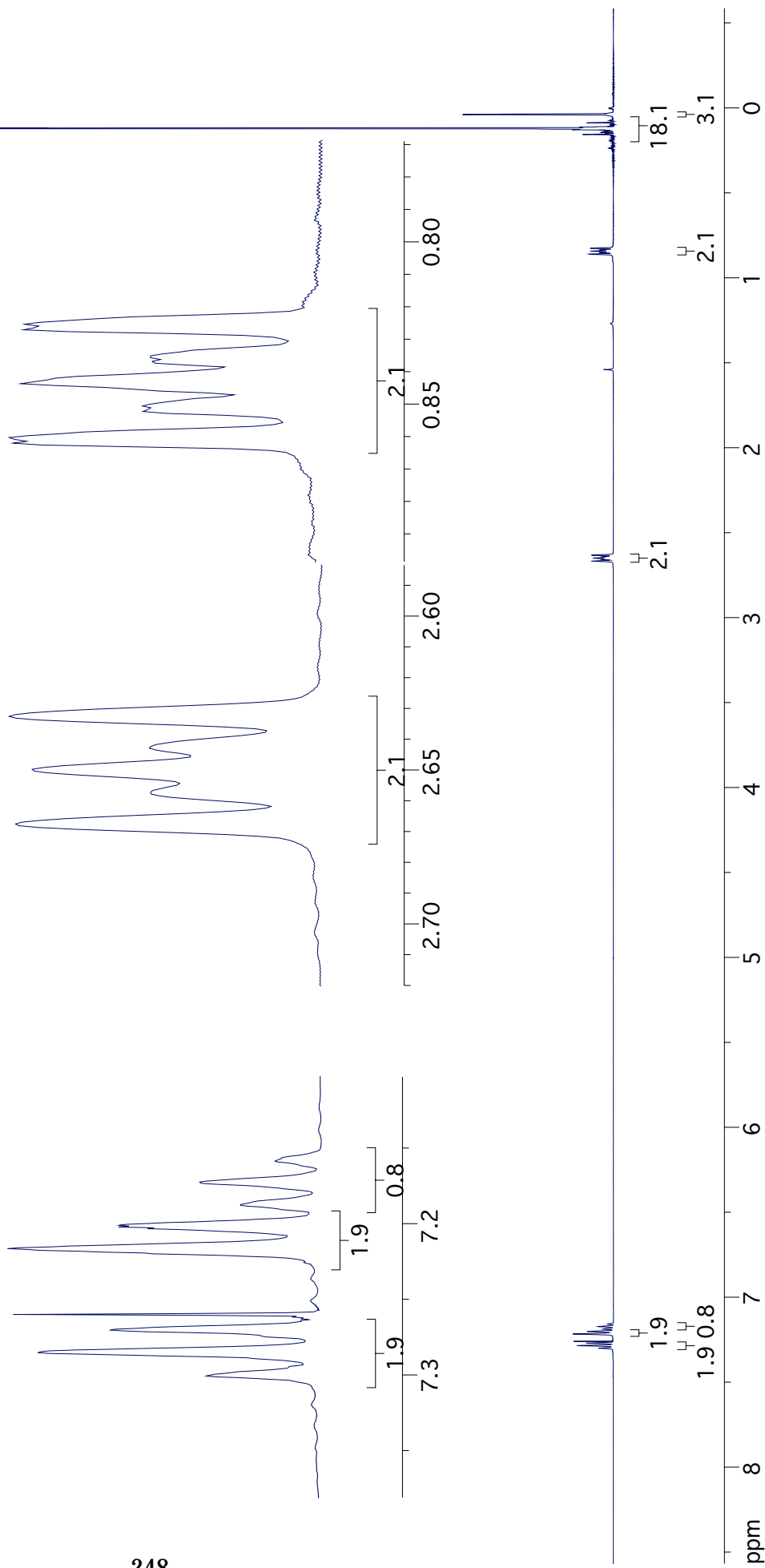
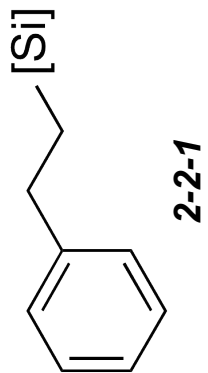
2-3-26

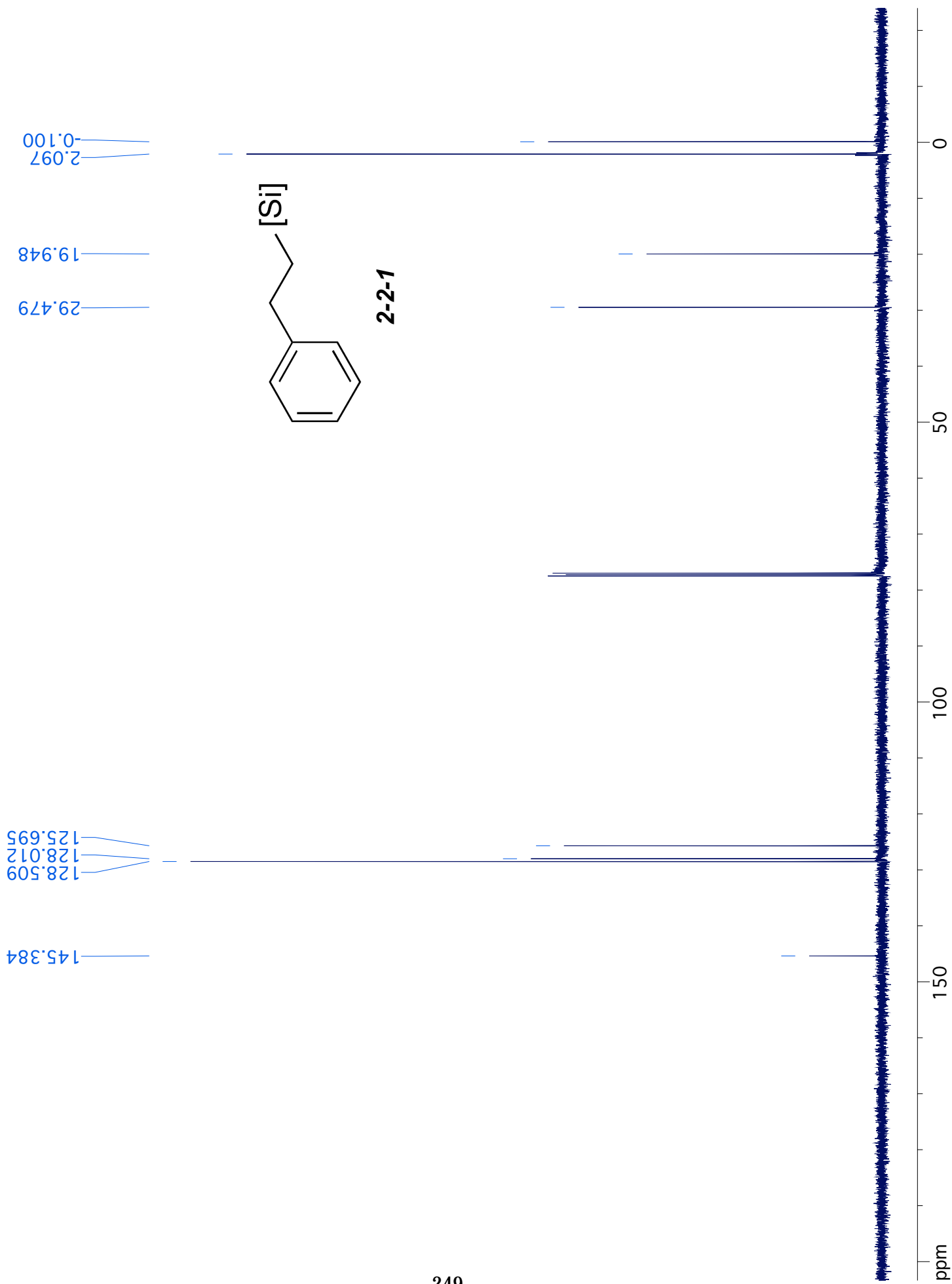


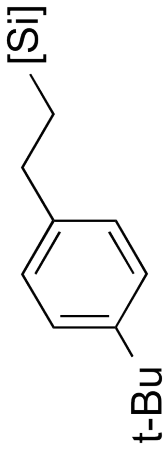




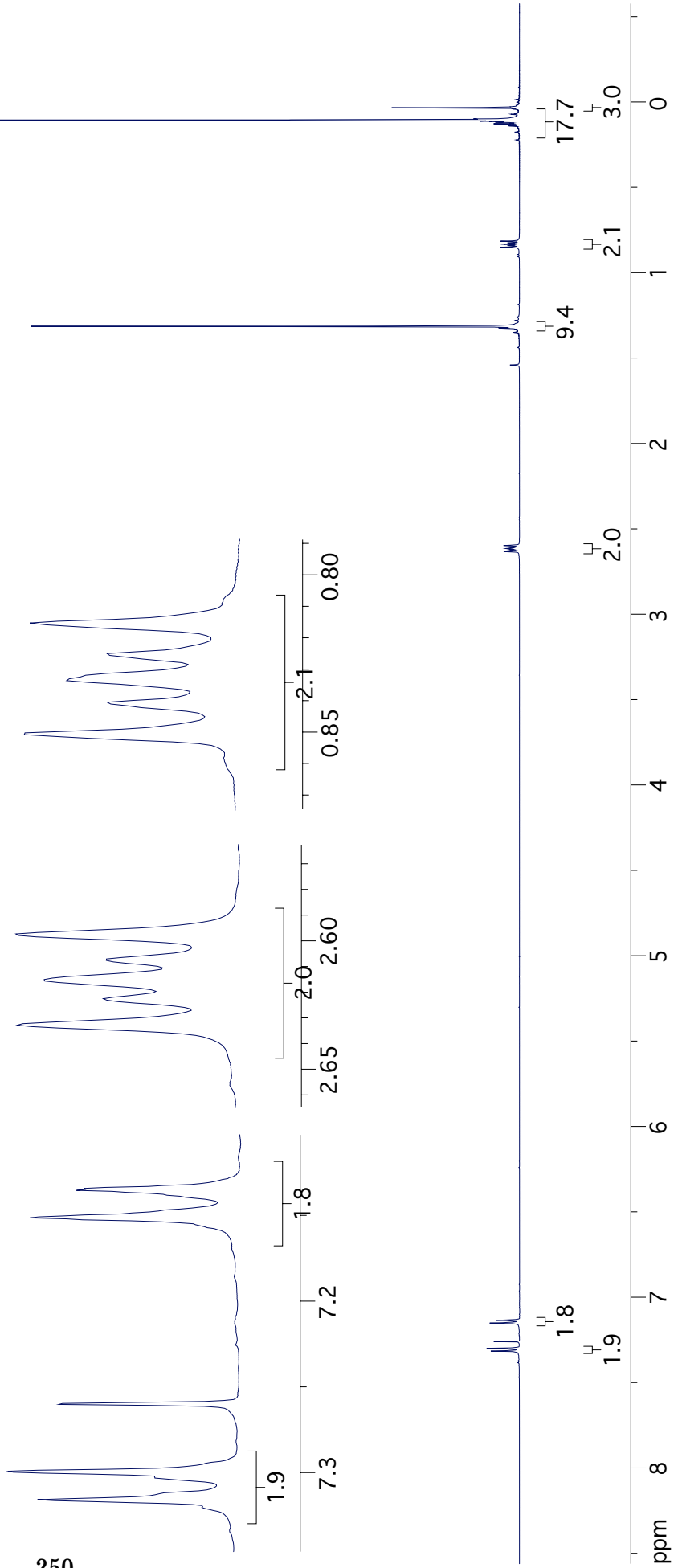


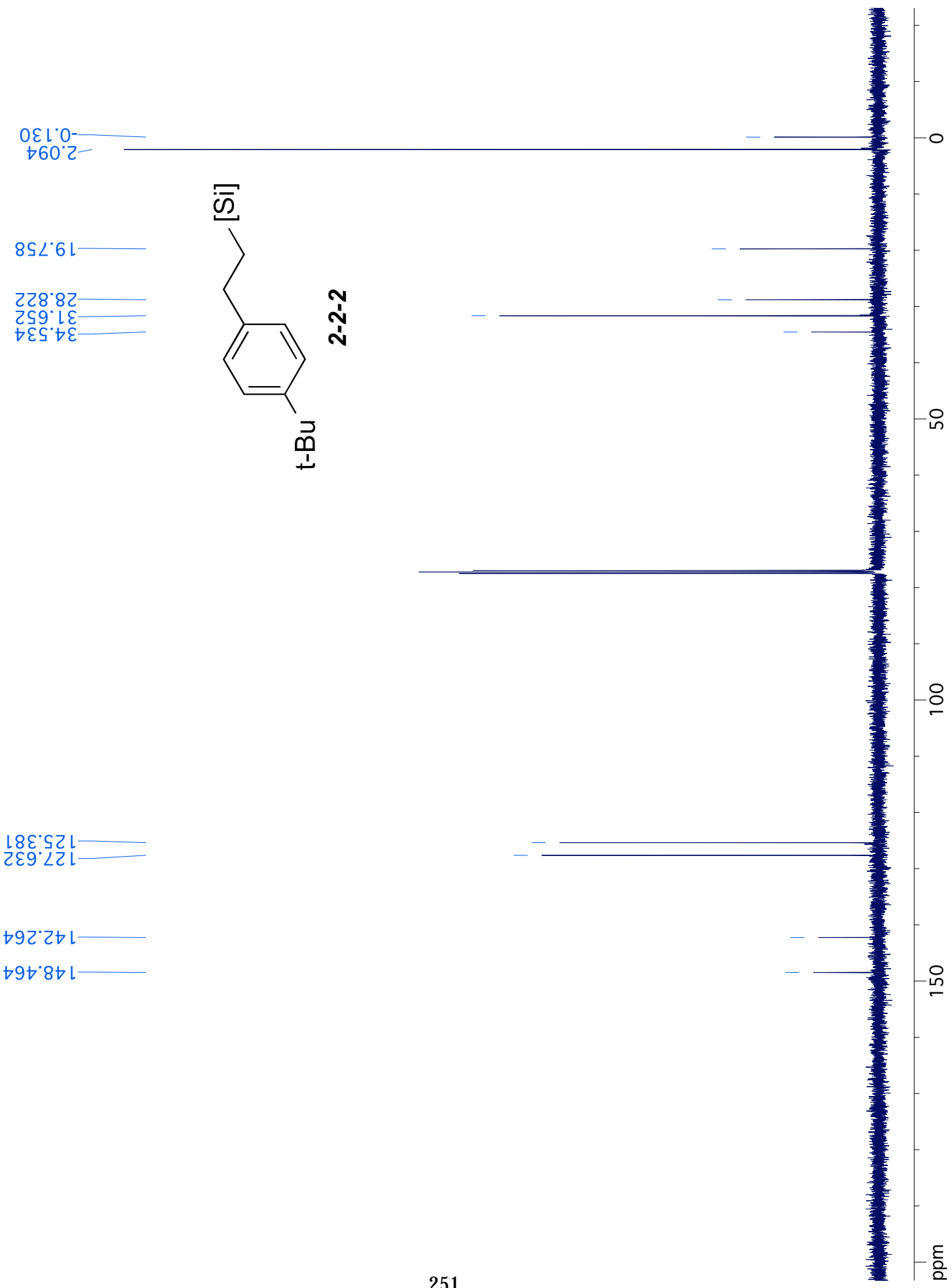


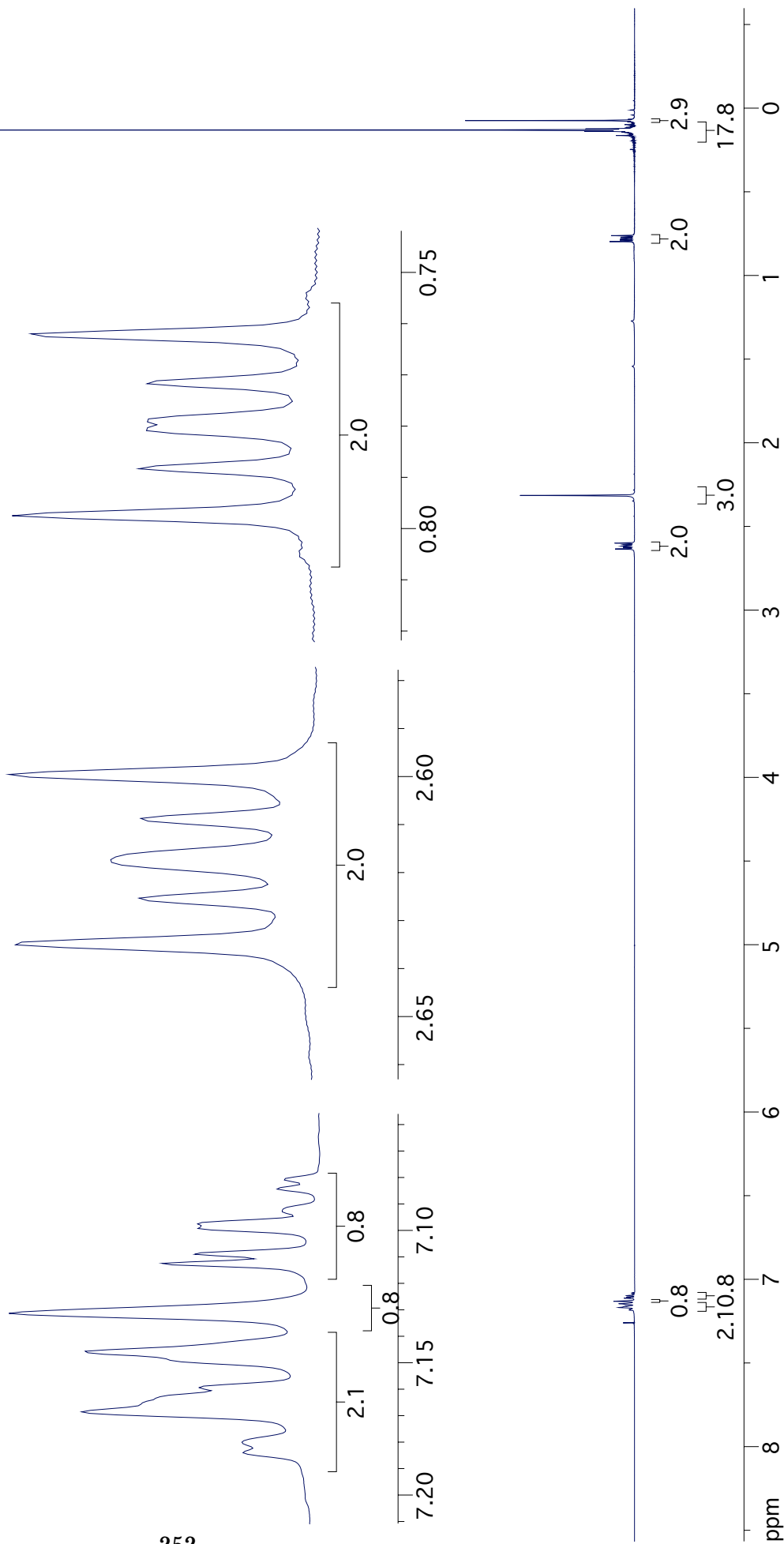
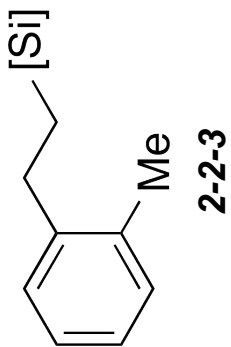


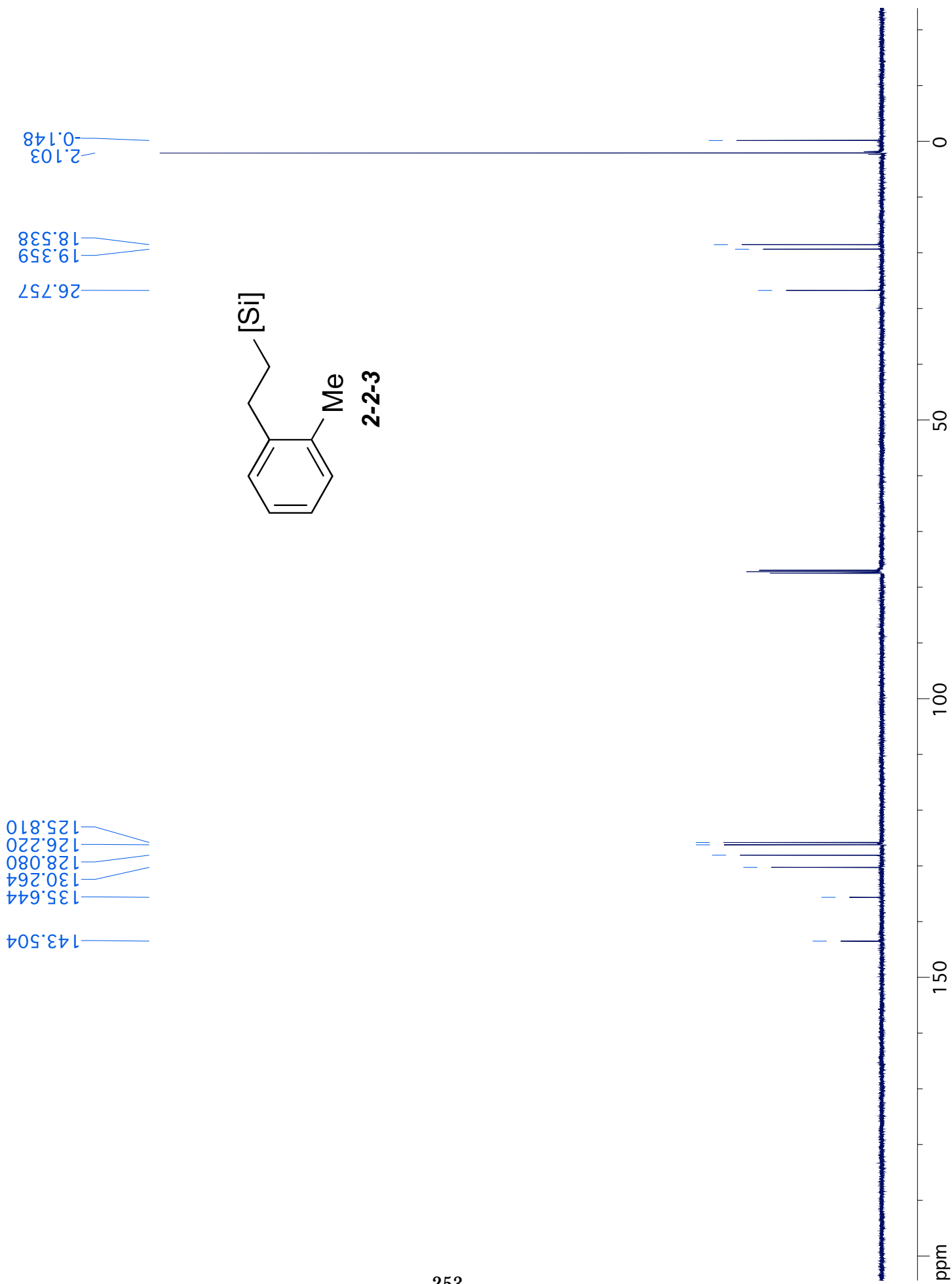


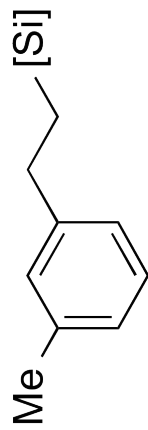
2-2-2



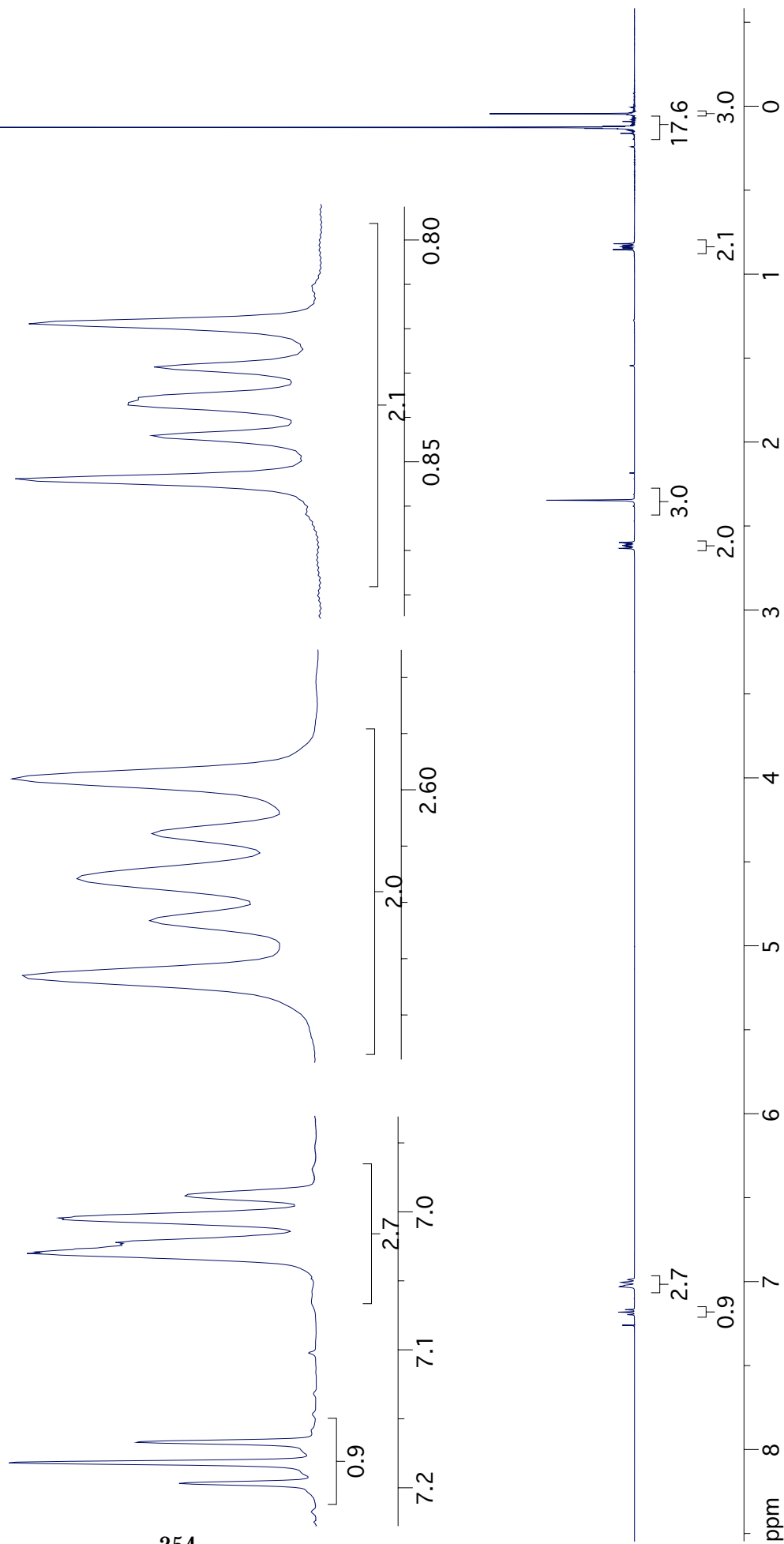


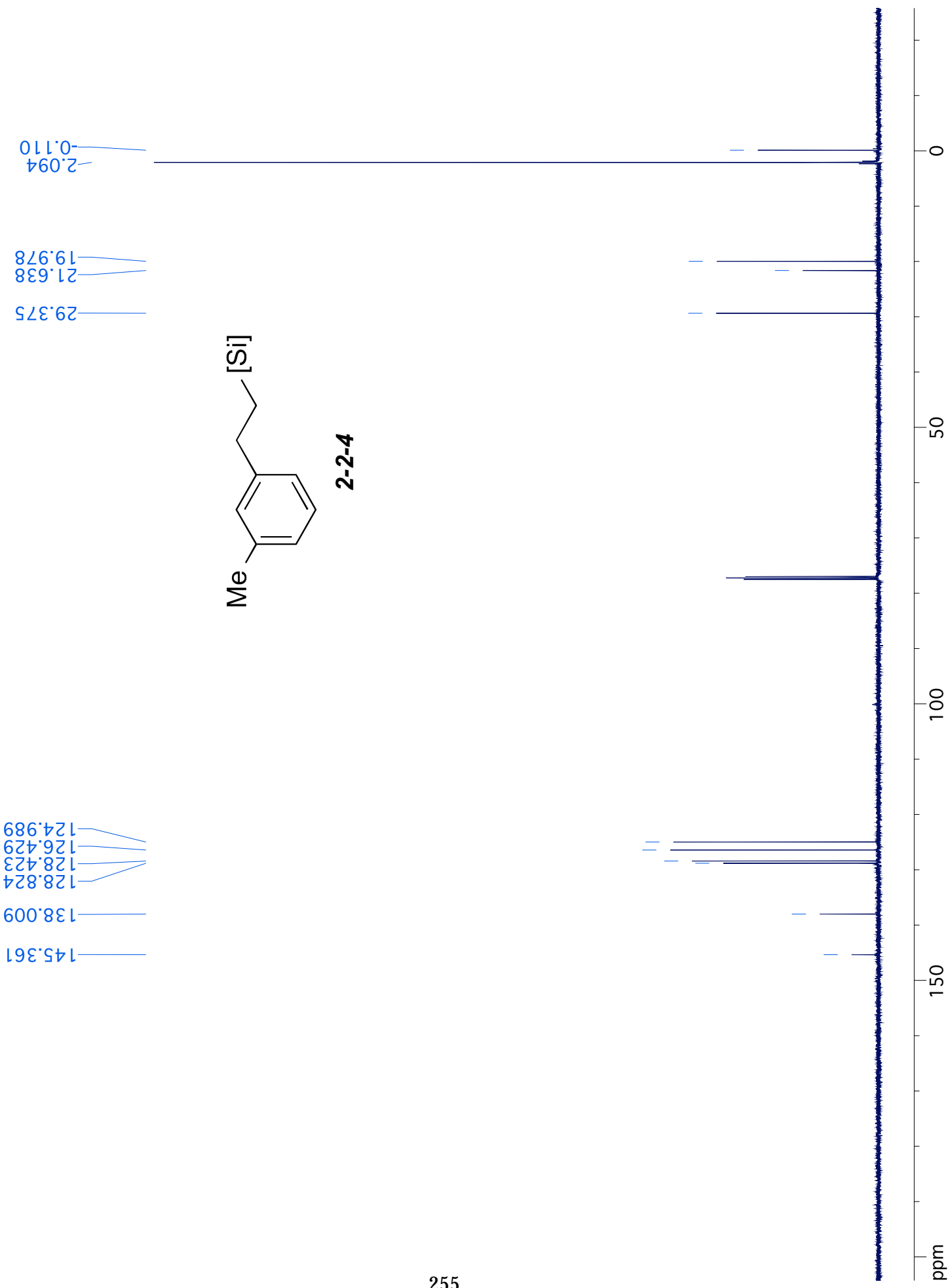


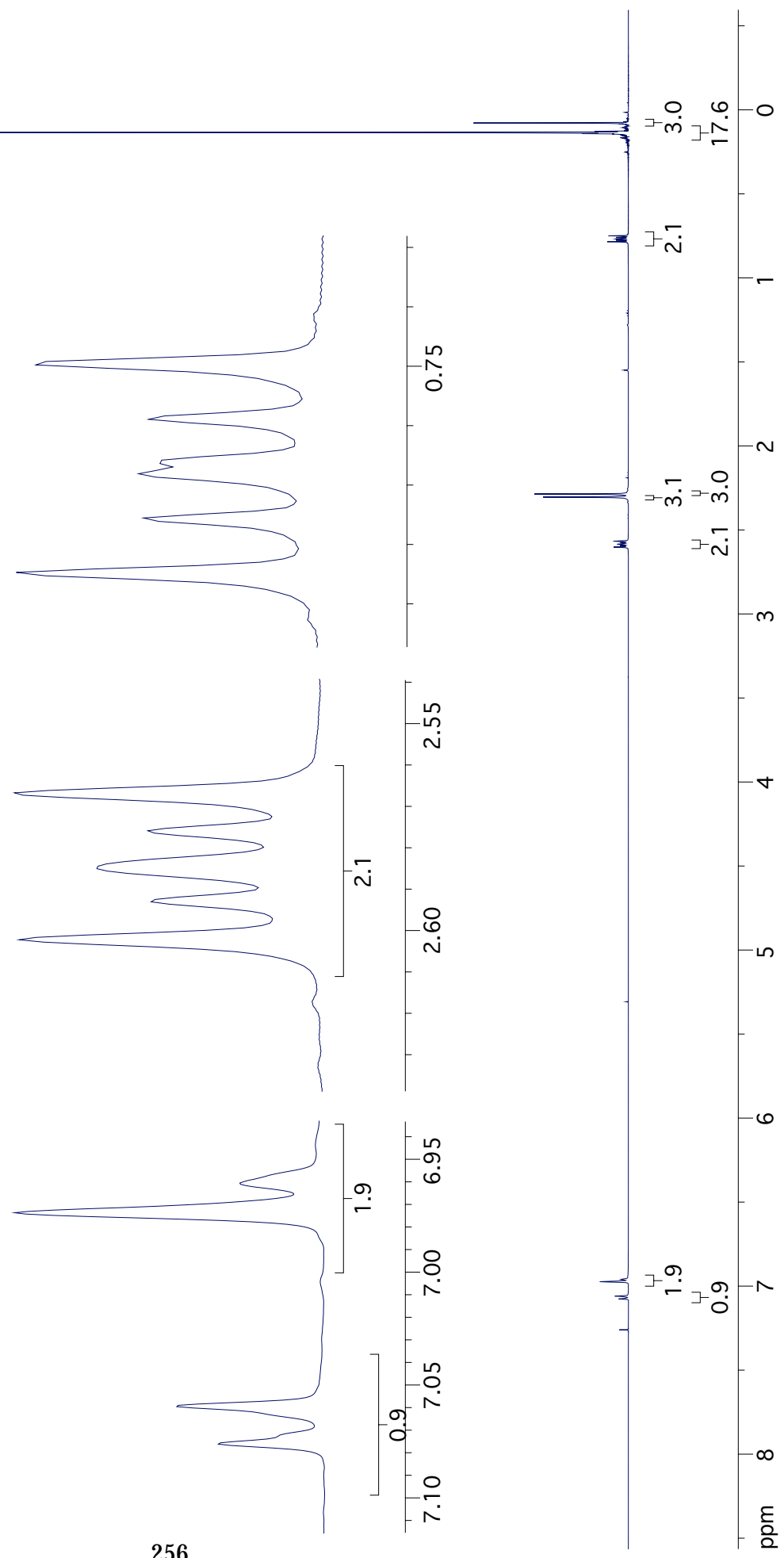
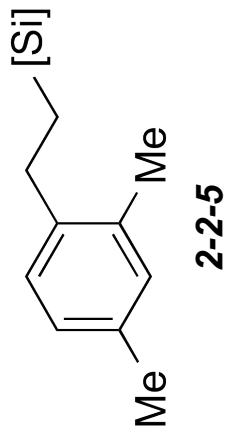




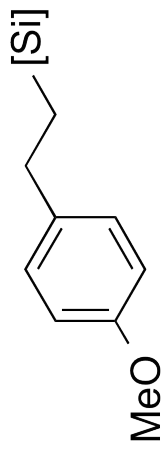
2-2-4



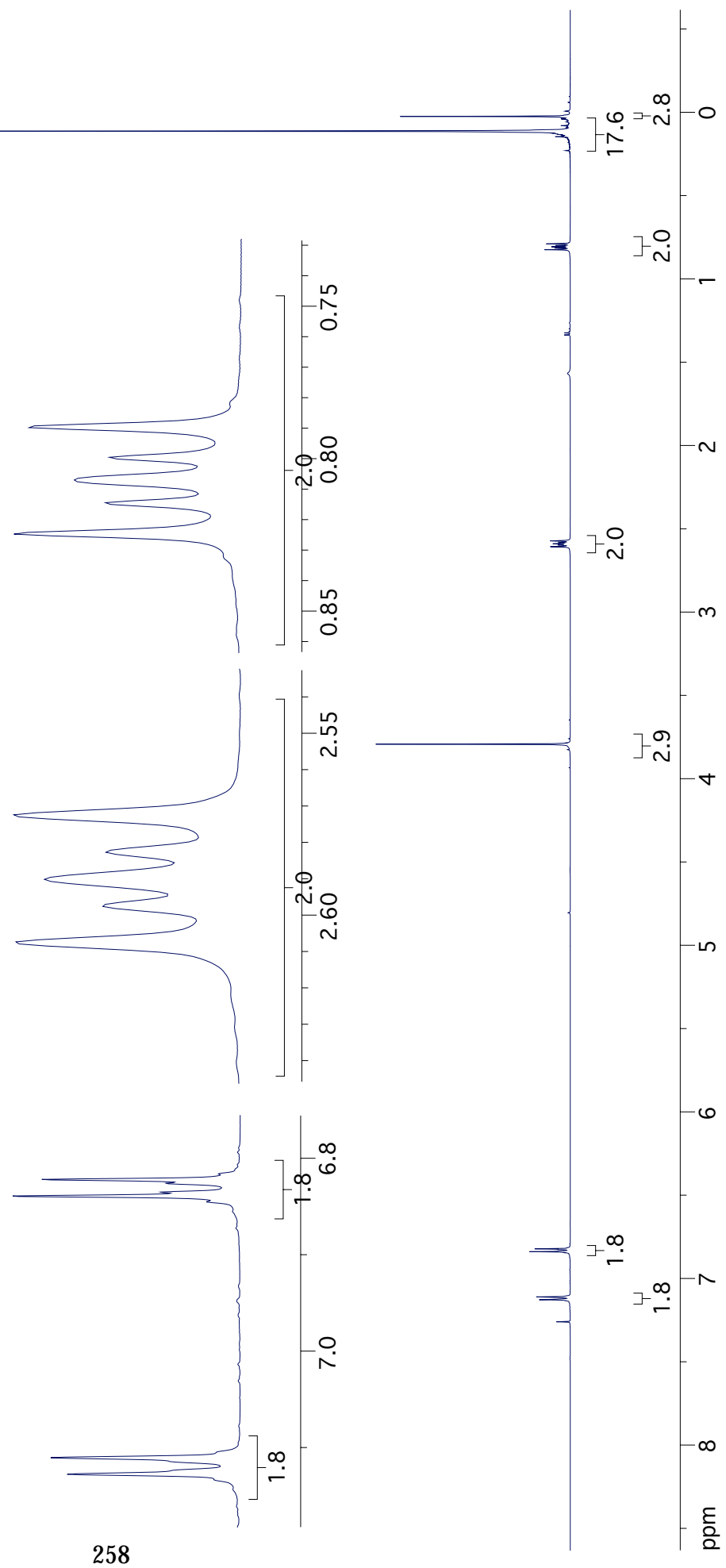


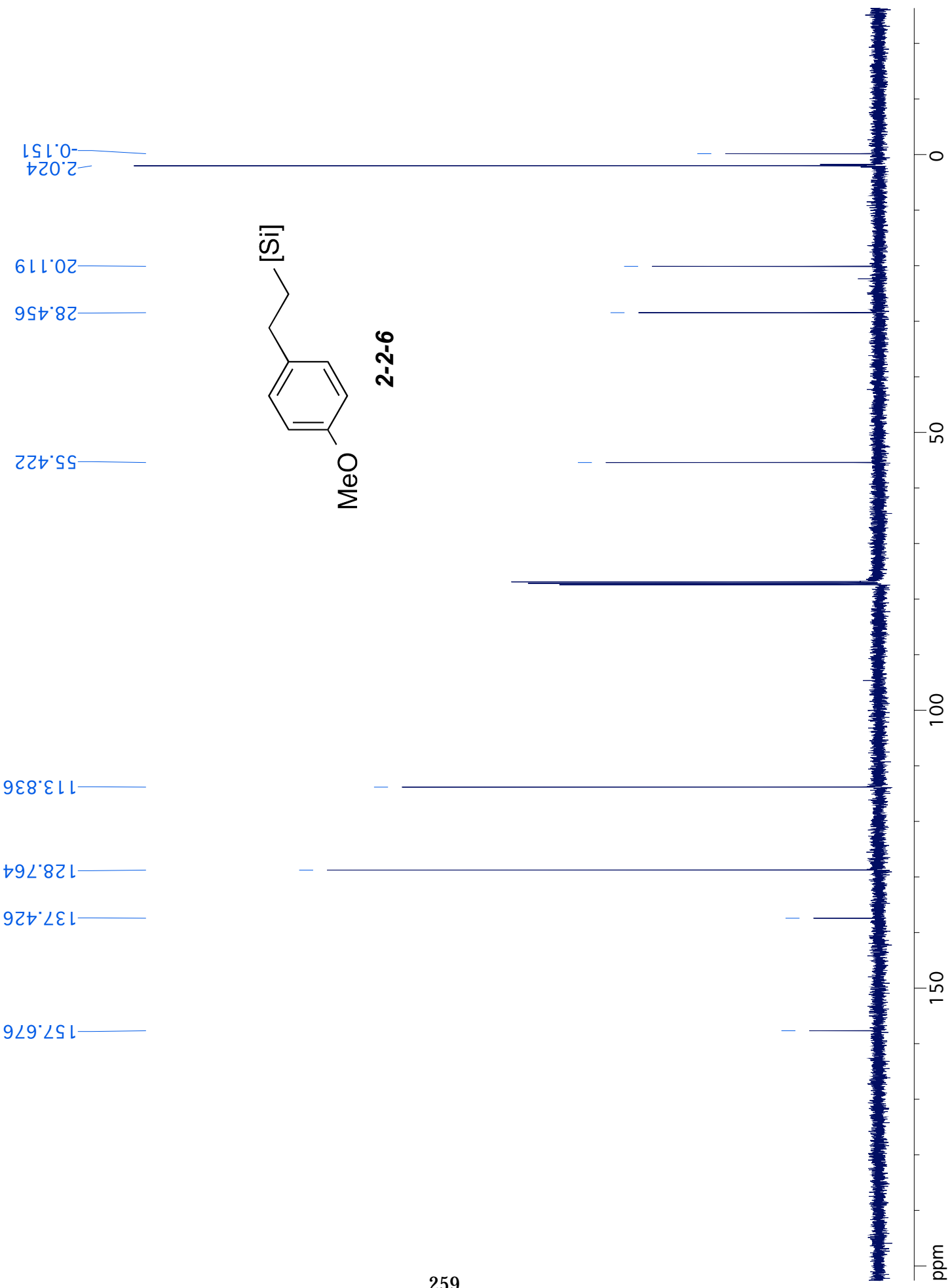


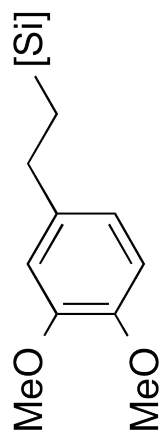




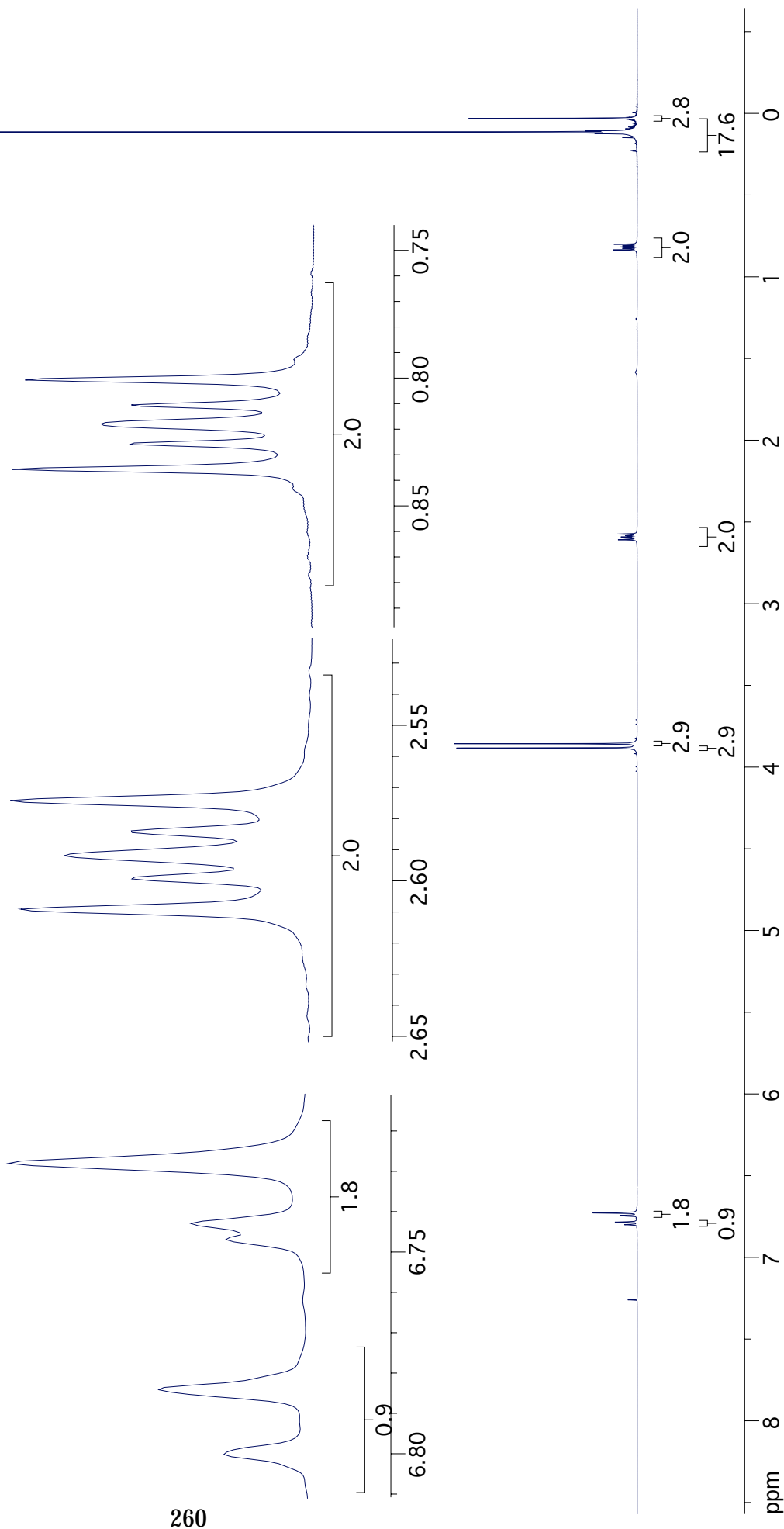
2-2-6

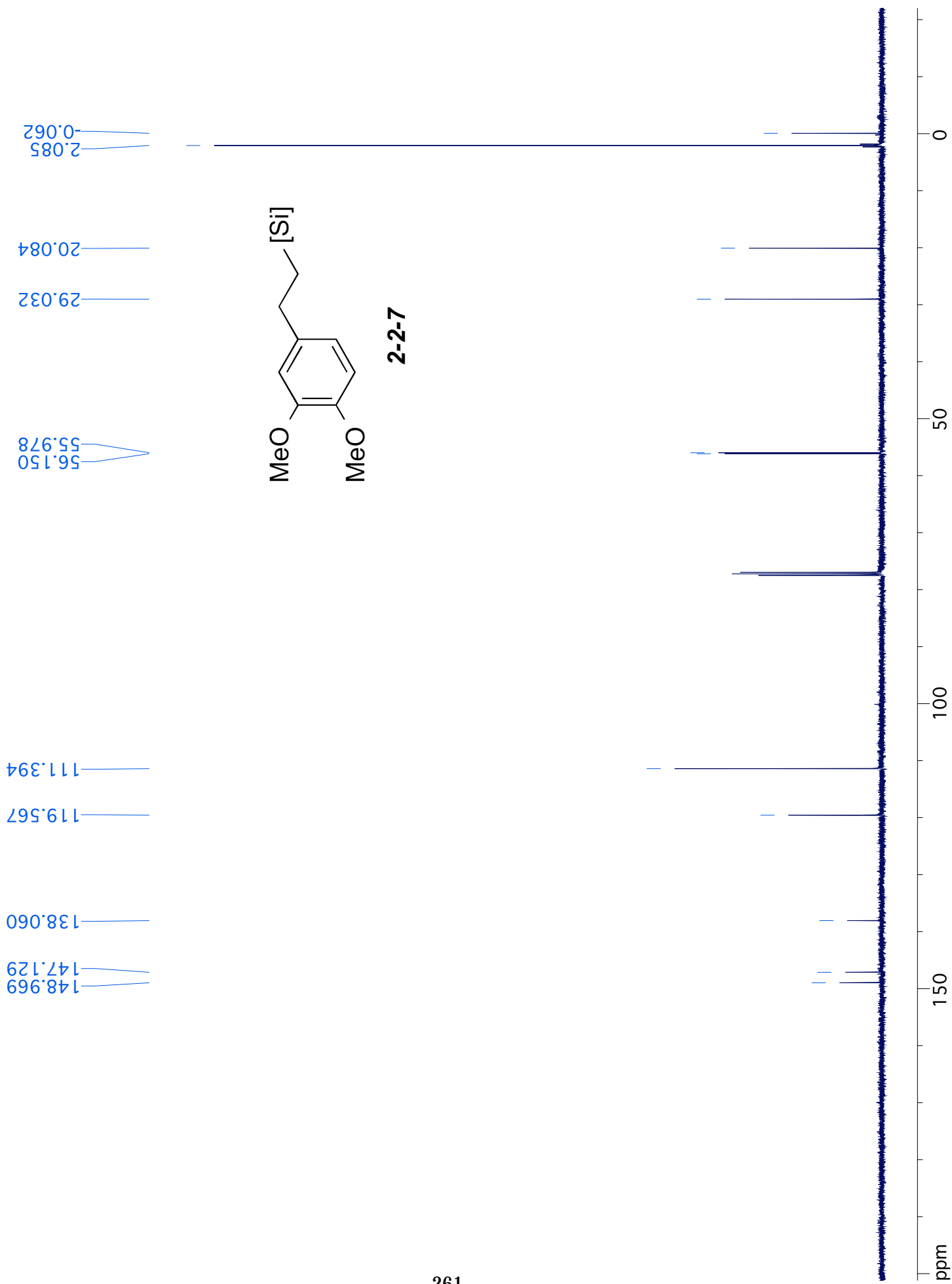


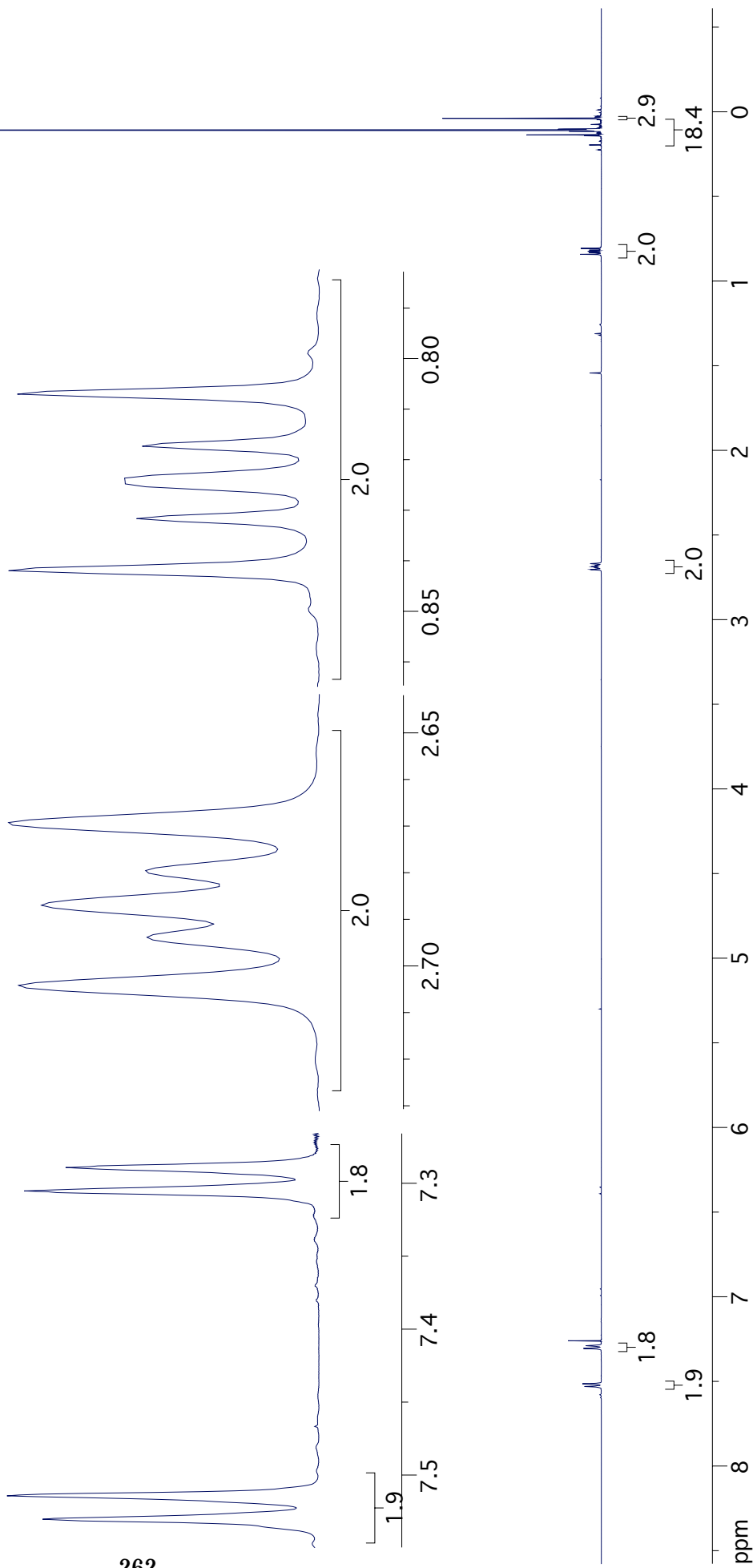
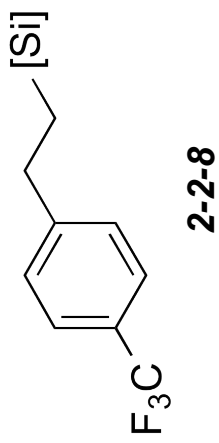


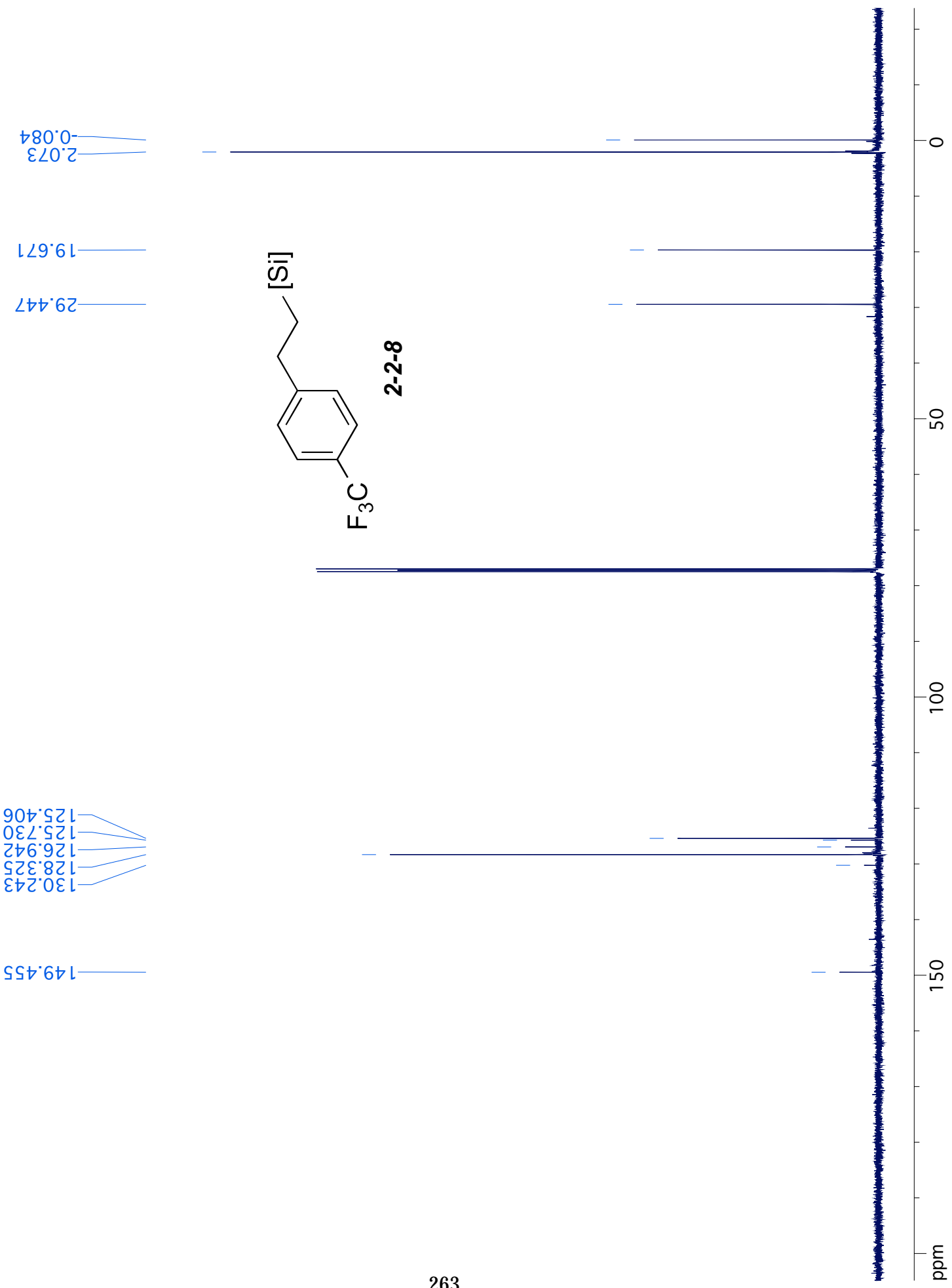


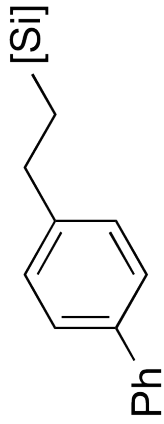
2-2-7



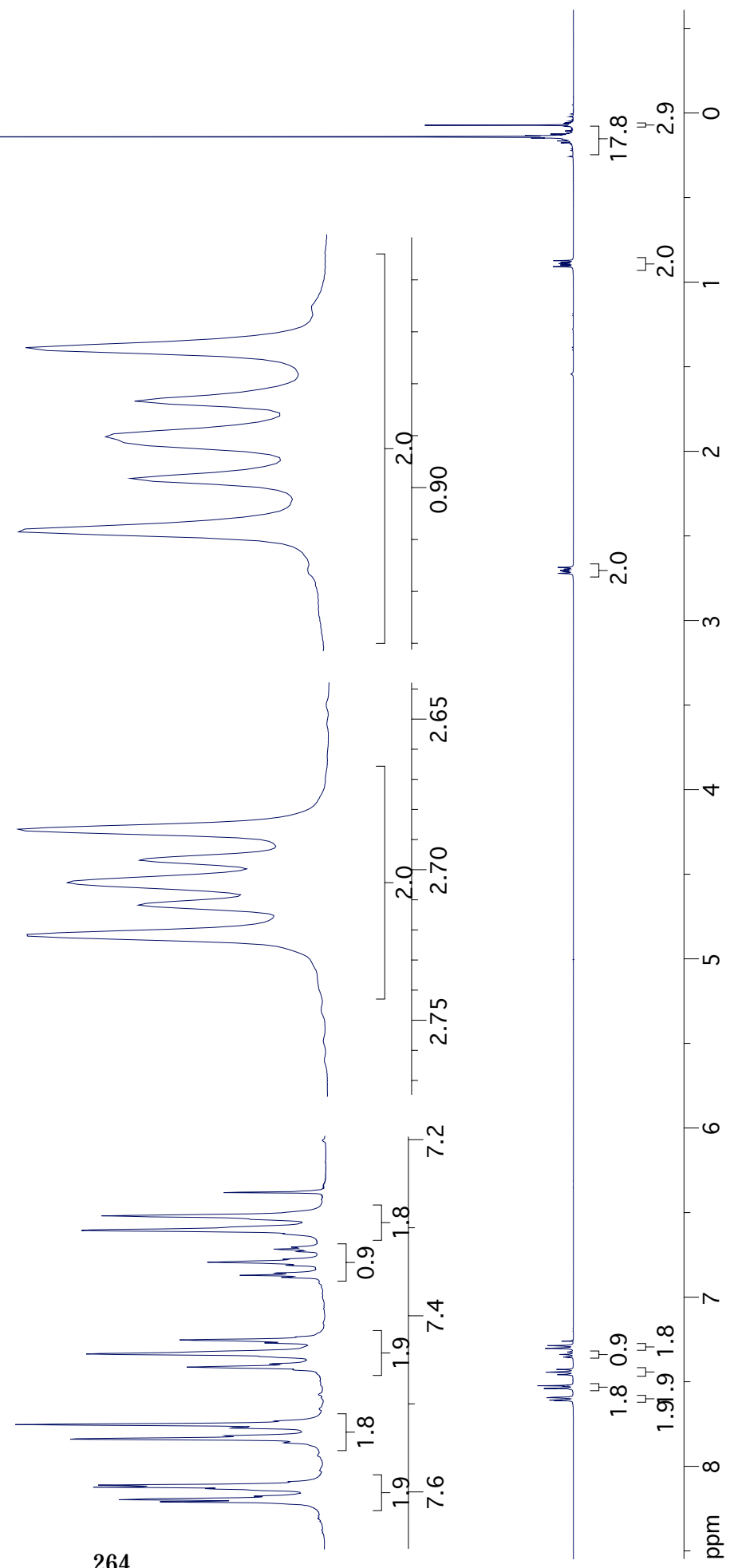




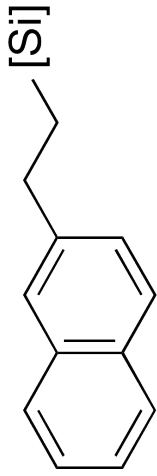




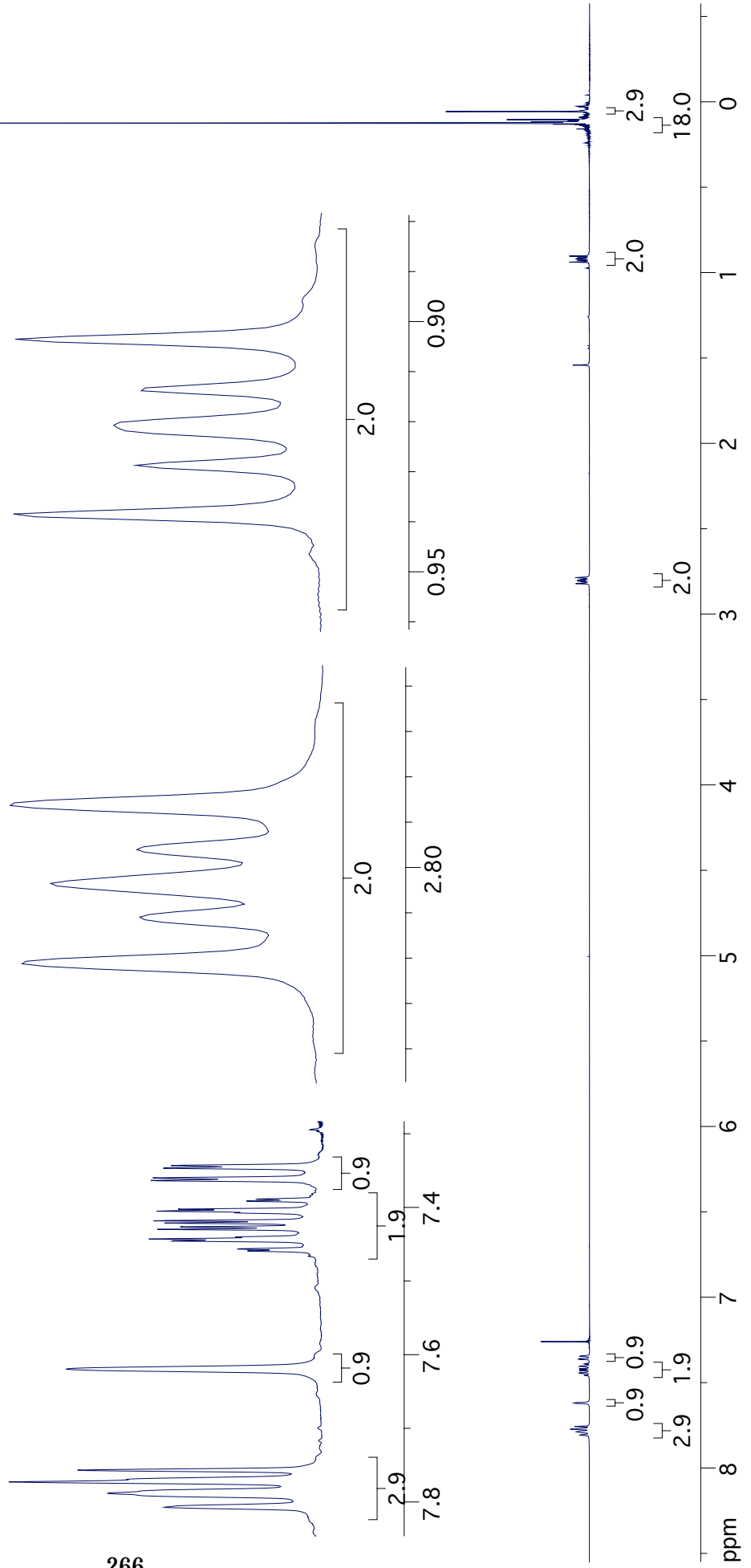
2-2-9

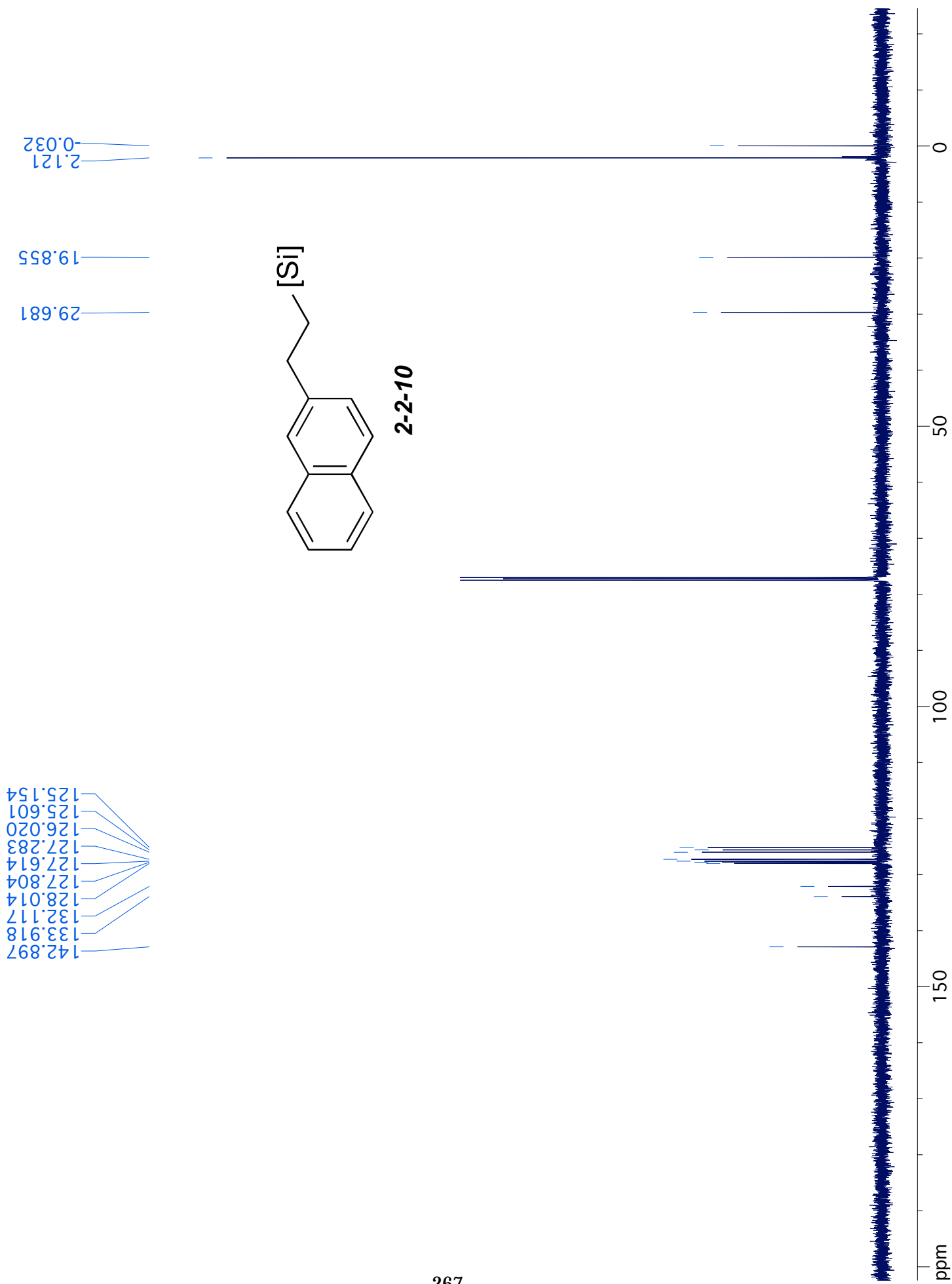


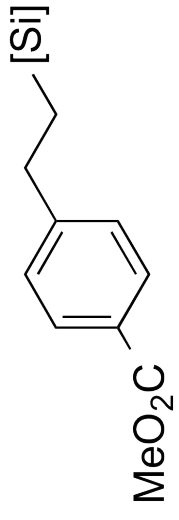




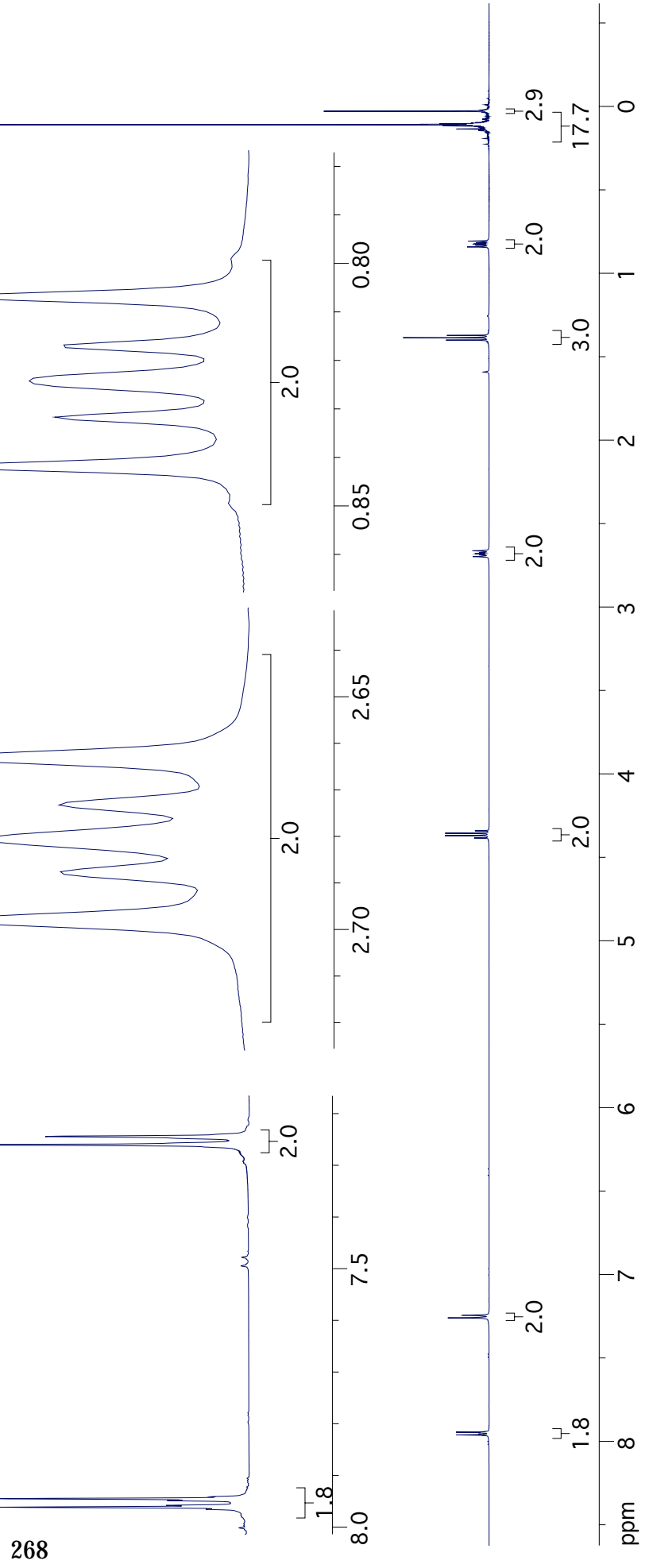
2-2-10

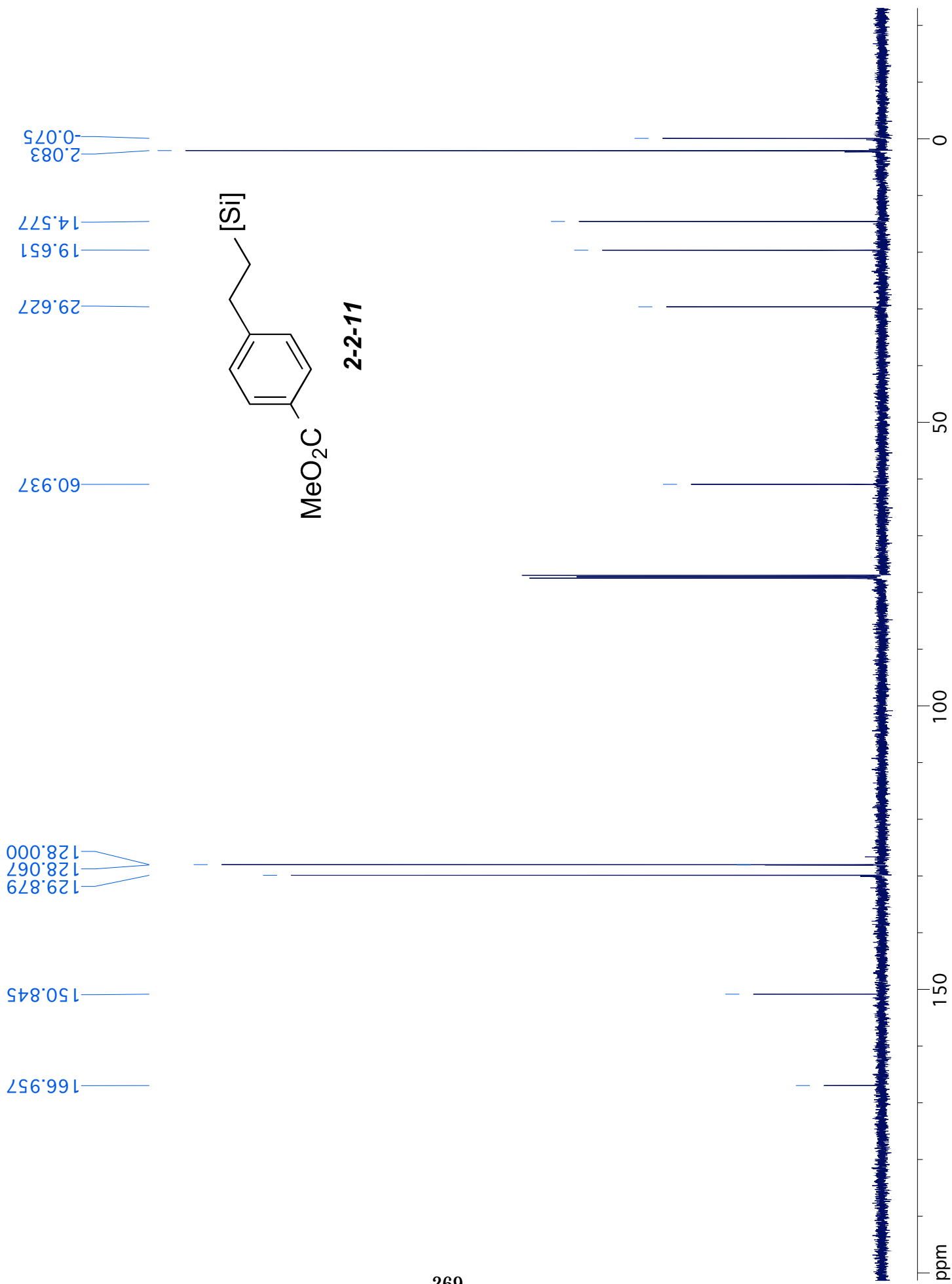


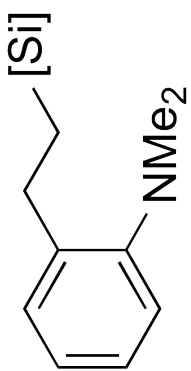




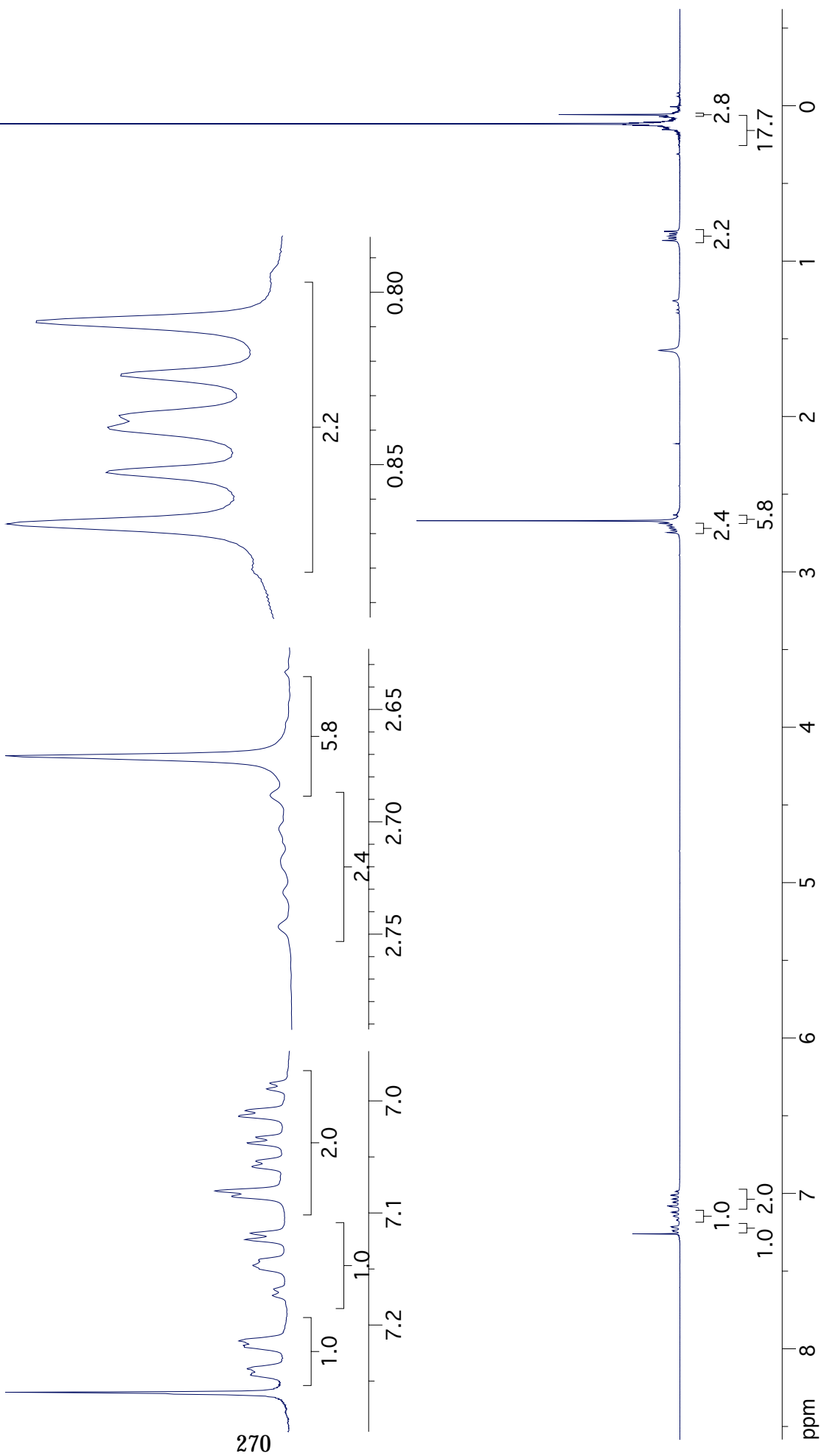
2-2-11

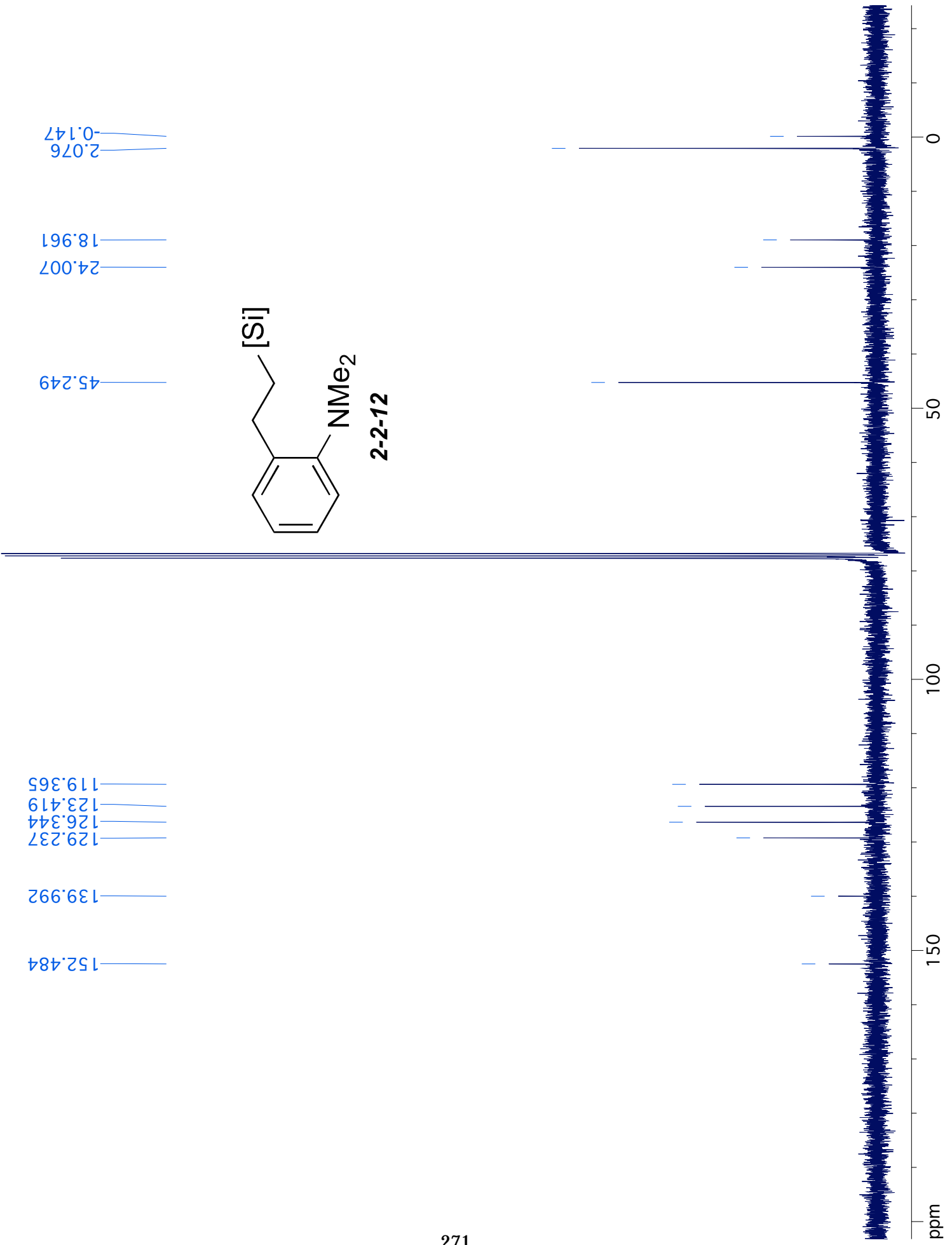


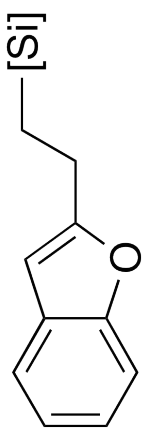




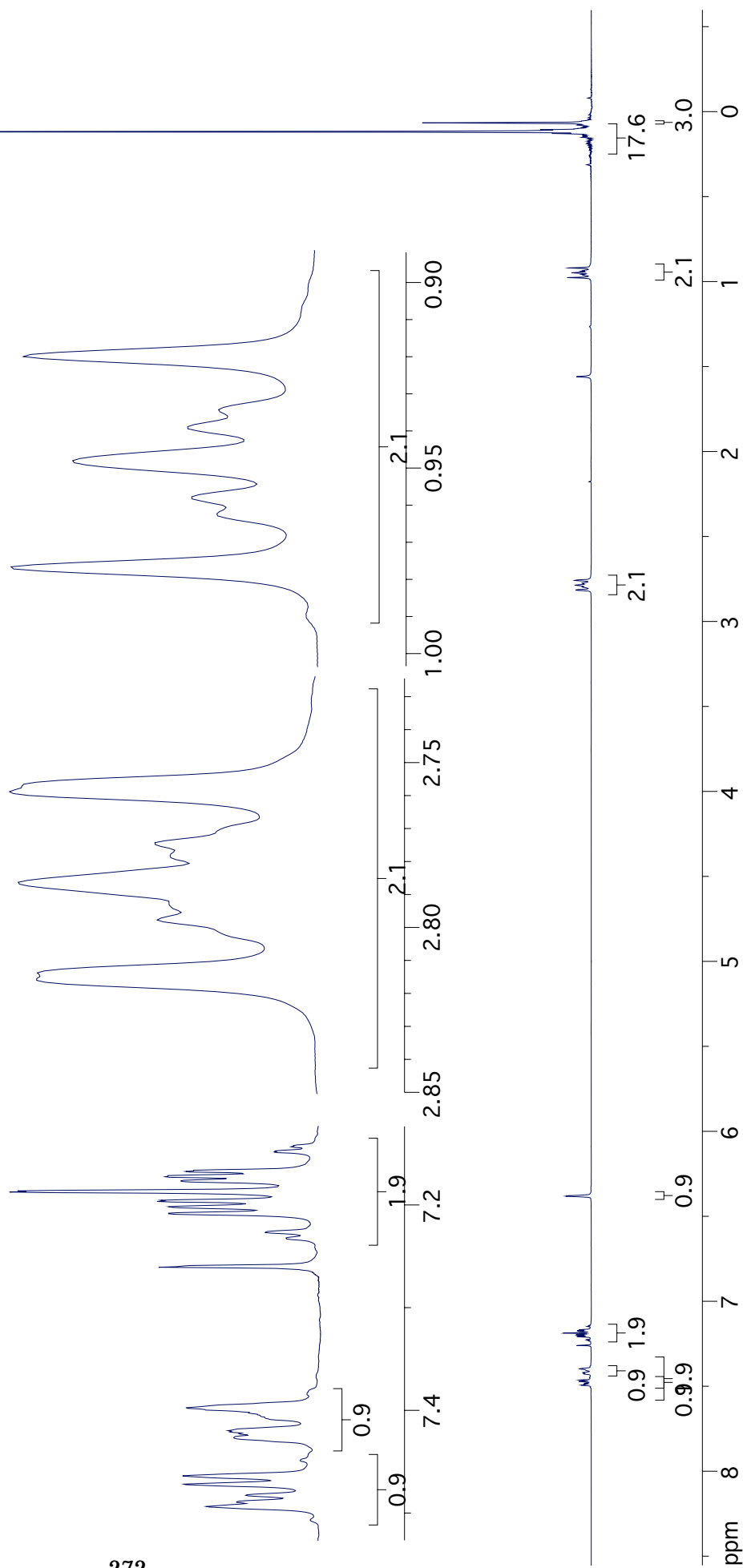
2-2-12

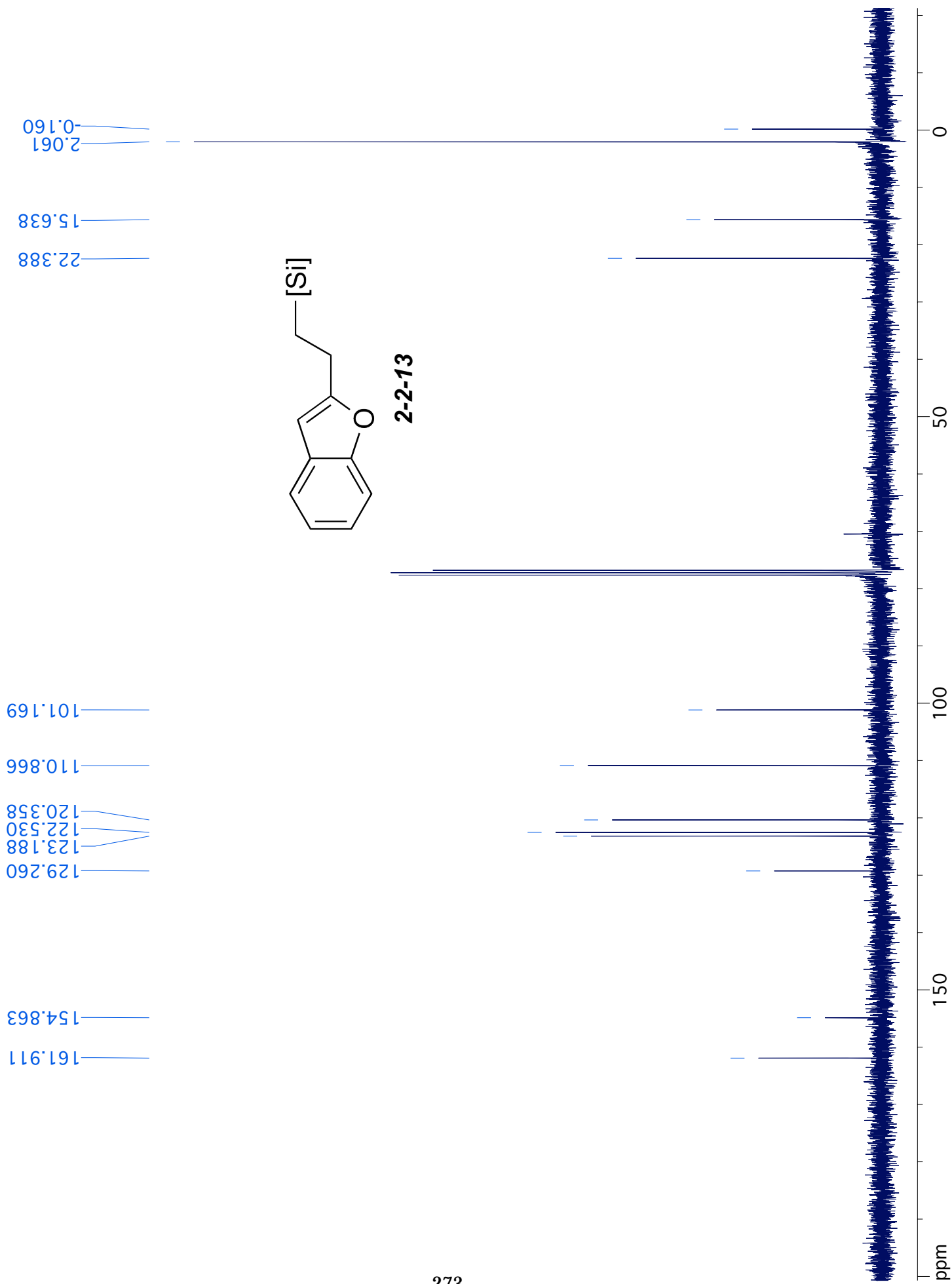


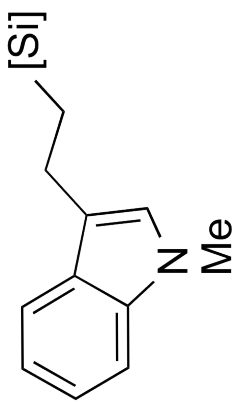




2-2-13

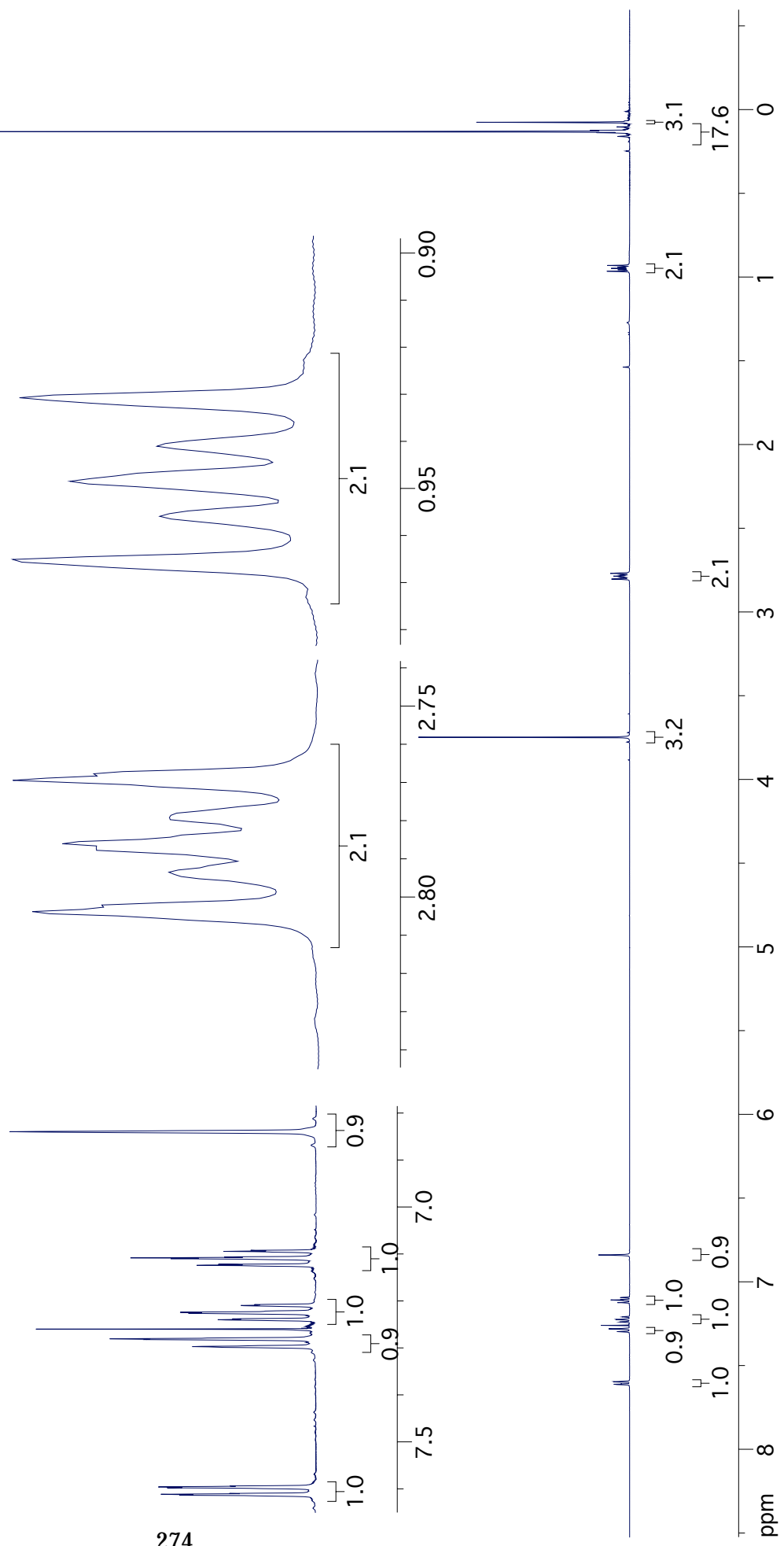






2-2-14

274





References:

1. Greene, T.; Wuts, P. G. M.; *Protecting Groups in Organic Synthesis*; 2nd ed.; Wiley: New York, 1991.
2. Kocienski, P. I.; *Protecting Groups*; Thieme: Stuttgart, **1994**.
3. Larson, G. L.; Fry, J. L.; *Ionic and Organometallic-Catalyzed Organosilane Reductions*. Denmark, S. E. Ed.; John Wiley and Sons: **2008**; Vol 71, pp. 1-737.
4. Denmark, S. E. Sweis, R. F. In *Metal-Catalyzed Cross-Coupling Reactions*; de Meijere, A., Diederich, F., Eds.; Wiley-VCH: New York, **2004**; Chapter 4.
5. Nakao, Y; Hiyama, T. *Chem. Soc. Rev.* **2011**, *40*, 4893–4901.
6. Denmark, S. E. *Acc. Chem. Res.* **2008**, *41*, 1486-1499.
7. Smith, A. B., III; Wuest, W. M. *Chem. Commun.* **2008**, 5883-5895.
8. Bains, W.; Tacke, R. Silicon Chemistry as a Novel Source of Chemical Diversity in Drug Design. *Curr. Opin. Drug. Discovery Dev.* **2003**, *6*, 526-543.
9. Franz, A. K.; Wilson, S. O. Organosilicon Molecules with Medicinal Applications. *J. Med. Chem.* **2013**, *56*, 388-405.
10. Ojima, I. In *The Chemistry of Organic Silicon Compounds*; Patai, S; Rappoport, Z. Eds.; John Wiley: New York, **1989**; Chapter 25, pp. 1479–1526.
11. Brook, M. A. *Silicon in organic, organometallic, and polymer chemistry*. J. Wiley: 2000.
12. Marciniak, B. *Coord. Chem. Rev.* **2005**, *249*, 2374.
13. Atienza, C. C. H.; Diao, T.; Weller, K. J.; Nye, S. A.; Lewis, K. M.; Delis, J. G. P.; Boyer, J. L.; Roy, A. K.; Chirik, P. J. *J. Am. Chem. Soc.* **2014**, *136*, 12108-12118.
14. Fleming, I.; Barbero, A.; Walter, D. *Chem. Rev.* **1997**, *97*, 2063-2192.
15. Brook, M. A. *Silicon in organic, organometallic, and polymer chemistry*. J. Wiley: **2000**.

16. Nakao, Y.; Hiyama, T. *Chem. Soc. Rev.* **2011**, *40*, 4893-4901.
17. Marciniak, B.; Maciejewski, H.; Pietraszuk, C.; Pawluc, P. *Hydrosilylation: A Comprehensive Review On Recent Advances*; Marciniak, B., Ed.; Springer: Berlin, **2009**; Vol. 1, pp 3–51.
18. Hiyama, T.; Kusumoto, T. In *Comprehensive Organic Synthesis*; Trost, B. M.; Fleming, I. Eds.; Pergamon: Oxford, **1991**; Vol 8, pp. 763-792.
19. Yamamoto, K.; Hayashi, T. In *Transition Metals for Organic Synthesis*, 2nd ed.; Beller, M., Bolm, C., Eds.; Wiley-VCH: Weinheim, **2004**; pp 167-191.
20. Showell, G. A.; Mills, J. S. *Drug Discov. Today* **2003**, *8*, 551-556;
21. Gately, S.; West, R. *Drug Dev. Res.* **2007**, *68*, 156-163.
22. Franz, A. K.; Wilson, S. O. *J. Med. Chem.* **2012**, *56*, 388-405.
23. Sommer, L. H.; Pietrusza, E. W.; Whitmore, F. C. *J. Am. Chem. Soc.* **1947**, *69*, 188.
24. Speier, J. L.; Zimmerman, R.; Webster, J. *J. Am. Chem. Soc.* **1956**, *78*, 2278.
25. Speier, J. L.; Webster, J. A.; Barnes, G. H. *J. Am. Chem. Soc.* **1957**, *79*, 974.
26. Speier, J. L.; Hook, E. D. *United States Pat.*, US2823218, 1958.
27. Karstedt, D.B. *France Pat.*, FR1548775, 1968.
28. Troegel, D.; Stohrer, J. *Coord. Chem. Rev.*, **2011**, *255*, 1440–1459.
29. Truscott, B. J.; Slawin, A. M. Z.; Nolan, S. P. *Dalton Trans.* **2013**, *42*, 270-276.
30. Trnka, T. M.; Grubbs, R. H. *Acc. Chem. Res.* **2001**, *34*, 18-29.
31. Vougioukalakis, G. C.; Grubbs, R. H. *Chem. Rev.* **2010**, *110*, 1746-1787. 3.
32. Tallarico, J. A.; Malnick, L. M.; Snapper, M. L. *J. Org. Chem.* **1999**, *64*, 344.
33. Grubbs, R. H.; Chang, S. *Tetrahedron* **1998**, *54*, 4413-4450.
34. Grubbs, R. H. *Tetrahedron* **2004**, *60*, 7117-7140.

35. Dragutan, V.; Dragutan, I.; Delaude, L.; Demonceaub, A. *Coord. Chem. Rev.* **2007**, *251*, 765-794.
36. Alcaide, B.; Almendros, P.; Luna, A. *Chem. Rev.* **2009**, *109*, 3817-3858.
37. Gonzalez-Gomez, A.; Dominguez, G.; Perez-Castells, J. *Tetrahedron Lett.* **2005**, *46*, 7267.
38. Dai, X.; Strotman, N. A.; Fu, G. C. *J. Am. Chem. Soc.* **2008**, *130*, 3302-3303.
39. Palmer, M.; Wills, M. *Tetrahedron: Asymmetry* **1999**, *10*, 2045.
40. Naota, T.; Takaya, H.; Murahashi, S.-I. *Chem. Rev.* **1998**, *98*, 2599.
41. Nishiyama, H. *Top. Organomet. Chem.* **2004**, *11*, 81.
42. Mass, G. *Chem. Soc. Rev.* **2004**, *33*, 183.
43. Rosillo, M.; Dominguez, G.; Casarrubios, L.; Amador, U.; Perez-Castells, J. *J. Org. Chem.* **2004**, *69*, 2084.
44. Rosillo, M.; Casarrubios, L.; Dominguez, G.; Perez-Castells, J. *Tetrahedron Lett.* **2001**, *42*, 7029.
45. Arico, C. S.; Cox, L. R. *Org. Biomol. Chem.* **2004**, *2*, 2558-2562.
46. Maifeld, S. V.; Tran, M. N.; Lee, D. *Tetrahedron Lett.* **2005**, *46*, 105-108.
47. Menozzi, C.; Dalko, P. I.; Cossy, J. *J. Org. Chem.* **2005**, *70*, 10717-10719.
48. Glaser, P. B.; Tilley, T. D. *J. Am. Chem. Soc.* **2003**, *125*, 13640-13641.
49. Marciniak, B.; Guliński, J.; *J. Organomet. Chem.* **1983**, *253*, 349-362.
50. Chalk, A. J.; Harrod, J. F. *J. Am. Chem. Soc.* **1965**, *87*, 16-21.
51. Randolph, C.L.; Wrighton, M. S. *J. Am. Chem. Soc.* **1986**, *108*, 3366-3374.
52. Fu, P.-f.; Brard, L.; Li, Y.; Marks, T. J. *J. Am. Chem. Soc.* **1995**, *117*, 7157-7168.

53. Cossy, J.; Arseniyadis, S.; Meyer, C. *Metathesis in Natural Product Synthesis: Strategies, Substrates and Catalysts*; Wiley-VCH: Weinheim, **2010**.
54. Denmark, S. E.; Sweis, R. F. In *Metal-Catalyzed Cross-Coupling Reactions*; de Meijere, A., Diederich, F., Eds.; Wiley-VCH: New York, **2004**; Chapter 4.
55. Tamao, K. *J. Syn. Org. Chem. Jpn.* **1988**, *46*, 861.
56. Bode, S. E.; Wolberg, M.; Müller, M. *Synthesis* **2006**, 557.
57. Rychnovsky, S. D. *Chem. Rev.* **1995**, *95*, 2021-2040.
58. Tortosa, M. *Angew. Chem. Int. Ed.* **2011**, *50*, 3950-3953.
59. Smitrovich, J. H.; Woerpel, K. A. *J. Org. Chem.* **1996**, *61*, 6044-6046.
60. Petit, M.; Chouraqui, G.; Aubert, C.; Malacria, M. *Org. Lett.* **2003**, *5*, 2037-2040.
61. Michael, R. G. N.; Jose, C. L. *Tetrahedron Lett.* **1999**, *40*, 8667-8670.
62. Petit, M.; Chouraqui, G.; Aubert, C.; Malacria, M. *Org. Lett.* **2003**, *5*, 2037-2040.
63. Schwab, P.; France, M. B.; Ziller, J. W.; Grubbs, R. H. *Angew. Chem., Int. Ed. Engl.* **1995**, *34*, 2039-2041.
64. Kingsbury, J. S.; Harrity, J. P. A.; Bonitatebus, P. J.; Hoveyda, A. H. *J. Am. Chem. Soc.* **1999**, *121*, 791-799.
65. Scholl, M.; Ding, S.; Lee, C. A.; Grubbs, R. H. *Org. Lett.* **1999**, *6*, 953-956.
66. Garber, S. B.; Kingsbury, J. S.; Gray, B. L.; Hoveyda, A. H. *J. Am. Chem. Soc.* **2000**, *122*, 8168-8179.
67. Stewart, I. C.; Douglas, C. J.; Grubbs, R. H. *Org. Lett.* **2008**, *10*, 441-444.
68. Schwab, P.; France, M. B.; Ziller, J. W.; Grubbs, R. H. *Angew. Chem., Int. Ed. Engl.* **1995**, *34*, 2039-2041.
69. Kingsbury, J. S.; Harrity, J. P. A.; Bonitatebus, P. J.; Hoveyda, A. H. *J. Am. Chem. Soc.*

- 1999**, *121*, 791–799.
70. Scholl, M.; Ding, S.; Grubbs, R. H. *Org. Lett.* **1999**, *1*, 953–956.
71. Sanford, M. S.; Love, J. A.; Grubbs, R. H. *J. Am. Chem. Soc.* **2001**, *123*, 6543–6554.
72. Wenzel, A. G.; Grubbs, R. H. *J. Am. Chem. Soc.* **2006**, *128*, 16048–16049.
73. Van der Eide, E. F.; Romero, P. E.; Piers, W. E. *J. Am. Chem. Soc.* **2008**, *130*, 4485–4491.
74. Garber, S. B.; Kingsbury, J. S.; Gray, B. L.; Hoveyda, A. H. *J. Am. Chem. Soc.* **2000**, *122*, 8168–8179.
75. Keitz, B. K.; Endo, K.; Patel, P. R.; Herbert, M. B.; Grubbs, R. H. *J. Am. Chem. Soc.* **2012**, *134*, 693–699.
76. Hartung, J.; Grubbs, R. H. *J. Am. Chem. Soc.* **2013**, *135*, 10183–10185.
77. Jung, E. M.; Piizzi, G. *Chem. Rev.* **2005**, *105*, 1735–1766.
78. Herrisson, J. L.; Chauvin, Y. *Makromol. Chem.* **1970**, *141*, 161–176.
79. Fellmann, J. D.; Tumer, H. W.; Schrock, R. R. *J. Am. Chem. Soc.* **1980**, *102*, 6608–6609.
80. Boukherroub, R.; Chatgililoglu, C.; Manuel, G. *Organometallics* **1996**, *15*, 1508–1510.
81. Kunai, A.; Ohshita, J. J. *Organomet. Chem.* **2003**, *686*, 3–15.
82. Karshtedt, D.; Bell, A. T.; Tilley, T. D. *Organometallics* **2006**, *25*, 4471–4482.
83. Ruiz, J.; Bentz, P. O.; Mann, B. E.; Spencer, C. M.; Taylor, B. F.; Maitlis, P. M. *J. Chem. Soc., Dalton Trans.* **1987**, 2709–2713.
84. Noyori, R.; Ohkuma, T. *Angew. Chem., Int. Ed.* **2001**, *40*, 40–73.
85. Tilley, T. D. Transition-Metal Silyl Derivatives. In *The Chemistry of Organic Silicon Compounds*; Patai, S., Rappoport, Z., Eds.; John Wiley and Sons: Chichester, UK, **1989**; pp 1415–1478.

86. Tilley, T. D. Appendix to Transition-Metal Silyl Derivatives. In *The Silicon–Heteroatom Bond*; Patai, S., Rappoport, Z., Eds.; John Wiley and Sons: Chichester, UK, **1991**; pp 309–364.
87. Dioumaev, V. K.; Procopio, L. J.; Carroll, P. J.; Berry, D. H. *J. Am. Chem. Soc.* **2003**, *125*, 8043–8058.
88. Gell, K. I.; Pain, B.; Schwartz, J.; Williams, G. M. *J. Am. Chem. Soc.* **1982**, *104*, 1846–1855.
89. Watson, P. L. *J. Am. Chem. Soc.* **1983**, *105*, 6491–6495.
90. Fendrick, C. M.; Marks, T. J. *J. Am. Chem. Soc.* **1984**, *106*, 2214–2216.
91. Thompson, M. E.; Baxter, S. M.; Bulls, A. R.; Burger, B. J.; Nolan, M. C.; Santarsiero, B. D.; Schaefer, W. P.; Bercaw, J. E. *J. Am. Chem. Soc.* **1987**, *109*, 203–225.
92. Hartwig, J. F.; Bhandari, S.; Rablen, P. R. *J. Am. Chem. Soc.* **1994**, *116*, 1839–1844.
93. Woo, H.-G.; Tilley, T. D. *J. Am. Chem. Soc.* **1989**, *111*, 3757–3758.
94. Woo, H.-G.; Tilley, T. D. *J. Am. Chem. Soc.* **1989**, *111*, 8043–8044.
95. Woo, H.-G.; Heyn, R. H.; Tilley, T. D. *J. Am. Chem. Soc.* **1992**, *114*, 5698–5707.
96. Woo, H.-G.; Walzer, J. F.; Tilley, T. D. *J. Am. Chem. Soc.* **1992**, *114*, 7047–7055.
97. Tilley, T. D. *Acc. Chem. Res.* **1993**, *26*, 22–29.
98. Tsuji, Y.; Funato, M.; Ozawa, M.; Ogiyama, H.; Kajita, S.; Kawamura, T. *J. Org. Chem.* **1996**, *61*, 5779–5787.
99. Verdaguer, X.; Hansen, M. C.; Berk, S. C.; Buchwald, S. L. *J. Org. Chem.* **1997**, *62*, 8522–8528.
100. Smith, E. E.; Du, G.; Fanwick, P. E.; Abu-Omar, M. M. *Organometallics* **2010**, *29*, 6527–6533.

101. Romero, P. E.; Piers, W. E. *J. Am. Chem. Soc.* **2007**, *129*, 1698–1704.
102. Stewart, I. C.; Keitz, B. K.; Kuhn, K. M.; Thomas, R. M.; Grubbs, R. H. *J. Am. Chem. Soc.* **2010**, *132*, 8534–8535.
103. Keitz, B. K.; Grubbs, R. H. *J. Am. Chem. Soc.* **2011**, *133*, 16277–16284.
104. Chatterjee, A. K.; Choi, T. L.; Sanders, D. P.; Grubbs, R. H. *J. Am. Chem. Soc.* **2003**, *125*, 11360–11370.
105. Zhang, L.; Chan, K. S. *Organometallics* **2006**, *25*, 4822–4829.
106. Ackermann, L.; Born, R.; Álvarez-Bercedo, P. *Angew. Chem., Int. Ed.* **2007**, *46*, 6364–6367.
107. Menozzi, C.; Dalko, P. I.; Cossy, J. *Synlett* **2005**, 2449–2452.
108. Denmark, S.; Baird, J. D. *Chem. - Eur. J.* **2006**, *12*, 4954–4963.
109. Jones, G. R.; Landais, Y. *Tetrahedron* **1996**, *52*, 7599–7662.
110. Ting, R.; Adam, M. J.; Ruth, T. J.; Perrin, D. M. *J. Am. Chem. Soc.* **2005**, *127*, 13094–13095.
111. Parrott, M. C.; Finnis, M.; Luft, J. C.; Pandya, A.; Gullapalli, A.; Napier, M. E.; DeSimone, J. M. *J. Am. Chem. Soc.* **2012**, *134*, 7978–7982.
112. Cheng, C.; Simmons, E. M.; Hartwig, J. F. *Angew. Chem., Int. Ed.* **2013**, *52*, 8984–8989.
113. Brough, P. A.; Fisher, S.; Zhao, B.; Thomas, R. C.; Snieckus, V. *Tetrahedron Lett.* **1996**, *37*, 2915–2918.
114. Sore, H.; Galloway, W.; Spring, D. *Chem. Soc. Rev.* **2012**, *41*, 1845–66.
115. Hosomi, A.; Endo, M.; Sakurai, H. *Chem. Lett.* **1976**, *5*, 941e942.
116. Masse, C. E.; Panek, J. S. *Chem. Rev.* **1995**, *95*, 1293–1316.
117. Denmark, S. E.; Fu, J. *Chem. Rev.* **2003**, *103*, 2763–2793.

118. Fleming, I.; Dunogues, J.; Smithers, R. In *Organic Reactions*; John Wiley & Sons: New York, NY, **2004**; pp 57-575.
119. Denmark, S. E.; Liu, J. H. C. *Angew. Chem., Int. Ed.* **2010**, *49*, 2978-2986.
120. Schroeder, M. A.; Wrighton, M. S. *J. Am. Chem. Soc.* **1976**, *98*, 551-558.
121. Mitchener, J. C.; Wrighton, M. S. *J. Am. Chem. Soc.* **1981**, *103*, 975-977.
122. Millan, A.; Towns, E.; Maitlis, P. M. *J. Chem. Soc., Chem. Commun.* **1981**, 673-674.
123. Carre, F. H.; Moreau, J. J. E. *Inorg. Chem.* **1982**, *21*, 3099-3105.
124. Millan, A.; Fernandez, M.-J.; Bentz, P.; Maitlis, P. M. *J. Mol. Catal.* **1984**, *26*, 89-104
125. Fernandez, M. J.; Esteruelas, M. A.; Jimenez, M. S.; Oro, L. A. *Organometallics* **1986**, *5*, 1519-1520.
126. Hori, Y.; Mitsudo, T.-a.; Watanabe, Y. *Bull. Chem. Soc. Jpn.* **1988**, *61*, 3011-3013.
127. Tanke, R. S.; Crabtree, R. H. *Organometallics* **1991**, *10*, 415-418.
128. Doyle, M. P.; Devora, G. A.; Nefedov, A. O.; High, K. G. *Organometallics* **1992**, *11*, 549-555.
129. Kakiuchi, F.; Tanaka, Y.; Chatani, N.; Murai, S. *J. Organomet. Chem.* **1993**, *456*, 45-47.
130. Takeuchi, R.; Yasue, H. *Organometallics* **1996**, *15*, 2098-2102.
131. LaPointe, A. M.; Rix, F. C.; Brookhart, M. *J. Am. Chem. Soc.* **1997**, *119*, 906-917.
132. Sakar, T. K. *Sci. Synth.* **2002**, *4*, 837.
133. Sprengers, J. W.; de Greef, M.; Duin, M. A.; Elsevier, C. J. *Eur. J. Inorg. Chem.* **2003**, *2003*, 3811-3819.
134. Hirano, K.; Yorimitsu, H.; Oshima, K. *J. Am. Chem. Soc.* **2007**, *129*, 6094-6095.
135. Nakamura, S.; Yonehara, M.; Uchiyama, M. *Chemistry—A European Journal* **2008**, *14*, 1068-1078.

136. Jiang, Y.; Blacque, O.; Fox, T.; Frech, C. M.; Berke, H. *Chemistry—A European Journal* **2009**, *15*, 2121-2128.
137. Naumov, R. N.; Itazaki, M.; Kamitani, M.; Nakazawa, H. *J. Am. Chem. Soc.* **2012**, *134*, 804-807.
138. Marciniak, B. *Silicon Chem.* **2002**, *1*, 155.
139. Marciniak, B. *Comprehensive Handbook on Hydrosilylation*; Pergamon Press: Oxford, UK, **1992**.
140. Hiyama, T.; Kusumoto, T. In *Comprehensive Organic Synthesis*; Trost, B. M., Fleming, I., Eds.; Pergamon: Oxford, U.K., **1991**; Vol. 8, p 769.
141. McAtee, R. J.; Martin, S. E. S.; Ahneman, T. D.; Johnson, A. K.; Watson, A. D. *Angew. Chem.* **2012**, *124*, 3723 – 3727; *Angew. Chem. Int. Ed.* **2012**, *51*, 3663 – 3667.
142. Na, Y.; Chang, S. *Org. Lett.* **2000**, *2*, 1887 – 1889.
143. Trost, M. B.; Ball, T. Z. *J. Am. Chem. Soc.* **2005**, *127*, 17644 – 17655.
144. Denmark, S. E.; Pan, W. *Org. Lett.* **2002**, *4*, 4163 – 4166.
145. Denmark, S. E.; Wehrli, D. *Org. Lett.* **2000**, *2*, 565 – 568.
146. Berthon-Gelloz, G.; Schumers M. J.; De Bo, G.; Mark, E. I. *J. Org. Chem.* **2008**, *73*, 4190 – 4197.
147. Takai, K.; Kataoka, Y.; Okazoe, T.; Utimoto, K. *Tetrahedron Lett.* **1987**, *28*, 1443 – 1446.
148. Hodgson, M. D.; Comina, J. P. *Tetrahedron Lett.* **1994**, *35*, 9469 – 9470.
149. Itami, K.; Nokami, T.; Yoshida, J. *Org. Lett.* **2000**, *2*, 1299 – 1302.
150. McNulty, J.; Das, P. *Chem. Commun.* **2008**, 1244 – 1245.
151. Murthi, K. K.; Salomon, G. R. *Tetrahedron Lett.* **1994**, *35*, 517 – 520.
152. Denmark, S. E.; Fujimori, S. *J. Am. Chem. Soc.* **2005**, *127*, 8971 – 8973.

153. Trost, M. B.; Frederiksen, U. M.; Papillon, P. N. J.; Harrington, E. P.; Shin, S.; Shireman, T. B. *J. Am. Chem. Soc.* **2005**, *127*, 3666 – 3667.
154. Trost, M. B.; Machacek, M. R.; Ball, T. B. *Org. Lett.* **2003**, *5*, 1895 – 1898.
155. Pietraszuk, C.; Fischer, H.; Kujawa, M.; Marciniak, B. *Tetrahedron Lett.* **2001**, *42*, 1175 – 1178.
156. Denmark, S. E.; Yang, M. S.; *Org. Lett.* **2001**, *3*, 1749 – 1752.
157. Denmark, S. E.; Wang, Z. *Org. Lett.* **2001**, *3*, 1073–1076.
158. Pietraszuk, C.; Fischer, H.; Rogalski, S.; Marciniak, B. *J. Organomet. Chem.* **2005**, *690*, 5912–5921.
159. Denmark, S. E.; Neuville, L.; Christy, M. E. L.; Tymonko, S. A. *J. Org. Chem.* **2006**, *71*, 8500–8509.
160. Li, J.; Sun, C.; Lee, D. *J. Am. Chem. Soc.* **2010**, *132*, 6640–6641.
161. Rooke, D. A.; Ferreira, E.M. *J. Am. Chem. Soc.* **2010**, *132*, 11926–11928.
162. Wang, P.; Yeo, X.-L.; Loh, T.-P. *J. Am. Chem. Soc.* **2011**, *133*, 1254–1256.
163. Miller, Z. D.; Li, W.; Belderrain, T. R.; Montgomery, J. *J. Am. Chem. Soc.* **2013**, *135*, 15282–15285.
164. Martin, S. E.; Watson, D. A. *J. Am. Chem. Soc.* **2013**, *135*, 13330–13333.
165. Lu, B.; Falck, J. R. *J. Org. Chem.* **2010**, *75*, 1701–1705.
166. Bokka, A.; Hua, Y.; Berlin, A. S.; Jeon, J. *ACS Catal.* **2015**, *5*, 3189–3195.
167. Brookhart, M.; Grant, B. E. *J. Am. Chem. Soc.* **1993**, *115*, 2151–2156.
168. Sadow, A. D.; Tilley, T. D. *J. Am. Chem. Soc.* **2005**, *127*, 643–656.
169. Schleyer, P. v. R.; Williams Jr, J. E.; Blanchard, K. *J. Am. Chem. Soc.* **1970**, *92*, 2377–2386.

170. Allinger, N. L.; Sprague, J. T. *J. Am. Chem. Soc.* **1972**, *94*, 5734-5747.
171. Bielawski, C. W.; Grubbs, R. H. *Prog. Polym. Sci.* **2007**, *32*, 1-29.
172. Our efforts toward observing the formation of a ruthenium silyl complex by crystallography were not fruitful.
173. Noyori, R.; Ohkuma, T. *Angew. Chem., Int. Ed.* **2001**, *40*, 40-73.
174. Hoye, T. R.; Zhao, H. *J. Org. Chem.* **2002**, *67*, 4014-4016.
175. Raptis, C.; Garcia, H.; Stratakis, M. *Angew. Chem. Int. Ed.* **2009**, *48*, 3133-3136.
176. Taillier, C.; Hameury, T.; Bellosta, V.; Cossy, J. *Tetrahedron*, **2007**, *63*, 4472-4479.

Biographical Information

Apparao Bokka earned a Bachelor of Science in Chemistry from Andhra University, located in Visakhapatnam, AP, India in 2002. He got his Master of Science in Chemistry with specialization in Organic Chemistry from the same university in 2004. He worked for different pharmaceutical companies in the field of research and development for about eight years. In 2012, Apparao began his doctoral studies under the supervision of Dr. Junha Jeon at the University of Texas at Arlington (UTA). Apparao has worked on various projects with emphasis on ruthenium alkylidene catalyzed alkene-silane cross-coupling reactions. He also worked as graduate summer intern at AbbVie Inc. during summer of 2016. He was involved in the development of Cu-H mediated asymmetric synthesis. Apparao plans to continue his career in industry after receiving his degree from UTA.